

**THE EFFECT OF HIGH VOLUMES OF UNGRADED FLY ASH
ON THE PROPERTIES OF FOAMED CONCRETE**

ELIZABETH PAULINA KEARSLEY

2

Submitted in accordance with the requirements for the degree of
DOCTOR OF PHILOSOPHY

The University of Leeds
School of Civil Engineering

August 1999

The candidate confirms that the work submitted is her own and that appropriate credit
has been given where reference has been made to the work of others

**THE EFFECT OF HIGH VOLUMES OF UNGRADED FLY ASH
ON THE PROPERTIES OF FOAMED CONCRETE**

ACKNOWLEDGEMENTS

I wish to express my appreciation to the following organizations and persons who made this thesis possible:

- The University of Pretoria for financial support and the use of laboratory facilities during the course of the study.
- Grinaker Duraset for financial support.
- The Joan Whitmore Scholarship Management Committee for financial support in the form of the Joan Whitmore Scholarship.
- Dr PJ Wainwright, my supervisor, and Professor SC van As, my co-supervisor for their guidance and support.
- Mr Derek Mostert, the concrete technologist at the University of Pretoria, for his technical assistance.
- My family for their encouragement and support during the study.

ABSTRACT

Foamed concrete is produced by combining foam and slurry thus entrapping numerous small bubbles of air in the cement paste or mortar. The density of foamed concrete is a function of the volume of foam added to the slurry and the strength decreases with decreasing density. In this study the effect on the properties of foamed concrete, of replacing large volumes of cement with both classified and unclassified fly ash (pfa) was investigated. The casting densities of the materials used in this investigation varied between 1000 and 1500 kg/m³ and 50%, 66.7% and 75% of the cement (by weight) was replaced with pfa. The properties measured included compressive strength, dry density, porosity, permeability, water absorption, drying shrinkage, elastic deformation, creep, and void size distribution.

The use of high volumes of unclassified ash did not appear to have any significant detrimental effects on the measured properties of the foamed concrete. Although the rate of gain in strength was reduced by the use of large volumes of ash, up to 67% of the cement can be replaced by ash without any significant reduction in the long-term strength. The permeability increased with increased air content but the water absorption did not appear to be influenced by the volume of air entrained. The elastic modulus of foamed concrete reduced while the creep increased with reducing density. The drying shrinkage of foamed concrete does not seem to be a function of density and the shrinkage values were similar to those of cement paste with similar water/binder ratios; these values were between two to three times greater than those of conventional concrete. An increase in ash content lead to a slight reduction in the drying shrinkage.

A mathematical model was developed relating the compressive strength of the foamed concrete to age, porosity and ash/cement ratio.

TABLE OF CONTENTS

	Page
CHAPTER 1: INTRODUCTION	1
1.1 BACKGROUND	1
CHAPTER 2 : REVIEW OF PREVIOUS RESEARCH	5
2.1 INTRODUCTION	5
2.2 FOAMED CONCRETE	5
2.2.1 PROPERTIES OF FOAMED CONCRETE	6
2.2.1.1 Compressive strength	6
2.2.1.2 Deformation	14
2.3 VOIDS IN HYDRATED CEMENT PASTE	17
2.3.1 BACKGROUND	17
2.3.2 TYPES OF VOIDS	19
2.3.2.1 Pore voids	19
2.3.2.2 Capillary voids	20
2.3.2.3 Air voids	21
2.3.3 THE EFFECT OF VOIDS ON DURABILITY AND STRENGTH	23
2.3.3.1 Effect on Durability	23
2.3.3.2 Effect on Strength	24
2.4 THE USE OF PFA IN CONCRETE	28
2.4.1 BACKGROUND	28
2.4.2 PFA SHAPE AND SIZE	30
2.4.3 HYDRATION AND MICROSTRUCTURE	31
2.4.4 CODE REQUIREMENTS FOR THE USE OF FLY ASH IN CONCRETE	33
2.4.5 THE EFFECT OF PFA ON THE PROPERTIES OF CONCRETE	34
2.4.5.1 Compressive Strength	34
2.4.5.2 Durability	44
2.4.5.3 Shrinkage and creep	47
2.5 CONCLUSIONS	48
CHAPTER 3 : EXPERIMENTAL PROCEDURE FOR THE MANUFACTURE OF FOAMED CONCRETE	50
3.1 INTRODUCTION	50
3.2 EQUIPMENT	50
3.3 MIX DESIGN	51
3.4 CASTING OF FOAMED CONCRETE	52
3.5 CURING	53
3.6 DENSITY	53
CHAPTER 4: EXPERIMENTAL PROGRAM	56
4.1 PRELIMINARY TESTS	56
4.1.1 MIX PROPORTIONS	56
4.1.2 REPEATABILITY	58
4.2 MAIN TEST PROGRAM	61

	Page
4.3 MATERIALS	63
4.3.1 FOAMING AGENT	63
4.3.2 CEMENT	63
4.3.3 FLY ASH	64
4.3.4 CONFORMITY TO STANDARD SPECIFICATION CRITERIA	68
4.4 MIXTURE COMPOSITION	68
4.5 TESTS CONDUCTED	69
4.5.1 COMPRESSIVE STRENGTH	69
4.5.2 DEFORMATION OF FOAMED CONCRETE	70
4.5.2.1 Shrinkage	70
4.5.2.2 Creep	71
4.5.2.3 Elastic modulus	71
4.5.3 POROSITY	72
4.5.4 PERMEABILITY	72
4.5.5 IMAGE ANALYSIS	74
CHAPTER 5: RESULTS	77
5.1 MIXTURES	77
5.2 RESULTS	77
CHAPTER 6: DISCUSSION OF RESULTS	88
6.1 INTRODUCTION	88
6.2 VOID STRUCTURE	88
6.2.1. ENTRAINED AIR VOIDS	88
6.2.1.1 Void size	89
6.2.1.2 Void spacing	92
6.2.1.3 Relation between dry density and void size	95
6.2.1.4 Relation between dry density, ash/cement ratio and void distribution	96
6.2.1.5 Combined particle size, void size and distribution	100
6.2.2 POROSITY	105
6.2.3 CONCLUSIONS ON VOIDS	111
6.3 COMPRESSIVE STRENGTH	112
6.3.1 CEMENT PASTE	112
6.3.2 PASTES CONTAINING ASH	112
6.3.3 MATHEMATICAL MODELING OF PASTE COMPRESSIVE STRENGTHS	114
6.3.4 FOAMED CONCRETE	118
6.3.5 MATHEMATICAL MODELING OF FOAMED CONCRETE COMPRESSIVE STRENGTHS	124
6.3.5.1 Volumetric ratios	124
6.3.5.2 Density ratios	125
6.3.6 EFFECT OF POROSITY ON COMPRESSIVE STRENGTH	131
6.3.7 EFFECT OF VOID STRUCTURE ON COMPRESSIVE STRENGTH	136
6.3.8 CONCLUSIONS ON COMPRESSIVE STRENGTH	137

	Page
6.4 WATER ABSORPTION AND PERMEABILITY	139
6.4.1 WATER ABSORPTION	139
6.4.2 WATER VAPOUR PERMEABILITY	143
6.4.3 CONCLUSIONS ON WATER ABSORPTION AND PERMEABILITY	147
6.5 DEFORMATION OF FOAMED CONCRETE	149
6.5.1 DRYING SHRINKAGE	149
6.5.2 ELASTICITY AND CREEP	152
6.5.3 CONCLUSIONS ON DEFORMATION	157
CHAPTER 7: COMPUTER SIMULATION	159
7.1 BACKGROUND	159
7.2 COMPRESSIVE STRENGTH MODEL	159
7.2.1 EFFECT OF ASH TYPE AND CONTENT	161
7.2.2 EFFECT OF AGE ON OPTIMUM COMPOSITION	163
7.2.3 MIXTURES OPTIMIZED FOR STRENGTH AND COSTS	165
7.3 CONCLUSION	172
CHAPTER 8: CONCLUSIONS AND RECOMMENDATIONS	174
8.1 CONCLUSIONS	174
8.2 RECOMMENDATIONS	176
CHAPTER 9 : REFERENCES	178

LIST OF TABLES

	Page
Table 2.1: Typical Properties of Foamed Concrete.	15
Table 2.2: Drying Shrinkage of A.A.C.	16
Table 4.1: Uniformity of Mixture.	59
Table 4.2: Binder Properties as Measured by Independent Outside Testing House.	64
Table 4.3: Conformity of Materials to Standards.	69
Table 4.4: Mix ratios.	69
Table 4.5: Typical Image Analysis Output	76
Table 5.1: Composition of Mixtures.	78
Table 5.2 : Volume Ratios of Mixtures.	79
Table 5.3: 7 Day and 28 Day Compressive Strength of Mixtures.	80
Table 5.4: 56 Day and 84 Day Compressive Strength of Mixtures.	81
Table 5.5: 180 Day and 270 Day Compressive Strength of Mixtures.	82
Table 5.6: 365 Day Compressive Strength of Mixtures.	83
Table 5.7: Porosity, Permeability and Water absorption.	84
Table 5.8: Drying Shrinkage.	85
Table 5.9: Creep Results.	86
Table 5.10: Void Diameter Distribution.	87
Table 6.1: Cumulative Void Diameter Distribution.	92
Table 6.2: Distance between Voids.	96
Table 6.3: Particle and Void Size Functions.	104
Table 6.4: Equations for the Strength-porosity Relationship of Foamed Concrete.	134
Table 6.5: Fitted Functions.	125
Table 6.5: Relation between Dry Density and Water Vapour Permeability.	140
Table 7.1: Constant for Compressive Strength Model.	161
Table 7.2: Optimum Ash Content.	164
Table 7.3: Mixtures for 28 day Strengths.	167
Table 7.4: Mixtures for 365 day Strengths.	169

LIST OF FIGURES

	Page
Figure 2.1: Effect of Sand Content on Compressive Strength of Foamed Concrete.	7
Figure 2.2: Influence of Type of Foaming Agent on Compressive Strength.	9
Figure 2.3: Water/cement Ratios to Achieve Adequate Foam Stability for Different Aggregate Contents.	10
Figure 2.4: Effect of Aggregate Content on Compressive Strength at Constant Density.	11
Figure 2.5: Effect of Water/cement Ratio on Compressive Strength.	12
Figure 2.6: Compressive Strengths using Fly ash or Sand.	13
Figure 2.7: Pore sizes.	18
Figure 2.8: Air Void Size Distribution of Foamed Concrete.	22
Figure 2.9: Effect of Cement Replacement on Compressive Strength.	34
Figure 2.10: Effect of Water Requirement on Compressive Strength.	36
Figure 2.11: Effect of Carbon Content on Water Requirement.	37
Figure 2.12: Effect of Carbon Content on Compressive Strength.	37
Figure 2.13: Effect of Particle Size on Compressive Strength.	38
Figure 3.1 : Compressive Strength as a Function of Wet Density.	54
Figure 3.2 : Dry Density as a Function of Wet Density.	55
Figure 4.1: Effect of Ash/cement Ratio on optimum Water/binder Ratio.	57
Figure 4.2: Effect of Ash/cement Ratio on Compressive Strength.	57
Figure 4.3: Effect of Ash/cement Ratio on Shrinkage.	58
Figure 4.4: Relationship between Standard Deviation and Characteristic Strength.	60
Figure 4.5: Particle Size Distribution of Binder.	63
Figure 6.1: Void Diameter Distribution of 1 500 kg/m ³ Mixtures with a/c=1.	89
Figure 6.2: Void Diameter Distribution of 1 000 kg/m ³ Mixtures with a/c=3.	90
Figure 6.3: Cumulative Void Diameter Distribution.	91
Figure 6.4: Calculation of Void Spacing.	93
Figure 6.5: Distance between Voids for Mixture with a/c =2.	94
Figure 6.6: Effect of Dry Density on Entrained Air Void Size.	97
Figure 6.7: Effect of Dry Density on the Distance between Voids.	98
Figure 6.8: Effect of Ash/cement Ratio on Distance between Voids.	99
Figure 6.9: Relation between Air Void Diameter and Air Void Spacing	100
Figure 6.10: Effect of Binder Particle Size on Void Size and Distribution.	102
Figure 6.11: Combined Binder and Void Sizes.	103
Figure 6.12: Effect of Dry Density on Median Combined Particle Size.	104
Figure 6.13: Porosity as a Function of Dry Density.	105
Figure 6.14: Effect of Porosity on Air Void Size and Distribution.	107
Figure 6.15: Effect of Ash/cement Ratio on Paste Porosity	108
Figure 6.16: Compressive Strength of Cement Paste as a Function of Time.	112
Figure 6.17: Compressive Strength of Pastes Containing Pfa.	113
Figure 6.18: Compressive Strength of Pastes Containing Pozz-fill.	114
Figure 6.19: Compressive Strength of Cement Paste versus Water/cement Ratio.	114
Figure 6.20: Calculated k-values.	117

	Page
Figure 6.21: Compressive Strength of 1500 kg/m ³ Mixtures as a Function of Time.	119
Figure 6.22: Compressive Strength of 1250 kg/m ³ Mixtures as a Function of Time.	120
Figure 6.23: Compressive Strength of 1000 kg/m ³ Mixtures as a Function of Time.	121
Figure 6.24: 28 Day Compressive Strength as a Function of Dry Density.	122
Figure 6.25: One Year Compressive Strength as a Function of Dry Density.	123
Figure 6.26: Measured Dry Density versus Calculated Dry Density.	127
Figure 6.27: Binder Weight Model Compared to 1500 kg/m ³ Mixtures.	128
Figure 6.28: Binder Weight Model Compared to 1250 kg/m ³ Mixtures.	129
Figure 6.29: Binder Weight Model Compared to 1000 kg/m ³ Mixtures.	130
Figure 6.30: Compressive Strength - Theoretical Porosity Relation at 365 days.	131
Figure 6.31: Measured versus Theoretical Porosity.	132
Figure 6.32: Effect of Porosity on Compressive Strength.	133
Figure 6.33: Predicted versus Measured Strengths.	136
Figure 6.34: Effect of Void Structure on Compressive Strength.	137
Figure 6.35: Effect of Dry Density on Percentage Water Absorption.	139
Figure 6.36: Effect of Dry Density on Water Absorption.	140
Figure 6.37: Effect of Porosity on Percentage Water Absorption.	141
Figure 6.38: Water Absorption as a Function of Porosity.	141
Figure 6.39: Effect of Void Size and Spacing on Water Absorption.	142
Figure 6.40: Water Absorption as a Function of Ash/cement Ratio.	143
Figure 6.41: Weight Loss as a Function of Dry Density.	144
Figure 6.42: Vapour Permeability as a Function of Dry Density.	144
Figure 6.43: Water Vapour Permeability versus Porosity.	145
Figure 6.44: Effect of Ash/cement Ratio on Water Vapour Permeability.	146
Figure 6.45: Effect of Void Size and Distribution on Water Vapour Permeability.	147
Figure 6.46: Water Absorption versus Water Vapour Permeability.	148
Figure 6.47: Shrinkage of 1500 kg/m ³ Mixtures Containing Pfa.	149
Figure 6.48: Drying Shrinkage versus Dry Density.	150
Figure 6.49: Effect of Porosity on the Drying Shrinkage of Foamed Concrete.	151
Figure 6.50: Effect of Ash/cement Ratio on the Drying Shrinkage of Foamed Concrete.	151
Figure 6.51: Modulus of Elasticity.	152
Figure 6.52: Creep of 1500 kg/m ³ Foamed Concrete.	153
Figure 6.53: Creep of 1250 kg/m ³ Foamed Concrete.	153
Figure 6.54: Creep of 1000 kg/m ³ Foamed Concrete.	154
Figure 6.55: Creep as a Function of Dry Density.	154
Figure 6.56: Specific Creep of 1500 kg/m ³ Foamed Concrete.	155
Figure 6.57: Specific Creep of 1250 kg/m ³ Foamed Concrete.	155
Figure 6.58: Specific Creep of 1000 kg/m ³ Foamed Concrete.	156
Figure 6.59: Specific Creep as a Function of Dry Density.	156
Figure 7.1: Predicted Strength versus Measured Strength.	161
Figure 7.2: Effect of Ash Type on Compressive Strength for 30% Porosity.	162
Figure 7.3: Effect of Ash Type on Compressive Strength for 60% Porosity.	162
Figure 7.4: Effect of Age on Strength Development of Foamed Concrete.	163
Figure 7.5: Optimum Ash Content as a Function of Time.	165
Figure 7.6: The effect of Required Compressive Strength on Material Cost.	171
Figure 7.7: Effect of Porosity on Material Cost.	172

LIST OF PLATES

Page

Plate 3.1: Equipment used for the Manufacture of Foamed Concrete.

51

Plate 4.1: SEM photos of cement, pfa and pozz-fill (x450).

66

Plate 4.2: SEM photos of cement, pfa and pozz-fill (x4500).

67

Plate 4.3: Typical Optical Microscope Image.

76

Plate 5.1: Typical Optical Microscope Image.

86

Plate 6.1: SEM photos of Paste, 1500 kg/m³ and 1000 kg/m³
Mixtures with pfa/c = 3 (x ± 400).

109

Plate 6.2: SEM photos of Paste, 1500 kg/m³ and 1000 kg/m³
Mixtures with pfa/c = 3 (x 5 000).

110

CHAPTER 1: INTRODUCTION

1.1 BACKGROUND

In South Africa there is currently a major shortfall in affordable, durable infrastructure and housing. The Reconstruction and Development Program underway in South Africa aims at giving all South Africans access to “A permanent residential structure with secure tenure, ensuring privacy and providing adequate protection against the elements”.¹

According to the White Paper on Housing¹ South Africa is characterized by large-scale unemployment in the formal sector of the economy. The lack of housing and infrastructure combined with the high unemployment figures, creates an environment perfectly suited for labour intensive projects where the unemployed in a disadvantaged community can be trained to uplift the community and provide the much needed infrastructure.

In order to address the needs of the country, modern specialized technology could be used to improve the quality of the building materials used in under developed areas. In a developing community the cost of the material and equipment as well as the ease of manufacture and construction plays a major role in determining the acceptability of a new building material. It is therefore essential to adapt any technology to local conditions.² By manufacturing lightweight building blocks, wall panels, roofing sheets, footings and floor slabs on the outskirts of undeveloped areas, the communities could use their own transport to obtain these building materials.³

Low density concrete is normally defined as concrete having an air-dry density of below 2000 kg/m^3 as opposed to normal concrete with a density in the region of 2350 kg/m^3 .⁴ Low density concrete has practical and economical advantages as the reduced weight of the superstructure can lead to savings in the cost of super- and substructures and components can be handled and erected relatively easily. Fire resistance⁵ and thermal insulation⁶ of low density concrete are superior to those of normal density concrete.

Low-density concrete can be manufactured with a density of between 300 and 1850 kg/m³. The strength of low-density concrete is a function of density and therefore density can be used to classify low density concrete according to the purpose for which it is to be used. Low density concrete can be classified as one of the following:⁶

- *Structural low-density concrete* has a density between 1350 and 1850 kg/m³ and minimum compressive cylinder strength of 17 MPa.
- *Low-density concrete* has a density between 300 and 800 kg/m³ and is used for non-structural applications, mainly for thermal insulation purposes.
- A third category between the previous two used for masonry units.

Replacing some of the solid material in the mixture by air voids can reduce the density of concrete. These voids can be located in one of the following three places:⁶

- In the aggregate particles; known as *low density aggregate concrete*.
- In the cement paste; known as *cellular or aerated concrete*.
- Between coarse aggregate particles (by omitting fine aggregate); known as *no-fines concrete*.

Cellular concrete is produced by introducing voids into the plastic mortar mixture, resulting in a material with a cellular structure, containing voids with a diameter of between 0.1 and 1 mm.⁷ As no coarse aggregate is used in cellular concrete, the term concrete is strictly speaking inappropriate.

The voids in cellular or aerated concrete can be produced by gas generated during a chemical reaction, normally caused by the addition of aluminum powder (gas concrete) or by the introduction of air. Cellular concrete produced by the introduction of a foaming agent, is called foamed concrete. The Dutch research centre “Civieltechnisch centrum uitvoering research en regelgeving” (C.U.R.), recommendation 14, defines foamed concrete as a cementitious material, with a minimum of 20% (per volume) foam entrained into the plastic mortar.⁸

Entrapping numerous small bubbles of air in cement paste or mortar forms foamed concrete by a mechanical process. Mechanical foaming can take place in two principal ways:⁹

- by pre-foaming a suitable agent with water and then combining the foam with the paste or mortar;
- by adding a quantity of foaming agent to the slurry and whisking the mixture into a stable mass with the required density.

The most commonly used foam concentrates are based on protein hydrolyzates or synthetic surfactants.¹⁰ They are formulated to produce air bubbles that are stable and able to resist the physical and chemical forces imposed during mixing, placing and hardening.

Foamed concrete is the most popular of all low-density concretes in developing countries.¹¹ The reasons for this are the low capital expenditure on equipment and the ready availability of the principal materials. The material can be produced on a small scale, even at site level and it is relatively easy to place and finish without heavy or expensive equipment. Foamed concrete is one of the few building materials combining good mechanical strength with low thermal conductivity and ease of working.⁹

Since the introduction of cellular concrete systems to the construction industry more than 50 years ago the use of foamed concrete has been almost exclusively limited to the following applications: non structural void filling, thermal insulation, acoustic damping, trench filling for reinstatement of roads and building blocks¹². In the Netherlands foamed concrete has been used not only for level corrections in housing developments, but also for fill-material where ground subsidence has taken place and as founding layer for road works on very weak soils¹³.

According to Benn¹² foamed concrete is self-compacting, free flowing and pumpable and therefore easy to place in inaccessible places. It has good thermal and acoustic properties and is frost resistant but it is too weak for direct exposure to traffic and hail and should be protected.

Foamed concrete is perceived to be weak, non-durable with high shrinkage characteristics. Neville⁶ states that untreated aerated concrete should not be exposed to an aggressive atmosphere and that unprotected reinforcement in aerated concrete would be vulnerable to corrosion even when the external attack is not very severe.

Neopor states that unstable foams have in the past resulted in foamed concrete having properties unsuitable for reinforced, structural applications.¹⁴ The development of protein-hydrolysis based foaming agents and specialized foam generating equipment have improved the stability of the foam, making it possible to manufacture foamed concrete for structural applications. In recent years foamed concrete has been used as a structural material in schools, apartments and housing developments in countries such as Brazil, Singapore, Kuwait, Nigeria, Botswana, Mexico, Indonesia, Libya, Saudi Arabia, Algeria, Iraq and Egypt.¹⁴

It is well known that the durability of normal concrete can be improved by reducing the permeability and porosity of the mortar through replacing small percentages (say up to 35%) of the cement with pulverized fuel ash (pfa). It would seem logical to expect that the inclusion of pfa into foamed concrete will have a similar effect but this fact has not yet been proven and it is one of the prime objectives of the study to prove this. A question that has to be answered is whether the use of pfa in foamed concrete can markedly improve the strength and durability of the material.

CHAPTER 2 : REVIEW OF PREVIOUS RESEARCH

2.1 INTRODUCTION

Little has been published on foamed concrete and the factors influencing its properties. In the first section of this review the published information on foamed concrete is discussed. As foamed concrete is produced by the inclusion of air voids in cement paste, the second section of this chapter reviews published research on the effect of voids on the properties of cement pastes and concrete. The third and final section of this chapter deals with the effect of pulverized-fuel ash (pfa) on the properties of normal concrete.

2.2 FOAMED CONCRETE

The production of foamed concrete involves the incorporation of a fairly large volume of air into a mixture consisting essentially of cement and water, with or without the addition of sand. This incorporation can be achieved by adding air to the mixture in the form of highly expanded foam consisting of innumerable small bubbles¹⁵. Forcing a foaming agent, diluted in water and a jet of air through baffles generates thick stable foam. The bubbles in this foam acts as temporary containers for the air, enabling accurate measurement of the air content to be made and producing a uniform distribution of the voids.

In conventional concrete the relationship between water content and strength is relatively straight forward; as a general rule and for a given mix of materials, as the water content increases the workability will increase and the strength will reduce. However for foamed concrete this relationship is not quite so simple and for the system to work correctly the amount of water that can be added is critical and lies within a very tight band. If too little water is added the cement will preferentially withdraw water from the foam causing rapid degeneration of the foam. On the other hand if too much water is added segregation will take place which causes the density to vary within any particular batch.³

Foamed concrete contains at least three constituents, namely cement, water and foam. Beside these constituents several fillers such as sand, pfa, crushed dust, expanded polystyrene granules and sintered pfa (Lytag) fines can be added to the mixture. Van Deijk¹⁶ states that various factors such as water-cement ratio, cement-water-aggregate ratio, nature of the foaming agent, hydration rate and workability have strong influences on the properties of foamed concrete.

2.2.1 PROPERTIES OF FOAMED CONCRETE

2.2.1.1 Compressive strength

According to L. B. Chemicals¹⁵ the strength of aerated concrete is closely related to the dry density and for any given mixture the strength rises rapidly as the density increases. The relationship between water-cement ratio and strength that exists in the case of normal or dense concrete is not so apparent where aerated mixes are concerned and the water-cement ratio required to achieve successful foaming might vary appreciably with the grading of the sand without affecting the compressive strength significantly, provided the ultimate dry density is not altered. The water/cement ratios used in these mixtures¹⁵ varied from 0.45 for the mixtures containing no sand to 0.85 for mixtures with a sand/cement ratio (by weight) of 4. The compressive strength values published in this article were used to draw the graph in Figure 2.1 indicating the effect of sand content on the relationship between dry density and compressive strength.

The compressive strengths in Figure 2.1 indicate that mixtures containing no sand yield significantly higher strengths than mixtures of the same density containing sand. A mixture containing only cement, water and foam can however only be affordable at very low densities (below 500 kg/m^3)¹⁵. For the mixtures containing sand the decrease in strength with increased sand content is only marginal for sand/cement ratios of between 2 and 4. Multiple regression analysis has been conducted by the author (Kearsley) to determine the numerical relations between the compressive strength and the water/cement ratio, sand/cement ratio and dry density. The empirical equation derived is:

$$f_c = 0.00000141 \gamma_D^2 + 0.00511 \gamma_D + 22.3w/c - 2.72s/c - 12.2 \quad (\text{Eq 2.1})$$

Where:

- f_c = compressive strength (MPa)
 w/c = water/cement ratio
 s/c = sand/cement ratio
 γ_D = dry density (kg/m^3).

The R-squared statistic indicates that the equation as fitted explains approximately 98 % of the variability in compressive strength. The adjusted R-squared statistic, which is more suitable for comparing models with different numbers of independent variables, is 98%. Stepwise regression indicates that 58% of the variation in strength can be explained by the square of the dry density while 90% of the variation can be explained by including the effect of the sand/cement ratio. The addition of the water/cement ratio as the third variable increases the R-squared value to 95%. The results of the stepwise regression clearly indicates that variations in both the density and the sand/cement ratio influences the strength by an order of magnitude more than that caused by variations in water/cement ratio. The fact that the water/cement ratios used for these mixtures only varied between 0.5 and 0.8 and all the compressive strengths were below 5.1 MPa limits the value of the equation as derived above and a different relation would have to be derived if a wider range of strengths and water contents are used.

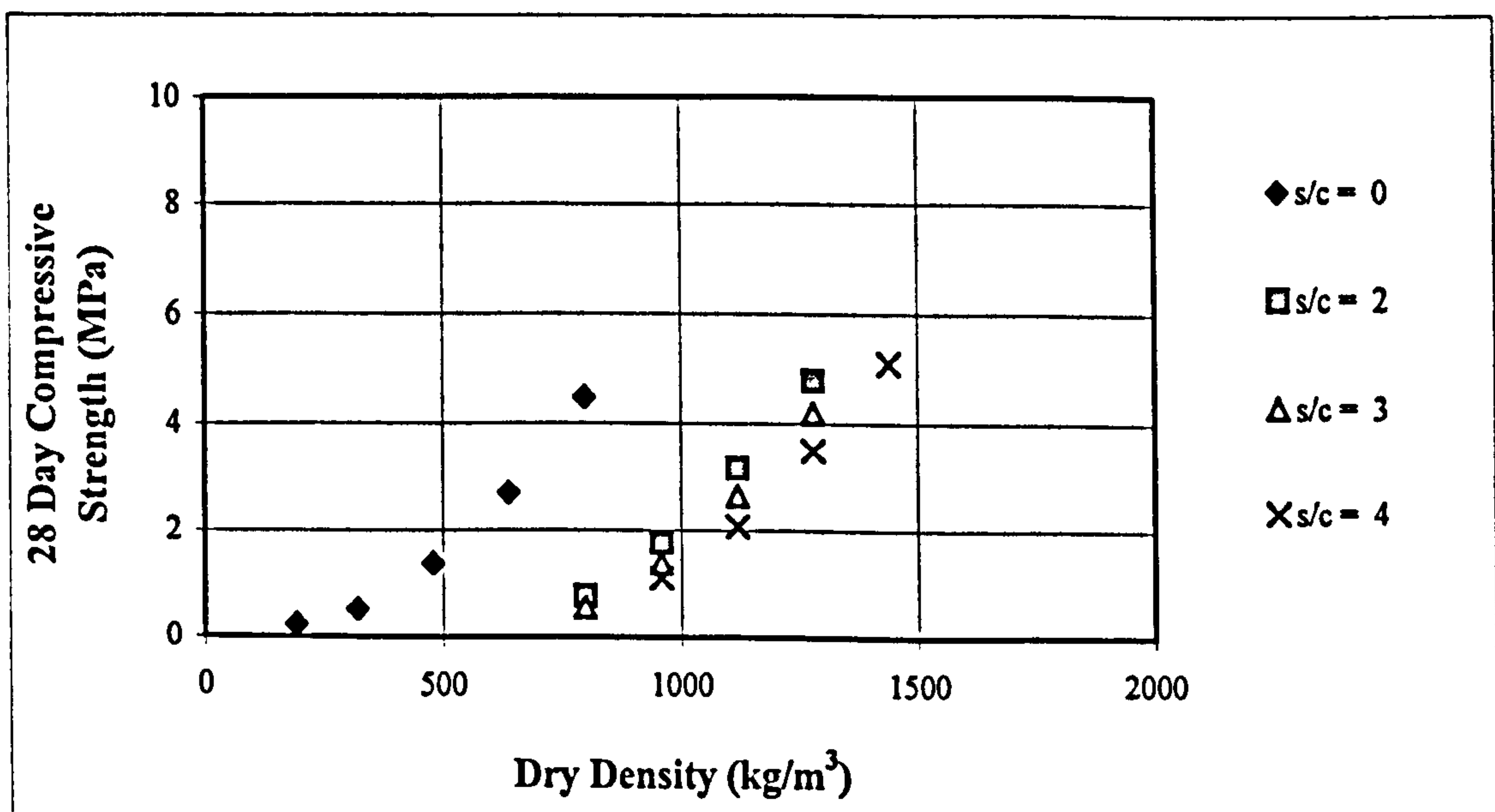


Figure 2.1: Effect of Sand Content on Compressive Strength of Foamed Concrete.

In their product information brochure Neopor¹⁴ states that foam concrete with densities from 400 to 1800 kg/m³ is produced with cement contents varying from 300 to 420 kg/m³. Foam concrete with densities up to 600 kg/m³ is normally produced using no sand but only water, cement and foam. According to Neopor an increase in cement content does not necessarily yield better compressive strengths, but it might rather have a negative influence on the shrinkage behaviour. Neopor claims that foaming agents based on protein hydrolysis are the most stable and as a result of their water retention abilities, the water in the foam is gradually released into the surrounding cement paste during the curing process, thereby contributing to the development of strength in the cellular concrete. This statement can be verified by comparing the results published by Neopor¹⁴ with results published by manufacturers of synthetic foaming agents¹⁵ (Figure 2.2). Figure 2.2 compares the 28-day compressive strengths of foam concrete manufactured using a protein based foaming agent to those manufactured using a synthetic foaming agent. The synthetic foam is an aqueous solution of a sodium alkylnaphthalene sulphonate and the compressive strengths are those published by L.B. Chemicals¹⁵. The sand cement ratio of both these sets of results vary from no sand at low densities to an approximate 3:1 ratio (by weight) at high densities. From these results it can be seen that the protein based foaming agent does result in higher compressive strengths than the synthetic foaming agent. At lower densities (below approximately 1 000 kg/m³), there does not seem to be much difference in the strengths, but the differences tend to increase with increased densities.

Widmann & Enoekl¹⁷ state that the cement content has a strong influence on the compressive strength of foamed concrete. They concluded that there is an optimum cement content for a given dry density and if the cement content is increased above the optimum content, the compressive strength decreases again because to prevent an increase in density more air voids have to be introduced into the mixture. According to Widmann & Enoekl the bulk density of the aggregates also has an influence on the compressive strength of the mixture as a more compact total structure is achieved with lighter aggregates. For a given cement content the compressive strength becomes greater with a lower bulk density of aggregate because fewer air voids need to be introduced into the cement matrix to achieve the same material bulk density.

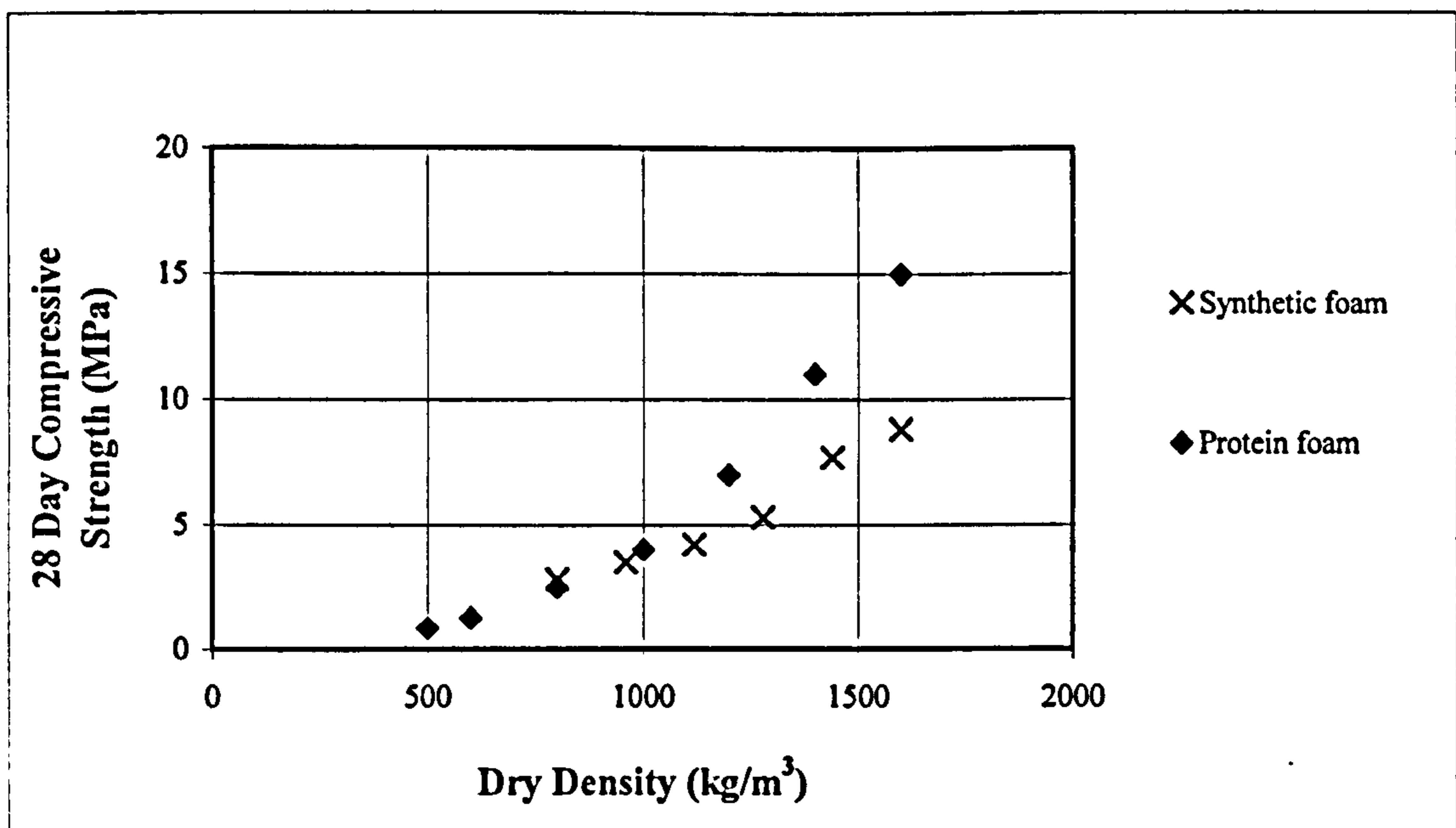


Figure 2.2: Influence of Type of Foaming Agent on Compressive Strength.^{14 15}

Mc Cormick¹⁸ tried to develop a rational method for proportioning foamed concrete mixtures by preparing 31 mixes using three different foaming agents (all were hydrolyzed proteins with different formulations), three types of sand and three types of expanded shale. The sand, with a relative density of 2.65, was a relatively non porous natural aggregate with rounded, smooth-textured particles and the expanded shale had the same fineness modulus as that of the sand. Water-cement ratios (by weight) varied between 0.35 and 0.57 (as indicated in Figure 2.3) and these were selected to satisfy the requirements for foam stability as determined from preliminary studies. The water/cement ratios as indicated in Figure 2.3 were determined for mixtures with a theoretical casting density of approximately 1250 kg/m³ and it is interesting to note that the finer sand, with the lower fineness modulus (FM) has a higher water demand than the sand with the higher FM. The fact that the water/cement ratio remains virtually unchanged while the aggregate/cement ratio increases from 1 to 1.5, may indicate that there is an optimum cement content, and the excess cement can be replaced with sand without any real changes in the water/cement ratio. When the aggregate/cement ratio is increased from 1.5 to 2 the water/cement ratio increases, indicating that the mixture now requires more water for the foam to remain stable.

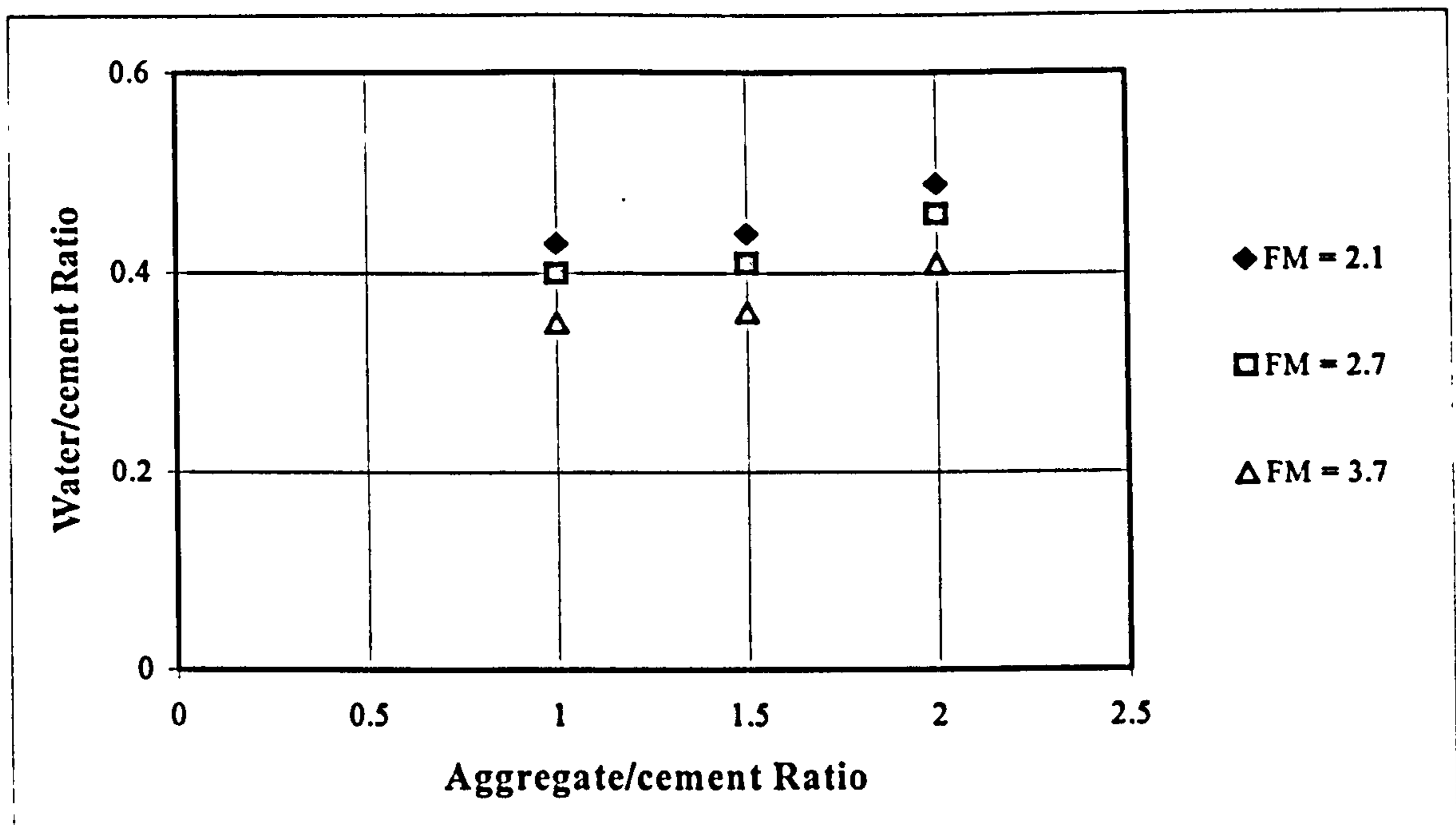


Figure 2.3: Water/cement Ratios to Achieve Adequate Foam Stability for Different Aggregate Contents.

The effect of fine aggregate content on the compressive strength was investigated by casting different mix combinations at the same design density. The effect of aggregate content on the compressive strength of foamed concrete can be seen in Figure 2.4. This graph has been compiled from the results published by Mc Cormick for foamed concrete with a target casting density of approximately 1250 kg/m^3 manufactured using three different sands. From these results it can be seen that the sand with a FM of 2.7 produces foamed concrete with much lower compressive strengths than both the coarser and the finer sand. The aggregate/cement ratio has a noticeable effect on the compressive strength but the trends observed for the different sands contradict each other as the fine sand seems to have a pessimum content, an increase in the coarse sand content seems to increase the compressive strength while the opposite is true for the third sample (medium sand).

Although the results are not conclusive, it is clear that the aggregate content and grading could have a significant influence on the compressive strength of foamed concrete. The fact that intermediate amounts of aggregate yield the highest strength in some sets might indicate an optimum aggregate content. In this experiment the water-cement ratio was increased with an increase in aggregate content and the effect of aggregate content on compressive strength cannot therefore be isolated.

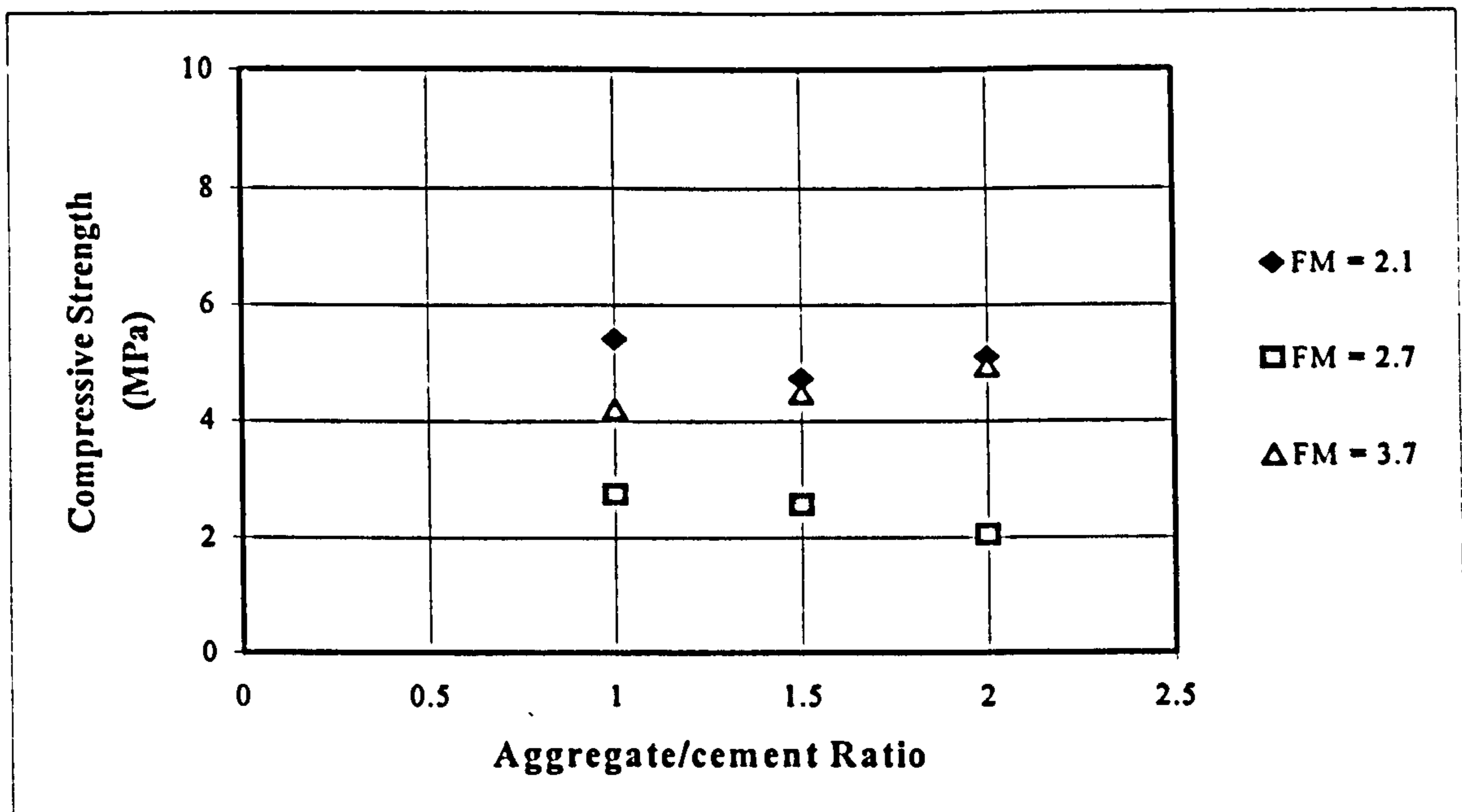


Figure 2.4: Effect of Aggregate Content on Compressive Strength at Constant Density.

The effect of water/cement ratio on the compressive strength of the different mixtures can be seen in Figure 2.5. From these results it can be seen that where for normal concrete lower water/cement ratios yields higher strengths, the water/cement ratio of foamed concrete does not seem to affect the compressive strength as significantly as the grading of the aggregate. The variation in water/cement ratio is however too small for any definitive conclusions to be drawn.

Based on seven sets of results, Mc Cormick concludes that the effect of varying the aggregate content appears to be inconsequential as two sets indicated increasing compressive strength with increasing aggregate content, one indicated decreasing compressive strength with increasing aggregate content and four indicated that the mixture containing an intermediate amount of aggregate was either the highest or lowest value of the set.

The results obtained by Mc Cormick were used by the author in multiple regression analysis and the mathematical relation between the compressive strength and four independent variables (water/cement ratio; sand/cement ratio; fineness modulus and density) was determined.

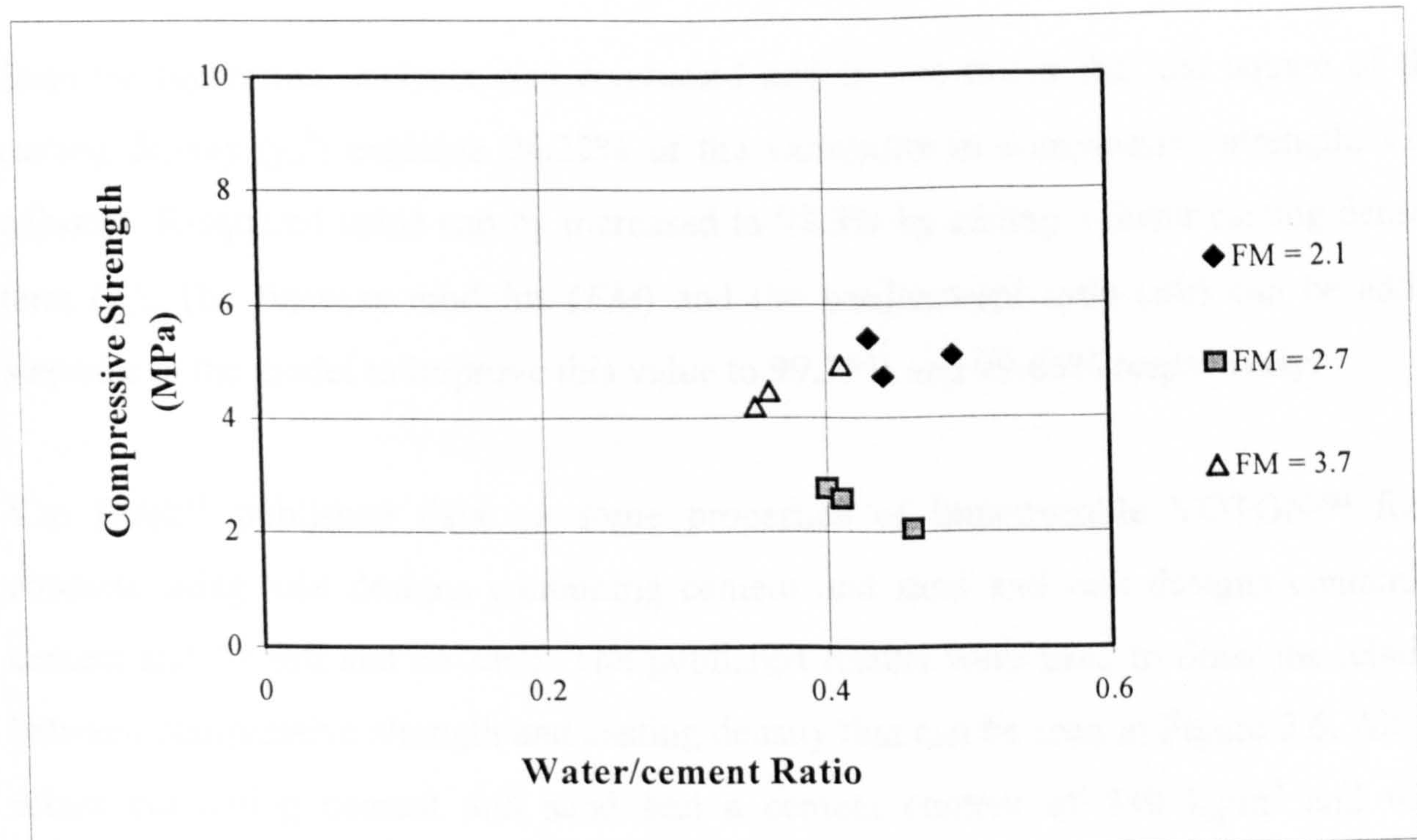


Figure 2.5: Effect of Water/cement Ratio on Compressive Strength.

The statistical analysis indicated that the water/cement ratio is not statistically significant at the 90% or higher confidence level and consequently it was removed from the model. The model was simplified to only include three independent variables and the following relation was derived:

$$f_c = 34.97 - 0.0577 \gamma_c + 0.0000302 \gamma_c^2 - 1.21 s/c - 1.77 FM \quad (\text{Eq 2.2})$$

Where:

f_c	=	compressive strength (MPa)
FM	=	fineness modulus of sand
s/c	=	sand/cement ratio
γ_c	=	casting density (kg/m^3).

The R-squared statistic indicates that the model as fitted explains more than 99% of the variability in compressive strength, while the adjusted R-squared statistic is 99.6%. The ANOVA* P-value is less than 0.01, which indicates that there is a statistically significant relationship between the variables at the 99% confidence level.

* ANOVA – Analysis of Variance

Stepwise regression analysis was conducted and it was found that the square of the casting density (γ_c^2) explains 94.22% of the variability in compressive strength. This adjusted R-squared value can be increased to 98.3% by adding a linear casting density term (γ_c). The fineness modulus (FM) and the sand/cement ratio (s/c) can be added stepwise to the model to improve this value to 99.35% and 99.66% respectively.

Van Deijk¹⁶ published data on some properties of impermeable VOTONTM foam concrete using mix designs containing cement and sand and mix designs containing cement and fly ash and no sand. The published results were used to draw the relation between compressive strength and casting density that can be seen in Figure 2.6. All the mixes containing cement and sand had a cement content of 340 kg/m³ and were produced with the wet mortar system where the cement, sand and water is mixed in a truck and transported to site where the foam is then added. All the mixes containing cement and fly ash were produced using the dry mortar method where the water is only added to the cement and fly ash on the construction site. The cement content of the mixes that contained fly ash varied and no indication of the fly ash-cement ratio was published, which makes meaningful comparisons between mixes very difficult.

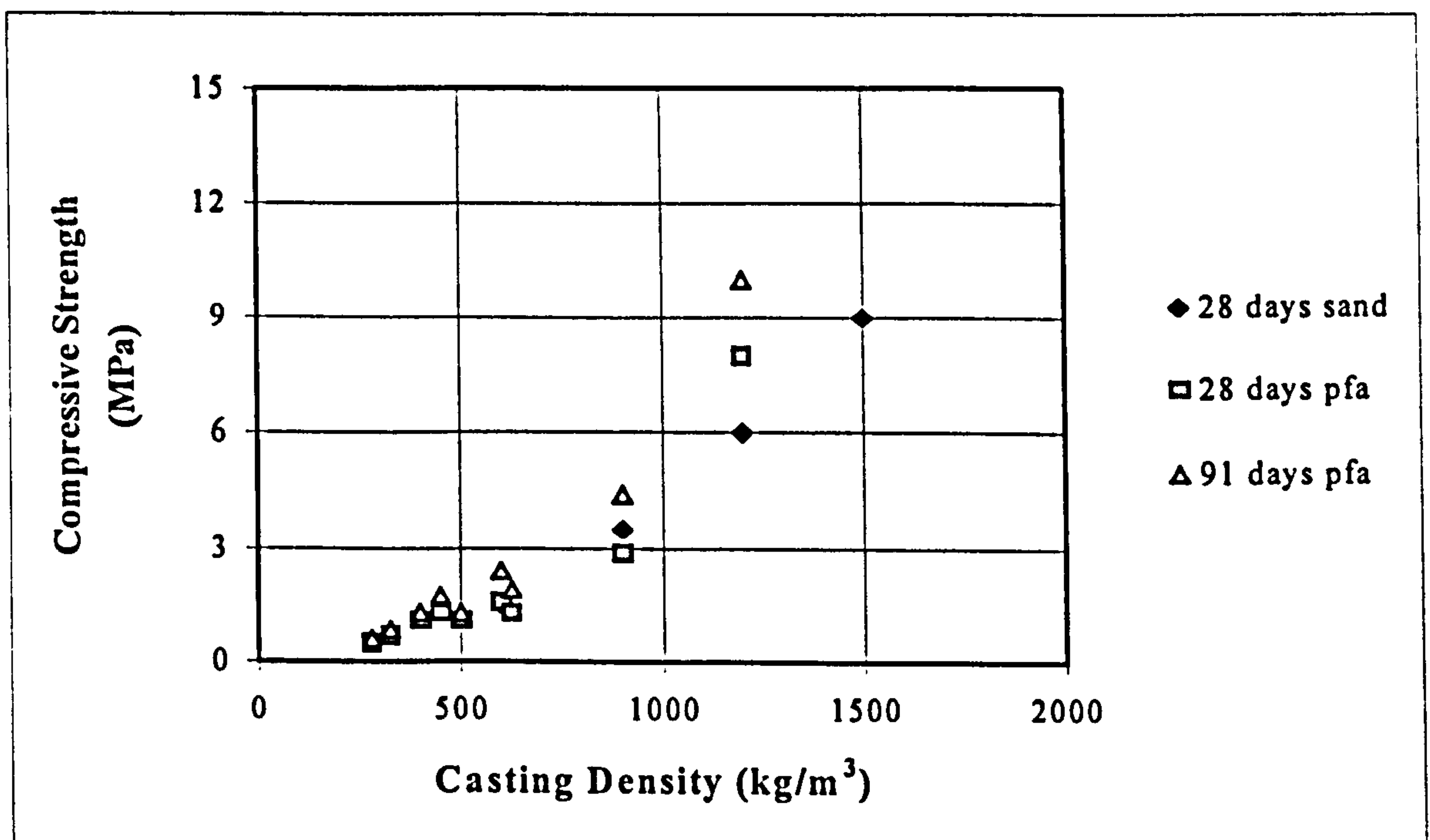


Figure 2.6: Compressive Strengths using Fly ash or Sand.

However from the results shown it can be seen that at densities above about 1000 kg/m^3 the mixes containing fly ash can yield higher compressive strengths than the mixes containing sand. Although 28 day and 91 day strengths were published for the mixes containing fly ash, only 28 day strengths were given for the sand mixes. At densities below 1000 kg/m^3 there is hardly any difference in the 28 or 91 day compressive strength for mixtures containing fly ash and those containing sand.

2.2.1.2 Deformation

Based on the results of their research Widmann & Enoekl¹⁷ state that the creep deformation (as measured under constant stress in an air-conditioned room) of foamed concrete is similar to that of normal concrete but the shrinkage contraction of foamed concrete is approximately four to six times that of normal concrete. They therefore concluded that building elements that are assembled under restrained conditions would be subject to a considerable risk of cracking. They further established that all test specimens showed cross-shaped hair cracks (<0.10 mm wide) on the surface at a spacing of approximately 15 to 25 cm after about 4 to 6 weeks.

To determine the effect of shrinkage on restrained building elements, panels (3 m long, 2.5 m high and approximately 28 days old) were built-in between reinforced concrete slabs. Within a relatively short time a vertical crack formed in the middle of these panels. These cracks increased in width to up to 1 mm after one year and after that no significant increases in crack widths could be detected. In an effort to minimize shrinkage the following measures were investigated:

- lower water-cement ratios
- curing regime
- heat treatment
- different cement qualities and types.

None of these methods resulted in a significant reduction in shrinkage and the authors concluded that damage to foamed concrete elements as a result of shrinkage can only be prevented by one of the following measures:

- assembling the building elements without contraction restraint, or
- storing the elements for at least 3 to 4 months without contraction restraint, or
- using foamed concrete only for small, as far as possible pre-stored elements (e.g. masonry blocks)

The British Cement Association (BCA) published typical properties of foamed concrete as indicated in Table 2.1.¹⁹ From these values it can be seen that the highest drying shrinkage can be associated with the lowest densities. The drying shrinkage of foamed concrete is perceived to be high when compared to that of normal concrete (where typical drying shrinkage is in the region of 0.04% to 0.12%).⁶ An advantage of the lower density foamed concrete is the lower thermal conductivity that gives better insulation properties. The thermal conductivity of foamed concrete is between 5% and 30% of that of dense concrete.⁶ The modulus of elasticity is less than that of dense concrete (where a value of 30 kN/mm² would be a typical value).⁶

Table 2.1: Typical Properties of Foamed Concrete.

Dry Density (kg/m ³)	Compressive Strength (MPa)	Thermal Conductivity (W/mK)	Modulus of Elasticity (kN/mm ²)	Drying Shrinkage (%)
400	0.5 – 1.0	0.10	0.8 – 1.0	0.30 – 0.35
600	1.0 – 1.5	0.11	1.0 – 1.5	0.22 – 0.25
800	1.5 – 2.0	0.17 – 0.23	2.0 – 2.5	0.20 – 0.22
1000	2.5 – 3.0	0.23 – 0.30	2.5 – 3.0	0.18 – 0.15
1200	4.5 – 5.5	0.38 – 0.42	3.5 – 4.0	0.11 – 0.09
1400	6.0 – 8.0	0.50 – 0.55	5.0 – 6.0	0.09 – 0.07
1600	7.5 – 10.0	0.62 – 0.66	10.0 – 12.0	0.07 – 0.06

ACI Committee 523⁵ reports that the cracking of cellular concrete at early ages due to thermal and moisture loss volume changes can be reduced by the addition of suitable fibers. These fibers must bond to the concrete and be of sufficient length, size and number to develop the required tensile force at any section.

Georgiades & Marinos²⁰ conducted research on the effect of the micropore structure on the shrinkage of autoclaved aerated concrete (A.A.C.). Eight series of A.A.C. specimens were prepared using different raw materials, rising agents, additives, mix proportions and autoclaving conditions. The autoclave pressure was kept constant at 12 bar while the curing time was varied. Either aluminum powder or stable foams were used as rising agents to obtain sample densities in the region of 500 kg/m^3 . The drying shrinkage of samples was determined by measuring the length changes of the specimens during moisture content variations, starting at maximum water saturation (approximately 40 to 45% by volume) to a moisture content of 1 to 1.2% by volume, at drying conditions of 35% relative humidity and 50 to 55 °C. The results of the shrinkage measurements are indicated in Table 2.2.

Table 2.2: Drying Shrinkage of A.A.C.

Sample Code	Drying Shrinkage (%)	Binder Ratio (cement/lime)	Additive	Curing Time	Rising Agent
A	0.098	9/1	None	6 hours	Foam
B	0.089	1/1	None	8 hours	Foam
C	0.094	1/1	None	10 hours	Foam
D	0.096	1/1	None	6 hours	Aluminium Powder
E	0.091	1/1	None	6 hours	Foam
F	0.068	1/1	Alumina	6 hours	Foam
G	0.066	1/1	Alumina & CaSO ₄	6 hours	Foam
H	0.071	1/1	Lime rich Fly ash	6 hours	Foam

From these results it can be seen that the drying shrinkage varied between 0.066 and 0.098%. The binder ratio is the only difference between specimens with sample codes A and E, indicating that the higher cement content results in marginally increased shrinkage. The use of different rising agents has an influence on the drying shrinkage and if samples D and E are compared it can be concluded that the use of aluminium as

rising agent results in marginally higher shrinkage than when foam is used. The use of alumina or fly ash as additive results in a marked reduction in shrinkage as can be seen when comparing the results of samples E, F, G and H. By comparing the drying shrinkage for mixtures B, C and E it can be seen that a curing time of 8 hours results in lower shrinkage values than for 6 or 10 hours of curing. This might indicate optimum autoclaving duration but more results than those published will be required before any trends could be defined.

2.3 VOIDS IN HYDRATED CEMENT PASTE

2.3.1 BACKGROUND

Progress in the field of materials science has primarily resulted from the recognition of the fact that the properties of a material are dictated by the nature of its internal structure. According to Metha and Monteiro²¹ hydrated cement paste (hcp) contains several types of voids which have an important influence on its properties. These voids include the interlayer space between calcium silica hydrate sheets, capillary voids and air voids. The major factors influencing the total volume of pores and the pore size distribution are:

- water/cement ratio
- cement content and type
- degree of hydration
- compaction
- plastic cracking.

The properties of hardened cement paste are a function of both the total pore volume and the relative sizes of the pores in the paste. The porosity, the pore size distribution, and the nature of the hydrated compounds of the hardened cement paste govern permeability and diffusivity of concrete to gases, water and harmful ions such as chlorides and sulfates.²² The type and relative size of pores and ions or gas molecules are shown schematically in Figure 2.7²³. The size of most ions and gas molecules that are harmful to concrete are smaller than the size of typical gel pores.

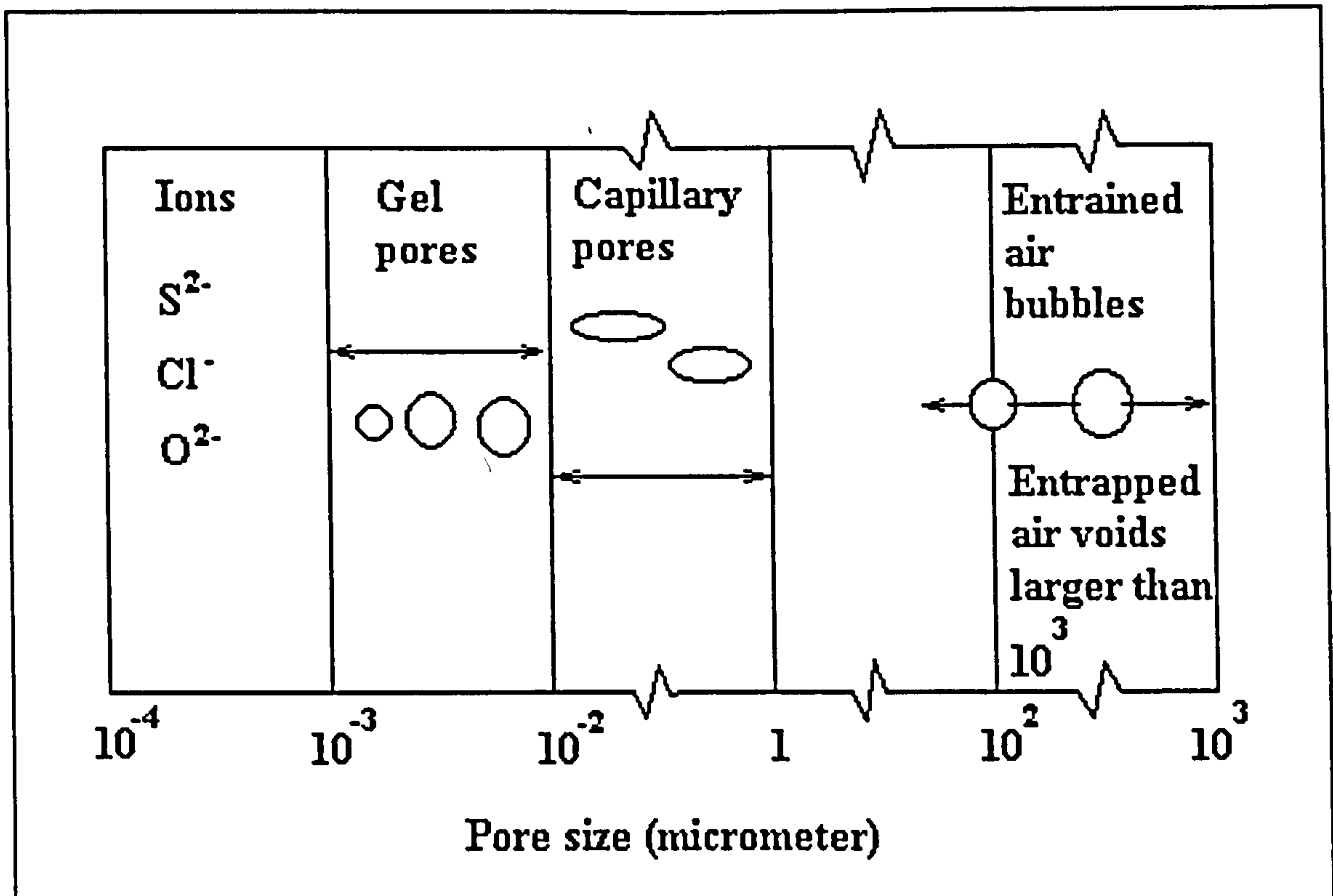


Figure 2.7: Pore sizes.

Fresh cement paste is a network of cement particles in water but as soon as hydration starts cement gel is formed. According to Powers²⁴ the hardened paste contains gel, crystals of calcium hydroxide, minor components, residues of the original cement and residues of the original water filled spaces in the fresh paste. These residues of water-filled space (known as capillary pores or cavities) exists in the hardened cement paste as interconnected channels or if the structure is dense enough, as cavities interconnected only by gel pores. The cement gel is composed of fibrous gel particles forming a cross-linked network containing gel pores. At any given stage of hydration, capillary- porosity depends on the original proportion of water in the cement paste, which is usually expressed as the ratio of water to cement in the original mixture. Cement gel can be produced only in water-filled capillary cavities, and when all these cavities are filled, no further hydration can take place. Powers states that the hydration products of cement require twice the volume of the unhydrated cement. The degree to which gel fills the available space can be expressed as a ratio of volume of gel to volume of available space. The compressive strength of cement paste increases in direct proportion to the cube of the increased gel-space ratio.

2.3.2 TYPES OF VOIDS

2.3.2.1 Pore voids

Metha & Monteiro²¹ state that the calcium silicate hydrate phase (C-S-H) accounts for up to 60% of the volume of solids in a completely hydrated Portland cement paste and therefore it is the most important phase in determining the properties of the paste. The interlayer space within the C-S-H structure accounts for up to 28% porosity in solid C-S-H but the size of this space is assumed to be less than 25 Å (1Å = 10⁻¹⁰ m). This void size is too small to have an adverse effect on the strength and the permeability of the hcp but the water in these voids can help by hydrogen bonding and the removal of this water could contribute to drying shrinkage and creep.

After their investigation on the effect of micropore structure on the shrinkage of A.A.C. Georgiades & Marinos²⁰ defined micropores as the pores in the walls of the air voids and stated that shrinkage is due to a change in disjoining pressure in the smallest pores of A.A.C. They found that the drying shrinkage of A.A.C. is a function of volume and specific surface of the micropores which have radii between 20 and 200 Å. These void sizes include the pore sizes as defined for gel pores as well as the lower range of pore sizes defined as capillary pores. The tests on pore size distribution were performed by means of mercury porosimetry using a porosimeter that can measure pores with radii greater than 18 Å. They concluded that the decisive effect on the A.A.C. shrinkage process is the structure of microporosity in the range of pore radii 20 – 55 Å and 55 - 200 Å. Using regression analysis they derived the following equations:

For pore radii 20 – 55 Å:

$$\varepsilon_d = \frac{V_p}{(0.023 + 9.657V_p)} \quad (\text{Eq 2.3})$$

For pore radii 55 – 200 Å:

$$\varepsilon_d = \frac{(V_p + 2.787)}{1.9} \quad (\text{Eq 2.4})$$

Where:

$$\begin{aligned} \varepsilon_{sf} &= \text{Drying shrinkage} \quad (\%) \\ V_p &= \text{Micropore volume} \quad (\text{cm}^3/\text{g}). \end{aligned}$$

2.3.2.2 Capillary voids

Capillary voids represents the space not filled by the solid components of the hcp.²¹ The total volume of the cement-water mixture remains virtually unchanged during the hydration process. The average bulk density of the hydration products is considerably lower than the density of the anhydrous Portland cement, and the process of cement hydration can be seen as a process during which the space originally occupied by cement and water is being replaced more and more by the space filled by hydration products. The space not taken up by the cement or hydration products consists of capillary voids and the volume and the original distance between the anhydrous cement particles and the degree of hydration determines ^{the} size of the capillary voids. The original distance between unhydrated cement particles is determined by the water/cement ratio.

The degree of hydration of Portland cement is dependent on the availability of free water within the pores of concrete.²⁵ When the degree of saturation of concrete is reduced to below 80% the hydration practically stops but fresh concrete normally contains water in excess of that required for full hydration. The hydration products have a volume which is approximately 2.5 times the sum of the volume of unhydrated cement and the volume of water, and therefore the void volume occupied by free water (the capillary voids) is reduced as hydration proceeds. The amount of water required for full hydration is approximately 0.28 of the weight of the cement and any water in excess of this value is not required for hydration but to reduce the viscosity of the material (increase the workability).

In well-hydrated, low water/cement ratio pastes the capillary voids may range in size from 10 to 50 nm while in high water/cement ratio pastes at early ages of hydration the capillary voids may be as large as 3 to 5 μm . According to Mehta and Monteiro²¹ it has been suggested that the pore size distribution, not the total capillary porosity is a better criterion for evaluating the characteristics of hcp. Capillary voids larger than 50 nm, also referred to as macropores, are assumed to be detrimental to strength and

impermeability, while voids smaller than 50 nm referred to as micropores are assumed to be more important to drying shrinkage and creep.

Metha & Manmohan²⁶ investigated the pore size distribution and permeability of Portland cement pastes with water/cement ratios varying from 0.3 to 0.9. The pastes with water/cement ratios of 0.6 to 0.9 contained substantial volumes of larger pores with diameters exceeding 1320 Å. In these high water/cement ratio pastes the pore size distribution at 28 days was found to remain essentially the same in the 45 to 1320 Å range indicating that the higher porosity manifests itself in pores with larger diameters.

Several investigators that studied the relationship between permeability and the pore size distribution of cement pastes and mortars have concluded that the flow of a fluid through concrete is associated with the larger capillary pores rather than total porosity.²² Gowripalan et al. concluded that blended cements containing 35% pulverized fuel ash (pfa) or 70% ground granulated blast furnace slag (ggbs) can be used in well cured cement pastes to produce a blocked pore structure resulting in a reduction in pores above 880 Å in diameter. The use of blended cements thus leads to a reduction in permeability.

2.3.2.3 Air voids

Entrapping or entraining air in the hcp forms air voids. The air voids are generally spherical where capillary voids are irregular in shape. Entrapped air voids may be as large as 3 mm while entrained air voids usually range from 50 to 200 µm. Both entrapped and entrained air voids are much larger than the capillary voids and are capable of adversely affecting the strength and permeability of the hcp.

Air-entrained concrete of quality is produced by introducing an increased quantity of air voids, duly graded according to size and uniformly distributed throughout the cement paste. According to Wilk and Dobrolubov²⁷ the mere determination of the total air void content of fresh concrete is not sufficient as shape, size and distribution of voids can affect the strength and durability of the concrete. Perfectly batched and mixed air-entrained concrete of high durability contains well-distributed spherical voids with diameters varying between 20 and 300 micrometer²⁷. The presence of void surface

defects, agglomerations of voids or large voids (with diameters exceeding 300 micrometer) indicate low quality air-entrained concrete.

Hengst & Tressler²⁸ investigated the microstructure of foamed cement with different densities manufactured using different cements and they concluded that the pores in the foamed cement are approximately spherical and no preferential distortion was detected when cross sections of various orientation to the horizontal casting plane were analyzed. The average measured pore diameter for the different mixtures varied between 0.131 mm and 0.532 mm. These values correlate with the values measured for voids formed by air entraining.

The pore size distribution of small pores can be measured by various well-established techniques, such as the value of porosity measured by mercury intrusion porosimetry (MIP)⁶, but macropores (with diameters exceeding 20 μ m) can be studied using image analysis²⁹. Visagie³⁰ determined the air void size distribution of foamed concrete with a casting density of 1500 kg/m³ and the distribution is shown in Figure 2.8. The histogram was compiled using the measured diameters of 182 voids. From this graph it can be seen that virtually all the voids formed by the foaming agent are less than 0.2 mm in diameter.

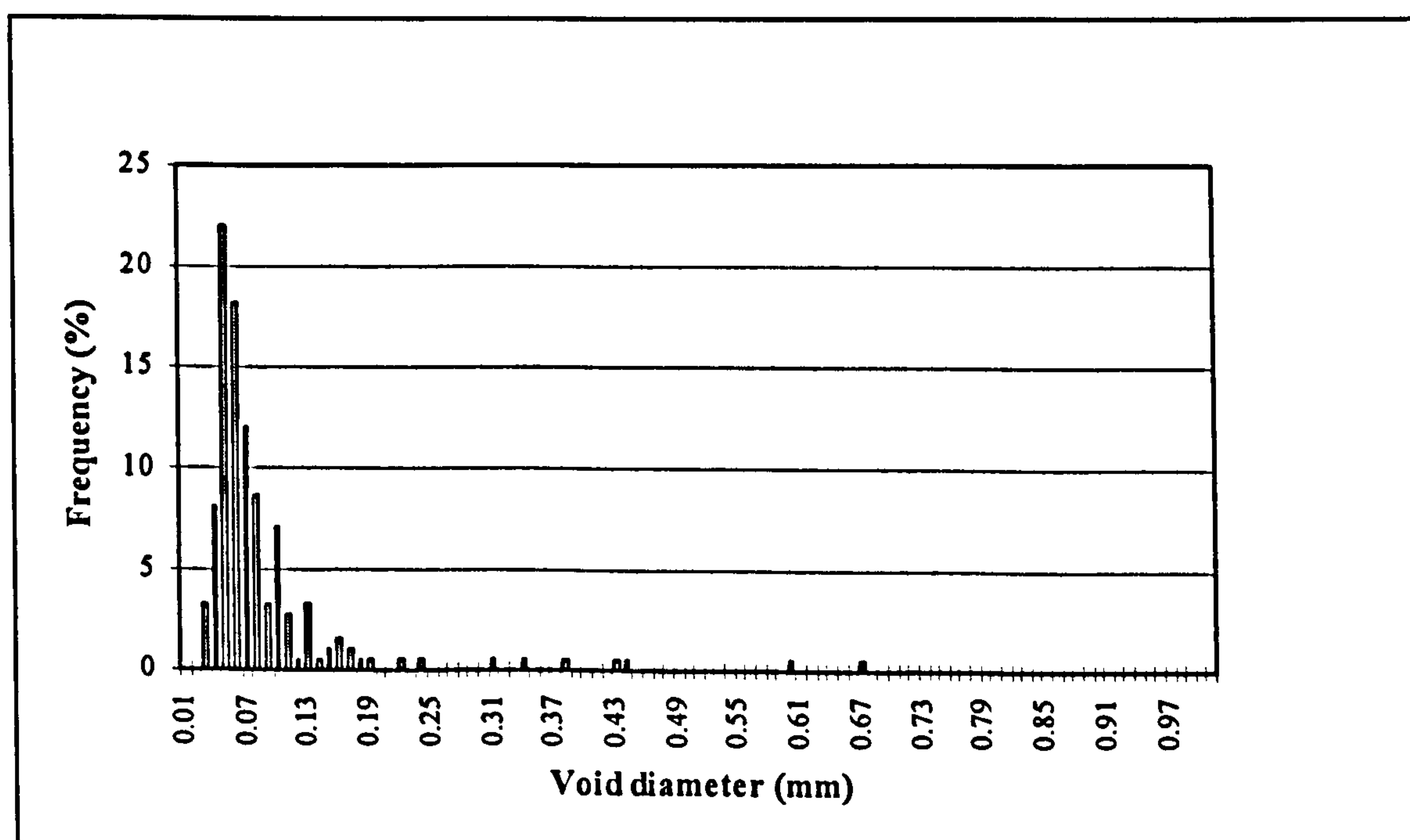


Figure 2.8: Air Void Size Distribution of Foamed Concrete.

2.3.3 THE EFFECT OF VOIDS ON DURABILITY AND STRENGTH

2.3.3.1 Effect on Durability

The durability of concrete can be defined as the capability of maintaining serviceability of a product, component or construction over a specified time³¹. With the exception of mechanical damage and alkali-silica reaction all the adverse influences on durability involve the transport of fluids through the concrete⁶. The permeability of concrete gives an indication of the ease of movement of various fluids through concrete.

Because of the existence of different types of pores of which only some contribute to the permeability of the concrete it is important to distinguish between porosity and permeability. Porosity is a measure of the proportion of the total volume of concrete occupied by pores. If the porosity is high and the pores are interconnected, they contribute to the transport of fluids so that the permeability is also high. If the pores are discontinuous the permeability of the concrete is low, although the porosity might be high.

Nyame and Illston³² investigated the relationship between permeability and pore structure of hardened cement paste and they concluded that porosity changes with time of hydration and water/cement ratio. This relationship between density and porosity can be expressed with the following equation:

$$\rho = 2.40 - 1.52 \varepsilon^{0.21} \quad (\text{Eq 2.5})$$

Where:

$$\begin{aligned} \rho &= \text{density} \quad (\text{g/cm}^3) \\ \varepsilon &= \text{porosity as determined by mercury intrusion porosimetry.} \\ &\quad (\text{cm}^3/\text{g}) \end{aligned}$$

The changes in porosity in relation to changes in water/cement ratio and time of hydration were fitted to the function:

$$\varepsilon(t) = \varepsilon_0 - m \log t \quad (\text{Eq 2.6})$$

Where:

t	=	time of hydration	(days)
$\varepsilon(t)$	=	porosity at a given age t	(cm^3/g)
ε_0	=	initial porosity (at $t = 0$)	(cm^3/g)
m	=	constant related to rate of change.	

In order to sustain the corrosion of reinforcing steel in concrete it is necessary that both oxygen and water be transported through the cover zone to the reinforcing bars. Both water and oxygen must penetrate the same depth of cover in order to reach the reaction site, and the one that has the slowest transport rate through concrete will thus limit the corrosion process. Cabrera & Claisse³³ investigated the transmission of oxygen and water vapor through mortars and they concluded that the rate of transport of water vapor was proportional to the porosity of the samples. Wainwright et al.³⁴ compared the performance properties of mortars made with ordinary Portland cement and pozzolanic cements containing pfa or ggbs after exposing the mixes to hot dry environments. The tests carried out to assess the performance properties and thus the durability of the mortars were total porosity, pore size distribution and gas permeability using oxygen. They derived a statistically valid function between the oxygen coefficient of permeability and the pore structure as measured using a mercury intrusion porosimeter. The function is:

$$\log_{10} OP = 0.5 \frac{1}{d^2 + p} + 5.3 \quad (\text{Eq 2.7})$$

Where:

OP	=	coefficient of oxygen permeability ($cm/s \times 10^{-8}$)
d	=	average pore diameter (micron)
p	=	porosity as a fraction.

2.3.3.2 Effect on Strength

When concrete is fully compacted the strength is taken to be inversely proportional to the water/cement ratio (Abrams rule).⁶ In 1896 René Féret formulated the following rule to relate the strength of concrete to the volumes of water, cement and air in the mixture:

$$f_c = K \left(\frac{c}{c + w + a} \right)^2 \quad (\text{Eq 2.8})$$

Where:

$$\begin{aligned} f_c &= \text{concrete compressive strength (MPa)} \\ c, w, a &= \text{absolute volumetric proportions of cement, water and air} \\ K &= \text{a constant.} \end{aligned}$$

The strength of concrete is influenced by the volume of all voids in the concrete (entrapped air, capillary pores, gel pores and entrained air) and a number of functions, including the following, have been proposed to express this strength-porosity relation^{35,36}:

$$f_c = f_{c,0} \cdot (1 - p)^n \quad (\text{Balshin}) \quad (\text{Eq 2.9})$$

$$f_c = f_{c,0} \cdot e^{-k_r \cdot p} \quad (\text{Ryshkevitch}) \quad (\text{Eq 2.10})$$

$$f_c = k_s \ln \left(\frac{p_0}{p} \right) \quad (\text{Schiller}) \quad (\text{Eq 2.11})$$

$$f_c = f_{c,0} - k_H p \quad (\text{Hasselman}) \quad (\text{Eq 2.12})$$

Where:

$$\begin{aligned} f_c &= \text{compressive strength of concrete with porosity } p \\ f_{c,0} &= \text{compressive strength at zero porosity} \\ p &= \text{porosity (volume of voids expressed as a fraction of the} \\ &\quad \text{total concrete volume)} \\ n &= \text{a coefficient, which need not be constant} \\ p_0 &= \text{porosity at zero strength} \\ k_r, k_s, k_H &= \text{empirical constants.} \end{aligned}$$

Rößler & Odler³⁵ determined the relationship between porosity and strength for a series of cement pastes with different water-cement ratios after different periods of hydration. They concluded for porosities between 5 and 28%, that although all four of the strength-porosity equations indicated above can be used, the relation between compressive strength and porosity can best be expressed in the form of a linear plot.

Fagerlund³⁶ states that it often seems as if one equation fits experimental data for porosities below a certain limiting porosity and another for porosities above this limit. At high porosities it is normally necessary to use an equation which indicates a critical porosity while these equations are too insensitive to change for use with low porosities. An equation that takes into consideration the effect of high as well as low porosity will include a critical porosity as well as a stress concentration factor. An example given by him of such an equation is:

$$f_c = f_l \left\{ 1 - \left(\frac{p}{p_{cr}} \right)^E \right\} \left\{ 1 + F \cdot \left(\frac{p}{p_{cr}} \right)^G \right\} \quad (\text{Eq 2.13})$$

Where:

f_c	=	compressive strength of concrete with porosity p
f_l	=	compressive strength at zero porosity
p	=	porosity (volume of voids expressed as a fraction of the total concrete volume)
p_{cr}	=	porosity at zero strength
E, F, G	=	empirical constants.

According to Fagerlund³⁶ it is important to use two quite different strength-porosity connections for a cement paste where the first is valid for different cement pastes with the same degree of hydration and the second is valid for a specific cement paste during curing. He determined a strength-porosity relation for cement mortars or concrete by first determining the strength porosity curve of the cement paste for different degrees of hydration. The concrete strength is then calculated as a function of the paste porosity and finally the paste porosity is translated to concrete porosity using the following equation:

$$p_c = p_p \cdot V_p + p_A \cdot (1 - V_p) \quad (\text{Eq 2.14})$$

Where:

p_c	=	porosity of the concrete
p_p	=	porosity of the paste
p_A	=	porosity of the aggregate
V_p	=	volume of the paste.

After studying aerated concrete manufactured at factories in China, Baozhen and Erda³⁷ concluded that the compressive strength decreases as the porosity increases with the same relationship as indicated in the strength-porosity equation derived by Balshin (as listed on page 25). It was found that n varied from 1 to 2.2 in different ranges of porosity, indicating that the strength of mixtures with low porosity were influenced more by small changes in porosity than the strength of mixtures with higher porosity.

Hengst & Tressler²⁸ concluded that the dominant parameter in controlling the strength of a foamed Portland cement at a given bulk density is the flaw size, which correlates with the pore size.

Hoff³⁸ conducted research on the porosity-strength relation of cellular concrete and he concluded that there is a single strength-porosity relation for given cement and this relation can be expressed in terms of water/cement ratio and density. Hoff³⁸ expressed the theoretical porosity of cellular concrete containing only water, cement and foam as the volume of voids as a fraction of the total volume. He used an average value of 0.2 for the ratio of the water bound by hydration to cement (by weight) and derived the following equation:

$$n = 1 - \frac{d_c (1 + 0.20 p_c)}{(1 + k) p_c \gamma_w} \quad (\text{Eq 2.15})$$

Where:

n	=	theoretical porosity
d_c	=	concrete density
p_c	=	specific gravity of the cement
γ_w	=	unit weight of water
k	=	water/cement ratio (by weight).

In the design of foamed concrete the use of the space occupied by the evaporable water plus the air void space as the total void space in the concrete permits the termination of a single strength-porosity relation for a given cement. The strength of cellular concrete in relation to any cement can, according to Hoff, be expressed using the following equation:

$$\frac{\sigma_y}{\sigma_0} = \left(\frac{d_c}{1+k} \right)^b \left(\frac{1+0.2 p_c}{p_c \gamma_w} \right)^b \quad (\text{Eq 2.16})$$

Where:

σ_y	=	compressive strength
σ_0	=	theoretical paste strength at zero porosity
k	=	water/cement ratio (by weight)
p_c	=	specific gravity of the cement
d_c	=	concrete density
γ_w	=	unit weight of water
b	=	empirical constant.

This equation does however only hold true for foamed concrete containing only air, water and cement. Adjustment will be required if additional components, such as fillers are used. Hoff evaluated bag-cured samples manufactured using different cements with water/cement ratios varying from 0.66 to 1.06 and casting densities varying from 320 to 1 000 kg/m³. The analysis produced values of $\sigma_0 = 245$ MPa and $b = 2.7$ with a correlation coefficient of 0.95 for cement with a Blaine fineness of between 4 500 and 4 650 cm²/g.

2.4 THE USE OF PFA IN CONCRETE

2.4.1 BACKGROUND

During the combustion of coal in modern power plants the volatile matter and carbon are burned off when the coal passes through the high temperature zone in the furnace. The impurities such as clay, quartz and feldspar melts at these high temperatures and the fused material is transferred to lower temperature zones, where it solidifies as spherical particles of glass²¹. Some of the mineral matter agglomerates forming bottom ash, but most of it flies out with the flue gas stream, is separated from the gas using electrostatic precipitators, and is called fly ash or pulverized fuel ash (pfa).

Fly ash or pulverized fuel ash (pfa) is a byproduct of the combustion of pulverized coal in thermal power plants. It is removed by mechanical collectors or electrostatic precipitators as a fine particulate residue from the combustion gases before they are discharged into the atmosphere. The fineness of the pulverized coal and the type of dust collection equipment used largely determine the range of particle sizes in any given pfa. The pfa collected from boilers where mechanical collectors alone are employed is coarser than pfa from plants using electrostatic precipitators³⁹. The types and relative amounts of mineral matter in the coal used determine the chemical composition of pfa. ×

The recognition that pfa frequently exhibits pozzolanic properties has led to its use as a constituent of concrete. A pozzolan can be defined as 'a finely divided siliceous material which reacts with lime in the presence of water to give cementitious products.'⁴⁰ The cementing action of the pozzolan is believed to be dependent upon the reaction between it and lime liberated from the cement during hydration. ASTM C 618-89 categorizes pozzolans into four classes namely class N, F, C and S.⁴¹ Class N refers to raw or calcined natural pozzolans such as diatomaceous earth derived from microscopic unicellular algae with siliceous wall cells, volcanic ashes or pumicites. Class S refers to certain processed pumicites, which are porous forms of volcanic glass and to certain calcified and ground diatomites, clays and shales. Class F and C pozzolans refer to fly ash derived from the burning of different coals. Class F refers to fly ash derived from burning anthracite or bituminous coal. Anthracite coal is hard coal with few volatile hydrocarbons. This coal burns with very little flame. Bituminous coal on the other hand is quite volatile. Class C refers to ashes derived from burning lignite or sub-bituminous coal and it contains less than 50% as oxides of silica, alumina and iron.

Pfa is normally used in concrete for economic and durability considerations as a partial replacement for Portland cement. In the amounts normally used, most low-calcium pfa's tend to reduce the early strengths up to 28 days, but improve the ultimate strength (after more than a year)⁶. When pfa is used as a partial replacement for fine aggregates, the strength at both early and later ages can be significantly improved. The strength gain at early ages is in part due to the slight acceleration in Portland cement hydration while the strength gain at later ages is mostly as a result of pozzolanic reaction, causing pore refinement and replacing the weaker calcium hydroxide with the stronger calcium silicate hydrate.

Pfa can be divided into two types which differ from each other mainly in terms of the calcium content ². Low-calcium pfa (class F) contains less than about 10% CaO and it is generally a product of combustion of anthracite and bituminous coals. The principal crystalline materials in low-calcium pfa are quartz, mullite and hematite or magnetite and as these materials are non-reactive at ordinary temperatures, their presence in large quantities tends to reduce the reactivity of pfa. High-calcium pfa (class C) is in general more reactive as it contains more calcium in the form of reactive crystalline compounds.

2.4.2 PFA SHAPE AND SIZE

Pfa particles are spherical and particle size distribution studies of pfa shows that the particles vary from 1 to 100 μm in diameter with more than 50% under 20 μm . The particle size distribution, morphology, and surface characteristics of the pfa has a considerable influence on the water requirement and workability of freshly made concrete and the rate of strength development in hardened concrete.

According to Sarkar & Ghosh⁴¹ fly ash particles of very small size are mostly made up of clear glass spheres. Spongy particles formed either by fusion of many fine particles or from ore mineral particles are also common in most fly ashes. The clear glass spheres are smaller than other particles and as a result they have higher specific areas than the spongy particles that are larger and generally have lower specific surface areas. About 60% of the particles in the ash have diameters less than 3 μm but these particles constitute less than 10% of the total weight. The particles in bituminous ash range from less than 1 μm to over 100 μm but the average particle size in such ashes vary from 7 μm to 12 μm . The surface area of fly ash particles have been reported to vary from about 2000 cm^2/g to 10 000 cm^2/g depending on the proportion of fine particles in the fly ash. ✕

Most pfa's contains up to 10% unburned carbon and this carbon is generally present in the form of cellular particles larger than 45 μm . Large amounts of carbon in pfa is considered harmful as the cellular particles of carbon tend to increase the water requirement for a given consistency and the admixture requirement for entrainment of a given volume of air.

In 1973 Cabrera & Gray⁴² published results from an investigation of nine pfas from different sources in the U.K. The relationship between the specific surface - as determined by different methods - the chemical composition, and the pozzolanic activity of the pfa was investigated and it was shown that the values obtained for specific surfaces of ashes vary according to the method of determination. Four different methods of measuring specific surface area were assessed and it was suggested that nitrogen absorption should be used to determine the specific area of pfa since only this method correlated with the strength of lime-pfa-sand mortars. The authors suggested that the air-permeability measurements determine only the external surfaces of the ash particles, whereas nitrogen adsorption measures both external and internal surfaces.

Hopkins and Cabrera⁴³ stated that the workability of concretes containing pfa is influenced by the properties of the ash used. Pfa is mainly composed of spherical particles but the material also contains irregularly shaped particles. The presence of large numbers of these irregular particles will adversely affect the ability of pfa to improve concrete workability. On storage pfa particles tend to agglomerate, and these agglomerated particles can also reduce workability. The authors suggest the use of a 'shape factor' to evaluate the suitability of a certain ash for use in concrete. This factor is a comparison of the measured specific surface area (MSA) obtained by the air permeability technique using a Fisher Sub Sieve Sizer, and the calculated specific surface area (CSA) derived from the particle size distribution by assuming that the ash consists of discrete spheres. Any agglomeration causes the MSA to be less than the CSA while irregular particles will result in the MSA being greater than the CSA. The MSA would be equal to the CSA if all the particles were perfectly spherical with no surface imperfections. Hopkins⁴⁴ stated that pfas with small differences between their measured and calculated specific surface areas are currently deemed best suited for use in concrete as this would mean that the pfa contains more rounded particles.

2.4.3 HYDRATION AND MICROSTRUCTURE

The chemical composition and reactivity of fly ashes vary with the mineralogy of impurities in the coal. All commercial fly ashes react with lime in the presence of water to produce highly cementitious products, which are insoluble in water. According to

Lea's Chemistry of Cement and Concrete the hydration products resulting from the hydration of pozzolanic cements are similar to those occurring in Portland cement pastes and the differences are as a result of variations in the ratio of the various compounds as well as their morphology.⁴⁵ The metastable silicates present in fly ash react with calcium ions in the presence of moisture to form water insoluble cementitious calcium silicates and aluminate hydrates⁴¹.

Berry et al.⁴⁶ investigated the hydration mechanism of high volume fly ash concrete binders using mixtures containing superplasticizers with a water-cementitious ratio of 0.3 and cement replacement of 58% per weight by fly ash. The authors concluded that these pastes appear to hydrate and gain strength by the interaction of at least three of the following mechanisms:

- Hydration of Portland cement by normal chemical reaction, slightly accelerated at early ages.
- Improved densification through particle packing, aided by the use of superplasticizers and the spherical form of fly ash.
- Reaction of fly ash particles that produce insoluble silicate and aluminate hydrates at particle boundary regions at late ages.
- Hydration of individual fly ash particles that remain physically intact and largely unchanged in morphology and thus capable of filling of void space.

The authors state that these functions are probably common to all cement-fly ash systems but they become measurable and contribute significantly to material properties only at high levels of cement substitution.

Sarkar & Ghosh⁴¹ state that fly ash acts as nucleation centers for the hydration of cement during the early stages of hydration. This is evidenced by the formation of precipitates on the fly ash surface which gradually grow to short acicular crystal-like phases which covers most of the fly ash particle to form a film-like layer (0.5 to 1 μm thick) that is very similar to the duplex film at the paste-aggregate interface in concrete. The thickness of this layer does not change much with hydration age and it is highly unlikely that the fly ash reacts chemically at an early age. As hydration progresses, fly ash particles become more and more etched. At the early stage of hydration (after 1 day) the

strength of the interlinked hydrated paste is still lower than that between the fly ash particle and the duplex layer and therefore the surface of the fly ash can not be observed in Scanning Electron Microscopy (SEM) studies. When the strength of the paste exceeds the bonding of the hydrates with the fly ash (generally after less than 7 days) the fly ash surface becomes exposed. The exterior glass hull starts to dissociate and the crystalline layer composed mainly of mullite emerges. Long time hydration (more than 90 days) eventually erodes away some of the fly ash glass phase but the crystalline phase layer retains its original spherical shape. In mature paste a gap occasionally exists between fly ash particles and the surrounding hydration products, indicating that the dissolved glass phase diffuses and precipitates far away from the fly ash particle.

2.4.4 CODE REQUIREMENTS FOR THE USE OF FLY ASH IN CONCRETE

ENV 197-1⁴⁷ states that “siliceous fly ash is a fine powder of mainly spherical particles having pozzolanic properties”. The fly ash should consist essentially of reactive SiO_2 and Al_2O_3 with the remainder containing Fe_2O_3 and other oxides. The proportion of reactive CaO is limited to less than 5% per mass while the reactive SiO_2 content shall not be less than 25% per mass. The suitability of a fly ash for incorporation in a Portland fly ash cement can according to this standard be judged by its “cementing efficiency index” as defined by Smith.⁴⁰ He assumed that each ash has a cementing efficiency K , such that a weight F of fly ash would be equivalent to a weight KF of cement and thus for a concrete containing weights W of water, C of cement and F of fly ash, the effective water-cement ratio can be calculated using the following equation:

$$(W/C)_e = \frac{W}{C+KF} = \frac{W}{C} \left[\frac{1}{1+(KF/C)} \right] \quad (\text{Eq 2-17})$$

The value for K varies between 0.15 and 0.38 for concrete at 20°C and between 0.61 and 1.22 for concrete at 50°C, illustrating the significant advantages of cements containing fly ashes for applications that involve humid high temperature curing.⁴⁵

ASTM Standard C 618 – 85 specifies that for a class F fly ash the sum of the silica, alumina, and ferric oxide should be at least 70% while the SO_3 should be less than 5% and the carbon content as determined by the loss on ignition (LOI) should be less than 6%⁴⁵. ENV 197-1⁴⁷ limits the loss on ignition of fly ash to 5% per mass. In order of complying to the South African standard specification for Portland cement extenders (SABS 1491: Part II – 1989)⁴⁸ not more than 12.5% of the particles in a fly ash should be retained on a sieve with square apertures with a nominal size of 45 μm .

2.4.5 THE EFFECT OF PFA ON THE PROPERTIES OF CONCRETE

2.4.5.1 Compressive Strength

The results of the first extensive study on the effect of pfa on the properties of concrete was published in 1937 by Davis et al.⁴⁹ In this study fifteen American fly ashes were blended with seven cements in blends of up to 50% fly ash (by weight of cement). These results indicated that fly ashes of moderate or low carbon content and moderately high fineness could be used as a replacement for Portland cement to produce concrete with properties equal or superior to those of concrete containing no fly ash. The results obtained from tests conducted using fly ash from Chicago ~~is~~ summarized in Figure 2.9 ~~are~~ that show the compressive strength of mixtures of different ages as a function of the percentage of cement that had been replaced with ash.

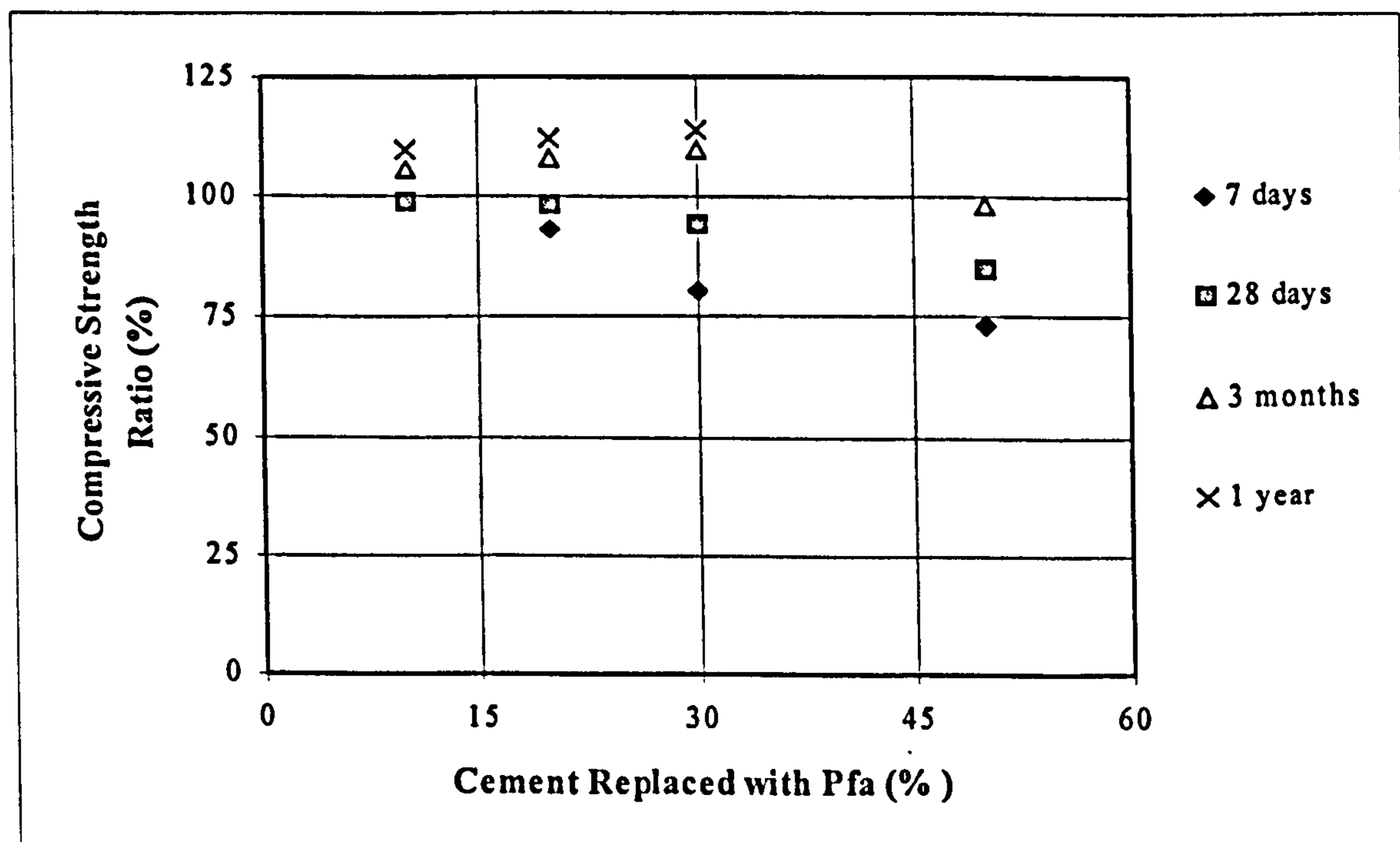


Figure 2.9: Effect of Cement Replacement on Compressive Strength.

The strength is indicated as a percentage of the strength obtained from a mixture containing no ash. The water/cement ratio of the mixtures varied between 0.43 for the mixture containing no ash and 0.40 for the mixtures containing 20 and 30% ash. Although early age compressive strength (up to 28 days) is lower than that of corresponding concrete containing normal Portland cement, the compressive strength obtained from mixtures containing up to 30% fly ash were found to be substantially higher at later ages (after 3 months and more). The researchers in this investigation found that the concrete strengths were lower for 50% replacement than for 30% replacement. From the results published this is true for ages up to 3 months, but no comparative results were published for testing ages of more than 3 months. As the results indicate that even 10% cement replacement leads to a marked reduction in the rate of gain in compressive strength, the ultimate compressive strength for 50% might be far higher than the 3 month strength and the conclusion that 30% replacement is an optimum might only be true for early ages.

Davis et al. concluded that the carbon content of fly ash appears to have a marked effect upon the properties of concrete. In their investigation the group of fly ashes of below 2% carbon content exhibited considerably higher concrete strengths at all ages than did the group of cements containing fly ashes of high average carbon content (22%). In this investigation the fly ashes with low carbon content were much finer than the fly ashes with higher carbon contents. The coarseness of the high-carbon fly ashes can in part be due to the fact that carbon particles are relatively large in size. The group of cements containing finer fly ashes (average specific surface area 3220 cm²/g) exhibited considerably higher concrete strengths at all ages than did the group of cements containing coarse fly ashes (average specific surface area 1730 cm²/g). Although there seems to be a correlation between the fineness of the fly ash and the compressive strength of the concrete in this investigation, both the fineness and the carbon content of the pfas varies and based on these results it is therefore not possible to isolate the effect of pfa particle size on the properties of concrete.

Brink & Halstead⁵⁰ investigated 34 fly ashes from 19 different sources and they concluded that the strength development of Portland cement fly ash mortars is related to the carbon content of the fly ash, the 45 μm sieve residue and the water requirement for mortars containing fly ash as compared to the water requirement for similar mortars

without fly ash. The effect of fly ash on the 28 day, 3 month and 1 year compressive strengths of mortar was determined by replacing up to 50% of the cement (by volume) with fly ash. The water added to each mixture was adjusted to maintain a uniform consistency. The researchers concluded that the compressive strength at 28 days and one year are usually reduced by partial replacement of the cement with fly ash. If however their compressive strengths of the 28 day and the 1 year results are investigated as a function of the water requirement (see Figure 2.10 for results of 35% ash replacement), it can be concluded that although the 28 day strength is reduced, the ultimate strength is higher than what it would have been for mixtures where the water content was not increased. From Figure 2.10 it can be concluded that the water requirement has a significant effect on the compressive strength of the mixture.

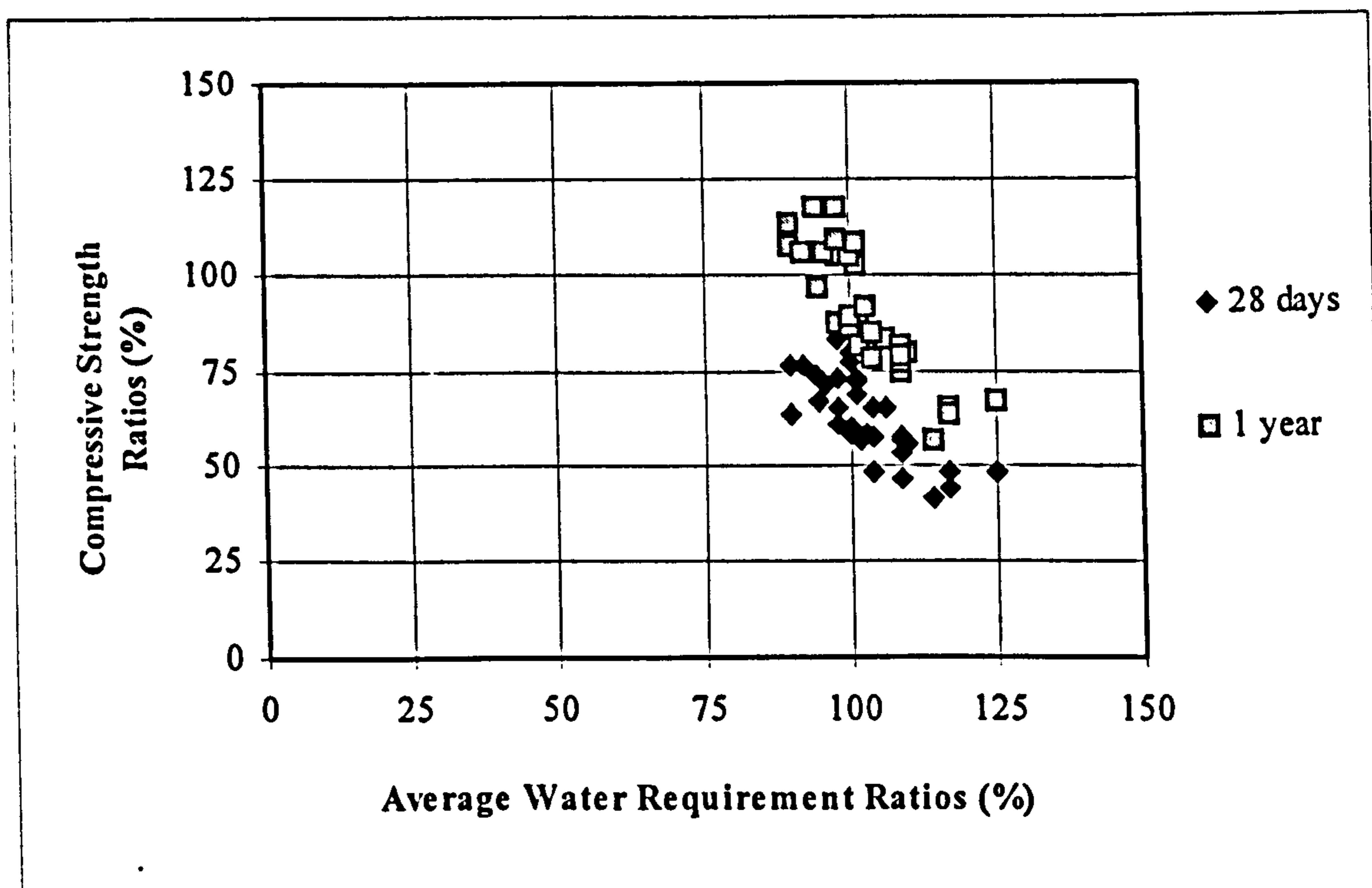


Figure 2.10: Effect of Water Requirement on Compressive Strength.

The water requirement for the different ash sources seems to be a function of the carbon content of the ash, as indicated in Figure 2.11. These results seem to indicate that the water requirement increase with an increase in carbon content. The higher carbon content would therefore result in lower compressive strengths as indicated in the graph in Figure 2.12. From this graph plotted for mixtures with constant workability it can be seen that, although all the 28 day compressive strengths of the mixtures containing 35% ash are lower than the compressive strength of the mixture without ash, the ultimate

strength (1 year strength) of the mixtures manufactured using ash with a low carbon content was higher than that obtained for the mixture containing no ash.

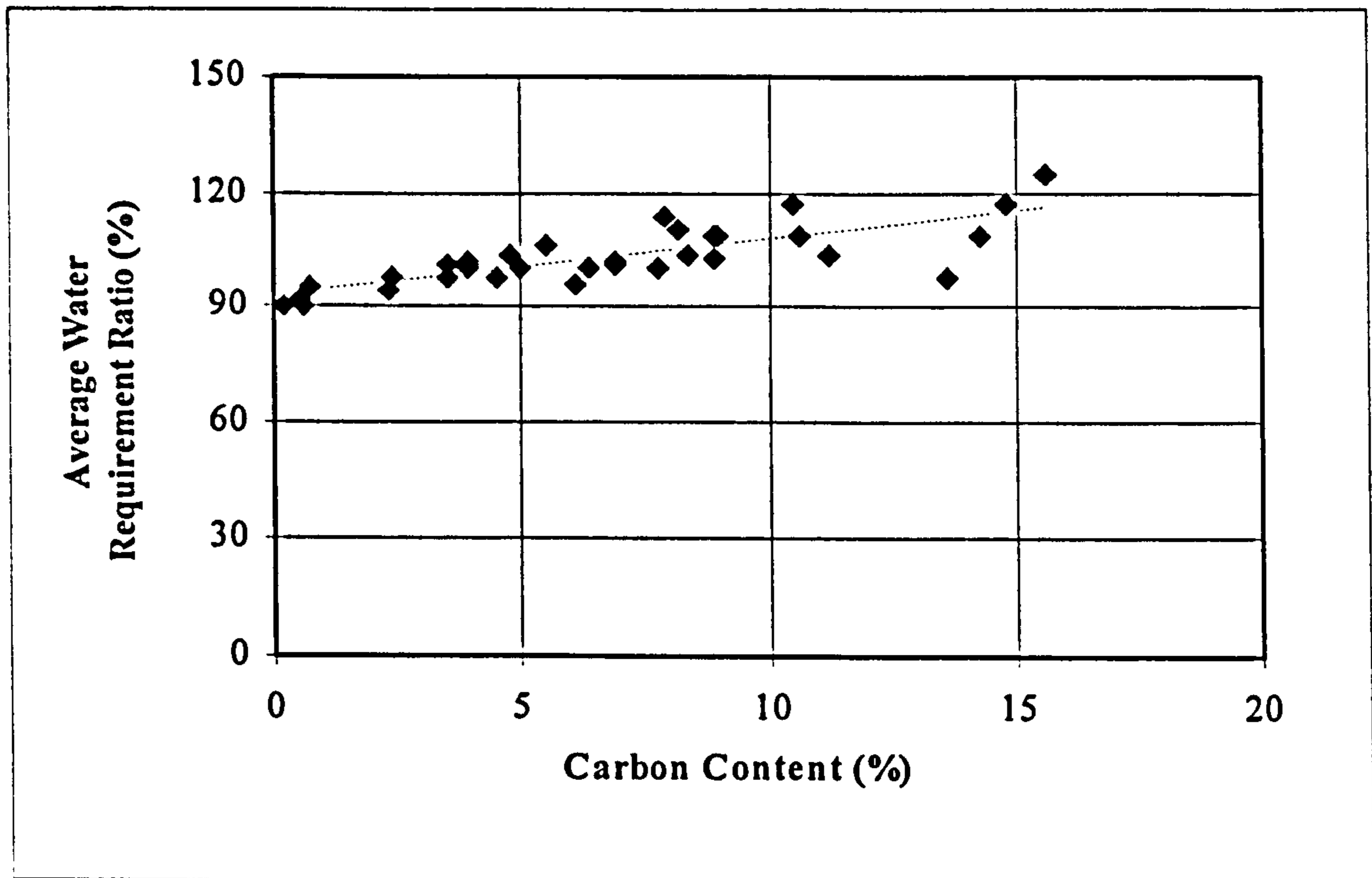


Figure 2.11: Effect of Carbon Content on Water Requirement.

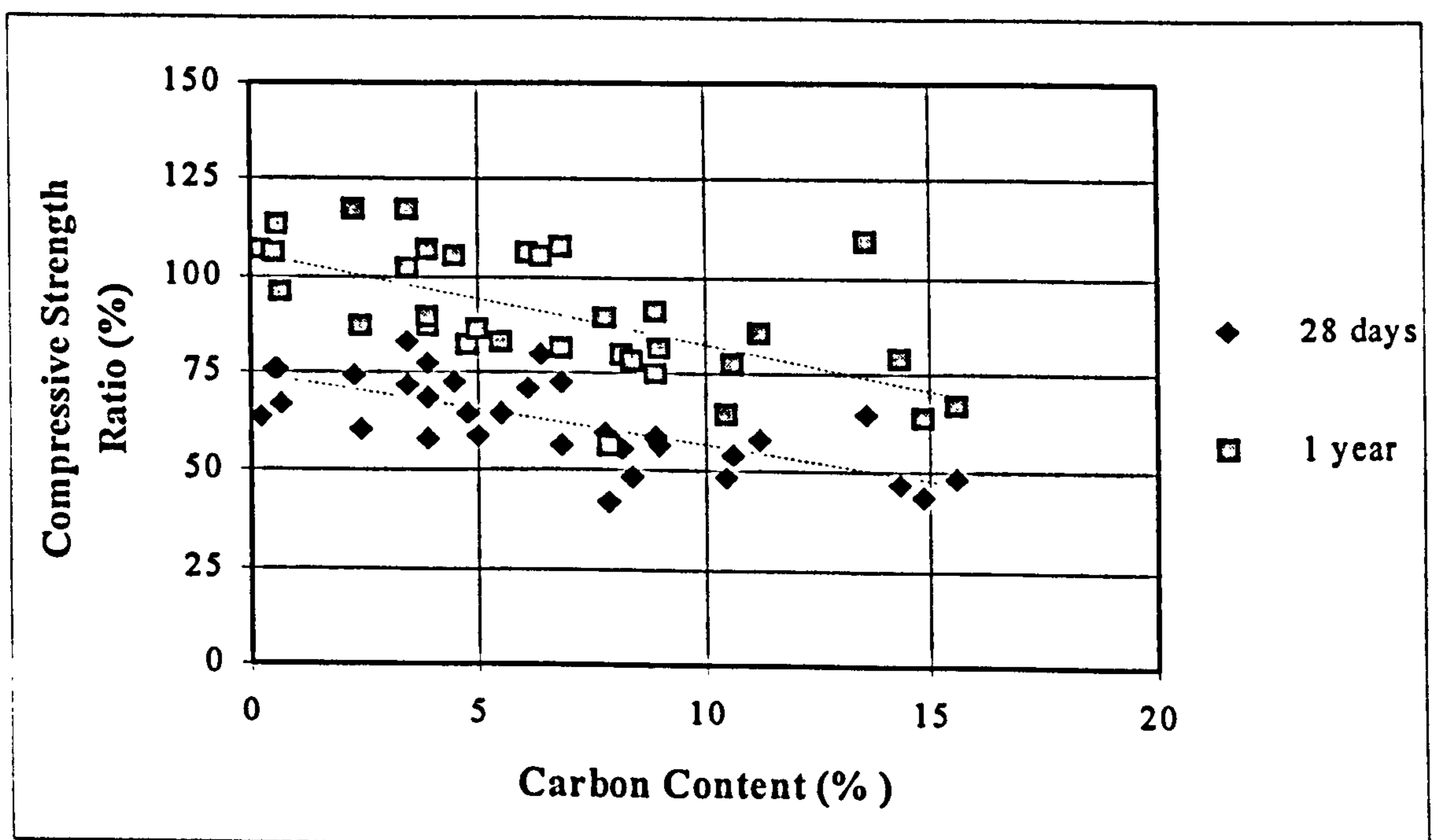


Figure 2.12: Effect of Carbon Content on Compressive Strength.

The effect of ash particle size on the compressive strength of a mixture with constant workability can be seen in Figure 2. 13. These results are again those published by Brink & Hallstead⁵⁰ for mixtures containing 35% ash. The surface area as measured using air permeability gives an indication of the ash particle size.

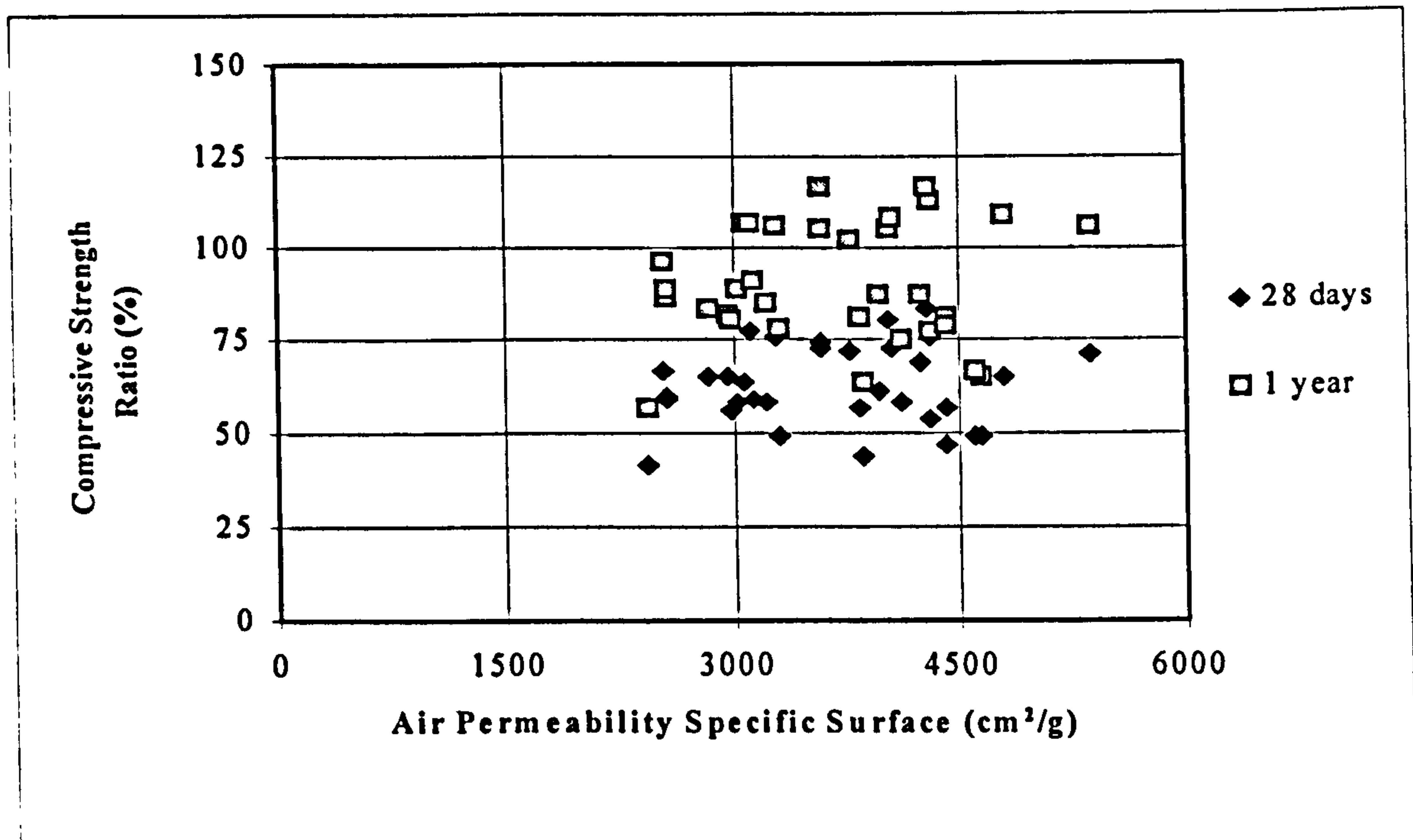


Figure 2.13: Effect of Particle Size on Compressive Strength.

From these results there does not seem to be any correlation between ash particle size (as indicated by surface area) and compressive strength. Based on these results where there does not seem to be a definite relationship between particle size and strength, one has to question the sense of limiting the particle size of the ash where the carbon content of a specific ash is already low.

The fact that Brink & Halstead simultaneously varied the age, water content, carbon content and ash particle size makes it impossible to determine the effect of any of these parameters on the compressive strength without taking all the other parameters into consideration. Stepwise regression analysis was conducted to determine what percentage of the variability in compressive strength can be attributed to each of these parameters. The equation of the multiple regression model fitted is:

$$F = 159.9 + 10.8 \ln(t) - 144 W + 0.004067 A \quad (\text{Eq 2.18})$$

Where:

F	=	compressive strength as a percentage of the strength of the mixture containing no ash
W	=	water requirement as a fraction of the water requirement of the mixture containing no ash
t	=	age (<i>days</i>)
A	=	specific surface (cm^2/g)

The R-squared statistic indicates that the model as fitted explains 84.4% of the variability in strength. The adjusted R-squared statistic, which is more suitable for comparing models with different numbers of independent variables, is 83.7%. Stepwise regression indicates that 51% of the variability in compressive strength can be explained by the age. Adding the water requirement ratio to the model as a second variable increases the R-squared value to 82%. The results of regression analysis indicate that the carbon content does not have a statistically significant effect (at the 90% or higher confidence level) on the compressive strength. The particle size as indicated by the air permeability has a relatively small influence on the compressive strength as the addition of this term through stepwise regression increases the R-squared value from 82% to only 84.4%.

First impressions indicate that Brink & Halstead obtained significantly lower compressive strength results when using ash than those obtained by Davis et al. The fact that the cement replacement was per volume in one study and per weight in the other means that the results can not be compared on face value. The relative density of pfa is much lower than that of cement and therefore the total volume of cementitious material used in the mixtures where cement was replaced per weight is much more than the total cementitious volume of the mixtures where replacement took place per volume. The larger volume of cementitious material should lead to higher strength as was obtained by Davis et al. Brink & Halstead again varied the water content of their mixtures and as the water/cement influences the compressive strength of cement pastes, the effect of using pfa can not be isolated. Lat

According to Smith⁴⁰ the two main factors influencing the strength of similar normal concretes are the type of cement and the water-cement ratio. If two cements which differ

in their rate of hydration are used in two concretes, then one concrete can be made to reach the same strength as the other at a given date by adjusting the water-cement ratio. Smith argues that concrete containing fly ash should be regarded as a new type of concrete and designed as such. His equation for cementing efficiency has been adopted for use by the European Prestandard for Common Cements. To calculate the value of K for each ash a control line of strength against water-cement ratio was first plotted from results of tests on control concretes containing no fly ash. The strengths reached by concretes containing ash were then used to find the effective water-cement ratios of these concretes against the control curve. The factor K was then calculated and Smith deemed a value of 0.25 to be a reasonable figure on which to base a rule for the design of fly ash concrete to reach a desired strength. He concluded that the K value remained virtually unchanged between 7 and 28 days but this seems unlikely as ash is known to reduce the initial rate of strength gain and therefore if a mixture containing fly ash is designed to have the same strength than a normal concrete mixture without ash after 7 days, the 28 day strength of the mixture containing fly ash should be much higher than that of the normal concrete mixture. The increase in K value (from 0.225 at 7 days to 0.352 at 6 months) that is found from the average value for all samples at all ages tested does seem to indicate that the K value increases with time.

In 1968 Cannon⁵¹ published an article on the proportioning of fly ash mixes for strength and economy discussing a method that was developed by the Tennessee Valley Authority (TVA) after using fly ashes for the previous twelve years in all classes of concrete. This method aims at designing the most economical mixture with a certain 28 day or 90 day strength. Based on the required strength and the cost of fly ash and cement an optimum fly ash content (% of cement content by weight) can be determined. The water-cement ratio that would yield the required strength in a control mix (without fly ash) is determined and this water content can now be adjusted according to the fly ash content by using a set of graphs produced by the TVA. The author concludes that fly ash should be proportioned in concrete on the basis of economy and equal strength requirements and not as a straight substitution for cement either on a weight or volume basis. He argues that economy should be the only restriction placed on the proportions of fly ash to cement used. Based on TVA's experience the author states that 'the addition of fly ash as an additional variable in concrete does not normally mean an increase in the coefficient of variation of the concrete as produced since fly ash concrete

at a given plant will almost always have an equal or lower coefficient of variation for a properly designed mix than a comparable mix without fly ash.' This statement is of interest especially if one takes into account the fact that when it was made it was TVA policy to use the source of fly ash which offered the greatest economy in the concrete for each particular construction project regardless of whether or not the fly ash met Federal and ASTM specifications for fineness.

Hassan et al.⁵² investigated the influence of fly ash content and curing temperature on the properties of high performance concrete. The effect of pozzolanic cements was examined by comparing the properties of mixes containing ordinary Portland cement to mixes with equal workability where 30, 50 or 70% of the cement (per weight) has been replaced with pfa. Equal workability was achieved by reducing the water/(opc+pfa) of the mix. This reduction was expressed mathematically using the following equation:

$$W_r = 0.36 fa + 0.11 \quad (\text{Eq 2.19})$$

Where:

$$\begin{aligned} W_r &= \text{reduction of water in mix (\%)} \\ fa &= \text{pfa content (\% by weight of cement)} \end{aligned}$$

The results of these tests not only confirmed that the water demand of a concrete mixture decreases with increased fly ash content but they also indicate that there is no unique relationship between fly ash content and strength, as the strength varies with the age of the concrete and the curing temperature. At early age (1 day) the compressive strength is inversely related to the fly ash content but this linear relationship is not valid at increasing curing time. At 3 days and beyond there is clearly an optimum fly ash content for maximum compressive strength. This optimum fly ash content increases from 5% at 3 days to 20% at 90 days for specimens cured at 20 °C, while the optimum increases from 15% at 3 days to 30% at 90 days for specimens cured at 45 °C. For specimens cured at 20 °C equal strength to the opc mix was obtained for mixes with between 30 and 40% cement replacement while for concrete cured at 45 °C equal strength to the opc mix was achieved at 3 days with a fly ash content of up to 30% and at 90 days with a fly ash content up to 60%. Hassan et al.⁵² concluded that there is a

linear relation between opc equivalent compressive strength (f_c) at varying age and fly ash content. The equation which describes these relations is:

$$f_c = a + b(fa) \quad (\text{Eq 2.20})$$

Where:

f_c	=	opc equivalent compressive strength (MPa)
a	=	the compressive strength of opc concrete without pfa at 1 day
b	=	“strength factor”
fa	=	pfa content (% by weight of cement).

The researchers used values for a of 19.52 and 20.00 for curing temperatures of 20 and 45 °C respectively while the corresponding slope (b) or strength factors were 1.34 and 0.80. They state that this method of determining a percentage fly ash replacement that would yield a specific strength after a certain period of time is far more logical and rational than the currently used k factor.

Timms & Grieb⁵³ conducted research on the use of four different sources of fly ash and two sources of cement in air-entrained concrete. These tests were conducted for 16.67% and 33.33% cement-replacement (per volume) and the water content of the mixtures were adjusted to have a constant workability. Where air entraining took place, the volume of sand was reduced to keep the volume of cement in the mixture the same than ~~than~~ a for no air entraining. Timms & Grieb reach conclusions that can be compared to those of Brink & Halstead but again the changes in water-cement ratio makes it impossible to quantify the effect of pfa alone. For the fly ashes of low carbon content the compressive strength after one year was higher than that for concrete without fly ash. The use of air-entrainment appeared to have little effect on the relative strengths, and for each combination of cement and fly ash, the concrete with and without air entrainment had similar relative compressive strengths. In general it was found that concrete containing fly ash showed less shrinkage upon drying than the concrete without fly ash.

Dhir et al.⁵⁴ studied the effect of in source variability of pfa upon the strength of concrete. They concluded that although the chemical composition appeared to be fairly

constant the physical characteristics of pfa samples showed in-source as well as between source variation when sampled over a period of time. The variability in quality of pfa does not however significantly alter the strength differences of concrete above those caused by the variability of the cement used.

Montgomery et al⁵⁵ conducted research on lean cement paste mixes and they suggested that the early age strength development is largely influenced by the physical presence of the ash particles rather than by a chemical reaction and that the continued increase in strength at greater ages might be the result of pozzolanic reaction. A constant solids-water volume ratio of 1.1:1 was maintained for mixtures with ash contents varying between 0% and 80% per volume and test were conducted on specimen cured at 20°C and 40°C, and autoclaved samples. The researchers concluded that cement paste with a dense and strong structure can be achieved either by using a high cement content or by replacing part of the cement with fly ash and then relying upon either time or elevated temperature to bring about the desired strength.

The results of this investigation indicates that although the 7 day strength of these mixtures reflect the effect of water-cement ratio on the compressive strength of concrete the long term strength development of the mixtures containing ash indicate that the strength is not purely a function of water-cement ratio but rather of water-cementitious or water/(cement + ash) ratio. Large increases in compressive strength takes place in the pastes with high ash contents after prolonged periods of curing and at an age of about 10 to 12 weeks the presumed pozzolanic reaction only starts contributing towards the strength.

The fact that constant solid-water volume ratios were used and that fly ash has a lower relative density than cement means that the weight of the solid material decreases with an increase in ash content. The water-cement ratio of concrete mixtures is normally expressed in terms of weight ratios and an increase in water-cement ratio normally leads to a decrease in compressive strength⁷. The water-cementitious weight ratio of these mixes increase with an increase in ash content and it is therefore possible that the compressive strengths obtained at higher ash contents would have been higher if the water-cementitious weight ratio was kept constant.

Ravina & Metha⁵⁶ conducted tests on low cement / high fly ash concrete and they concluded that it was possible to replace up to 50% of the cement in a lean mix with fly ash and obtain the design compressive strength after 75 days curing. The researchers concluded that this curing period could be considerably reduced when a part of the aggregate in the concrete is replaced with additional fly ash. The authors used two high-calcium and two low-calcium fly ashes and concluded that the reactivity of low-calcium fly ashes is governed by the fineness but as the chemical composition of the two low-calcium ashes differed significantly factors other than fineness might contribute to the difference in reactivity and their conclusion might therefore be unfounded.

Other researchers such as Stuart et al.⁵⁷ that studied the compressive strength of cement mortars containing fly ash replaced up to 60% of the cement with fly ash but where replacement was conducted based on volume replacement the use of ash seemed to have a detrimental effect on the compressive strength at all ages. The researchers that substituted the cement based on weight replacement in stead of volume replacement all concluded that ash increases the long term compressive strength.^{6,52,49,41,57}

2.4.5.2 Durability

Neville⁶ states that one of the consequences of the slow reaction of fly ash in concrete is that, initially, the concrete has a higher permeability than concrete with a similar water/cementitious ratio. Fly ash concrete can however with time acquire a very low permeability, thereby reducing the possibility of aggressive agents penetrating the concrete. Fly ash in adequate quantities is beneficial in reducing alkali-silica reaction, improving resistance to chloride penetration, sulfate resistance and freezing and thawing resistance. The incorporation of fly ash in concrete is desirable not only from the economic benefit ensuing from its use but most importantly from the environmental benefits such as disposal of waste and the improvement of long term properties.⁵²

Wainwright et al.³⁴ concluded that a hot dry environment is detrimental to the durability related properties of the ordinary Portland cement (opc) mixtures but favorable to the improvement of properties of the opc/pfa mortar mixture. Samples were tested after different periods of curing and the permeability and pore structure characteristics of all mixtures were adversely affected by a total lack of curing. They further concluded that

the critical curing period is three days regardless of cement type or curing environment used in their program. After this period there is little change in permeability or average pore diameter although the porosity of pfa mixtures was still reducing. The reduction in porosity observed after more than 7 days of curing was negligible. Regardless of curing time the specimens containing pfa that were stored in the hot environments had a finer pore structure than the specimens containing only opc. Wainwright et al. pointed out that a constant water/cementitious ratio was used in their tests to simplify the analysis of the results but that in practice it would be possible to reduce the water content in the pfa mixes and still maintain the same workability. This reduction in water content would result in a further improvement in the properties of the pfa mixes.

In their investigation on the influence of fly ash content and curing temperature on the properties of high performance concrete Hassan et al.⁵² found that the opc control mix exhibited the highest porosity value at both (20 and 45 °C) curing temperatures and at all curing ages, whilst the mixes containing pfa showed relatively large reductions in porosity with increasing pfa content and curing temperature. This reduction is mainly due to the important role the pfa plays in controlling the porosity by reducing the water demand and increasing the packing capacity of the concrete ingredients.

Hassan et al.⁵² also investigated the influence of fly ash content and curing temperature on the oxygen and water permeability of concrete and they found that the oxygen permeability of samples decreased with increasing curing time but at different rates depending on the pfa content. For specimens cured in water at 20 °C increasing the pfa content to more than 30% causes high permeability at early ages, but it provides significant reduction at later ages (28 days). While the concrete with different levels of pfa substitution required a curing period of 3 to 28 days in water of 20 °C to reach lower oxygen permeability than the opc concrete, the period is reduced to 3 days when the concrete is cured at 45 °C. The water permeability values obtained for the different concrete mixes were similar to those obtained for oxygen permeability, also indicating lower permeability values for the mixes containing pfa. This reduction in permeability is due not only to the pore refinement and pore blockage resulting from the additional volume of reaction product generated by the pfa and the lime present in the hydrated cement but also to the improved packing of the mineral aggregate structure which results from the addition of pfa.

Taylor & Kruger⁵⁸ conducted research on the effect of fly ash particle size on concrete properties using a constant water-cement ratio of 0.6 and 40% cement replacement. The fly ash was split into samples containing particles smaller than 20 μm , 45 μm and 70 μm , and samples containing particles larger than 20 μm , 45 μm and 70 μm . The properties of concrete manufactured using the split samples was compared to that of concrete made using unclassified samples (identical to the other samples before splitting) and classified fly ash containing less than 12.5 % particles larger than 45 μm . The water requirement for constant slump was the lowest for the fine fractions followed by the classified ash, while the coarse fraction mixes all required more water than the OPC mix. The fact that the finer particles required less water is not what would normally be expected, but the shape of the larger particles could be irregular, thus affecting the ability of the ash to reduce workability. It may also be argued that the slump test does not fully quantify workability and the results might have been different if a different workability test was used. The highest strengths at all ages up to 56 days were obtained using the finer particles. The compressive strength obtained using OPC was virtually the same as that for the mixes containing the coarse ash particles, indicating that the coarse particles do not significantly contribute to the hydration process during the first 56 days. This finding correlates with the findings of Montgomery et al.⁵⁵

Air-permeability tests conducted indicated that the mixtures containing the coarse ash particles are more permeable than the OPC or the mixtures containing the fine fractions. The tests were conducted after 28 days of water curing and as the samples contained relatively large volumes of fly ash the full benefit of the fly ash might not be apparent in the results. Fly ash is known to reduce the permeability of concrete⁷ but yet the results of these tests indicate that even the mixes containing the fine ash particles had virtually the same permeability than the OPC mixes. This seems to indicate that the tests were conducted on samples that were too young to show the benefits of using fly ash. Taylor & Kruger concluded that there was a reduction in potential durability with the use of unclassified and coarser fraction fly ashes. They further stated that the current means of specifying fly ash fineness (less than 12.5% particles larger than 45 μm) is satisfactory as there is little difference between the results obtained from the classified ash and that fraction of the ash with particles less than 45 μm in diameter. These statements seem to be based on pre-conceived ideas as the tests indicating durability

were only conducted after 28 days for one specific curing condition. From the results there is little difference between the mixes manufactured using particles smaller than 45 μm and particles smaller than 70 μm . The reasoning for using 45 μm as a specification cut-off point remains unclear. The fact that the results of this investigation might indicate that the coarse fly ash particles when separated from the rest are detrimental to the properties of concrete manufactured using the coarse particles it does not necessarily mean that these particles when used with finer ash particles would have a detrimental effect on any properties of concrete.

2.4.5.3 Shrinkage and creep

Neville⁶ states that shrinkage of hydrated cement paste is directly proportional to water/cement ratio as the water/cement ratio determines the amount of evaporable water in the cement paste and the rate at which water can move towards the surface of the specimen. If the water/cementitious ratio is kept constant a higher percentage of fly ash in a blended cement would result in up to 20% higher shrinkage. When the water/cementitious ratio is reduced so as to maintain the same workability as the control concrete shrinkage is either unchanged or slightly reduced.⁵⁹

Various authors have conducted research on the effect of fly ash on the drying shrinkage of concrete.^{45,59} Shrinkage is sensitive to the replacement level of fly ashes for Portland cement, only when initial curing is limited to 3 days, where the shrinkage increases with increased fly ash content. When concrete is however cured for up to 28 days before drying, the shrinkage is not affected for up to 40% replacement.⁶⁰

Carette et al.⁶¹ investigated the mechanical properties of air-entrained concrete incorporating high volumes of fly ash. Eight fly ashes and two Portland cements from the U.S. were used in mixtures with a constant water-cementitious ratio of 0.33 and 58% cement replacement (by weight). Prisms cast from all the mixtures were subjected to drying shrinkage measurements after initial storage in lime-saturated water for periods of 7 and 91 days. For most of the 7-day water cured samples the drying shrinkage strains at the end of 224 days of drying ranged from 400 to 600 $\times 10^{-6}$, whereas for the 91 day water-cured concrete, these values ranged from 350 to 450 $\times 10^{-6}$.

Carrette et al. concluded that these values are either comparable to or lower than those observed for Portland cement concretes of similar proportions.

Sirivivatnanon and Khatri⁶² conducted research on the selective use of fly ash. Their results indicate that the volume stability properties (drying shrinkage and creep) of concrete where between 40% and 50% of the cement (by weight) had been replaced with fly ash are better than those of OPC concrete.

Creep is strictly related to the concrete strength at the time of loading and it therefore depends on the strength of the cement paste, the water/cement ratio and the curing period.⁴⁵ As the use of ash reduces the early age strength of concrete, the specific creep of mixtures containing ash will be greater than that of the plain concrete if the concrete has been loaded too early. The difference tends to reduce as the curing proceeds. Results of many studies tend to suggest that long-term-cured fly ash concretes exhibit lower creep than similar Portland cement concretes.^{63, 59}

2.5 CONCLUSIONS

Little work has been published on foamed concrete and the factors influencing its properties. The strength of foamed concrete decreases as the density is reduced but it behaves differently to normal concrete in that the water/cement ratio does not have a major influence on the strength of the material. Foamed concrete with any specific density can only be manufactured with a small range of water/cement ratios because if the water in foamed concrete is insufficient, the foam degenerates and if too much water is added segregation takes place. The cement and aggregate content has a strong influence on the compressive strength of foamed concrete and there seems to be optimum contents for both. The compressive strengths obtained are significantly higher when protein foams is used in stead of synthetic foams. For a specific density the strength of the material can be improved by replacing some of the cement with pfa.

From the literature reviewed it can be concluded that the use of pfa in cement pastes retards the initial gain in strength, but if cement is replaced per weight the long term

strength of mixtures containing up to 80% pfa can be improved. The use of pfa can reduce shrinkage and long term porosity and permeability.

Although many researchers have investigated the properties influencing the performance of pfa no conclusive evidence could be found to support claims that the inclusion of coarse particles in pfa has any detrimental effect on the long term properties of pfa-cement pastes. The shape of the pfa particles as indicated by the shaped factor does seem to have a definite effect on the workability, and therefore the water requirement and thus the ultimate compressive strength of pfa-cement pastes.

High and low calcium pfas react differently in cement pastes and the carbon content as measured by the L.O.I. seems to have a significant influence on the efficiency of pfa. No conclusive evidence could be found that suggests that any other aspects relating to chemical composition has any significant influence on the properties of pfa-cement pastes.

Foamed concrete is manufactured by introducing air voids into a cement based mortar. The compressive strength of a brittle materials is a function of the number of voids in it. In addition to their volume, the shape and size of pores also has an influence and generally at a given porosity, smaller pores lead to a higher strength of the cement paste.

CHAPTER 3 : EXPERIMENTAL PROCEDURE FOR THE MANUFACTURE OF FOAMED CONCRETE

3.1 INTRODUCTION

Although foamed concrete is a cement based material, it is strictly speaking not concrete as it contains large volumes of air and no coarse aggregate. Conventional concrete mixing and casting procedures and equipment can not be used for the manufacture of foamed concrete and this chapter will deal with the experimental procedure used for the manufacture of foamed concrete. The procedures and equipment have been developed in the laboratories of the University of Pretoria as a result of several years of experience using this material.

3.2 EQUIPMENT

Concrete should be mechanically mixed to produce a uniform distribution of the materials with a suitable uniformity and the required wet density. Precautions should be taken to avoid excessive mixing that could cause changes in density⁵. A forced action mixer should be used¹⁷ but from experience the best results are obtained when using a paddle type whisk rotating around an axis.⁹

When mixing foamed concrete the mixing sequence for the materials differs from that normally used for concrete. It is recommended that the required amount of water is placed in the mixer first, followed by the cement, fine aggregate and lastly the pre-formed foam⁵.

The foam is produced using a foam generator that adds compressed air to the diluted foaming agent in a pre-determined ratio. The foam is pumped directly into the mixer and the volume of foam is batched in seconds using a time switch. The foam generator needs to be accurately set and the flow rate of the foam calibrated regularly.

The foamed concrete used for this investigation is manufactured using a custom-built foam generator and foamed concrete mixer. The equipment, as can be seen in Plate 3.1,

has been fixed to a trailer to enable easy movement and the power requirements have been adjusted such that the equipment can be plugged into a standard single phase power point. These changes will make it possible to use the equipment in any location where electricity and water is available.

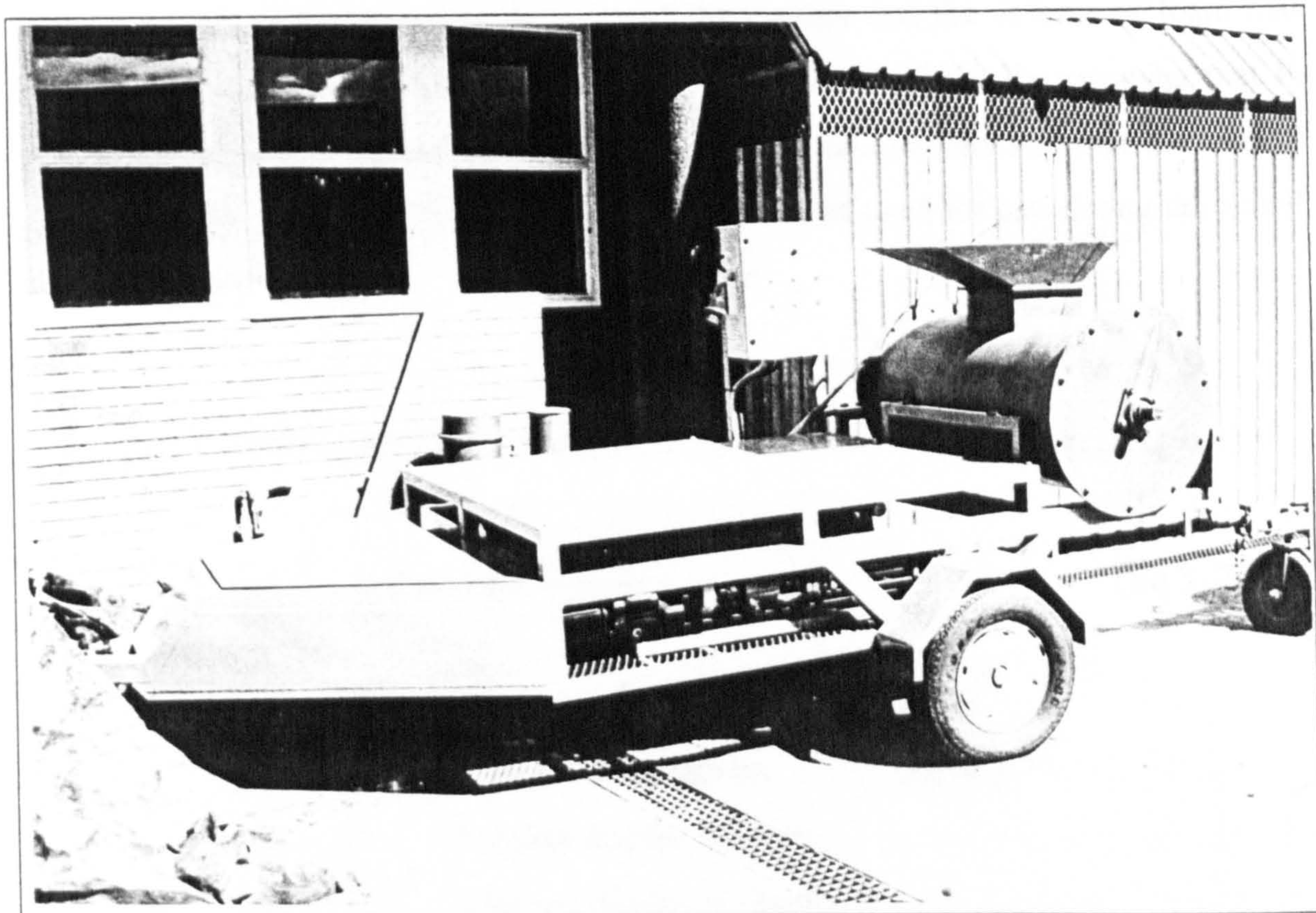


Plate 3.1: Equipment used for the Manufacture of Foamed Concrete

3.3 MIX DESIGN

When undertaking the mix design for a normal concrete mix, the compressive strength required normally dictates the water/cement ratio and the workability gives an indication of the volume of water needed.⁶⁴ Fine and coarse aggregates are then added to fill up the rest of the volume. From experience it has been found that, for a given mixture, there is only a narrow range of water/cement ratios that yield uniform, stable foamed concrete. If too little water is added to the mixture, the foam breaks down as a result of the cement withdrawing water for hydration from the foam. If too much water is added to the mixture, segregation takes place and the particles with higher densities migrate towards

the bottom of the batch and the voids move upwards resulting in a non-homogeneous mixture.

When designing foamed concrete a target casting density is determined and the water/cement (w/c) and sand/cement (s/c) ratios are chosen.⁵ Using these ratios and the relative densities of the materials the mass of the cement and the volume of foam that should be added to obtain the required density can be determined. By assuming that V_f liters of foam should be added per cubic meter of foamed concrete and that the cement content of a mix is x kg/m³ the following equations can be used for calculating the actual mix compositions:

$$\rho_m = x + xw/c + xs/c + RD_f V_f \quad (\text{Eq 3. 1})$$

$$1000 = \frac{x}{RD_c} + xw/c + \frac{xs/c}{RD_s} + V_f \quad (\text{Eq 3. 2})$$

where:

ρ_m	=	Target casting density	(kg/m ³)
RD_f	=	Relative density of foam	
RD_c	=	Relative density of cement	
RD_s	=	Relative density of sand.	

In mixtures where the sand has been replaced by ash an ash/cement ratio (a/c) is used in stead of the sand/cement ratio and the relative density of sand is replaced by that of ash. Due to the variable results found by other authors that used sand in foamed concrete¹⁸ the scope of this investigation was limited to mixtures containing no sand.

3.4 CASTING OF FOAMED CONCRETE

After mixing foamed concrete the material should be placed in moulds as soon as possible to maximize the time available for the mortar to set around the voids before the foam that forms the voids starts breaking down. The time available before stable foam starts breaking down varies, but experience has shown that it is not advisable to place foamed concrete more than half an hour after mixing.

Normal density concrete is compacted during placing to expel entrapped air, thereby achieving maximum density and strength and minimum permeability⁶⁵. Foamed concrete is used where a reduction in density is required and excessive compaction should be avoided as it would be counter productive. The formation of large voids as a result of entrapped air rather than entrained air can be prevented by softly tapping the outside of the mould with a rubber hammer during the filling operation⁶⁶. A smooth surface can be obtained by floating directly after casting.

3.5 CURING

In South Africa the standard method of curing normal concrete is under water in a curing tank at 22 to 25 °C, but as a result of the high void content of the foamed concrete, large volumes of moisture can be absorbed if curing takes place under water. As this unknown volume of absorbed water could affect the properties of the samples it was decided not to cure in water.

All the specimens used in this investigation were covered in plastic and placed in a constant temperature room at 22 ± 2 °C and 60 ± 5 % relative humidity immediately after casting. Within 24 hours after casting all samples were de-moulded, individually wrapped in polythene wrapping and stored in the constant temperature room up to the date of testing.

3.6 DENSITY

The density of foamed concrete is directly related to the percentage of foam that is added to the slurry. The maximum compressive strength of the material decreases as the foam content increases, and the density decreases as indicated in Figure 3.1⁶⁷. The results as indicated in this graph were obtained from tests conducted at the University of Pretoria over a eight year period. The fact that a small change in density can cause a large difference in strength means that it is essential to place strict control on density.

When designing foamed concrete mixtures a design density is specified and during the manufacturing process the actual density of the mixture can be compared to this target density. This initial density is the *casting density* and it is determined by filling a small container of known weight and volume with foamed concrete from the mixer and measuring the increase in weight. After casting all specimens are placed in the constant temperature room (22 ± 2 °C and 60 ± 5 % relative humidity) and covered with plastic sheeting.

Test specimens are demoulded within 24 hours of casting and the density of each specimen is determined. This *demoulding density* is used as the *wet density* of that specific specimen. After demoulding, each specimen is wrapped in plastic wrapping and cured in the constant temperature room up to the date of testing.

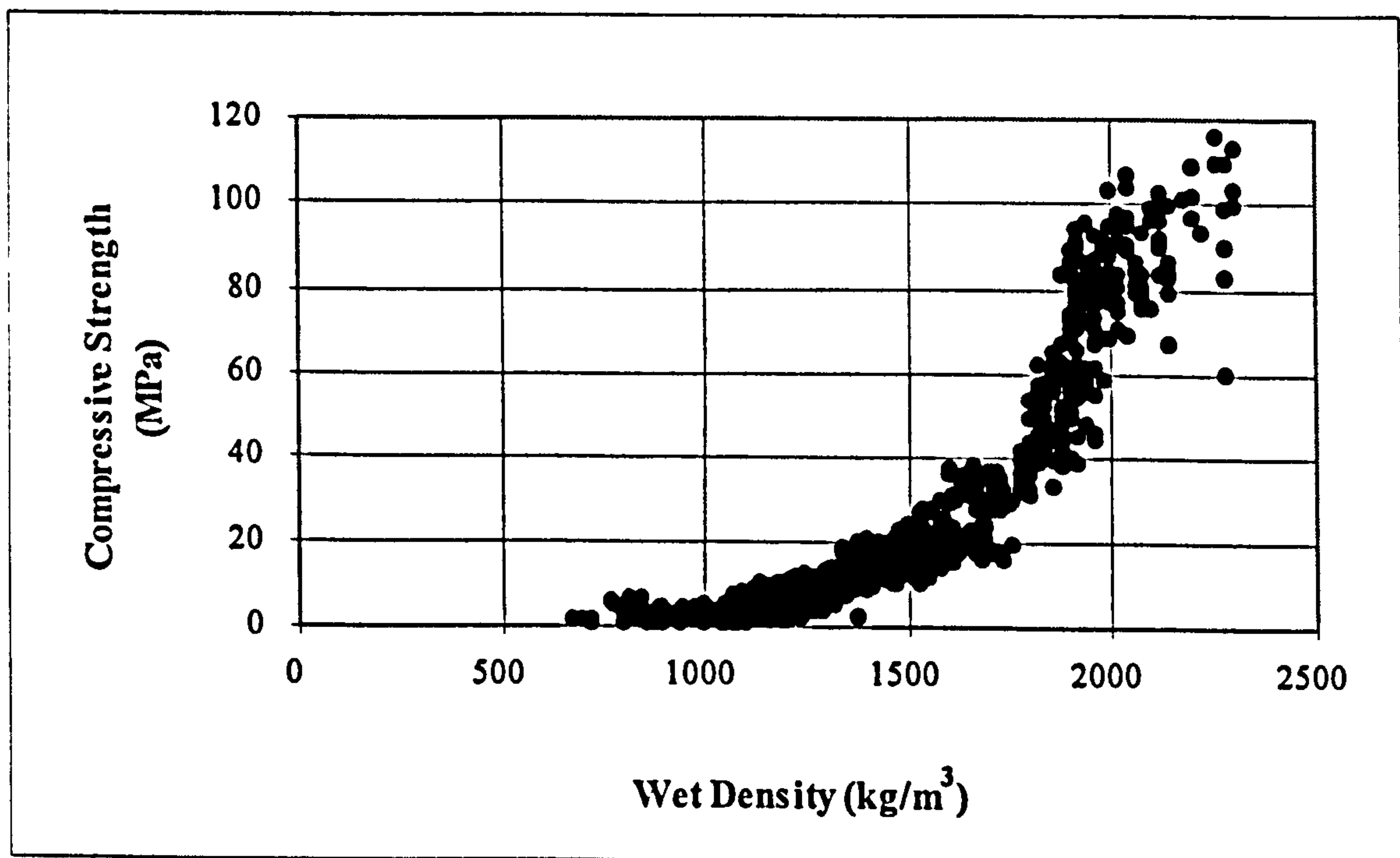


Figure 3.1 : Compressive Strength as a Function of Wet Density.

The density of each specimen is again determined just before the specimen is tested and this density is called the *testing density*. Notable changes in density between demoulding and testing indicate that the moisture content of the specific specimen has changed. A marked reduction in density would indicate moisture loss and can mean that that specimen was not cured to the same extent as other samples.

One cube in every batch is cast with the specific aim of determining the dry density of that mixture. The cube is cured for seven days in the constant temperature room whereafter the cube is weighed to determine the testing density. The cube is then placed in an oven at 100 ± 5 °C until constant mass is reached and the *dry density* is then determined. Over 2000 results from tests conducted over a period of eight years and preliminary tests conducted at the beginning of this investigation were used to establish the linear relation between wet and dry density that can be seen in Figure 3.2⁶⁷. Some authors have published properties of foamed concrete as a function of dry density^{14, 15} while others^{16, 67} have used wet or casting density and the relation between wet and dry density can be used to compare the results obtained from the different studies.

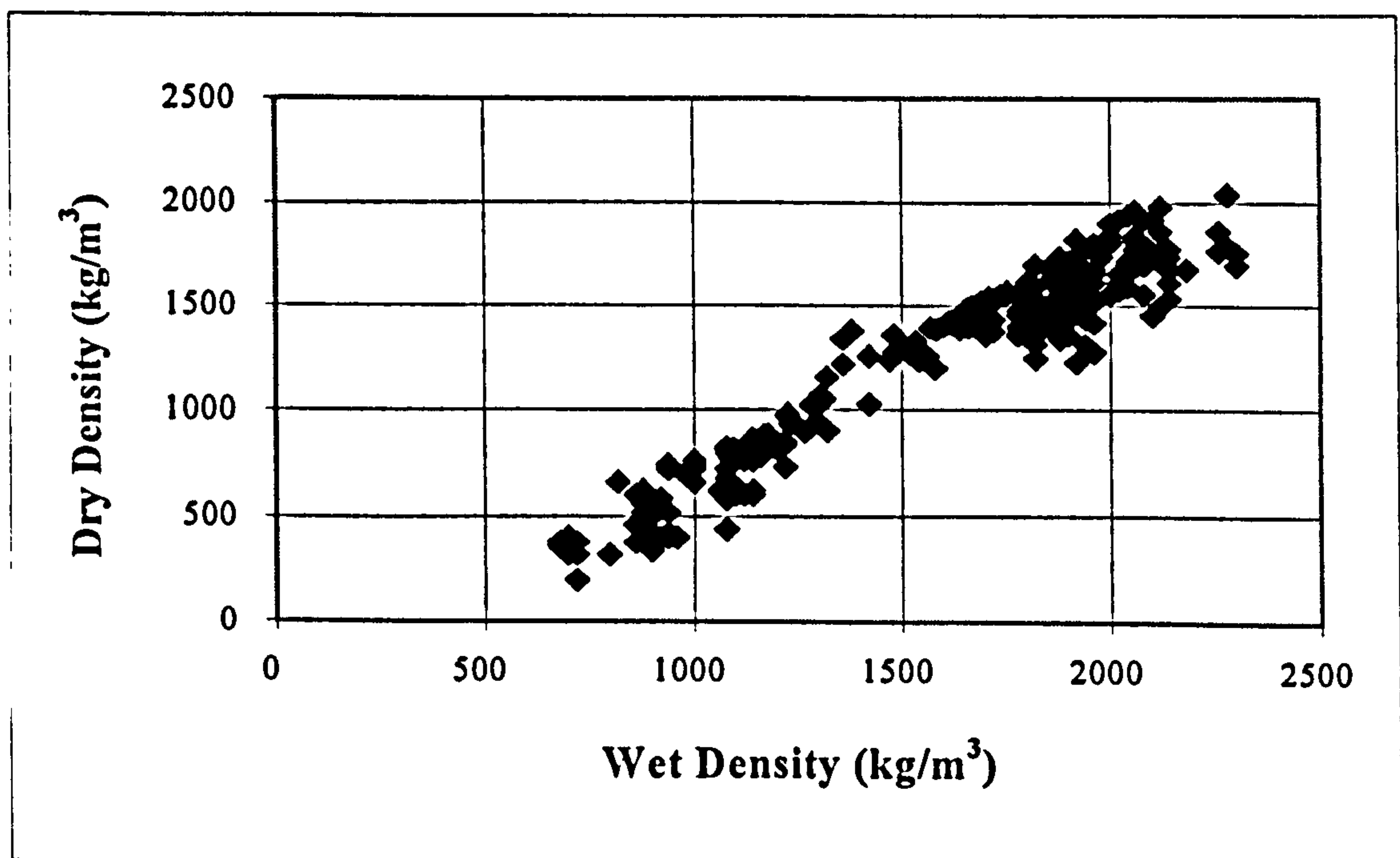


Figure 3.2 : Dry Density as a Function of Wet Density.

CHAPTER 4: EXPERIMENTAL PROGRAM

4.1 PRELIMINARY TESTS

Preliminary tests were conducted to establish a workable range of ash/cement ratios and optimum water/cement ratios for the mixes to be used in the main program. The within-batch variability of the foamed concrete was also established.

4.1.1 Mix Proportions

The water/cement ratios that were required to manufacture stable foamed concrete were first determined using samples consisting of only cement, water and foam. The water demand for different percentages of foam was obtained by slowly increasing the water/cement ratio to the point where no visual breakdown of foam took place. This ratio was used as a basis and a range of mixes both dryer and wetter than these mixtures were tested. For each of the foam contents an optimum water/cement ratio, resulting in the highest 28-day compressive strength, was obtained.³ By replacing cement with pfa different ash/cement ratios (by weight) were obtained and for these ash/cement ratios the optimum water/cement ratios were determined for different foam contents. The mixtures containing no foam reached an optimum strength when much dryer than the mixtures containing foam. The effect of ash/cement ratio on the optimum water/binder ratio can be seen in the graph in Figure 4.1. From this graph it can be seen that the optimum water requirement of the mixtures containing no foam decreases with an increase in pfa content, up to an ash/cement ratio of 1, and thereafter there is no further reduction in the optimum water/binder ratio. The optimum water/binder ratio of mixtures containing foam seems to be inversely related to the ash/cement ratio (up to a ratio of 3) and the percentage foam added to the mixture does not seem to have a large influence on the optimum water/binder ratio for a specific ash/cement ratio.

The effect of ash/cement ratio on the 28-day compressive strength of the foamed concrete was determined by crushing 100 mm cubes, the results of these tests are shown in Figure 4.2. As ash is less reactive than cement a reduction in strength is expected with an increase in ash/cement ratio. For mixtures containing no foam increases in ash/cement ratio resulted in a marked decrease in 28-day compressive strength but for

mixtures containing foam the compressive strength remained almost unaltered with increased ash contents.

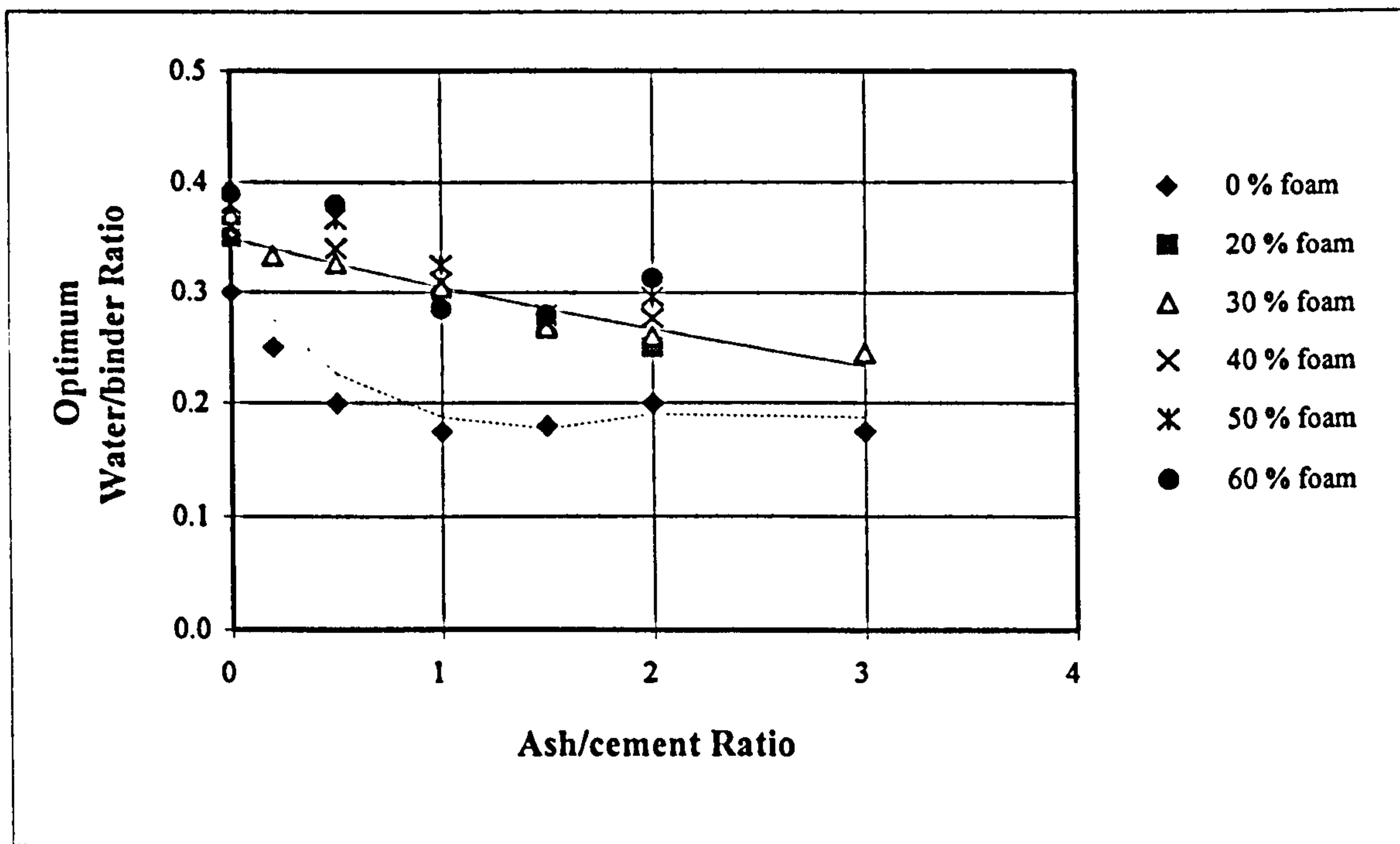


Figure 4.1: Effect of Ash/cement Ratio on optimum Water/binder Ratio.

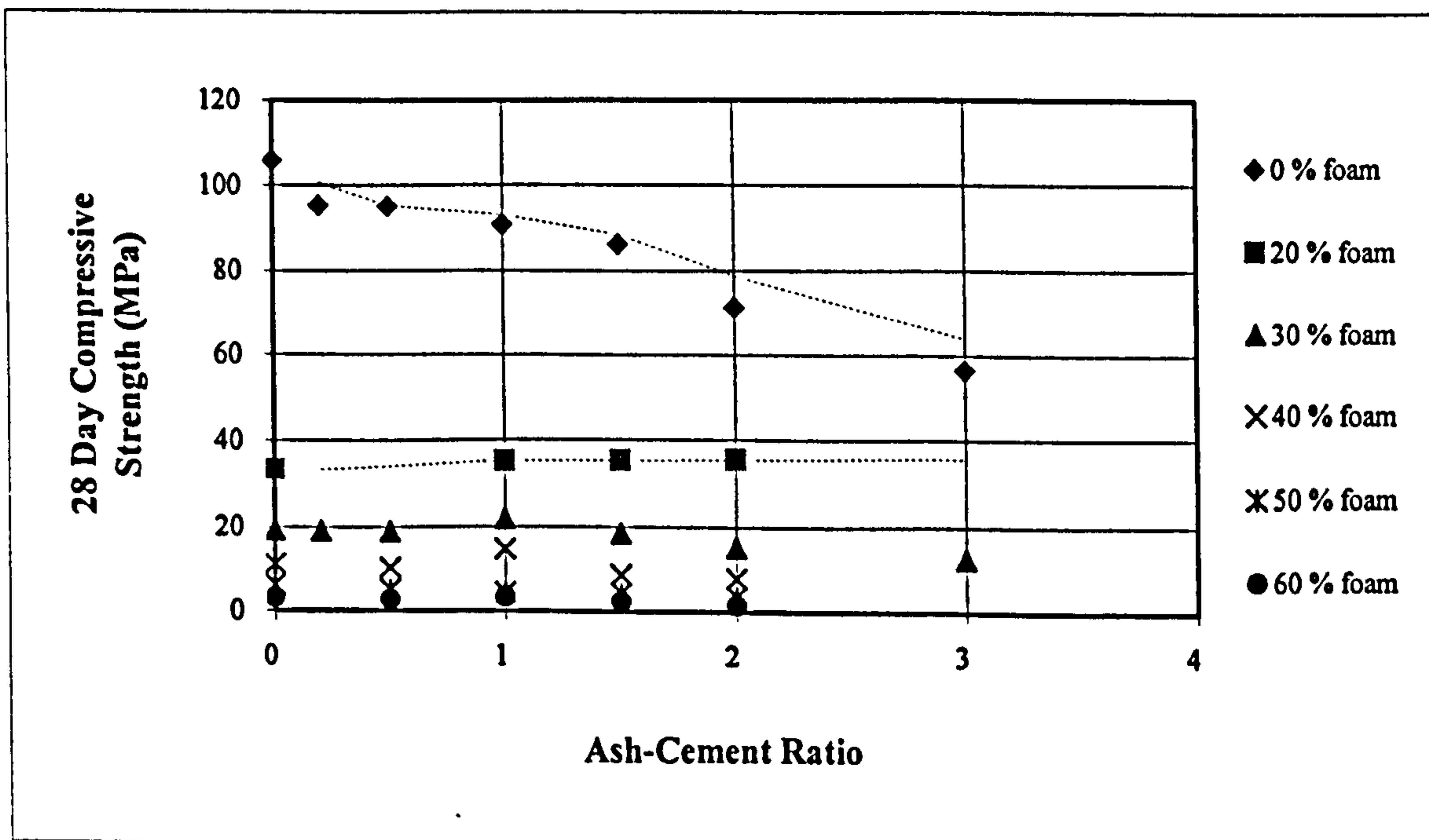


Figure 4.2: Effect of Ash/cement Ratio on Compressive Strength.

Tests have been conducted by Kearsley & Mostert² to determine what the effect of the large percentage pfa in foamed concrete is on the drying shrinkage. Samples (40mm x 40mm x 250mm) were cured in a water bath for 7 days where after the samples were removed and placed in a shrinkage oven at 50 ± 2 °C and 20 ± 5 % humidity and the change in length was recorded at regular time intervals. Initial results indicate that foamed concrete shrinks between four and ten times as much as normal concrete. The shrinkage as measured after 28 days is shown in Figure 4.3. These results indicate that replacing some of the cement with pfa can reduce the drying shrinkage of foamed concrete.

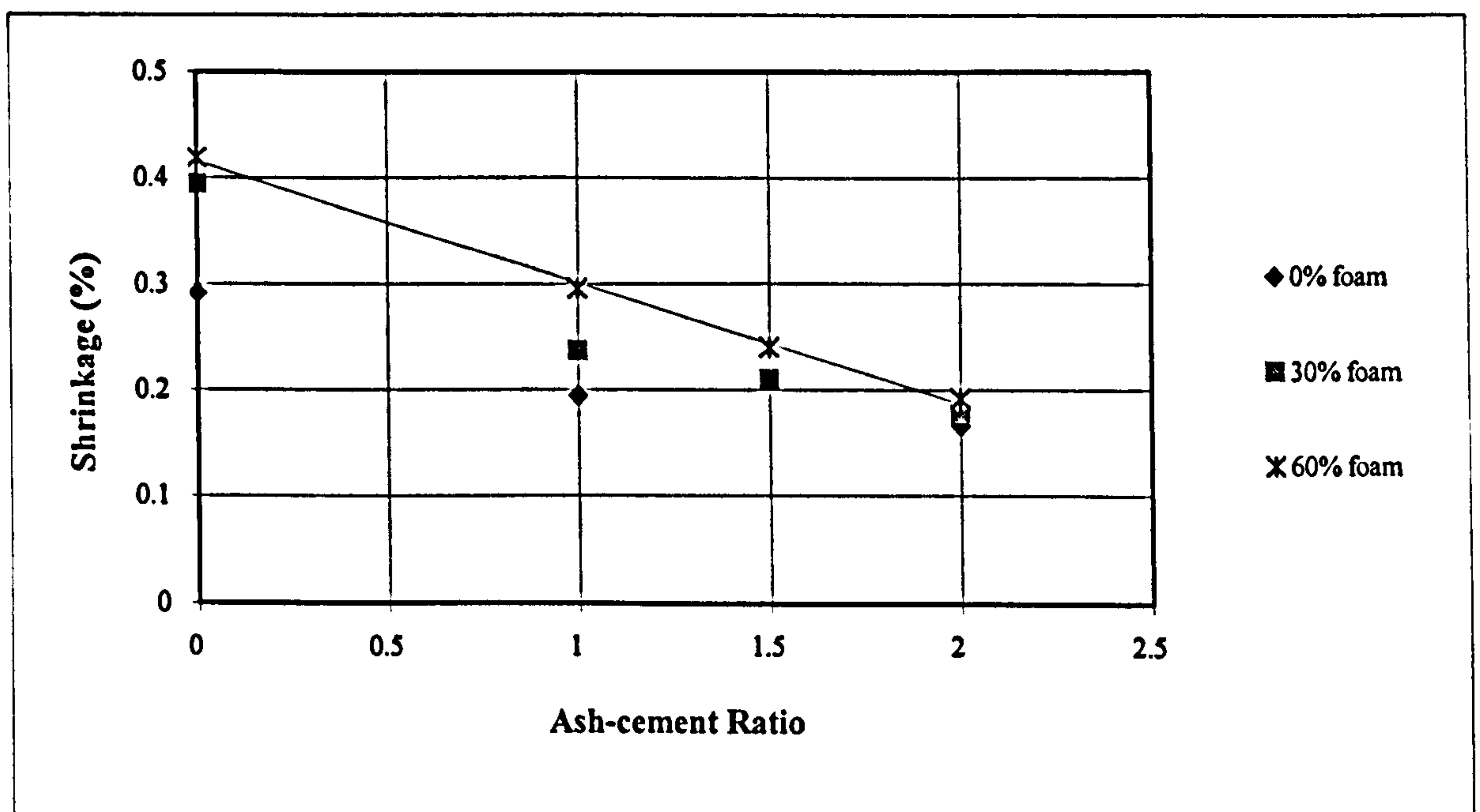


Figure 4.3: Effect of Ash/cement Ratio on Shrinkage.

Based on these preliminary test results it was decided to maintain a constant water binder ratio of approximately 0.3 and a range of ash/cement ratios varying from 0 to 3 for the main test program.

4.1.2 Repeatability

Concrete is normally classified in terms of characteristic compressive strength obtained from cubes, crushed after 28 days.⁶⁸ The characteristic strength is defined as the value below which not more than 5% of the cube results are expected to fall and this value is

dependent on the average or mean cube strength as well as the standard deviation or scatter of the cube strengths.⁶⁹

When foamed concrete is produced, it is important to determine whether a certain, predictable density and compressive strength can be maintained throughout a batch. To determine the within-batch homogeneity of specific mixtures, target densities of 1000 and 1250 kg/m³ were used and for each density 58 cubes were cast from one batch. These cubes were crushed after 3 months (84 days) and the average and standard deviation for density and strength were calculated. These values can be used to determine whether the mixture is consistent. By comparing the actual casting densities with these target densities the accuracy of the mixing process can be evaluated. The results obtained from these tests are shown in Table 4.1.

Table 4.1: Uniformity of Mixture.

Target Density (kg/m³)	1000	1250
Casting Density (kg/m³)	1019	1305
Demoulding Density (kg/m³)		
Average:	998	1280
Standard Deviation:	9	14
56 Day Density (kg/m³)		
Average:	989	1267
Standard Deviation:	11	15
84 Day Density (kg/m³)		
Average:	988	1266
Standard Deviation:	10	14
84 Day Compressive Strength (MPa)		
Average:	6.2	15.1
Standard Deviation:	0.7	1.5

The casting densities as indicated in Table 4.1, are the average of three measurements taken during casting and these averages are 19 and 55 kg/m³ from the target densities of 1000 and 1250 kg/m³ respectively. The casting densities vary less than 5% from the target densities, indicating good control of the mixing process. The demoulding

densities of the lighter mixtures are slightly lower than the casting densities, and all the testing densities are slightly lower than the demoulding densities but the differences are negligible. The low standard deviations in density indicate that the in-batch variations are small and the mixing and casting method results in homogeneous mixtures. For both sets of results shown in Table 4.1 the standard deviation in compressive strength is approximately 10% of the average strength. The standard deviation of the compressive strength has to be compared to that normally found in normal concrete. The D. O. E. mix design method for normal concrete uses the standard deviation to determine the target mean strength.⁶⁹ This method permits a minimum standard deviation of 4 MPa to be used for designing mixtures with characteristic strengths above 20 MPa. For strengths below 20 MPa the minimum value that should be used for the standard deviation decreases linearly. The values as permitted with the D. O. E method are shown in Figure 4.4. Using the results in Table 4.1 the permissible standard deviations were calculated as 3 MPa for a compressive strength of 15 MPa and 1.2 MPa for a compressive strength of 6.2 MPa. Both the standard deviations obtained for foamed concrete are lower than the minimum value used to design normal concrete mixtures. These results indicate that the variability in strength of the foamed concrete is no more than that of normal concrete. It can thus be concluded that the equipment and mixing process used to manufacture foamed concrete is suitable for manufacturing foamed concrete with uniform density and strength.

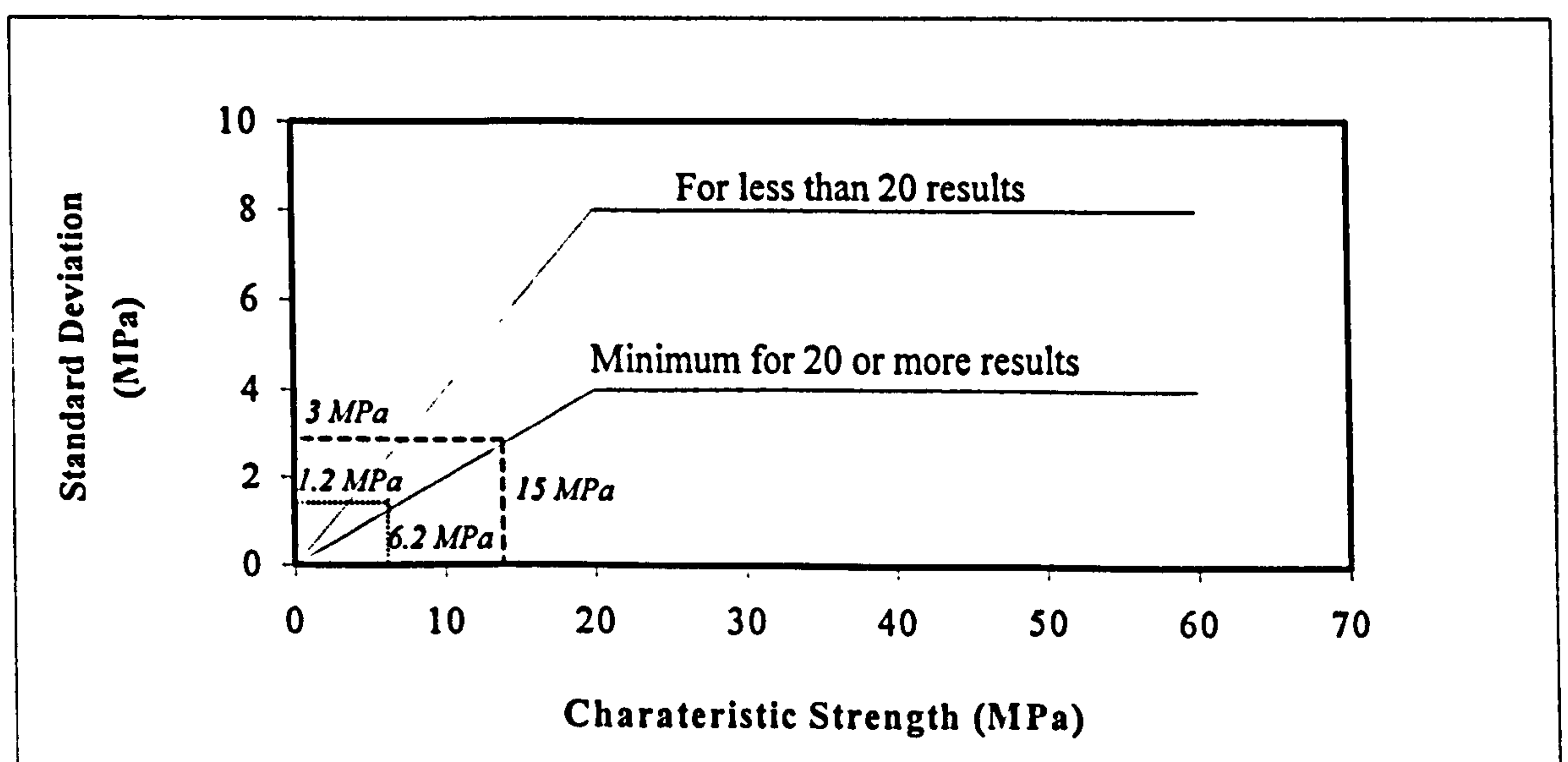


Figure 4.4: Relationship between Standard Deviation and Characteristic Strength.

4.2 MAIN TEST PROGRAM

This research on foamed concrete has been conducted using the laboratories of the University of Pretoria in South Africa, with the aim of developing a material suitable for affordable development in South African conditions. Foamed concrete consists of cement paste and voids and the properties of both these components should have a measurable effect on the properties of the combined material. This investigation aimed to determine and optimize the contribution of each of these components to the properties of the foamed concrete.

Literature reviewed indicates that replacing small percentages (per weight) of cement with pfa can enhance the properties of cement paste. The main aim of this investigation was to determine whether the use of unclassified pfa as replacement for large percentages of the cement in foamed concrete has a significant influence on the compressive strength and the durability of the material. Durability was measured in terms of permeability and porosity.

The shape, size and distribution of voids in mortar and concrete have an influence on the properties of the material. A secondary aim of this investigation was to determine whether there is an optimum ash content that leads to an optimum void distribution in foamed concrete. The possibility of a relationship between the characteristics of the voids and the material properties was investigated.

Tests have shown that the production of foamed concrete with predictable densities and strengths is only possible with pre-foamed protein foams.¹⁷ This investigation was therefore conducted using only pre-foaming. All the materials used in this investigation are produced or manufactured in South Africa. Only one source of foaming agent, cement and ash was used and the possible effect of different sources was therefor~~not~~ taken into account.

In establishing whether foamed concrete can be used for affordable development, it was essential to determine the short and the long-term properties of the material. The properties of a building material that are normally of concern to engineers are strength,

elasticity, shrinkage, creep and durability. These properties were investigated and the effect of mix composition on each of these properties determined.

Properties of mortars containing different percentages of pfa were compared to cement paste with the same water-binder ratio to determine the effect of pfa-replacement. Thereafter the properties of mortars containing pfa were compared to that of mortars containing ungraded ash (Pozz-fill). Once the effect of high ash content had been determined, the effect of adding foam to the mortar was established.

Although foamed concrete can be manufactured with a density of as low as 300 kg/m^3 and as high as 1850 kg/m^3 , the density of the material used in this study varied between approximately 1000 and 1500 kg/m^3 , unless indicated differently. The compressive strength, permeability and porosity of the following mixtures were determined after 28 days, 56 days, 3 months, 6 months, 9 months and 1 year:

- Cement pastes with water-cement ratios of 0.3, 0.4 and 0.6.
- Mixtures with pfa where 50%, 66.7% and 75% of the cement (by weight) had been replaced with pfa (ash/cement ratios of 1, 2 and 3). The water/binder ratio was kept constant at approximately 0.3.
- Mixtures with ungraded ash where 50%, 66.7% and 75% of the cement (by weight) had been replaced with ungraded ash (ash/cement ratios of 1, 2 and 3). The water/binder ratios of these mixtures were the same as that of the mixtures containing pfa.
- Foamed concrete mixtures of different densities (1000 , 1250 and 1500 kg/m^3) with different percentages of ash replacement (50%, 66.7% and 75%).

Prior experience has shown that it is not possible to produce foamed concrete of quality using only cement and water. Control foamed concrete mixtures were therefore not cast.

The entrained air-void size, shape and distribution were determined for the foamed concrete mixtures and the drying shrinkage of all mixtures were recorded at regular time intervals. Multi-variable analysis was employed to develop a mathematical model that takes account of the age, ash and void content on some of the properties of foamed concrete.

4.3 MATERIALS

4.3.1 Foaming Agent

Foamed concrete is produced under controlled conditions from cement, filler, water and a liquid chemical⁷⁰ that is diluted with water and aerated to form the foaming agent. The foaming agent used is “Foamtech”, consisting of hydrolyzed proteins and manufactured in South Africa. The foaming agent is diluted with water in a ratio of 1:40 (by volume) and then aerated to a density of 70 kg/m³.

4.3.2 Cement

The cement used in this investigation was rapid hardening Portland cement from Pretoria Portland Cement (PPC), Hercules, Pretoria. The cement can be classified as CEM I 42,5R according to the South African Specification SABS EVN 197-1:1992.⁷¹ The cement has a relative density of 3.15 and an average Blaine specific surface area of 431 m²/kg. The results of cement analysis as supplied by the manufacturer can be seen in Table 4.2. The average cement particle size is about 20 μm and the particle size distribution as determined by the supplier, using a Malvern instrument, can be seen in Figure 4.5. A range of cements were tested but this cement was used as it yielded the highest early age strengths.

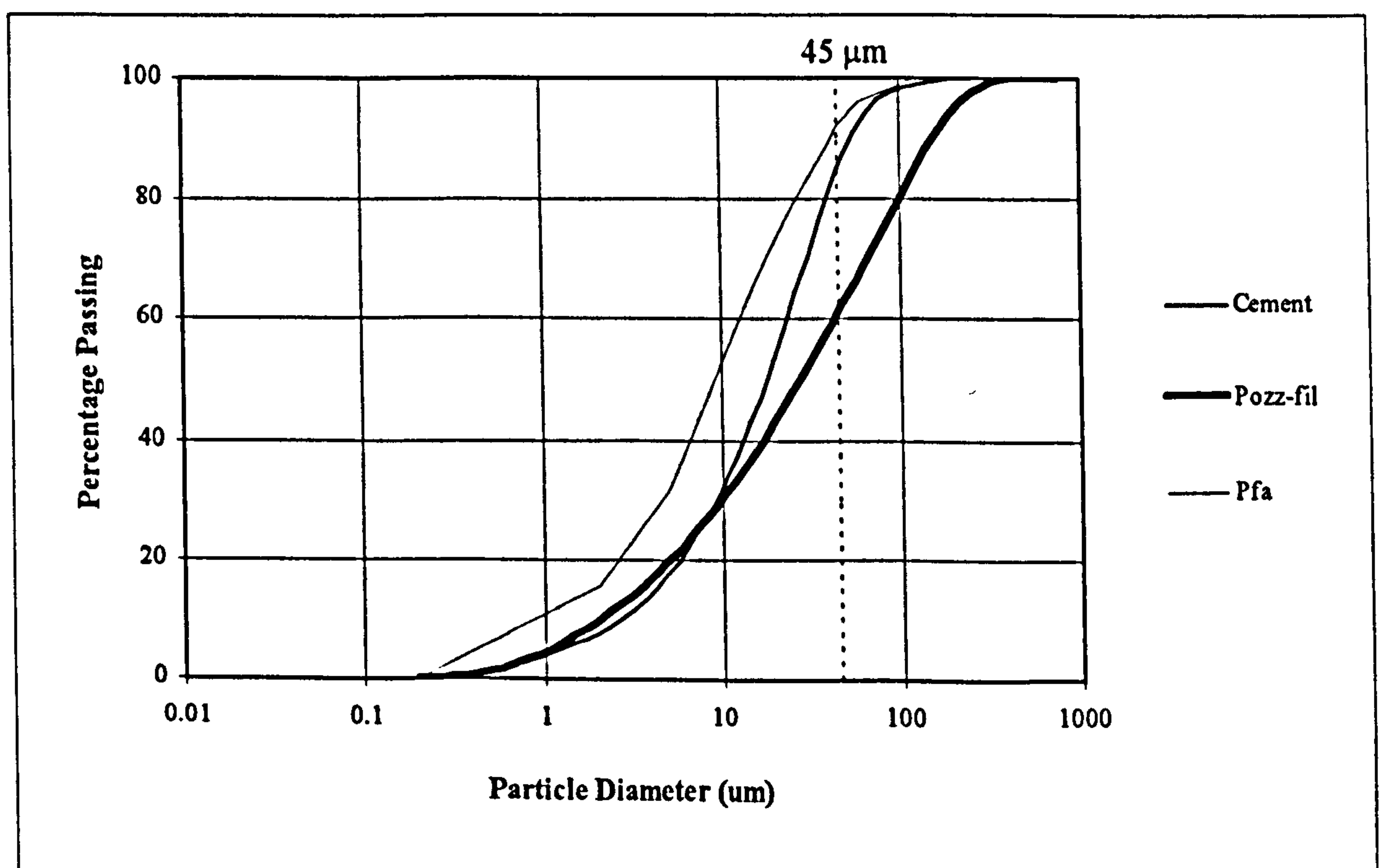


Figure 4.5: Particle Size Distribution of Binder.

Table 4.2 : Binder Properties as Measured by Independent Outside Testing House.

Oxides	RHPC from PPC Hercules (percentages)	Processed Pfa from Lethabo (percentages)	Pozz-fill from Lethabo (percentages)
CaO	61.7	4.7	5.0
SiO ₂	21.2	53.9	54.8
Al ₂ O ₃	4.6	33.5	31.7
Fe ₂ O ₃	1.8	3.7	3.8
Na ₂ O	0.1	0.7	0.8
K ₂ O	0.7	0.7	0.8
MgO	4.3	1.3	1.1
SO ₃	2.0	0.1	0.3
CO ₂	2.6		
Free CaO	1.2		
Loss On Ignition		0.8	0.8
Blaine Surface Area (m ² /kg)	431	350	280
Calculated Surface Area (m ² /kg)		408	469
Relative Density	3.15	2.2	2.2
Bogue:			
C ₃ S	45.8		
C ₂ S	26.2		
C ₃ A	9.2		
C ₄ AF	5.5		

4.3.3 Fly Ash

In South Africa the production of electricity and liquid fuel from coal causes the accumulation of vast quantities of coal ash. In 1990 it was estimated that approximately 350 million tons of coal ash was stored in South Africa and that this amount was growing by 23 million tons annually⁷². A large proportion of this ash can be used at low cost as a cement extender. By processing the ash and removing the coarse particles pulverized fuel ash (pfa) complying with SABS 1491 is produced.⁷³ The properties of the processed pfa from Lethabo power station as supplied by Ash Resources was

measured by an independent outside testing house as indicated in Table 4.2. The processed pfa has a relative density of 2.2 and a typical particle size distribution as indicated in Figure 4.5. The measured Blaine surface area is approximately 350 m²/kg while the calculated surface area is 408 m²/kg, which, according to Hopkins & Cabrera⁴³ indicates that some agglomeration takes place in the pfa.

Since 1992 Pozz-fill has been marketed in South Africa. Pozz-fill is an unclassified ash with a similar chemical composition to pfa, but the coarse particles are not removed and therefore more than 12.5% of the particles may have a diameter exceeding 45 µm.⁷³ As no classifying is required the Pozz-fill is much cheaper than pfa which is one of the main reasons why its use in foamed concrete is being investigated by the author. Pozz-fill, with properties as indicated in Table 4.2 was obtained in bulk from Lethabo and used as a cement extender. The grading of a typical Pozz-fill sample can be seen in Figure 4.5. From the grading it can be seen that nearly 40% of the Pozz-fill sample consists of particles larger than 45 µm. The Pozz-fill has a measured specific surface area (assuming spherical particles) of 280 m²/kg (Blaine), compared with a specific surface area of 469 m²/kg, calculated using the grading. As expected the fact that Pozz-fill is coarser than pfa results in a smaller measured surface area but is interesting to note that the difference between measured surface area (MSA) and calculated surface area (CSA) is much larger than that obtained for pfa, which could indicate more agglomeration.⁴³ The suppliers of the pfa and the independent chemists used to measure the surface area of the pfa and the Pozz-fill expressed their concern about the repeatability and the accuracy of the results obtained from the Blaine surface area tests as they experienced great difficulty with the large influence that the inclusion of different agglomerations has on the final result. It was therefore decided to obtain scanning electron microscope (SEM) photographs of the cement, pfa and the Pozz-fill to compare both the particle sizes and shapes. The photographs as taken at two different magnifications (450 x and 4 500 x) can be seen in Plate 4.1 and Plate 4.2. From these micro-photographs it can be seen that while the particle sizes of the cement and the pfa seem to be similar, the cement is more angular with a rough surface texture while the majority of the pfa particles are spherical with smooth surfaces. In the Pozz-fill sample compared with pfa, the larger particles are noticeable and these particles seem to be more angular in shape with rougher surface textures.

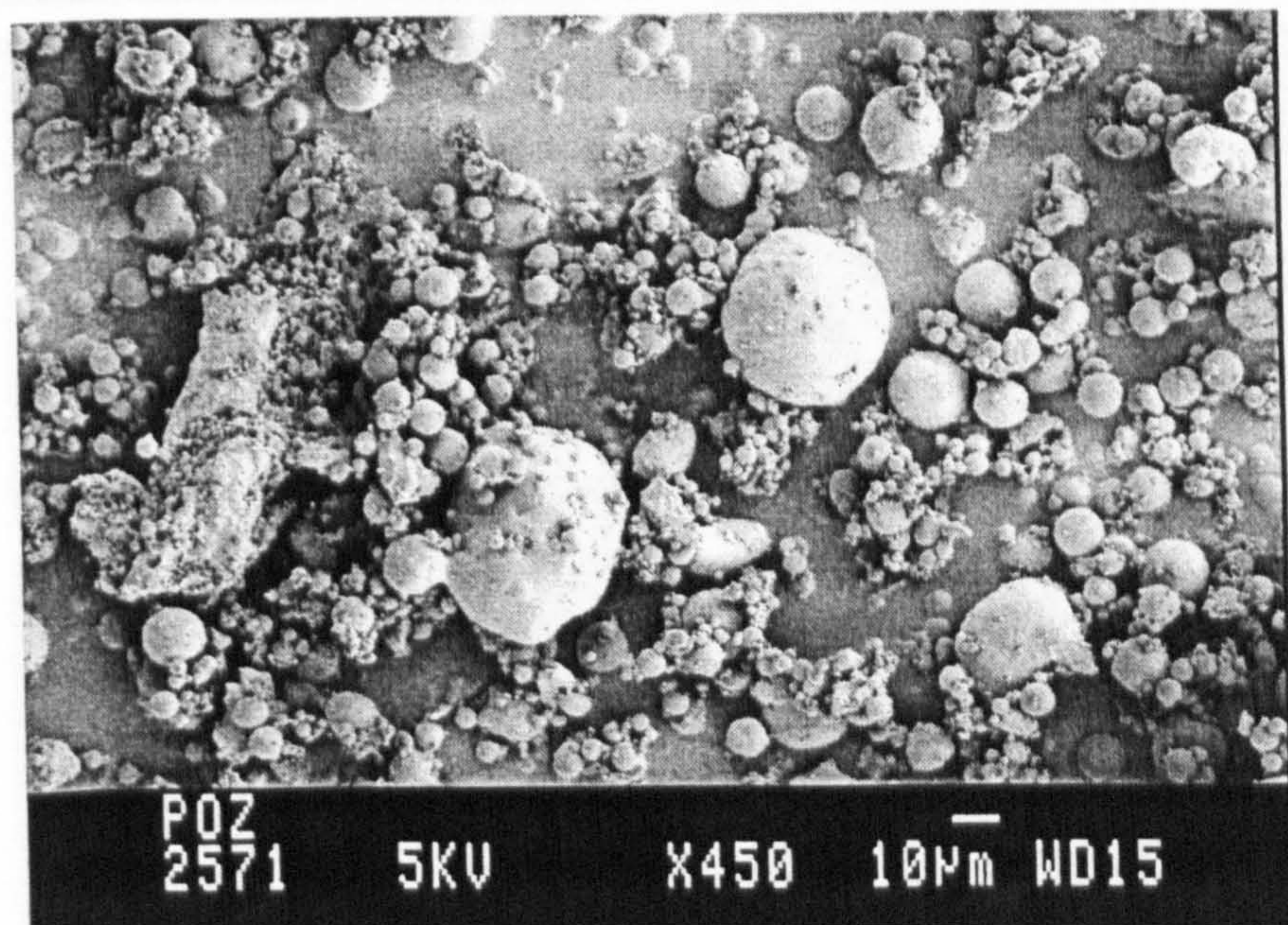
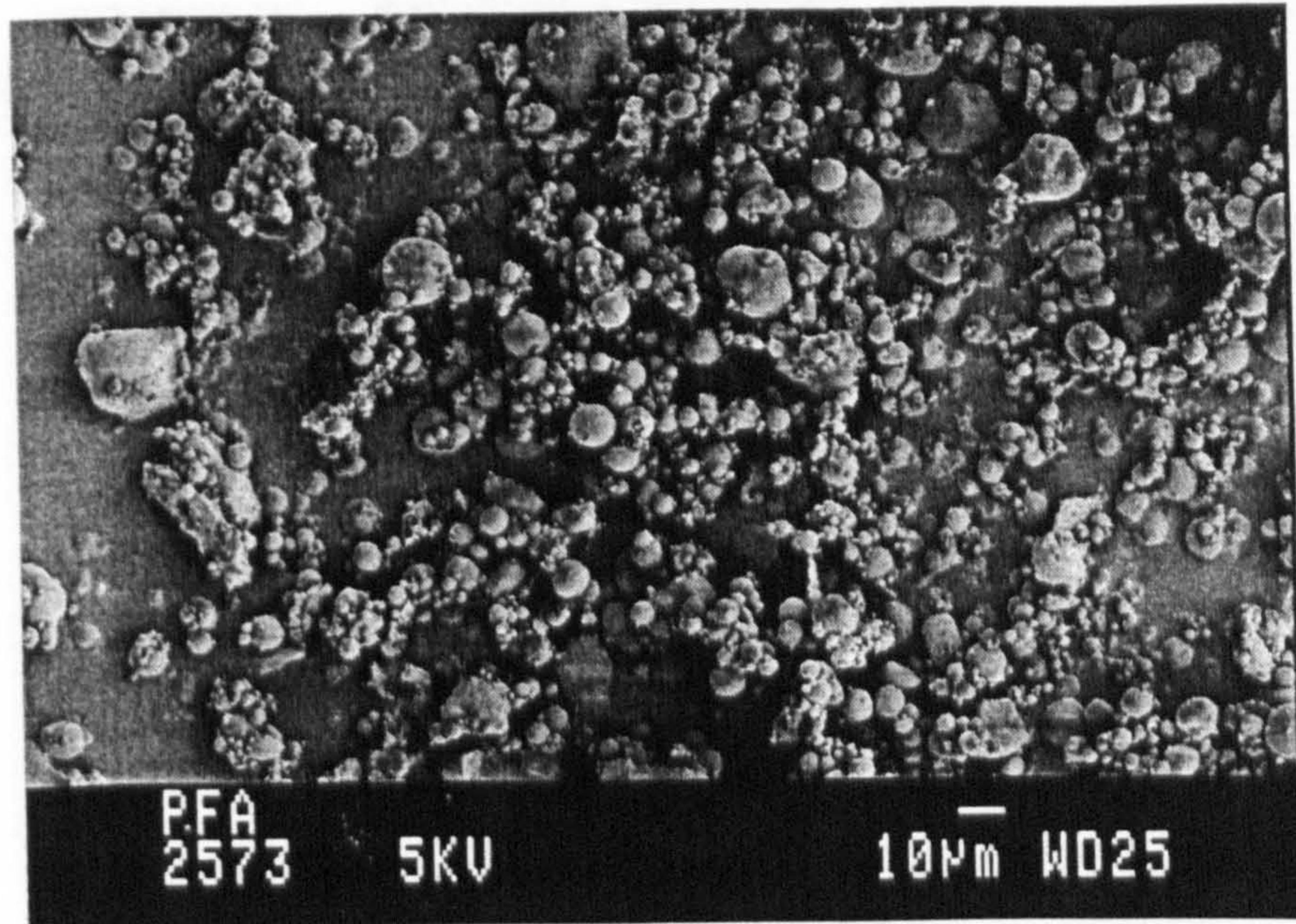
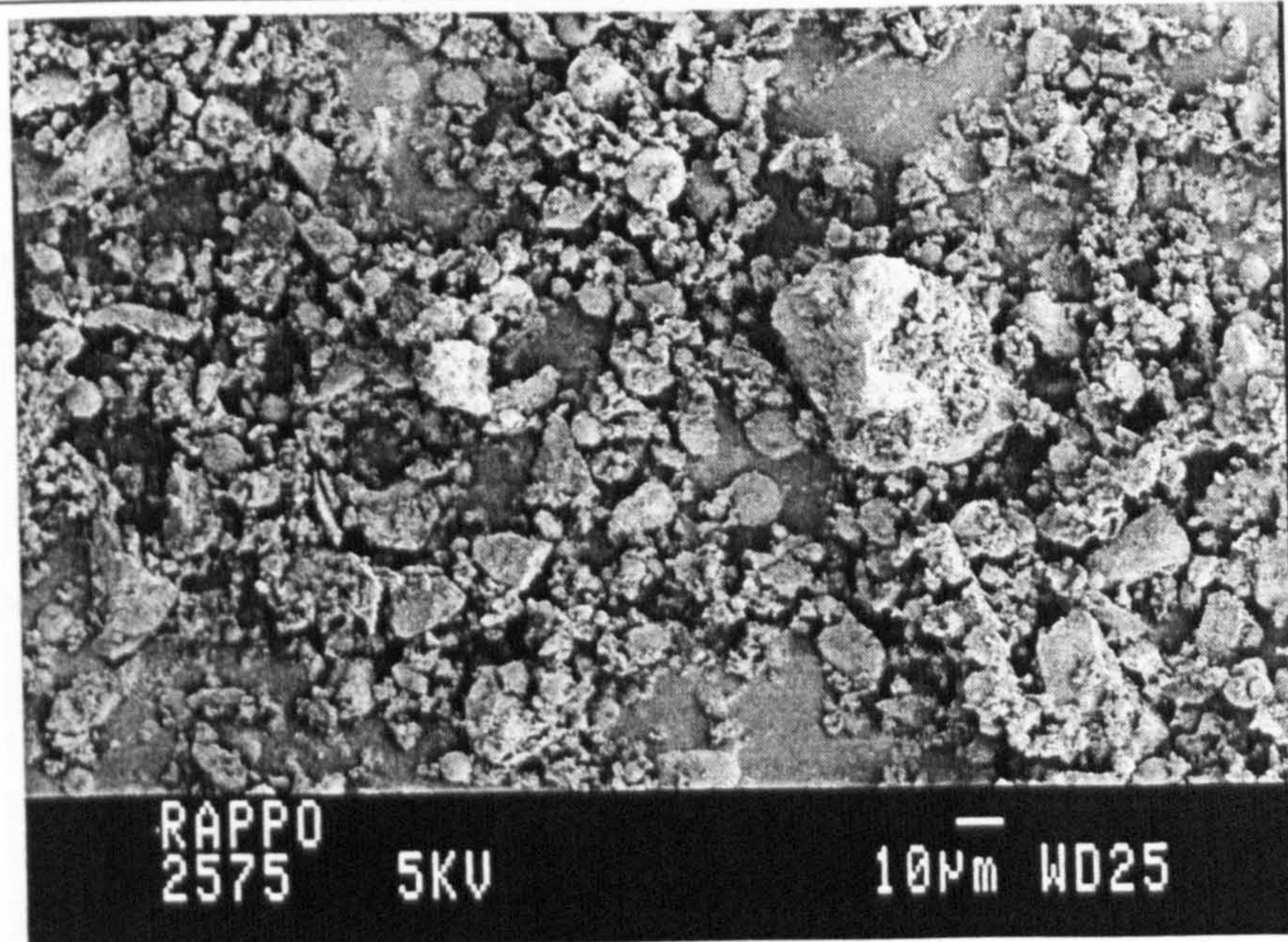
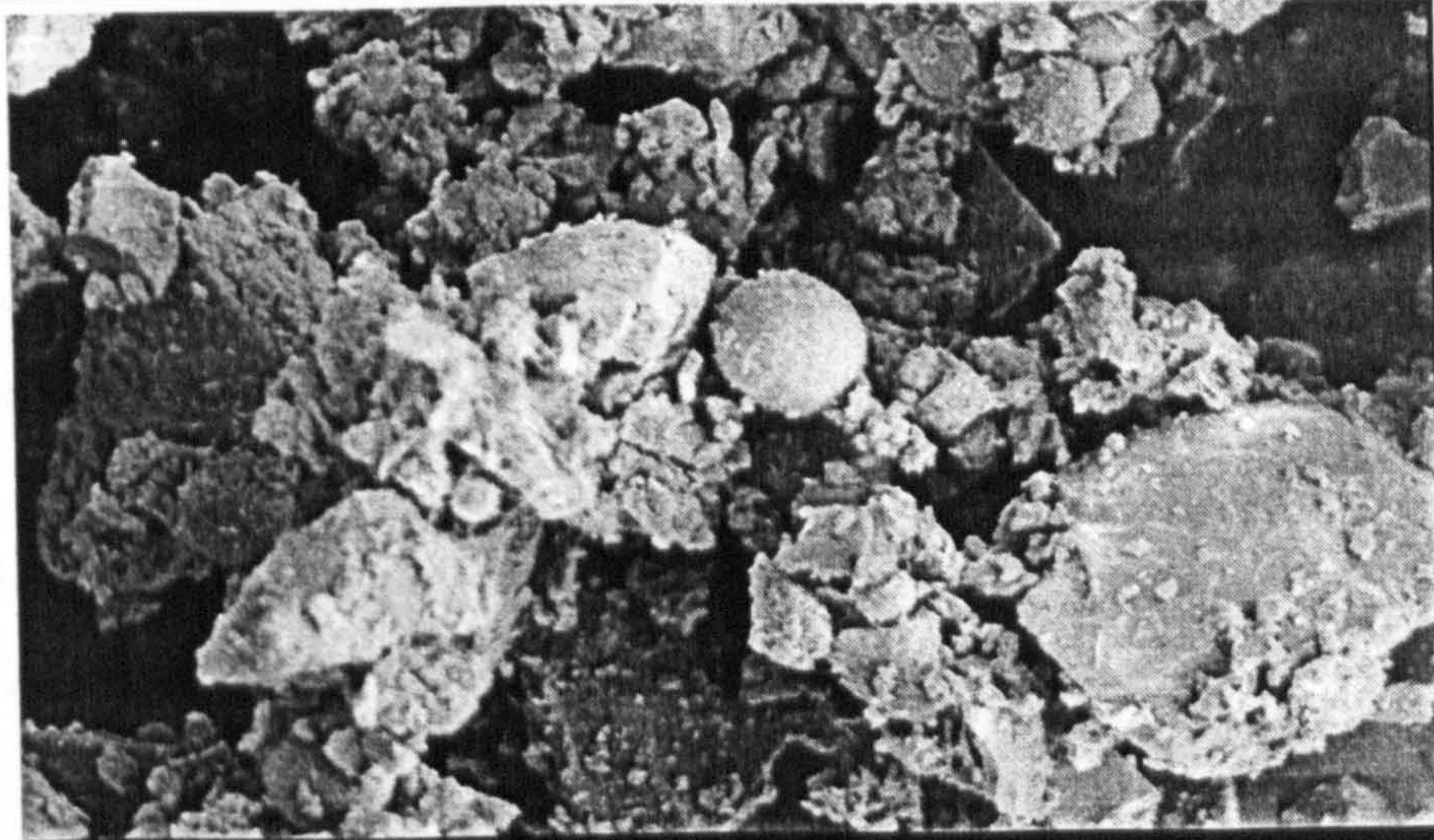
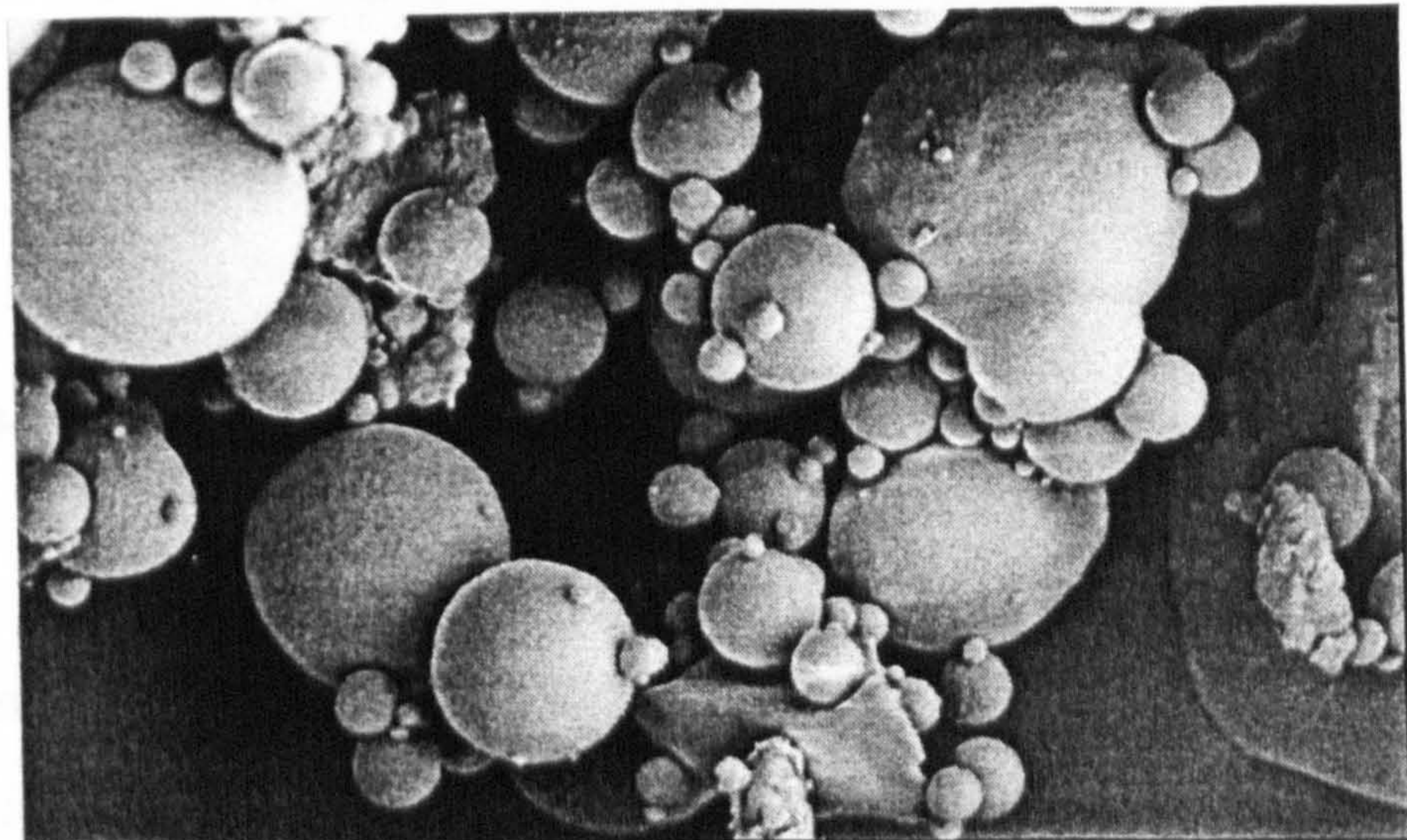


Plate 4.1: SEM photographs of cement, pfa and Pozz-fill (x450).



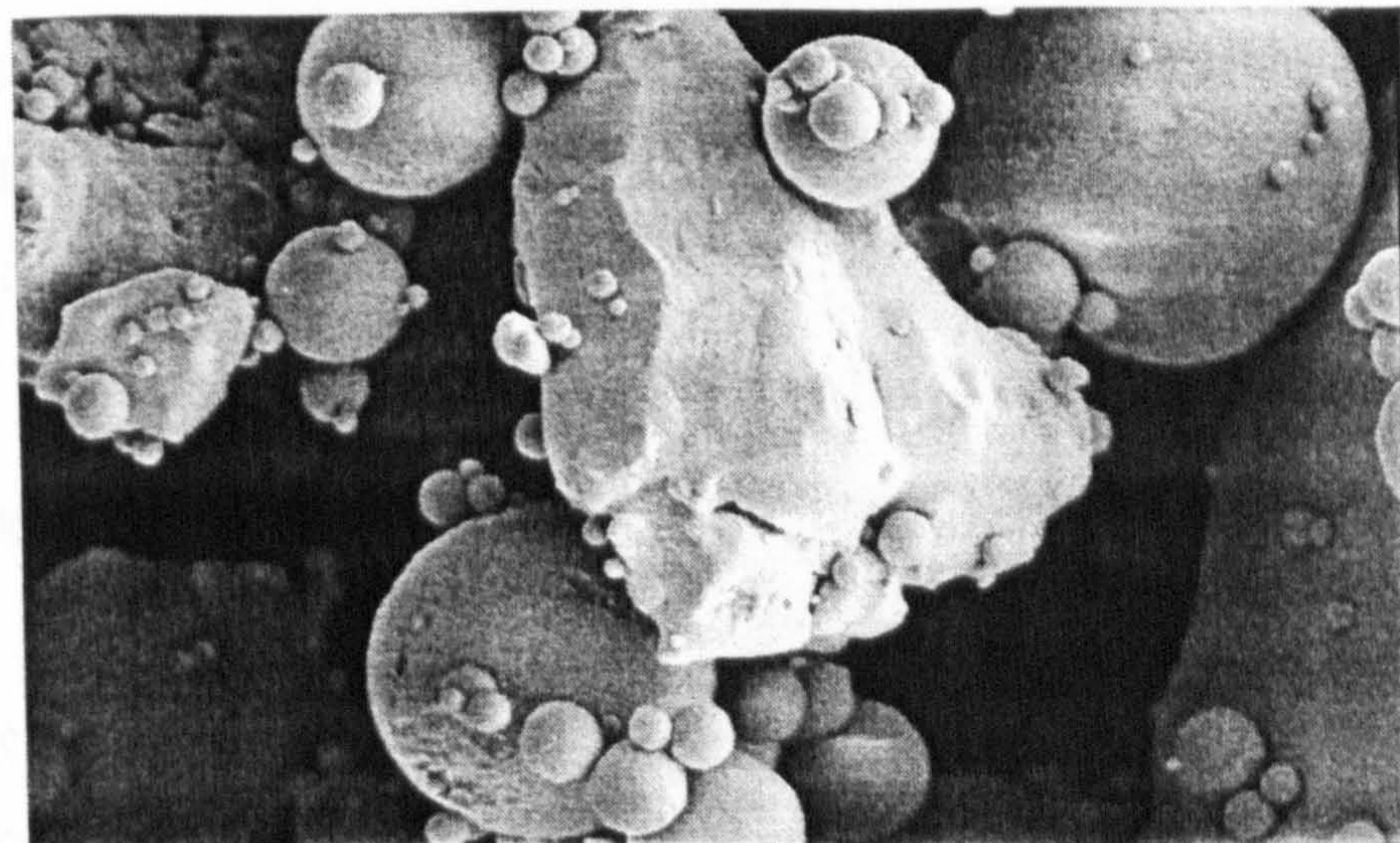
RAPP0
2576 5KV

1µm WD25



PFA
2574 5KV

1µm WD25



POZ
2572 5KV

1µm WD15

Plate 4.2: SEM photographs of cement, pfa and Pozz-fill (x4500).

These photographs seem to correlate with the result obtained from the particle size distributions shown in Figure 4.5. For both the pfa and Pozz-fill there does seem to be groups of particles clinging to each other, explaining the relatively low measured Blaine surface areas. The inclusion of relatively large, angular particles in the Pozz-fill could lead to some increase in water demand.

The typical chemical composition of the cement, pfa and the Pozz-fill used can be seen in Table 4.2. The Bogue composition of the cement was calculated using the following equations:⁶

$$C_3S = 4.07(CaO) - 7.60(SiO_2) - 6.72(Al_2O_3) - 1.43(Fe_2O_3) - 2.85(SO_3) \quad (\text{Eq 4. 1})$$

$$C_2S = 2.87(SiO_2) - 0.75(3CaO.SiO_2) \quad (\text{Eq 4. 2})$$

$$C_3A = 2.65(Al_2O_3) - 1.69(Fe_2O_3) \quad (\text{Eq 4. 3})$$

$$C_4AF = 3.04(Fe_2O_3) \quad (\text{Eq 4. 4})$$

4.3.4 Conformity to standard specification criteria

Standards for composition and conformity criteria for cement and fly ash are given in SABS ENV 197-1:1992⁷¹ and SABS 1491:Part II – 1989⁷³ respectively. The binder properties of the materials used in this investigation are compared to the specifications in Table 4.3. From the values listed in this table it can be seen that the cement and the pfa meets all the requirements while the Pozz-fill contains too high a percentage coarse particles to meet the fineness requirement.

4.4 MIXTURE COMPOSITION

The target casting densities used in this investigation were 1000, 1250 and 1500 kg/m³ unless stated differently. The water/cement ratio was kept constant for the different casting densities, but with different ash/cement ratios the water/cement ratios had to be adjusted. The relevant water/cement and water/binder ratios are indicated in Table 4.4. These ratios do not include the water added to the mixture as part of the foam.

Table 4.3: Conformity of Materials to Standards.

Property	Code Requirement	RHPC from PPC Hercules	Processed Pfa from Lethabo	Pozz-fill from Lethabo
CaO & SiO ₂	≥ 67%	82.9%		
(CaO/SiO ₂) Ratio	≥ 2	2.9		
MgO	≤ 5%	4.3%		
SO ₃	≤ 4%	2 %		
Loss on ignition	< 5%		0.8 %	0.8 %
CaO	< 5%		4.7 %	5 %
Reactive SiO ₂	≥ 25%		53.9 %	54.8 %
Residue retained on 45 μm sieve	< 12.5 %		8 %	39 %
SO ₃	2.5 %		0.1 %	0.3 %

Table 4.4: Mix ratios (by weight).

Ash/cement ratio	Water/cement ratio	Water/binder ratio
0	0.3, 0.4 & 0.6	0.30, 0.40 & 0.60
1	0.6	0.30
2	0.86	0.287
3	1.17	0.293

4.5 TESTS CONDUCTED

4.5.1 COMPRESSIVE STRENGTH

The compressive strength of foamed concrete was determined from 100 mm cubes. The cubes were cast in steel moulds, de-moulded after 24±2 hours, wrapped in polythene wrapping and kept in a constant temperature room up to the day of testing. Before

testing each cube was unwrapped and weighed. The testing weight is compared with the de-moulding weight and any large reduction in weight would indicate that the cube dried out, and that hydration might have been reduced by the lack of moisture available.

The cube test consisted of crushing three cubes from the same sample of concrete. Strength is defined as the average of the three results and for the results to be valid the range of results must not be more than 15% of the average.⁷⁰ The cement paste cubes were crushed on a standard cube press, but as the foamed concrete strengths were relatively low these cubes were crushed on a more sensitive press with a 50 MPa capacity. It was decided to record the compressive strength to the nearest 0.1 MPa instead of 0.5 MPa⁷ that is normally used for concrete.

4.5.2 DEFORMATION OF FOAMED CONCRETE

With any stress there is always an associated strain, but strain can also arise from other causes than applied stress. A material is said to be perfectly elastic if strain appears and disappears immediately on application and removal of stress. Concrete is elastic to a degree but when concrete is subjected to a sustained loading, strain increases with time and creep takes place. Furthermore concrete contracts on drying, undergoing shrinkage. For normal concrete the magnitude of shrinkage and creep are of the same order as elastic strain under the usual range of stresses, and therefore the various types of strain must at all times be taken into account.⁶

4.5.2.1 Shrinkage

The type of volume change that is of most concern in structural performance is that associated with an interchange of moisture between the hardened concrete and the environment. If the net flow of moisture is from the environment to the concrete, the result is an increase in volume, called swelling, while drying shrinkage is the decrease in volume as a result of a net outflow of moisture from the concrete to the environment.

Shrinkage tests were conducted on 40 x 40 x 250 mm shrinkage beams. A set of two beams were cast from each mixture and these beams were wrapped in polythene and

cured at $22\pm 2^\circ\text{C}$ in the constant temperature room for 7 days where after the distance between the stainless steel studs that have been cast into the ends of the beam was measured using a micrometer. Seven days after casting the beams were unwrapped and placed in the constant temperature room at 60% humidity. Measurements were taken at regular time intervals and the change in length was recorded to the nearest micrometer and the shrinkage calculated in microstrain.

4.5.2.2 Creep

Creep can be defined as the increase in strain under a sustained stress. Creep tests were conducted according to ASTM C512-87⁷⁴ on 300 mm long cylinders with a diameter of 150 mm. Three cylinders were cast from a mixture, wrapped in polythene and cured in the constant temperature room for 28 days. These cylinders were then capped and placed in a spring-loaded creep frame in a constant temperature room at $22\pm 2^\circ\text{C}$ and $60\pm 5\%$ humidity. Two of the cylinders were loaded to 40% of the average 28 day cube compressive strength while the third cylinder was used as an unloaded control to monitor possible volume changes caused by moisture changes. The strain was measured using a 200 mm long mechanical strain gauge on four sets of targets placed on each cylinder. The change in length was measured at regular time intervals and recorded to the nearest micrometer. Creep was calculated in microstrain. The polythene wrapping was kept in place throughout the test period to ensure that the deformation measured was a result of basic creep and not caused by drying shrinkage.

4.5.2.3 Elastic modulus

The elastic modulus of foamed concrete was determined more than 780 days by loading 300 mm long cylinders with a diameter of 150 mm to approximately 30% of their failure load. The deformation was measured over the central 100 mm of the length of the cylinder. The load was then reduced to a nominal load (approximately 5% of the failure load) and the deformation was measured at this reduced load. The load cycle was repeated and the readings checked. The change in strain of each sample was calculated as the deformation change over the initial 100 mm length while the change in stress is the difference between the maximum and the nominal load applied. The elastic modulus was calculated as the change in stress divided by the change in strain. Due to the low compressive strengths of the foamed concrete no standard test method was used.

4.5.3 POROSITY

The porosity of the foamed concrete was determined using the Vacuum Saturation Apparatus as developed by Cabrera and Lynsdale at the University of Leeds⁷⁵. According to Gaafar⁷⁶ the porosity that is calculated using the mercury porosimetry technique is always lower than that determined from vacuum saturation. As foamed concrete contains a relatively large percentage voids, that might not be easily accessible to mercury, it was decided to use the vacuum saturation technique. Porosity measurements were conducted on slices of 68 mm diameter cores that were drilled out of the center of a 100 mm cube. This technique should ensure that results are not affected by possible casting edge effects. The slices were dried at 100 ± 5 °C until all the evaporable water had evaporated and weight became constant. This weight was recorded as the dry weight of the sample. After drying the samples were packed in a desiccator and placed under vacuum for at least three hours, whereafter the desiccator was filled with de-aired, distilled water. The vacuum pump was left running for another three hours, whereafter the vacuum was removed and the samples remained under water over night. The day after submerging the samples they were removed from the desiccator and both the wet and submerged weight of each sample was measured. The porosity was calculated using the following formula⁷⁵:

$$P = \frac{(W_{sat} - W_{dry})}{(W_{sat} - W_{wat})} * 100 \quad (\text{Eq 4. 5})$$

where:

- P = Vacuum saturation porosity (%)
- W_{sat} = Weight in air of saturated sample
- W_{wat} = Weight in water of saturated sample
- W_{dry} = Weight of oven dried sample.

4.5.4 PERMEABILITY

Inadequate durability manifests itself by deterioration, which can be due to either external factors or to internal causes within the concrete itself. The various actions can be physical, chemical or mechanical, and the deterioration of concrete is rarely the result

of one isolated cause. The permeability of concrete gives an indication of the ease with which fluids, gases or vapours can enter into and move through the concrete and it is therefore a good indicator of the quality of the concrete⁶. The ease with which a fluid can penetrate foamed concrete was determined by measuring both the water absorption and the water vapour permeability. The water absorption was measured by drying a 100 mm cube (after 28 days curing in a constant temperature room) to a constant mass at 100 ± 5 °C, immersing it in water for 7 days, and measuring the increase in mass as a percentage of the dry mass.

A water vapour permeability test was set up in accordance to the RILEM recommendation LC7 for Autoclaved Aerated Concrete⁷⁷. The water vapour permeability can be defined as “the amount of mass transfer due to diffusion of water vapour resulting from a difference in water vapour pressure on the two parallel surfaces of a disc of aerated concrete”⁷⁷. One year after casting, a core with a diameter of 100 mm was drilled from a 150 mm cube and sliced into 40 ± 2 mm slices. Specimens were dried at 50 ± 3 °C and then stored over a saturated solution of potassium nitrate in a closed container for 7 days. After conditioning the samples were placed in plastic containers filled with a saturated solution of potassium nitrate to a depth of 30 ± 2 mm below the bottom surface of the specimen. The sides of the specimens were covered with vapour-impermeable tape and rubber packing whereafter the assemblies were placed in the constant temperature room at 22 ± 2 °C and 60 ± 5 % humidity. Each assembly was weighed every 48 hours until a constant rate of weight loss was obtained. After completion of the test each sample was removed and dried at 100 ± 5 °C in order to determine the dry density.

The water vapour permeability k_d is a material constant which is a function of the density of the aerated concrete and its pore structure. The permeability can be calculated using the following equation:

$$k_d = \frac{G d}{A_c t \Delta p} \quad (\text{Eq 4.6})$$

where :

k_d	=	Time rate of vapour flow through unit area (<i>Perm cm</i>) or $kg\ m/m^2\ s\ MN/m^2$ assuming $1\text{mm Hg} = 0.133\ MN/m^2$)
G	=	Weight loss during t hours
A_c	=	Cross-sectional area of specimen perpendicular to flow (m^2)
d	=	Thickness of specimen in m
t	=	Time in hours
Δp	=	Difference in water vapour partial pressure between the dry side and the moist side of the specimen in mm of mercury.

4.5.5 IMAGE ANALYSIS

Image analysis was conducted using an *Axiolab-A Reflected Light Microscope* (manufactured by Zeiss). The objective used was an Epiplan 10 x / 0.20. A black and white microscope camera was used to transfer images to the computer, where *Optimate* image analysis software was used. Specimens were cut from the center of a 100 mm cube with a diamond saw and the surfaces ground and polished with care to prevent damage to the void structure⁷⁸. Initially the voids in samples were impregnated with a low viscosity epoxy⁷⁸, but the impregnation process damaged the edges of the voids to the extent that less damage occurred when preparing the samples without epoxy in the voids. The experimental results as discussed in this document are obtained from samples without epoxy in the voids. The European Standard ENV 480 Part II⁷⁹ prescribes a process where polished samples of concrete are examined microscopically along a series of regularly spaced lines of traverse to determine the void spacing. Every air-void encountered on the traverse must be recognized and recorded and its chord length measured. Image acquisition and analysis can be used to identify voids along these traverse lines by using threshold grey scale values⁸⁰, but major discrepancy exists between results obtained using this automatic measurement method and that obtained from measuring void by physically determining the areas of visible voids. The grey scale image analysis method results in large numbers of very small voids (that can not be seen on the photograph by the naked eye) being counted.

The aim of the image analysis conducted on the foamed concrete is to determine the size, shape and distribution of the entrained air voids. As the linear traverse method as described before assumes that voids are spherical this method was deemed unsuitable and it was decided to take discreet microscope photographs and measure the voids on these photos. The area, coordinates, maximum and minimum diameter and circumference of each void on the photograph is measured. Photographs are taken on a predetermined grid and enough photographs are taken on one sample of each mixture so that the statistics of voids can be calculated for every mixture. To ensure that the voids measured are representative of that specific mixture the number of voids taken into account must be sufficient. As this investigation includes mixtures with different densities, the volume of voids and therefore the number of voids on a given area will vary. It was decided to measure a minimum number of 250 voids of each mixture and this number of voids should give an indication of any trends in void size that might exist. Image analysis was conducted on samples from all the mixtures containing foam to determine the void size, shape and distribution. Plate 4.3 is a typical optical microscope image, with the voids caused by the foam clearly visible. The optical microscope is linked to a computer and an example of typical image analysis output can be seen in Table 4.5. The value in the first column of this table indicates that 15 voids were counted on this specific microscope photo. The second column gives the area of each of these voids (in μm^2), while the circumference of each void, as measured from the length of the line that was drawn around the void (using the computer mouse), is given in column 3. The next two columns gives the x and y co-ordinate of the centre-point of each void. The circularity is the ratio between the area and the circumference of each void and for a perfect circle this value would be 4π . The more imperfect the shape of the void is, the higher this circularity value would become. The longest axis is calculated as the longest straight line that can be drawn through the center-point coordinates with end points on the circumference. By using the measured perimeter and longest axis, the width is calculated as the second main axis assuming that the void is a perfect ellipse. The fact that the voids have irregular perimeters results in the width often being longer than the longest axis. The program used for image analysis has an option for gray scale analysis and the last three columns are used for automatic gray scale analysis. The longest axis, width and gray scale values were not used for this investigation.

Although optical microscope image analysis is a two dimensional technique, it is used in this investigation to analyze a three dimensional problem. The results in this investigation are therefor not absolute but they are comparative and they are not used as definitive answers but rather as a tool to define possible trends.

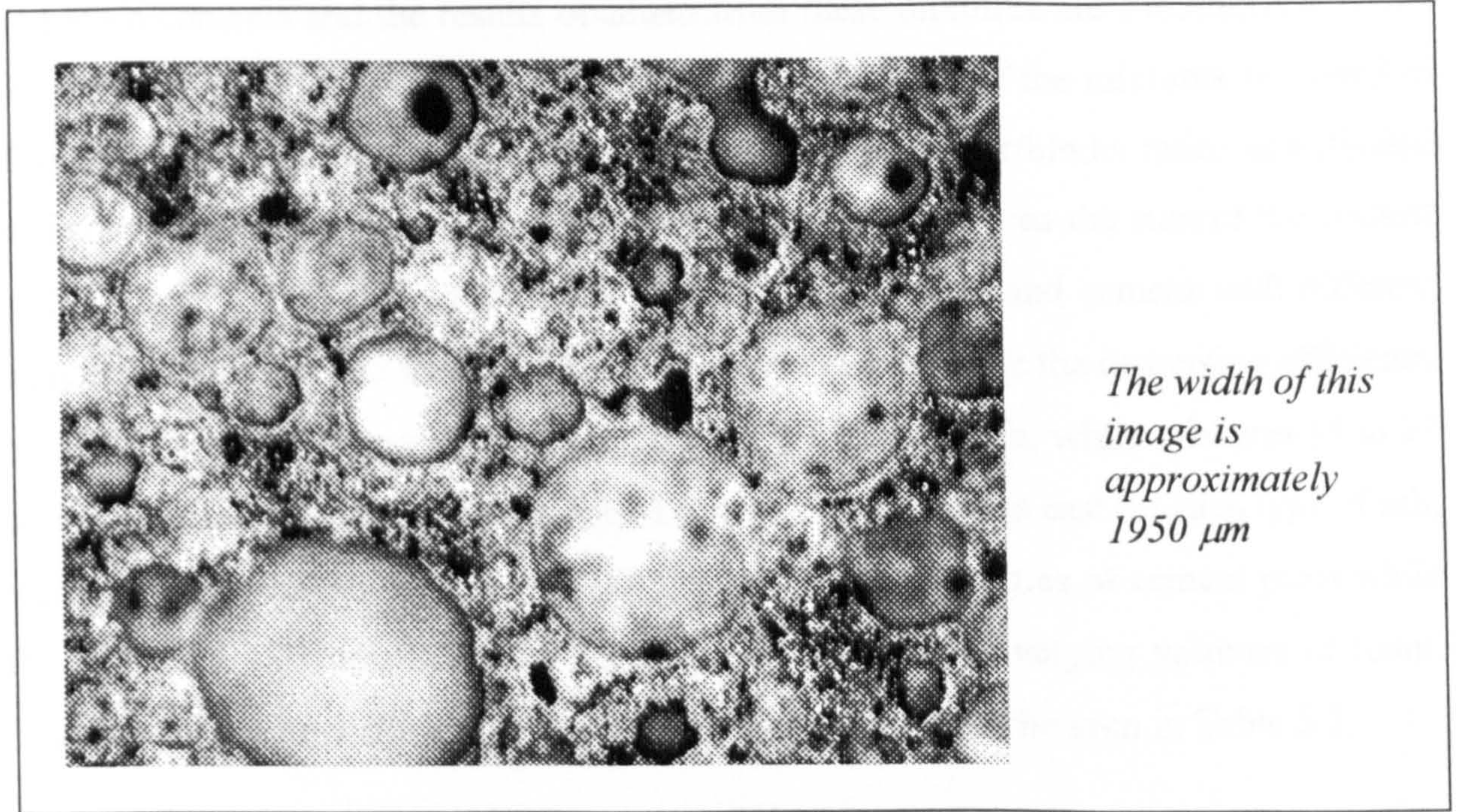


Plate 4.3: Typical Optical Microscope Image.

Table 4.5: Typical Image Analysis Output.

Count	Area	Perimeter	X - Position	Y - Position	Circularity	Longest Axis	Width	Mean Gray	Std. Dev. Gray	Var. of Gray
15	3713.32	228.31	631.64	1132.91	14.04	68.37	70.65	163.59	6.64	44.12
	51565.81	1112.4	900.6	1088.51	24	248.78	419.86	142.41	6.73	45.28
	5487.67	273.35	699.28	1059.72	13.62	82.87	85.71	162.67	8.73	76.27
	527484.1	2909.07	1271.25	601.11	16.04	779.75	1023.93	149.19	10.94	119.67
	23450.65	552.76	276.48	945.1	13.03	170.4	175.53	155.07	10.11	102.28
	6865.69	305.32	636.58	971.93	13.58	92.23	95.75	145.4	15.34	235.21
	1874.95	163.3	166.42	947.52	14.22	49	50.88	130.85	8.54	73
	35361.94	673.91	771.45	801.19	12.84	209.01	215.39	165.06	12.16	147.76
	6124.85	288	406.33	849.99	13.54	87.26	90.7	159.76	8.97	80.47
	24667.08	563.52	564.09	769.47	12.87	175.27	180.96	157.09	10.7	114.52
	104707.8	1155.9	421.25	359.75	12.76	360.1	370.56	162.84	14.61	213.36
	71964.71	1207.84	853.62	82.49	20.27	236.04	461.01	155.1	11.35	128.82
	2283.48	185.95	1301.57	176.81	15.14	54.39	56.33	151.7	5.63	31.7
	51233.51	1058.36	186.31	68.28	21.86	220.77	410.9	144.83	10.09	101.72
	3710.28	227.86	1486.56	110.97	13.99	68.97	70.65	141.97	5.91	34.9

CHAPTER 5: RESULTS

5.1 MIXTURES

The aim of this investigation was to determine the effect of high volumes of coal ash on the properties of foamed concrete. Twenty-seven mixtures were cast with different ash and foam contents and the results obtained from these mixtures are summarized in this chapter. The cement, ash, water and foam content for each of the mixtures are listed in Table 5.1. The water/cement (w/c), ash/cement (a/c) and water/binder ratios as indicated in Table 5.1 are weight ratios and the binder content is taken as the sum of the cement and the ash. The first three mixtures contained only water and cement with different water/cement ratios and these mixtures were used to determine the cementing efficiency of the ash used. Mixtures number 4 to 15 contain classified pfa, while mixtures 16 to 27 contain the unclassified ash (Pozz-fill). The first three mixtures cast for each type of ash, were used to establish the effect of ash content on the properties of cement paste while the other nine mixtures cast with each type of ash contains varying volumes of foam. The volumetric proportional composition of each mixture can be seen in Table 5.2.

5.2 RESULTS

The compressive strengths for the different mixtures after 7 and 28, 56 and 84, 180 and 270 and 365 days are given in Table 5.3, Table 5.4, Table 5.5 and Table 5.6 respectively. The demould and test densities are listed with the compressive strengths and each value represents the average of three cubes. Table 5.7 contains the permeability, porosity, dry and wet density of each of the 27 mixtures. The permeability and porosity as indicated in the table were measured approximately one year after casting. Porosities were measured at different ages (such as 28 days, 180 days, 270 days and 365 days) and all these values are indicated in Appendix A. Experimental problems were however experienced with the initial porosity measurements and it is believed that air remained entrapped in some of the voids, making the results inaccurate. The process was changed to include the use of de-aired distilled water and a magnetic stir to drive off the air and the later measurements does seem to be more reliable. The dry density was determined after 28 days of curing and 7 days of drying. The saturated density was determined from the same cubes as the dry densities, after submerging these cubes in water for 7 days.

Table 5.1: Composition of Mixtures.

Mix No	Type of Ash	Target Density (kg/m ³)	a/c	w/c	w/binder	Composition of Mixture (per m ³)			
						Water (l)	Cement (kg)	Ash (kg)	Foam (l)
1	NONE	FULL	0	0.30	0.30	486	1620	0	0
2	NONE	FULL	0	0.40	0.40	558	1394	0	0
3	NONE	FULL	0	0.60	0.60	654	1090	0	0
4	PFA	FULL	1	0.60	0.30	437	729	729	0
5	PFA	FULL	2	0.86	0.29	412	479	958	0
6	PFA	FULL	3	1.17	0.29	411	351	1053	0
7	PFA	1500	1	0.60	0.30	346	577	577	208
8	PFA	1500	2	0.86	0.29	335	389	778	188
9	PFA	1500	3	1.17	0.29	339	290	870	173
10	PFA	1250	1	0.60	0.30	289	481	481	340
11	PFA	1250	2	0.86	0.29	279	324	648	324
12	PFA	1250	3	1.17	0.29	283	242	726	310
13	PFA	1000	1	0.60	0.30	231	385	385	472
14	PFA	1000	2	0.86	0.29	223	259	518	460
15	PFA	1000	3	1.17	0.29	226	193	579	450
16	POZ	FULL	1	0.60	0.30	437	729	729	0
17	POZ	FULL	2	0.86	0.29	412	479	958	0
18	POZ	FULL	3	1.17	0.29	411	351	1053	0
19	POZ	1500	1	0.60	0.30	346	577	577	208
20	POZ	1500	2	0.86	0.29	335	389	778	188
21	POZ	1500	3	1.17	0.29	339	290	870	173
22	POZ	1250	1	0.60	0.30	289	481	481	340
23	POZ	1250	2	0.86	0.29	279	324	648	324
24	POZ	1250	3	1.17	0.29	283	242	726	310
25	POZ	1000	1	0.60	0.30	231	385	385	472
26	POZ	1000	2	0.86	0.29	223	259	518	460
27	POZ	1000	3	1.17	0.29	226	193	579	450

Table 5.2 : Volume Ratios of Mixtures.

Mix No	Type of Ash	Target Density (kg/m ³)	a/c	w/c	w/binder	Composition of Mixture (per Volume)			
						Water (%)	Cement (%)	Ash (%)	Foam (%)
1	NONE	FULL	0	0.30	0.30	48.6	51.4	0.0	0.0
2	NONE	FULL	0	0.40	0.40	55.8	44.2	0.0	0.0
3	NONE	FULL	0	0.60	0.60	65.4	34.6	0.0	0.0
4	PFA	FULL	1	0.60	0.30	43.7	23.1	33.1	0.0
5	PFA	FULL	2	0.86	0.29	41.2	15.2	43.6	0.0
6	PFA	FULL	3	1.17	0.29	41.0	11.1	47.8	0.0
7	PFA	1500	1	0.60	0.30	36.1	18.3	26.2	19.4
8	PFA	1500	2	0.86	0.29	34.8	12.3	35.4	17.5
9	PFA	1500	3	1.17	0.29	35.1	9.2	39.5	16.1
10	PFA	1250	1	0.60	0.30	31.2	15.3	21.9	31.6
11	PFA	1250	2	0.86	0.29	30.1	10.3	29.5	30.1
12	PFA	1250	3	1.17	0.29	30.5	7.7	33.0	28.8
13	PFA	1000	1	0.60	0.30	26.4	12.2	17.5	43.9
14	PFA	1000	2	0.86	0.29	25.5	8.2	23.5	42.7
15	PFA	1000	3	1.17	0.29	25.7	6.1	26.3	41.8
16	POZ	FULL	1	0.60	0.30	43.7	23.1	33.1	0.0
17	POZ	FULL	2	0.86	0.29	41.2	15.2	43.6	0.0
18	POZ	FULL	3	1.17	0.29	41.0	11.1	47.8	0.0
19	POZ	1500	1	0.60	0.30	36.1	18.3	26.2	19.4
20	POZ	1500	2	0.86	0.29	34.8	12.3	35.4	17.5
21	POZ	1500	3	1.17	0.29	35.1	9.2	39.5	16.1
22	POZ	1250	1	0.60	0.30	31.2	15.3	21.9	31.6
23	POZ	1250	2	0.86	0.29	30.1	10.3	29.5	30.1
24	POZ	1250	3	1.17	0.29	30.5	7.7	33.0	28.8
25	POZ	1000	1	0.60	0.30	26.4	12.2	17.5	43.9
26	POZ	1000	2	0.86	0.29	25.5	8.2	23.5	42.7
27	POZ	1000	3	1.17	0.29	25.7	6.1	26.3	41.8

Table 5.3: 7 Day and 28 Day Compressive Strength of Mixtures.

Mix No	Type of Ash	Target Density (kg/m ³)	a/c	w/c	w/binder	7 Day Results			28 Day Results		
						Demould Density (kg/m ³)	Testing Density (kg/m ³)	Cube Strength (MPa)	Demould Density (kg/m ³)	Testing Density (kg/m ³)	Cube Strength (MPa)
1	NONE	FULL	0	0.30	0.30	2058.7	2053.7	63.1	2053.7	2046.3	79.0
2	NONE	FULL	0	0.40	0.40	1937.0	1933.0	47.6	1942.3	1927.0	59.0
3	NONE	FULL	0	0.60	0.60	1705.3	1700.0	20.5	1709.0	1688.0	32.0
4	PFA	FULL	1	0.60	0.30	1838.0	1832.3	31.5	1840.7	1833.3	43.3
5	PFA	FULL	2	0.86	0.29	1831.0	1823.3	23.1	1820.7	1808.0	37.5
6	PFA	FULL	3	1.17	0.29	1770.0	1762.7	9.9	1771.7	1750.7	16.5
7	PFA	1500	1	0.60	0.30	1451.3	1450.0	11.9	1445.3	1441.0	18.1
8	PFA	1500	2	0.85	0.29	1441.3	1438.3	8.6	1445.0	1441.0	14.6
9	PFA	1500	3	1.17	0.29	1466.7	1465.0	6.6	1452.7	1454.0	13.9
10	PFA	1250	1	0.60	0.30	1239.3	1232.0	5.5	1225.7	1215.3	9.3
11	PFA	1250	2	0.86	0.29	1208.3	1208.7	4.7	1206.0	1204.0	8.0
12	PFA	1250	3	1.17	0.29	1231.3	1227.3	3.6	1241.7	1233.0	7.2
13	PFA	1000	1	0.60	0.30	986.0	986.0	2.2	988.7	987.7	3.8
14	PFA	1000	2	0.86	0.29	997.3	995.0	2.6	995.0	991.0	4.0
15	PFA	1000	3	1.17	0.29	988.3	982.3	1.7	986.3	976.7	2.8
16	POZ	FULL	1	0.60	0.30	1836.3	1833.3	35.0	1837.7	1828.3	45.7
17	POZ	FULL	2	0.86	0.29	1772.3	1765.0	15.3	1772.3	1767.7	27.0
18	POZ	FULL	3	1.17	0.29	1729.7	1720.3	10.2	1733.7	1711.7	18.9
19	POZ	1500	1	0.60	0.30	1474.0	1474.3	14.9	1474.7	1470.0	20.0
20	POZ	1500	2	0.86	0.29	1462.7	1461.0	11.2	1473.0	1470.0	17.4
21	POZ	1500	3	1.17	0.29	1500.0	1496.7	8.6	1490.7	1483.7	14.3
22	POZ	1250	1	0.60	0.30	1236.0	1231.0	7.9	1243.3	1226.0	9.6
23	POZ	1250	2	0.86	0.29	1213.0	1209.3	5.0	1216.7	1210.0	8.8
24	POZ	1250	3	1.17	0.29	1236.7	1229.0	4.6	1228.0	1221.3	5.6
25	POZ	1000	1	0.60	0.30	981.7	973.7	2.9	976.0	962.7	4.3
26	POZ	1000	2	0.86	0.29	969.7	965.0	2.3	975.0	956.3	3.8
27	POZ	1000	3	1.17	0.29	947.3	942.7	1.2	960.3	952.0	2.2

Table 5.4: 56 Day and 84 Day Compressive Strength of Mixtures.

Mix No	Type of Ash	Target Density (kg/m ³)	a/c	w/c	w/binder	56 Day Results			84 Day Results		
						Demould Density (kg/m ³)	Testing Density (kg/m ³)	Cube Strength (MPa)	Demould Density (kg/m ³)	Testing Density (kg/m ³)	Cube Strength (MPa)
1	NONE	FULL	0	0.30	0.30	2064.0	2047.5	80.4	2043.0	2028.3	80.4
2	NONE	FULL	0	0.40	0.40	1924.8	1902.3	64.1	1925.3	1919.7	62.0
3	NONE	FULL	0	0.60	0.60	1718.0	1700.0	37.1	1719.3	1697.7	38.9
4	PFA	FULL	1	0.60	0.30	1851.0	1843.5	52.6	1828.0	1820.0	58.1
5	PFA	FULL	2	0.86	0.29	1837.8	1820.3	47.4	1842.0	1824.3	58.9
6	PFA	FULL	3	1.17	0.29	1769.5	1751.3	28.3	1762.3	1743.3	36.5
7	PFA	1500	1	0.60	0.30	1447.5	1438.8	25.0	1459.3	1455.7	30.8
8	PFA	1500	2	0.86	0.29	1442.5	1437.8	18.5	1443.0	1436.3	26.9
9	PFA	1500	3	1.17	0.29	1459.0	1452.3	18.0	1468.0	1456.7	24.6
10	PFA	1250	1	0.60	0.30	1232.5	1221.0	12.0	1224.7	1212.0	14.1
11	PFA	1250	2	0.86	0.29	1206.3	1205.3	10.6	1210.0	1205.3	13.3
12	PFA	1250	3	1.17	0.29	1237.8	1221.8	10.3	1240.7	1222.0	13.6
13	PFA	1000	1	0.60	0.30	986.0	985.8	5.8	982.0	983.0	6.2
14	PFA	1000	2	0.86	0.29	997.8	991.3	4.6	1000.0	993.3	6.9
15	PFA	1000	3	1.17	0.29	987.3	974.5	5.2	981.3	963.0	5.6
16	POZ	FULL	1	0.60	0.30	1831.8	1819.8	52.2	1841.3	1827.7	55.2
17	POZ	FULL	2	0.86	0.29	1770.8	1755.8	42.1	1771.7	1752.7	44.7
18	POZ	FULL	3	1.17	0.29	1741.0	1722.5	30.0	1747.0	1709.0	35.2
19	POZ	1500	1	0.60	0.30	1475.5	1460.8	23.8	1480.0	1475.3	29.7
20	POZ	1500	2	0.86	0.29	1462.5	1456.8	25.6	1464.3	1460.3	24.8
21	POZ	1500	3	1.17	0.29	1490.0	1479.5	21.1	1496.0	1482.0	27.2
22	POZ	1250	1	0.60	0.30	1237.3	1225.5	11.9	1234.7	1218.3	14.5
23	POZ	1250	2	0.86	0.29	1213.8	1207.3	11.6	1210.0	1200.7	14.0
24	POZ	1250	3	1.17	0.29	1232.5	1217.5	9.7	1247.3	1229.0	12.8
25	POZ	1000	1	0.60	0.30	970.0	953.5	5.0	972.0	952.7	6.5
26	POZ	1000	2	0.86	0.29	971.0	945.5	4.6	966.3	947.7	5.6
27	POZ	1000	3	1.17	0.29	949.0	940.3	2.9	950.0	936.7	4.2

Table 5.5: 180 Day and 270 Day Compressive Strength of Mixtures.

Mix No	Type of Ash	Target Density (kg/m ³)	a/c	w/c	w/binder	180 Day Results			270 Day Results		
						Demould Density (kg/m ³)	Testing Density (kg/m ³)	Cube Strength (MPa)	Demould Density (kg/m ³)	Testing Density (kg/m ³)	Cube Strength (MPa)
1	NONE	FULL	0	0.30	0.30	2041.0	2015.0	84.5	2048.7	1999.7	81.6
2	NONE	FULL	0	0.40	0.40	1937.7	1904.7	68.0	1925.7	1872.7	68.9
3	NONE	FULL	0	0.60	0.60	1666.7	1632.3	39.5	1710.0	1665.3	43.5
4	PFA	FULL	1	0.60	0.30	1843.0	1826.0	69.2	1832.7	1807.7	84.6
5	PFA	FULL	2	0.86	0.29	1838.7	1812.7	64.7	1845.3	1812.7	78.3
6	PFA	FULL	3	1.17	0.29	1761.7	1733.0	54.7	1760.7	1722.3	61.2
7	PFA	1500	1	0.60	0.30	1460.3	1447.7	29.3	1470.7	1453.7	37.0
8	PFA	1500	2	0.86	0.29	1437.3	1426.0	33.2	1443.3	1421.3	36.1
9	PFA	1500	3	1.17	0.29	1479.7	1459.7	30.8	1473.0	1446.7	33.7
10	PFA	1250	1	0.60	0.30	1220.3	1203.7	15.5	1245.7	1220.3	20.1
11	PFA	1250	2	0.86	0.29	1204.3	1194.7	16.0	1196.0	1179.0	18.5
12	PFA	1250	3	1.17	0.29	1234.3	1214.0	15.2	1240.0	1214.3	18.7
13	PFA	1000	1	0.60	0.30	984.7	978.3	9.0	986.7	977.7	9.6
14	PFA	1000	2	0.86	0.29	1001.7	985.3	8.2	990.3	970.3	8.2
15	PFA	1000	3	1.17	0.29	985.0	963.0	7.8	990.0	959.0	7.9
16	POZ	FULL	1	0.60	0.30	1837.7	1810.3	68.8	1829.7	1806.3	80.1
17	POZ	FULL	2	0.86	0.29	1764.0	1726.7	66.0	1770.3	1742.3	75.3
18	POZ	FULL	3	1.17	0.29	1729.0	1690.0	48.9	1742.7	1676.0	60.0
19	POZ	1500	1	0.60	0.30	1468.0	1449.0	33.8	1476.7	1442.0	39.7
20	POZ	1500	2	0.86	0.29	1467.0	1457.0	35.2	1459.7	1442.7	39.7
21	POZ	1500	3	1.17	0.29	1485.7	1462.3	30.1	1492.0	1461.0	36.9
22	POZ	1250	1	0.60	0.30	1238.3	1208.0	16.9	1241.7	1207.3	19.7
23	POZ	1250	2	0.86	0.29	1214.0	1200.0	15.1	1212.0	1192.7	18.8
24	POZ	1250	3	1.17	0.29	1241.7	1198.0	15.8	1233.7	1196.7	18.1
25	POZ	1000	1	0.60	0.30	971.3	937.7	5.7	974.3	939.7	6.3
26	POZ	1000	2	0.86	0.29	970.0	936.7	6.6	971.7	919.0	6.5
27	POZ	1000	3	1.17	0.29	943.0	925.3	5.8	954.7	933.7	6.1

Table 5.6: 365 Day Compressive Strength of Mixtures.

Mix No	Type of Ash	Target Density (kg/m ³)	a/c	w/c	w/binder	365 Day Results		
						Demould Density (kg/m ³)	Testing Density (kg/m ³)	Cube Strength (MPa)
1	NONE	FULL	0	0.30	0.30	2024.7	1992.7	85.4
2	NONE	FULL	0	0.40	0.40	1923.7	1877.3	78.9
3	NONE	FULL	0	0.60	0.60	1704.7	1641.0	46.7
4	PFA	FULL	1	0.60	0.30	1858.0	1828.7	80.3
5	PFA	FULL	2	0.86	0.29	1847.0	1817.0	81.5
6	PFA	FULL	3	1.17	0.29	1762.3	1727.3	58.1
7	PFA	1500	1	0.60	0.30	1463.7	1449.3	39.5
8	PFA	1500	2	0.86	0.29	1450.7	1431.7	35.6
9	PFA	1500	3	1.17	0.29	1483.0	1460.3	36.1
10	PFA	1250	1	0.60	0.30	1239.7	1219.3	19.8
11	PFA	1250	2	0.86	0.29	1205.0	1194.0	18.4
12	PFA	1250	3	1.17	0.29	1234.3	1208.0	19.1
13	PFA	1000	1	0.60	0.30	984.0	982.0	9.2
14	PFA	1000	2	0.86	0.29	987.3	973.3	8.6
15	PFA	1000	3	1.17	0.29	985.7	955.0	7.1
16	POZ	FULL	1	0.60	0.30	1833.7	1798.0	93.4
17	POZ	FULL	2	0.86	0.29	1776.7	1742.3	78.7
18	POZ	FULL	3	1.17	0.29	1736.0	1680.3	63.1
19	POZ	1500	1	0.60	0.30	1473.7	1439.3	37.0
20	POZ	1500	2	0.86	0.29	1463.3	1448.3	41.3
21	POZ	1500	3	1.17	0.29	1494.0	1451.7	38.8
22	POZ	1250	1	0.60	0.30	1240.3	1204.7	19.8
23	POZ	1250	2	0.86	0.29	1211.3	1193.3	19.8
24	POZ	1250	3	1.17	0.29	1227.7	1195.3	17.6
25	POZ	1000	1	0.60	0.30	972.3	937.0	7.0
26	POZ	1000	2	0.86	0.29	973.0	932.0	7.5
27	POZ	1000	3	1.17	0.29	951.3	928.7	5.8

Table 5.7: Porosity, Permeability and Water absorption.

Mix No	Type of Ash	Target Density (kg/m ³)	a/c	w/c	w/binder	Vapour Permeability (after 365 days)				Porosity After 365 Days (%)	Dry Density (kg/m ³)	Saturated Density (kg/m ³)
						Sample Thickness (mm)	Weight Loss (g/100 days)	k _d (kg s MN/m ³)	k _a (Perm cm)			
1	NONE	FULL	0	0.30	0.30	18.4	5.2	0.0045	0.0508	28.2	1958.3	2057.5
2	NONE	FULL	0	0.40	0.40	17.9	7.6	0.0062	0.0718	31.0	1817.3	1968.5
3	NONE	FULL	0	0.60	0.60	18.4	18.6	0.0163	0.1911	37.2	1450.3	1753.0
4	PFA	FULL	1	0.60	0.30	18.9	5.7	0.0059	0.0566	29.8	1751.0	1920.0
5	PFA	FULL	2	0.86	0.29	23.2	4.4	0.0047	0.0540	27.0	1715.5	1889.5
6	PFA	FULL	3	1.17	0.29	16.9	13.6	0.0114	0.1234	30.6	1570.8	1819.0
7	PFA	1500	1	0.60	0.30	20.7	18.2	0.0183	0.2107	43.3	1287.3	1530.5
8	PFA	1500	2	0.86	0.29	21.6	19.5	0.0204	0.2335	43.6	1273.3	1509.5
9	PFA	1500	3	1.17	0.29	23.7	14.2	0.0164	0.1862	43.1	1274.3	1531.5
10	PFA	1250	1	0.60	0.30	21.1	25.3	0.0255	0.2953	48.4	1055.8	1304.5
11	PFA	1250	2	0.86	0.29	21.7	19.6	0.0405	0.4726	52.5	1023.5	1254.0
12	PFA	1250	3	1.17	0.29	22.8	31.6	0.0351	0.4024	49.5	1040.8	1318.5
13	PFA	1000	1	0.60	0.30	17.1	68.8	0.0539	0.6237	59.3	833.0	1079.0
14	PFA	1000	2	0.86	0.29	21.7	64.4	0.0677	0.7810	62.6	820.8	1064.5
15	PFA	1000	3	1.17	0.29	23.2	62.2	0.0698	0.8105	61.9	810.0	1111.0
16	POZ	FULL	1	0.60	0.30	19.6	7.9	0.0077	0.0867	31.7	1695.5	1871.5
17	POZ	FULL	2	0.86	0.29	23.3	3.1	0.0031	0.0357	31.6	1561.0	1800.0
18	POZ	FULL	3	1.17	0.29	20.8	8.9	0.0087	0.0999	33.2	1524.5	1789.0
19	POZ	1500	1	0.60	0.30	21.2	12.8	0.0131	0.1493	43.0	1341.5	1545.5
20	POZ	1500	2	0.86	0.29	24.0	11.3	0.0125	0.1449	41.1	1327.0	1537.5
21	POZ	1500	3	1.17	0.29	17.5	20.6	0.0170	0.1990	38.2	1308.5	1560.5
22	POZ	1250	1	0.60	0.30	22.1	25.8	0.0275	0.3185	50.0	1058.0	1303.0
23	POZ	1250	2	0.86	0.29	20.9	33.7	0.0339	0.3918	51.1	1055.0	1281.0
24	POZ	1250	3	1.17	0.29	21.6	34.5	0.0368	0.4218	48.3	1014.0	1280.5
25	POZ	1000	1	0.60	0.30	16.3	68.0	0.0537	0.6205	58.7	823.5	1097.5
26	POZ	1000	2	0.86	0.29	20.8	56.9	0.0575	0.6650	60.6	849.5	1088.0
27	POZ	1000	3	1.17	0.29	16.4	93.6	0.0724	0.8313	62.6	772.5	1023.5

The volumetric changes of the mixtures over a period of time as measured in drying shrinkage can be seen in Table 5.8, while creep values are given in Table 5.9.

Table 5.8: Drying Shrinkage.

Mix No	Type of Ash	Target Density (kg/m ³)	a/c	w/c	w/binder	Shrinkage (microstrain)		
						1 month	6 months	20 months
1	NONE	FULL	0	0.30	0.30	1198	2614	2663
2	NONE	FULL	0	0.40	0.40	1892	3536	3610
3	NONE	FULL	0	0.60	0.60	2570	5544	5720
4	PFA	FULL	1	0.60	0.30	1504	2952	2818
5	PFA	FULL	2	0.86	0.29	1608	2700	2832
6	PFA	FULL	3	1.17	0.29	1058	2146	2257
7	PFA	1500	1	0.60	0.30	1600	2750	3137
8	PFA	1500	2	0.86	0.29	1826	2938	2980
9	PFA	1500	3	1.17	0.29	1462	2430	2694
10	PFA	1250	1	0.60	0.30	1600	2496	2354
11	PFA	1250	2	0.86	0.29	1684	2898	3183
12	PFA	1250	3	1.17	0.29	1640	2768	STUD LOOSE
13	PFA	1000	1	0.60	0.30	1996	3162	3643
14	PFA	1000	2	0.86	0.29	2078	3268	3644
15	PFA	1000	3	1.17	0.29	1628	2778	2981
16	POZ	FULL	1	0.60	0.30	1494	2788	2845
17	POZ	FULL	2	0.86	0.29	1182	2192	2208
18	POZ	FULL	3	1.17	0.29	1170	2160	2201
19	POZ	1500	1	0.60	0.30	1956	3116	3375
20	POZ	1500	2	0.86	0.29	1524	2526	2747
21	POZ	1500	3	1.17	0.29	1484	2456	2597
22	POZ	1250	1	0.60	0.30	2108	3104	3621
23	POZ	1250	2	0.86	0.29	1926	2824	3308
24	POZ	1250	3	1.17	0.29	2034	2440	2663
25	POZ	1000	1	0.60	0.30	2118	3230	3415
26	POZ	1000	2	0.86	0.29	1424	2384	STUD LOOSE
27	POZ	1000	3	1.17	0.29	1416	2508	2613

Table 5.9: Creep Results.

Mix	Type	Target density (kg/m ³)	A/c	W/c	W/binder	Dry density (kg/m ³)	28 Day Compressive strength (MPa)	Modulus of Elasticity (GPa)*	Creep load (MPa)	Creep after 28 months (μstrain)	Specific creep after 28 months (μstrain/MPa)
A	POZ	1500	1	0.60	0.30	1260	24.2	12.2	8.0	1606	200
B	POZ	1500	2	0.86	0.29	1274	20.3	13.2	6.8	741	109
C	POZ	1500	3	1.17	0.29	1205	12.5	10.9	7.1	1742	245
D	POZ	1250	1	0.60	0.30	1101	15.3	6.9	4.6	1405	286
E	POZ	1250	2	0.86	0.29	988	8.5	8.1	2.6	1121	436
F	POZ	1250	3	1.17	0.29	1014	6.0	6.0	3.7	830	219
G	POZ	1000	0.5	0.5	0.33	851	4.8	3.9	2.0	1924	950
H	POZ	1000	1	0.60	0.30	770	4.7	3.1	1.3	1337	1000
J	POZ	1000	1.5	0.70	0.28	769	3.7	2.9	1.4	1923	1382
K	POZ	1000	2	0.86	0.29	877	5.8	4.2	1.7	898	540
L	POZ	1000	2.5	0.95	0.271	774	3.6	2.5	1.0	1115	1133

*- Measured on creep samples after completion of creep tests.

The creep tests were performed in advance of the main series of tests. It was originally intended to use these tests as preliminary tests and to repeat them again as part of the main test programme. However, due to circumstances beyond the control of the author, when the time came to repeat them the creep frames were no longer available for use. For completeness it was decided to include these preliminary test results in this report. With the exception of the mixtures cast to a target density of 1000 kg/m³, where ash/cement ratios of 0.5, 1.0, 1.5, 2.0 and 2.5 were used instead of 1.0, 2.0 and 3.0, all the other mix proportions were nominally the same as those used in the main series. Although all the materials used were from the same source they were not taken from the same batches as those used in the main series and allowance must be made for this when discussing the results in chapter 6.

The deformation reading taken directly after loading was used as the datum for creep measurements and therefore creep results as indicated in Table 5.9 excludes the initial elastic deformation at loading. Corrections were made for changes in moisture content by adjusting readings with values obtained from unloaded cylinders.

The shape, size and distribution of air voids were determined from 20 microscope photographs taken from each foamed concrete mixture. For each mixture the shape, size and distribution of at least 250 voids were measured. The void diameters as indicated in Table 5.10 have been estimated from the area assuming that the voids are circular.

Table 5.10: Void Diameter Distribution.

Mix No	Type of Ash	Target Density (kg/m ³)	a/c	w/c	w/binder	Cumulative Percentage Voids with Diameters Larger				
						100 μ m (%)	200 μ m (%)	300 μ m (%)	400 μ m (%)	500 μ m (%)
7	PFA	1500	1	0.60	0.30	44.92	4.69	0.78	0.00	0.00
8	PFA	1500	2	0.86	0.29	38.69	5.47	1.82	0.36	0.36
9	PFA	1500	3	1.17	0.29	30.65	3.23	1.21	0.81	0.81
10	PFA	1250	1	0.60	0.30	66.79	22.50	7.50	3.93	2.14
11	PFA	1250	2	0.86	0.29	49.36	7.38	0.76	0.00	0.00
12	PFA	1250	3	1.17	0.29	58.78	18.64	8.24	3.94	1.79
13	PFA	1000	1	0.60	0.30	55.54	9.54	1.69	0.62	0.31
14	PFA	1000	2	0.86	0.29	52.45	9.43	0.38	0.00	0.00
15	PFA	1000	3	1.17	0.29	52.76	14.48	5.86	3.45	0.34
19	POZ	1500	1	0.60	0.30	50.44	7.04	1.76	0.59	0.59
20	POZ	1500	2	0.86	0.29	46.82	12.36	2.25	1.12	0.75
21	POZ	1500	3	1.17	0.29	42.75	7.81	1.86	0.37	0.37
22	POZ	1250	1	0.60	0.30	57.01	12.67	4.30	1.13	0.23
23	POZ	1250	2	0.86	0.29	54.05	13.51	2.08	0.21	0.00
24	POZ	1250	3	1.17	0.29	74.21	9.13	1.59	0.40	0.40
25	POZ	1000	1	0.60	0.30	58.86	22.07	8.70	4.68	2.68
26	POZ	1000	2	0.86	0.29	61.03	25.13	8.46	3.08	2.05
27	POZ	1000	3	1.17	0.29	74.01	25.99	9.90	3.96	1.98

CHAPTER 6: DISCUSSION OF RESULTS

6.1 INTRODUCTION

Due to the nature of foamed concrete the results from this work and previous experience has shown that it is not possible to change one parameter without affecting some of the others. This makes analysis and discussion of the results somewhat difficult and this should be borne in mind when reading this chapter.

The parameters that are assumed to have the greatest effect on the properties of foamed concrete are the age, curing regime, water/cement ratio, density, relative density of materials, reactivity of the binder, material grading, void size and void size distribution. The curing conditions were kept constant and the ash samples were taken from a single batch and therefore the grading of the materials were assumed to remain constant. The rest of the listed parameters will be addressed in such a manner that the effect of age and water/cement ratio will be determined from the results of the neat cement pastes before the reactivity (and thus contribution) of the ash is determined from pastes containing varying quantities of the two different ashes. Once the effects of the parameters that affect the properties of the dense cement paste have been quantified, the effect of changing the density by addition of foam will be addressed.

6.2 VOIDS STRUCTURE

6.2.1 Entrained air voids

The foam in foamed concrete is used to contain the air until the surrounding cement paste has set. After about one hour the foam breaks down into water, containing proteins, and air. The water can now partake in the hydration process leaving only the air in the voids. The effects of shape, size and distribution of these voids on the properties of foamed concrete were investigated and will be discussed in this section.

The magnification on the optical microscope that was used to determine the void sizes was chosen such that voids with diameters in excess of 20 μm could be easily identified.

Each photograph that was taken represented an area 1 954 μm wide and 1872 μm high. Twenty photos were taken in a predetermined pattern on one sample from each mixture. The circumference of each void was identified and traced, where after image analysis software was used to automatically calculate the void properties. The fact that entrapped air voids usually have diameters in excess of 1 000 μm and capillary pores usually have diameters smaller than 1 μm , means that by using this manual method of measurement it is highly likely that only the entrained air voids are measured.

6.2.1.1 Void size

An effective diameter was calculated for each void by taking the measured void area and assuming that the void is a perfect sphere. The distribution of void sizes was determined by plotting a histogram of frequency as a function of void diameter. Typical void diameter distributions are indicated in Figures 6.1 and 6.2.

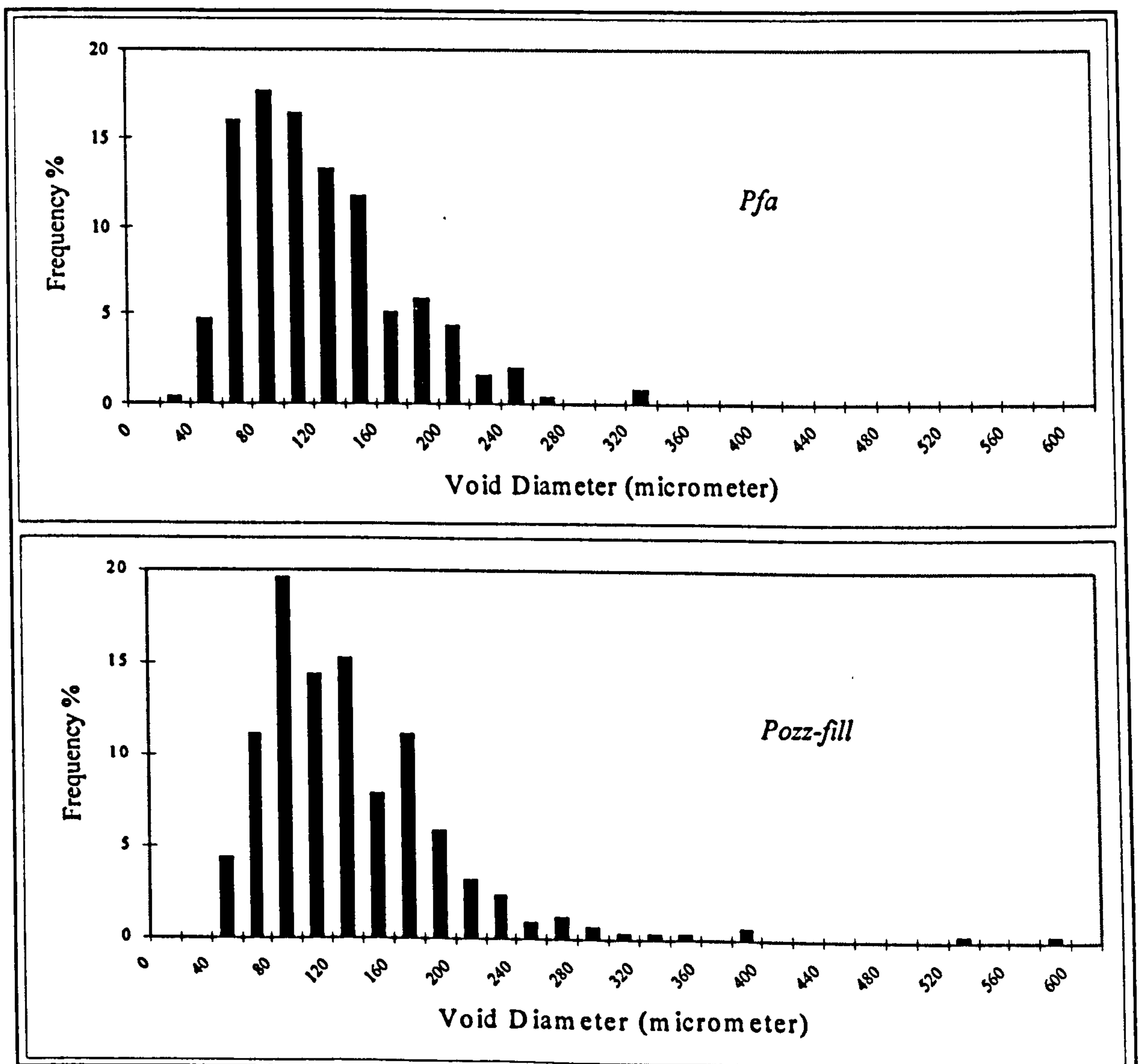


Figure 6.1: Void Diameter Distribution of 1 500 kg/m^3 Mixtures with $a/c=1$.

In Figure 6.1 the top graph gives an indication of the void diameters measured in a foamed concrete mixture with a casting density of $1\,500\text{ kg/m}^3$ and a pfa/cement ratio of 1, while the bottom graph is for a similar mixture containing Pozz-fill instead of pfa. From Figure 6.1 it can be concluded that there is no obvious difference between the void sizes observed in this pfa and this Pozz-fill mixture. The entrained air void diameters measured vary between approximately 40 and 300 μm , indicating, according to Wilk & Dobrolubov²⁷, a good quality air entraining. At lower densities (such as $1\,000\text{ kg/m}^3$) and high ash contents (such as $a/c=3$) there does seem to be a noticeable difference between the two ash types as can be seen in Figure 6.2.

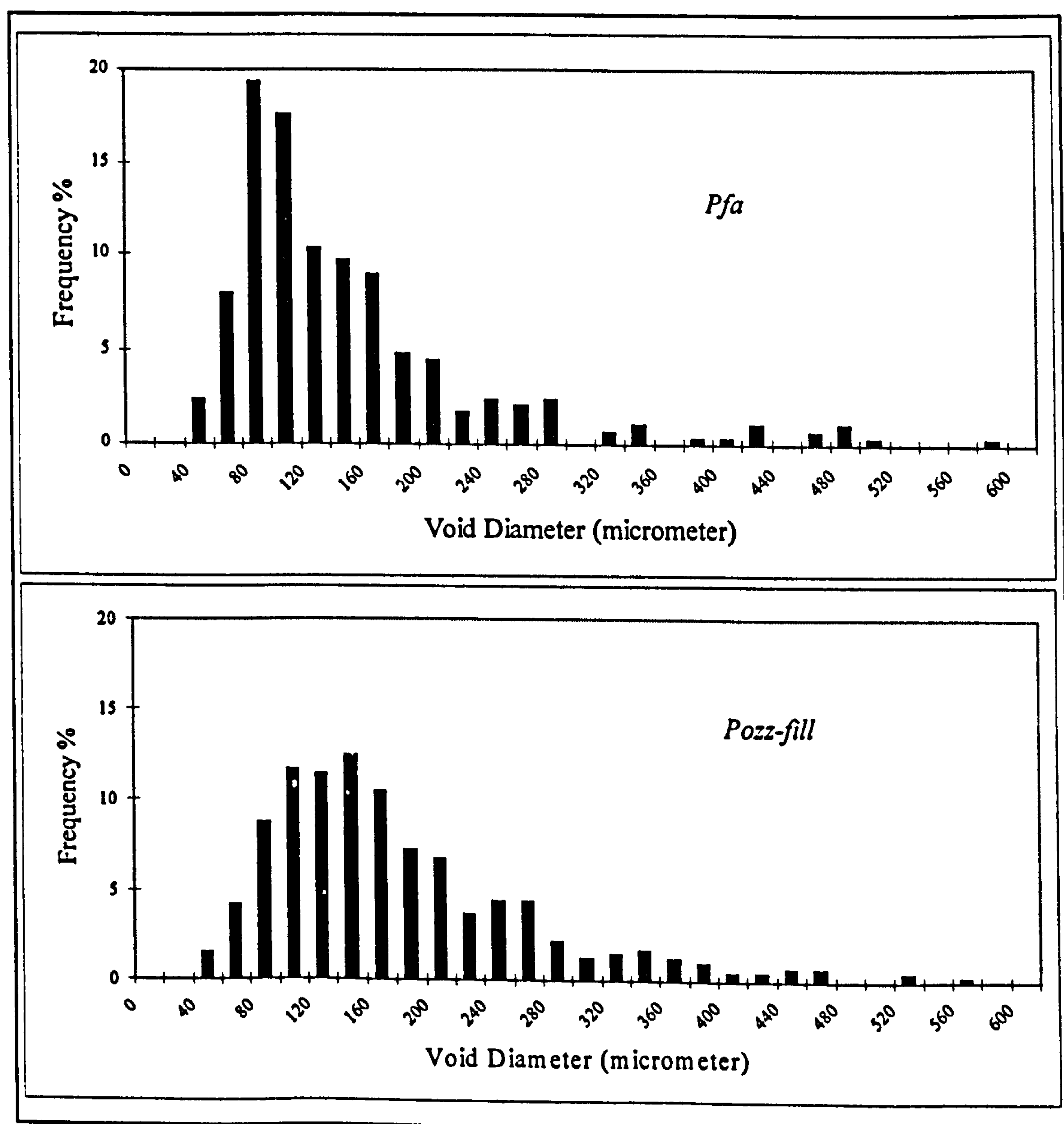


Figure 6.2: Void Diameter Distribution of $1\,000\text{ kg/m}^3$ Mixtures with $a/c=3$.

There appears to be an increase in the number of larger voids (above about 240 micrometer) in the Pozz-fill mixtures compared to that of the pfa.

The distribution in void sizes for all the mixtures is lognormal and a normal distribution can be found by plotting the void diameters on a logarithmic scale. The void diameter distribution of all the foamed concrete mixtures (plotted both on a linear and a logarithmic scale) can be seen in Appendix B.

In order to establish the effect of entrained air void size on the properties of foamed concrete a parameter has to be established that can be used to compare the void sizes of the different mixes. The cumulative void size distribution of each mixture was plotted and these cumulative distributions are attached in Appendix C. As an illustration of the variation in cumulative distribution the values obtained for the mixtures with the frequency distributions as shown in Figure 6.1 and Figure 6.2 are plotted in Figure 6.3. In an attempt to try and make a quantitative comparison between the air void distribution of the different mixes it was decided to calculate:

- (i) The median void size (the diameter for which 50% of the voids have larger diameters).
- (ii) The 90th percentile value (the diameter for which 90% of the voids have smaller diameters).

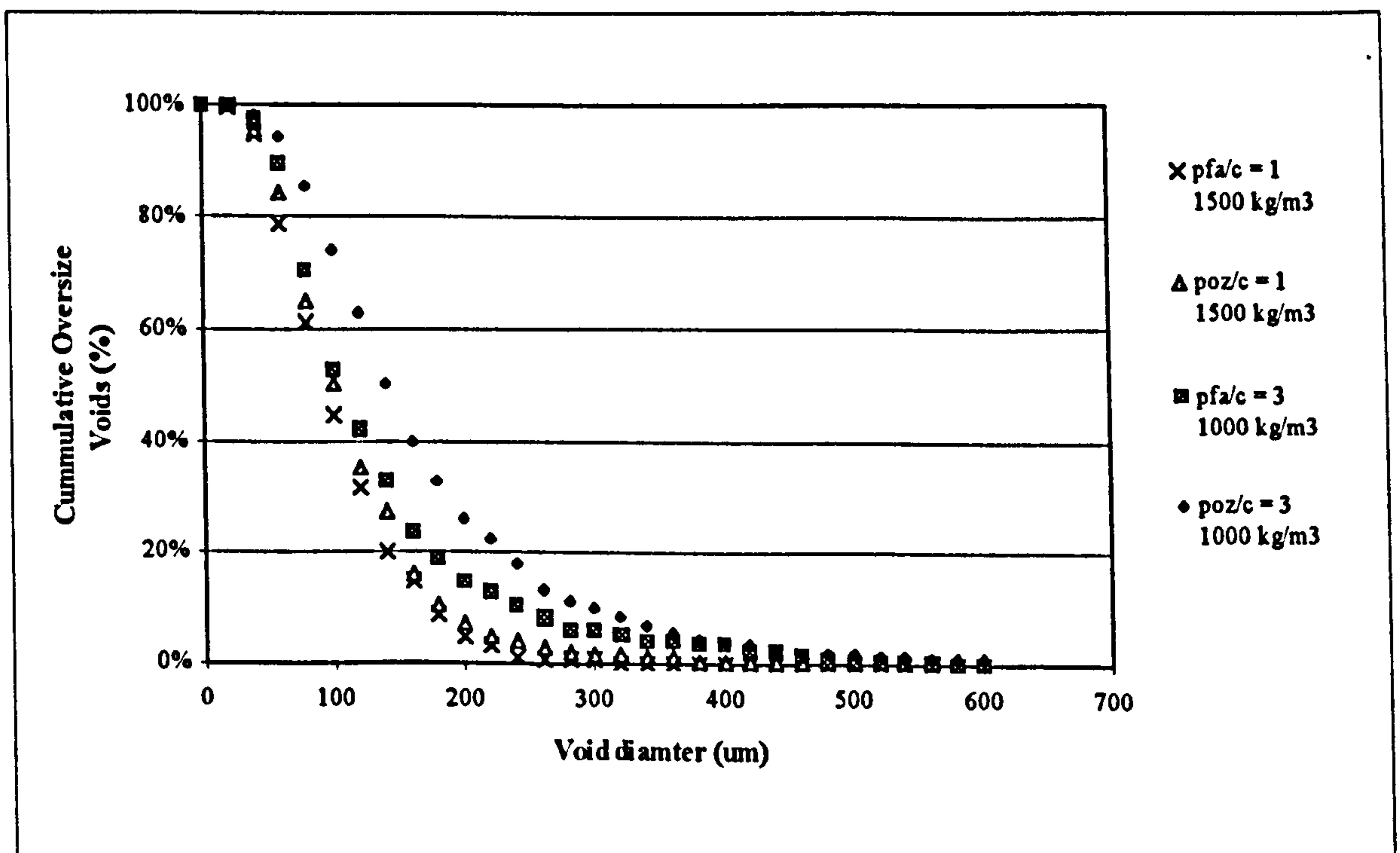


Figure 6.3: Cumulative Void Diameter Distribution.

The 5% largest and the 5% smallest voids that were counted for each mixture were assumed to be statistical outliers and they were not taken into account when an equation was fitted through each of these cumulative distributions. The fitted equations as well as the calculated median and 90th percentile values for all the mixtures are shown in Table 6.1.

Table 6.1: Cumulative Void Diameter Distribution.

Mix nr	Type of Ash	Target Density (kg/m ³)	a/c	Cumulative Distribution Equation: $y = a e^{bx}$ (fraction voids larger)		Median Void Diameter (micrometer)	90 th Percentile of Void Diameter (micrometer)
				a	b		
7	PFA	1500	1	2.201	-0.017	87.2	181.9
8	PFA	1500	2	2.355	-0.019	82.0	167.1
9	PFA	1500	3	2.550	-0.021	76.9	152.8
10	PFA	1250	1	1.937	-0.011	126.6	277.0
11	PFA	1250	2	2.731	-0.017	98.1	191.2
12	PFA	1250	3	1.377	-0.010	105.5	273.2
13	PFA	1000	1	2.754	-0.017	102.8	199.7
14	PFA	1000	2	2.785	-0.017	99.3	192.3
15	PFA	1000	3	1.614	-0.011	102.8	244.0
19	POZ	1500	1	2.844	-0.018	96.6	186.0
20	POZ	1500	2	2.160	-0.015	96.9	203.5
21	POZ	1500	3	2.327	-0.017	89.9	184.0
22	POZ	1250	1	1.963	-0.013	103.6	225.5
23	POZ	1250	2	2.414	-0.015	104.3	210.8
24	POZ	1250	3	4.556	-0.019	118.8	205.3
25	POZ	1000	1	1.359	-0.009	113.6	296.5
26	POZ	1000	2	1.673	-0.010	124.5	290.4
27	POZ	1000	3	1.906	-0.010	135.2	297.7

6.2.1.2 Void spacing

The size of the entrained air voids is not the only aspect of the voids that could affect the properties of the foamed concrete, the void spacing may also have an influence on the material properties. Based on the principle that a chain is only as strong as its weakest link, the minimum paste thickness around each void was established. The area and center-point coordinates of each void were used to establish this minimum paste thickness. The method used to calculate the minimum paste thickness for each void can best be described by referring to the drawing representing the microscopic image of the

best be described by referring to the drawing representing the microscopic image of the voids in Figure 6.4. In this drawing there are three voids, each represented by an x -coordinate, a y -coordinate and a radius (R). The coordinates for each void were obtained directly from the image analysis software while the radii were calculated from the measured areas by assuming that all voids are perfect spheres. The distance between the first and the second void ($S_{1;2}$) in Figure 6.4 can be calculated by using basic trigonometry in the form of the following equation:

$$S_{1;2} = \sqrt{((x_1 - x_2)^2 + (y_1 - y_2)^2)} - R_1 - R_2 \quad (\text{Eq 6.1})$$

Where:

$S_{1;2}$	=	distance between void 1 and void 2
x_1, x_2	=	x -coordinates of void 1 and void 2
y_1, y_2	=	y -coordinates of void 1 and void 2
R_1, R_2	=	radii of void 1 and void 2.

By sequentially replacing the properties of void 2 in Equation 6.1 with each of the voids on the photo the distance between void 1 and each of the other voids can be calculated. These distances are compared and the minimum distance is recorded as the space between void 1 and its closest neighbour. After determining the minimum spacing for void 1 the procedure can be repeated for each of the other voids.

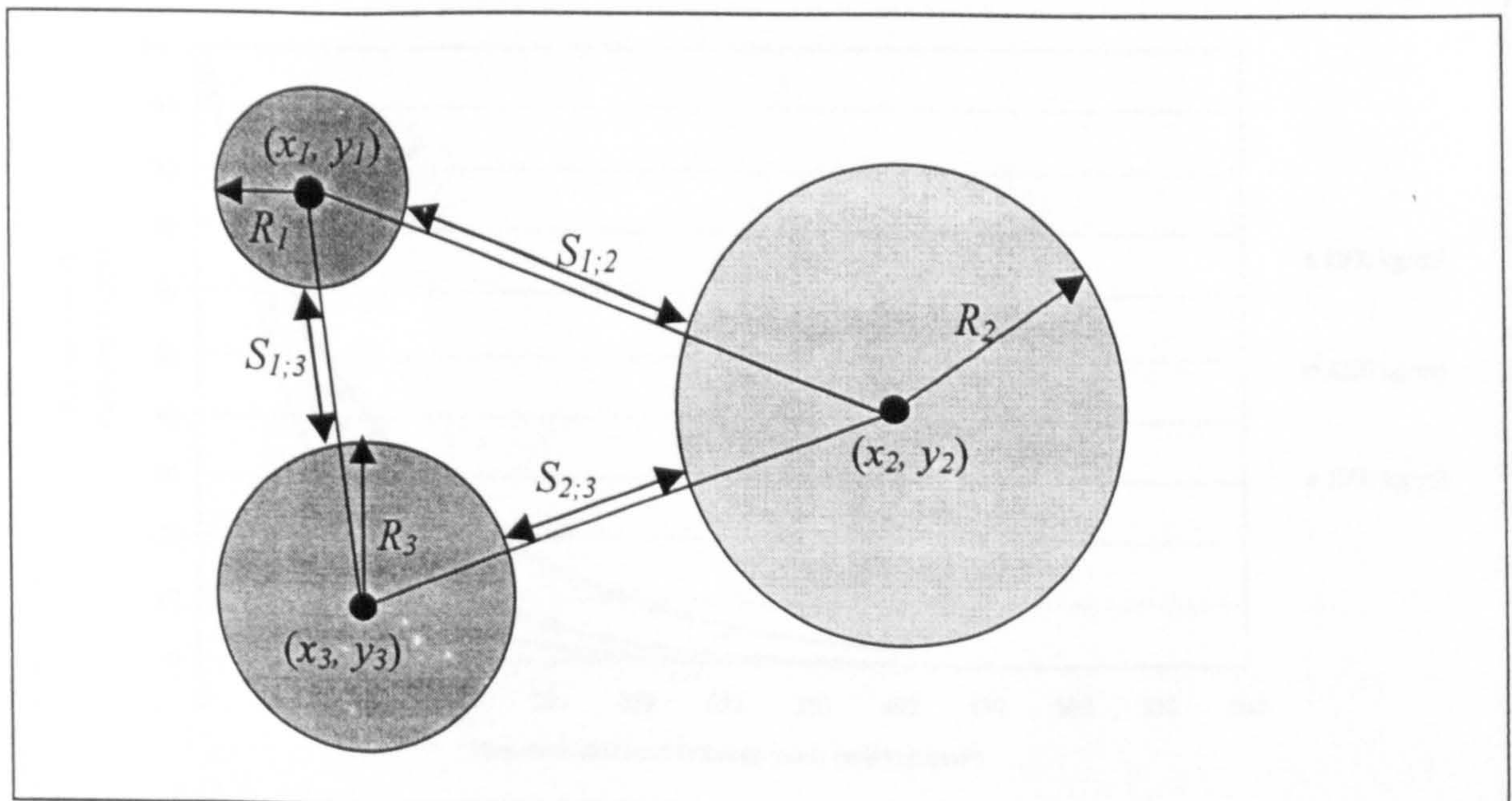


Figure 6.4: Calculation of Void Spacing.

The image analysis software produces a text file listing the properties of each void on every photograph and these text files were imported into spreadsheets using Microsoft Excel. A macro was written in excel (see Appendix D) to take each void and calculate the thickness of the paste between that void and all the other voids. These calculated values were compared and the minimum space between voids was noted as the minimum paste thickness around that void. The cumulative frequency distribution of the minimum void spacing was determined for each mixture and as can be seen from Figure 6.5 the cumulative frequency of the space between voids follows an exponential distribution.

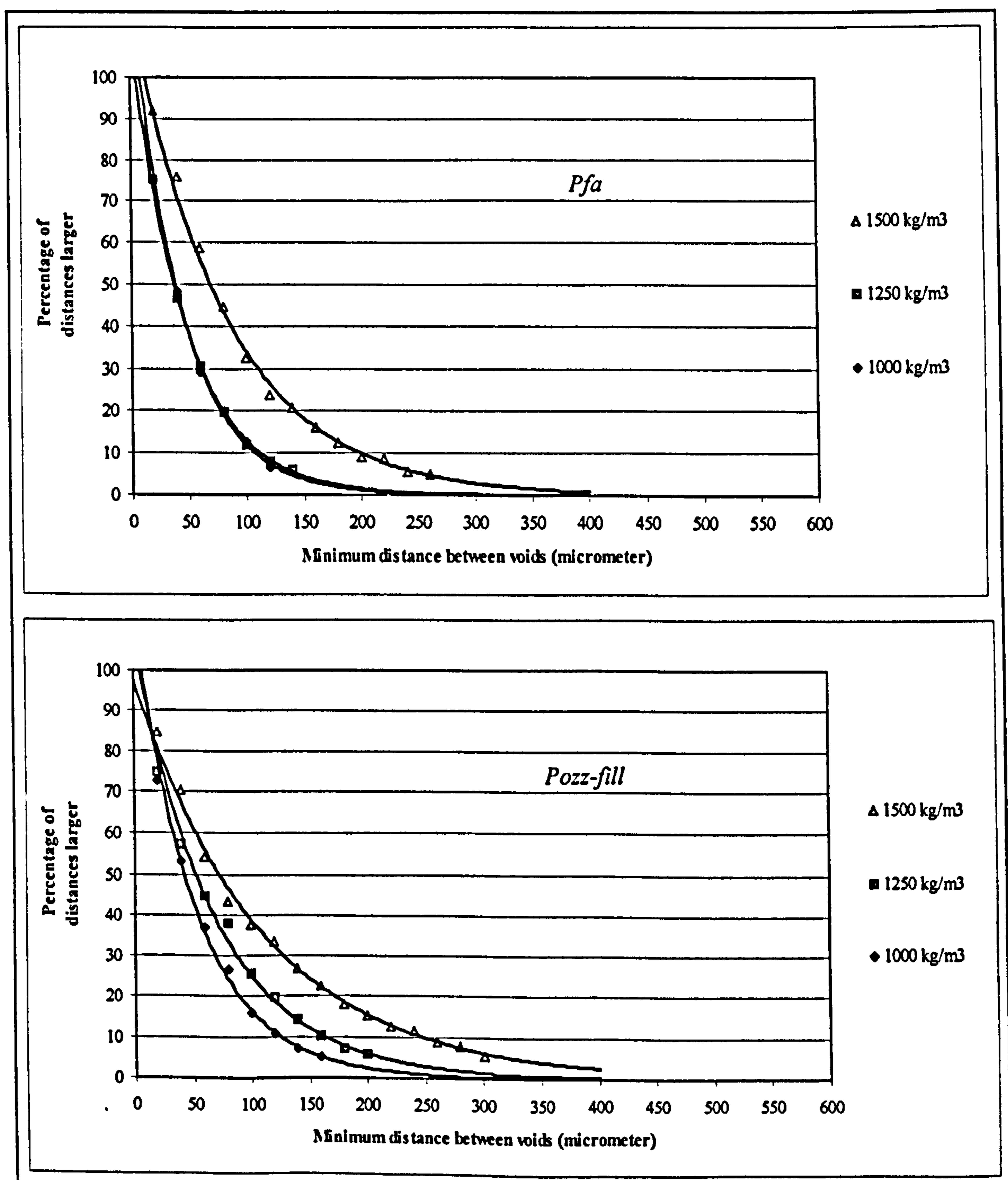


Figure 6.5: Distance between Voids for Mixture with $a/c = 2$.

The distributions that are shown in Figure 6.5 are the minimum distances between voids for mixtures with an ash/cement ratio of 2 and target densities of 1500, 1250 and 1000 kg/m³. The values in the top graph were obtained for mixtures containing pfa and those in the bottom graph for mixtures containing Pozz-fill. From these two sets of frequency distributions it can be seen that the distance between voids tend to be smaller in the mixture with the lower densities. Most of the voids in the higher density mixtures tend to be less than about 350 µm apart whereas this distance decreases to less than about 200 µm for the mixtures with the lower density. This trend can be expected as more foam is used in lower density mixtures, resulting in more voids, which would be closer to each other. The type of ash used does not seem to have a significant effect on the distances between voids. The cumulative frequency distribution of distances between voids for all the foamed concrete mixtures can be seen in Appendix E.

The void spacing was treated in a similar way to void size in an attempt to quantify the effect on the concrete properties. Regression analysis was used to fit exponential functions through these distributions for all the foamed concrete mixtures. Provision was made for statistical outliers by omitting the top and bottom 5%, in other words the 5% voids with the smallest distance to their nearest neighbour and the 5% voids with the largest distance to their nearest neighbour. These functions were used to calculate a median minimum distance between voids (where 50% of the minimum distances between voids are smaller than the value) as well as a 10th percentile (where 10% of the minimum distances are smaller than the value) for each mixture. The constants obtained for the fitted functions, the R-squared values as well as the calculated median and 10th percentile values are summarized in Table 6.2.

6.2.1.3 Relation between dry density and void size

The effect of the dry density, ash type and ash/cement ratio on the median void size and the void size distribution (or 90th percentile of void diameter) are shown in Figure 6.6. From these graphs it can be seen that the voids are smaller in the mixtures with the higher dry densities, irrespective of the ash/cement ratio or type of ash used. Both the median and the 90th percentile void diameter decrease with increasing dry density. Between nominal dry densities of 750 kg/m³ and 1000 kg/m³ the decrease is marginal but between 1000 kg/m³ and 1250 kg/m³ it is much more significant. One possible

reason for the larger voids in the low-density mixtures is that there are more voids in these mixtures and therefore there is a greater possibility of the voids merging. The general trend seems to indicate a larger median void size in mixtures containing pozz-fill. The ash/cement ratio does not seem to have a distinguishable effect on the air void sizes.

Table 6.2: Distance between Voids.

Mix Nr	Type of Ash	Target Density (kg/m ³)	a/c Ratio	Fitted Cumulative Distance Distribution Equation: $y = a e^{bx}$ (% distances larger)			Median Distance between Voids (micrometer)	10 th Percentile of Distances between Voids (micrometer)
				a	b	R ²		
7	PFA	1500	1	110.67	-0.0122	0.993	65.1	16.9
8	PFA	1500	2	116.92	-0.0123	0.995	69.1	21.3
9	PFA	1500	3	135.84	-0.0105	0.993	95.2	39.2
10	PFA	1250	1	104.8	-0.0101	0.997	73.3	15.1
11	PFA	1250	2	110.04	-0.0213	0.996	37.0	9.4
12	PFA	1250	3	120.11	-0.0122	0.994	71.8	23.7
13	PFA	1000	1	104.53	-0.0213	0.997	34.6	7.0
14	PFA	1000	2	122.07	-0.0233	0.995	38.3	13.1
15	PFA	1000	3	115.07	-0.0127	0.986	65.6	19.3
19	POZ	1500	1	117.22	-0.0119	0.988	71.6	22.2
20	POZ	1500	2	97.593	-0.0092	0.997	72.7	8.8
21	POZ	1500	3	111.68	-0.0083	0.996	96.8	26.0
22	POZ	1250	1	107.57	-0.0146	0.995	52.5	12.2
23	POZ	1250	2	117.21	-0.0168	0.987	50.7	15.7
24	POZ	1250	3	130.83	-0.0115	0.990	83.6	32.5
25	POZ	1000	1	117.68	-0.0127	0.940	67.4	21.1
26	POZ	1000	2	115.25	-0.0195	0.997	42.8	12.7
27	POZ	1000	3	102.68	-0.0155	0.996	46.4	8.5

6.2.1.4 Relation between dry density, ash/cement ratio and void distribution

The effect of density on the void distribution can be seen in Figure 6.7, where the median and 10th percentile distances between voids are plotted as a function of dry

density. The median distance between voids tend to increase with increasing density confirming that fewer entrained air voids would be situated further apart in the cement paste. The large variation in 10th percentile distances at high dry density, seems to indicate that the distribution of voids becomes more random with a decreasing number of voids being present.

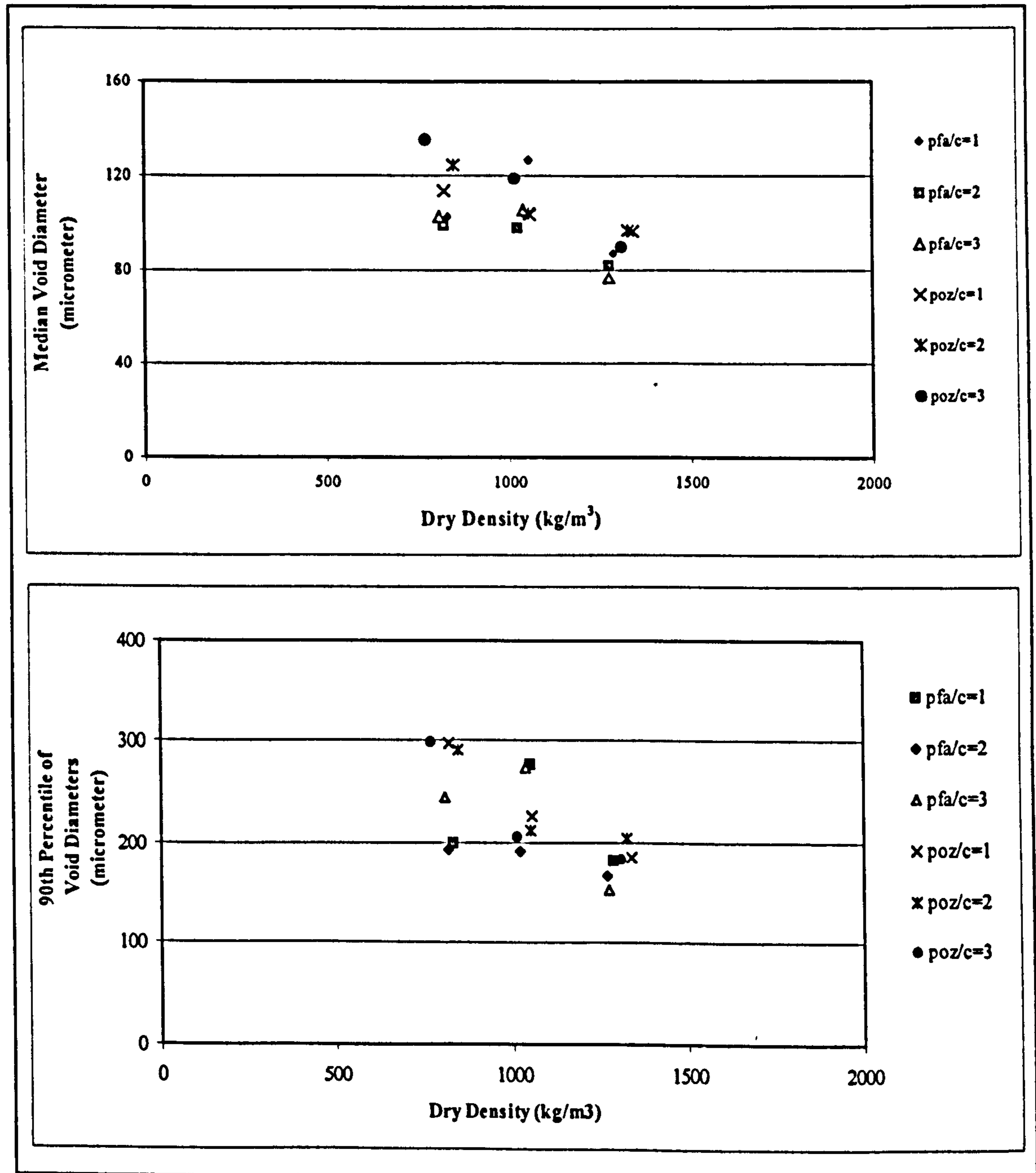


Figure 6.6: Effect of Dry Density on Entrained Air Void Size.

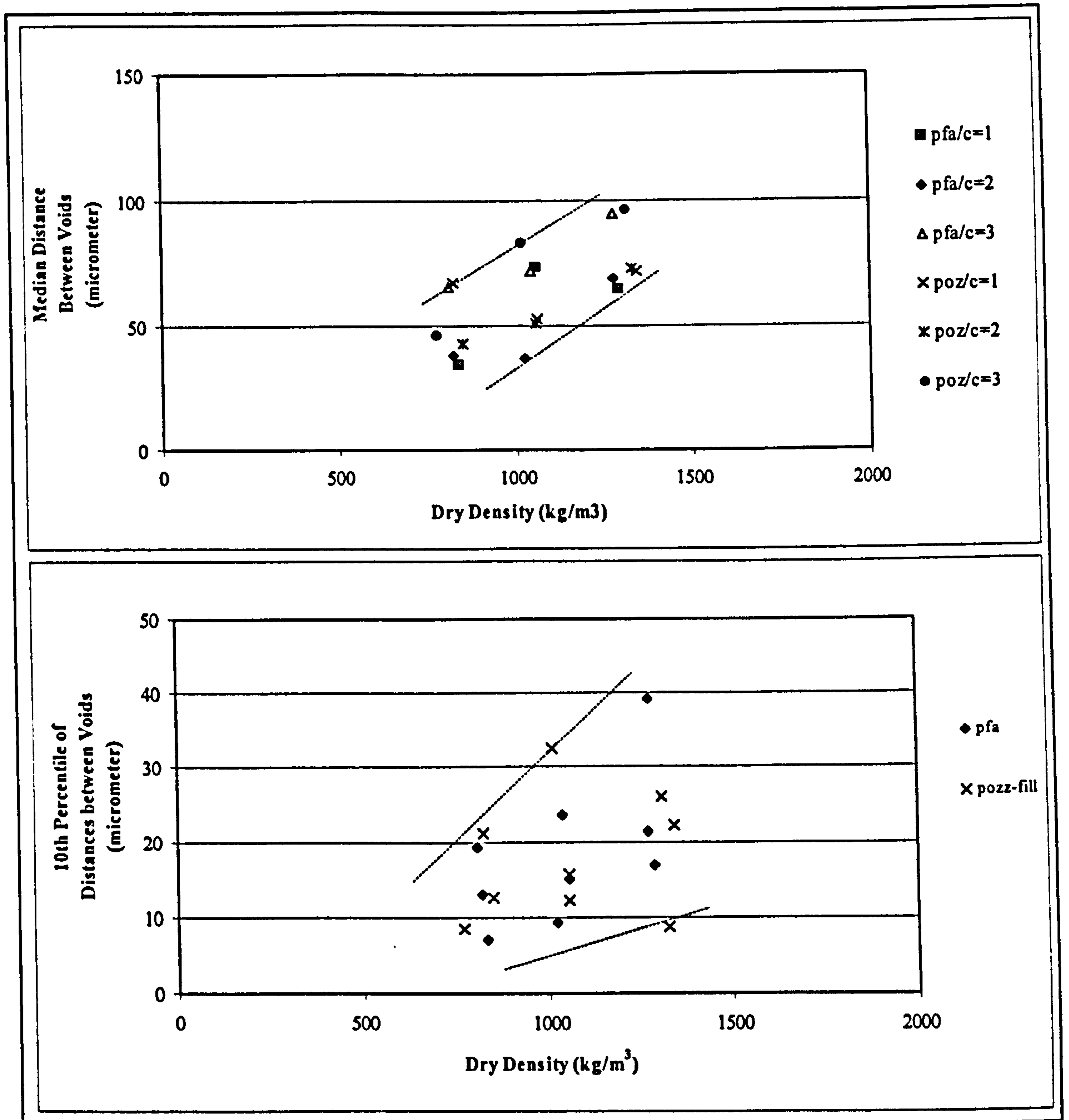


Figure 6.7: Effect of Dry Density on the Distance between Voids.

The graphs in Figure 6.7 confirm that there is no noticeable difference between the void spacing of mixtures containing pfa and those containing Pozz-fill. There seems to be a slight increase in the minimum distance between voids with increasing ash/cement ratio. This increase in distance between voids could be caused by the fact that the mixtures containing large volumes of ash requires less foam to be added for a certain density. Less foam would result in fewer air voids that should be further apart.

The effect of ash/cement ratio on the distance between voids can be seen more clearly in Figure 6.8. Both the median distance between voids and the 10th percentile of distances between voids indicate that the voids are further apart in the mixtures with ash/cement ratios of 3. The large variation in 10th percentile distances at this high ash content seems to indicate a larger variation in void distribution at higher ash content.

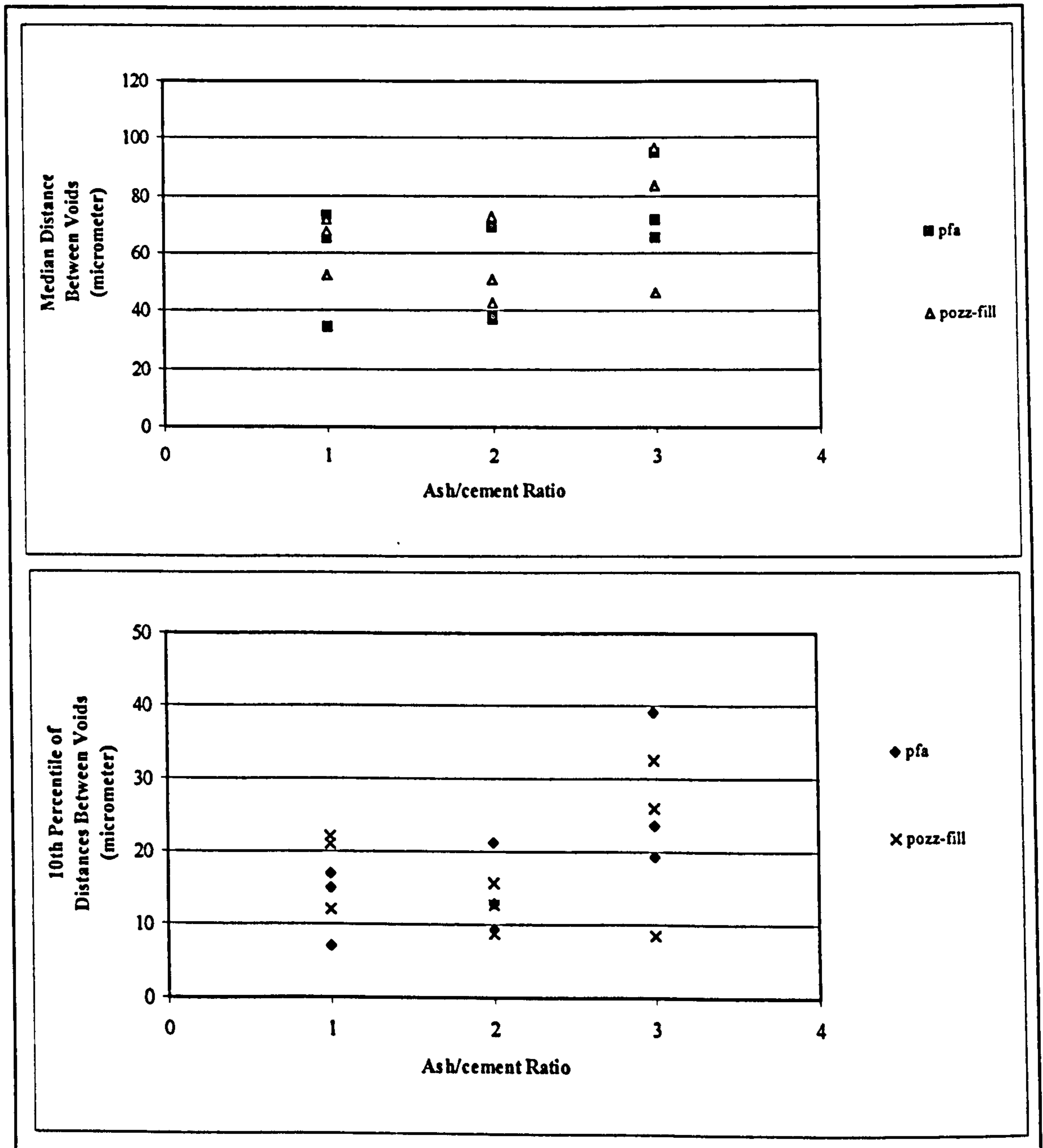


Figure 6.8: Effect of Ash/cement Ratio on Distance between Voids.

6.2.1.5 Combined particle size, void size and distribution

Increased void content can manifest itself in larger diameter voids or more voids of similar diameter with reduced distances between them or perhaps a combination of both. To establish whether there is any relation between the void diameters and the void spacing the distance between voids was plotted as a function of void diameter in Figure 6.9. In the top graph of this figure the distances between voids is plotted as a function of the median void diameter while they are plotted as a function of the 90th percentile of void diameter in the bottom graph. From these graphs it can be seen that there does seem to be a reduction in median distance between voids for increased void diameter. This indicates that increased void content manifests itself as a combination of increased diameter and reduced spacing.

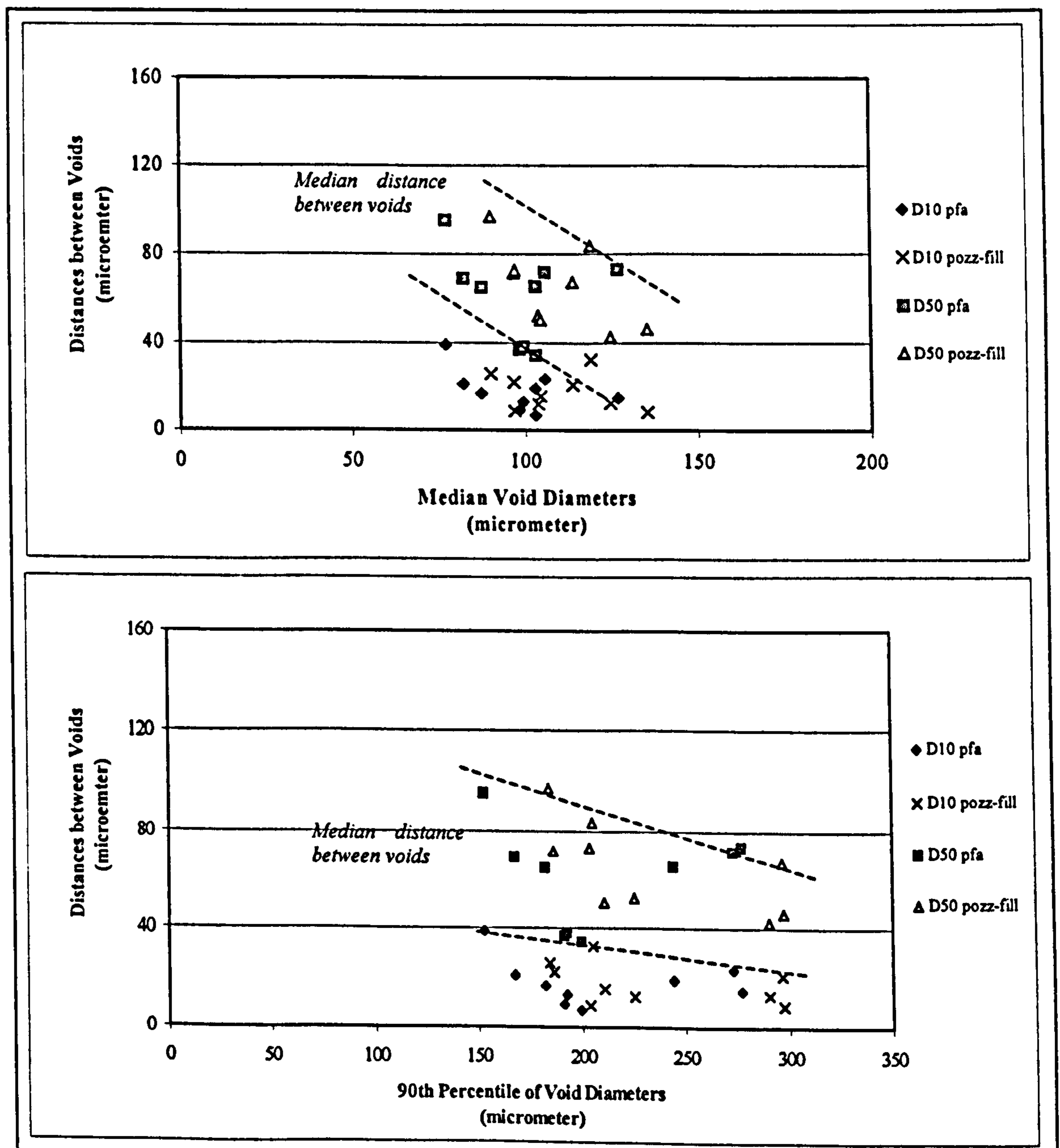


Figure 6.9: Relation between Air Void Diameter and Air Void Spacing.

The diameters measured for the entrained air voids are in the same order of magnitude as the particle sizes of the cement, pfa and pozz-fill as recorded in Chapter 4. The particle sizes of the cement and ash could therefore have a significant effect on the size and the shape of the air voids that are formed during initial set of the foamed concrete. If the particles used are relatively coarse and single sized a smaller number of large voids are likely to be left between these particles and these voids will initially be filled with foam. As the foam starts breaking down the bubbles will tend to merge together resulting in larger bubbles with a high circularity factor (far from circular). If however the particles are relatively fine and varied in size, the particles will have a higher packing density with a larger number of smaller voids, the voids formed by the foam will be less likely to merge resulting in smaller voids with lower circularity factors.

In an effort to establish the effect of particle size distribution of the solids on the void sizes, the particle size distributions of the cement, pfa and pozz-fill were used and the effective binder particle size distributions were calculated for ash/cement ratios of 1, 2 and 3. The effect of binder particle size on the void size and distribution can be seen in Figure 6.10 where both the 90th percentile of the void diameters and the 10th percentile of distances between voids are plotted as functions of the 90th percentile of the binder particle size (the diameter for which only 10% of the binder particles have larger diameters). These graphs clearly indicate that neither the void diameter nor the distances between voids is significantly influenced by the binder particle size. The fact that no trend was observed could be because the variation in binder particle size is not sufficient to affect the voids and the effect of particle size on void size and distribution could become more noticeable if a wider range of binder particle sizes were used.

As the binder particle size does not seem to influence the void sizes the question arises whether the void sizes follows a predictable trend at all. To establish the existence of any trend the total particle size distribution of each mixture was determined. This total particle size distribution is a combination of the binder and the void size distributions. The volumetric mix proportions (as indicated in Chapter 5) were used to combine the particle size distribution of the binder with the measured entrained air void size distribution of each mixture. The cumulative percentages of these combined particle size distributions of all 18 foamed concrete mixtures are plotted as a function of the particle size in Figure 6.11.

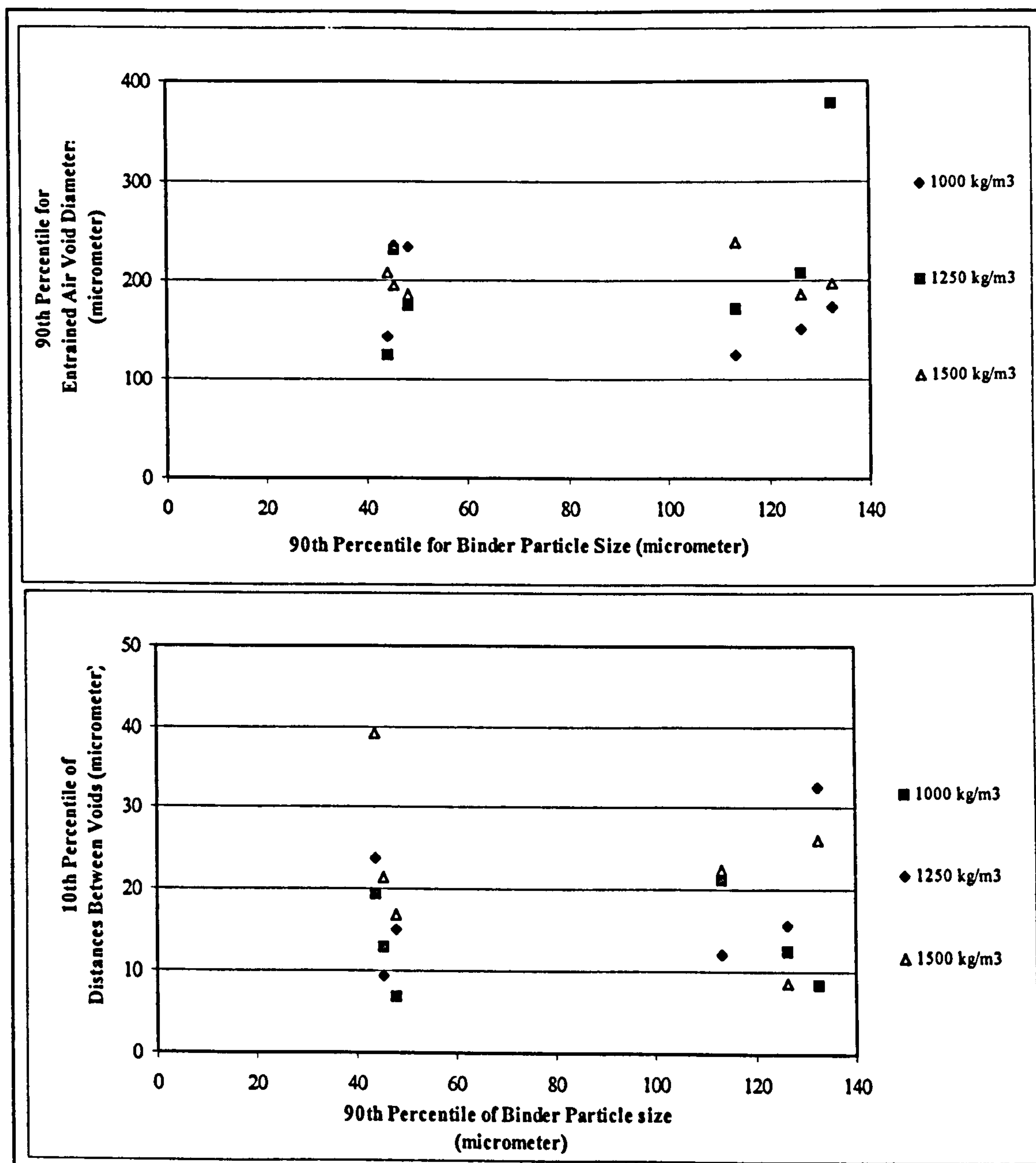


Figure 6.10: Effect of Binder Particle Size on Void Size and Distribution.

The values as plotted in Figure 6.11 indicate that the total particle size distribution of the different mixtures fall within a relatively narrow band. These distributions can best be described with power functions and regression analysis was used to determine an optimum function for each mixture. These functions and the correlating R-squared values are listed in Table 6.3. The particle size distributions of the different mixtures can be compared to each other by comparing the median particle diameters as calculated using the fitted equations.

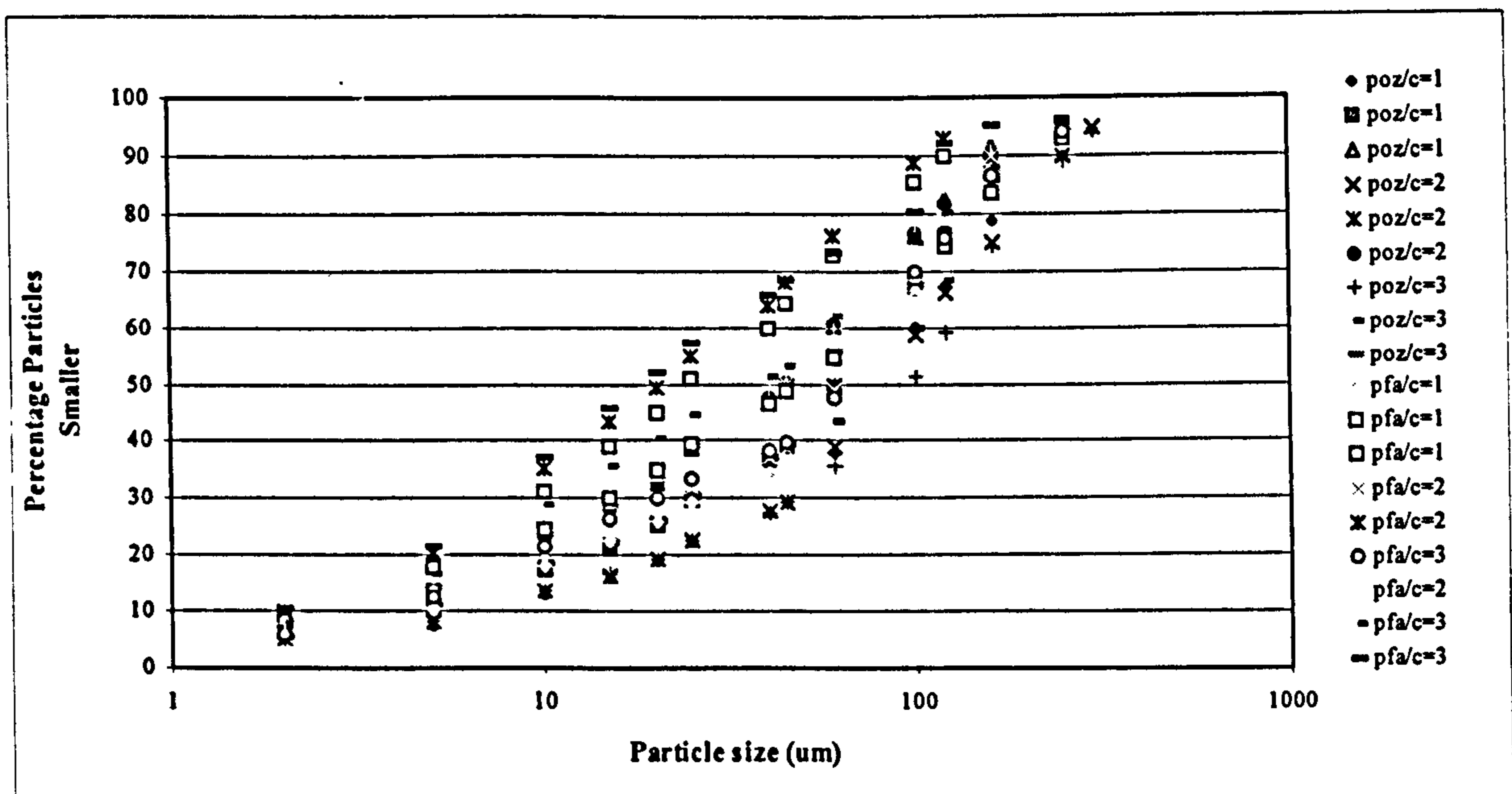


Figure 6.11: Combined Binder and Void Sizes.

The effect of dry density on the median combined particle size can be seen in Figure 6.12. From this graph it can be seen that the mixtures with lower densities have larger median particle diameters. As the binder size remains unchanged it can be assumed that this increase in particle size is caused by the increase in larger voids. It is interesting to note that there is a very strong relationship between dry density and median particle size, indicating that the void sizes are not random but predictable for a given density and binder particle size distribution. The particle sizes of the pfa blends are smaller than those of the Pozz-fill and therefore the lower median particle diameter for pfa as indicated in Figure 6.12 could be expected.

It is worth noting (Figure 6.12) that the difference between the combined particle size of the pfa and the Pozz-fill increases with decreasing density. Since the volume of binder decreases with decreasing density one would expect the difference to remain constant or decrease with decreasing density. At this stage no explanation can be given for this trend and a larger variety of binder particle sizes will have to be used to determine whether this trend is significant.

From Figure 6.12 it can also be seen that the effect of ash content on the combined binder and void particle sizes is negligible for the range of ash/cement ratios used in this investigation.

Table 6.3: Particle and Void Size Functions.

Mix nr	Type of Ash	Target Density (kg/m ³)	a/c	Y=mx ^c			Median Combined Particle Diameter (micrometer)
				c	m	R ²	
4	PFA	FULL	1	18.94	1.0461	0.9582	12.5
5	PFA	FULL	2	20.751	0.9927	0.9559	11.3
6	PFA	FULL	3	21.591	0.9695	0.9545	10.8
7	PFA	1500	1	11.763	1.2558	0.9858	23.7
8	PFA	1500	2	13.583	1.1955	0.9889	19.6
9	PFA	1500	3	14.715	1.1386	0.9918	18.7
10	PFA	1250	1	8.8268	1.3114	0.9814	42.6
11	PFA	1250	2	10.188	1.266	0.9773	33.6
12	PFA	1250	3	11.076	1.2134	0.985	31.9
13	PFA	1000	1	3.821	1.814	0.9613	62.0
14	PFA	1000	2	7.2857	1.3679	0.9467	59.6
15	PFA	1000	3	7.6759	1.3544	0.9541	54.0
16	POZ	FULL	1	12.623	1.2249	0.9818	21.7
17	POZ	FULL	2	12.704	1.2036	0.9853	22.7
18	POZ	FULL	3	12.737	1.1939	0.9864	23.2
19	POZ	1500	1	8.0432	1.3942	0.9673	40.8
20	POZ	1500	2	8.6619	1.3415	0.9667	40.2
21	POZ	1500	3	8.9936	1.3069	0.9727	41.1
22	POZ	1250	1	7.2857	1.3679	0.9467	59.6
23	POZ	1250	2	6.4833	1.4212	0.9436	67.3
24	POZ	1250	3	6.8641	1.3519	0.9497	77.0
25	POZ	1000	1	2.0815	2.1397	0.9619	82.9
26	POZ	1000	2	2.3073	2.0677	0.96	83.6
27	POZ	1000	3	2.4805	1.9939	0.9571	91.0

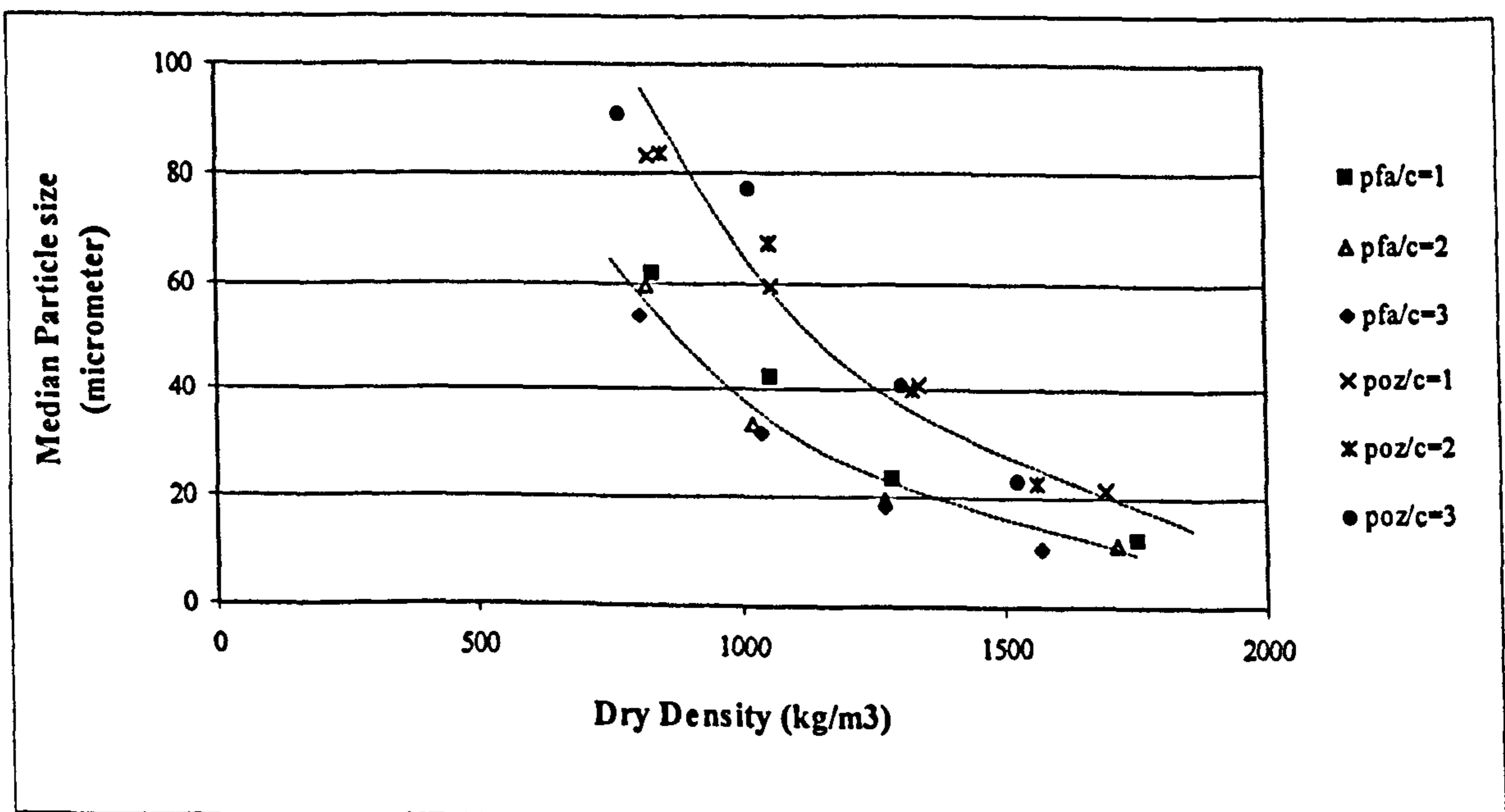


Figure 6.12: Effect of Dry Density on Median Combined Particle Size.

6.2.2 Porosity

The porosity of the foamed concrete is the sum of the air voids and the voids in the paste. The relation between dry density and porosity can be seen in Figure 6.13. From this graph it can be seen that porosity is largely dependant on dry density and not on ash type or ash content. The porosities as shown in Figure 6.13 vary between 29% (for cement paste with a water/cement ratio of 0.3) and 67% (for foamed concrete with a casting density of 1000 kg/m³ and a pfa/cement ratio of 3). The lowest porosity, at 29%, was measured for the cement paste with a water/cement ratio of 0.3 containing no ash. This value correlates well with the 28% porosity that is characteristic of the volume of gel water in fully hydrated cement paste.⁶ The cement paste with a water/cement ratio of 0.6 has a porosity of 40% which is virtually the same as the porosity of the foamed concrete mixtures with a casting density of 1 500 kg/m³ and an ash/cement ratio of 3. The expected reduction in porosity with increased ash content as reported by other researchers^{6, 34, 52} was not observed here because unlike other workers the authors mixes were based on equal water/binder ratio and not on equal workability.

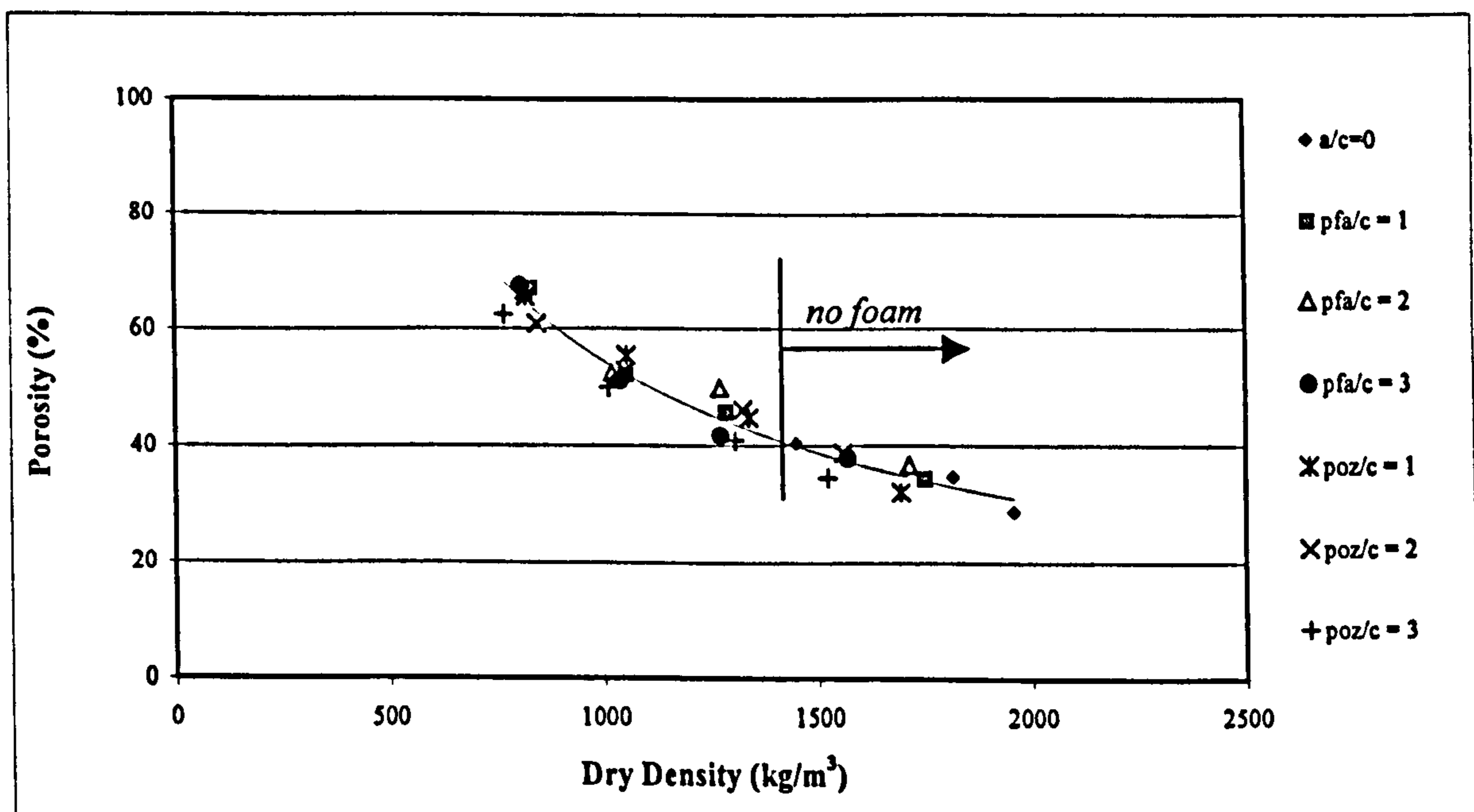


Figure 6.13: Porosity as a Function of Dry Density.

The porosity of foamed concrete as a function of the dry density (as shown in Figure 6.13) can best be described using the following equation:

$$\rho = 18665 \gamma_d^{-0.844}$$

Where:

$$\begin{aligned} \rho &= \text{porosity (\%)} \\ \gamma_d &= \text{dry density (kg/m}^3\text{)}. \end{aligned}$$

Regression analysis indicates that comparing the actual measured porosities to the values calculated using equation Eq 6.10 yields an R-squared value of 0.95, indicating a relatively strong relation between dry density and porosity.

The relation between the porosity of foamed concrete and the air void size and distribution can be seen in Figure 6.14 where the void sizes and the distances between voids are plotted as a function of porosity. From this graph it can be seen that although there is no marked difference in the relationship between porosity and median void size of mixtures containing pfa and those containing Pozz-fill, the large voids in the Pozz-fill mixtures (90th percentile) seem to be larger than that of pfa mixtures at any porosity. Porosity increases with increases in both the median and the 90th percentile of the void size. From the bottom graph in Figure 6.14 it can be concluded that smaller distances between voids result in increased porosity. Both the median distance between voids and the least distance between voids (as expressed by the 10th percentile value) decreases with increased porosity.

There is some doubt as to what happens to the water that is added to the mixtures as part of the foam. The water/cement ratio that was used for a certain ash/cement ratio was constant for different densities cast and therefore the porosity of the paste fractions of one ash/cement ratio should not vary. The foam does however contain approximately 70 kg of water per cubic meter of foam. When the foam breaks down this water becomes available to partake in the hydration process. Depending on when the foam actually breaks down this water can be mixed in, thereby affecting the porosity of the paste, or this water can be trapped in the air voids, which should not affect the porosity of the paste. The porosity of the paste fraction of each mixture can be estimated by subtracting the volume of air voids from the measured porosity and then dividing the remaining porosity by the fraction of the mixture that consists of paste. The calculated paste porosities for the different mixtures is plotted as a function of ash/cement ratio in

Figure 6.15. From the graph in Figure 6.15 it can be seen that the mixtures with a relatively high foam content (1000 kg/m^3 mixtures) tend to have higher paste porosities than the corresponding cement paste without foam. This increase in porosity with increased foam content suggests that some of the water in the foam is contributing to the water/ cement ratio of the mixture thus increasing the paste porosity. The porosity of the paste in the foamed concrete mixtures with higher densities is marginally lower than the porosity of the pastes containing no foam. A possible explanation for this slight reduction in porosity is that the water in the foam is trapped in the air voids and when the hydration products are formed they grow into these voids, thus reducing the actual air void volumes. It is therefore probably not the paste that is less porous but the volume of the air voids that is slightly over estimated by using the volumetric proportions.

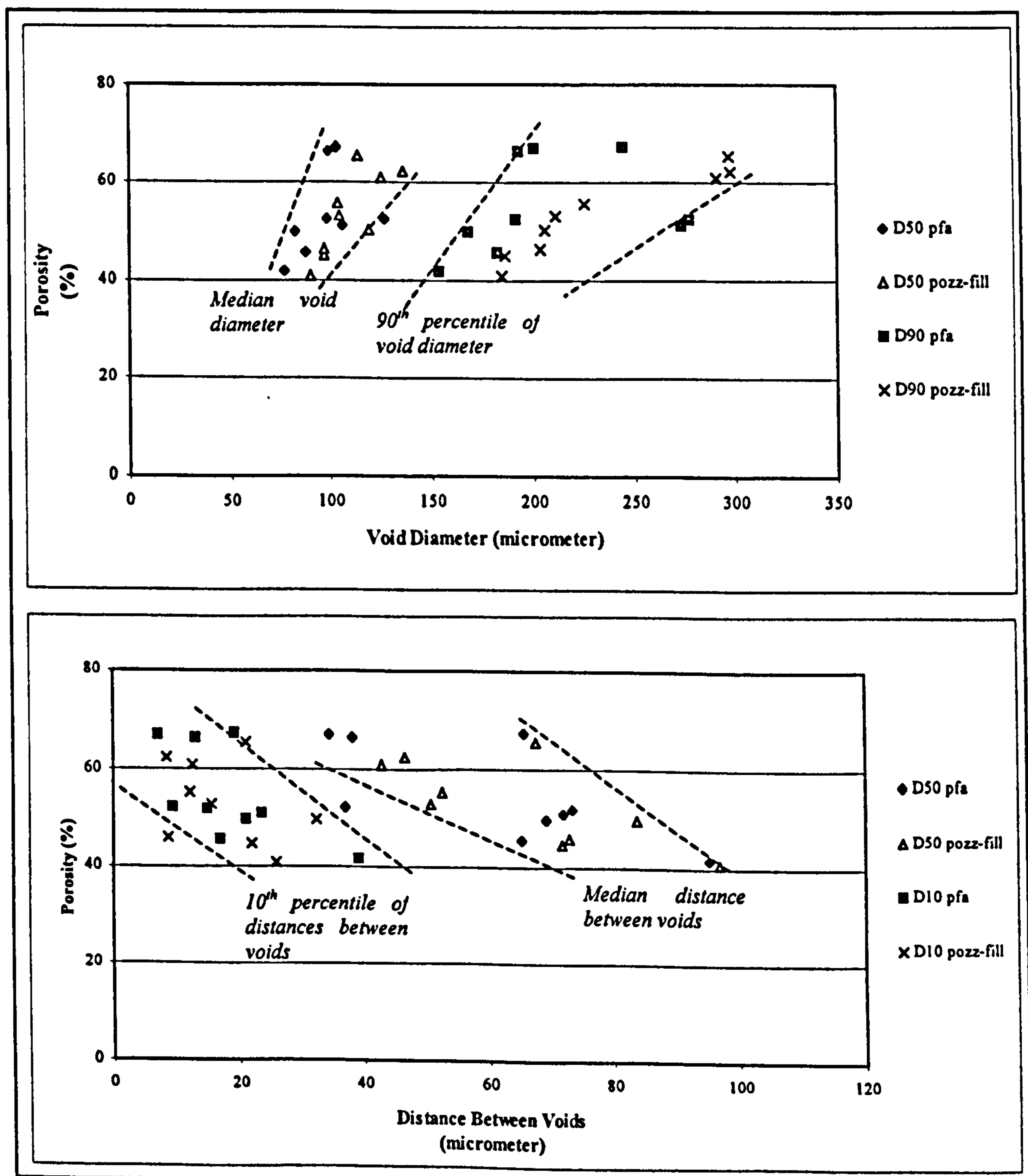


Figure 6.14: Effect of Porosity on Air Void Size and Distribution.

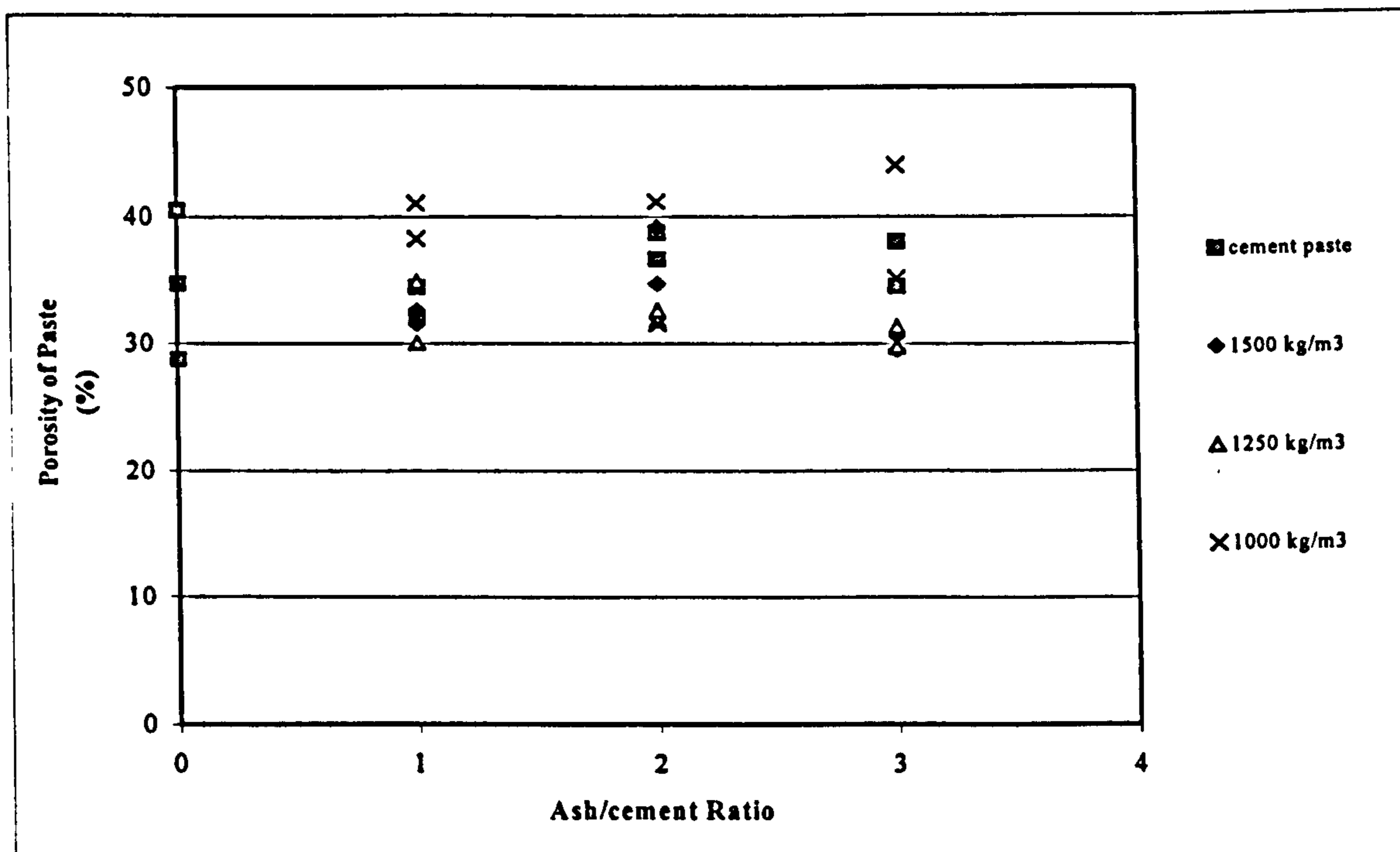
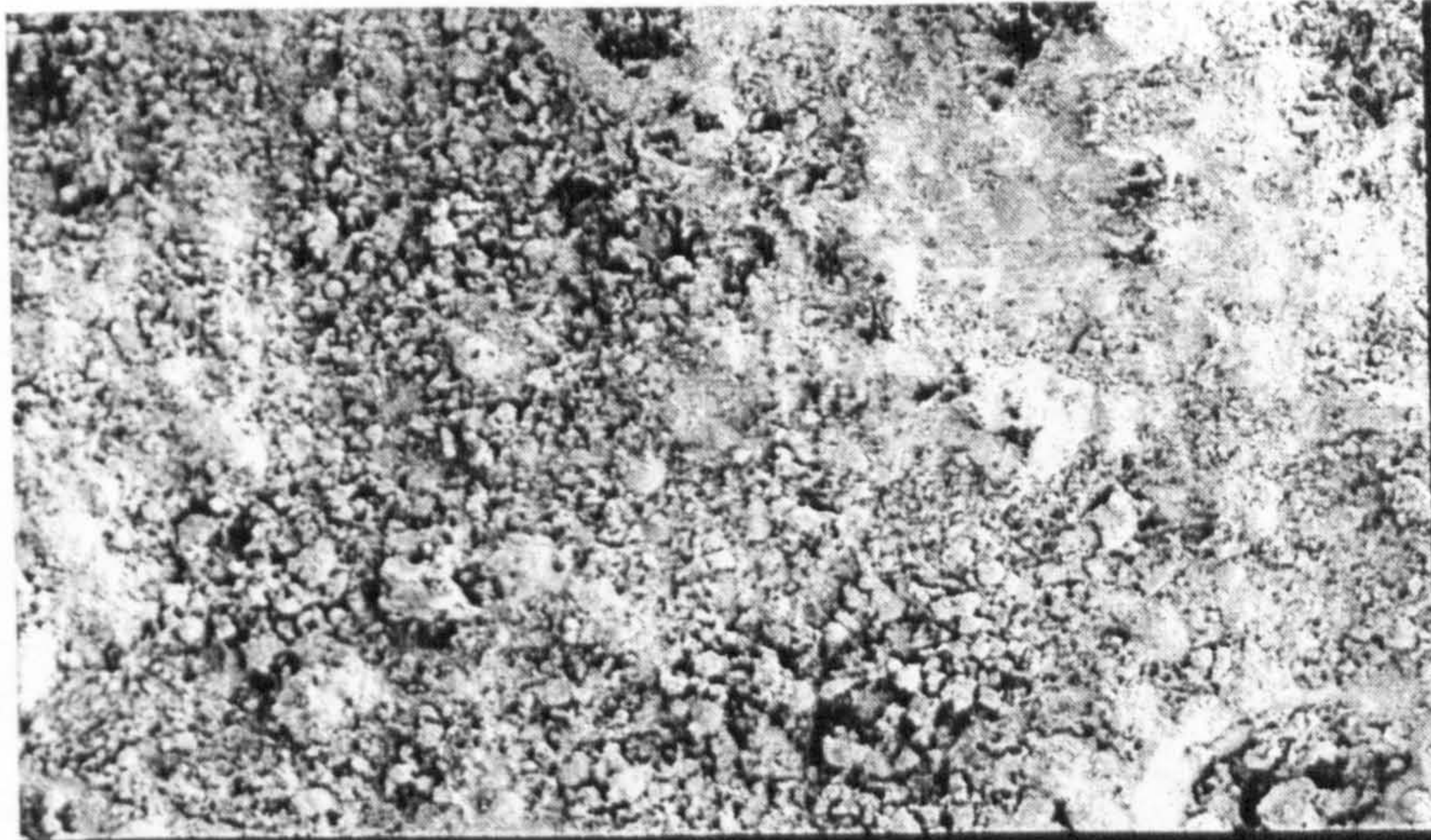
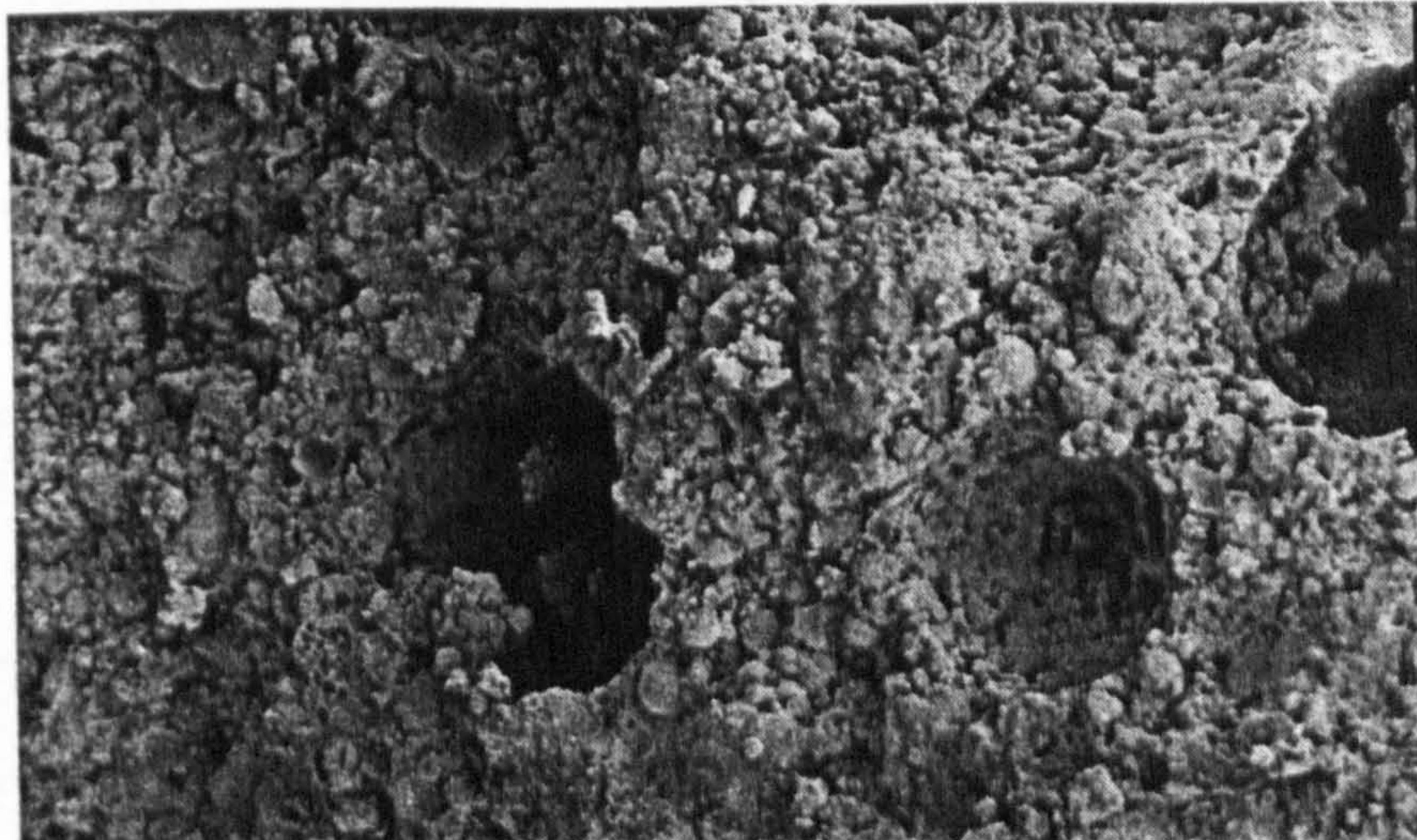


Figure 6.15: Effect of Ash/cement Ratio on Paste Porosity.

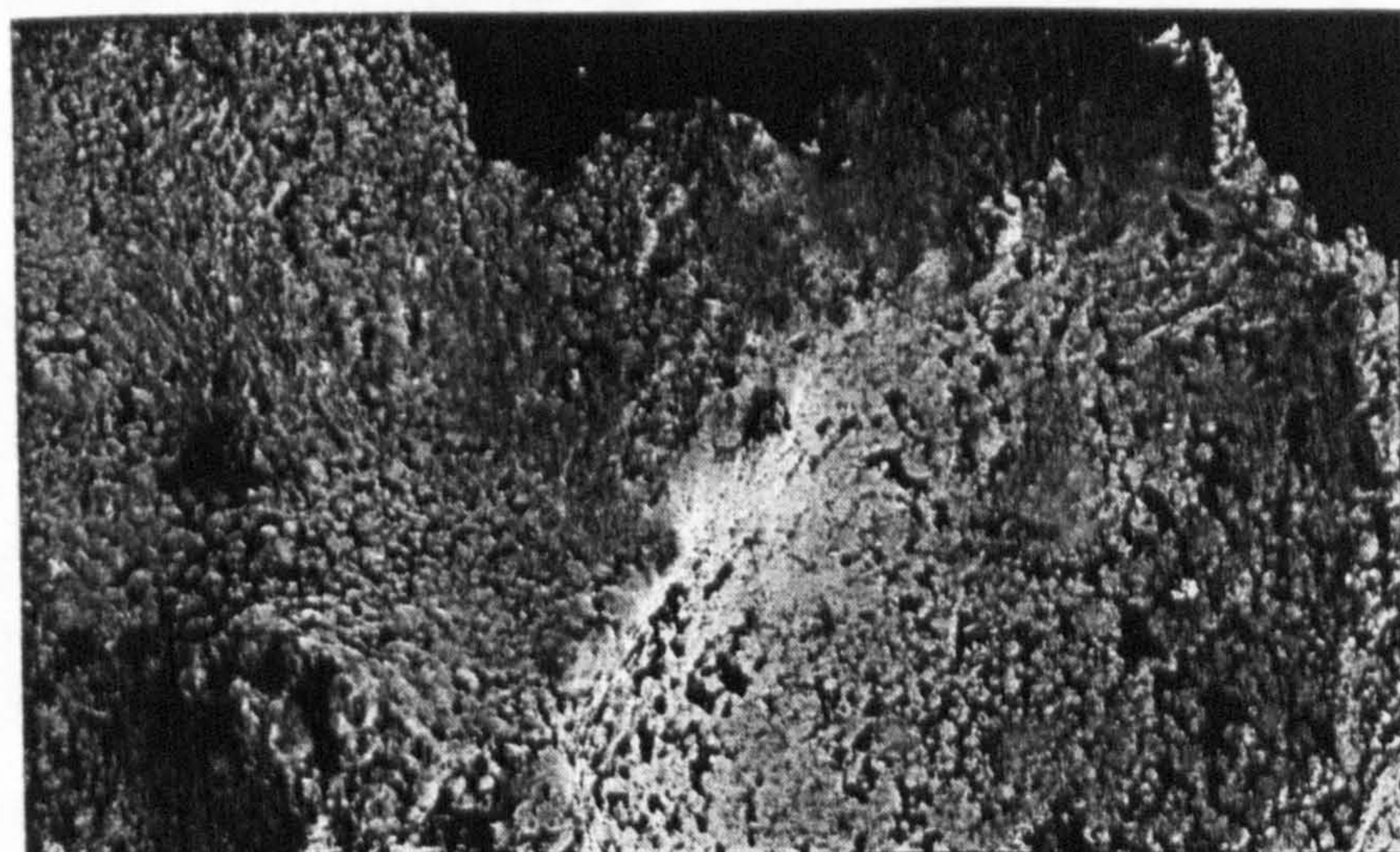
In an effort to confirm the postulation as explained above scanning electron microscope (SEM) photographs were taken. The photographs in Plate 6.1 and Plate 6.2 were taken from mixtures with a pfa/cement ratio of 3 at different magnifications. The first photo in each plate is that of the mixture containing no foam, the second photo is that of the 1500 kg/m³ mixture and the third photo was taken of the 1000 kg/m³ mixture. The lowest possible magnification (in the region of 400 times) was used to obtain the photos in Plate 6.1 and in these photos the porosity of the paste can be seen. The air voids in the second and third photo on this plate can clearly be seen and while the edge of the air voids in the 1500 kg/m³ mixture is clearly defined and fairly smooth the edges of the voids in the 1000 kg/m³ mixture are more rugged and less uniform. The shape of the edge of the voids does seem to indicate that at higher densities (such as 1500 kg/m³) the paste set around the foam bubbles before the foam broke down, while at lower densities a degree of foam breakdown had to occur before the paste set, resulting in the rugged edges. With decreasing density the paste seems to become more coarse and the paste at lower density does seem to be more porous. The effect of density (or foam content) on the porosity of the paste can be seen in Plate 6.2 where the magnification was increased to 5000 times. From the SEM photographs in Plate 6.2 it can be seen that there is no noticeable difference in paste porosity between the full density paste and the foamed concrete with a target density of 1500 kg/m³.



No Foam



1500 kg/m³



1000 kg/m³

Plate 6.1: SEM photos of Paste, 1500 kg/m³ and 1000 kg/m³ Mixtures with pfa/c = 3 ($x \pm 400$).

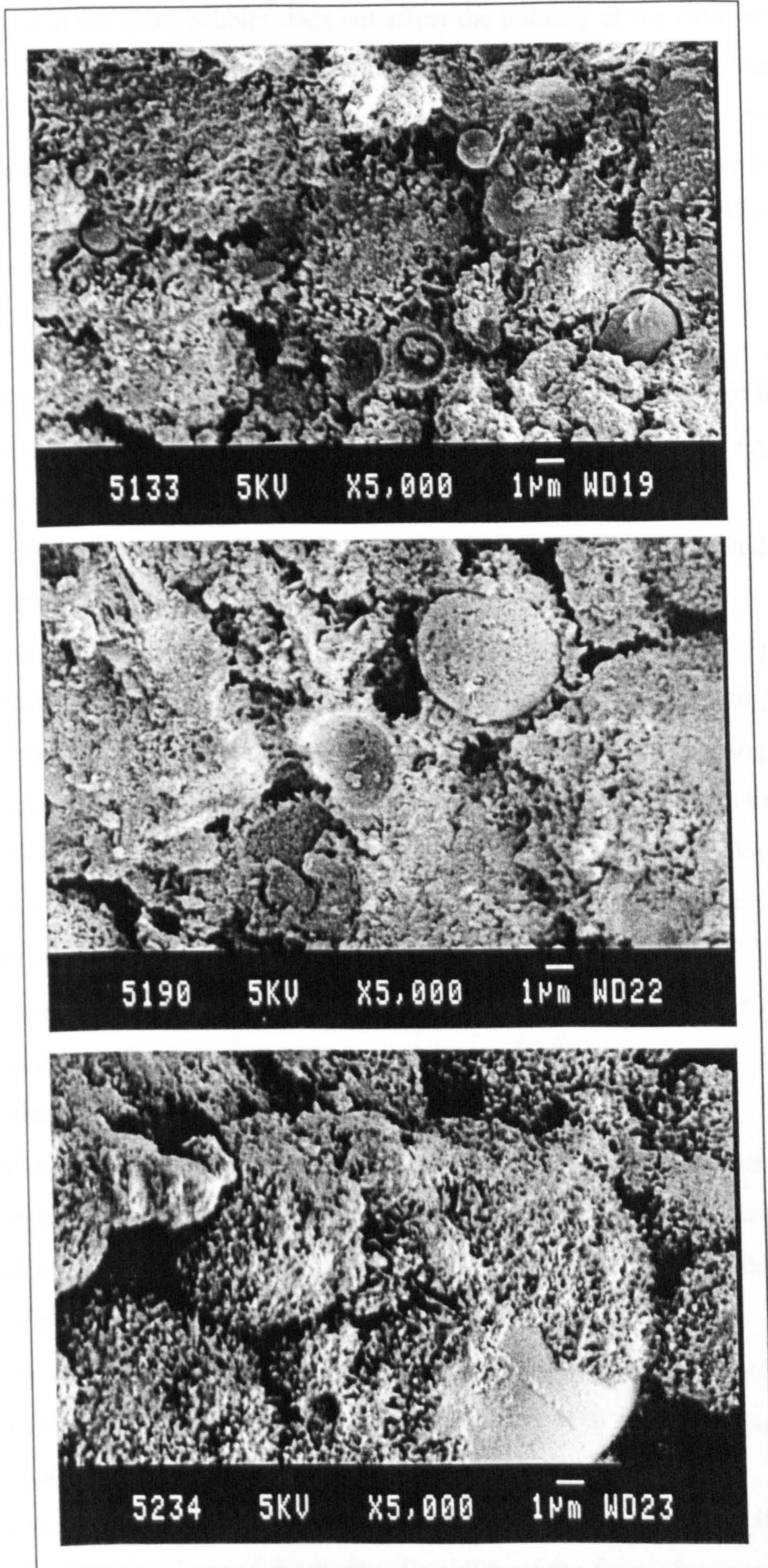


Plate 6.2: SEM photos of Paste, 1500 kg/m³ and 1000 kg/m³ Mixtures with pfa/c = 3 (x 5 000).

These photographs do seem to confirm that at relatively high density the water contained in the foam bubbles does not affect the porosity of the paste surrounding the voids. The third photograph in Plate 6.2 clearly shows that the paste in the $1\,000\text{ kg/m}^3$ mixture seems to be much coarser and more porous than the paste in the mixtures containing less foam. It is therefore probable that at relatively low target densities, the water contained in the foam bubbles does increase the porosity of the cement paste surrounding the air voids.

6.2.3 Conclusions on voids

- The distribution in size of the air voids in the foamed concrete under investigation is log normal. The majority of the air voids have diameters of less than $300\mu\text{m}$, indicating a good quality air entraining.
- A decrease in dry density results in an increase in entrained air void diameters and a decrease in distances between voids.
- Although there is no noticeable difference at relatively high casting densities (say above 1250 kg/m^3) between the void sizes in the mixtures containing pfa and those containing pozz-fill the voids in the mixtures with lower casting densities that contains pozz-fill seems to be larger than those in the mixtures containing pfa.
- The binder particle size (for the range used in this investigation) does not influence the void diameters or the distances between voids. The ash type or content does not appear to have a significant effect on the entrained air void size and distribution.
- Porosity is largely dependant on dry density and not on ash type or content.
- Void diameters increases with increased porosity.
- Distances between voids decreases with increased porosity.
- At high porosities the calculated paste porosity is higher than the porosity of the cement paste containing no foam. It is therefore possible that some of the water added to mixtures as part of the foam is increasing the effective water/binder ratio of the paste surrounding the entrained air voids.
- The casting densities and mix proportions used in this investigation were chosen within the range where the foaming agent had been proven to yield stable foam. Although the effect of the voids is minimal in this investigation, the voids could have a significant effect on the properties of foamed concrete if mixtures were manufactured closer to the limits of stability of the foam (for example much lower casting densities or higher ash contents).

6.3 COMPRESSIVE STRENGTH

6.3.1 Cement paste

The compressive strengths of the cement pastes as a function of time are shown in Figure 6.16. From this graph it can be seen that, as expected, the compressive strength increases rapidly during the first 28 days where after the increase in strength is only marginal. As expected an increase in water/cement ratio results in a decrease in compressive strength. The mixture with a water/cement ratio of 0.6 gains about 14.5 MPa in strength between the age of 28 days and 365 days while the mixture with the water/cement ratio of 0.3 only gains 6.5 MPa. This indicates that more water was available for later age hydration in the mixtures with the higher water/cement ratio.

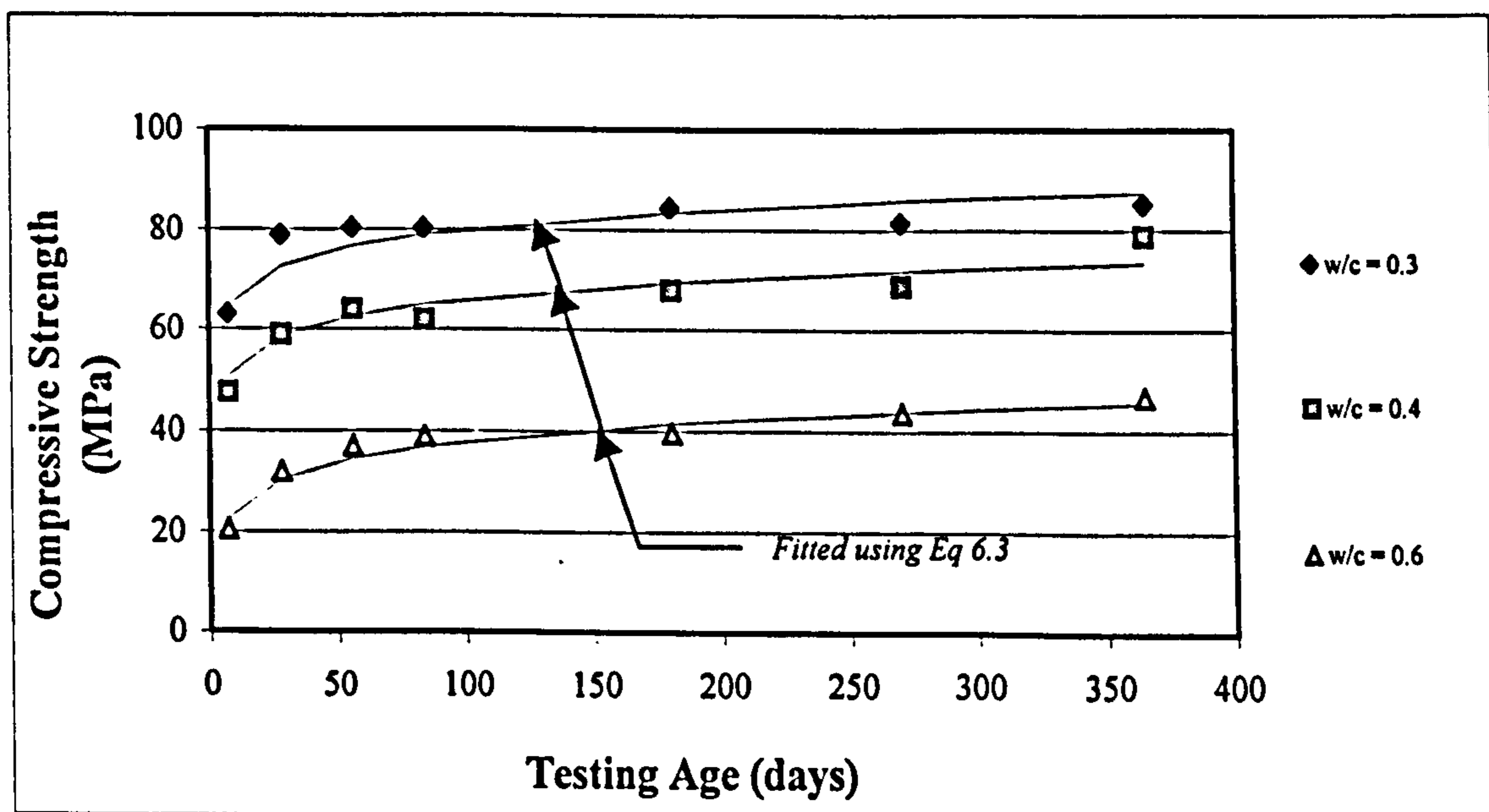


Figure 6.16: Compressive Strength of Cement Paste as a Function of Time.

6.3.2 Pastes containing ash

From literature ^{6,21,41,45,55,56} it is clear that pulverized coal ash on its own does not hydrate, and a paste containing only water and ash will never gain strength. When ash is added to a cement paste it can therefore be assumed that initially the gain in strength is caused by the hydration of the cement and the ash acts as filler. As time passes, the ash starts contributing towards the strength, and although a certain percentage of the ash will always merely act as filler, an increasing percentage of the ash acts as a cement-extender. The compressive strength of mixtures containing pfa is plotted as a function of time in Figure 6.17. Although the ash/cement ratio of these mixtures varies from 1 to 3,

the water/binder ratio was kept constant at approximately 0.3. From this graph it is clear that the compressive strength of these mixtures increase over a much longer period of time than that of mixtures containing no ash. The gain in strength between 28 days and 365 days is 37 MPa and 44 MPa for the mixtures with the pfa/cement ratios of 1 and 2 respectively. After 270 days the mixtures with pfa/cement ratios of 1 and 2 have reached compressive strengths of approximately 80 MPa, which is similar to the compressive strength of the cement paste (containing no ash) with the water/cement ratio of 0.3 at the same age. After a period of one year the mixture with the pfa/cement ratio of 3 yields a compressive strength of 58 MPa, which is significantly lower than the other mixtures (at ± 80 MPa). From the results as indicated in Figure 6.17 the difference in strength between this mixture and the mixtures with pfa/cement ratios of 1 and 2 remains virtually unchanged, regardless of age.

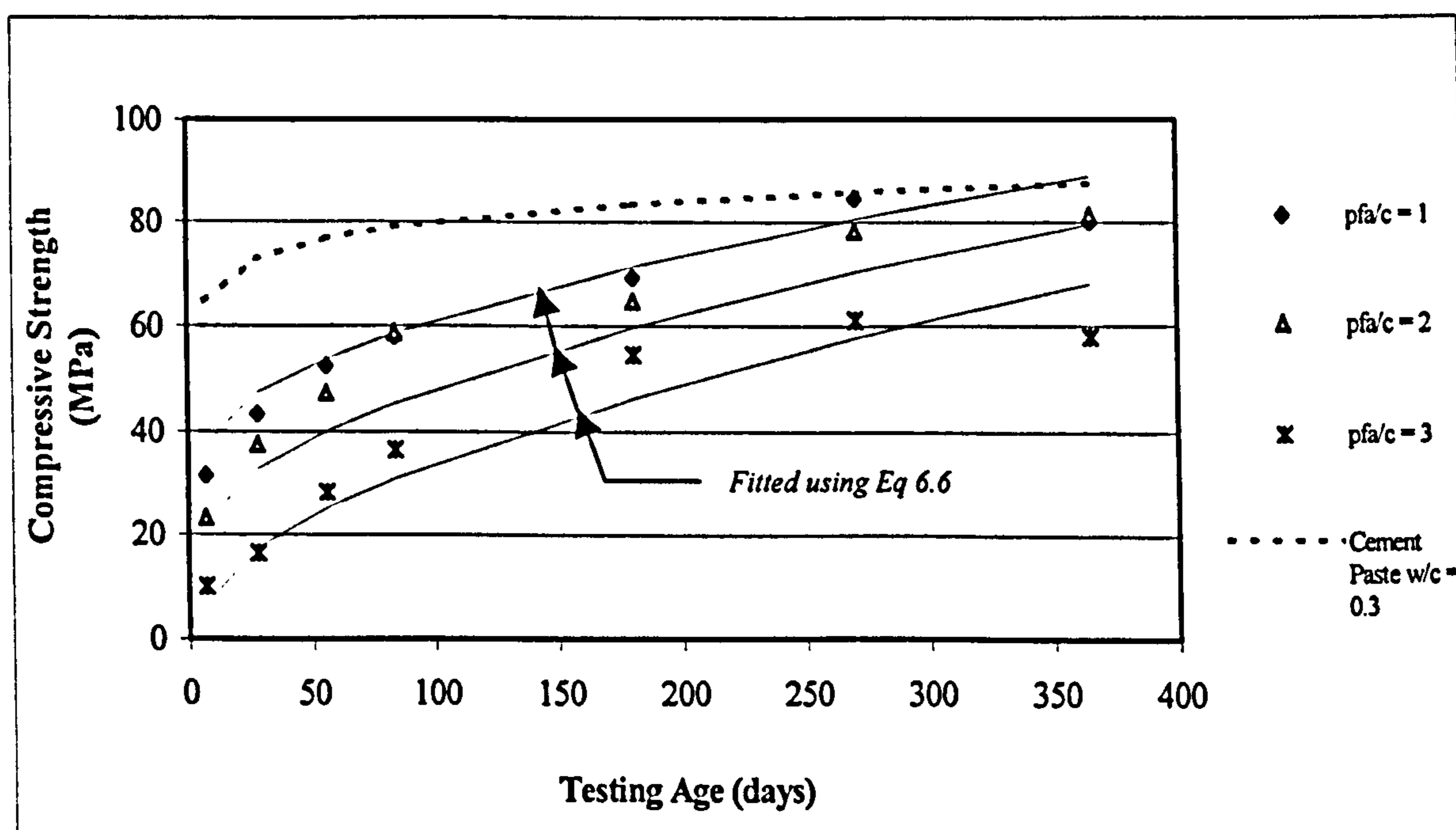


Figure 6.17: Compressive Strength of Pastes Containing Pfa.

The compressive strength of mixtures containing Pozz-fill is plotted as a function of time in Figure 6.18. These results show a similar trend to that observed for the mixtures containing pfa. As far as ultimate compressive strength is concerned there seems to be no significant difference between the mixtures containing pfa and those containing Pozz-fill. These results seem to indicate that the classification of the ash does not improve the effectiveness of the ash as far as contribution towards compressive strength is concerned.

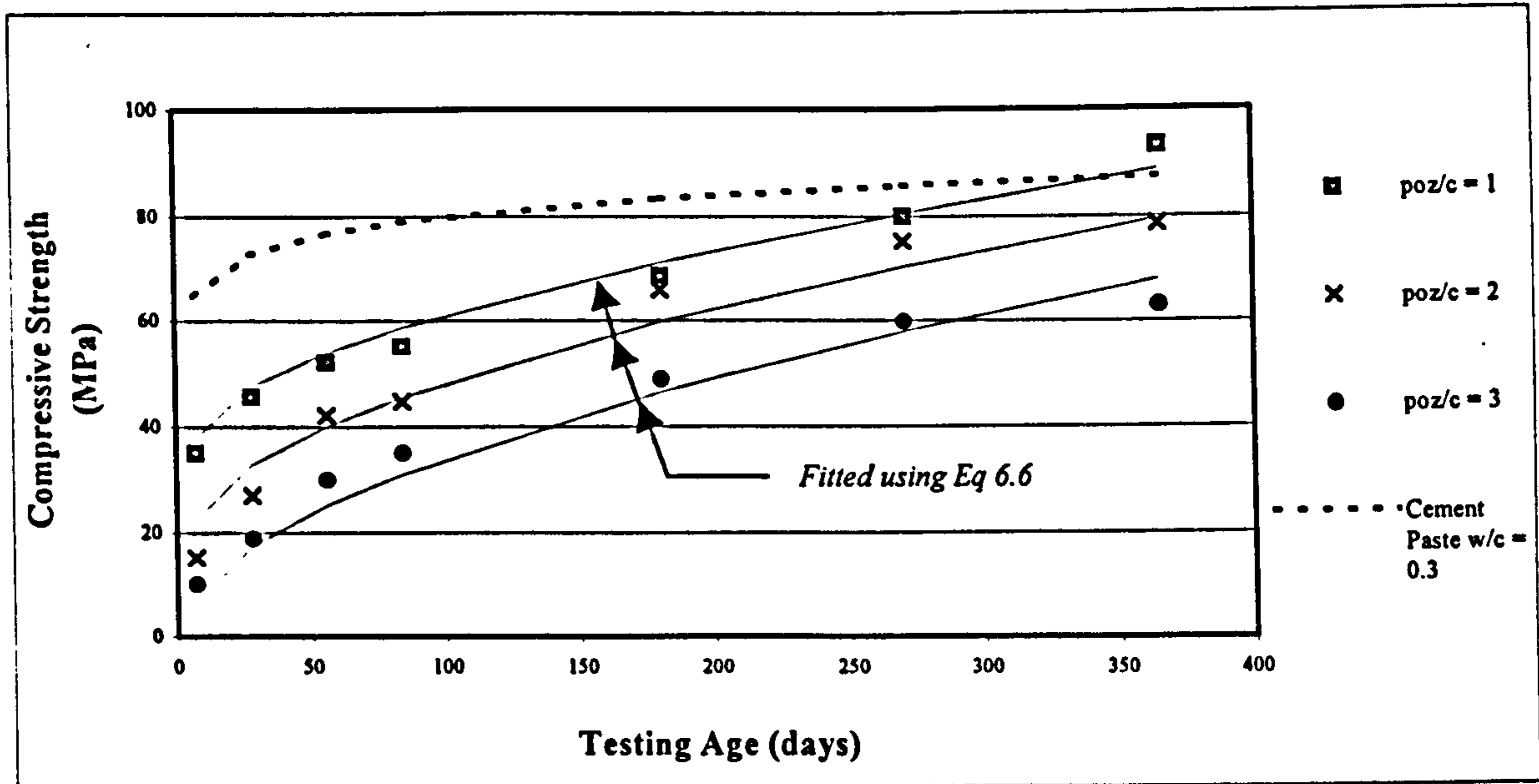


Figure 6.18: Compressive Strength of Pastes Containing Pozz-fill .

6.3.3 Mathematical modeling of paste compressive strengths

By plotting the compressive strength of the cement paste (at different ages) as a function of water/cement ratio (as indicated in Figure 6.19) it can be seen that there is a linear relation between the two.

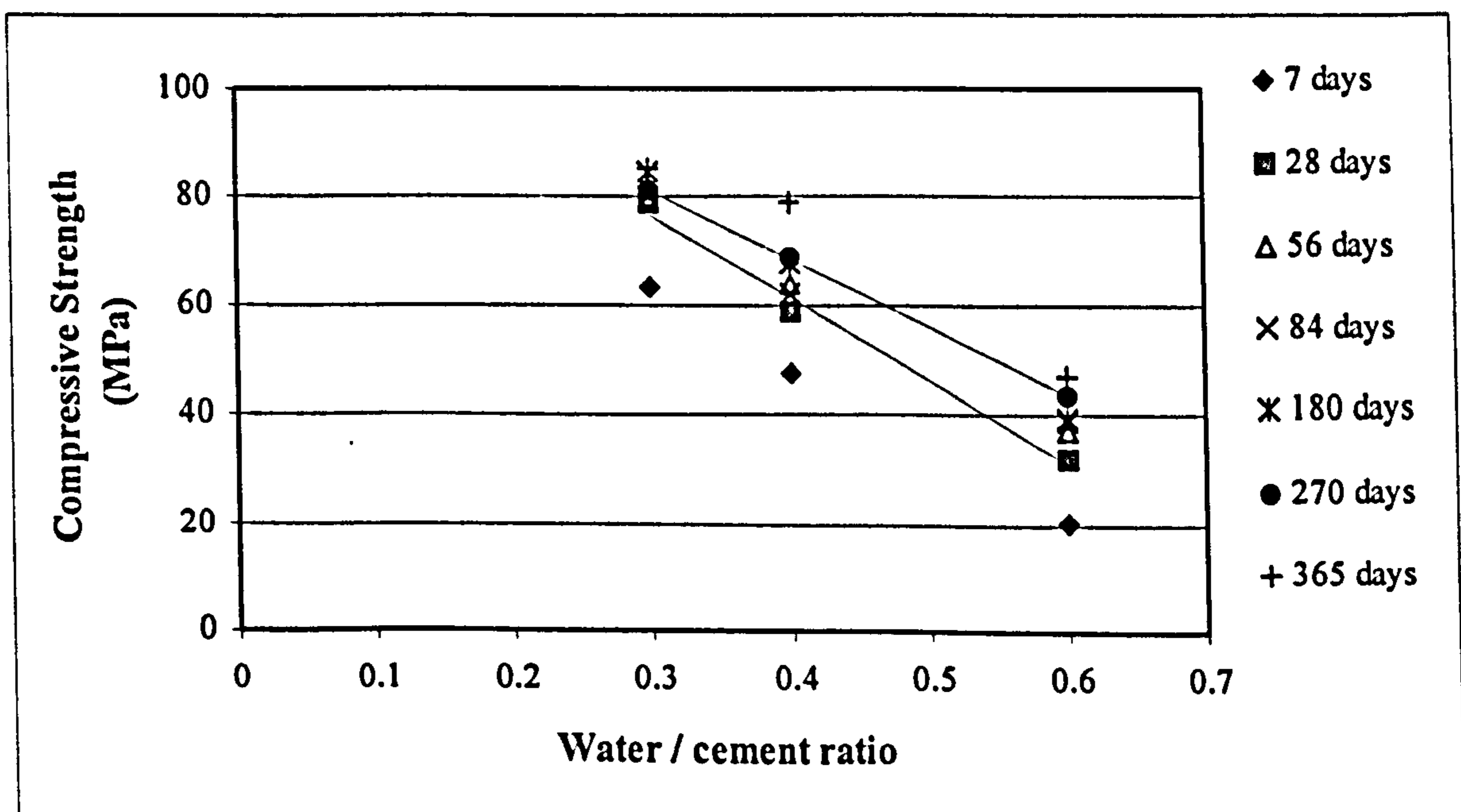


Figure 6.19: Compressive Strength of Cement Paste versus Water/cement Ratio.

Although the strengths increase over time, the linear relation between water/cement ratio and compressive strength remains. Using a multiple linear regression model to describe the relationship between the compressive strength and the two independent variables (time and water/cement ratio), the following equation was derived:

$$f_c(t; w/c) = 95.5 + 5.8 \ln(t) - 140.4 w/c \quad (\text{Eq 6.3})$$

Where:

$$\begin{aligned} f_c &= \text{cube compressive strength (MPa)} \\ t &= \text{time since casting (days)} \\ w/c &= \text{water/cement ratio.} \end{aligned}$$

The R-squared statistic indicates that the model as fitted explains 97.9% of the variability in the compressive strength of the cement paste. The adjusted R-squared statistic, which is more suitable for comparing models with different numbers of independent variables, is 97.7%. The standard error of the estimate shows the standard deviation of the residuals to be 2.89. Stepwise regression indicates that 82.7% of the variation in compressive strength of the cement paste can be explained by the water/cement ratio. The addition of the natural logarithm of age as a second independent variable increases the correlation to 97.9%. The solid lines in Figure 6.16 are fitted using (Eq 6.3) for different water/cement ratios and ages.

The mathematical analysis to determine the contribution of the ash towards the compressive strength of the cement paste is simplified by assuming that the water/cement ratio and age of the paste are the only factors affecting the compressive strength of the paste. A fraction of the ash is taken to be active, and this fraction of the ash is added to the actual cement content when the water/cement ratio is calculated. The compressive strength is used to determine what the actual size of the active fraction at any given time should be.

The effective water/cement ratio of the cement paste at any given age can be calculated (based on the work conducted by Smith 1967)⁴⁰ using the following equation:

$$W/C (w/c;k;a/c) = w/c \left[\frac{1}{1+k(a/c)} \right] \quad (\text{Eq 6.4})$$

Where:

W/C	=	effective water/cement ratio
w/c	=	actual water/cement ratio
a/c	=	ash/cement ratio
k	=	cementing efficiency.

The cementing efficiency is dependent on not only the source and quality of the ash but also on the age of the cement paste, the water/cement ratio and the ash/cement ratio of the paste. Mathematical modeling was simplified by assuming that there is no marked difference between the cementing efficiency of pfa and that of Pozz-fill. The cementing efficiency for the mixtures containing ash was determined using a multiple linear regression model and the following equation was derived:

$$k(t;a/c) = \left(0.457 + 0.00315 \frac{t}{(a/c + 1)} \right)^2 \quad (\text{Eq 6.5})$$

Where:

k	=	cementing efficiency
t	=	time since casting (days)
a/c	=	ash/cement ratio (by weight).

The R-squared statistic indicates that the model as fitted explains 85.6% of the variability in k . The calculated cementing efficiencies (k -values) for the different ash contents is plotted as a function of time in the graph in Figure 6.20. The k -value increases from approximately 0.21 after 7 days to between 0.55 and 1.1 after 365 days. Smith⁴⁰ recommended a k -value of 0.25 based on 7 and 28 day concrete strengths and these results seem to confirm his recommendation. These results do however suggest that his assumption of a constant k -value might be conservative as the efficiency definitely increases with time up to ages of at least one year.

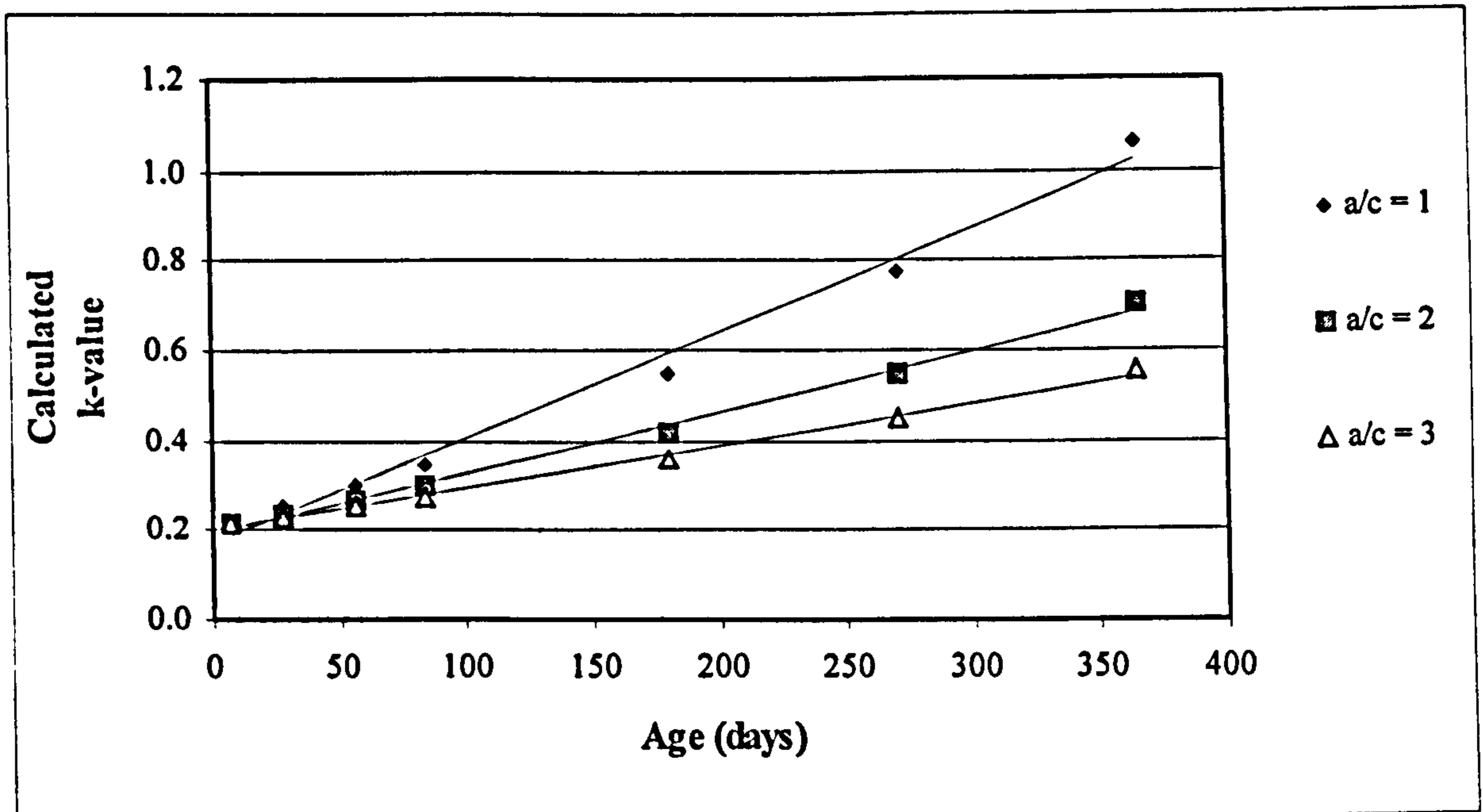


Figure 6.20: Calculated k-values.

A new relationship between compressive strength, effective water/cement ratio and time can now be established using the calculated k-value. The k-value is used to calculate an effective water/cement ratio that can be used as an independent variable in a multiple regression analysis. The relationship between compressive strength and time since casting as well as effective water/cement ratio can be expressed using the following equation:

$$f_c(t; W/C) = 88.04 + 6.569 \ln(t) - 130.5 W/C \quad (\text{Eq 6.6})$$

Where:

$$\begin{aligned} f_c &= \text{cube compressive strength (MPa)} \\ t &= \text{time since casting (days)} \\ W/C &= \text{effective water/cement ratio.} \end{aligned}$$

The R-squared statistic indicates that the model as fitted explains 96.3 % of the variability in strength, while the adjusted R-squared statistic is 96.2 %. The standard error of the estimate shows the standard deviation of the residuals to be 4.2 MPa. Stepwise regression indicates that 83.5% of the variation in compressive strength can be explained by the variation in effective water/cement ratio. Adding the time since casting as a second independent variable increases the percentage of variation in compressive

strength that can be explained by the fitted equation to 96.3%. The calculated k-values were used to adjust the water/cement ratios of the mixtures containing ash, and the effective water/cement ratios was used in Eq 6.6 to calculate the compressive strengths as indicated with the solid lines on the graphs in Figure 6.17 and Figure 6.18.

6.3.4 Foamed concrete

The compressive strength of foamed concrete mixtures with different ash contents and densities are plotted as function of time in Figure 6.21, Figure 6.22 and Figure 6.23 for mixtures with a casting density of 1500, 1250 and 1000 kg/m³ respectively. The top graph in each of these figures is for mixtures containing pfa while the bottom graph is that for mixtures containing Pozz-fill .

From the graphs in Figure 6.21 it can be seen that after one year (365 days) the compressive strength of all six mixtures with casting densities of 1500 kg/m³ is approximately 40 MPa. Neither the ash/cement ratio nor the type of ash used (pfa or Pozz-fill) seems to have a significant effect on the long term strength of these foamed concrete mixtures. After nine months (270 days) the compressive strength of the mixtures containing pfa seems to be slightly lower than that for mixtures containing Pozz-fill but this difference does not seem to be significant. The one year compressive strengths of the mixtures is approximately double the 28 day strength, indicating a similar trend in long term strength gain to that observed for the mortars containing ash (see Figure 6.17 and Figure 6.18).

From the graphs in Figure 6.22 it can be seen that after one year (365 days) the compressive strength of all six mixtures with casting densities of 1250 kg/m³ is approximately 20 MPa. Again neither the ash/cement ratio nor the type of ash used (pfa or Pozz-fill) seems to have a significant effect on the long term strength of these foamed concrete mixtures. The 28 day strength is yet again approximately 50% of the one year strength.

From the graphs in Figure 6.23 it can be seen that after one year (365 days) the compressive strength of six mixtures with casting densities of 1000 kg/m³ varies between 6 MPa and 10 MPa. Although the ash/cement ratio does not seem to have a

significant effect on the compressive strength, the type of ash used (pfa or Pozz-fill) does seem to have a significant effect on the long term strength of these foamed concrete mixtures. The compressive strength of mixtures containing Pozz-fill are significantly lower than the strength of the mixtures containing pfa.

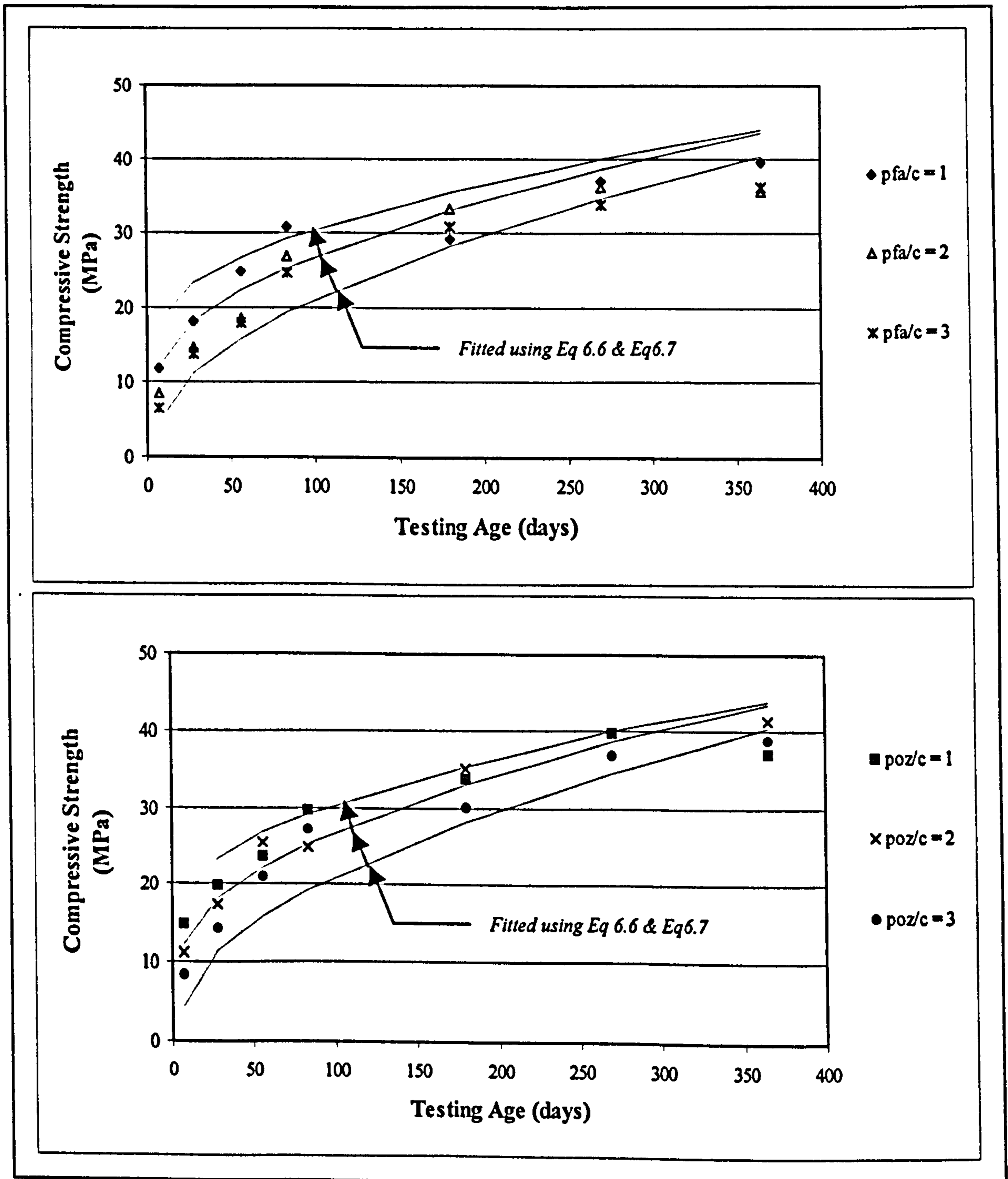


Figure 6.21: Compressive Strength of 1500 kg/m³ Mixtures as a Function of Time.

It is important to note that, unlike those mixtures with higher casting densities, there seems to be virtually no increase in compressive strength after more than 180 days. The contribution to the long-term gain in strength of the ash seems to be reduced at these low densities.

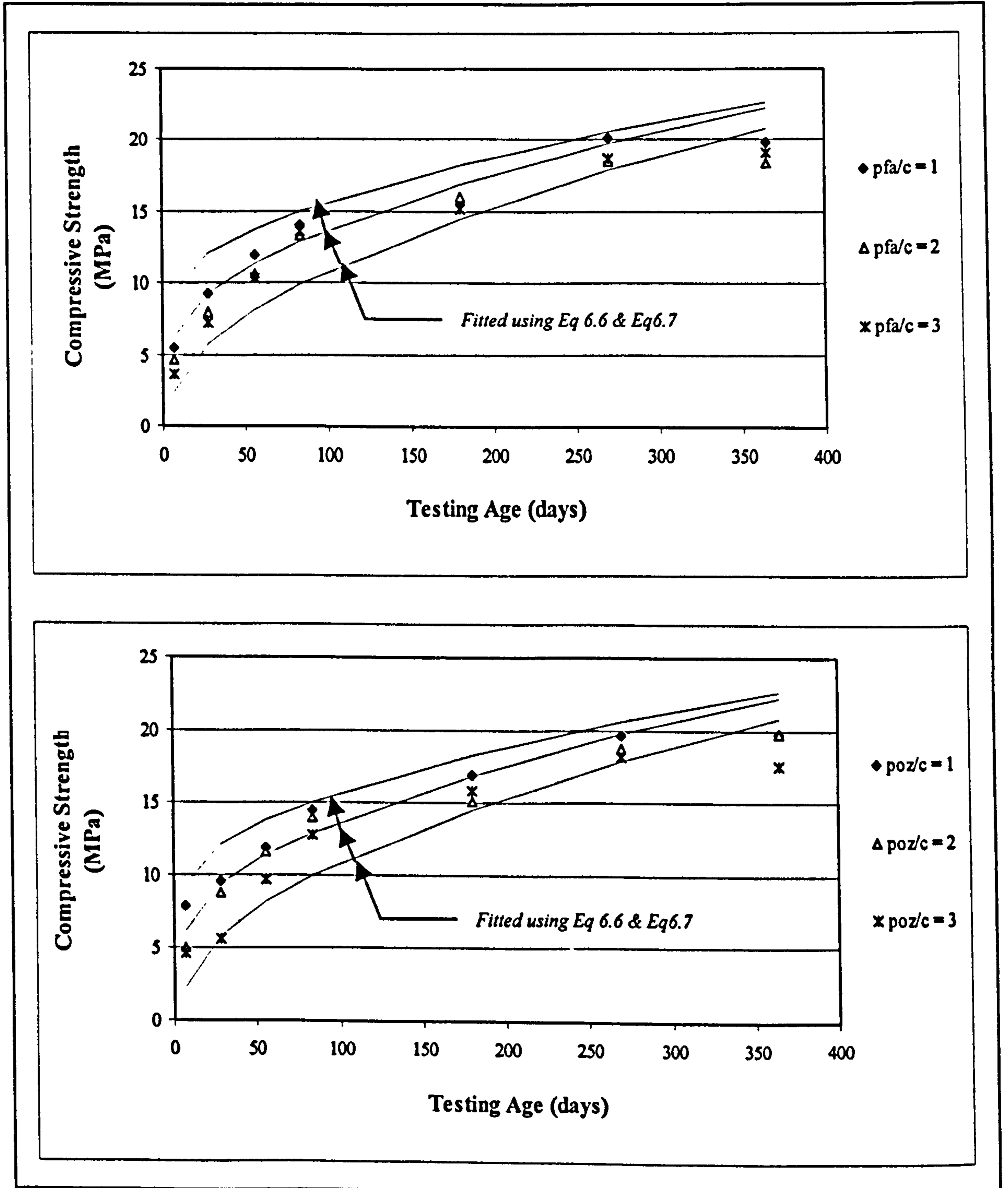


Figure 6.22: Compressive Strength of 1250 kg/m³ Mixtures as a Function of Time.

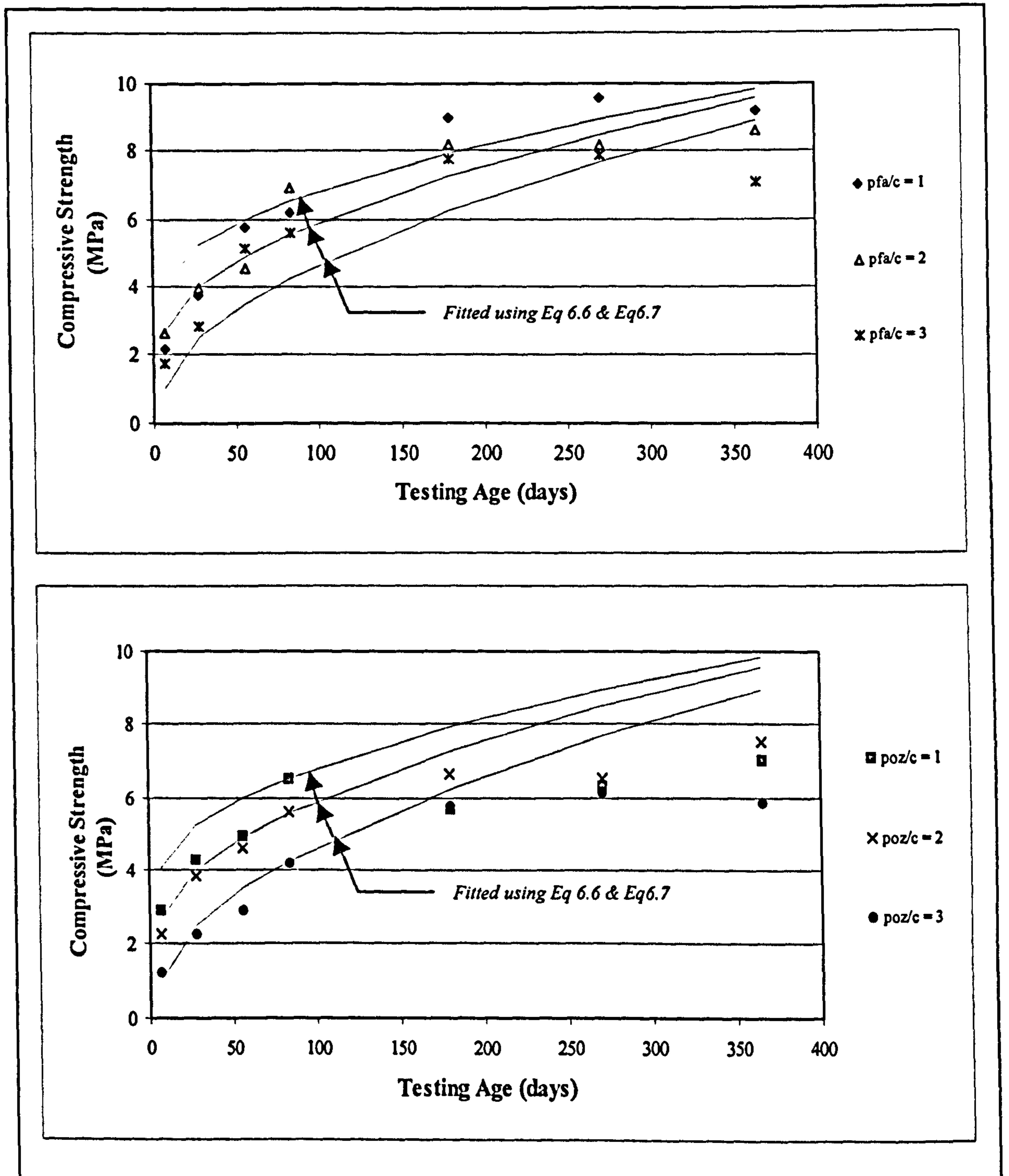


Figure 6.23: Compressive Strength of 1000 kg/m^3 Mixtures as a Function of Time.

The 28 day and one year compressive strength are plotted as a function of density in Figure 6.24 and Figure 6.25 respectively. In each of these figures the top graph shows the results obtained for pfa while the bottom graph shows the results obtained for Pozz-fill. The dry density was only determined from cubes that were cured for 28 days before drying and it has been assumed that the dry density would not change significantly with longer periods of curing.

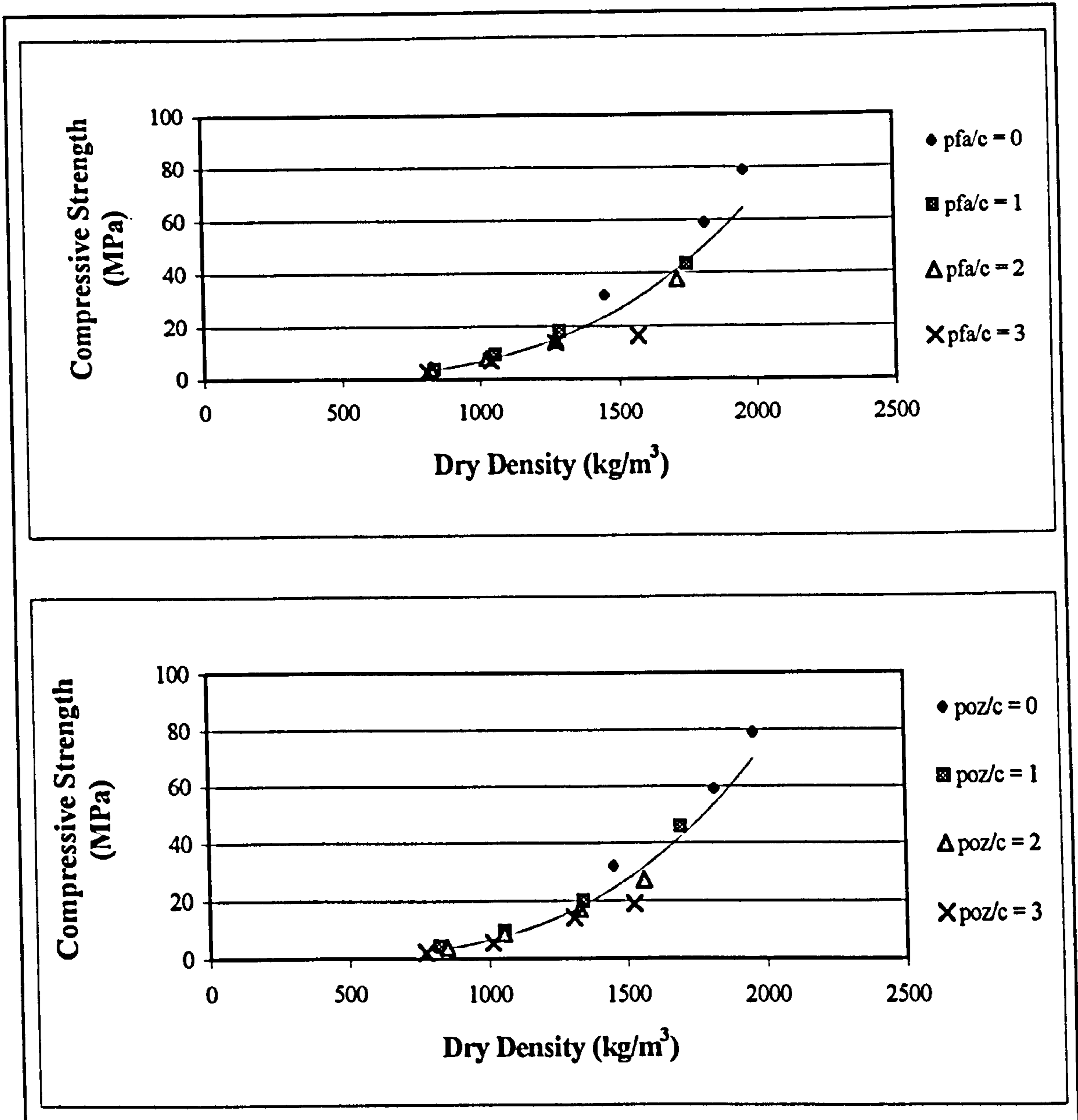


Figure 6.24: 28 Day Compressive Strength as a Function of Dry Density.

From Figure 6.24 it can be seen that there is an exponential relationship between dry density and compressive strength (as indicated with the solid line). After 28 days there seems to be little difference between the strengths obtained from mixtures containing pfa and those obtained from mixtures containing Pozz-fill. The mixtures containing no ash seem to have slightly higher strengths than the mixtures containing ash, confirming the fact that the early strength (up to 28 days) is reduced with high ash contents. The 28-day strengths of all the foamed concrete mixtures are however significantly higher than those obtained by others. The strengths as shown in Figure 6.24 (approximately 15 MPa for a dry density of $\pm 1250 \text{ kg/m}^3$) are approximately double those published for other protein foams (7 MPa for a dry density of $\pm 1200 \text{ kg/m}^3$)¹⁴.

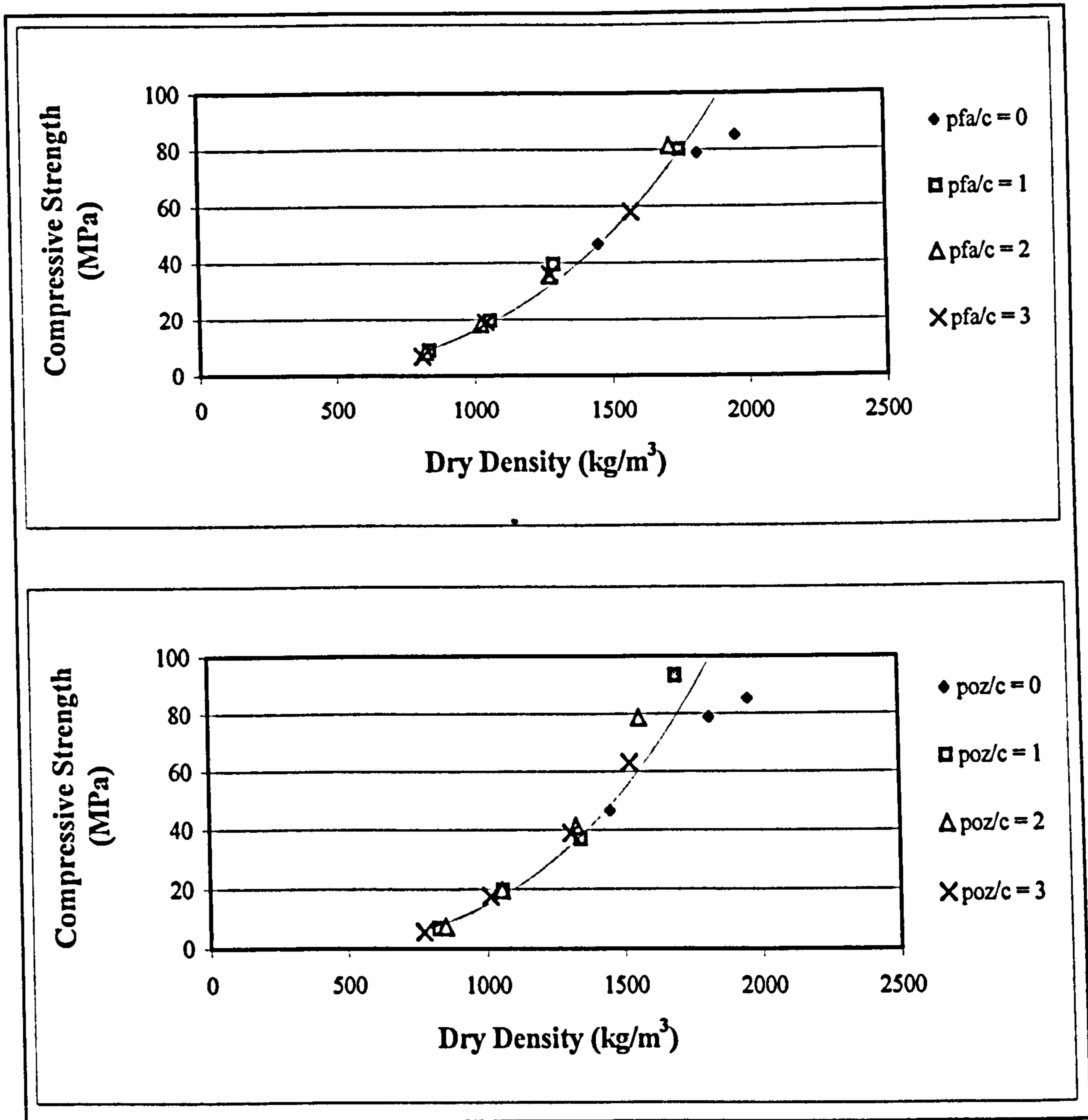


Figure 6.25: One Year Compressive Strength as a Function of Dry Density.

From the graphs in Figure 6.25 it can be seen that after one year, for the same dry density, the mixtures containing ash have marginally higher compressive strengths than those without ash. Yet again there is virtually no difference between the pfa and the Pozz-fill mixtures, with the Pozz-fill mixture strengths being marginally higher than those of the pfa mixtures at high densities. Both the 28-day and one year results indicate that the compressive strength of foamed concrete is primarily a function of dry density and the percentage cement replaced by ash does not have a significant effect on the compressive strength. Based on the results of this investigation it can therefore be concluded that replacing high proportions of cement with fly ash does not significantly affect the long-term compressive strength of foamed concrete. These results indicate

that although the foamed concrete mixtures with high ash contents might need a longer period of time to reach their ultimate strength, this strength could be higher than the ultimate strength that can be achieved using only cement. The fact that ungraded ash (Pozz-fill) yields similar results to pfa indicates that the cost of foamed concrete mixtures could be reduced by replacing large volumes of cement with Pozz-fill, without significantly affecting the long term strength.

6.3.5 Mathematical modeling of foamed concrete compressive strengths

6.3.5.1 Volumetric ratios

The compressive strength of concrete is not only a function of the water/cement ratio but also a function of the density ratio of the concrete.⁶ The density ratio is defined as the ratio between the actual density of the concrete and the density of the concrete when fully compacted. The compressive strength of the paste in the foamed concrete can be expressed in terms of the age and the effective water/cement ratio of the paste. If one assumes that the paste in the foamed concrete has the same strength as the paste on its own, the only factor that should cause a reduction in strength should be the volume of air added to the mixture. As even the mixtures containing no foam might contain significant volumes of entrapped air, the theoretical volumes of binder were used as a base for comparison.

The binder contents (per volume) of the foamed concrete mixtures were expressed as a fraction of the binder content of the pastes and the compressive strengths as calculated with (Eq 6.6) for pastes containing ash was adjusted taking the binder ratios into account. The effect of binder ratio on the compressive strength of foamed concrete can be expressed as follows:

$$f_{c_c} = 1.172 f_c \alpha_b^{3.7} \quad (\text{Eq 6.7})$$

Where:

- f_{c_c} = compressive strength of foamed concrete
- f_c = compressive strength of paste as calculated using (Eq 6.6)
- α_b = binder ratio.

Regression analysis was conducted on all the compressive strengths obtained for foamed concrete mixtures and it was concluded that the combination of equations Eq 6.6 and Eq 6.7 explains 97.9% of the variation in compressive strength of the foamed concrete. Since Eq 6.7 does not contain a constant the correlation percentage as calculated can not be compared to that of models containing a constant, and the value of 97.9% might be misleadingly high. The solid lines plotted on the graphs in Figure 6.21 to Figure 6.23 were calculated using Eq 6.6 and Eq 6.7. On each graph three lines are shown with the top line (the highest compressive strength at any given age) representing an ash/cement ratios of 1, while the bottom line (the lowest compressive strength at any given age) represents ash/cement ratios of 3. Relatively large differences occurred between some of the calculated strengths and the actual measured values, suggesting that some factor other than age, effective water/cement ratio and binder ratio may be having an effect on the compressive strength of the foamed concrete mixtures. The difference between the predicted and the actual behavior of the foamed concrete seems to increase with increased air content, indicating that the nature as well as the volume of air voids might have an effect on the compressive strength of foamed concrete. In the volumetric approach used here only the volumes of binder were taken into account and it was assumed that the water/binder remains constant and therefore does not influence the results. From the discussion on porosity there does seem to be a possibility that the water that was added as part of the foam might affect the water/binder ratio and this effect should become more noticeable with increased foam or void content. It was therefore decided to use a different approach, where the possible increase in bound water can be taken into account. As dry density takes the bound water into account it was decided to investigate the effect of density ratios on the compressive strength of the mixtures.

6.3.5.2 Density ratios

The compressive strength of foamed concrete can be expressed as a function of age, effective water/binder ratio and dry density. If it is assumed that the paste between the voids in the foamed concrete have identical strength properties to the mortars at the same age, water/cement and ash/cement ratios, the effect of age and effective water/binder ratio is already taken into account in Equation 6.6. The effect of the dry density on the compressive strength can be taken into account by using the ratio between the dry density of the foamed concrete and the dry density of the mortar without any

foam added. Regression analysis was used to fit a square root-Y model describing the relation between the compressive strength of foamed concrete and the dry density ratio. The equation of the fitted model is:

$$f_{c_c} = f_c (-0.324 + 1.325 \alpha_d)^2 \quad (\text{Eq 6.8})$$

Where:

- f_{c_c} = compressive strength of foamed concrete
- f_c = compressive strength of paste as calculated using (Eq 6.6)
- α_d = dry density ratio.

The R-squared statistic indicates that the model as fitted explains 95.35% of the variability in compressive strength of the foamed concrete after transforming to a square root scale to linearize the model. The correlation coefficient equals 0.976, indicating a relatively strong relationship between the variables. The dry densities used to fit this equation were measured after 28 days of curing. The dry density should be a function of time as the evaporable water content is reduced through increased cement hydration. A more exact relation between dry density and compressive strength could be determined if the dry density was determined on the same day as that when the cubes were crushed. The fact that using the 28 day dry densities results in a relatively strong relationship means that the 28 day dry density could be used as an indicator of the ultimate strength of a specific foamed concrete mixture. Mix designs could be optimized for ultimate strength if the factors influencing the dry density were known.

When a mixture is cast it consists of water, air, cement and ash in specific volumetric proportions. Before any hydration takes place the dry density of the mixture would be the actual weight of the cement and the ash divided by the total volume of the mixture. As hydration takes place a percentage of the water will be chemically bound and will therefore not evaporate during oven drying. The fact that the chemically bound percentage of water increases with time and the hydrated cement has a lower density than unhydrated cement causes the measured dry density to differ from the theoretical dry density. From Figure 6.26 it can be seen that all the measured dry densities are higher than the calculated values. For all the mixtures containing ash there seems to be a definite linear relation between the calculated and the measured densities, which is

independent of the type of ash or the ash/cement ratio. This relation does not hold true for the mixtures containing no ash. Linear regression conducted on the mixtures containing ash shows that 98.3% of the variation in measured dry density can be explained by the variation in calculated dry density. The fact that there is an exponential relation between measured dry density and compressive strength and a linear relation between measured and calculated dry density, means that there should be an exponential relation between the calculated dry density and the compressive strength. As the calculated dry density is the weight of binder (ash and cement) per cubic meter, the compressive strength of foamed concrete mixtures should be a function of binder content (per weight). Using regression analysis a model was fitted, using results from all mixtures containing ash, to describe the relationship between the compressive strength of foamed concrete and the binder content and paste strength. The equation of the fitted model is:

$$f_{c_c} = 2.075 + 2.012 E - 12 (f_c \cdot \rho_b^{3.7}) \quad (\text{Eq 6.9})$$

Where:

- f_{c_c} = compressive strength of foamed concrete
 f_c = compressive paste strength calculated using (Eq 6.6)
 ρ_b = binder content per cubic meter of foamed concrete (per weight).

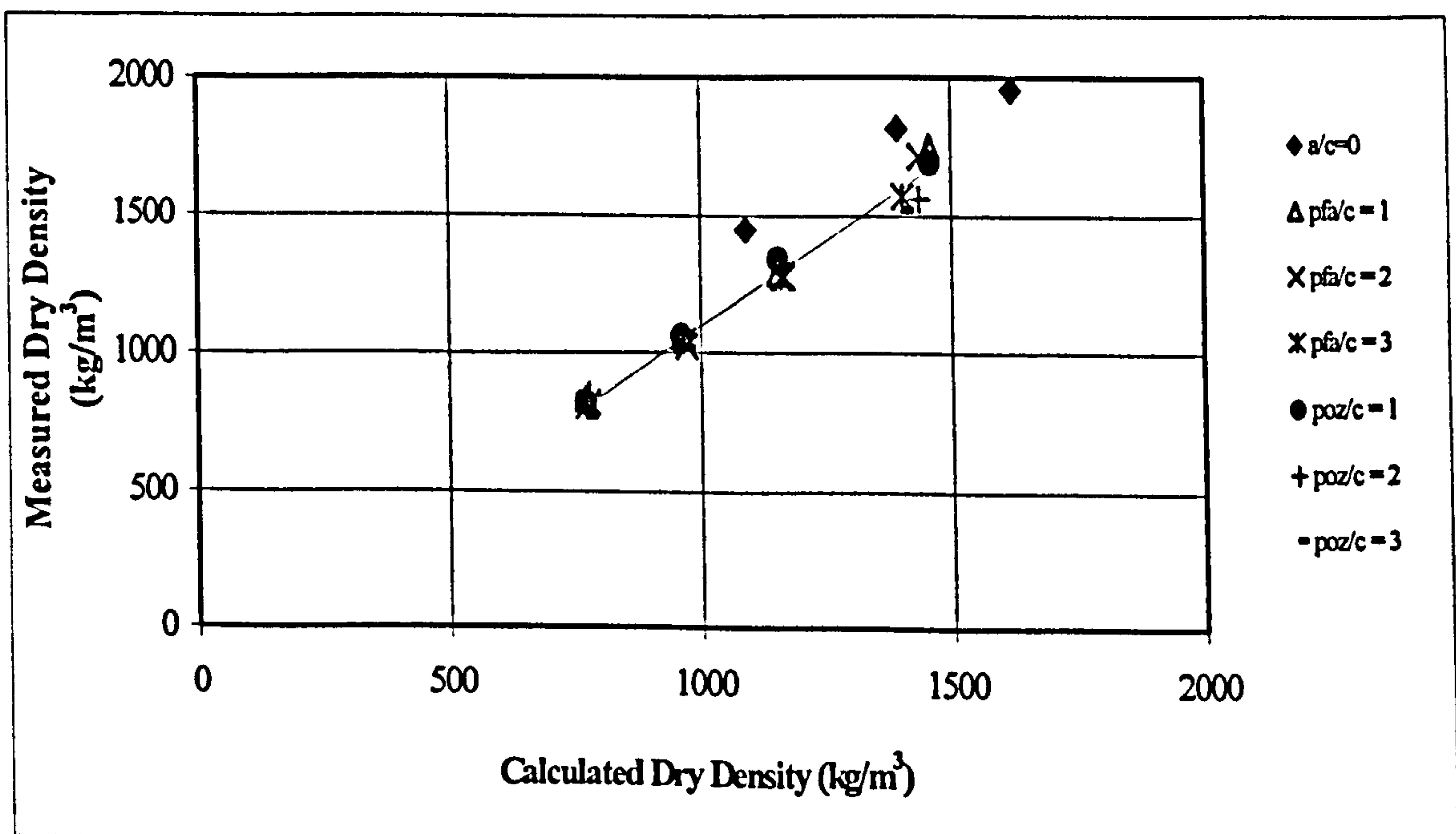


Figure 6.26: Measured Dry Density versus Calculated Dry Density.

The R-squared statistic indicates that the model as fitted explains 96.9% of the variability in the compressive strength of the foamed concrete. The correlation coefficient equals 0.984, indicating a relatively strong relationship between the variables. This fitted model is plotted with the measured compressive strengths of foamed concrete mixtures with casting densities of 1500 kg/m^3 , 1520 kg/m^3 , and 1000 kg/m^3 in Figure 6.27, Figure 6.28 and Figure 6.29 respectively. From the solid lines in Figure 6.27 it can be seen that this model fits the results of the high density foamed concrete well and the over estimation of the one year strength (see Figure 6.21), that occurred with the model based on volumetric proportions, does not occur here.

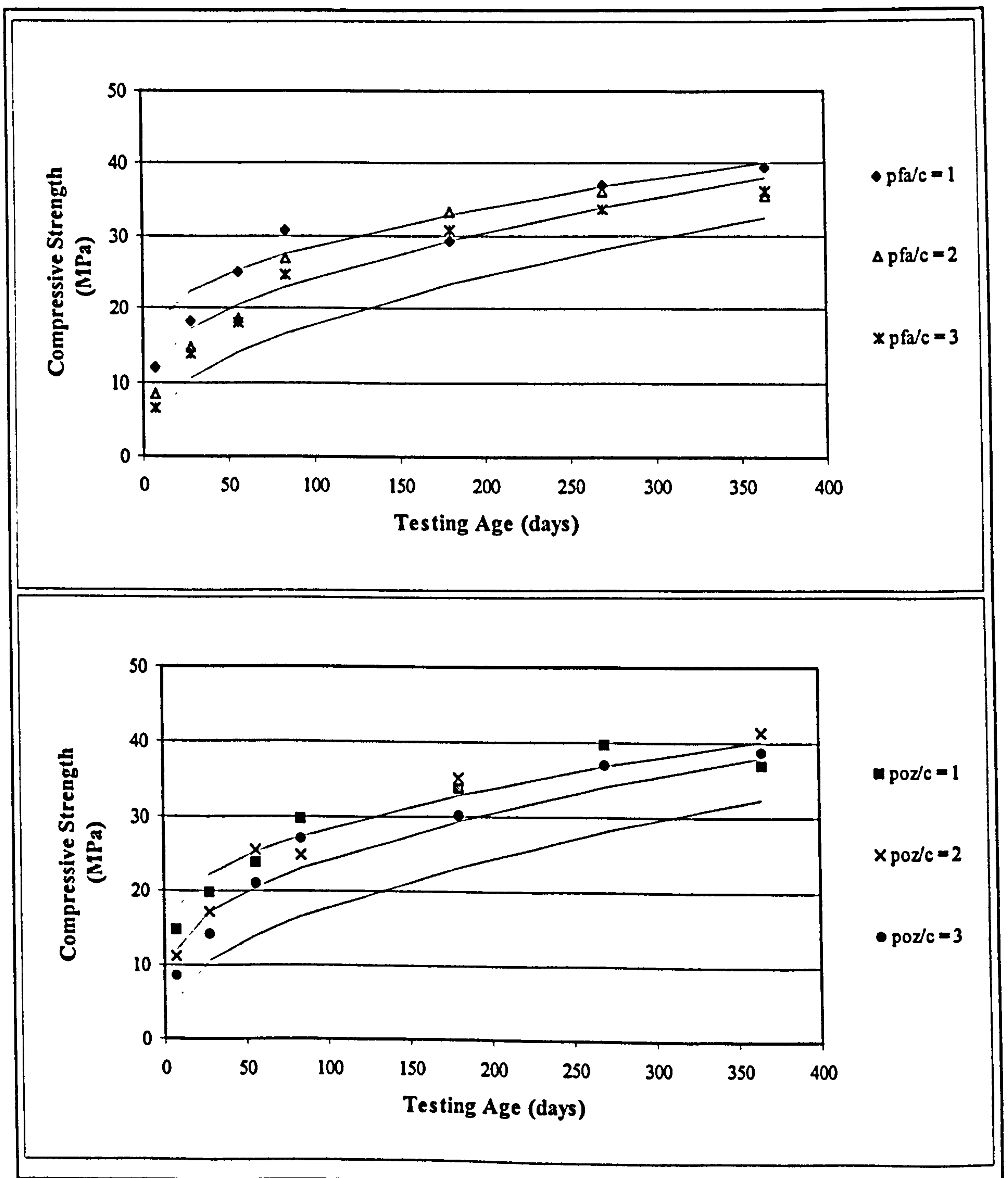


Figure 6.27: Binder Weight Model Compared to 1500 kg/m^3 Mixtures.

From Figure 6.28 it can be seen that the binder weight model also fits the actual measured strengths of the foamed concrete mixtures with a casting density of 1250 kg/m^3 well. The three fitted lines in each of the graphs in these figures represents the model as fitted for ash/cement ratios of 1, 2 and 3, where the line with the highest strength represents the ratio of 1 and the line with the lowest strength represents the ratio of 3. It is interesting noting that the actual difference in compressive strength for different ash contents is much less than that predicted by the model.

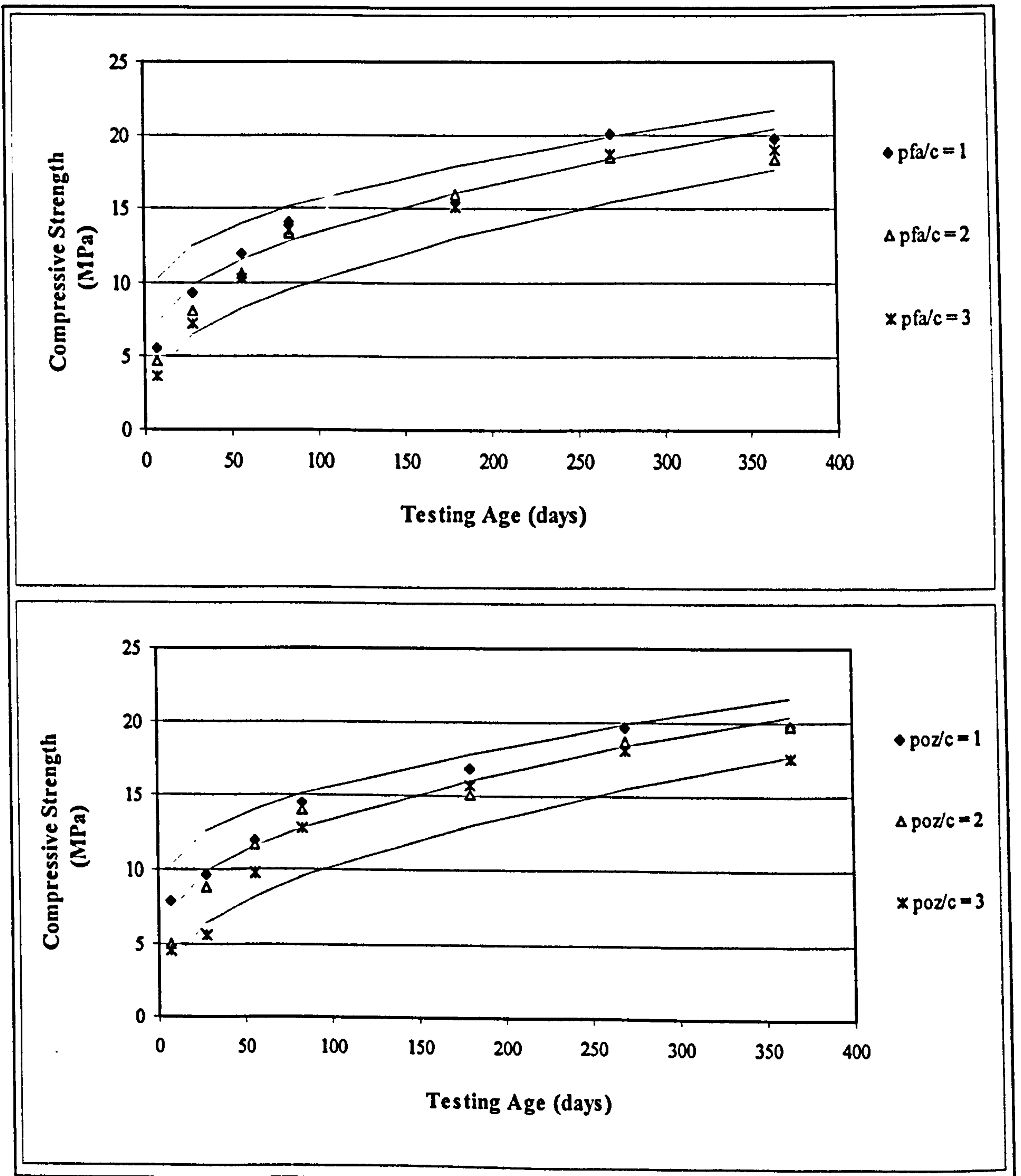


Figure 6.28: Binder Weight Model Compared to 1250 kg/m^3 Mixtures.

The results as indicated in Figure 6.29 clearly shows that the model fits the actual compressive strength of the low density ($1\,000\text{ kg/m}^3$) mixtures containing pfa reasonably well but the compressive strength of mixtures containing Pozz-fill is significantly lower than that predicted by the model. The fact that the model fits the mixtures with higher densities well might indicate that the compressive strength of high density foamed concrete mixtures is primarily a function of only binder weight, age and effective water cement ratio.

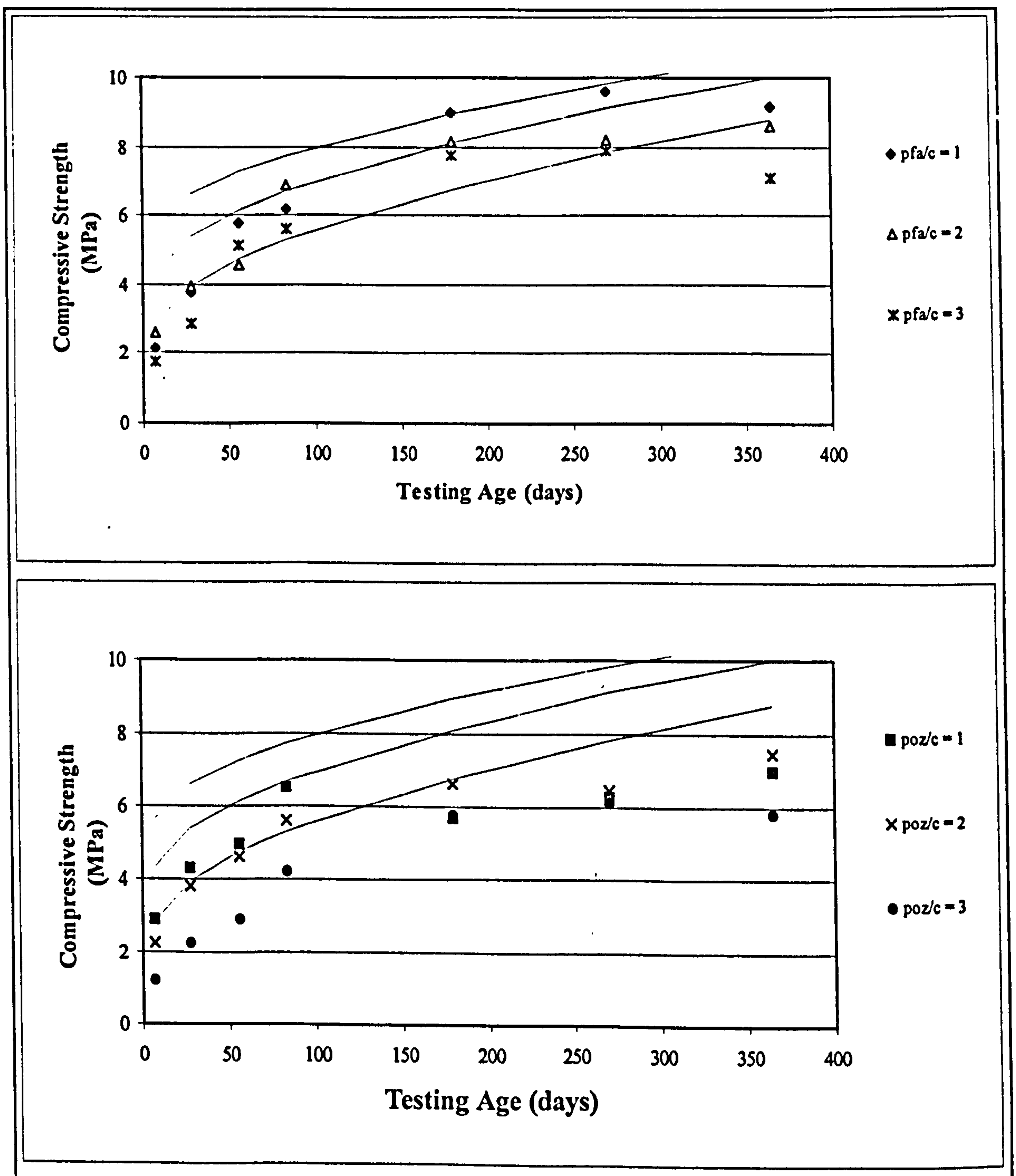


Figure 6.29: Binder Weight Model Compared to 1000 kg/m^3 Mixtures.

The fact that the model does not fit the low density mixtures containing coarser ash particles could indicate that additional factors (such as particle or air void shape, size and distribution) may have a significant effect on the compressive strength of mixtures with high air contents.

6.3.6 Effect of Porosity on Compressive Strength

Using the equations derived by Hoff³⁸ (see Eq 2.15 and Eq 2.16), a theoretical porosity can be calculated for any mixture with a specific dry density, water/cement ratio and cement specific gravity. Although these equations take into account the volume of water bound through hydration, they were derived for mixtures containing only water, cement and foam and they might not be valid for mixtures containing ash. The theoretical porosity of mixtures containing ash was calculated using the water/binder ratio and the binder specific gravity, where the term binder is defined as all the cementitious material in the mixture. The binder specific gravity was calculated by dividing the total binder weight by the total binder volume. The relation between compressive strength (as measured one year after casting) and theoretical porosity can be seen in the graph in Figure 6.30. The solid line in this graph was fitted using Hoff's equation for compressive strength with coefficients $\sigma_0 = 188$ MPa and $b = 3.1$. The R-squared statistic indicates that the model as fitted explains 92.3% of the variability in compressive strength. The correlation coefficient equals 0.961, indicating a relatively strong relationship between theoretical porosity and compressive strength.

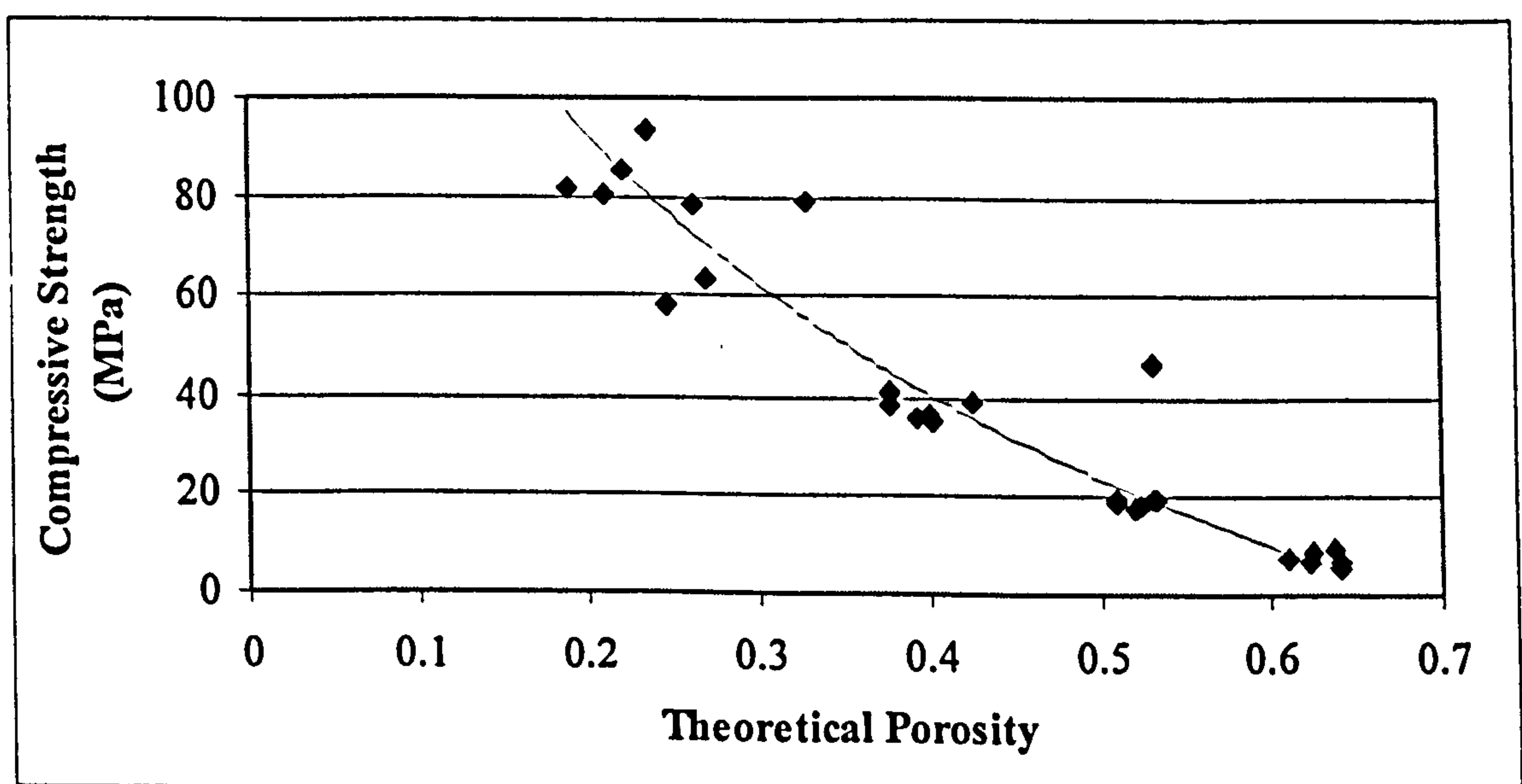


Figure 6.30: Compressive Strength - Theoretical Porosity Relation at 365 days.

It is interesting to note that the variation in strength for a given porosity decreases as the porosity increases. This trend indicates that the single strength-porosity relation for a given cement (as concluded by Hoff) might only be valid at relatively high porosities. When Hoff did his analysis, he calculated coefficients of σ_0 between 115 and 290 MPa and b between 2.7 and 3.0. The coefficients calculated for mixtures containing high volumes of ash compares well with his values and the fact that σ_0 is relatively low (at 188 MPa) for a relatively fine cement can be explained by the fact that, even one year after casting all the ash does not partake in the hydration process. Although Hoff only proved his equations for foamed concrete with densities below 1120 kg/m^3 , it can at this stage be concluded that the equation for calculating compressive strength is not only valid for mixtures containing large volumes of ash, but it is also valid for higher densities (even for pastes without any foam added).

The porosity of each mixture was determined one year after casting and these measured porosities are compared to the theoretical porosities calculated using the equations derived by Hoff³⁸ (see Figure 6.31). From Figure 6.31 it can be seen that there is a relatively strong relation between the theoretical and actual porosities. At low porosities the equation under-estimates the porosity (mixtures with a theoretical porosity in the region of 0.2 have a measured porosity in the region of 0.3 to 0.4). It may be concluded, that when using the author's results, although Hoff's equation may be used to calculate compressive strengths it is not deemed suitable to calculate the porosity of high-density (above say 1500 kg/m^3) mixtures.

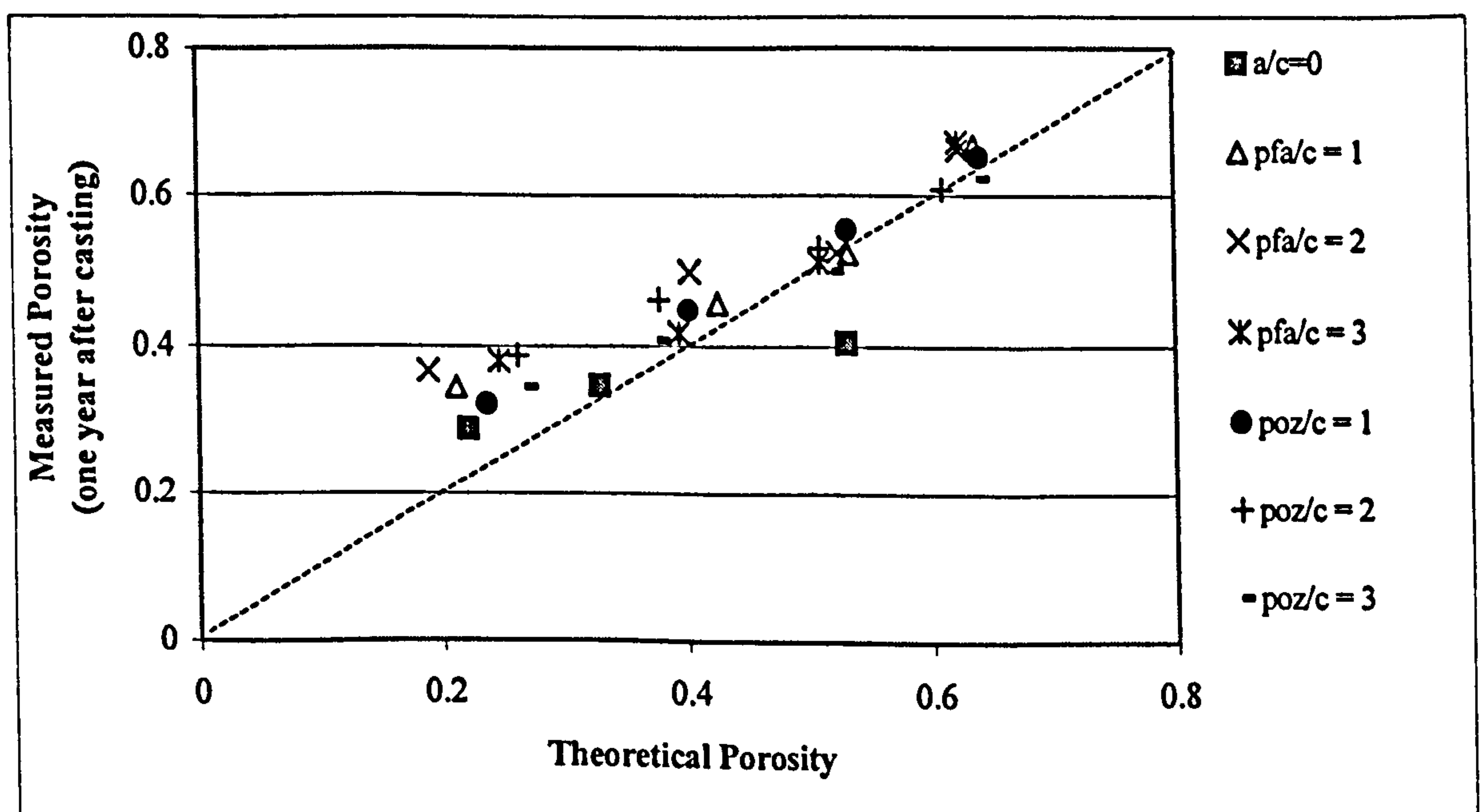


Figure 6.31: Measured versus Theoretical Porosity.

There are no marked trends as far as ash type or content is concerned, indicating that the use of large volumes of ungraded ash does not affect the suitability of the equations for calculating the theoretical porosity of low density foamed concrete mixtures. The measured porosities of the mixtures containing no ash ($a/c=0$) seem to follow a different trend line to the mixtures containing ash with slightly lower measured porosities for a given theoretical porosity.

The relationship between measured porosity and the compressive strength of foamed concrete can be seen in Figure 6.32 where the compressive strength (measured one year after casting) is plotted as a function of the porosity (measured one year after casting). From this graph it can be seen that the relationship is not significantly influenced by the use of pfa or Pozz-fill. Mixtures with an ash/cement ratio of 2 seem to yield marginally higher strengths for a given porosity and mixtures with no ash or an ash/cement ratio of 3 seem to yield marginally lower strengths for a given porosity. These differences are however only small and it can be concluded that for the results available the volume of ash used does not significantly influence the porosity strength relationship of foamed concrete.

Rößler & Odler³⁵ used four expressions that had been derived by other workers to express the relationship between porosity and compressive strength of porous solids. They determined the optimum values of the constant terms and sought the equation that best expressed the existing relationship between strength and total porosity of their set of portland cement pastes.

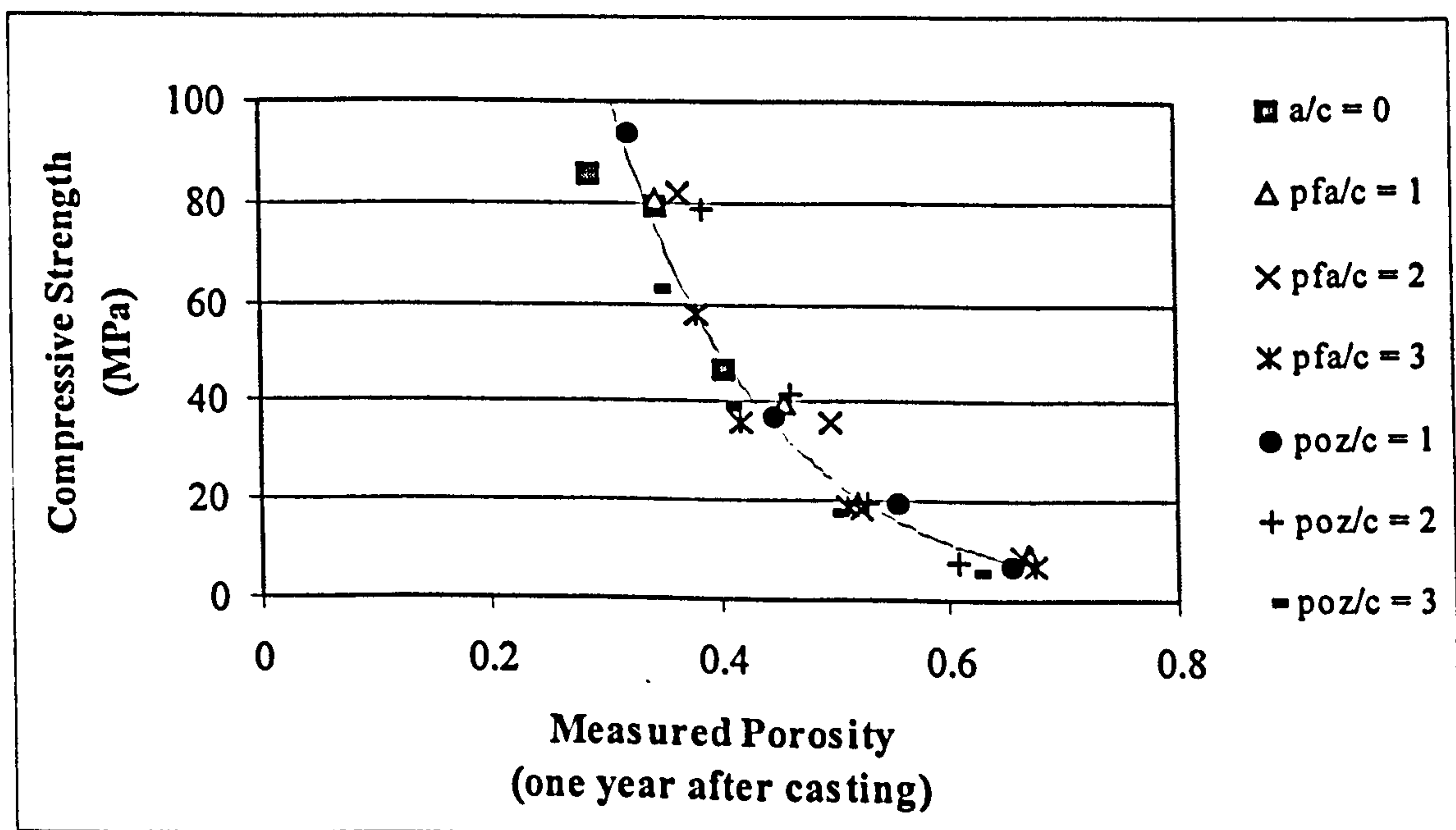


Figure 6.32: Effect of Porosity on Compressive Strength.

The same procedure was used to determine whether these equations could be used to express the relation between porosity and strength of the author's foamed concrete mixtures with high ash contents. The results in Table 6.4 indicate that one year after casting any one of the four equations can be fitted, resulting in a relatively strong relationship between the compressive strength and the porosity of the foamed concrete. While Rößler & Odler³⁵ concluded that the linear relation (Hasselmann) fits their results best, the author's results are best fitted to an exponential function (Ryshkevitch). The solid line in Figure 6.32 fits the exponential function ($f_c = 981 e^{-7.43p}$) as shown in Table 6.4. The porosity of the cement pastes analyzed by Rößler & Odler were below 0.3 (30%) while the porosity of the foamed concrete samples were as high as 0.66 (66%). From Figure 6.32 it can be seen that a linear function would fit the foamed concrete mixtures with lower porosities (say below 0.4) and these results do therefore seem to concur with the conclusions drawn by Rößler & Odler.

Table 6.4: Equations for the Strength-porosity Relationship of Foamed Concrete.

Equation	Equation fitted by Rößler & Odler ³⁵	Authors Foamed Concrete		
		Equation fitted	R-squared	Correlation coefficient
Balshin	$\sigma_c = 540 (1-p)^{14.47}$	$f_c = 321 (1-p)^{3.6}$	0.926	0.962
Ryshkevitch	$\sigma_c = 636 e^{-17.04p}$	$f_c = 981 e^{-7.43p}$	0.936	0.967
Schiller	$\sigma_c = 81.5 \ln(0.31/p)$	$f_c = 109.5 \ln(0.66/p)$	0.89	0.943
Hasselmann	$\sigma_c = 158 - 601p$	$f_c = 147 - 226p$	0.848	0.921

The multiplicative model (Balshin) fitted as shown in Table 6.4 has a power of 3.6 which is much higher than the values of up to 2.2 calculated for aerated concrete by Baozhen and Erda³⁷. The fact that the current investigation contains data with a larger spectrum of porosities as well as higher strengths could explain this difference.

For the foamed concrete mixtures used in this investigation, the strength-porosity equation fitted using an exponential function explains the relation best, and the correlation coefficient of 0.967 indicates a marginally better fit than that obtained using

the strength-theoretical porosity equation derived by Hoff (where the correlation coefficient was 0.961). All the foamed concrete strengths and porosities used to fit these functions were however measured one year after casting. The compressive strength of the mixtures increased significantly between 28 days and 365 days after casting while based on literature reviewed^{34,52} it was assumed that the change in porosity during this period should be negligible. The equations as fitted can therefore only be valid for the one-year results and another factor will have to be added to the equation, taking time since casting into account. When the equations shown in Table 6.4 are fitted for strengths at different ages the equation derived by Balshin gives the best result for the combination of all ages. The effect of age can be taken into account by taking the equation as derived by Balshin and expanding it to use a variable strength at zero porosity (changing σ_0 to a function of time instead of using the fixed value of 321 that was derived for the one year strengths). Fitting a multiplicative model through linear regression results in the following:

$$f_c = 39.6 (\ln(t))^{1.174} (1-p)^{3.6} \quad (\text{Eq 6.10})$$

Where:

f_c	=	compressive strength of foamed concrete	(MPa)
t	=	time since casting	(days)
p	=	mature porosity.	

The R-squared statistic indicates that this model as fitted explains 89.6% of the variability in compressive strength. A correlation coefficient of 0.946 indicates a relatively strong relationship between these variables. The relation between the compressive strength as predicted using Eq 6.10 and the actual measured values can be seen in Figure 6.33. Although the equation seems to predict the strengths reasonably accurately at low values the compressive strength seems to be underestimated at higher strengths (between 50 and 80 MPa).

The mathematical analysis of the compressive strength of foamed concrete indicates that the age and porosity of foamed concrete affects the compressive strength significantly. The effect of ash type and content has been addressed in that (apart from the 1000 kg/m³ mixtures) no large differences between compressive strength of mixtures containing pfa and those containing Pozz-fill could be observed.

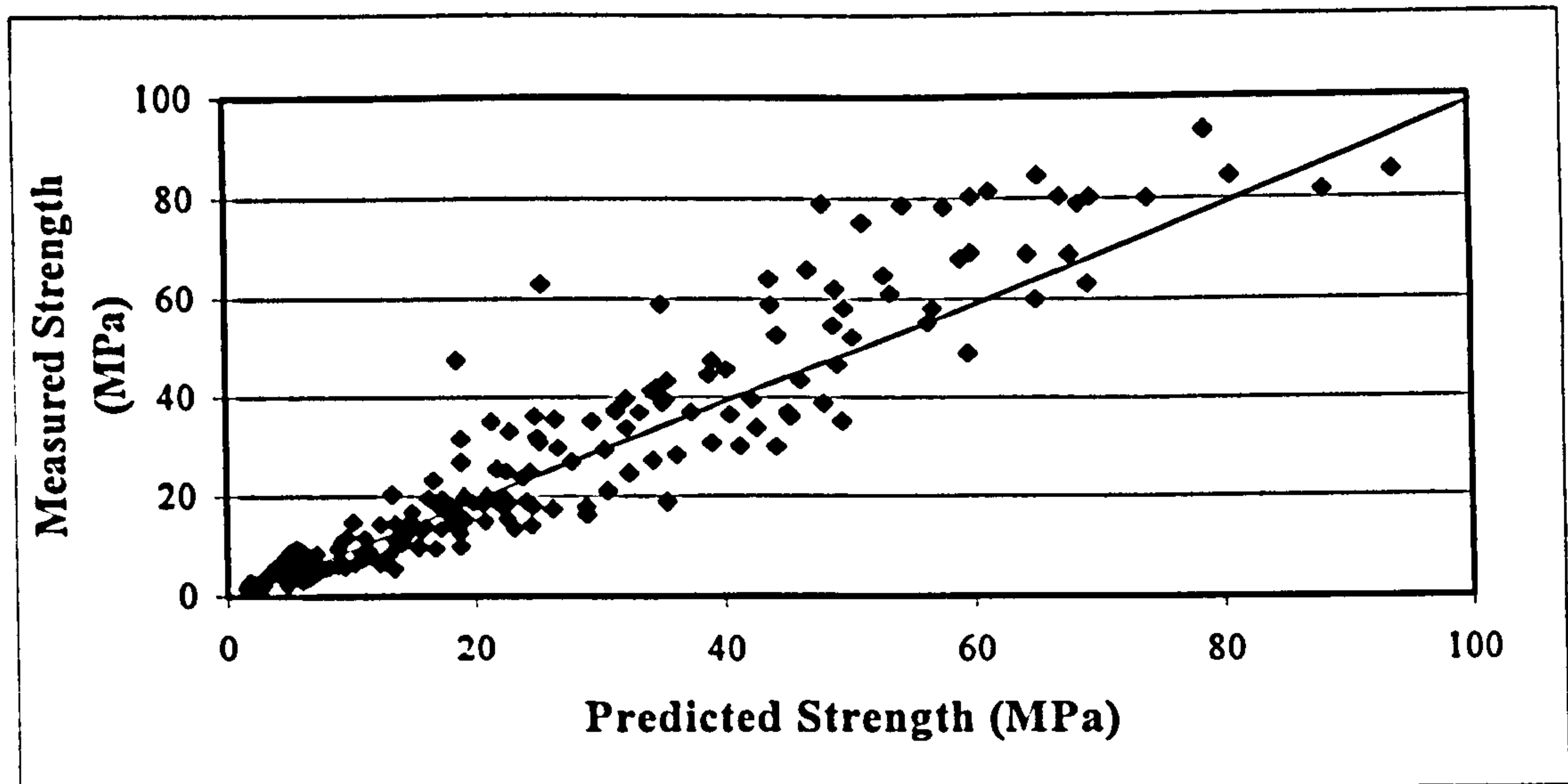


Figure 6.33: Predicted versus Measured Strengths.

The effect of ash/cement ratio on the compressive strength has however not been taken into account at this stage and a detailed computer simulation will be conducted in Chapter 7 to establish possible optimum ash contents.

6.3.7 The effect of void structure on compressive strength

The effect of void diameter and distance between voids on the compressive strength of foamed concrete can be seen in Figure 6.34. The top graph in Figure 6.34 shows the 365-day compressive strength as a function of median void diameter while the bottom graph shows the 365-day strength as a function of median distance between voids. On both these graphs there are three distinct clusters of results, which represents the three different casting densities. Although the density does have an effect on the void sizes and distances between voids, the results within each cluster (for any given density) does not show any relationship between the compressive strength of foamed concrete and the void diameters or the distances between voids.

The effect of void size on the compressive strength might become noticeable at lower densities than that used in this investigation or if a less stable foam is used. The effect of void structure on the compressive strength of foamed concrete should be further investigated in future by comparing voids formed using different foaming agents.

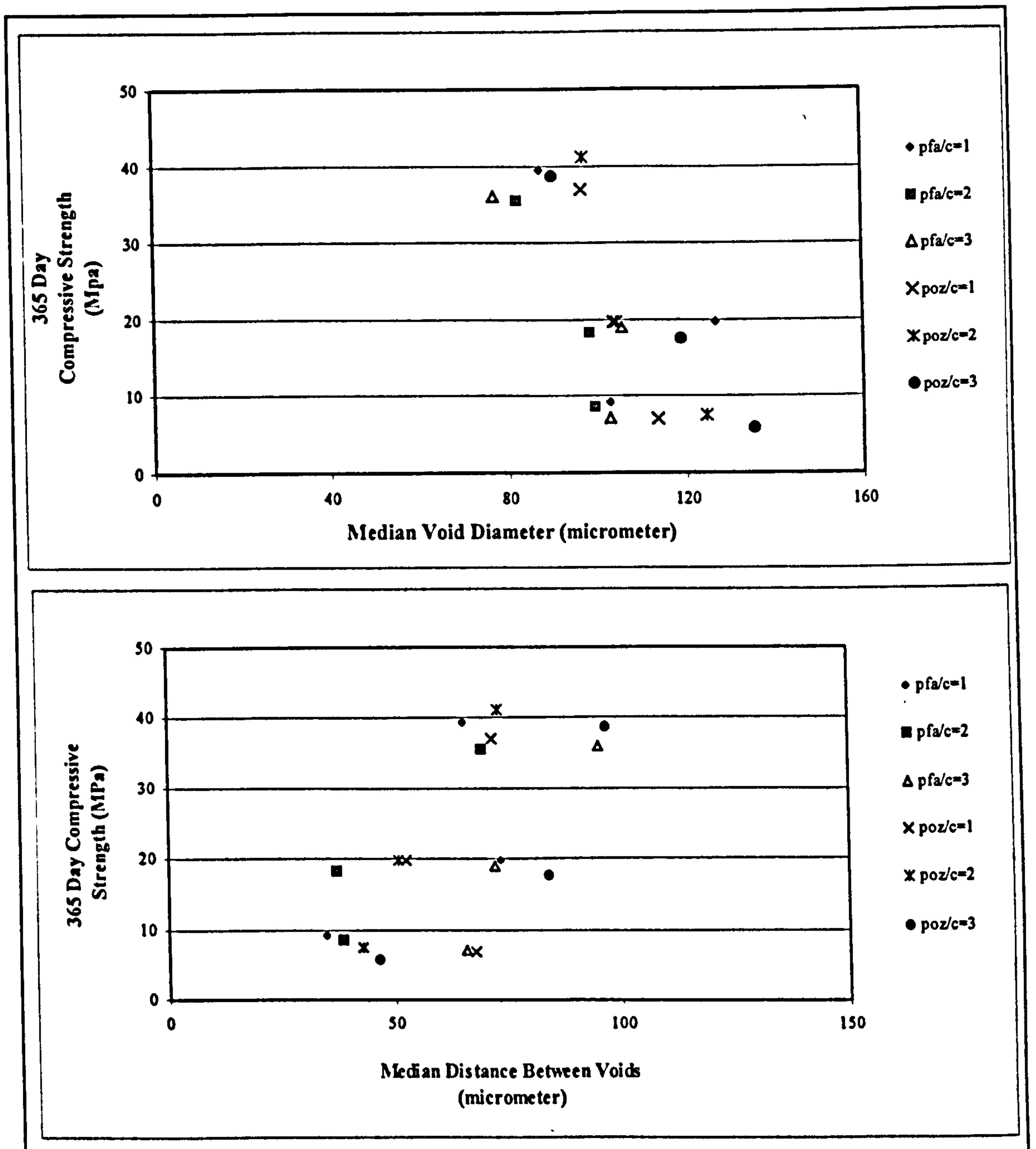


Figure 6.34: Effect of Void Structure on Compressive Strength.

6.3.8 Conclusions on compressive strength

- The compressive strength of neat cement paste is a function of water/cement ratio and the strength gained after more than 28 days is only marginal.
- The compressive strength of foamed concrete is a function of dry density and at a density of 1500 kg/m^3 strengths of up to 20 MPa and 40MPa are attained after 28 days and 1 year respectively.

- The rate of gain in strength of the foamed concrete is reduced by the use of large volumes of ash but up to 67% of the cement (ash/cement ratio of 2) can be replaced by ash without any large reduction in long term strength (up to 1 year).
- The cementing efficiency of the ash used in this investigation varied between 0.21 after 7 days to between 0.55 and 1.1 after 365 days. The efficiency is a function of age and ash/cement ratio and it can be calculated using the following equation:

$$k = \left(0.457 + 0.00315 \frac{t}{(a/c+1)} \right)^2$$

- At higher densities (1500 kg/m³ and 1250 kg/m³) the use of unclassified ash does not yield significantly lower strengths than the use of classified ash. The use of large volumes of unclassified ash in foamed concrete could therefore result in significant cost savings without any real reduction in strength. At lower casting densities (say below 1000 kg/m³) the use of unclassified ash does result in a noticeable reduction in compressive strength.
- The ultimate compressive strength of foamed concrete mixtures is strongly influenced by dry density and a decrease in dry density results in a decrease in compressive strength.
- The compressive strength of foamed concrete was shown to be a function of porosity and age. A multiplicative model (such as the equation derived by Balshin³⁵) best fits the results at all ages of this investigation.
- The effect of ash/cement ratio has not yet been established and in Chapter 7 an attempt will be made to establish whether there are optimum ash contents at different ages and porosities.
- At any given density the void diameters and distances between voids does not seem to have an effect on the compressive strength of foamed concrete.

6.4 WATER ABSORPTION AND PERMEABILITY

6.4.1 Water absorption

The water absorption of foamed concrete mixtures (as expressed by the increase in mass as a percentage of dry mass) is plotted as a function of dry density in Figure 6.35. There seems to be a linear relation between the dry density and the percentage water absorbed, with mixtures with lower dry densities absorbing significantly higher percentages of water than the mixtures with higher densities. Based on percentage water absorption it could thus be concluded that the mixtures with lower densities absorb more water and are therefore potentially less durable than the mixtures with higher densities.

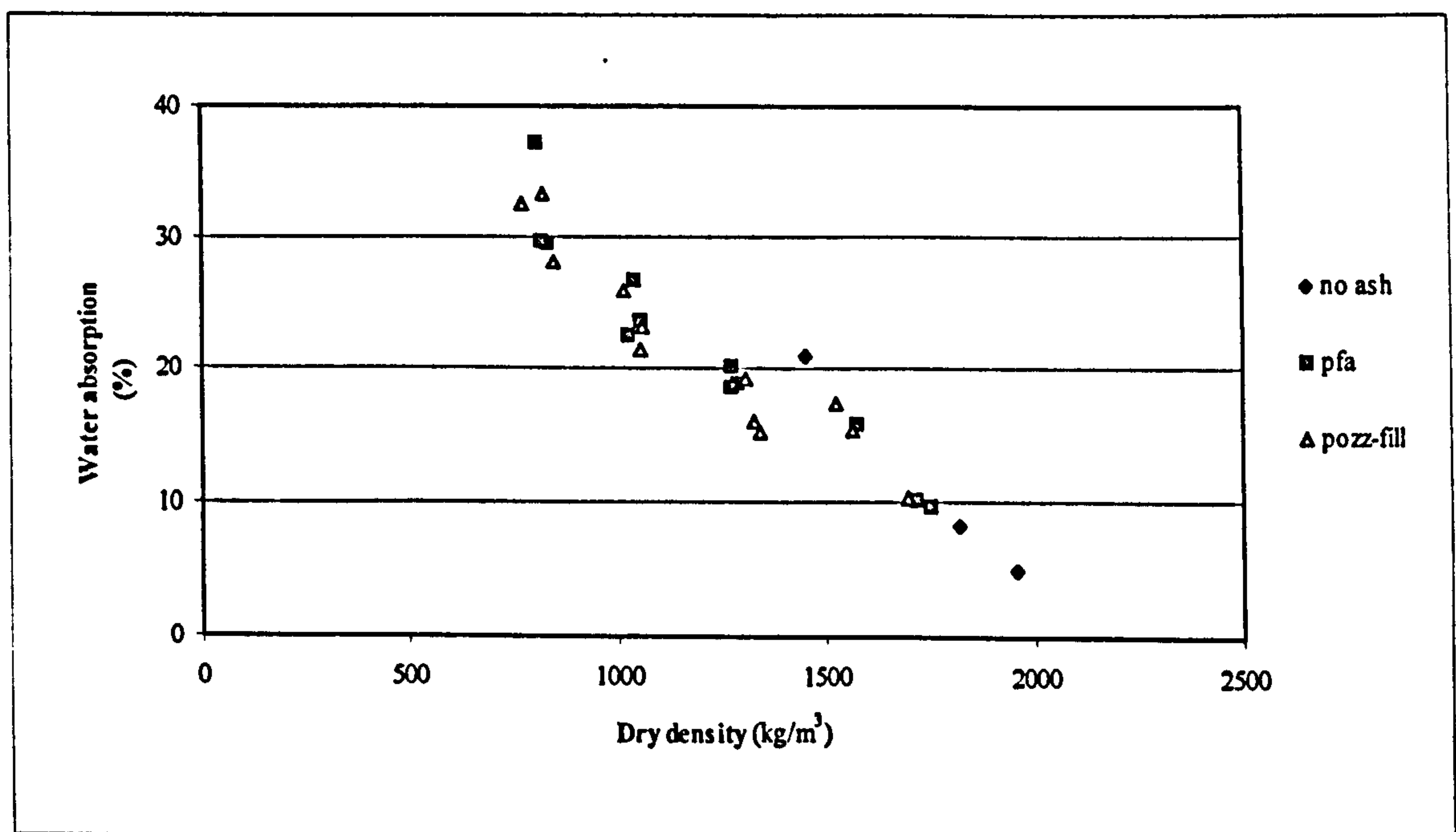


Figure 6.35: Effect of Dry Density on Percentage Water Absorption.

Water absorption may be expressed as the increase in mass per unit of dry mass (as in Figure 6.35) or as the increase in mass per unit volume. For conventional concrete where densities normally vary very little the results are likely to be similar no matter which way they are expressed. However for the foamed concrete mixtures reported here there are significant differences in density (1000 to 1500 kg/m³) and expressing water absorption as the increase in mass per unit volume (see Figure 6.36) presents a different picture to that discussed previously in Figure 6.35. It is now apparent that the foamed concrete mixtures with low density absorb only marginally more water than those with higher densities. It is also apparent that the cement paste mixture containing no ash

(w/c = 0.6) absorbs more water than any of the foamed concrete mixtures. From Figure 6.36 it can be seen that there is a trend of increased absorption with decreasing density but a reduction in density for the paste mixtures containing no foam results in a much more drastic increase in absorption than that found for the mixtures containing foam.

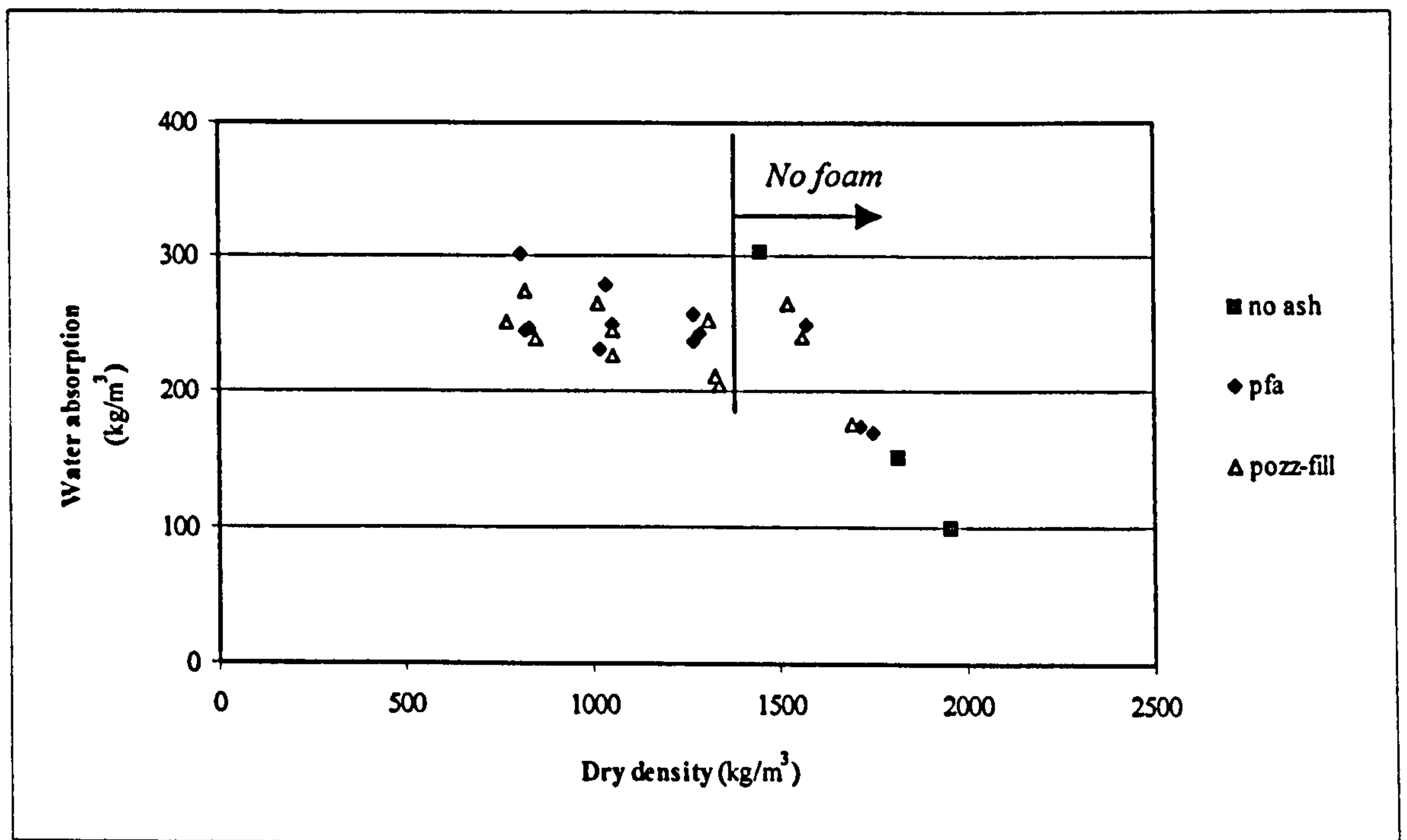


Figure 6.36: Effect of Dry Density on Water Absorption.

The relationship between porosity and water absorption, per unit weight and per volume, are shown in Figure 6.37 and Figure 6.38 and it is not surprising to see similar trends to those for dry density shown in Figure 6.35 and Figure 6.36. Figure 6.37 shows a linear relationship between porosity and water absorption (% increase per unit weight). Linear regression indicates that 85.9 % of the variation in water absorption can be explained by the variation in porosity. The relationship between porosity and the water absorption (% increase per unit volume) is shown in Figure 6.38 and this confirms the fact that higher porosity does not necessarily result in higher water absorption. The majority of the foamed concrete mixtures have water absorption between 200 to 280 kg/m³ which is greater than that of the cement paste with a water/cement ratio of 0.30 (100 kg/m³) and less than that of the paste with water/cement ratio of 0.6 (300 kg/m³). As the water/binder ratio of all the foamed concrete mixtures were nominally the same at 0.30 these results would suggest that about 50% of their water absorption can be accounted for by their paste fraction. The inclusion of the entrained air results in an

approximate doubling of the water absorption but the fact that this increase appears to remain almost the same regardless of the amount of air entrained would suggest that only some of the voids are either filled or part filled with water.

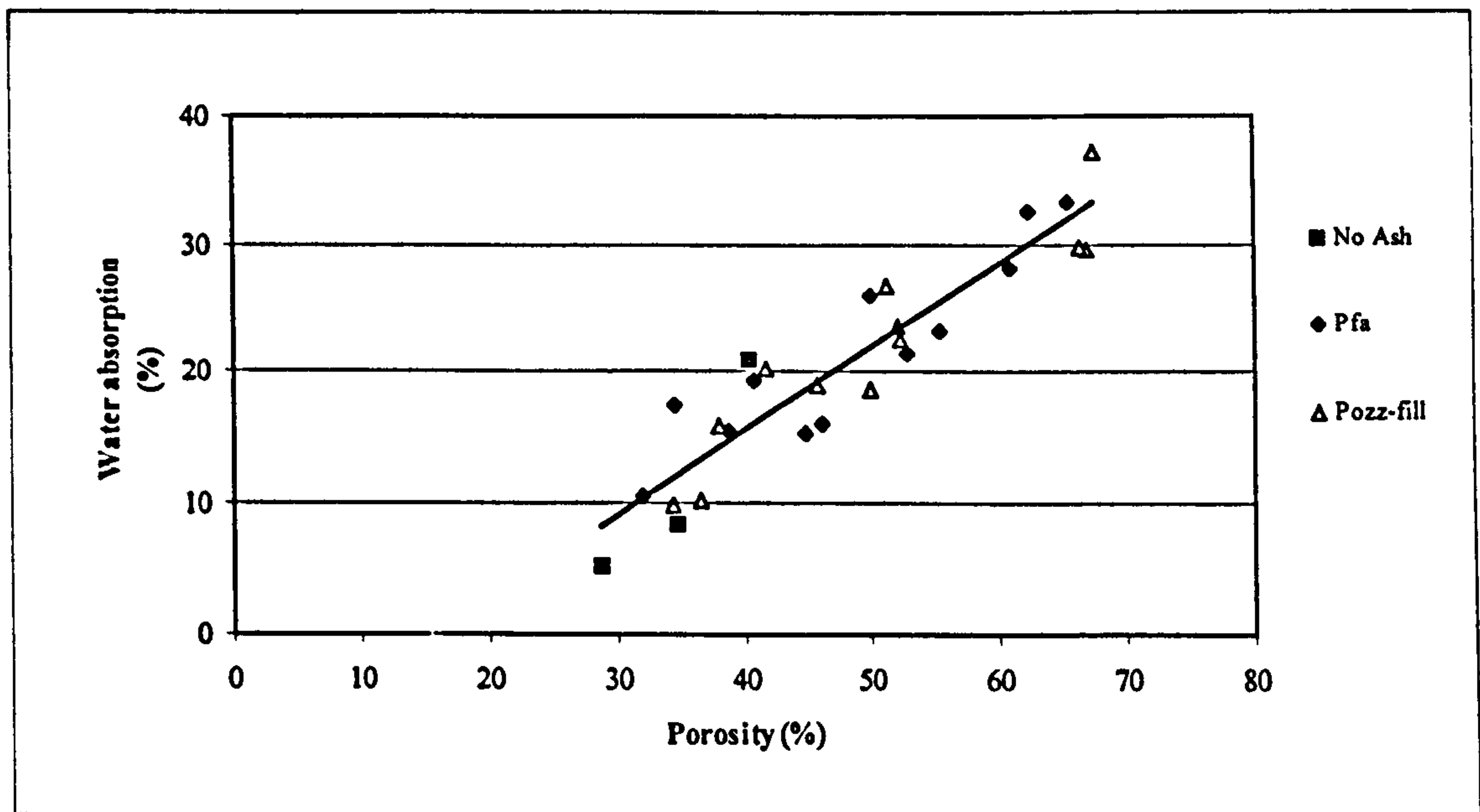


Figure 6.37: Effect of Porosity on Percentage Water Absorption.

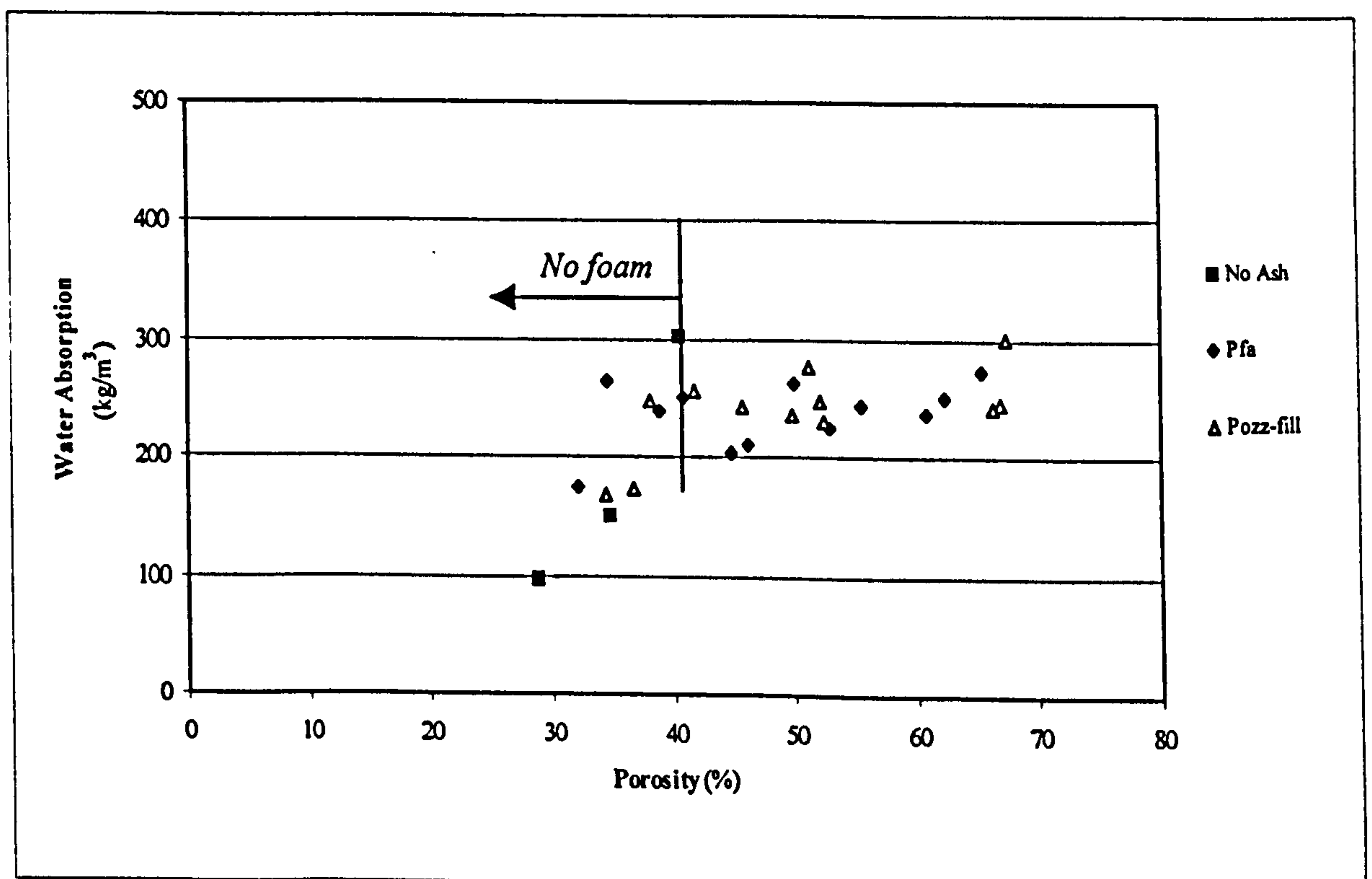


Figure 6.38: Water Absorption as a Function of Porosity.

The effect of the void size and spacing on water absorption can be seen in Figure 6.39. The water absorption seems to increase marginally with increased void diameters. It is interesting to note that increasing distances between voids results in a marginal increase in absorption. This slight trend would suggest that the voids might be acting as a buffer and stop the water from migrating deeper into the sample.

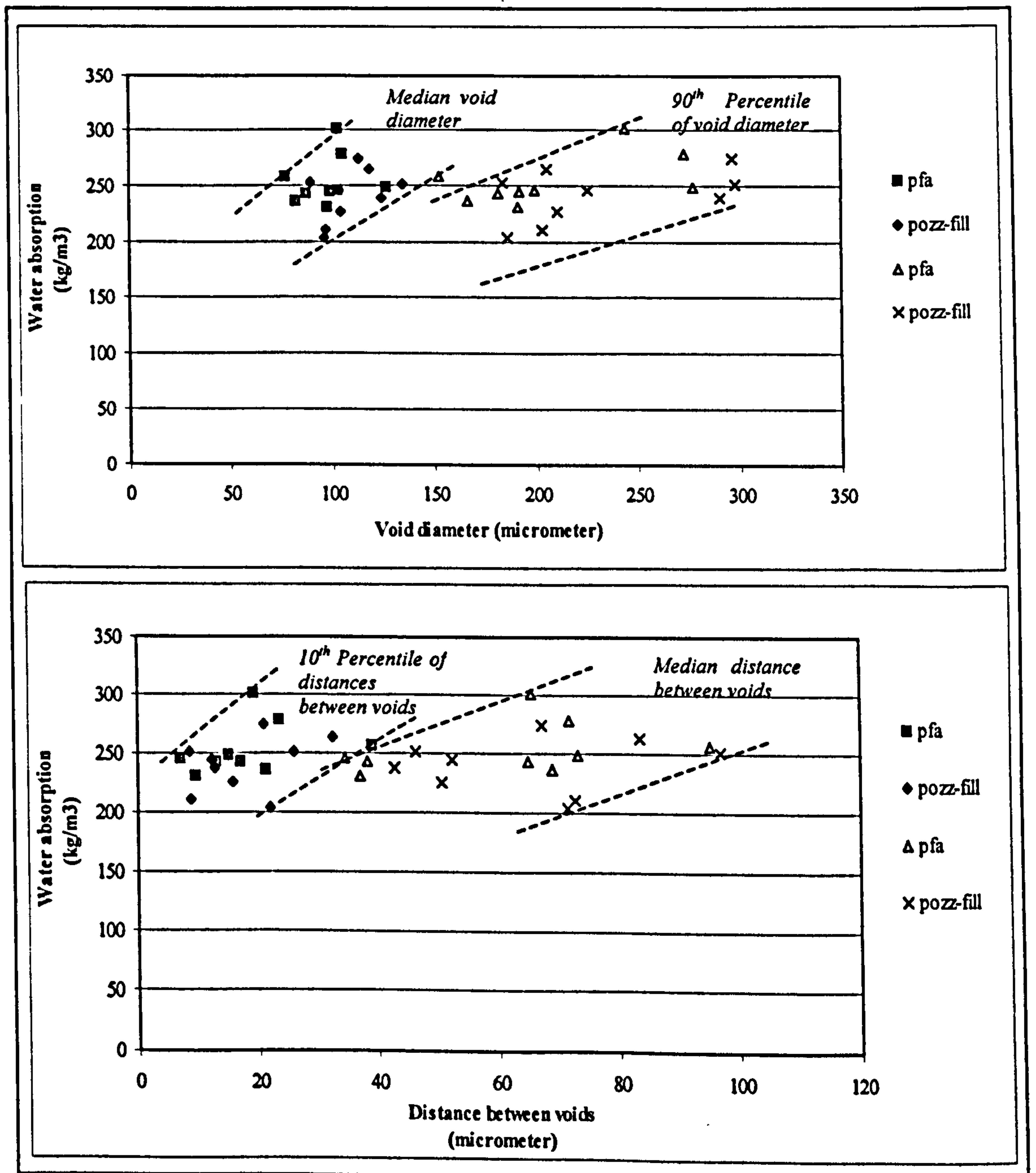


Figure 6.39: Effect of Void Size and Spacing on Water Absorption.

The effect of ash type and content on the water absorption of foamed concrete can be seen in Figure 6.40. Neither the ash type nor content seems to have a significant effect on the water absorption.

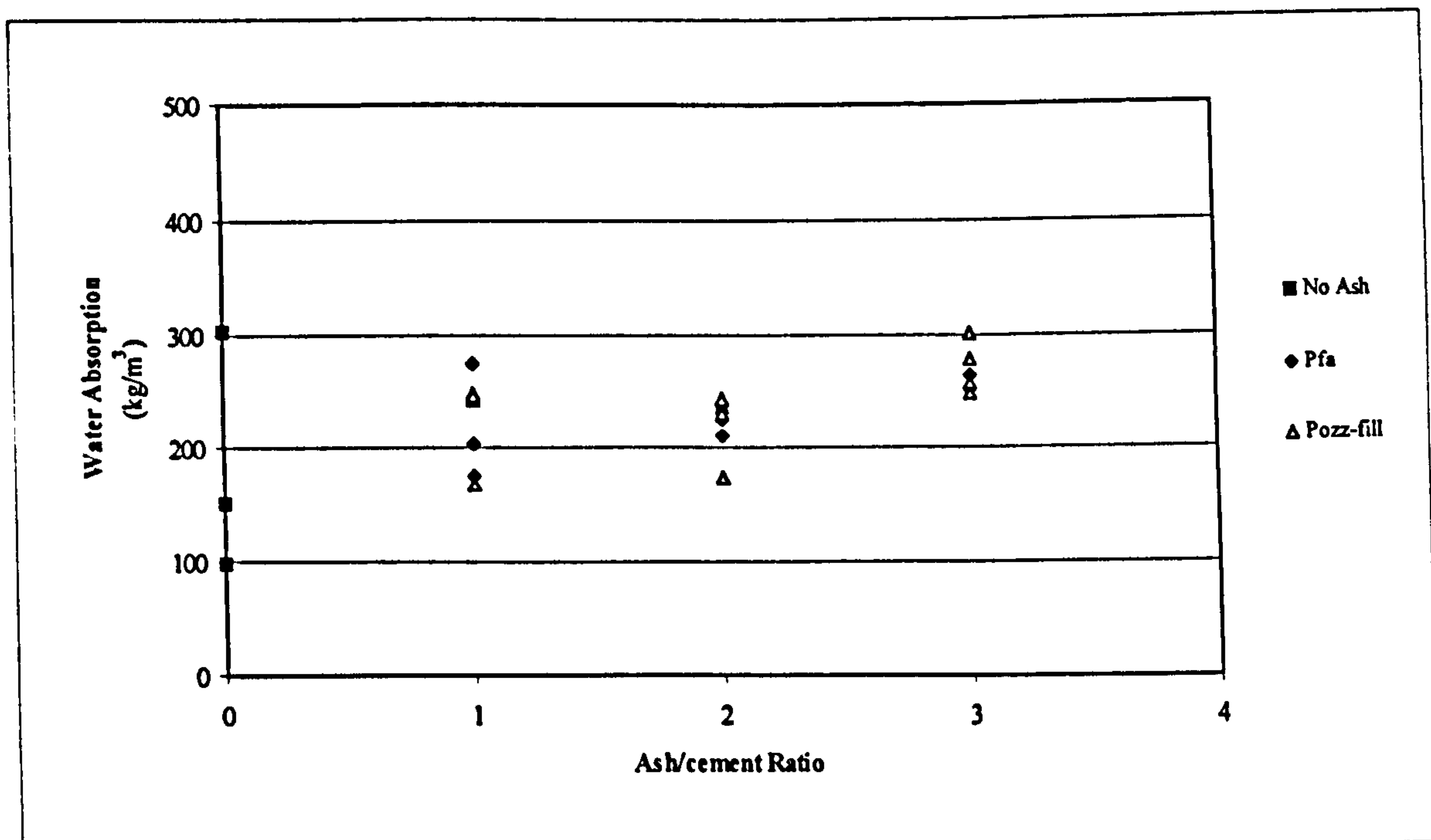


Figure 6.40: Water Absorption as a Function of Ash/cement Ratio.

6.4.2 Water vapour permeability

The water vapour permeability of foamed concrete was determined by measuring the amount of mass transfer due to diffusion of water vapour resulting from a difference in water vapour pressure on the two parallel surfaces of a foamed concrete disc. Two specimens were set up for each mixture and the weight loss was measured as a function of time as can be seen in Appendix F where the measurements are reported graphically. The permeability is a function of the rate of weight loss and all the specimen rapidly reached a steady condition where the rate of weight loss (or the slope of the graphs in Appendix F) is constant.

The average rate of weight loss was determined for each mixture, and the loss over a 100-day period was calculated and plotted as a function of dry density, as can be seen in Figure 6.41. The weight loss through the foamed concrete specimen is a function of the dry density as can be seen in the graph in Figure 6.41. The weight loss of mixtures increases with decreasing dry density, but the spread of results indicate that factors other than dry density affects the water vapour permeability. The discs used to determine the water vapour permeability did not all have the same thickness, and this variation in thickness would increase the variability in the relation between weight loss and dry density. The effect of variation in thickness was eliminated by calculating the water

vapour permeability (k_d), which according to RILEM Recommendation LC 7⁷³ is a material constant which is a function of density and pore structure. The water vapour permeability is plotted as a function of dry density in Figure 6.42, which indicates there is a strong relation between dry density and permeability.

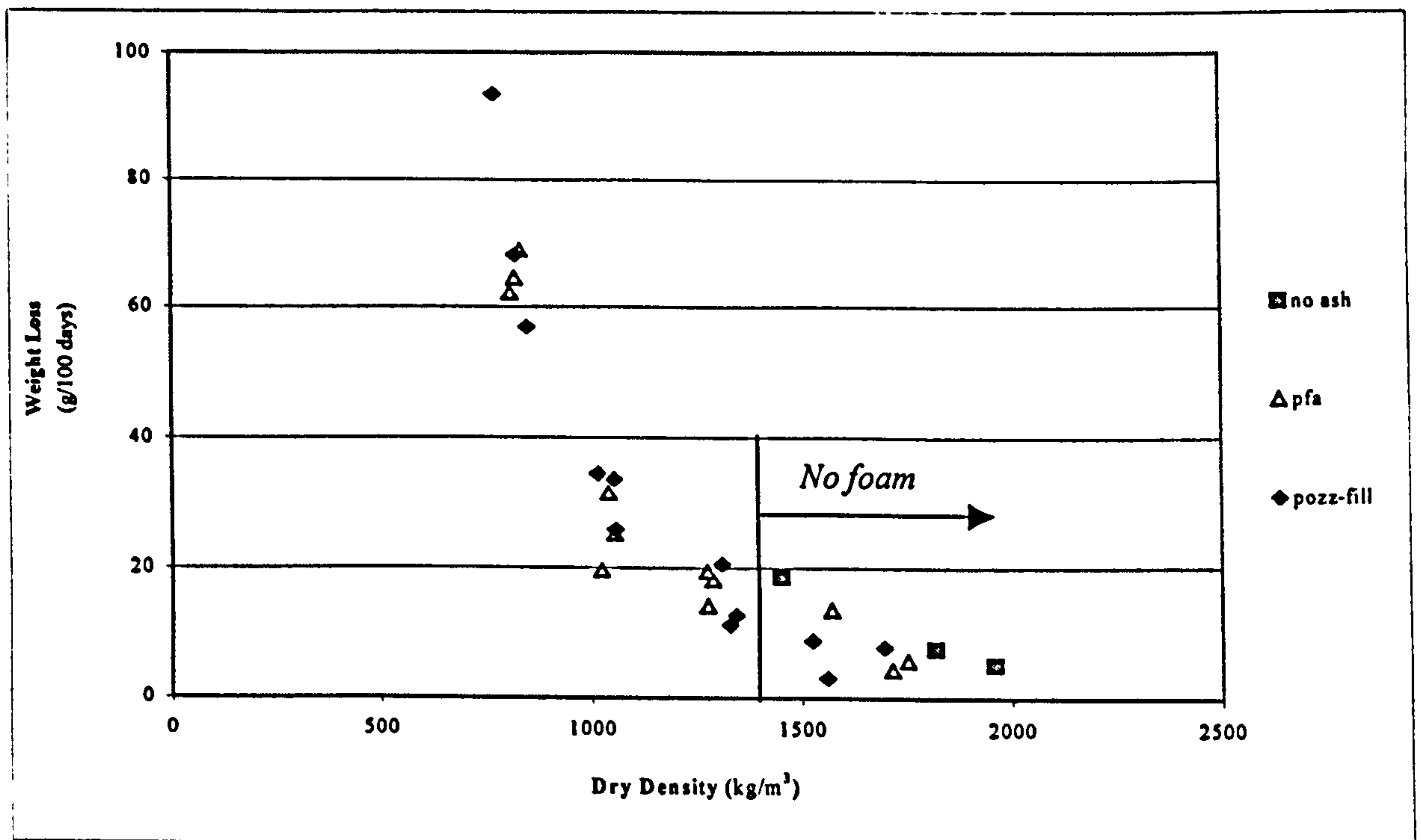


Figure 6.41: Weight Loss as a Function of Dry Density.

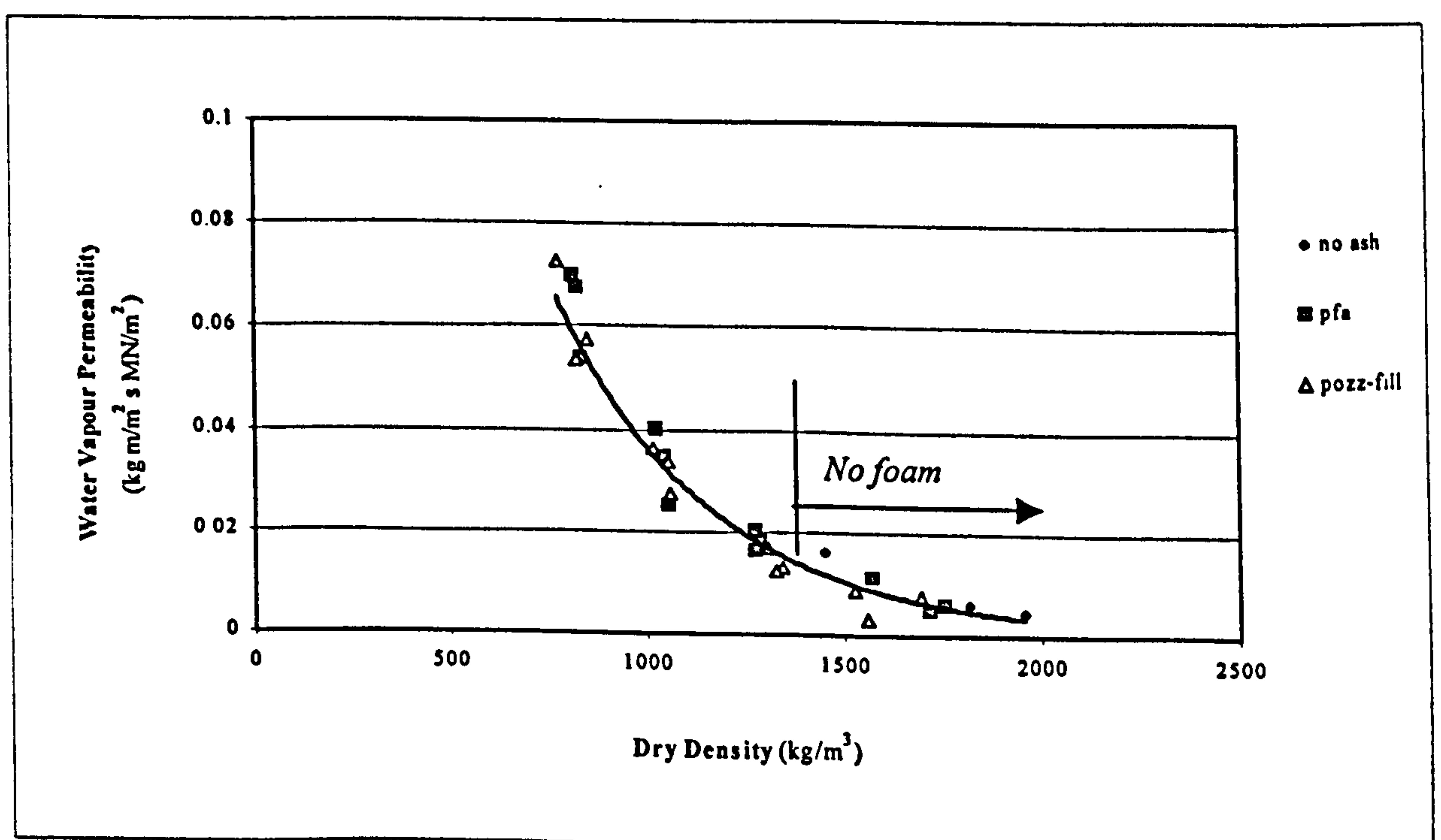


Figure 6.42: Vapour Permeability as a Function of Dry Density.

A similar but slightly less defined trend is observed when plotting water vapour permeability against porosity (Figure 6.43). It is interesting to note that the same trend line fits the results both with and without foam which is in contrast to the case for water absorption (Figure 6.36 and Figure 6.38). An increase in the volume of voids (as indicated by a reduction in density or increase in porosity) leads to a marked increase in water vapour permeability. This suggests that perhaps all the voids are playing a part in the transfer mechanism of water vapour through the specimen, which does not appear to be the case with water absorption.

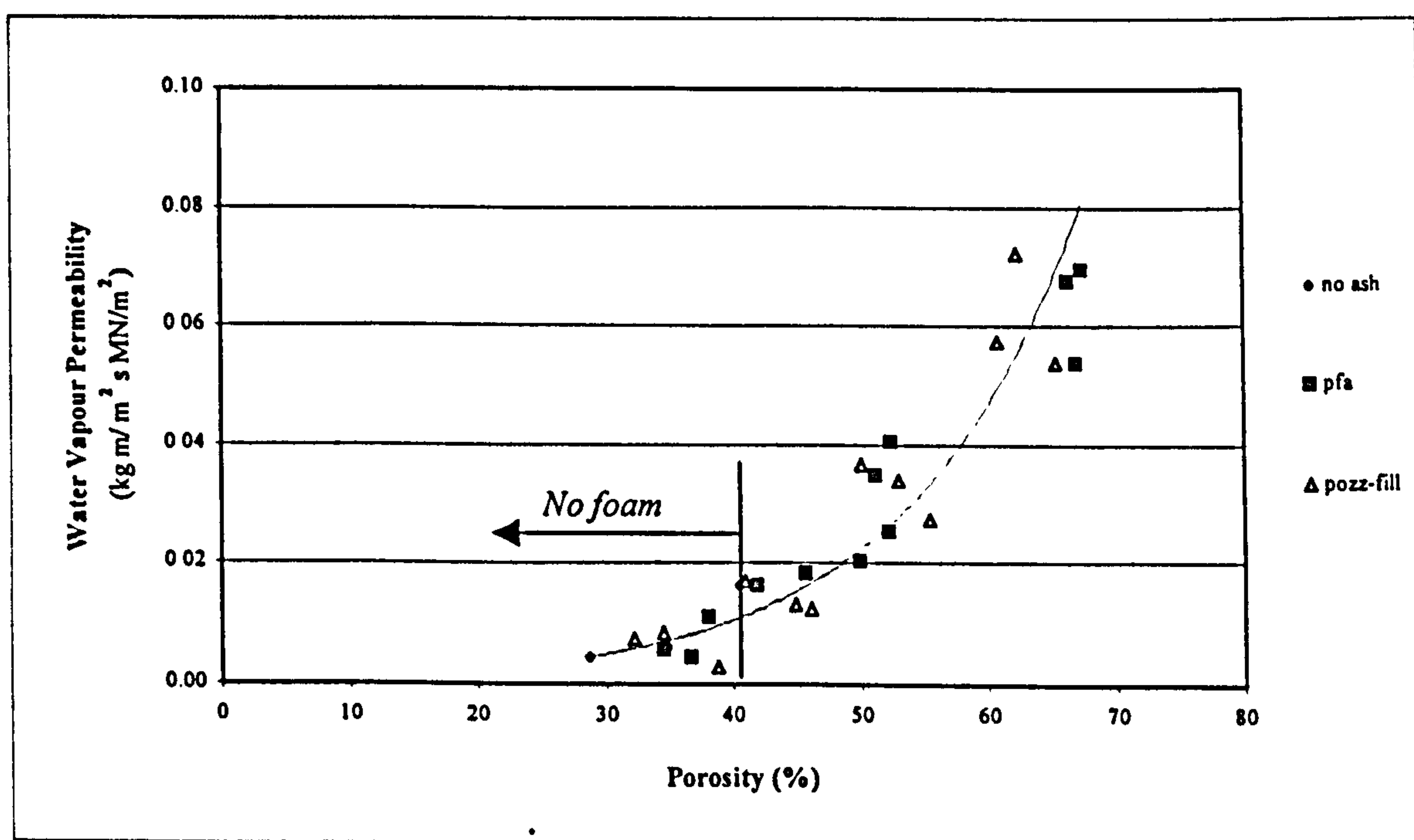


Figure 6.43: Water Vapour Permeability versus Porosity.

The volume of ash (pfa or pozz-fill) used has an effect on the water vapour permeability of foamed concrete as can be seen in Figure 6.44. The water vapour permeability of the foamed concrete mixtures increase with increasing ash/cement ratio and this trend becomes more significant at the lower densities.

The effect of void size and distribution on the water vapour permeability of foamed concrete can be seen in Figure 6.45. It is difficult to see any clear trends from these results although there would appear to be an overall increase in permeability with an increase in the diameter of the larger voids as indicated by the 90th percentile values. In

addition an increase in the median distance between the voids appears to lead to an overall reduction in permeability. There does not seem to be any relationship between the 10th percentile of distances between voids and the water vapour permeability, indicating that the permeability of foamed concrete is not dependant on the minimum distances between voids.

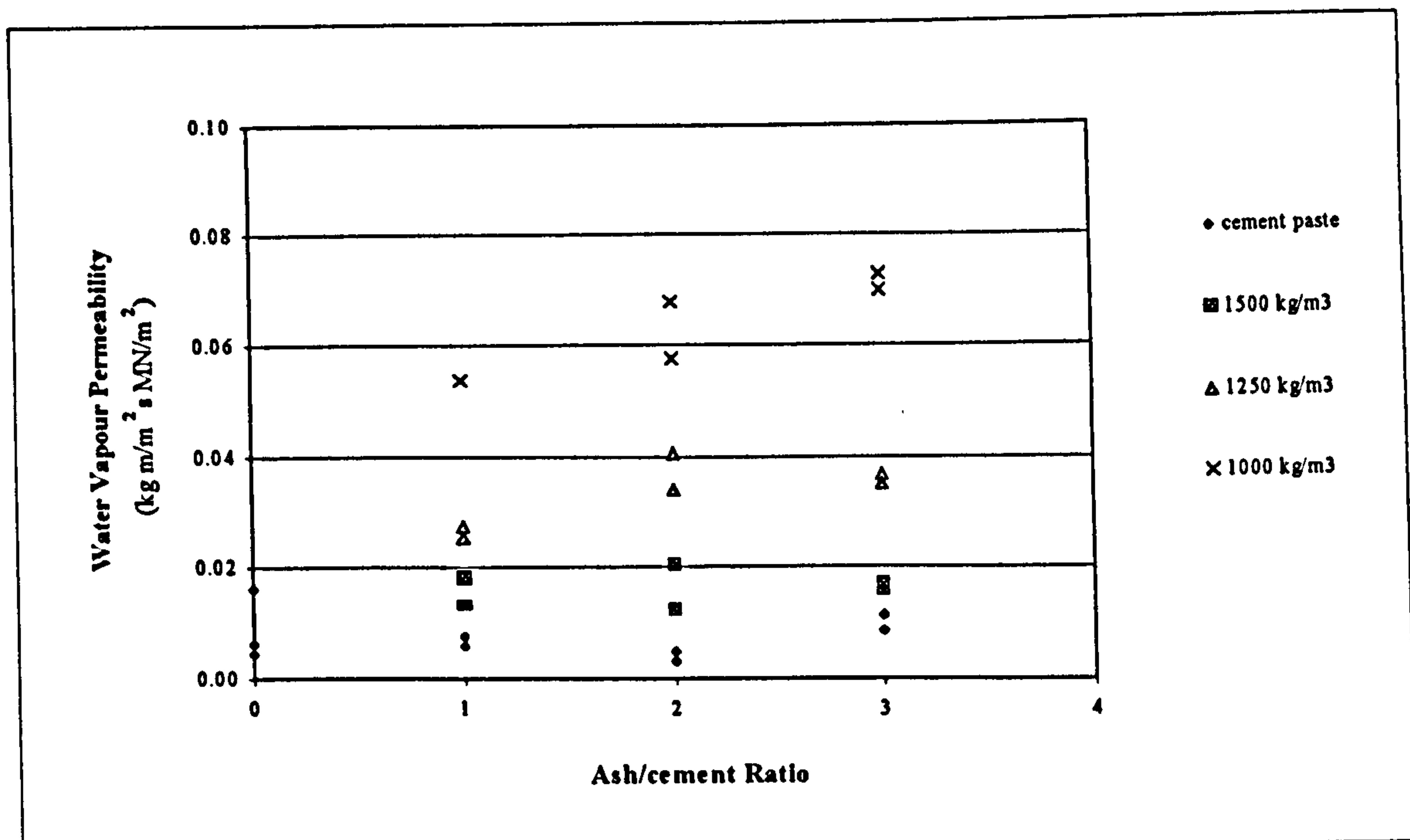


Figure 6.44: Effect of Ash/cement Ratio on Water Vapour Permeability.

The relation between the water absorption and the water vapour permeability of foamed concrete can be seen in Figure 6.46. For the mixtures containing no foam the water absorption can increase dramatically without any noticeable increase in water vapour permeability. For the mixtures containing foam relatively small increases in water absorption results in significant increases in water vapour permeability. These results would suggest as discussed earlier that the mechanism of water absorption and water vapour permeability are fundamentally different and influenced by different factors.

Of the two tests reported in this section the water vapour permeability tests could arguably be considered as the more realistic in terms of reproducing the conditions that concrete might be subjected to in service. The results from this test indicate that reinforcing steel in foamed concrete with relatively high density is probably no more prone to corrosion than that in normal concrete.

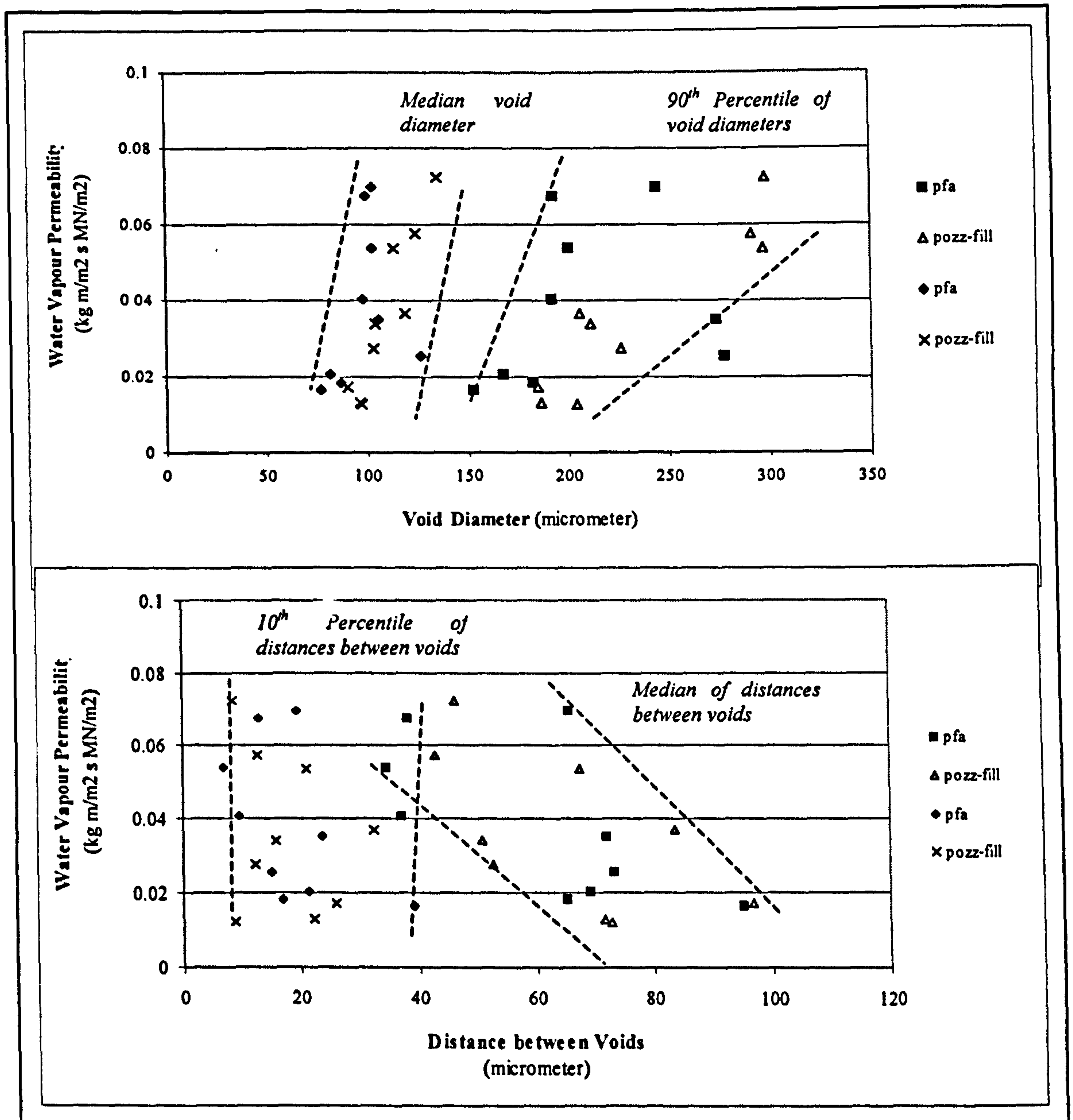


Figure 6.45: Effect of Void Size and Distribution on Water Vapour Permeability.

6.4.3 Conclusions on water absorption and permeability

- Expressing water absorption as a percentage increase in mass can give misleading results where foamed concrete is concerned because of the large differences in density.
- The volume of water, expressed in kg/m^3 absorbed by the foamed concrete is approximately twice that absorbed by a cement paste with similar water/binder ratio.

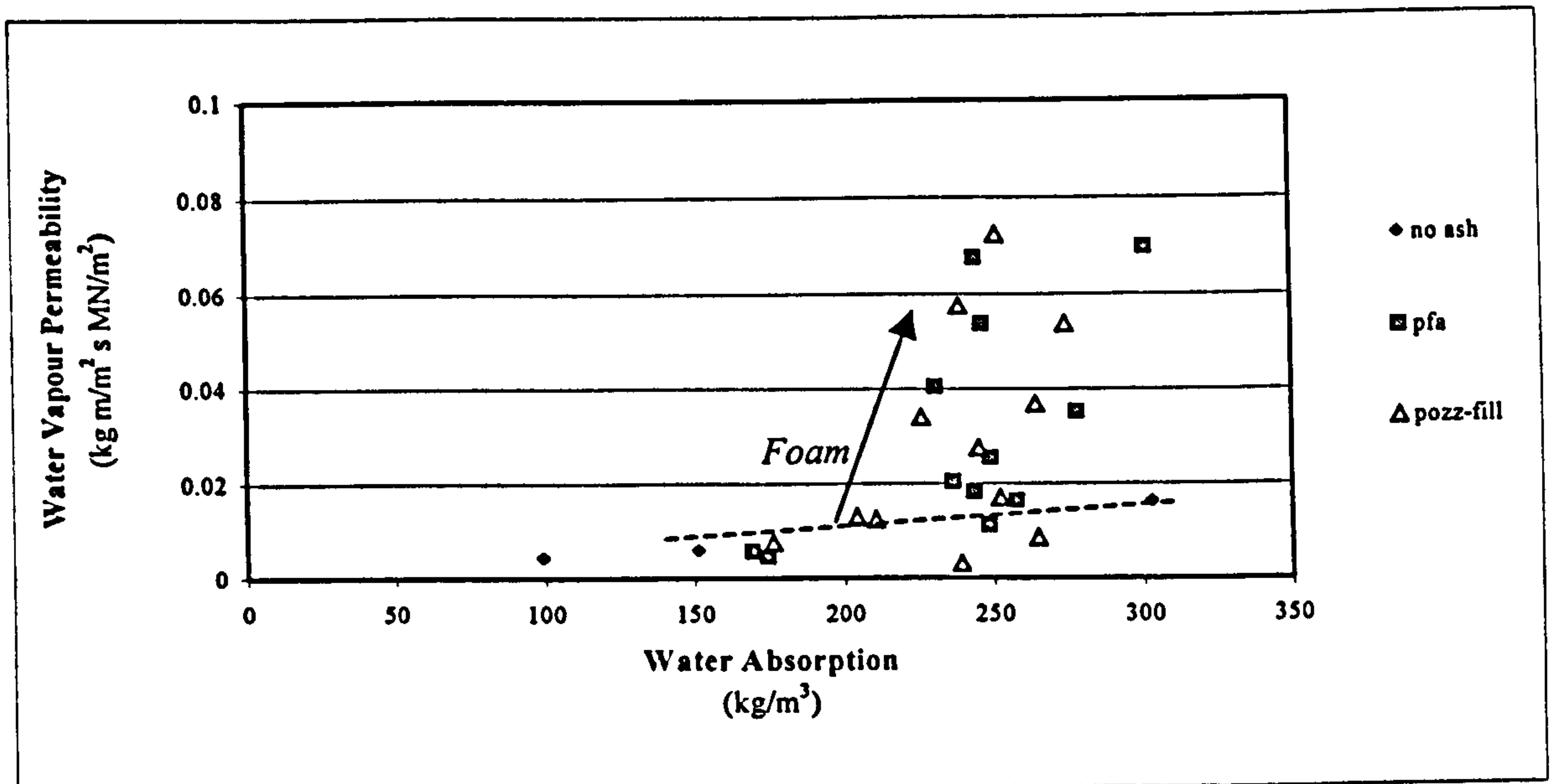


Figure 6.46: Water Absorption versus Water Vapour Permeability.

- The volume of water, expressed in kg/m^3 absorbed by the foamed concrete appears to be little influenced by the volume of air entrained which suggests that not all the voids are filled with water.
- Neither ash type nor content has an effect on the water absorption of foamed concrete. The fact that the water/binder ratio was kept constant with changing ash content possibly eliminated any reduction in water absorption that could be caused by the use of ash.
- Although the water absorption of cement pastes increases with increasing porosity, there is no trend between the water absorption of foamed concrete and its porosity.
- Water absorption increases with increased void size.
- Water vapour permeability increases with increasing porosity (or reducing density) and the trend lines appear to be similar for mixtures both with and without foam.
- The water vapour permeability of foamed concrete mixtures increase with increasing ash/cement ratios and this trend becomes more significant at lower densities.
- The water vapour permeability of mixtures containing pozz-fill is marginally lower than that of mixtures containing pfa.
- For mixtures containing no foam large increases in water absorption results in marginal increases in water vapour permeability.
- For mixtures containing foam small increases in water absorption results in significant increases in water vapour permeability.

6.5 DEFORMATION OF FOAMED CONCRETE

6.5.1 Drying shrinkage

The drying shrinkage of two beams from each mixture were recorded for a period of 30 months and in Appendix G the average of these two sets of readings is plotted as a function of time for each of the mixtures cast in this test program. An example of these graphs can be seen in Figure 6.47 where the shrinkage of 1500 kg/m^3 pfa mixtures are shown as a function of time.

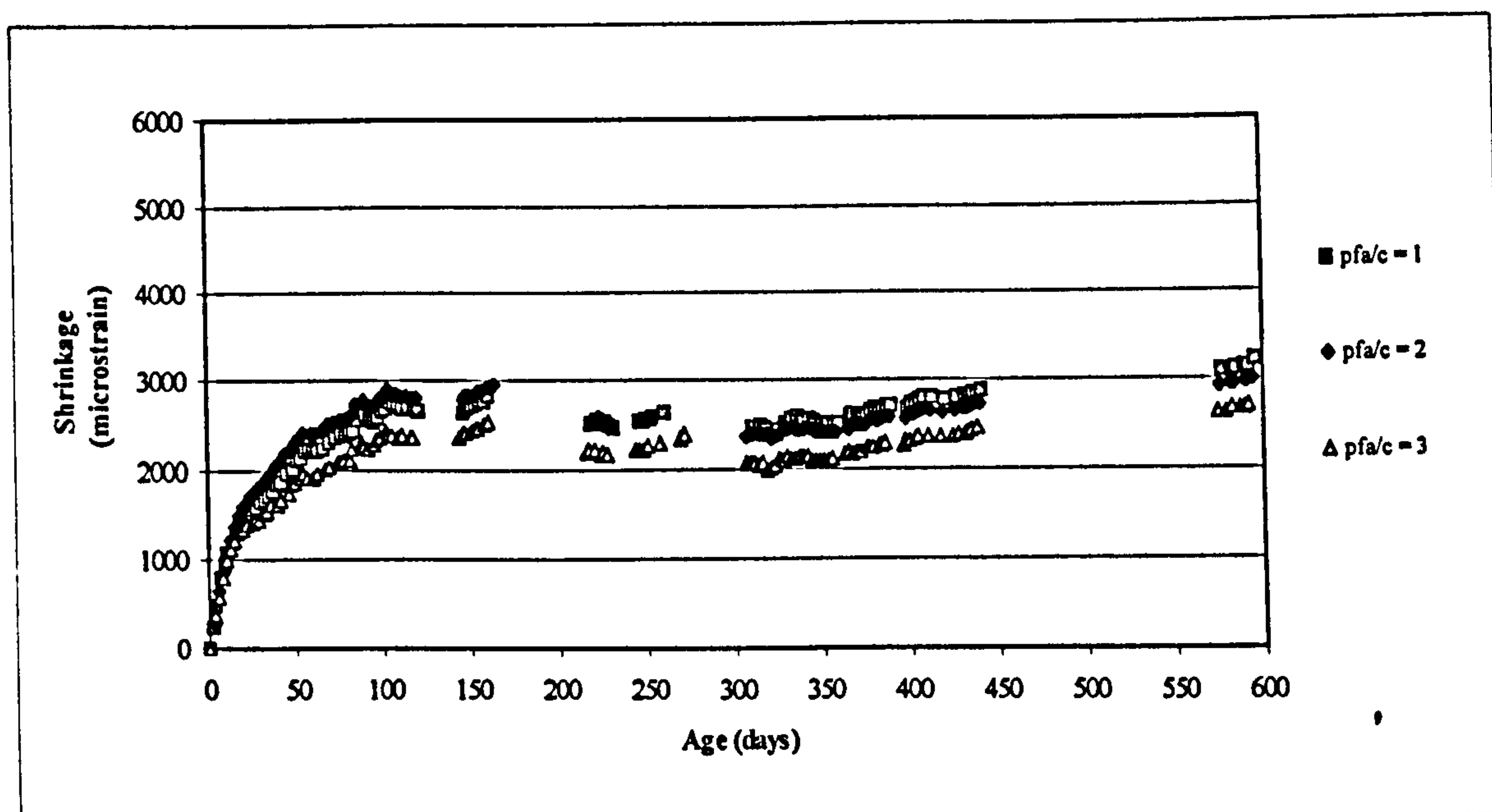


Figure 6.47: Shrinkage of 1500 kg/m^3 Mixtures Containing Pfa.

After 150 days of drying the rate of shrinkage had reduced to such an extent that a relatively constant value was reached. In an effort to establish the effect of high content ungraded fly ash on the drying shrinkage of foamed concrete the shrinkage of all mixtures after six months were compared. These values are plotted as a function of dry density in Figure 6.48. From this graph it can be seen that the shrinkage of the cement paste is inversely related to dry density which is only to be expected since the density is directly related to water/cement ratio. In other words a higher density corresponds to a lower water/cement ratio which results in a lower shrinkage. The drying shrinkage of the pastes containing ash are similar to or slightly lower than those of the cement pastes which again is to be expected because the water/binder ratio in all cases is kept

nominally the same at 0.3. The slight reduction in shrinkage of those pastes containing higher ash contents may be the result of some of the ash acting as an inert filler and thus restraining some of the shrinkage. The introduction of foam into the mixtures appears to have little effect on the shrinkage with all the values being similar to the pastes with the same nominal water/binder ratio of 0.30. This is a similar trend to that observed earlier for water absorption (Figure 6.36) and suggests that the drying shrinkage is influenced more by the cement paste than the volume of air entrained. As the volume of air is increased the stiffness of the concrete would be expected to fall (which might be expected to result in increased shrinkage) but this is presumably offset by the reduction in the volume of paste resulting in little overall change in the shrinkage. As might be expected similar trends to these discussed above are observed if drying shrinkage is plotted against porosity as shown in Figure 6.49. The author's results seem to disagree with other investigators¹⁹ who have indicated that the shrinkage of foamed concrete is a function of the volume of air entrained with lower densities resulting in higher shrinkage.

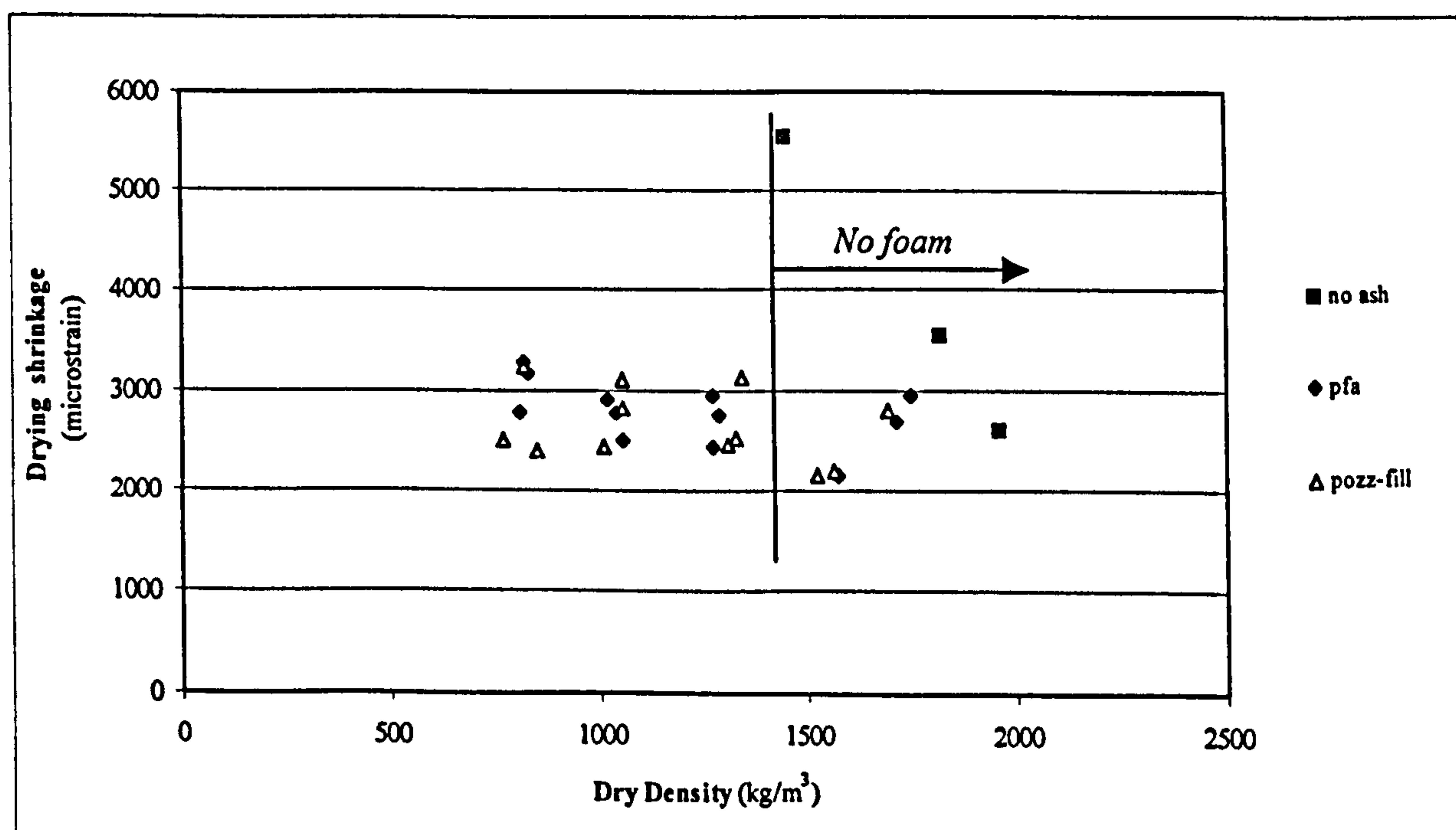


Figure 6.48: Drying Shrinkage versus Dry Density.

The slight reduction in drying shrinkage with increased ash content was referred to earlier. This trend can be seen more clearly in Figure 6.50 where it is also apparent that the type of ash has little influence over shrinkage.

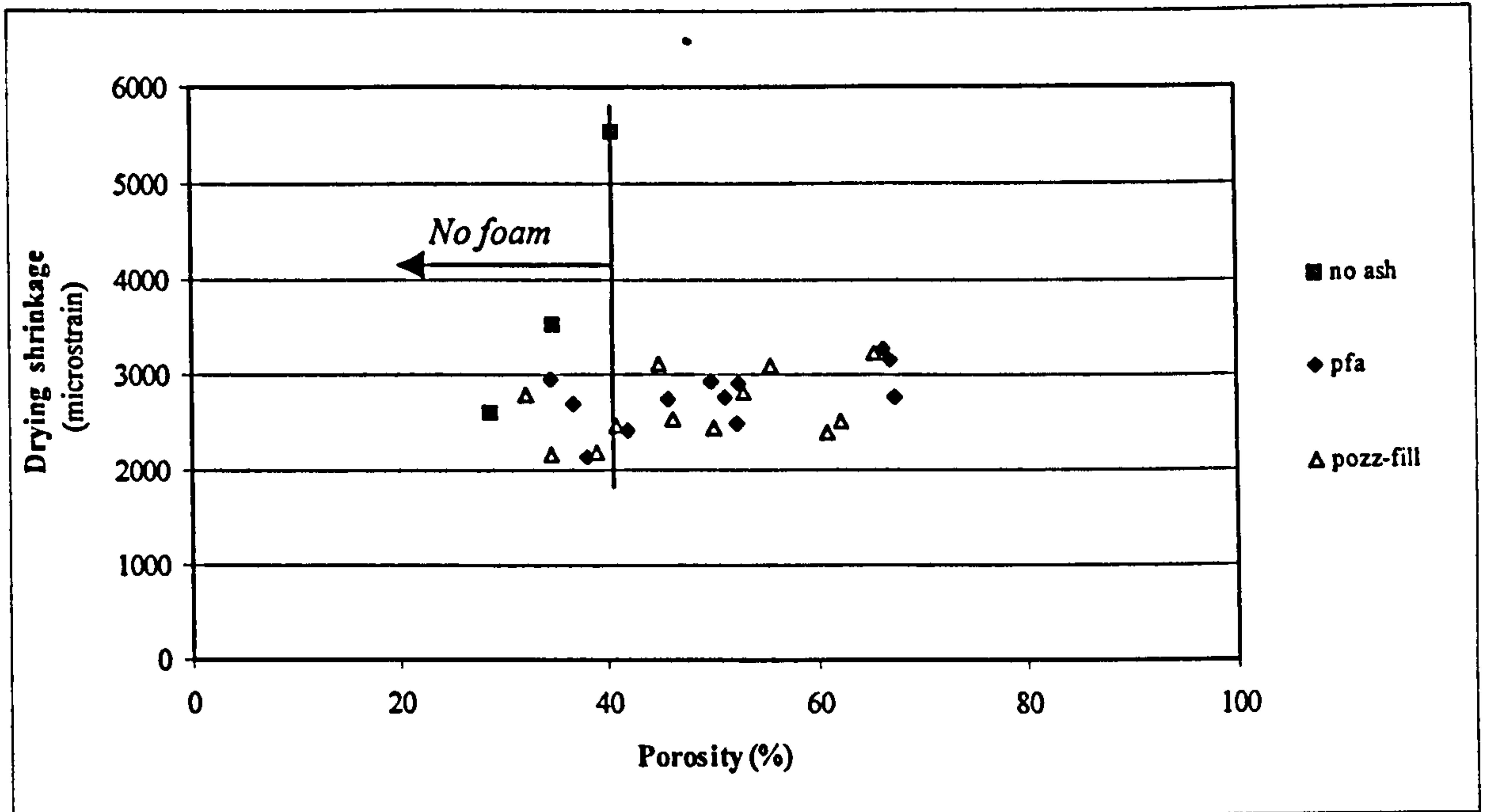


Figure 6.49: Effect of Porosity on the Drying Shrinkage of Foamed Concrete.

The shrinkage results referred to here and those shown in Appendix G are all in the region of 2000 to 3000 microstrains at six months which is some two to three times greater than that of normal concrete¹⁶. Such high values are not surprising in view of the fact that the stiffer aggregate is being replaced by the less stiff air voids.

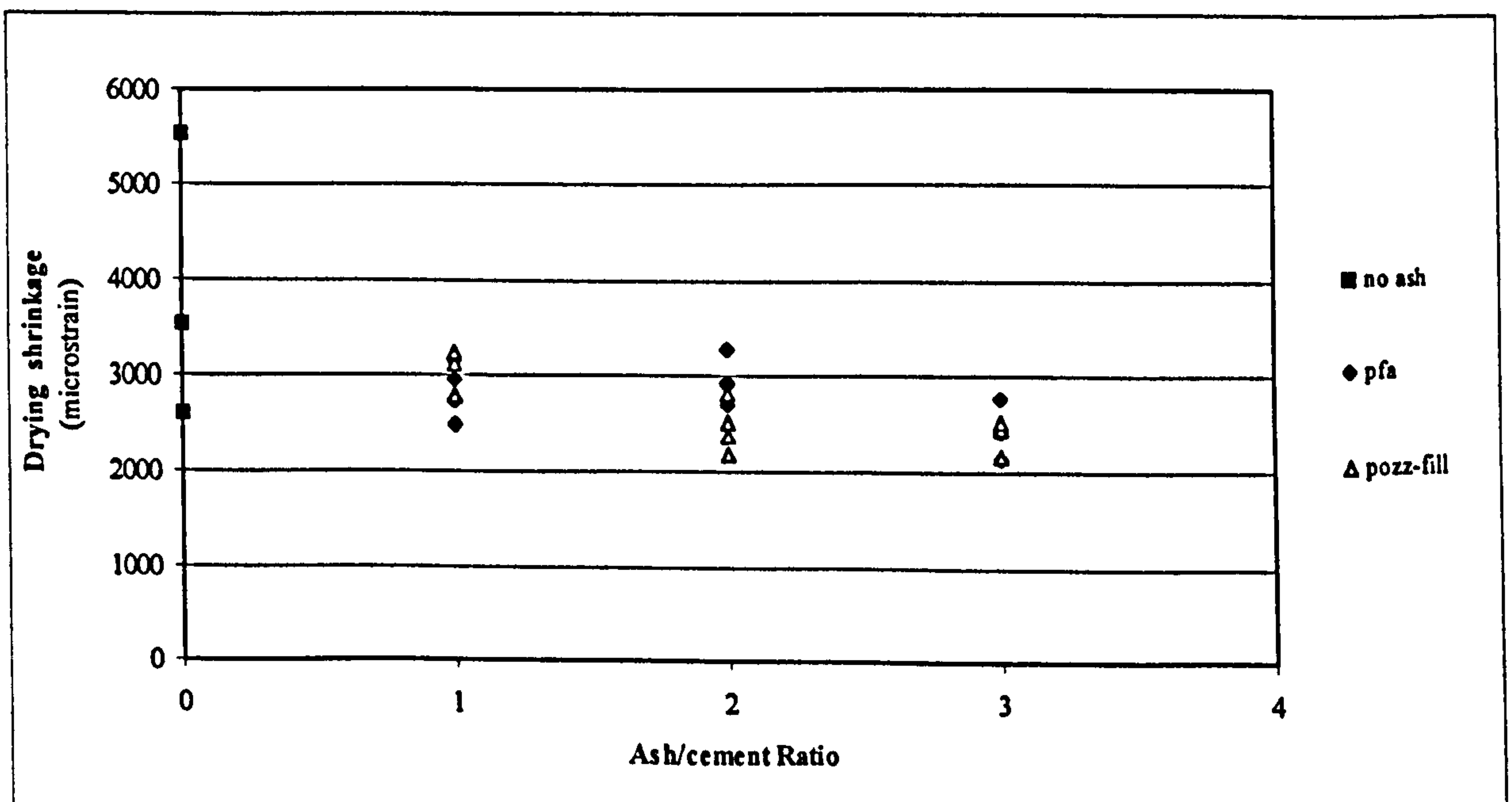


Figure 6.50: Effect of Ash/cement Ratio on the Drying Shrinkage of Foamed Concrete.

However it is interesting to note that increasing the air content (and thus reducing the density to approximately 1000 kg/m³) resulted in no significant increases in shrinkage. Increasing the volume of ash at the expense of the cement resulted in a small reduction but more significant reductions can only be achieved by the introduction of an inert filler (e.g. sand), a study which is outside the bounds of this investigation.

6.5.2 Elasticity and Creep

Elasticity and creep results are presented in Table 5.9. The creep tests were carried out under sealed conditions at a constant stress/strength ratio of 0.4 and the creep measured is therefore defined as “basic creep”.

The measured modulus of elasticity for the foamed concrete is significantly lower than that of normal concrete and the value ranges from 13.2 GPa to 2.5 GPa. There is a good relationship between dry density and elastic modulus (see Figure 6.51) which does not appear to be dependent on the ash/cement ratio.

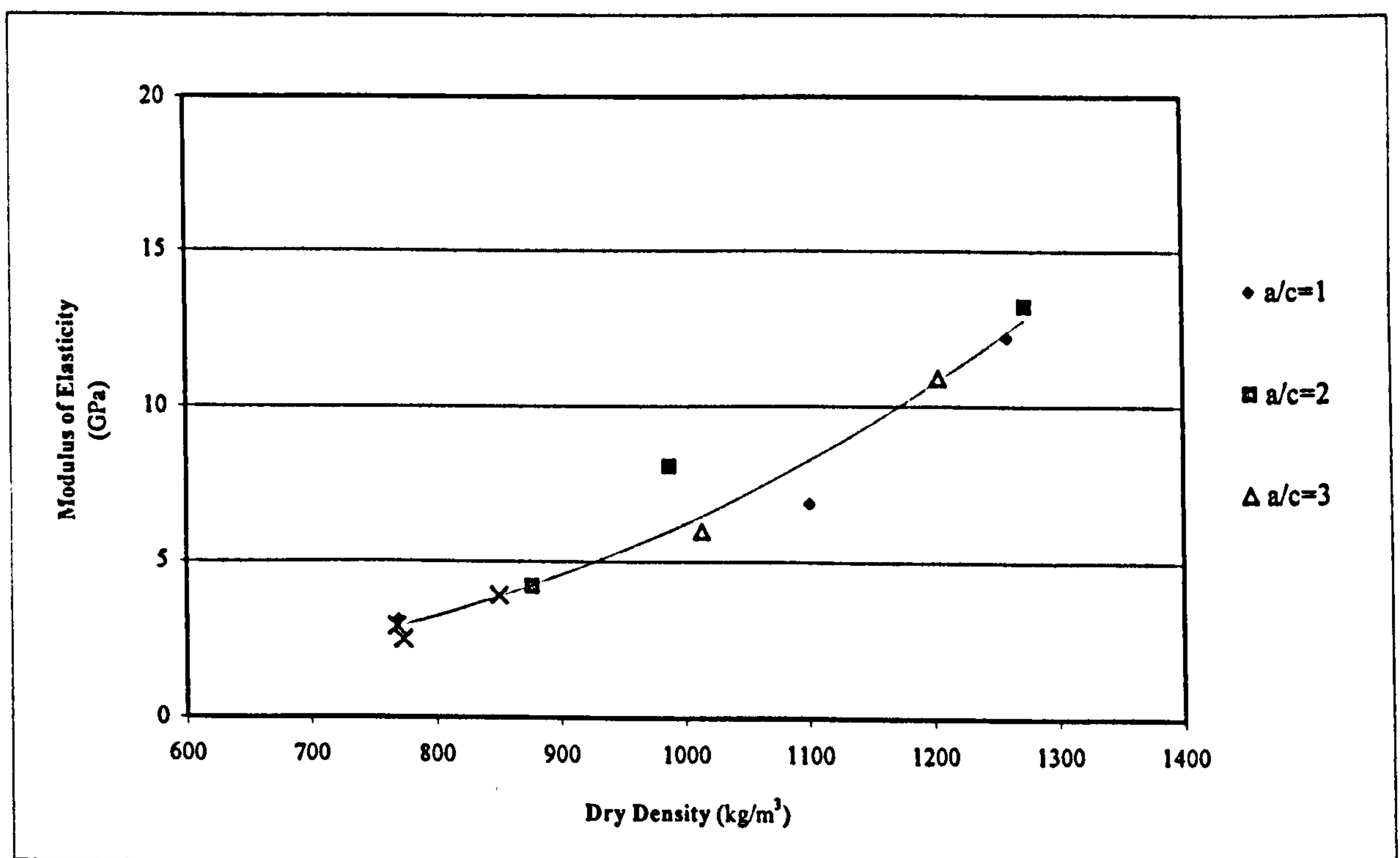


Figure 6.51: Modulus of Elasticity.

The basic creep/time curves for mixes up to 780 days of loading are shown in Figure 6.52 to Figure 6.54. These graphs show no clear pattern either with respect to density or

ash/cement ratio. The highest values were recorded in the specimens with the lowest densities with ash/cement ratios of 0.5 and 1.0, yet on the other hand, one of the other low-density mixtures, with an ash/cement ratio of 2.0, produced one of the lowest values.

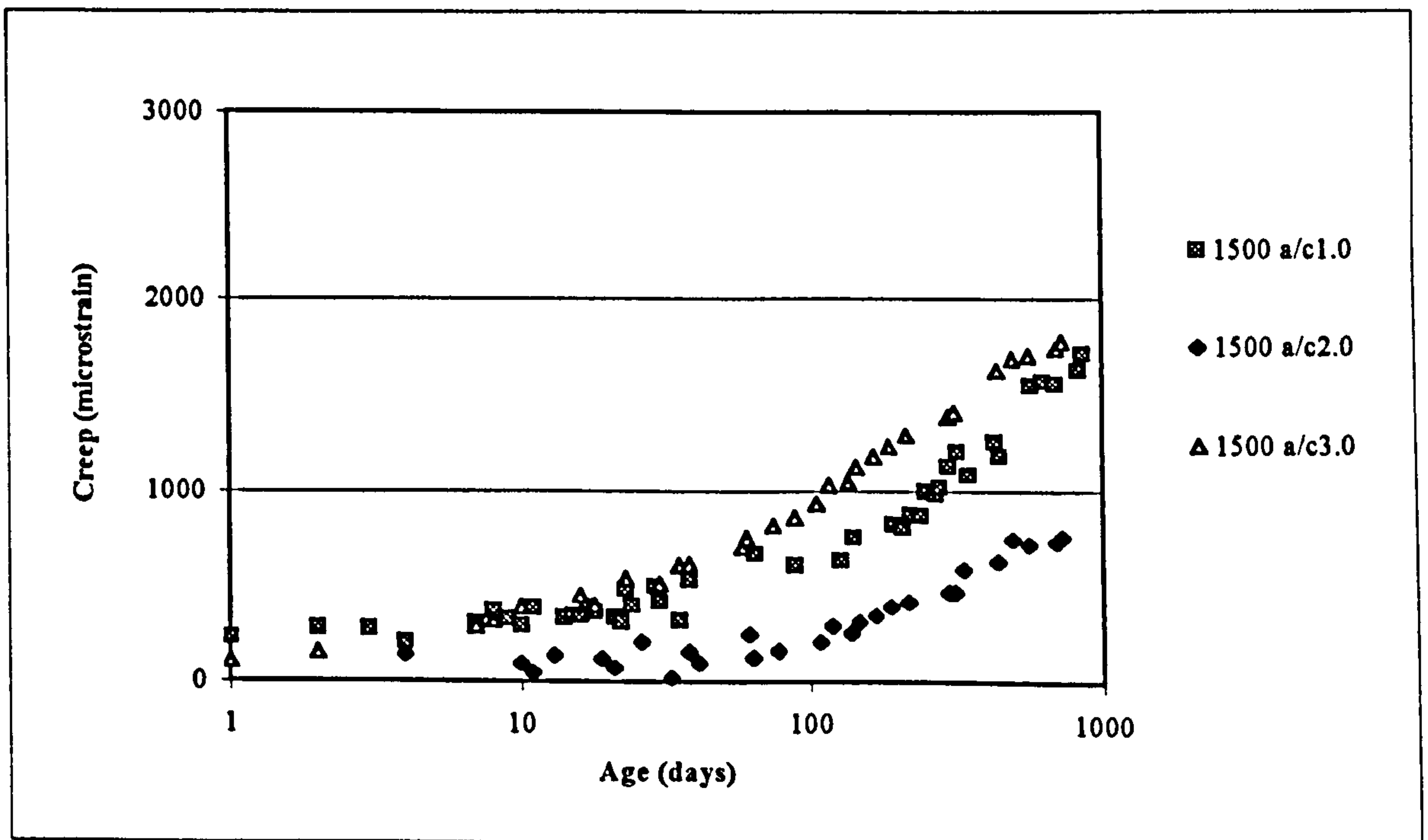


Figure 6.52: Creep of 1500 kg/m³ Foamed Concrete.

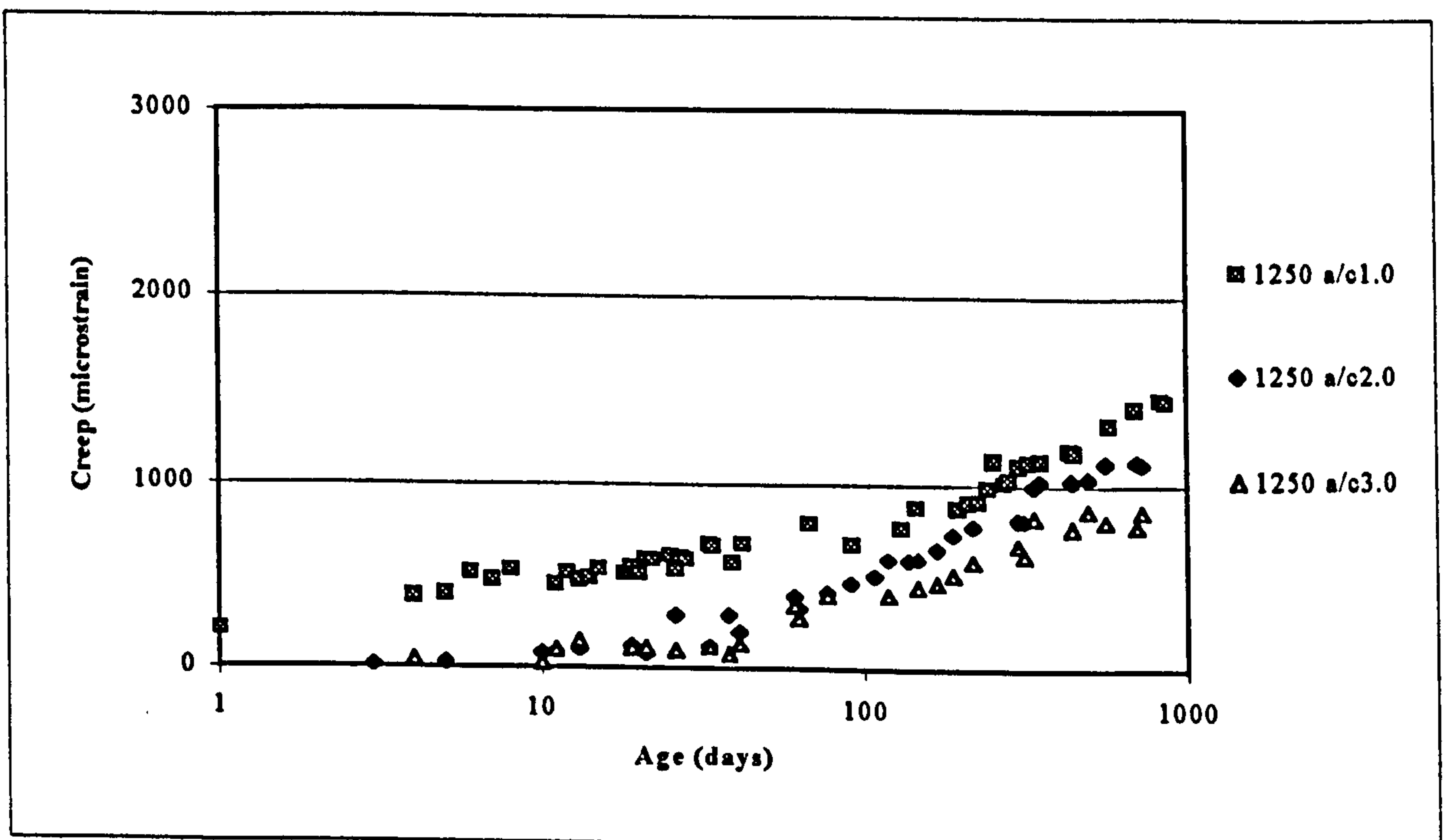


Figure 6.53: Creep of 1250 kg/m³ Foamed Concrete.

The lack of trend with respect to ash/cement ratio is also surprising because mixtures with the higher ash/cement ratio were expected to creep less because their rate of gain in strength over the test period was more than those mixtures with a lower ash/cement ratio. Figure 6.55 shows basic creep at 780 days against dry density and confirms the lack of trend discussed above.

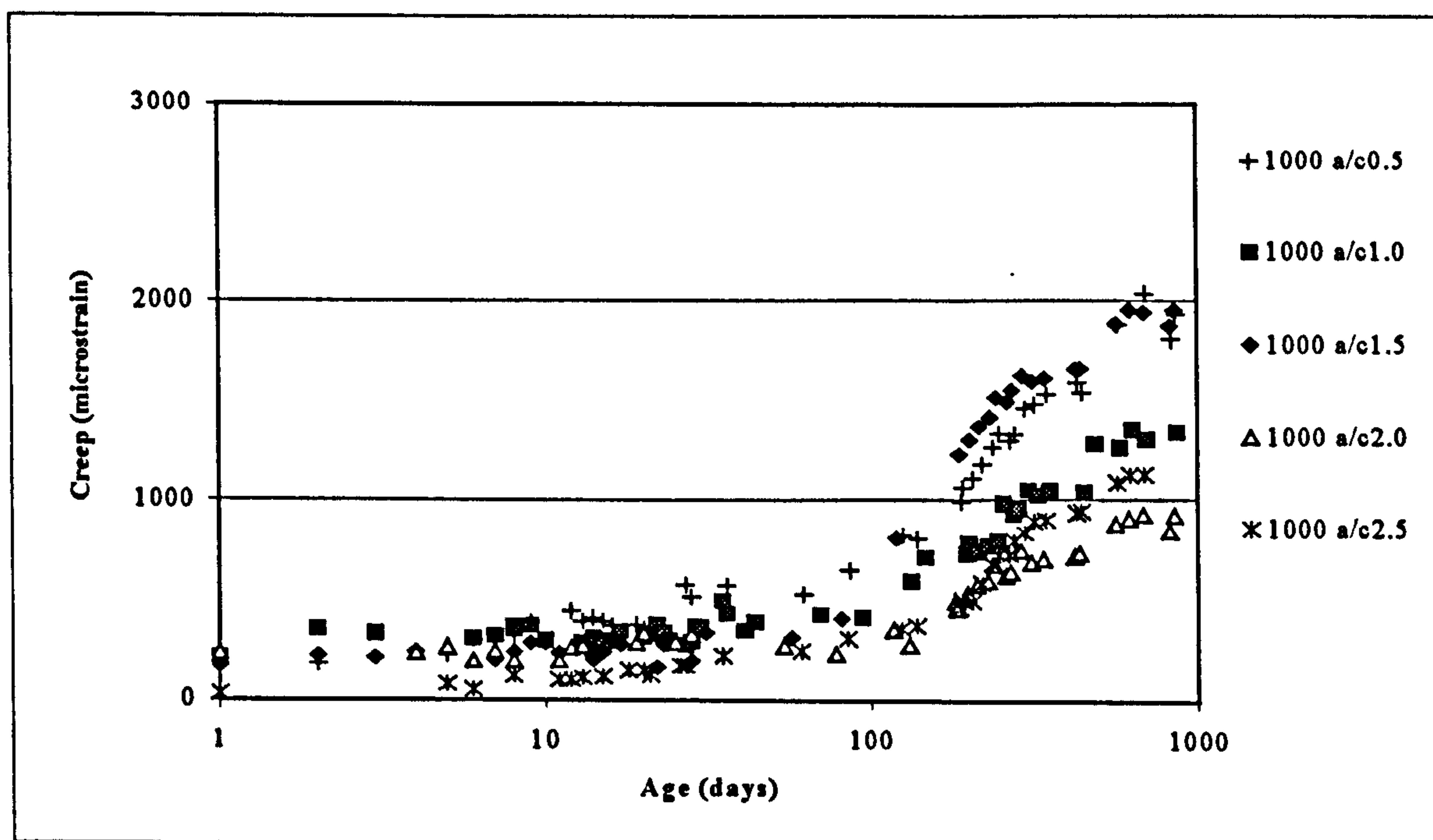


Figure 6.54: Creep of 1000 kg/m^3 Foamed Concrete.

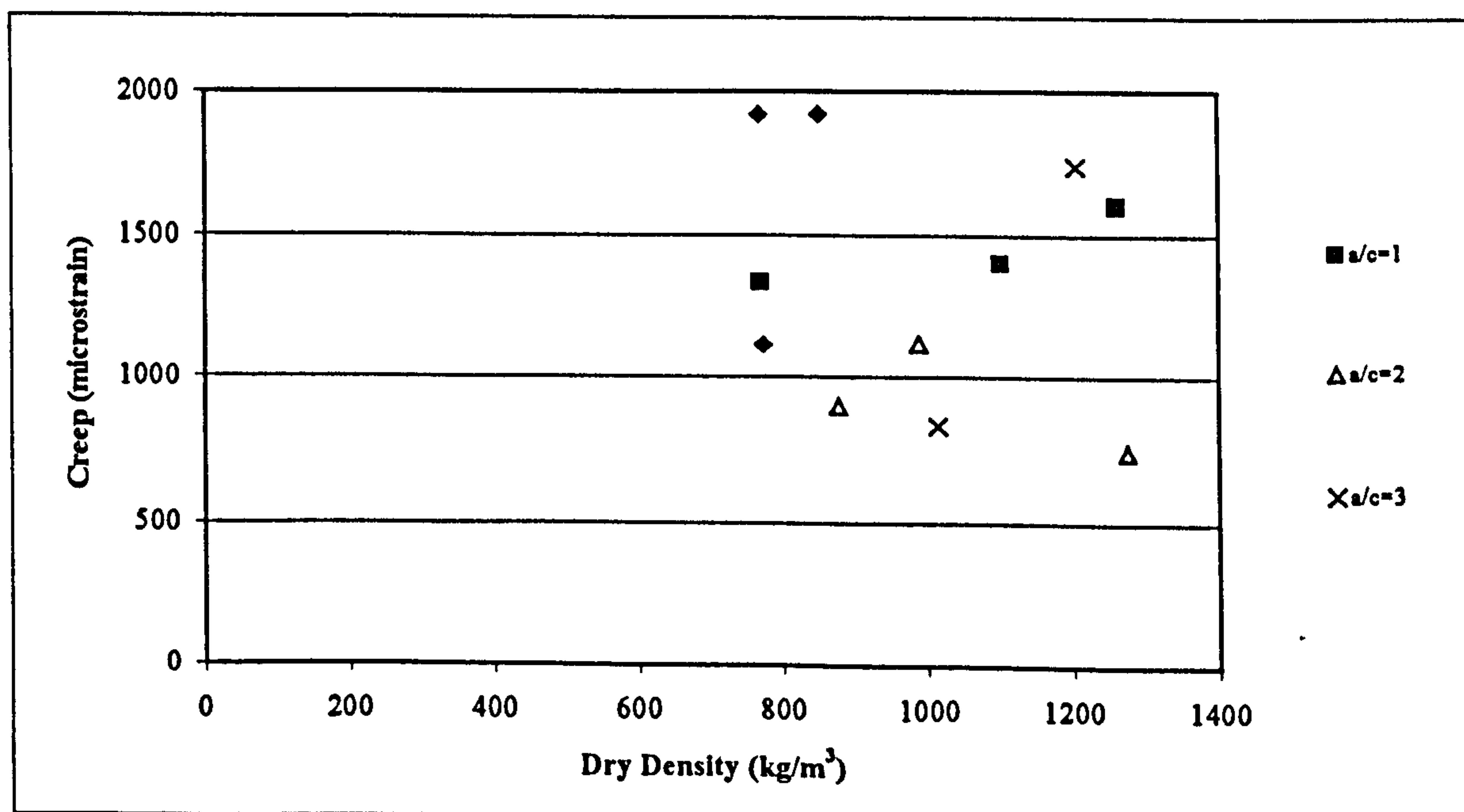


Figure 6.55: Creep as a Function of Dry Density. (◆ - Indicate results of mixtures with a target density of 1000 kg/m^3 and ash/cement ratios of 0.5, 1.5 and 2.5.)

An alternative way of presenting the creep data is on the basis of specific creep, which is defined as creep per unit of stress and is calculated by dividing the basic creep by the applied stress. The specific creep time curves for all the mixtures are shown in Figure 6.56 to Figure 6.58.

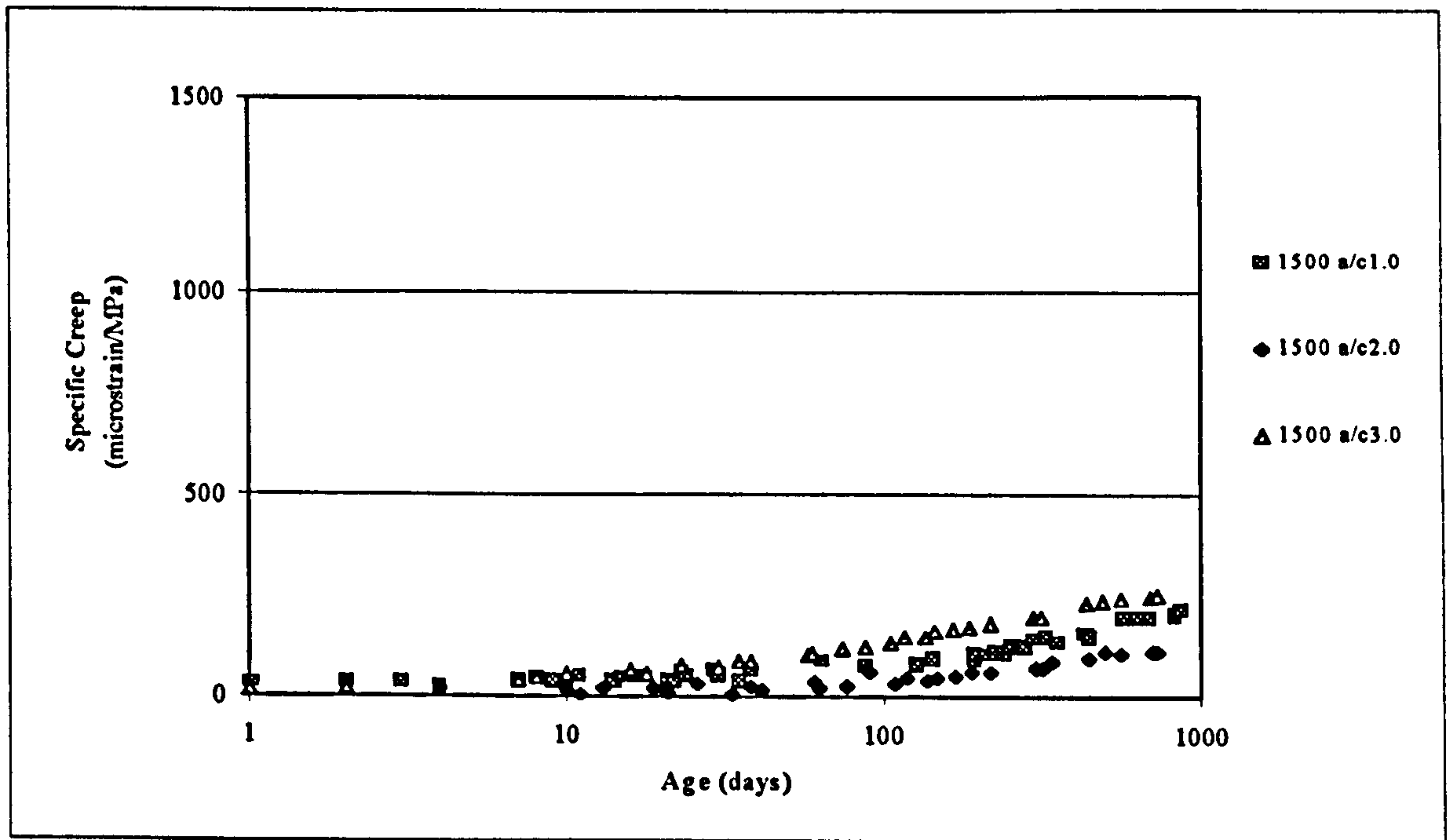


Figure 6.56: Specific Creep of 1500 kg/m³ Foamed Concrete.

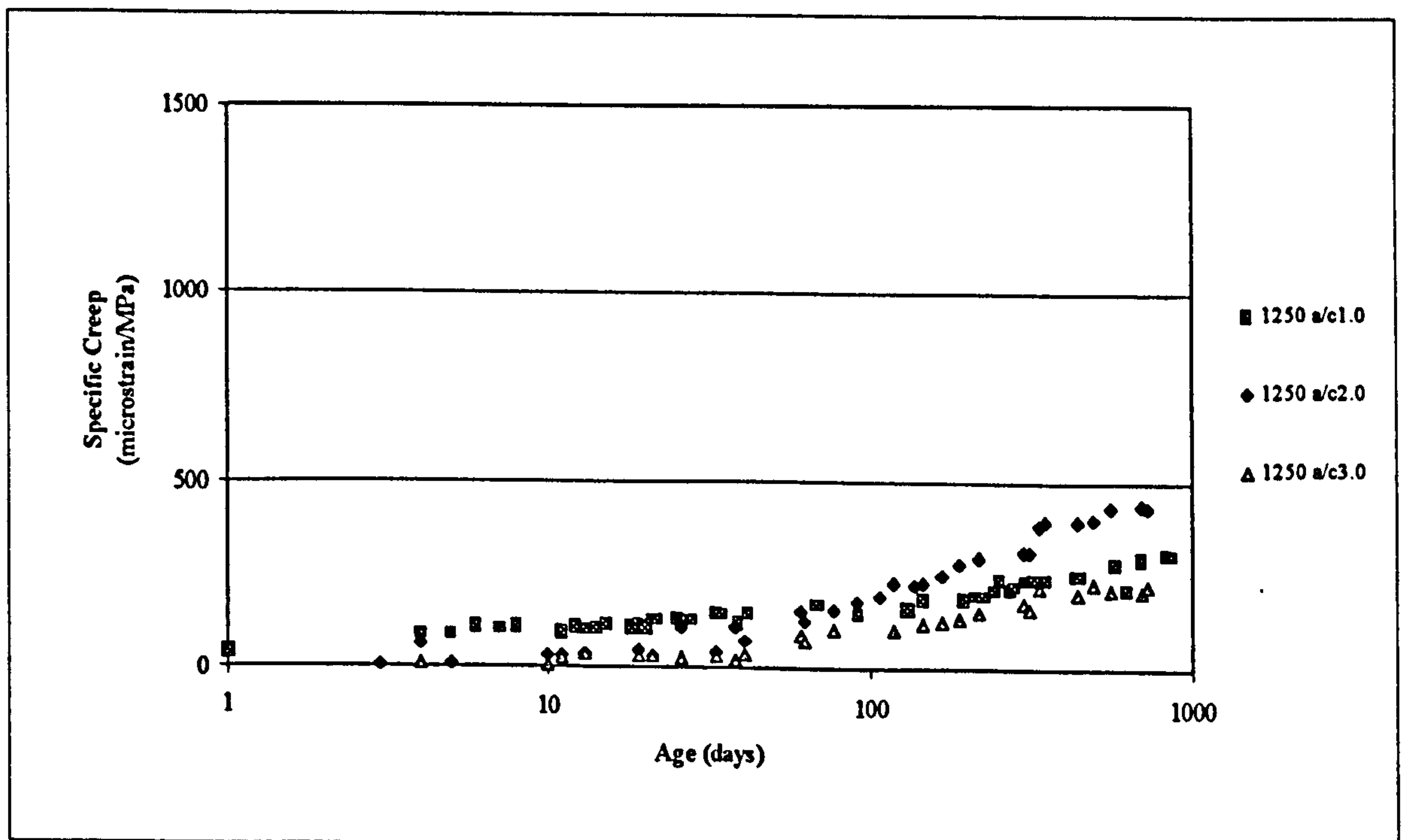


Figure 6.57: Specific Creep of 1250 kg/m³ Foamed Concrete.

The lack of trend with regard ash/cement ratio is again apparent but there is a definite trend of increasing creep with reduced density. This is shown more clearly in Figure 6.59 where the specific creep after 780 days are plotted against density.

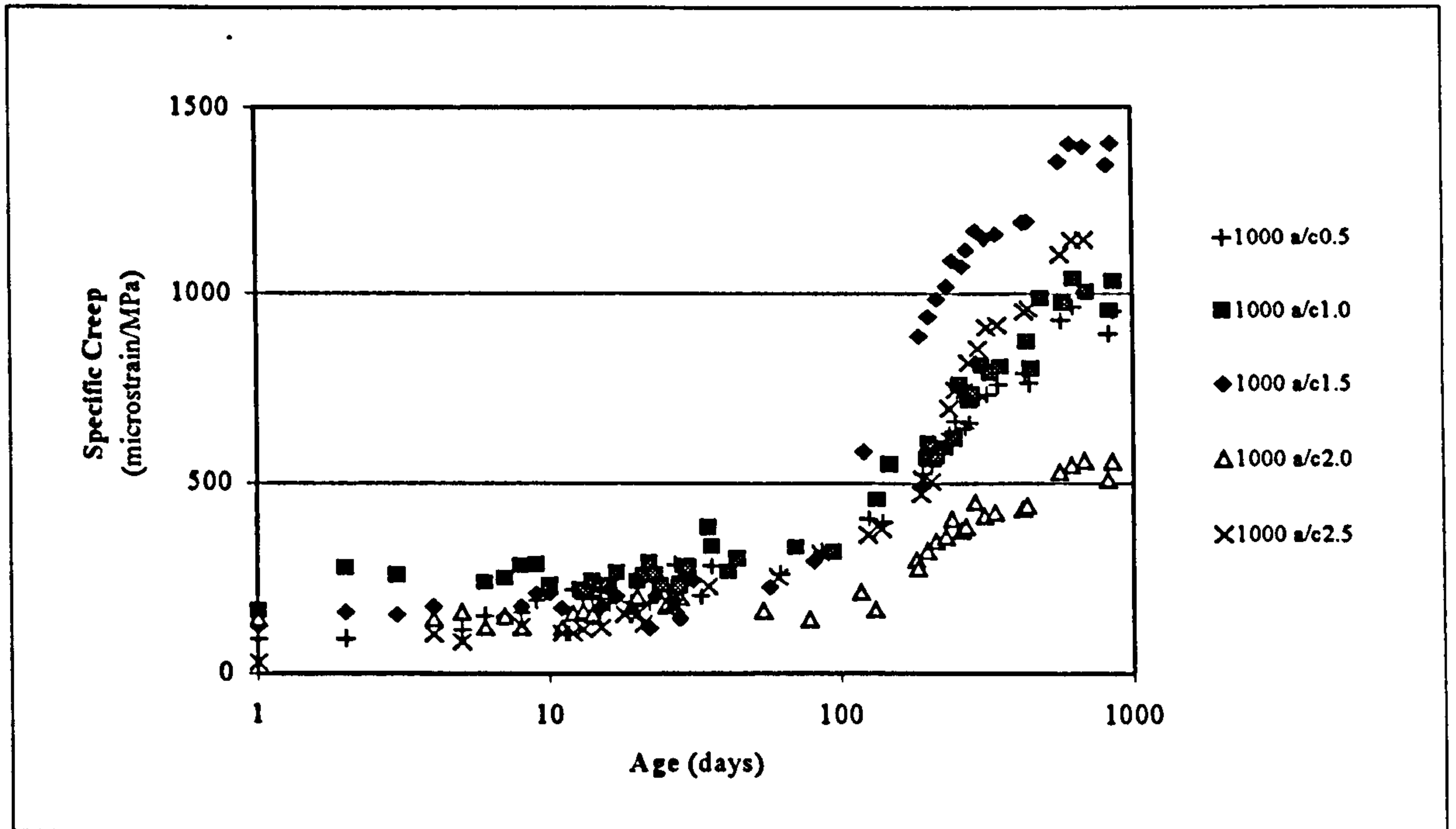


Figure 6.58: Specific Creep of 1000 kg/m^3 Foamed Concrete.

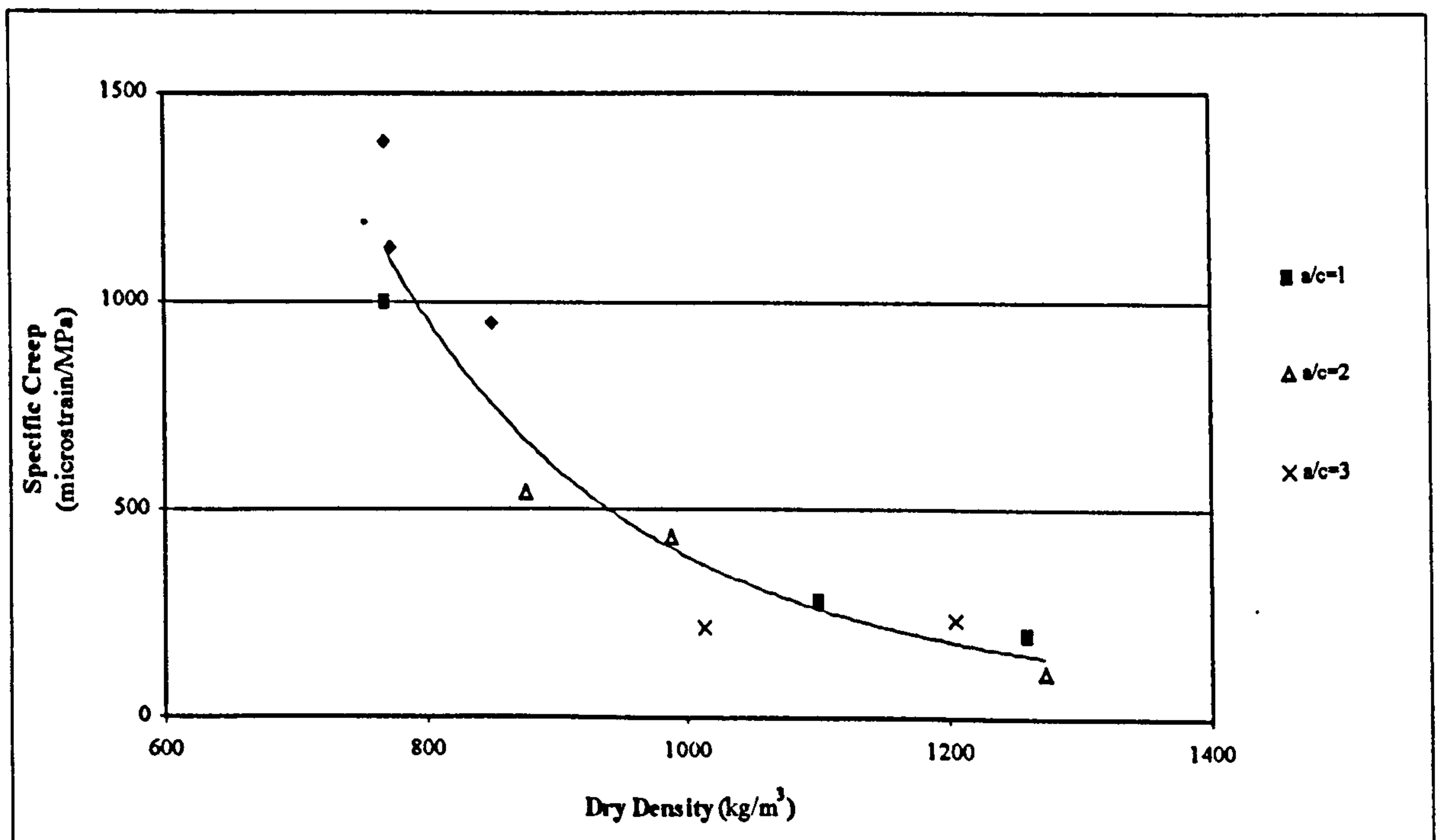


Figure 6.59: Specific Creep as a Function of Dry Density. (◆ - Indicate results of mixtures with a target density of 1000 kg/m^3 and ash/cement ratios of 0.5, 1.5 and 2.5.)

This increase in creep with reduction in density is probably related to the resulting reduction in elastic modulus as illustrated in Figure 6.51. The relationship between specific basic creep and dry density shown in Figure 6.59 can be represented by the following power function:

$$C_f = 6 \times 10^{14} \gamma_d^{-4.05} \quad (\text{Eq 6.11})$$

Where:

$$\begin{aligned} C_f &= \text{Specific creep after 2 years (microstrain)} \\ \gamma_d &= \text{Dry density after 28 days (kg/m}^3\text{)}. \end{aligned}$$

Using Equation 6.11, 90.7% of the variation can be explained by variation in dry density. While the specific creep measured for the mixtures with target densities of 1250 kg/m³ and 1500 kg/m³ are in the same order of magnitude as the values published for normal concrete (up to about 200×10^{-6} /MPa)⁶, the 1000 kg/m³ mixtures creep significantly more.

Had circumstances allowed these tests would have been repeated during the main test programme. It is possible that clearer more meaningful trends may have been produced than was apparent with these preliminary tests. In addition creep tests would also have been carried out under drying conditions to help build up a clearer picture of how the material is likely to perform in service.

6.5.3 Conclusions on Deformation

- The drying shrinkage of cement and cement/ash pastes increases with reducing density (or increasing water/cement ratio).
- The introduction of foam into the pastes appears to have little influence on the drying shrinkage. This is a similar trend to that observed with water absorption.
- There is a slight reduction in drying shrinkage with increasing ash content.
- On average the drying shrinkage of foam concrete is between two and three times greater than that of conventional concrete.
- The elastic modulus of the foamed concrete reduces with reducing density and this relationship is independent of ash/cement ratio or ash type.

- The elastic modulus of the foamed concrete mixtures at more than 800 days ranged from 13.2 GPa to 2.5 GPa.
- The basic creep versus time curves for the foamed concrete mixtures show no clear pattern with respect to density or ash/cement ratio.
- The specific creep of foamed concrete increases with reducing density but this relationship is not influenced by the ash/cement ratio.
- The specific creep of foamed concrete mixtures with densities of 1250 kg/m³ and 1500 kg/m³ are similar to those for normal concrete. The values for the lower density mixtures (1000 kg/m³) are significantly higher.

CHAPTER 7: COMPUTER SIMULATION

7.1 BACKGROUND

The aim of this investigation was to determine the effect of high levels of ungraded fly ash on the properties of foamed concrete. Twenty seven (27) different mixtures were cast with varying ash contents and densities, and the results obtained from these mixtures have been used to develop models that can be used to predict the compressive strength of foamed concrete. Through computer simulation, the output of these models were used to determine optimum ash contents and to establish the effect of high contents of ungraded ash on the compressive strength of foamed concrete.

7.2 COMPRESSIVE STRENGTH MODEL

From the discussion of results in Chapter 6, it has been concluded that the compressive strength of foamed concrete is not only a function of time but also of porosity and ash content. Previously it has been established that the function that best describes the relation between porosity and strength is a multiplicative function while the relation between time and strength is best fitted by a logarithmic function. The effect of ash content on the compressive strength has not yet been quantified and this effect was established by using all 180 sets of strength results. The effect of ash type, ash content, porosity and age on compressive strength was taken into account simultaneously. The fact that the variables are not only interdependent but their influences are also not linear complicated the interpretation of results and it ruled out the use of a standard statistical program to conduct multiple linear regression analysis. A specially written program⁸² was obtained to optimize the fitted model. The general shape of the age and porosity relations as established in the discussion of results (Chapter 6) was used for fitting the model. The two different types of ash was treated as two separate samples. It was decided to use a second order polynomial function to represent the effect of ash content on the compressive strength. The reason for using a second order function was that the best-fit result of the third (or quadratic) term would be zero unless there is an optimum ash content. If both the third and the second (or linear) term are zero one could conclude that the ash content has no influence on the compressive strength.

The strength of foamed concrete is deemed to be represented by the following equation:

$$f_c = (\lambda + \beta \ln(t))(1 - p)^\alpha \quad (\text{Eq 7.1})$$

with

$$\beta = \beta_1 + \beta_2 (a/c) + \beta_3 (a/c)^2 \quad (\text{Eq 7.2})$$

$$\lambda = \lambda_1 + \lambda_2 (a/c) + \lambda_3 (a/c)^2 \quad (\text{Eq 7.3})$$

Where:

f_c	=	compressive strength (MPa)
t	=	time since casting (days)
p	=	porosity (as a fraction)
a/c	=	ash/cement ratio (by weight)
$\alpha, \beta \text{ \& } \lambda$	=	constants.

The test results were divided into two groups with one group being results for samples containing pfa and the other group results for samples containing pozz-fill. The two groups of results were used separately and a set of constants was determined for each of these groups. The source code of the computer program used can be seen in Appendix H. The program was written in Fortran 77 and it uses an iterative process, where default values are used to calculate the first set of fitted strengths. The differences between the actual measured strengths and the calculated values are taken as the errors and the squares of these errors are summated. Stepwise regression is used to alter one variable at a time by one increment at a time and each time the new sum of the square of the errors is compared to the previous value. The process is repeated until the sum of the square of the errors is minimized. The constants that produced the best fit for each of the sets of data can be seen in Table 7.1.

The function as fitted for the pfa explains 96.3 % of the variation in compressive strength while the function as fitted for the pozz-fill explains 95.9 % of the variation. The strengths as predicted using the model are plotted versus the measured strength in Figure 7.1 and it can be seen that the model accurately predicts the strength and there is no skewness in fit. This model can now be used to evaluate the effect of ash type, ash content, porosity and age on the compressive strength of foamed concrete.

Table 7.1: Constant for Compressive Strength Model.

Constant	Pfa	Pozz-fill
α	3.7	3.7
β_1	24.91	23.74
β_2	52.89	56.78
β_3	-12.27	-14.31
λ_1	172.8	176.9
λ_2	-196.0	-229.7
λ_3	34.02	46.04

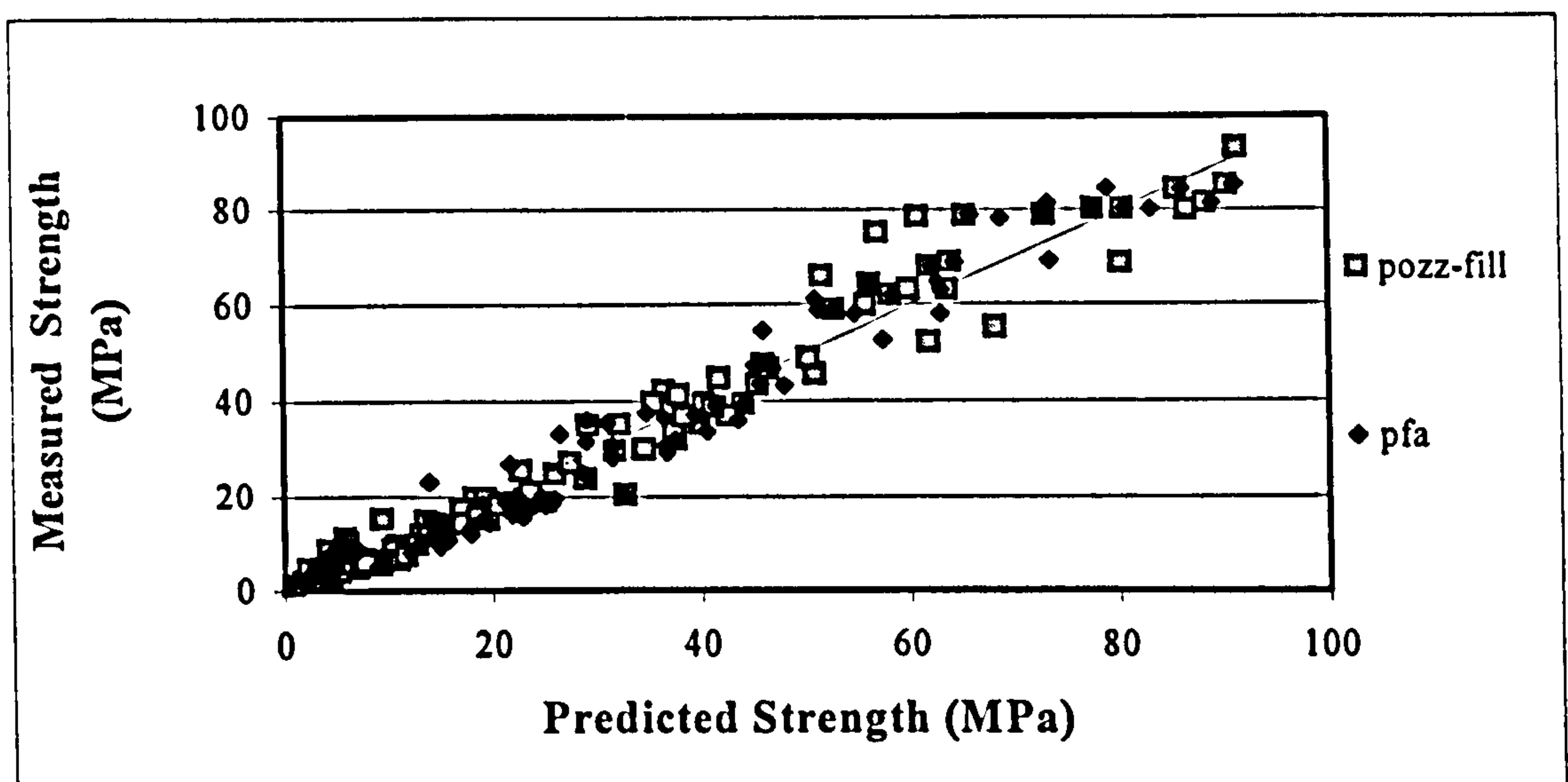


Figure 7.1: Predicted Strength versus Measured Strength.

7.2.1 Effect of ash type and content

The effect of ash type on the compressive strength of foamed concrete can be established by comparing the calculated strength of pfa and pozz-fill mixtures for a given porosity, age and ash/cement ratio. In Figure 7.2 the 28- and 365-day compressive strengths of mixtures with a porosity of 30% are plotted as a function of ash/cement ratio. From this graph it can be seen that the 28-day compressive strength decreases with increased ash content and for constant porosity the highest 28-day strength is achieved with no ash in the mixture. The 365-day strengths indicate an optimum ash

content with maximum strength obtained at ash/cement ratios in the region of 1.5. The trends observed are similar regardless of the ash type used, but the compressive strengths obtained when using the pozz-fill are marginally lower than when using pfa. Although pozz-fill yields marginally lower strengths than pfa, the 365-day strength of mixtures containing pozz-fill for mixtures with ash/cement ratios below 2.75 are higher than those of mixtures containing no ash. The trends observed for mixtures with 30% porosity are not unique and although increased porosity results in decreased strength the trends remain unchanged with changes in porosity. In Figure 7.3 the effect of ash type and content on the compressive strength of mixtures with 60% porosity can be seen.

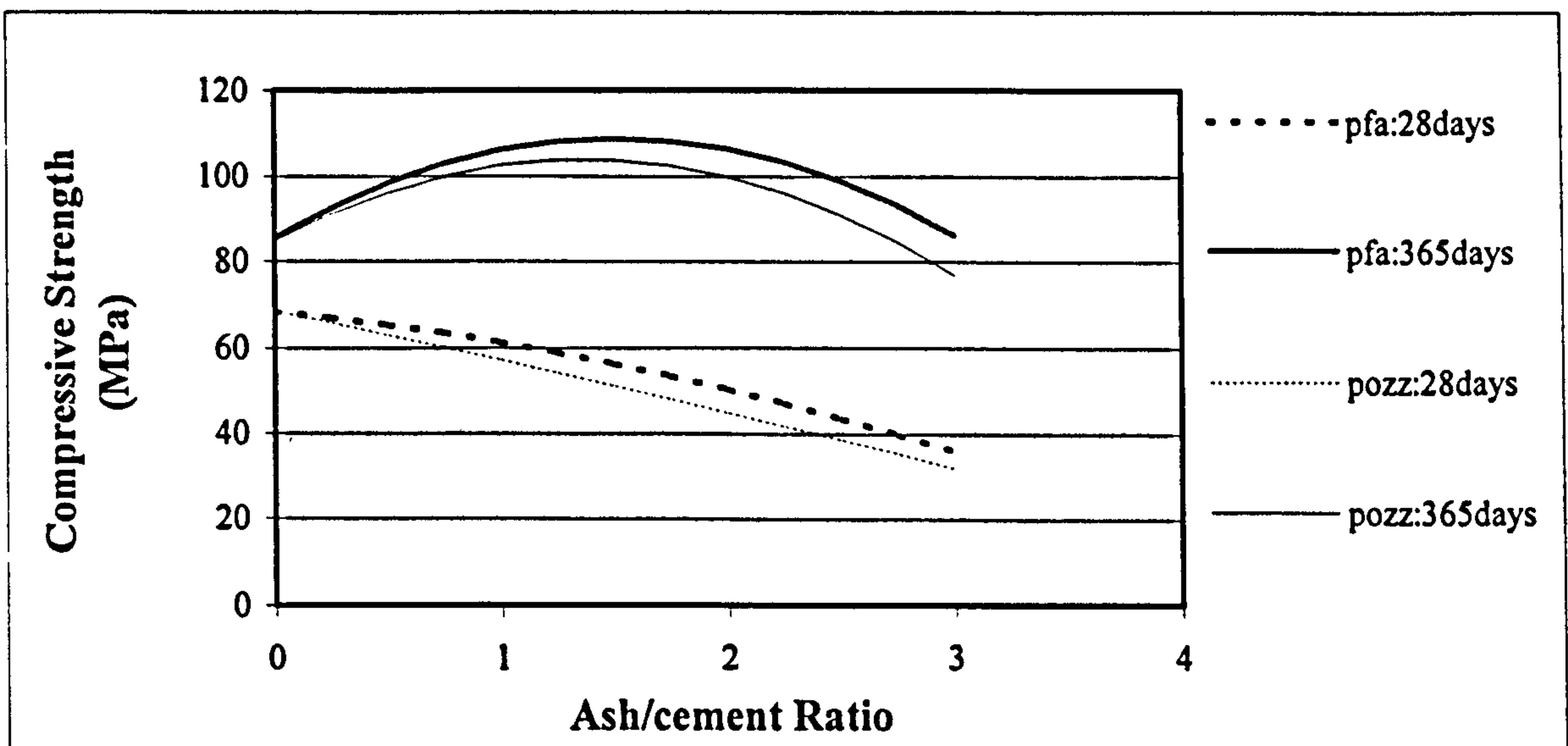


Figure 7.2: Effect of Ash Type on Compressive Strength for 30% Porosity.

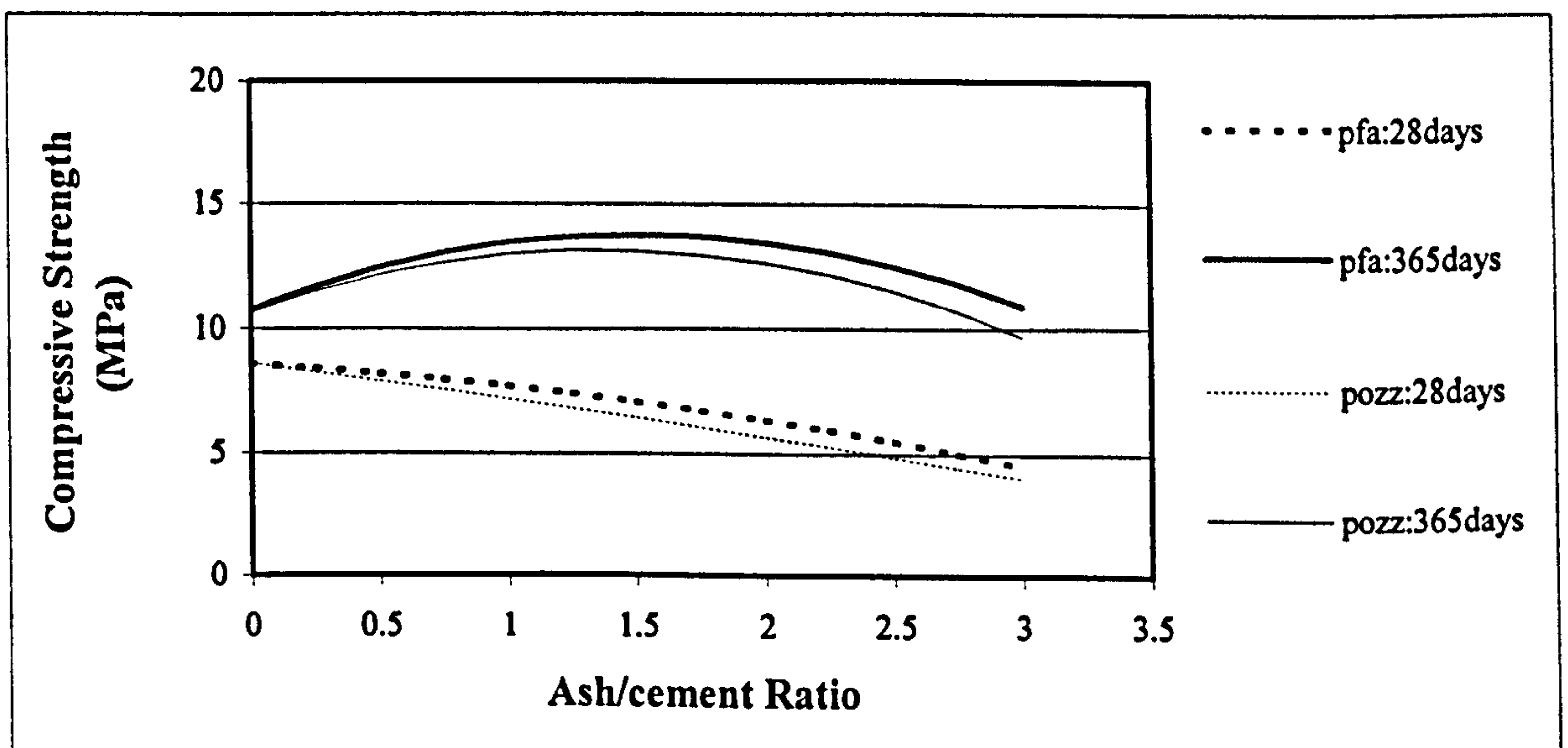


Figure 7.3: Effect of Ash Type on Compressive Strength for 60% Porosity.

7.2.2 Effect of age on optimum composition

The effect of age on the strength development of foamed concrete containing Pozz-fill can be seen in Figure 7.4. This graph contains values for a porosity of 30% and it can be seen that the ash content resulting in the maximum strength for a given porosity increases with time. This finding correlates with the findings of Hassan et al⁵² for normal concrete where up to 70% of the cement was replaced by ash.

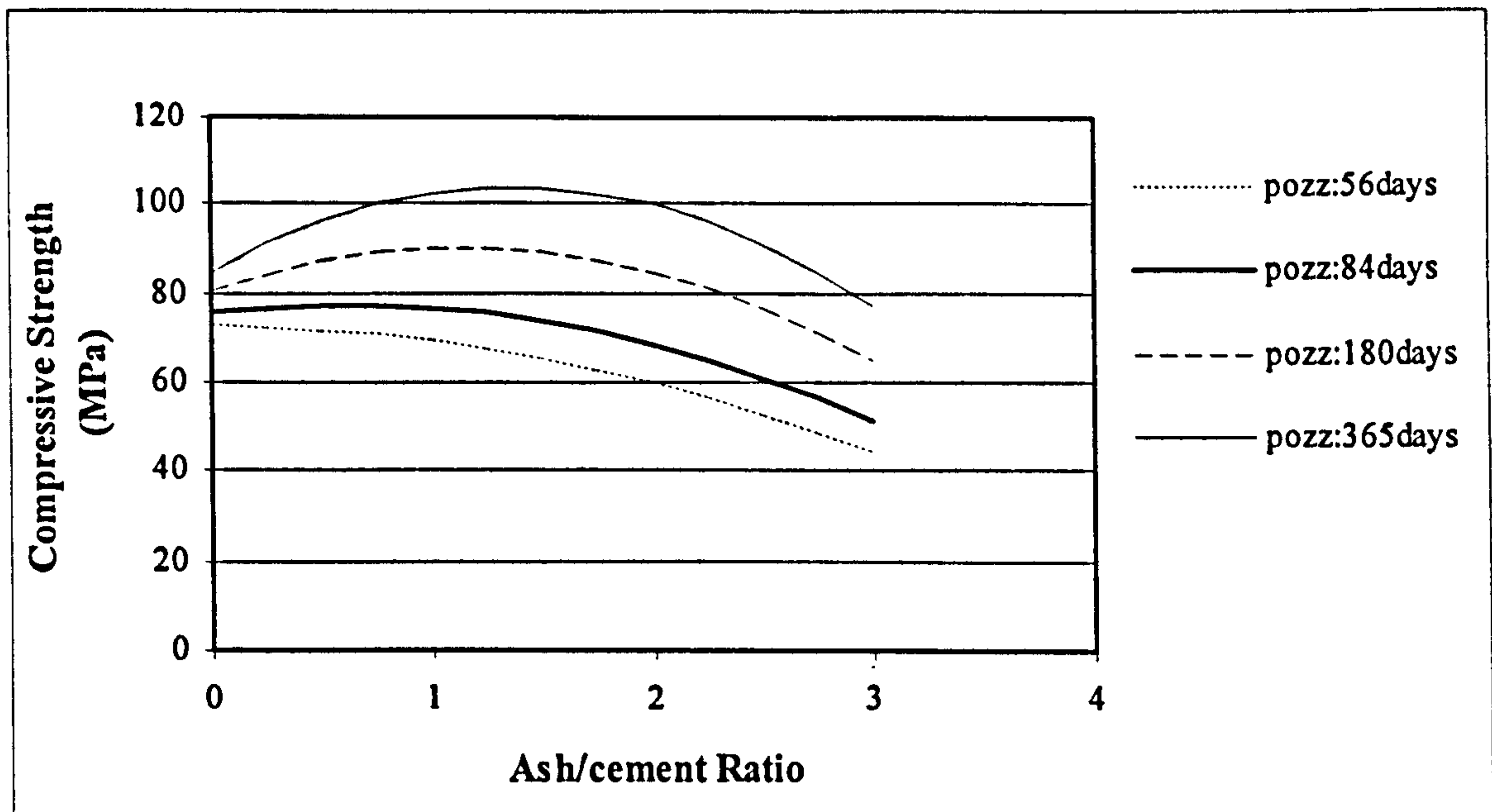


Figure 7.4: Effect of Age on Strength Development of Foamed Concrete.

The optimum composition at a given time and porosity can be determined by fitting a second order polynomial function through the strengths obtained at different ash/cement ratios from the simulation model. The function fitted has the general form:

$$f_c = l(a/c)^2 + m(a/c) + n \quad (\text{Eq 7.4})$$

Where:

$$\begin{aligned} f_c &= \text{compressive strength (MPa)} \\ a/c &= \text{ash/cement ratio (by weight)} \\ l, m \text{ and } n &= \text{constants.} \end{aligned}$$

The values calculated for l , m and n at different ages, using the strengths obtained from the simulation model for pfa and pozz-fill can be seen in Table 7.2 for a constant porosity of 30%. The optimum ash content at any given age can be determined through calculating the turning point of the polynomial function by setting the slope of the

strength function (the derivative of Eq 7.4) equal to zero. These calculated optimum ash contents are plotted as a function of time in Figure 7.5.

Table 7.2: Optimum Ash Content.

pfa	Age	56	84	180	270	365
	l	-4.107	-5.437	-7.936	-9.265	-10.254
	m	4.516	10.247	21.018	26.748	31.009
	n	72.971	75.67	80.743	83.46	85.449
	optimum a/c	0.550	0.942	1.324	1.443	1.512
	maximum a/c	1.100	1.885	2.649	2.887	3.024
pozz-fill	Age	56	84	180	270	365
	l	-3.090	-4.640	-7.555	-9.105	-10.258
	m	-0.305	5.847	17.411	23.563	28.137
	n	72.808	75.38	80.215	82.787	84.7
	optimum a/c	-	0.630	1.152	1.294	1.371
	maximum a/c	-	1.260	2.305	2.588	2.743

From Figure 7.5 it can be seen that the optimum ash/cement ratio increases to a value of approximately 1.5, indicating that the highest long term compressive strength is obtained for mixtures where 60% of the cement (by weight) has been replaced with ash. The optimum ash/cement ratio of pozz-fill follows the same trend that of pfa, with the optimum ash content for the pozz-fill always being marginally lower than for pfa. The difference in optimum ash/cement ratio decreases with increasing age. Curing temperature is known to have a considerable influence on the strength development of mixtures containing large volumes of fly ash⁵² and increased curing temperature, should reduce the time it takes for the ash to start contributing towards the compressive strength and the time scale of Figure 7.5 would therefore be temperature dependent.

The optimum ash content at a specific age is the ash/cement ratio that yields the highest strength at that age, but equal strength to the mixture containing no ash is obtained at much higher ash/cement ratios. The maximum ash/cement ratio that yields a strength equal to or higher than that obtained when no ash is used at different ages are indicated in Table 7.2. These values indicate that mixtures where up to 75% of the cement has

been replaced with pfa yields higher one-year strengths than that obtained from mixtures containing no ash. This maximum value is marginally lower (at approximately 73%) for pozz-fill.

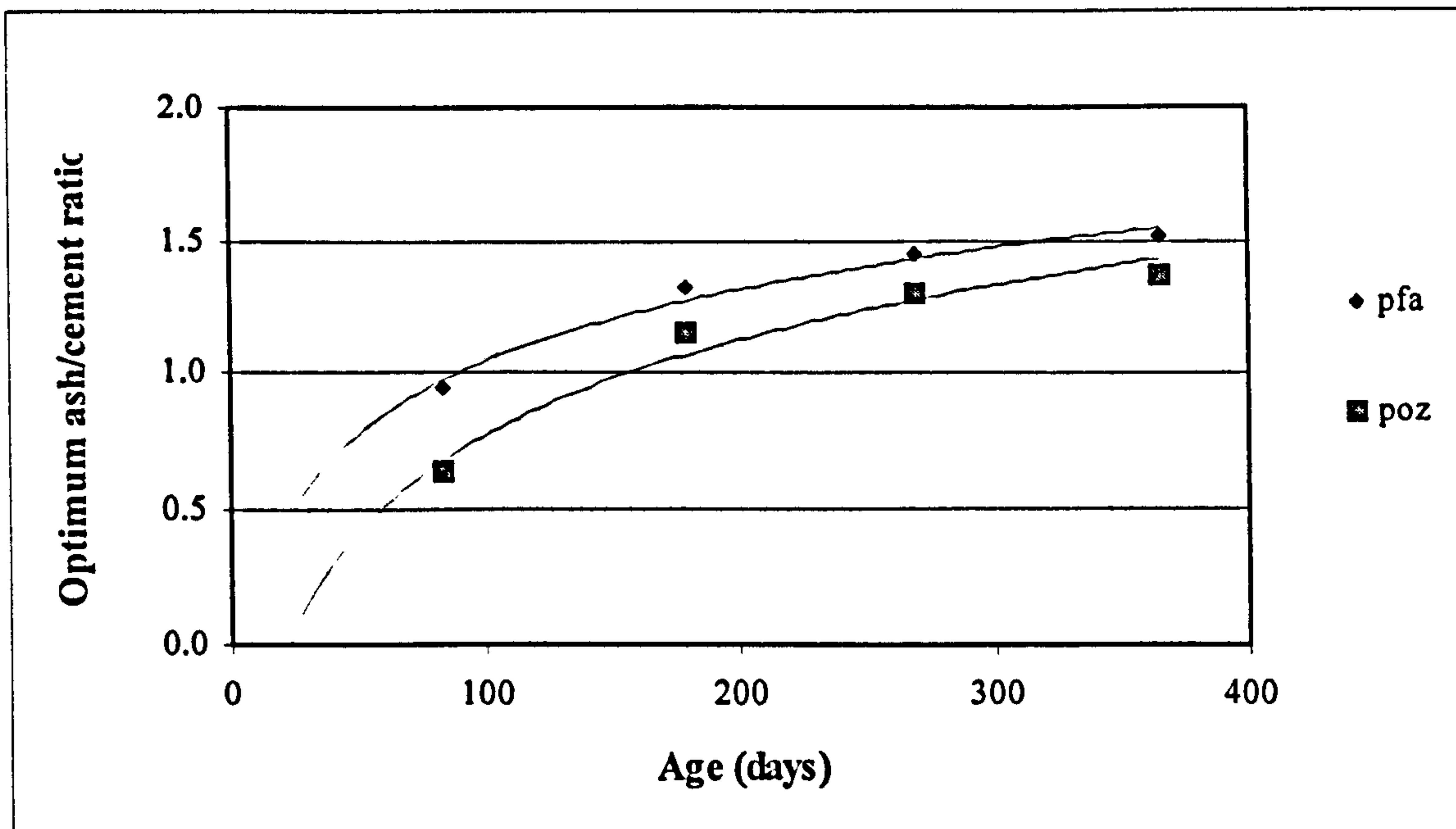


Figure 7.5: Optimum Ash Content as a Function of Time.

The calculated values as indicated in Table 7.2 are independent of porosity and although the actual values for l , m and n varies with varying porosity, the optimum ash/cement ratio for any given age does not vary with varying porosity.

7.2.3 Mixtures optimized for strength and costs

When foamed concrete is used it is not only the casting density that is important but a certain compressive strength would also be required at a given age. Although it might be possible to obtain higher strengths from mixtures of the required density, it would be a waste of money producing foamed concrete with compressive strengths much higher than that required. The optimum mixture would be the mixture that meets the strength and density requirements at the lowest cost. The actual material cost of the mixtures were compared using the following bulk costs:

- Cement: R18-00 per 50 kg bag (R0-36/kg)
- Pfa: R 6-67 per 40 kg bag (R0-167/kg)

- Pozz-fill: R55-29 per ton (R0-055/kg)
- Water: R 3-50 per kiloliter (R0-004/kg)
- Foaming agent: R 30 per liter of concentrate.

The foaming agent is diluted in water to a ratio of 1:40 and then aerated to a density of 70 kg/m³. The actual cost of the foam can therefore be taken as R52-50 per m³. From the material costs as listed above it can clearly be seen that replacing cement with pfa could result in large savings. Using pozz-fill in stead of pfa could increase these savings.

A given porosity, age and compressive strength were used in Equation 7.1 with the constants as indicated in Table 7.1 to calculate a maximum ash/cement ratio that would yield the required strength. The mix compositions (and costs) for mixtures yielding compressive strengths of up to 40 MPa for mixtures with different densities containing pfa or pozz-fill can be seen in Table 7.3 and Table 7.4 for ages of 28 days and 365 days respectively. Mixtures for specific strengths at other ages can be seen in Appendix I. Where the calculated ash/cement ratio was higher than 3.3 a value of 3.30 is indicated in these tables. A value of 3.30 is already 10% higher than the ash/cement ratios used in this investigation and the use of higher ash/cement ratios has not been scientifically proven. Using mixtures where more than 75% of the cement has been replaced with ash ($a/c > 3$) causes problems with early age strength development and demoulding within 24 hours becomes problematic. The maximum ash/cement ratio in Table 7.3 and Table 7.4 has therefore for practical reasons been limited to 3.30 and if set accelerators are used the use of higher ash/cement ratios might be a possibility.

The water/cement ratio of the mixtures in Table 7.3 and Table 7.4 were calculated using the following equation:

$$w/c = 0.4 + 0.18(a/c) + 0.027(a/c)^2 \quad (\text{Eq 7.4})$$

Where:

$$\begin{aligned} w/c &= \text{water/cement ratio (by weight)} \\ a/c &= \text{ash/cement ratio (by weight)}. \end{aligned}$$

Table 7.3: Mixtures for 28 day Strengths.

		PFA				Pczz-fill				
Strength (MPa)	Approximate Casting Density (kg/m ³)	1750	1500	1250	1000	Approximate Casting Density (kg/m ³)	1750	1500	1250	1000
	Approximate Porosity	30%	40%	50%	60%	Approximate Porosity	30%	40%	50%	60%
5	a/c	3.30 *	3.30 *	3.30 *	2.77	a/c	3.30 *	3.30 *	3.30 *	2.42
	w/c	1.27	1.27	1.27	1.09	w/c	1.27	1.27	1.27	0.98
	water (l)	399	341	282	220	water (l)	399	341	282	218
	cement (kg)	314	268	222	201	cement (kg)	314	268	222	222
	pfa (kg)	1037	884	731	557	pozz-fill (kg)	1037	884	731	537
	foam (l)	29	172	315	463	foam (l)	29	172	315	467
	Cost (R/m ³)	289	254	219	191	Cost (R/m ³)	173	156	138	135
	Density (kg/m ³)	1752	1505	1258	1011	Density (kg/m ³)	1752	1505	1258	1012
10	a/c	3.30 *	3.30 *	3.08		a/c	3.30 *	3.30 *	2.80	
	w/c	1.27	1.27	1.19		w/c	1.27	1.27	1.10	
	water (l)	399	341	279		water (l)	399	341	278	
	cement (kg)	314	268	234		cement (kg)	314	268	252	
	pfa (kg)	1036	884	721		pozz-fill (kg)	1037	884	705	
	foam (l)	29	172	318		foam (l)	29	172	322	
	Cost (R/m ³)	289	254	222		Cost (R/m ³)	173	156	148	
	Density (kg/m ³)	1752	1505	1258		Density (kg/m ³)	1752	1505	1258	
15	a/c	3.30 *	3.30 *	1.87		a/c	3.30 *	3.30 *	1.43	
	w/c	1.27	1.27	0.82		w/c	1.27	1.27	0.70	
	water (l)	399	341	275		water (l)	399	341	278	
	cement (kg)	314	268	335		cement (kg)	314	268	395	
	pfa (kg)	1037	884	625		pozz-fill (kg)	1037	884	562	
	foam (l)	29	172	334		foam (l)	29	172	341	
	Cost (R/m ³)	289	254	243		Cost (R/m ³)	173	156	192	
	Density (kg/m ³)	1752	1505	1259		Density (kg/m ³)	1752	1505	1260	
20	a/c	3.30 *	3.04			a/c	3.30 *	2.75		
	w/c	1.27	1.18			w/c	1.27	1.08		
	water (l)	399	338			water (l)	399	335		
	cement (kg)	314	286			cement (kg)	314	309		
	pfa (kg)	1037	869			pozz-fill (kg)	1037	849		
	foam (l)	29	176			foam (l)	29	181		
	Cost (R/m ³)	289	258			Cost (R/m ³)	173	169		
	Density (kg/m ³)	1752	1505			Density (kg/m ³)	1752	1506		

* - To prevent extrapolation of results, the ash/cement ratio has been limited to within 10% of ratios tested (therefore a/c=3.3 where larger ratios were calculated).

Table 7.3 (continue): Mixtures for 28 day Strengths.

		PFA				Pozz-fill				
Strength (MPa)	Approximate Casting Density (kg/m ³)	1750	1500	1250	1000	Approximate Casting Density (kg/m ³)	1750	1500	1250	1000
	Approximate Porosity	30%	40%	50%	60%	Approximate Porosity	30%	40%	50%	60%
25	a/c	3.30 *	2.46			a/c	3.30 *	2.06		
	w/c	1.27	0.99			w/c	1.27	0.88		
	water (l)	399	333			water (l)	399	332		
	cement (kg)	314	335			cement (kg)	314	379		
	pfa (kg)	1037	825			pozz-fill (kg)	1037	782		
	foam (l)	29	185			foam (l)	29	192		
	Cost (R/m ³)	289	269			Cost (R/m ³)	173	191		
	Density (kg/m ³)	1752	1506			Density (kg/m ³)	1752	1506		
30	a/c	3.30 *	1.79			a/c	3.15	1.34		
	w/c	1.27	0.80			w/c	1.22	0.68		
	water (l)	399	333			water (l)	397	337		
	cement (kg)	314	416			cement (kg)	326	493		
	pfa (kg)	1037	744			pozz-fill (kg)	1027	663		
	foam (l)	29	197			foam (l)	32	205		
	Cost (R/m ³)	289	285			Cost (R/m ³)	177	226		
	Density (kg/m ³)	1752	1507			Density (kg/m ³)	1752	1507		
35	a/c	3.06	0.92			a/c	2.77	0.59		
	w/c	1.19	0.58			w/c	1.09	0.51		
	water (l)	396	348			water (l)	393	364		
	cement (kg)	333	595			cement (kg)	359	711		
	pfa (kg)	1020	550			pozz-fill (kg)	997	417		
	foam (l)	34	213			foam (l)	39	220		
	Cost (R/m ³)	293	318			Cost (R/m ³)	188	292		
	Density (kg/m ³)	1752	1508			Density (kg/m ³)	1753	1508		
40	a/c	2.75				a/c	2.39			
	w/c	1.08				w/c	0.97			
	water (l)	393				water (l)	390			
	cement (kg)	362				cement (kg)	401			
	pfa (kg)	995				pozz-fill (kg)	959			
	foam (l)	40				foam (l)	46			
	Cost (R/m ³)	300				Cost (R/m ³)	201			
	Density (kg/m ³)	1753				Density (kg/m ³)	1753			

- - To prevent extrapolation of results, the ash/cement ratio has been limited to within 10% of ratios tested (therefore a/c=3.3 where larger ratios were calculated).

Table 7.4: Mixtures for 365 day Strengths.

		PFA				Pozz-fill				
Strength (MPa)	Approximate Casting Density (kg/m ³)	1750	1500	1250	1000	Approximate Casting Density (kg/m ³)	1750	1500	1250	1000
	Approximate Porosity	30%	40%	50%	60%	Approximate Porosity	30%	40%	50%	60%
5	a/c	3.30 *	3.30 *	3.30 *	3.30 *	a/c	3.30 *	3.30 *	3.30 *	3.30 *
	w/c	1.27	1.27	1.27	1.27	w/c	1.27	1.27	1.27	1.27
	water (l)	399	341	282	223	water (l)	399	341	282	223
	cement (kg)	314	268	222	175	cement (kg)	314	268	222	175
	pfa (kg)	1037	884	731	579	pozz-fill (kg)	1037	884	731	579
	foam (l)	29	172	315	458	foam (l)	29	172	315	458
	Cost (R/m ³)	289	254	219	185	Cost (R/m ³)	173	156	138	120
	Density (kg/m ³)	1752	1505	1258	1011	Density (kg/m ³)	1752	1505	1258	1011
10	a/c	3.30 *	3.30 *	3.30 *	3.21	a/c	3.30 *	3.30 *	3.30 *	2.92
	w/c	1.27	1.27	1.27	1.24	w/c	1.27	1.27	1.27	1.14
	water (l)	399	341	282	222	water (l)	399	341	282	220
	cement (kg)	314	268	222	179	cement (kg)	314	268	222	193
	pfa (kg)	1037	884	731	576	pozz-fill (kg)	1037	884	731	564
	foam (l)	29	172	315	459	foam (l)	29	172	315	462
	Cost (R/m ³)	289	254	219	186	Cost (R/m ³)	173	156	138	126
	Density (kg/m ³)	1752	1505	1258	1011	Density (kg/m ³)	1752	1505	1258	1011
15	a/c	3.30 *	3.30 *	3.30 *		A/c	3.30 *	3.30 *	3.30 *	
	W/c	1.27	1.27	1.27		W/c	1.27	1.27	1.27	
	Water (l)	399	341	282		Water (l)	399	341	282	
	Cement (kg)	314	268	222		Cement (kg)	314	268	222	
	Pfa (kg)	1037	884	731		Pozz-fill (kg)	1037	884	731	
	Foam (l)	29	172	315		Foam (l)	29	172	315	
	Cost (R/m ³)	289	254	219		Cost (R/m ³)	173	156	138	
	Density (kg/m ³)	1752	1505	1258		Density (kg/m ³)	1752	1505	1258	
20	a/c	3.30 *	3.30 *	3.30 *		A/c	3.30 *	3.30 *	3.21	
	W/c	1.27	1.27	1.27		W/c	1.27	1.27	1.24	
	Water (l)	399	341	282		Water (l)	399	341	281	
	Cement (kg)	314	268	222		Cement (kg)	314	268	227	
	Pfa (kg)	1037	884	731		Pozz-fill (kg)	1037	884	727	
	Foam (l)	29	172	315		Foam (l)	29	172	316	
	Cost (R/m ³)	289	254	219		Cost (R/m ³)	173	156	140	
	Density (kg/m ³)	1752	1505	1258		Density (kg/m ³)	1752	1505	1258	

*- To prevent extrapolation of results, the ash/cement ratio has been limited to within 10% of ratios tested (therefore a/c=3.3 where larger ratios were calculated).

Table 7.4 (continue): Mixtures for 365 day Strengths.

		PFA				Pozz-fill				
Strength (MPa)	Approximate Casting Density (kg/m ³)	1750	1500	1250	1000	Approximate Casting Density (kg/m ³)	1750	1500	1250	1000
	Approximate Porosity	30%	40%	50%	60%	Approximate Porosity	30%	40%	50%	60%
25	a/c	3.30 *	3.30 *	2.98		a/c	3.30 *	3.30 *	2.67	
	w/c	1.27	1.27	1.16		w/c	1.27	1.27	1.06	
	water (l)	399	341	279		water (l)	399	341	277	
	cement (kg)	314	268	240		cement (kg)	314	268	261	
	pfa (kg)	1037	884	716		pozz-fill (kg)	1037	884	697	
	foam (l)	29	172	319		foam (l)	29	172	323	
	Cost (R/m ³)	289	254	224		Cost (R/m ³)	173	156	151	
	Density (kg/m ³)	1752	1505	1258		Density (kg/m ³)	1752	1505	1259	
30	a/c	3.30 *	3.30 *	2.19		a/c	3.30 *	3.30 *		
	w/c	1.27	1.27	0.91		w/c	1.27	1.27		
	water (l)	399	341	275		water (l)	399	341		
	cement (kg)	314	268	301		cement (kg)	314	268		
	pfa (kg)	1037	884	659		pozz-fill (kg)	1037	884		
	foam (l)	29	172	330		foam (l)	29	172		
	Cost (R/m ³)	289	254	237		Cost (R/m ³)	173	156		
	Density (kg/m ³)	1752	1505	1259		Density (kg/m ³)	1752	1505		
35	a/c	3.30 *	3.30 *			a/c	3.30 *	3.30 *		
	w/c	1.27	1.27			w/c	1.27	1.27		
	water (l)	399	341			water (l)	399	341		
	cement (kg)	314	268			cement (kg)	314	268		
	pfa (kg)	1037	884			pozz-fill (kg)	1037	884		
	foam (l)	29	172			foam (l)	29	172		
	Cost (R/m ³)	289	254			Cost (R/m ³)	173	156		
	Density (kg/m ³)	1752	1505			Density (kg/m ³)	1752	1505		
40	a/c	3.30 *	3.30 *			a/c	3.30 *	3.17		
	w/c	1.27	1.27			w/c	1.27	1.23		
	water (l)	399	341			water (l)	399	339		
	cement (kg)	314	268			cement (kg)	314	276		
	pfa (kg)	1037	884			pozz-fill (kg)	1037	877		
	foam (l)	29	172			foam (l)	29	174		
	Cost (R/m ³)	289	254			Cost (R/m ³)	173	158		
	Density (kg/m ³)	1752	1505			Density (kg/m ³)	1752	1505		

*- To prevent extrapolation of results, the ash/cement ratio has been limited to within 10% of ratios tested (therefore a/c=3.3 where larger ratios were calculated).

From the costs of mixtures as indicated in Table 7.3 and Table 7.4 it can be seen that the cost of a mixture yielding a certain strength can not only be reduced by increasing the ash content but also by reducing the density (or increasing the porosity). For a certain strength the cost of foamed concrete mixtures containing large volumes of ash can further be reduced by increasing the age when the strength is required. It is however often impractical to wait for long periods (up to one year) before the required strength is reached and therefore the effect of accelerated curing on the strength development of foamed concrete containing large volumes of ash needs to be investigated.

The effect of strength requirement on the material cost of foamed concrete mixtures can be seen in the graph in Figure 7.6. For each given strength the cost of the mixture with the lowest material cost was used (regardless of porosity) for both pfa and pozz-fill after 28 days and 365 days. After 28 days mixtures with higher porosities required relatively low ash/cement ratios to yield the required strengths and therefore the lowest cost for a given 28 day strength was not necessarily obtained from the mixture with the highest porosity. From Figure 7.6 it can be seen that although the material cost increases with increased required strength, the material cost for a given strength can be reduced by waiting longer to obtain the strength or by using pozz-fill in stead of pfa.

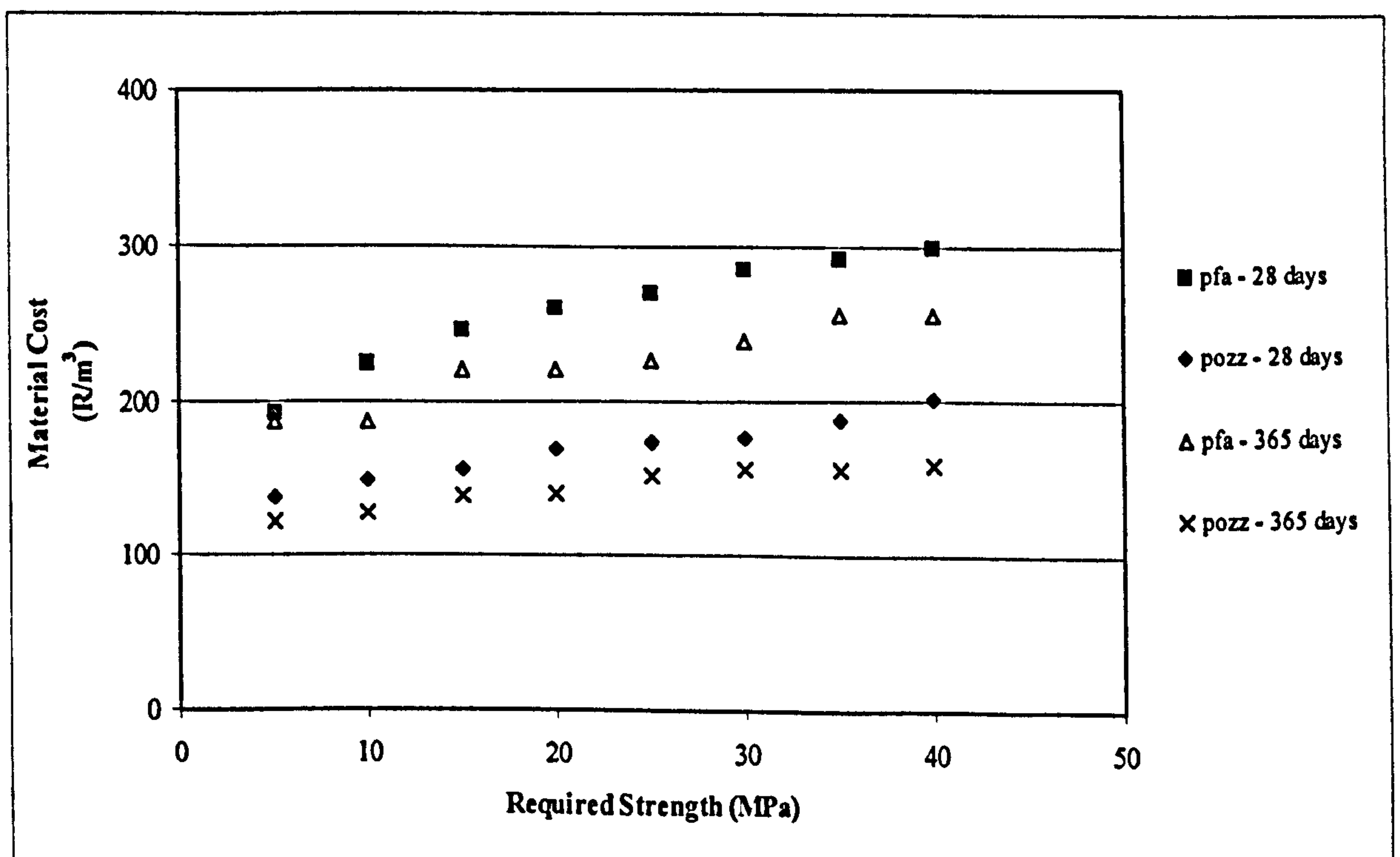


Figure 7.6: The effect of Required Compressive Strength on Material Cost.

The effect of porosity on material cost can be seen in Figure 7.7 where mixtures were used that would yield a compressive strength of at least 10 MPa after 365 days. These results indicate that in the long term (more than 365 days) the mixtures with the highest porosity that would yield the required strength, would be the mixture with the lowest material cost.

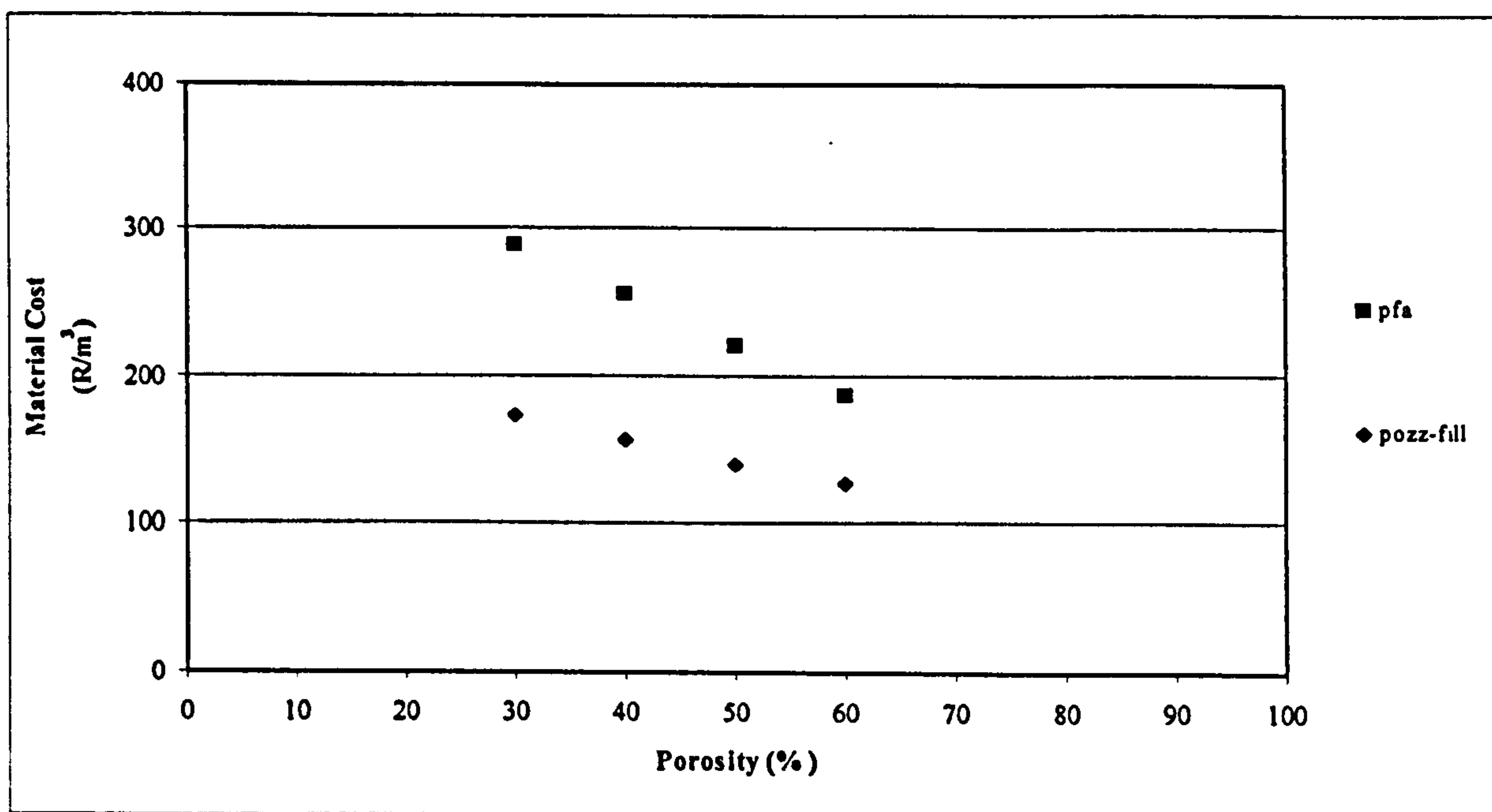


Figure 7.7: Effect of Porosity on Material Cost.

7.3 CONCLUSION

Based on the compressive strengths calculated using the simulation model it can be concluded that:

- Although high ash content results in a reduction in compressive strength at early ages, the long term strength (say after one year) is improved by replacing up to 75% of the cement (by weight) with ash.
- There seems to be an optimum ash content, resulting in the highest compressive strength for a given porosity, and this optimum increases with increased age. This optimum content is dependent on age only and although the porosity affects the compressive strength it does not affect the optimum ash/cement ratio.
- The trends observed for classified ash (pfa) and unclassified ash (pozz-fill) are similar, with the pozz-fill mixtures yielding marginally lower strengths than the mixtures containing pfa. The pozz-fill mixtures (with up to more than 70% of the

cement replaced with pozz-fill) do however still yield higher long-term strengths than the mixtures containing no ash.

- Replacing large volumes of cement with pfa can significantly reduce the cost of foamed concrete mixtures. The cost can be reduced even more if pozz-fill is used in stead of pfa.
- At any given age, the most cost efficient mixture would be the mixture with the highest ash content that still yields the required strength.

CHAPTER 8: CONCLUSIONS AND RECOMMENDATIONS

8.1 CONCLUSIONS

The properties of foamed concrete as established in this investigation indicate that the mixtures with relatively high density could be used as a structural material although some problems could be encountered due to the high drying shrinkage. The use of high volumes of ungraded fly ash do not have any negative effect on the properties of foamed concrete. Replacing large volumes of cement (up to 75%) with ash can significantly reduce the cost of foamed concrete. The most important conclusions that can be drawn from this research are:

- Although the rate of gain in strength is reduced by the use of large volumes of ash, up to 67% of the cement can be replaced by ash without any significant reductions in long-term strength.
- The properties of foamed concrete manufactured using unclassified ash (Pozz-fill) are as least as good as that of foamed concrete manufactured using classified ash (Pfa).
- The single most important factor that seems to affect all the properties of foamed concrete is the dry density. Other factors such as the ash type and content and the entrained air void characteristics only seems to have a marginal effect on the properties.

Other useful conclusions are:

8.1.1 Compressive strength

- The compressive strength of foamed concrete is a function of age, ash/cement ratio and porosity and for a given porosity and age there seems to be an

optimum ash content, resulting in the highest compressive strength. The optimum ash content increases with time.

- A mathematical model was developed relating the compressive strength of the foamed concrete to age, porosity and ash/cement ratio. The mathematical model (as indicated on page 160) was used to predict the values for optimum ash content at different ages. A good correlation was obtained between the experimental results and those predicted from the model.

8.1.2 Void structure

- Image analysis using optical microscopy was used to study the characteristics of the entrained air voids. The distribution of the sizes was found to be log normal with the majority less than 300 μm . The void diameter increases and spacing decreases with increased porosity.
- It was not possible to identify any strong relationship between void size distribution and any of the properties measured. This is possibly a reflection of the high quality of the foaming agent used producing a stable consistent foam with little variation in void size distribution.

8.1.3 Water absorption and permeability

- The water absorption (expressed in kg/m^3) of foamed concrete is approximately twice that of a paste with similar water/binder ratio but appears to be little influenced by the volume of air entrained.
- Expressing water absorption as a percentage in mass can give misleading high results where foamed concrete is concerned because of the low densities involved.

- Water vapour permeability increases with an increase in the volume of air entrained.

8.1.4 Deformation

- The drying shrinkage of foamed concrete is similar to that of cement paste with similar water/binder ratios. The volume of air entrained has little influence over the shrinkage.
- The average drying shrinkage of foamed concrete is between two and three times greater than conventional concrete. Increasing the ash/cement ratio results in a slight reduction in shrinkage.
- The elastic modulus of the foamed concrete ranged from 13.2 GPa to 2.5 GPa and reduced with a reduction in density.
- The specific basic creep of foamed concrete increases with reducing density and is not influenced by ash/cement ratio. The creep values for foamed concrete with densities of 1250 kg/m³ and 1500 kg/m³ are similar to conventional concrete but are significantly higher for the lower density mixtures of 1000 kg/m³.

8.2 RECOMMENDATIONS FOR FUTURE WORK

The reasons for the differences between the foamed concrete properties obtained in this investigation and that published by others should be further investigated.

The compressive strength of foamed concrete mixtures containing large volumes of ash increases significantly after more than 28 days and therefore the full benefit of the strength can not be used in standard construction practice where the 28 day strength is the standard measure of strength. The possibility of steam curing to increase early age strength development should be investigated.

The casting densities and mix proportions used in this investigation were chosen within the range where the foaming agent had been proven to yield stable foam. Although the effect of voids was found to be minimal in this investigation, the voids could have a significant effect on the properties of foamed concrete if mixtures were manufactured closer to the limits of stability of the foam. The effect of voids at lower casting densities should be investigated.

This research was executed using only one source of materials and the effect of different cement, ash and foam sources on the properties of foamed concrete should be investigated.

The influence of sand grading and content, when used as an inert filler, on the properties of foamed concrete should be further investigated.

By using a mathematical strength model an optimum ash content for different ages was determined. The calculated optimum ash contents are relatively high and further research should be conducted on mixtures with ash/cement ratios higher than 3. Further research should also be conducted to establish whether the relationship developed holds true for other ashes and even for normal concrete.

Owing to problems encountered in this investigation and the lack of availability of test rigs the long-term movement properties of the foamed concrete mixtures could not adequately be determined. Further and more extensive test programs are recommended which would examine the long-term behaviour of foamed concrete under sealed and dry conditions. The data obtained could then be incorporated in recognized code prediction methods to ascertain the adequacy of these methods to predict the elastic and long term movement of foamed concrete.

The use of fiber reinforcing and inert fillers to reduce the shrinkage and prevent shrinkage cracks from forming should be investigated.

The difference in trend between water absorption and water vapour permeability needs further investigation. This needs to be linked to a study of the corrosion behaviour of reinforcing steel embedded in foamed concrete mixtures.

CHAPTER 9: REFERENCES

- 1) Government Gazette; Republic of South Africa. *The White Paper on Housing*. December 1994.
- 2) Kearsley, E. P. & Mostert, H.F. The use of Foamcrete in Southern Africa. ACI 1997 International Conference on High Performance Concrete: Design and Materials and Recent Advances in Concrete Technology, December 1997, Kuala Lumpur, Malaysia.
- 3) Kearsley, E. P. The use of Foamcrete for Affordable Development in Third World Countries. *Proceedings Conference on Concrete in Service of Mankind (Congress on Appropriate Concrete Technology)*, Dundee, UK, 1996. E & FN Spon, London, UK, 1996, pp. 233 – 243.
- 4) Goodman, H.J. 1994. Low-density Concrete. *Fulton's Concrete Technology*, Ed Addis, B.J. Seventh (revised) Edition. Portland Cement Institute, Midrand, South Africa, pp. 281-285.
- 5) ACI Committee 523. 1975. Guide for Cellular Concretes Above 50 pcf, and for Aggregate Concretes Above 50 pcf with Compressive Strengths Less Than 2500 psi. *ACI Journal*, February 1975, Title no. 72-7, pp. 50-66.
- 6) Neville, A. M. 1995. *Properties of Concrete*. Fourth Edition, Longman Group Limited, Essex, England.
- 7) Neville, A. M. & Brooks J.J. 1987. *Concrete Technology*. Longman Scientific & Technical, Essex, England.
- 8) CUR-onderzoekcommissie B 34 'Schuimbeton'. CUR-aanbeveling 14: Vervaardiging en beproeving van schuimbeton. Redactionele bijlage bij *Cement* 1989 nr 12.
- 9) Taylor, W. H. The production, properties and uses of foamed concrete. *Precast Concrete*, February 1974, pp. 83-96.
- 10) BRE Digest. *Autoclaved Aerated Concrete*. Building Research Establishment Digest 342, March 1989.
- 11) Leitch, F. N. The Properties of Aerated Concrete in Service. *Proceedings of the Second International Congress on Lightweight Concrete*, London, April 1980, pp. 97 - 111.
- 12) Benn, B. T. *Foamed Cement - Information Sheet*. Portland Cement Institute, Midrand, South Africa. 1994.
- 13) CUR - onderzoekcommissie B 34 'Schuimbeton'. *Literatuurstudie Schuimbeton* 86/3. Gouda, Netherlands. 1986.

- 14) Neopor System GMBH. *Neopor Lightweight Cellular Concrete* - Product Information Sheet. Nürtingen, Germany.
- 15) L. B. Chemicals. *Product Information Sheet*. Cheshire, UK.
- 16) Van Deijk, S. Foam Concrete. *Concrete*, July / August 1991, pp. 49 - 54.
- 17) Widmann, H. & Enoekl, V. *Concrete Precasting Plant and Technology*, Issue 6/1991, pp. 38 - 44.
- 18) Mc Cormick, F. C. Rational Proportioning of Preformed Foam Cellular Concrete. *ACI Journal*, February 1967, pp. 104 - 110.
- 19) Clark, A. J. 1991. *Foamed Concrete: Composition and Properties*. British Cement Association Publication Ref 46.042. BCA, Wexham Springs, Slough, UK.
- 20) Georgiades, A. & Marinos, J. 1991. Effect of Micropore Structure on Autoclaved Aerated Concrete Shrinkage. *Cement and Concrete Research*, Volume 21, 1991, pp. 655 - 662.
- 21) Mehta, P. K. & Monteiro, P. J. M. 1986. *Concrete Structure, Properties and Materials*, Second Edition. Prentice-Hall Inc., New Jersey, USA.
- 22) Gowripalan, N, Cabrera, J. G., Cusens, A. R. & Wainwright, P. J. Effect of Curing on Durability. *Concrete International*, February 1990, pp. 47 - 53.
- 23) Cabrera, J. G. & Wainwright, P. J. Educational Packages in Concrete Construction: Lecture EP10 Durability of Concrete Structures.
- 24) Powers, T. C. Structure and Physical Properties of Hardened Portland Cement Paste. *Journal of the American Ceramic Society*, Volume 41, No1, January 1958, pp. 1 - 6.
- 25) Cabrera, J. G. & Lynsdale, C. J. 1993. The effect of Superplasticisers on the Hydration of Normal Portland Cement. *full detail required*
- 26) Metha, P. K. & Manmohan, D. 1980. *Pore Size Distribution and Permeability of Hardened Cement Pastes*. Proceedings of the seventh International Conference on the Chemistry of Cement, Paris, 1980, Volume II, pp. 1-5.
- 27) Wilk, W. & Dobrolubov, G. 1984. *Microscopic Quality Control of Concrete during Construction*. Proceedings of the sixth International Conference on Cement Microscopy, Albuquerque, 1984, pp. 330 - 343.
- 28) Hengst, R. R. & Tressler, R. E. Fracture of Foamed Portland Cements. *Cement and Concrete Research*, Volume 13, 1983, pp. 127 - 134.
- 29) Nasser, K. W. & Singh, B. P. A New Method and Apparatus for Determining the Air-Void Parameters in Fresh and Hardened Concrete. *Adam Neville Symposium on Concrete Technology*, 1995, pp. 239 - 256.

- 30) Visagie, M. The Effect of Microstructure on the Properties of Foamed Concrete. *The Young Concrete Engineers' and Technologists' Conference*, Midrand, South Africa, October 1997, pp. 101 – 109.
- 31) Basson, J. J. & Ballim, Y. 1994. Durability of Concrete. *Fulton's Concrete Technology*, Ed Addis, B.J. Seventh (revised) Edition. Portland Cement Institute, Midrand, South Africa, pp. 153-179.
- 32) Nyame, B. K. & Illston, J. M. Relationship between Permeability and Pore Structure of Hardened Cement Paste. *Magazine of concrete Research*: Volume 33, No 116: September 1981, pp. 139 – 146.
- 33) Cabrera, J. G. & Claisse, P. A. 1997. *Assessment of the Durability of Cement-Silica Fume Pastes and Mortars Measuring Oxygen and Water Vapour Transport*. Proceedings of the International Seminar on the use of Microsilica in Concrete, Islamic Republic of Iran, April 1997, pp. 13 – 30.
- 34) Wainwright, J. G., Cabrera, J. G. & Alamri, A. M. 1992. Performance Properties of Pozzolanic Mortars cured in Hot Dry Environments. *Concrete in Hot Climates: Proceedings of the Third International RILEM Conference*. E & FN Spon, Torquay, England, 1992, pp. 115 - 128.
- 35) Rößler, M. & Odler, I. 1985. Investigations on the Relationship between Porosity, Structure and Strength of Hydrated Portland Cement Pastes. I Effect of Porosity. *Cement and Concrete Research*. Volume 15, 1985, pp. 320 – 330.
- 36) Fagerlund, G. 1973. *Strength and Porosity of concrete*. Proceedings of the International RILEM Symposium on Pore Structure, Prague, 1973, Part 2, pp. D51 – D73.
- 37) Baozhen, S. & Erda, S. 1987. *Relation between Properties of Aerated Concrete and its Porosity and Hydrates*. Pore Structure and Materials Properties. Proceedings of the First International Congress held by RILEM, Versailles, France, September 1987, pp.232 - 237.
- 38) Hoff, G. C. 1972. Porosity – Strength Considerations for Cellular Concrete. *Cement and Concrete Research*. Volume 2, 1972, pp. 91 – 100.
- 39) Berry, E. E. & Malhotra, V. M., Fly Ash for use in Concrete - A Critical Review. *ACI Journal*, March-April 1980, pp. 59 - 73.
- 40) Smith, I. A. The Design of Fly-Ash Concretes. *Proceedings of the Institution of Civil Engineers (London)*, Volume 36, 1967, pp. 769 - 790.
- 41) Sarkar, L. S & Ghosh, S. N. 1993. *Progress in Cement and Concrete: Mineral Admixtures in Cement and Concrete, Volume 4*. ABI Books Private Limited. New Delhi, India.

- 42) Cabrera, J. G. & Gray, M. N. Specific surface, pozzolanic activity and composition of pulverized-fuel ash. *Fuel*, Volume 52, July 1973, pp. 213 - 219.
- 43) Hopkins, C. J. & Cabrera, J. G. The Shape Factor: A Parameter to Assess the Effect of Pulverized Fuel Ash on the Flow Properties of Cement Pastes and Concrete. *International Symposium on Cement and Concrete Science*. Beijing, Peoples Republic of China. 1994.
- 44) Hopkins, C. J. The Properties of Pulverized Fuel Ash and their Influence on the Flow Behaviour of Cement Pastes and Concrete. Ph. D. Thesis, Department of Civil Engineering, University of Leeds, 1984.
- 45) Hewlett, P. C. 1998. *Lea's Chemistry of Cement and Concrete, Fourth Edition*. Arnold, London.
- 46) Berry, E. E., Hemmings, R. T., Zhang, M. H., Cornelius, B. J. & Golden, D. M. Hydration in High-Volume Fly Ash Concrete Binders. *ACI Materials Journal*, July - August 1994, pp. 382 - 389.
- 47) British Standards Institution. *ENV 197-1: Cement – composition, specifications and conformity criteria. Part 1. Common cements*. BSI, 1995, London.
- 48) South African Standard. *SABS 1491 Part II - 1989: Standard Specification for Portland Cement Extenders. Part II: Fly ash* (amended in 1992) SABS, Pretoria.
- 49) Davis, R. E., Carlson, R. W., Kelly, J. W. & Davis, H. E.; Properties of Cements and Concretes containing Fly Ash. *Proceedings of the American Concrete Institute*, Volume 33, May-June 1937, pp. 577 - 612.
- 50) Brink, R. H. & Halstead, W. J. Studies related to the Testing of Fly Ash for Use in Concrete. *Proceedings of the ASTM*, Volume 56, 1956, pp. 1161 - 1214.
- 51) Cannon, R. W. Proportioning Fly Ash Concrete Mixes for Strength and Economy. *ACI Journal*, November 1968, pp. 969 - 978.
- 52) Hassan, K. E., Cabrera, J. G. & Bajracharya, Y. M. 1997. *The Influence of Fly Ash Content and Curing Temperature on the Properties of High Performance Concrete*. Bahrain, 1997.
- 53) Timms, A. G. & Grieb, W. E. Use of Fly Ash in Concrete. *Proceedings of the ASTM*, Volume 56, 1956, pp. 1139 - 1160.
- 54) Dhir, R. K., Apte, A. G. & Munday, J. G. L. Effect of In-source Variability of Pulverized-fuel Ash upon the Strength of OPC/pfa Concrete. *Magazine of Concrete Research* : Volume 33, No 117 : December 1981, pp. 199 - 207.
- 55) Montgomery, D. G., Hughes, D. C. & Williams, R. I. T. Fly Ash in Concrete - A Microstructure Study. *Cement and Concrete Research*, Volume 11, Number 4, 1981, pp. 591 - 603.

- 56) Ravina, D & Metha, P. K. Compressive Strength of Low Cement / High Fly Ash Concrete. *Cement and Concrete Research*, Volume 18, 1988, pp. 571 - 583.
- 57) Stuart, K. D., Anderson, D. A. & Cady, P. D. Compressive Strength Studies on Portland Cement Mortars Containing Fly Ash and Superplasticizers. *Cement and Concrete Research*, Volume 10, 1988, pp. 823 - 832.
- 58) Taylor, P. C. & Kruger, R. A. Effect of fly Ash Particle Size on Concrete Properties. The Concrete Way to Development - *FIP Symposium 1997*, The Concrete Society of Southern Africa, Midrand, South Africa. 1997, pp.631 - 640.
- 59) Brooks, J. J. & Neville, A. Creep and Shrinkage of Concrete as affected by Admixtures and Cement Replacement Materials. Creep and Shrinkage of Concrete: Effect of Materials and Environment. *American Concrete Institute Special Publication 129*, 1992. pp. 19 - 36.
- 60) Sri Ravindraraja, R. & Tam, C. T. Properties of Concrete Containing Low Calcium Fly Ash under Hot and Humid Climate. Proceedings of the 3rd International Congress on Fly Ash, Silica Fume, Slag, and Natural Pozzolans in Concrete, Trondheim, 1989. *American Concrete Institute Special Publication 114*. Volume I: pp. 139 - 155.
- 61) Carette, G., Bilodeau, A., Chevrier, R. L. & Malhotra, V. M. Mechanical Properties of Concrete Incorporating High Volumes of Fly Ash from Sources in the U.S. *ACI Materials Journal*, Volume 90, Number 6, November-December 1993, pp. 535 - 544.
- 62) Sirivivatnanon, V. & Khatri, R.P. Selective use of Fly Ash Concrete. Proceedings of the 6th International Congress on the Use of Fly Ash, Silica Fume, Slag and Natural Pozzolans in Concrete, Bangkok, Thailand, 1998. *American Concrete Institute Special Publication 178*. Volume I: pp. 37 - 57.
- 63) Swamy, R. N. & Mahmud H. B. Shrinkage and Creep Behaviour of High Fly Ash Concrete. Proceedings of the 3rd International Congress on Fly Ash, Silica Fume, Slag, and Natural Pozzolans in Concrete, Trondheim, 1989. *American Concrete Institute Special Publication 114*. Volume I: pp. 453 - 475.
- 64) Daly, D.D. 1994. Concrete mix design. *Fulton's Concrete Technology*, Ed Addis, B.J. Seventh (revised) Edition. Portland Cement Institute, Midrand, South Africa, pp. 209-217.
- 65) Kellerman, J. & du Preez, H.T.R. 1994, Manufacture of concrete. *Fulton's Concrete Technology*, Ed Addis, B.J. Seventh (revised) Edition. Portland Cement Institute, Midrand, South Africa, pp. 219-244.
- 66) ASTM Committee C-9. ASTM Standard C495 - 1980: *Standard Test Method for Compressive Strength of Lightweight Insulating Concrete*.

- 67) Kearsley, E.P. & Mostert H.F. Foamcrete in Developing Communities. *Proceedings FIP Symposium 1997: The Concrete Way to Development*, Johannesburg, South Africa, March 1997. The Concrete Society of Southern Africa, Midrand, South Africa, 1997, pp.735 - 745.
- 68) Mosley, W.H. & Bungey, J.H. 1990. *Reinforced Concrete Design*. Fourth Edition. MacMillan Educational Ltd., Hong Kong.
- 69) Wilby, C.B. 1991. *Concrete Materials and Structures*. Cambridge University Press, Cambridge, UK.
- 70) Vine-Lott, K. Production of "foam" concrete by microcomputer. *Concrete* November 1985, pp. 12 - 14.
- 71) South African Bureau of Standards. SABS ENV 197-1:1992: *Cement - Composition, specifications and conformity criteria, Part I: Common cements*. SABS, Pretoria.
- 72) Kruger, R.A. Ten years of research into ASH utilisation. *Proceedings of the First National Symposium of the South African Coal Ash Association*. Pretoria, South Africa. May 1990, pp. 1 - 13.
- 73) South African Bureau of Standards. SABS 1491: Part II - 1989: *Portland cement extenders Part II: Fly ash*. SABS.
- 74) ASTM Committee C-9. 1992. ASTM C512 - 87 (Reapproved 1992): *Standard Test Method for Creep of Concrete in Compression*.
- 75) Cabrera, J. G. & Lynsdale, C. J. A New Gas Permeameter for Measuring the Permeability of Mortar and Concrete. *Magazine of Concrete Research*. 1988. Volume 40, Number 144, September, pp. 177 - 182.
- 76) Gaafar, B. A. 1995. *The Effect of Environmental Curing Conditions on the Gas and Water Permeability of Concrete*. Ph.D. Thesis, University of Leeds, Leeds, UK, 1995.
- 77) RILEM. 1978. RILEM Recommendation LC7: *Water vapour permeability of autoclaved aerated concrete*.
- 78) Ahmed, W. U. 1994. Petrographic Methods for Analysis of Cement Clinker and Concrete Microstructure. *Petrography of Cementitious Materials ASTM STP1215*. Ed De Hayes, S. M. & Stark, D. American Society for Testing and Materials, Philadelphia, USA, 1994, pp. 1 - 12.
- 79) CEN/TC 104. *ENV 480 Part II:1993 Admixtures for Concrete, Mortar and Grout - Test methods - Determination of Air Void Characteristics in Hardened Concrete*. European Committee for Standardization, Brussels, 1993.

- 80) Cahill, J., Dolan, C. D. & Inward, P. W. 1994. The Identification and Measurement of Entrained Air in Concrete using Image Analysis. *Petrography of Cementitious Materials ASTM STP1215*. Ed De Hayes, S. M. & Stark, D. American Society for Testing and Materials, Philadelphia, USA, 1994, pp. 111 - 124.
- 81) Wainwright, P. J. & Boni, S. P. K. Some Properties of Concrete Containing Sintered Domestic Refuse as a Coarse Aggregate. *Magazine of Concrete Research*. 1983. Volume 35, Number 123, June 1983, pp. 75 - 85.
- 82) Van As, S. C. Fortran Computer Program written at the University of Pretoria.

APPENDIX A: POROSITIES

Mix nr	Type of Ash	Target Density (kg/m ³)	a/c	w/c	w/binder	Porosity			
						After 28 Days (%)	After 180 Days (%)	After 270 Days (%)	After 365 Days (%)
1	NONE	FULL	0	0.30	0.30	23.3*	28.0	28.8	28.2
2	NONE	FULL	0	0.40	0.40	31.3	31.8	34.7	31.0
3	NONE	FULL	0	0.60	0.60	40.9	39.3	40.5	37.2
4	PFA	FULL	1	0.60	0.30	18.3*	32.6	34.5	29.8
5	PFA	FULL	2	0.86	0.29	16.2*	30.9	36.7	27.0
6	PFA	FULL	3	1.17	0.29	33.5	35.4	39.1	30.6
7	PFA	1500	1	0.60	0.30	50.6	46.6	45.7	43.3
8	PFA	1500	2	0.86	0.29	45.9	40.6	49.9	43.6
9	PFA	1500	3	1.17	0.29	38.1	35.2*	41.8	43.1
10	PFA	1250	1	0.60	0.30	56.0	44.6*	52.2	48.4
11	PFA	1250	2	0.86	0.29	64.2	43.8*	52.4	52.5
12	PFA	1250	3	1.17	0.29	43.8*	51.8	51.1	49.5
13	PFA	1000	1	0.60	0.30	64.1	63.2	66.9	59.3
14	PFA	1000	2	0.86	0.29	63.4	59.7	66.3	62.6
15	PFA	1000	3	1.17	0.29	51.9*	65.9	67.4	61.9
16	POZ	FULL	1	0.60	0.30	25.6*	30.6	32.2	31.7
17	POZ	FULL	2	0.86	0.29	33.9	32.5	38.8	31.6
18	POZ	FULL	3	1.17	0.29	31.9	35.4	34.6	33.2
19	POZ	1500	1	0.60	0.30	28.2*	38.8	44.8	43.0
20	POZ	1500	2	0.86	0.29	26.0*	38.1	46.2	41.1
21	POZ	1500	3	1.17	0.29	27.4*	43.0	40.9	38.2
22	POZ	1250	1	0.60	0.30	57.7	47.8	55.5	50.0
23	POZ	1250	2	0.86	0.29	61.6	48.6*	52.9	51.1
24	POZ	1250	3	1.17	0.29	31.3*	41.3*	50.0	48.3
25	POZ	1000	1	0.60	0.30	64.8	49.2	65.4	58.7
26	POZ	1000	2	0.86	0.29	72.4	64.8	60.8	60.6
27	POZ	1000	3	1.17	0.29	67.6	66.0	62.3	62.6

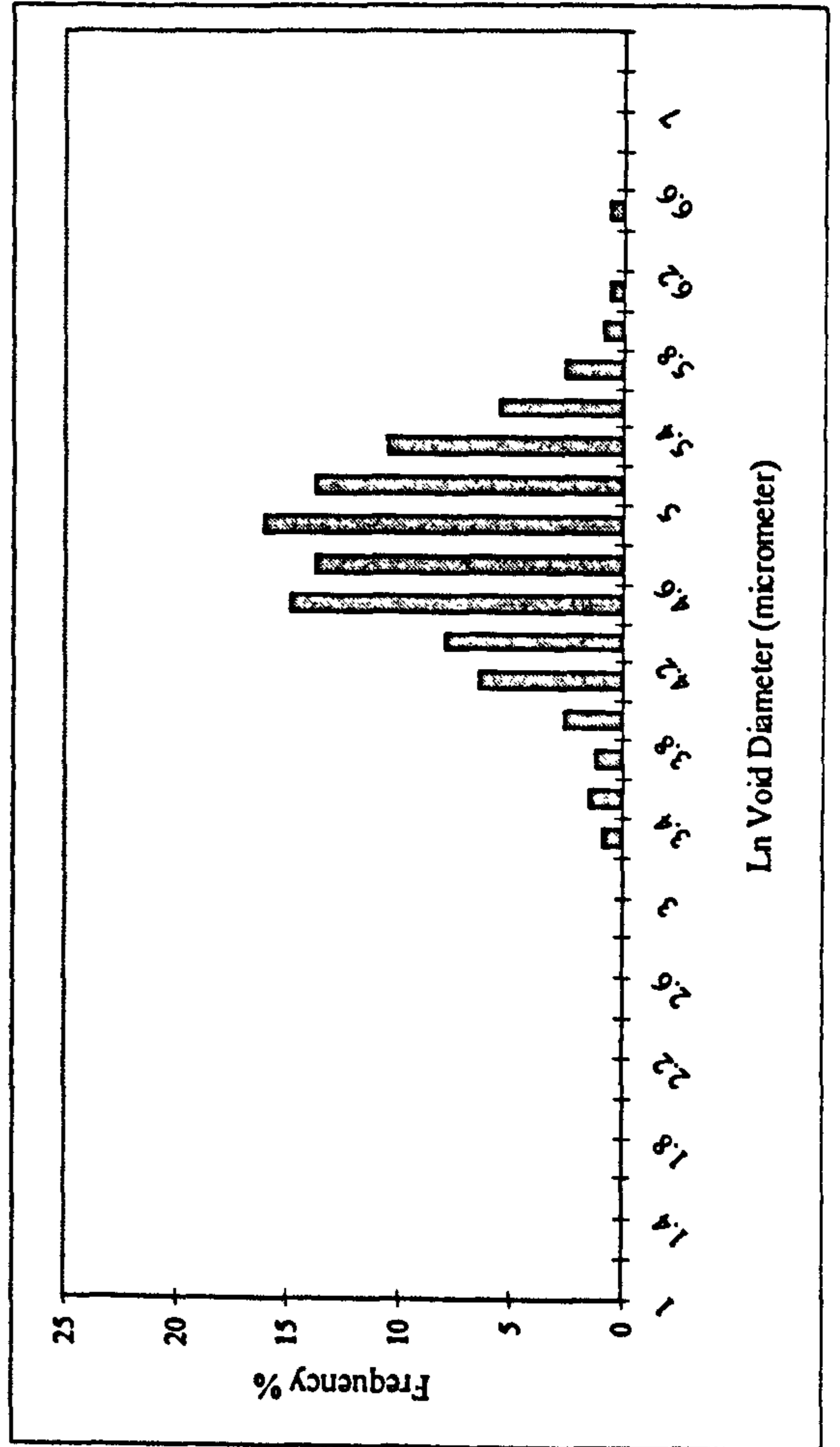
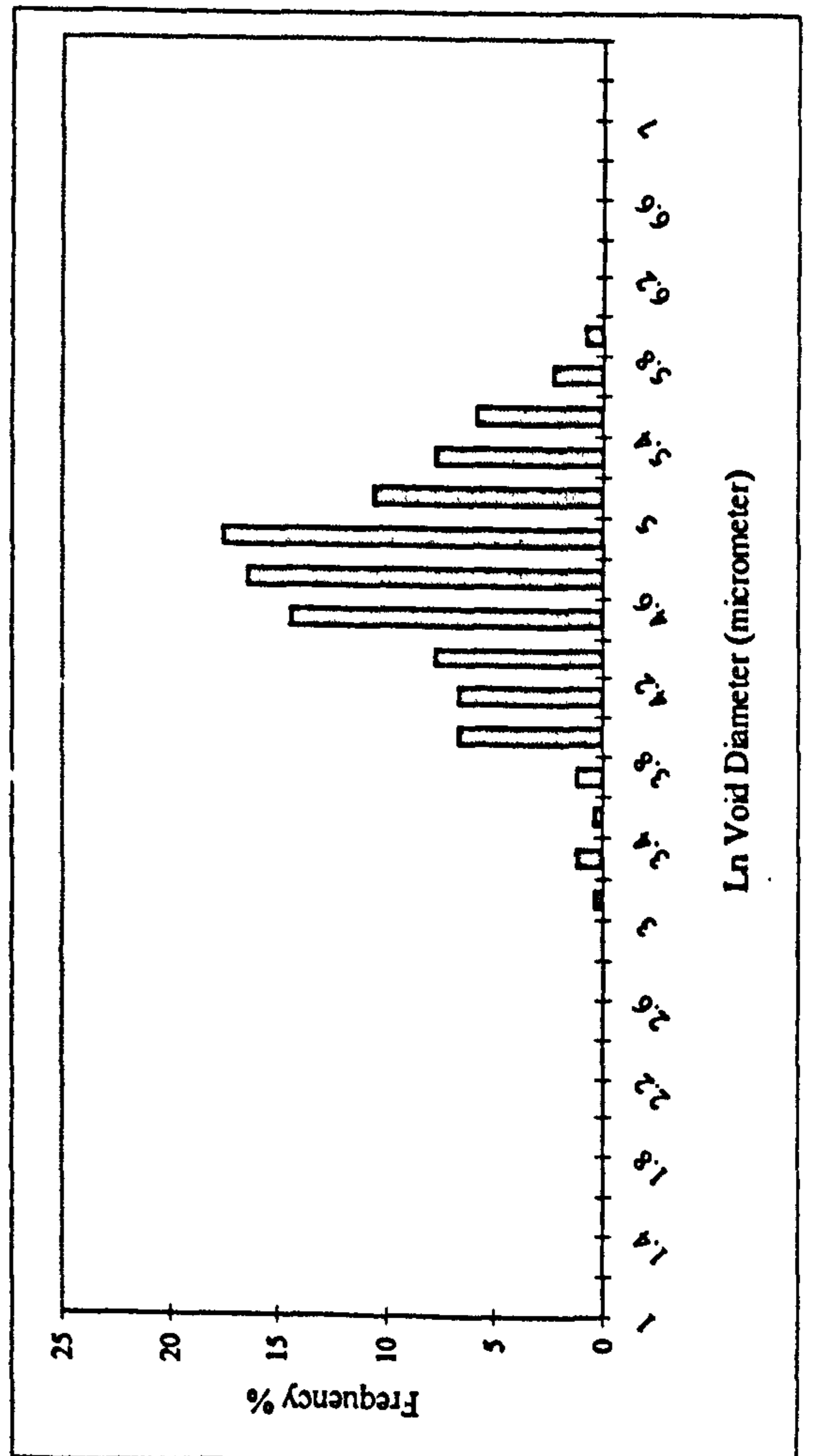
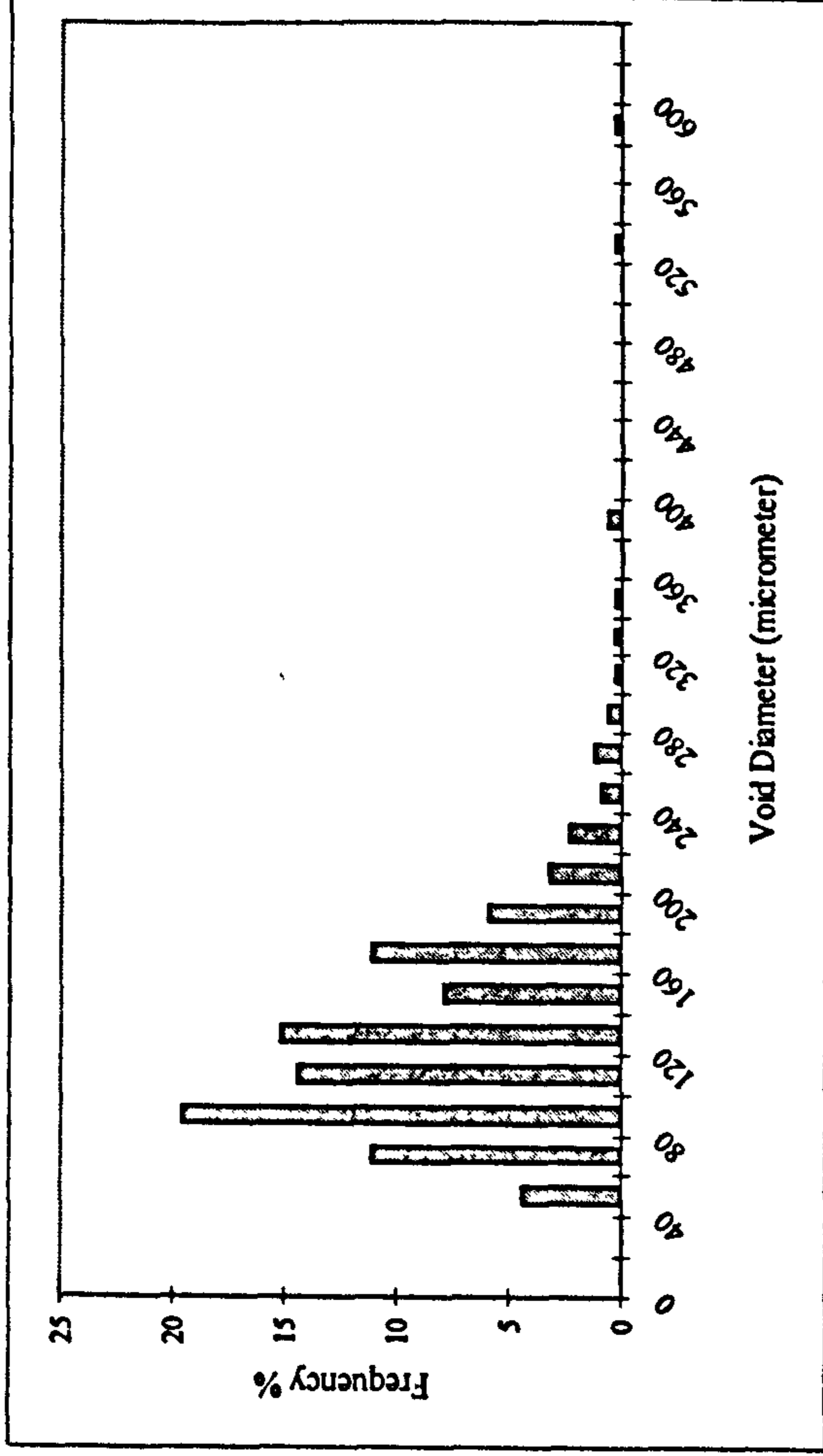
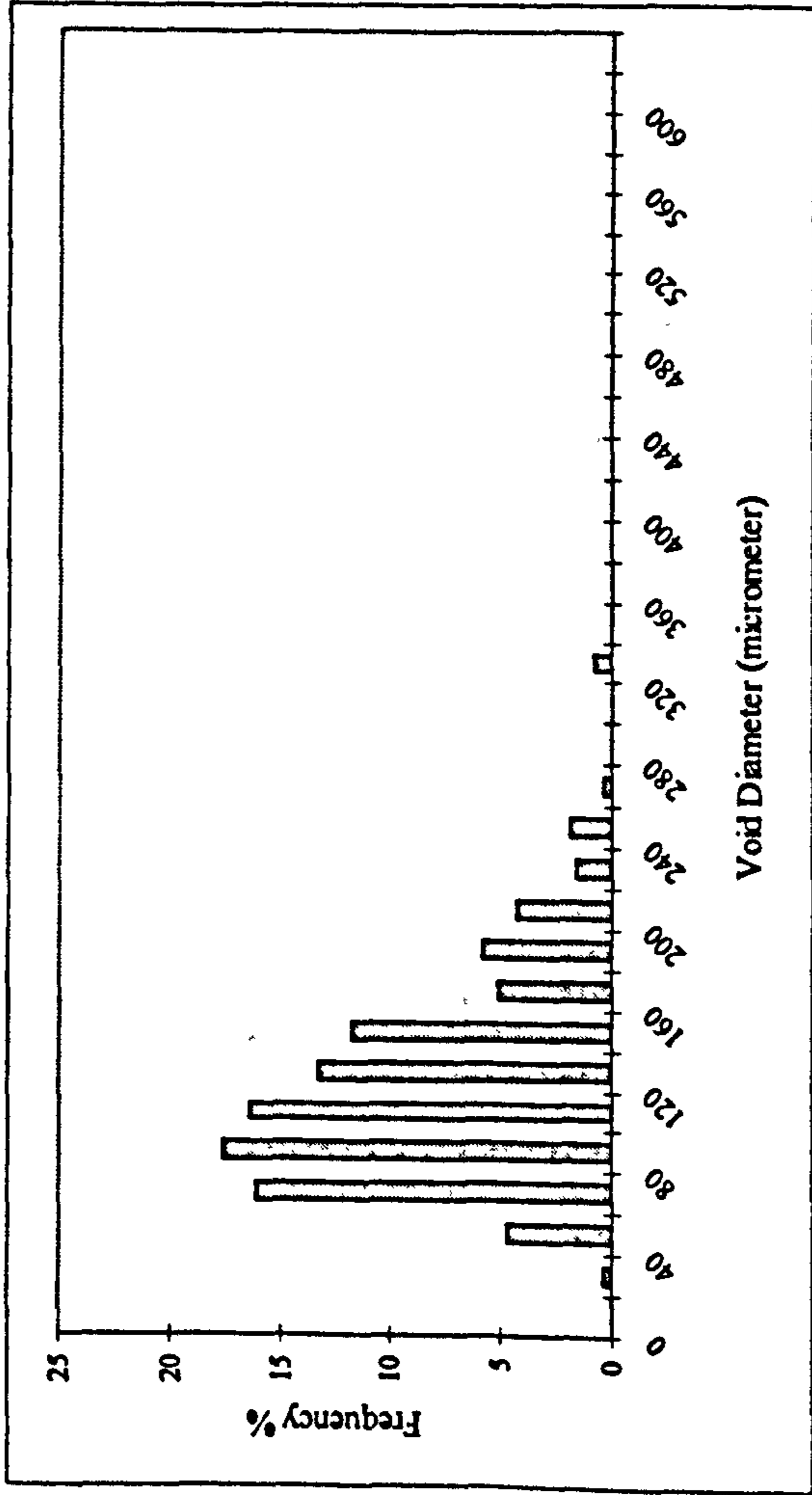
* Results suspect.

APPENDIX B: VOID SIZE DISTRIBUTIONS

1500 kg/m³ a/c=1

PFA

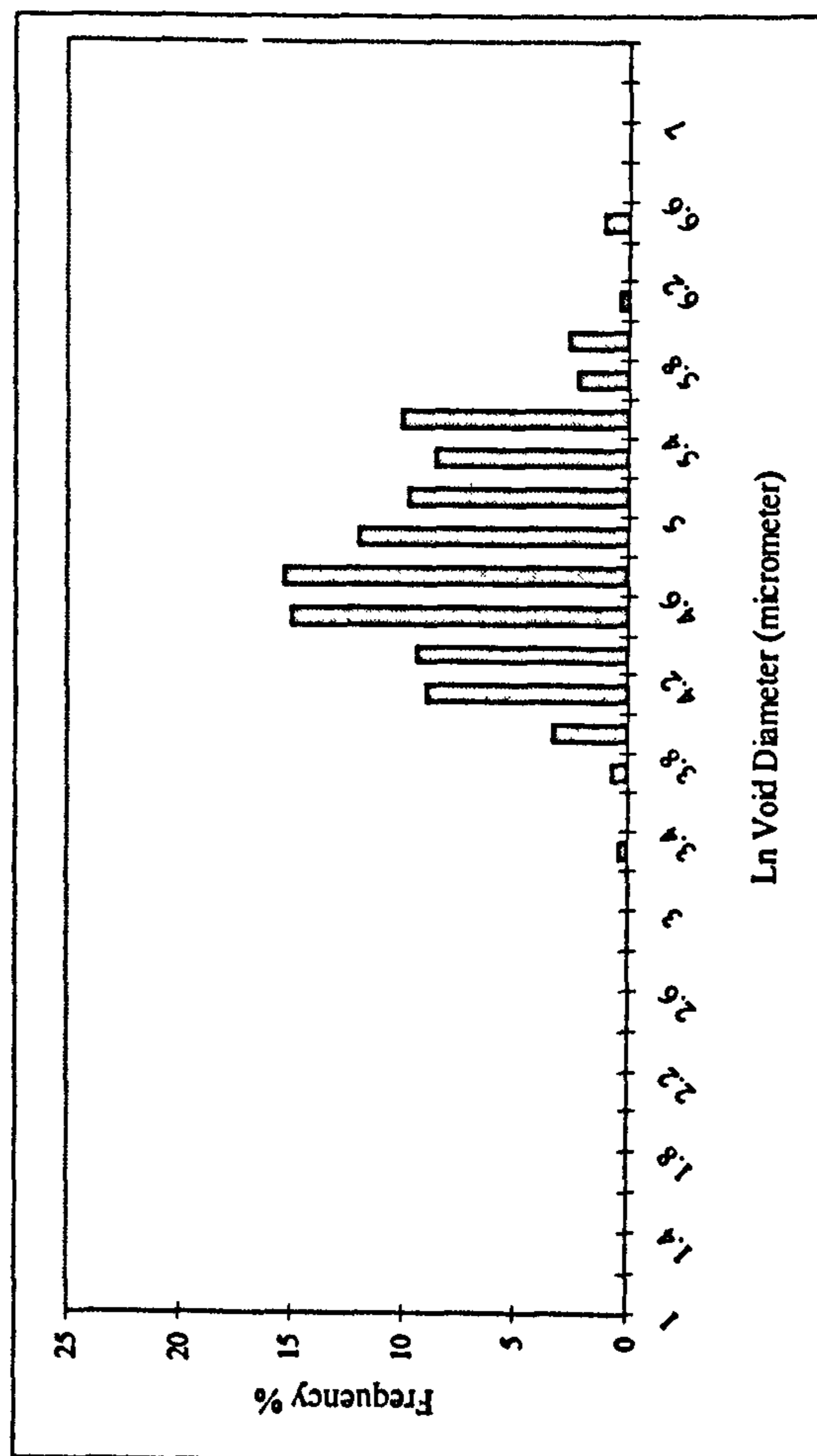
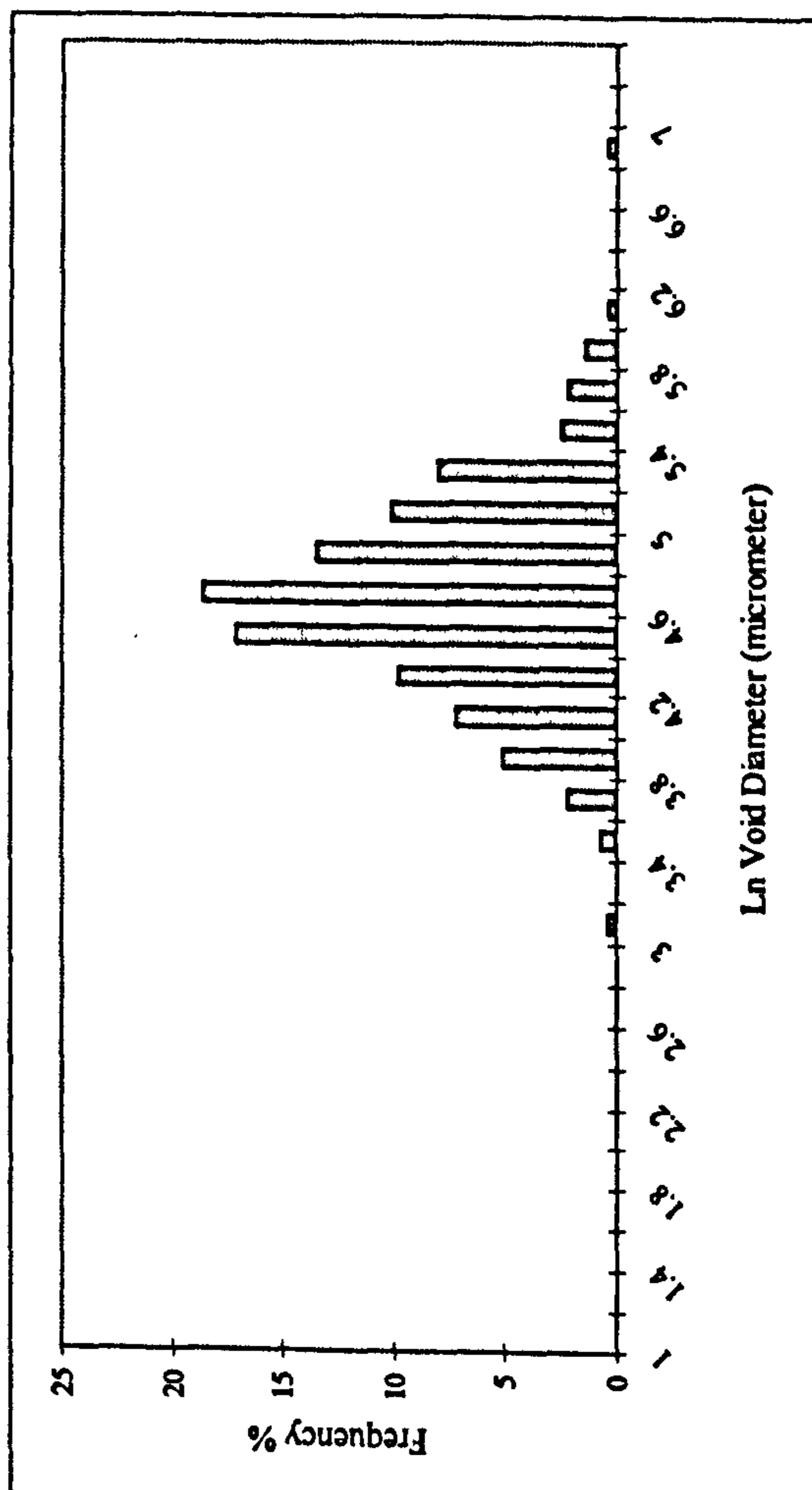
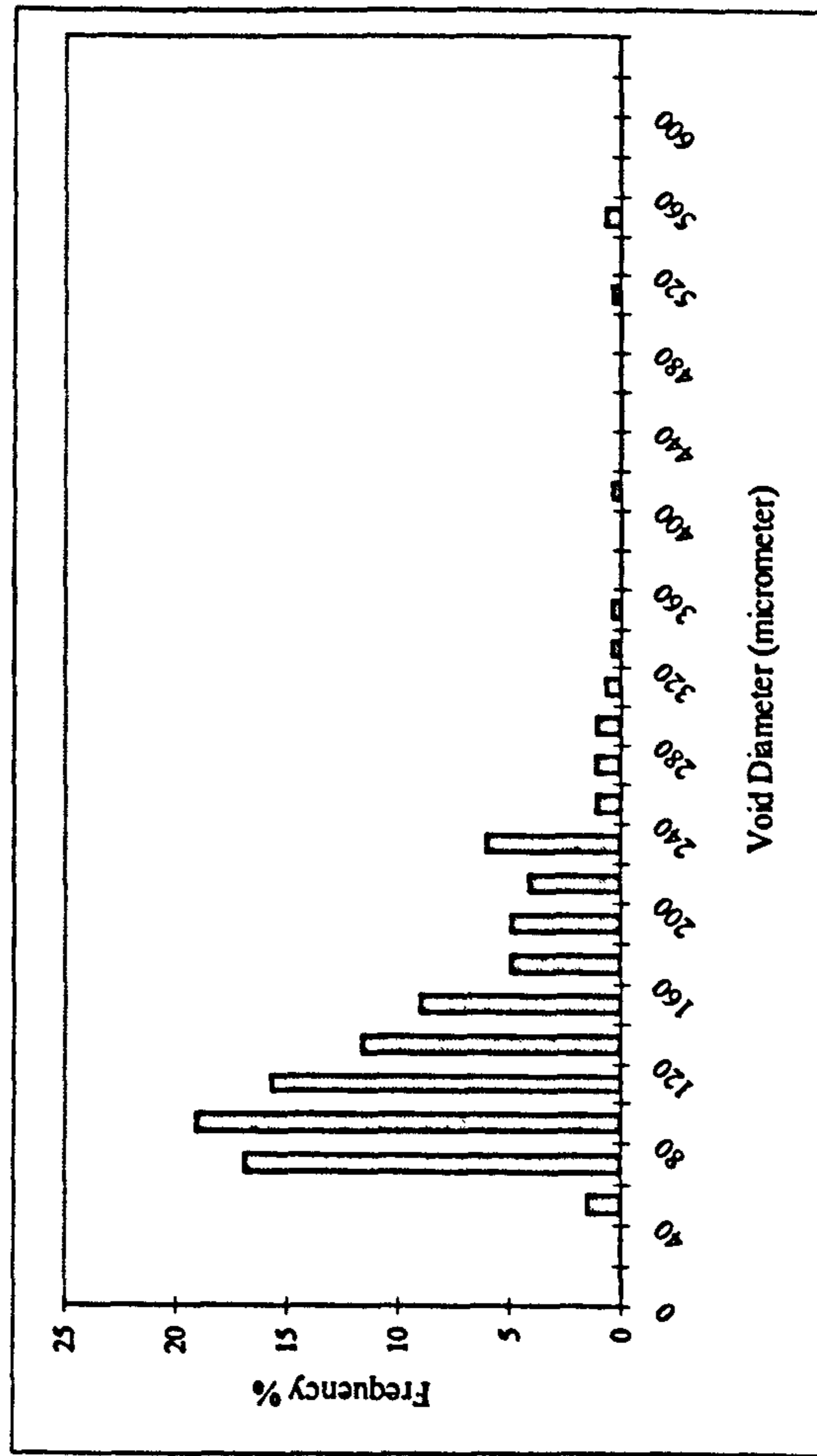
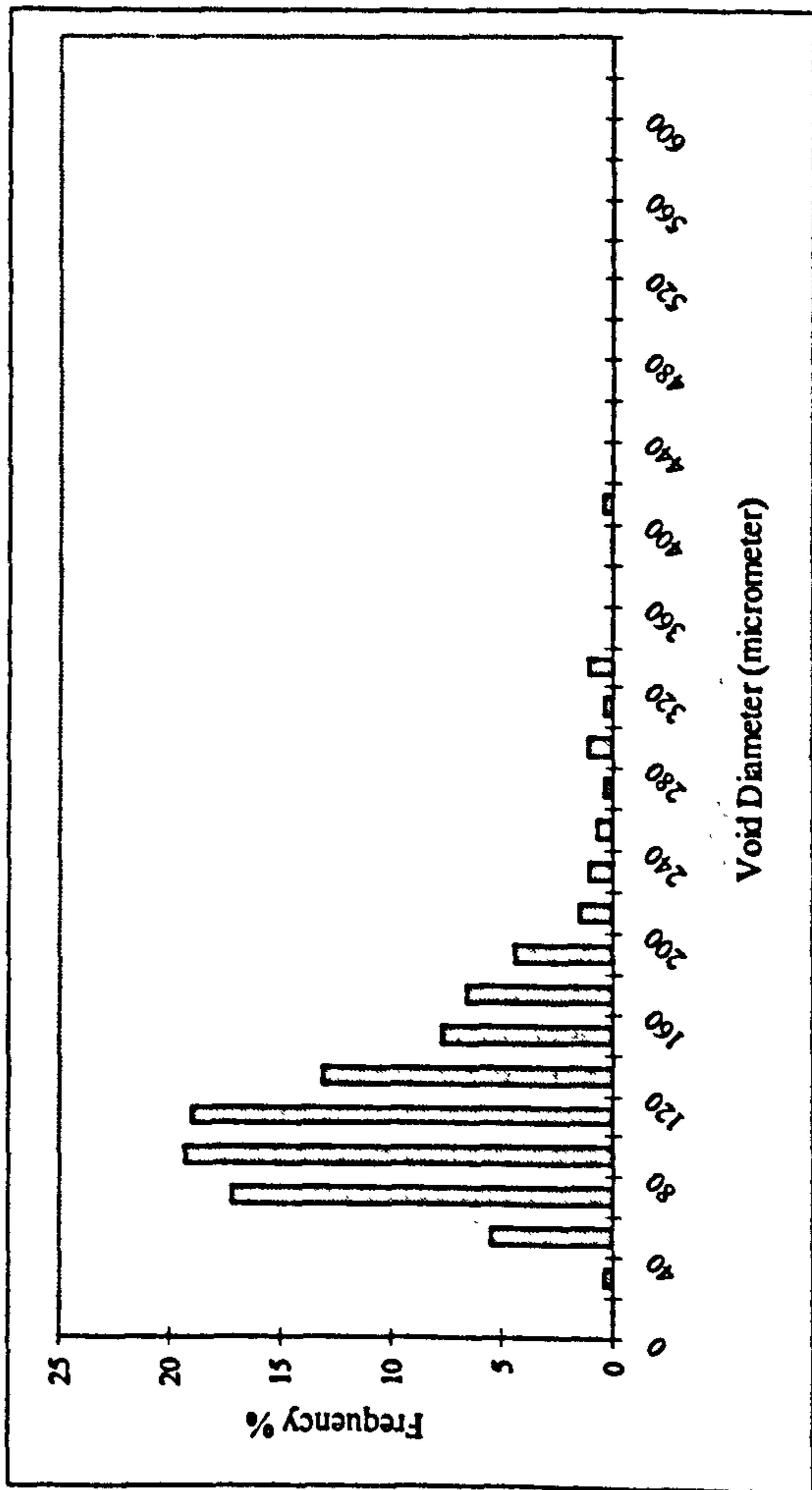
POZZ-FILL



1500 kg/m³ a/c=2

PFA

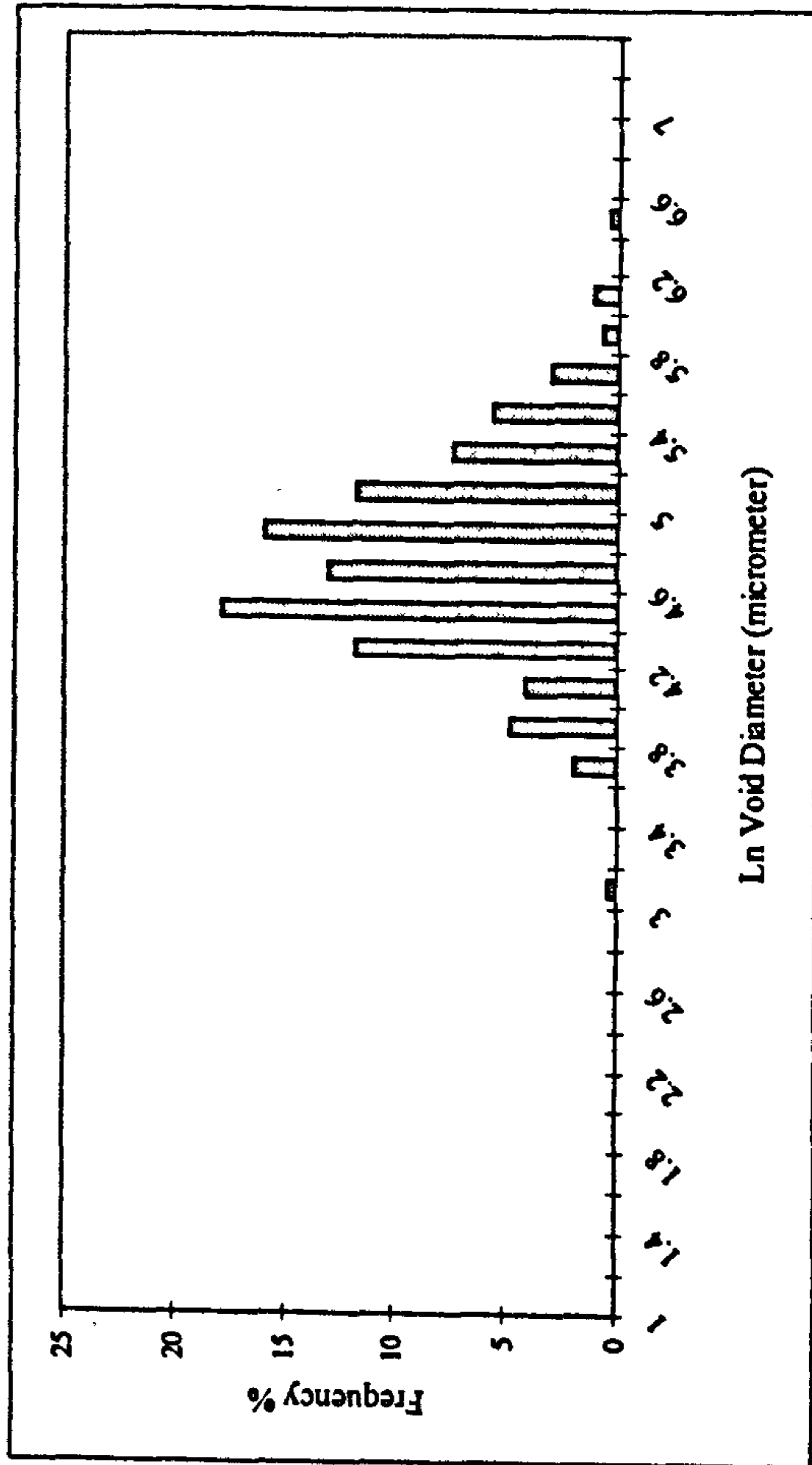
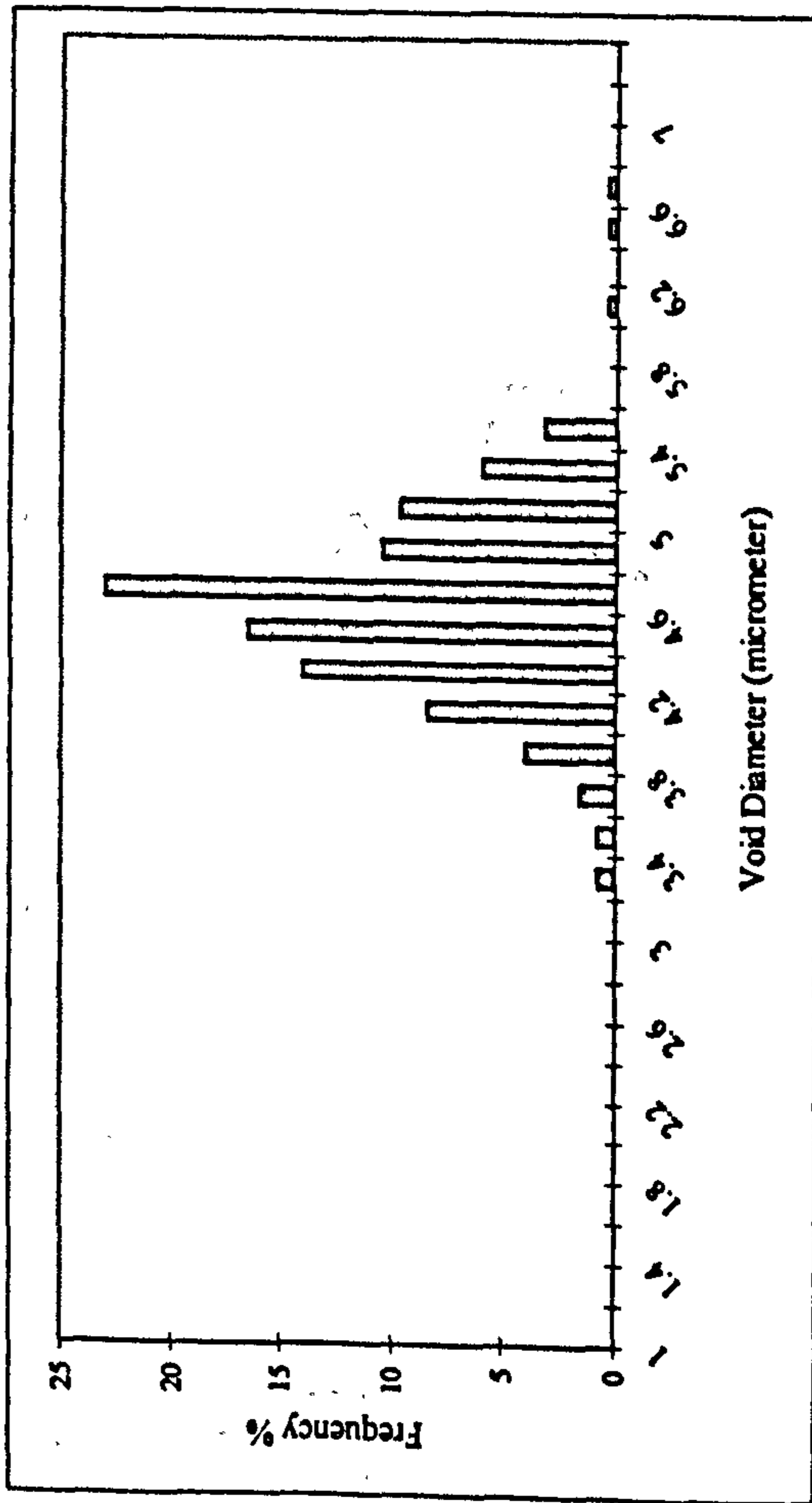
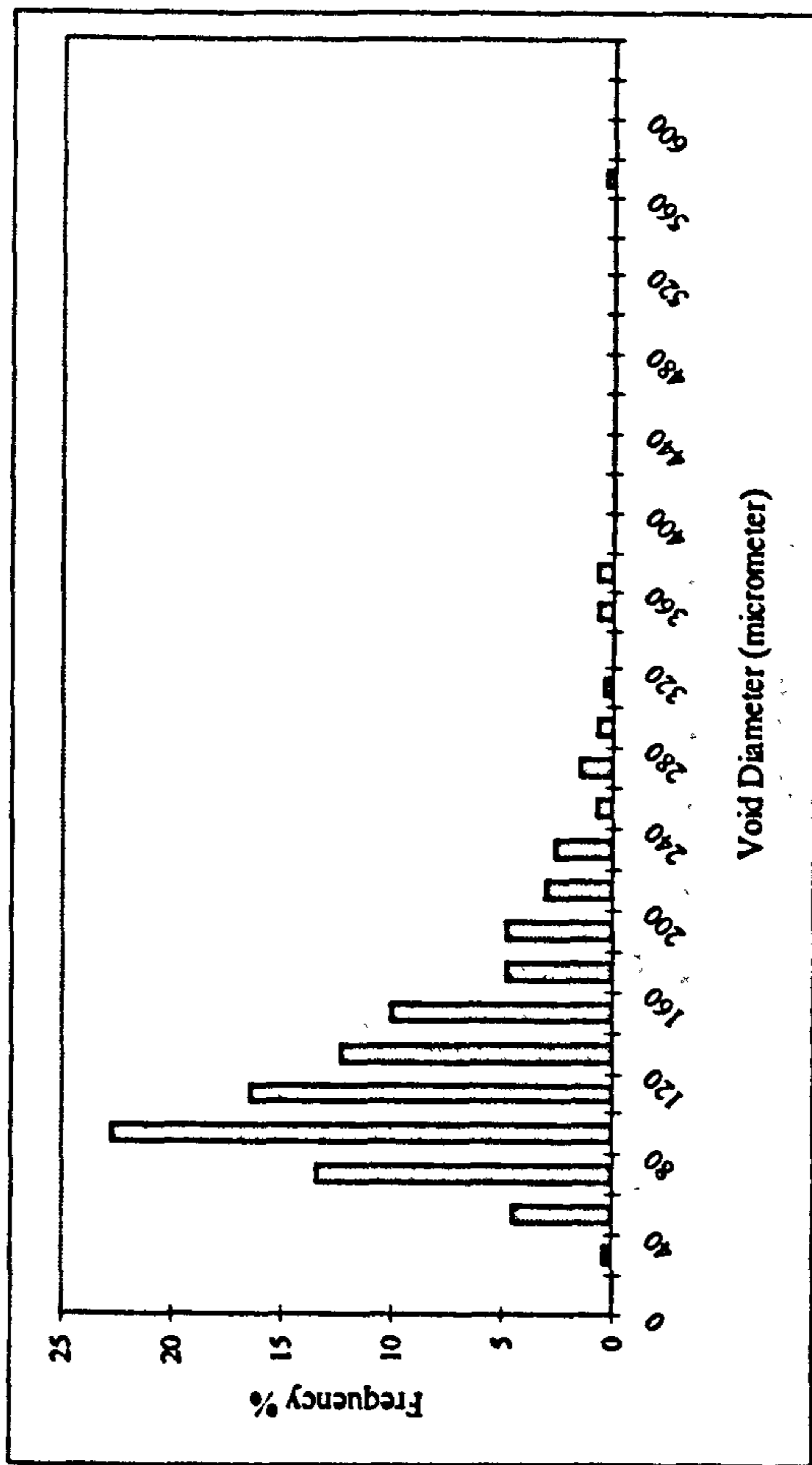
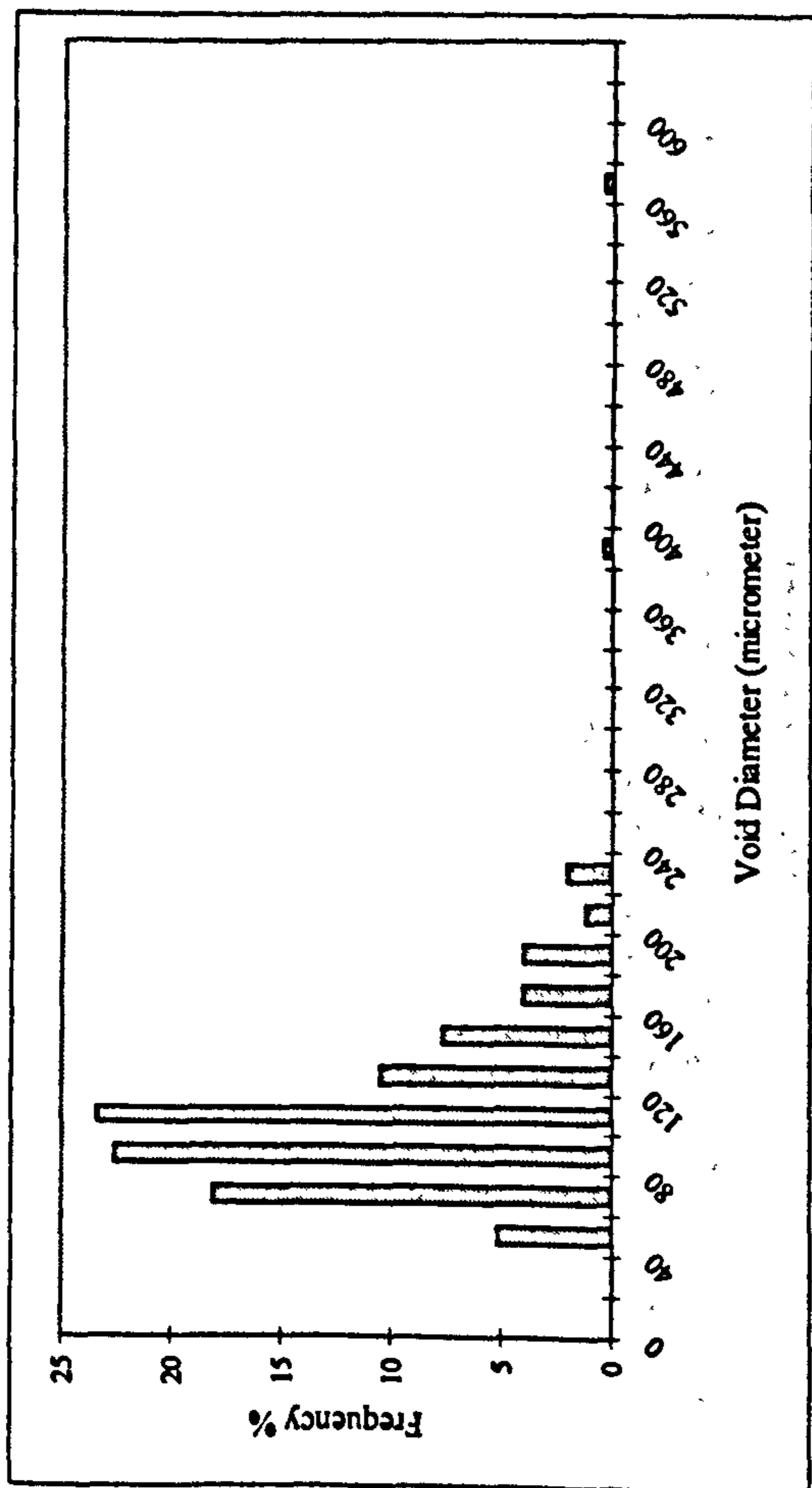
POZZ-FILL



1500 kg/m³ a/c=3

PFA

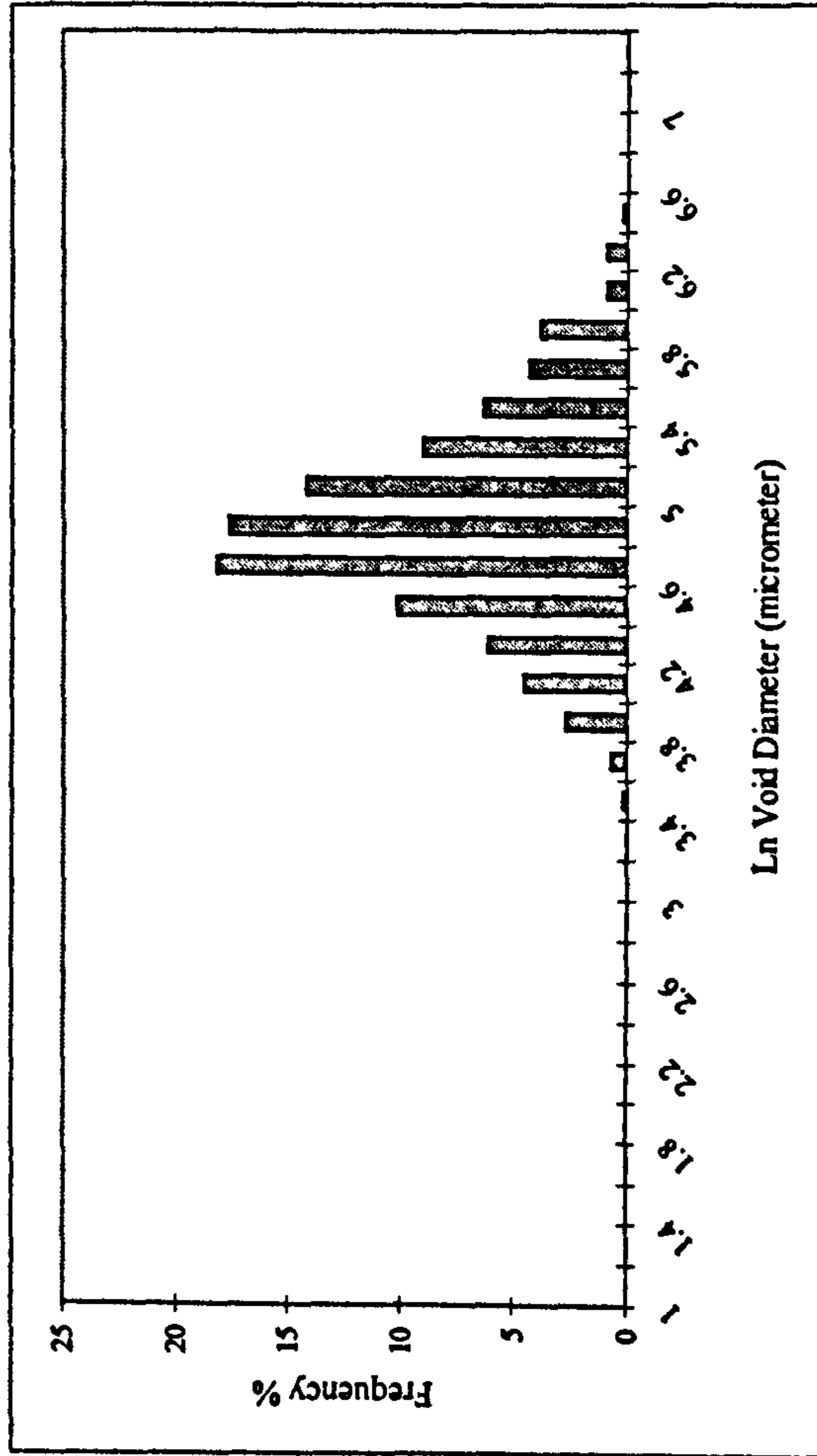
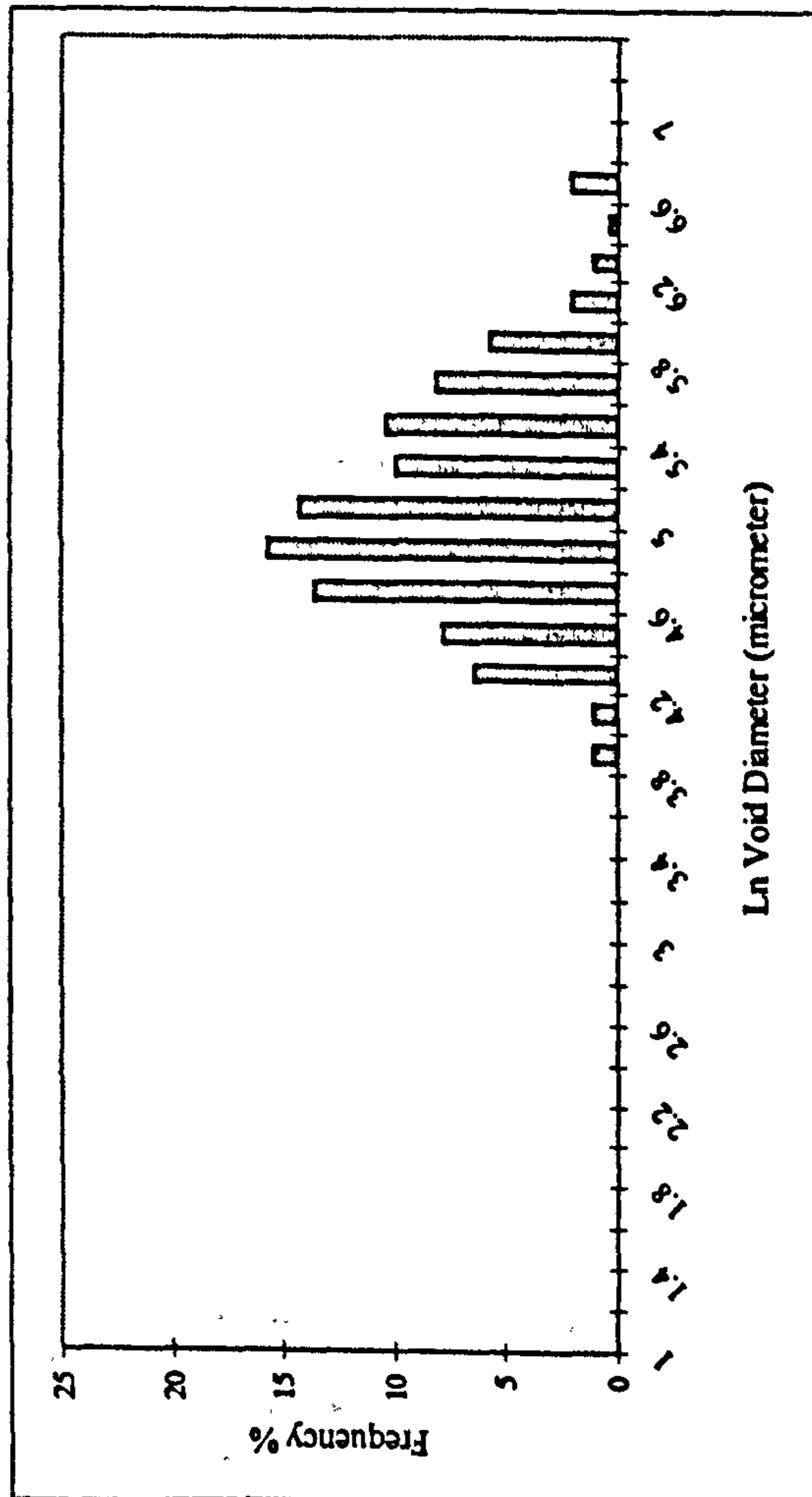
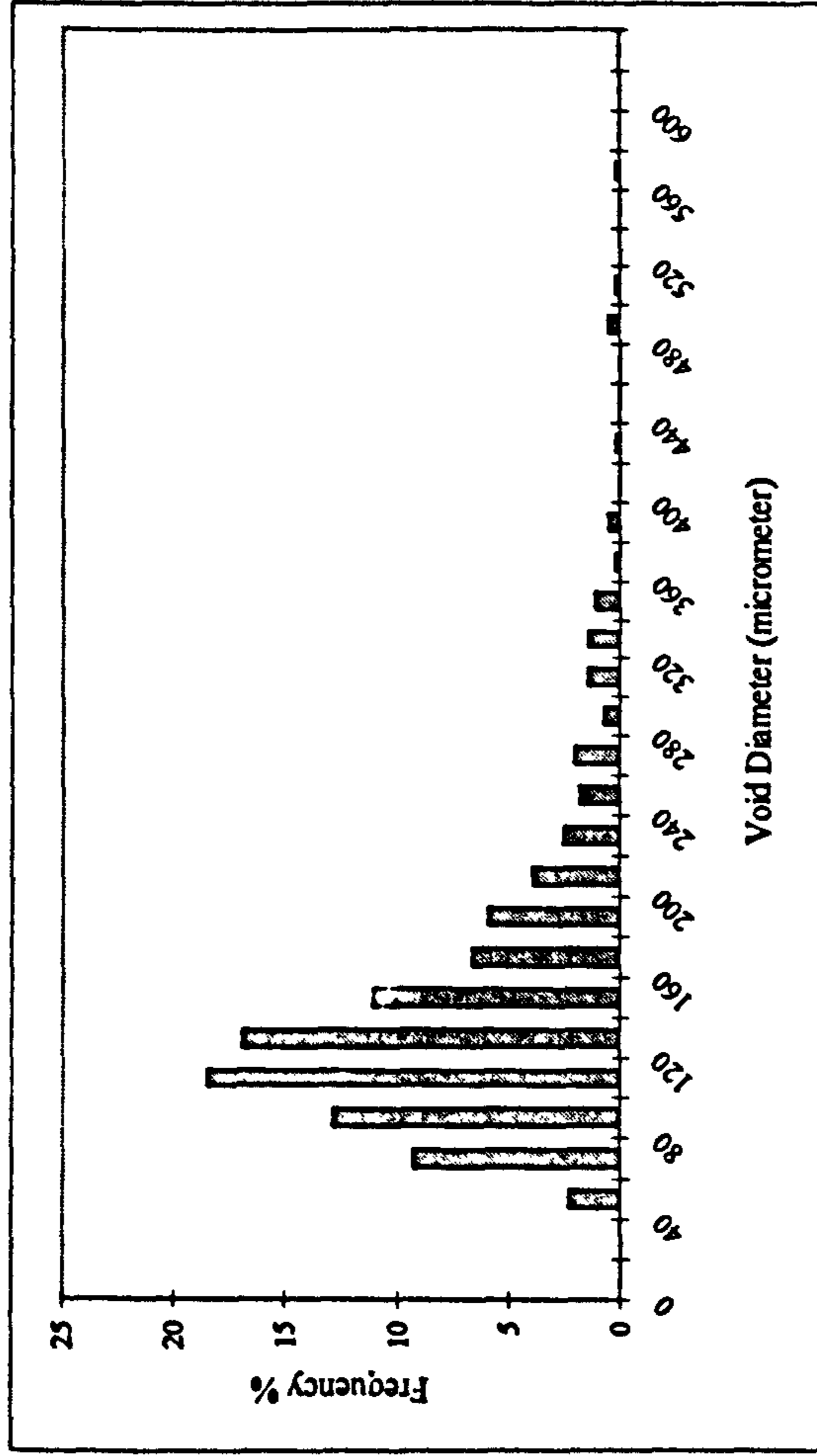
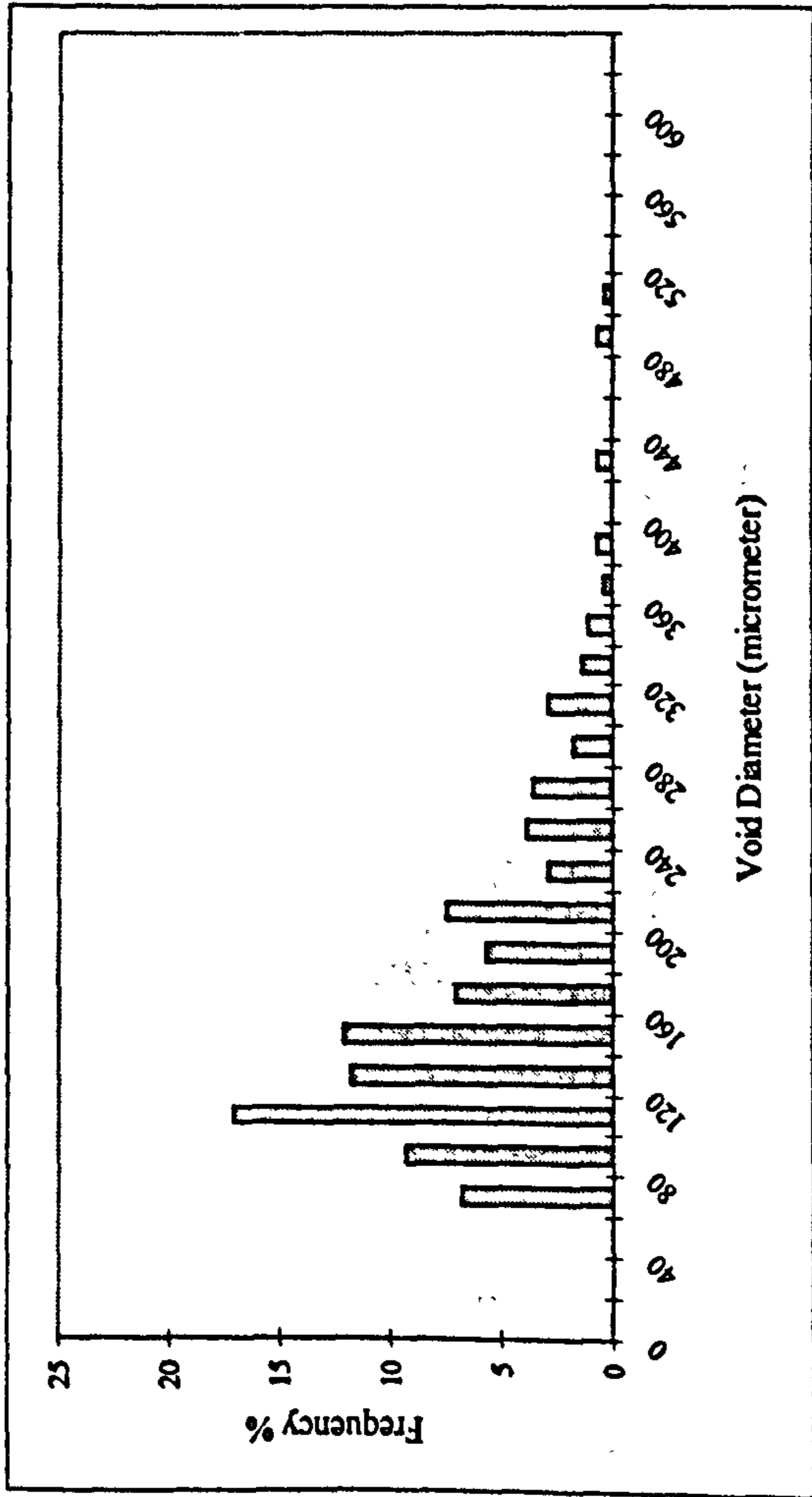
POZZ-FILL



1250 kg/m³ a/c=1

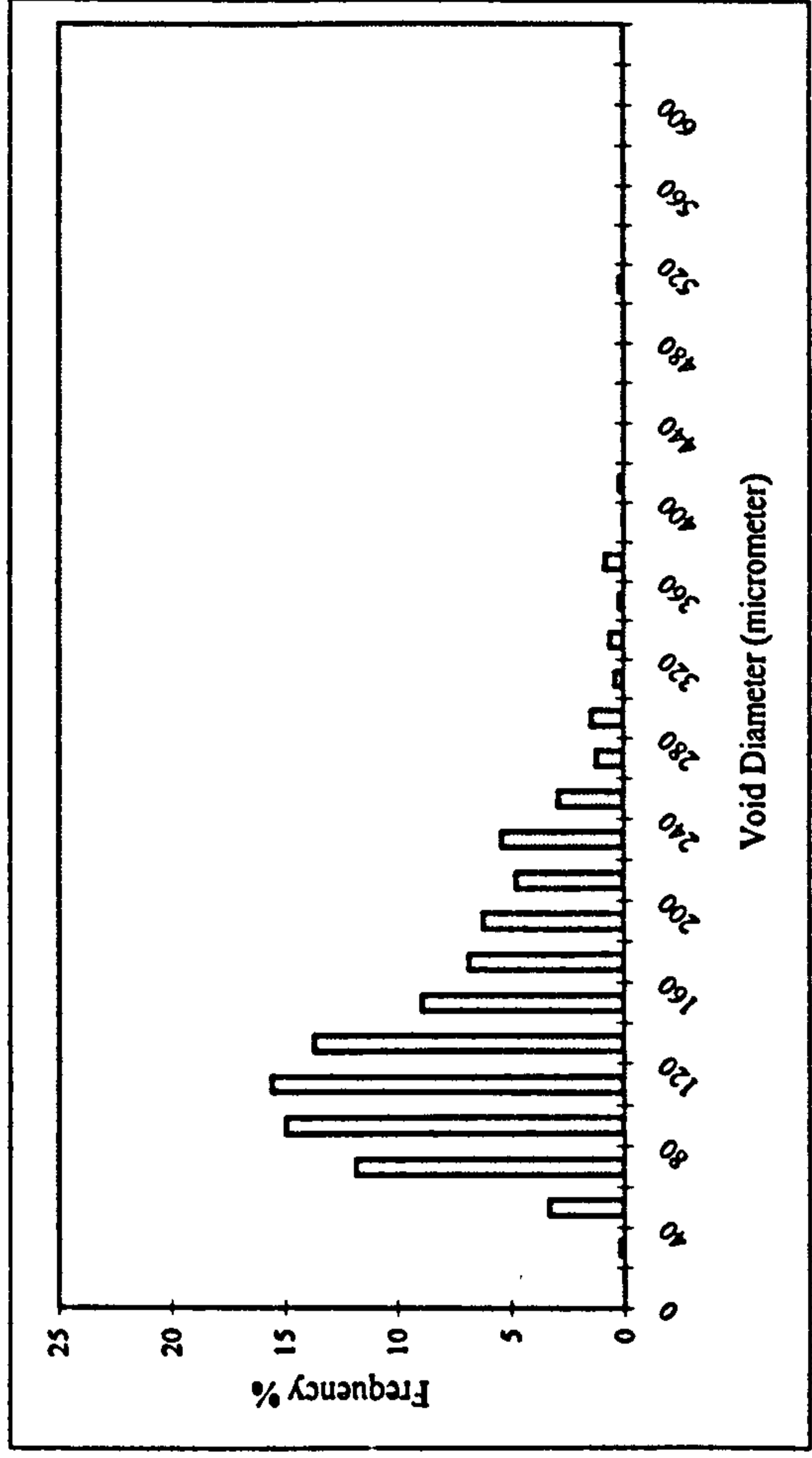
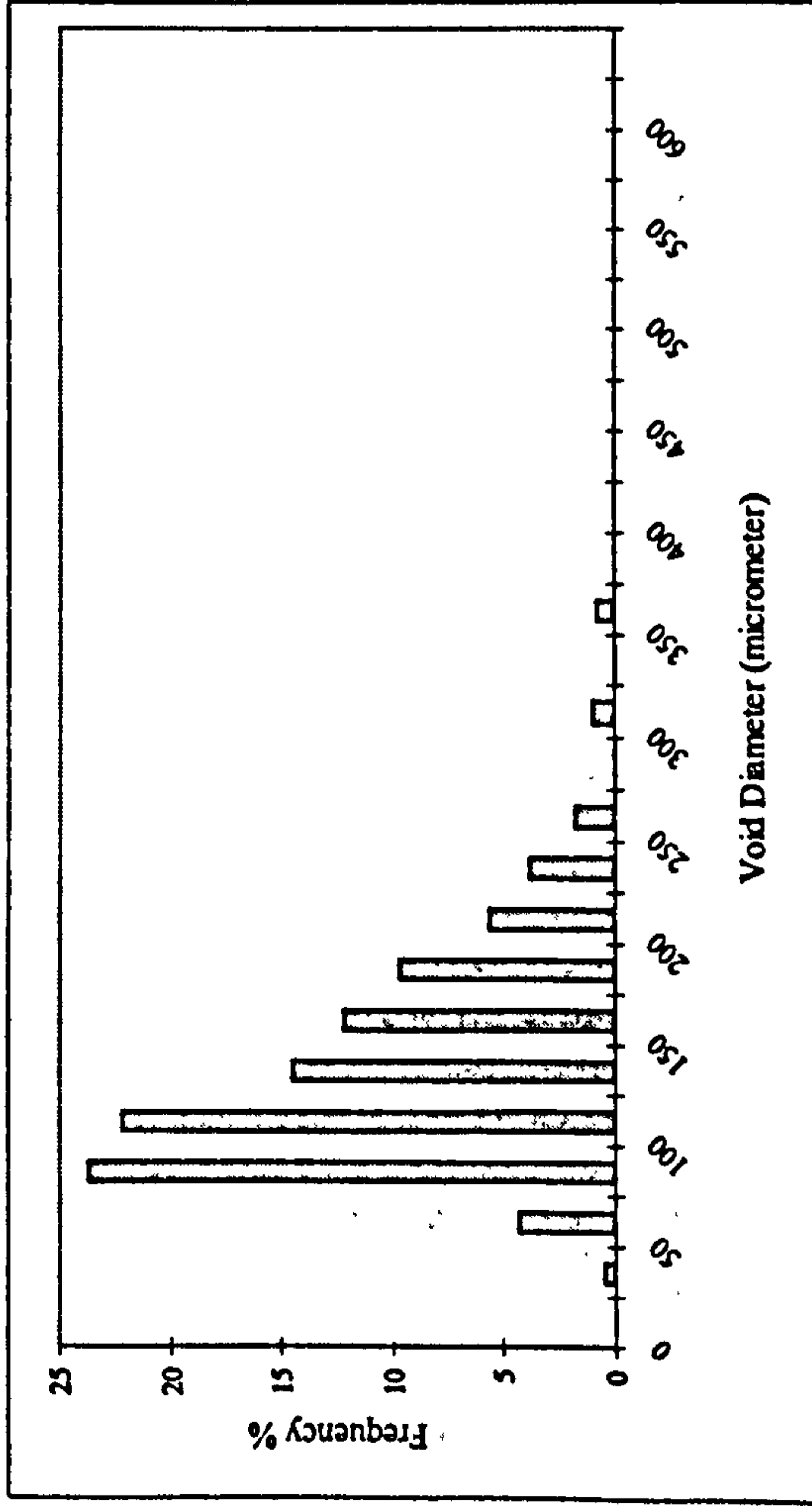
PFA

POZZ-FILL

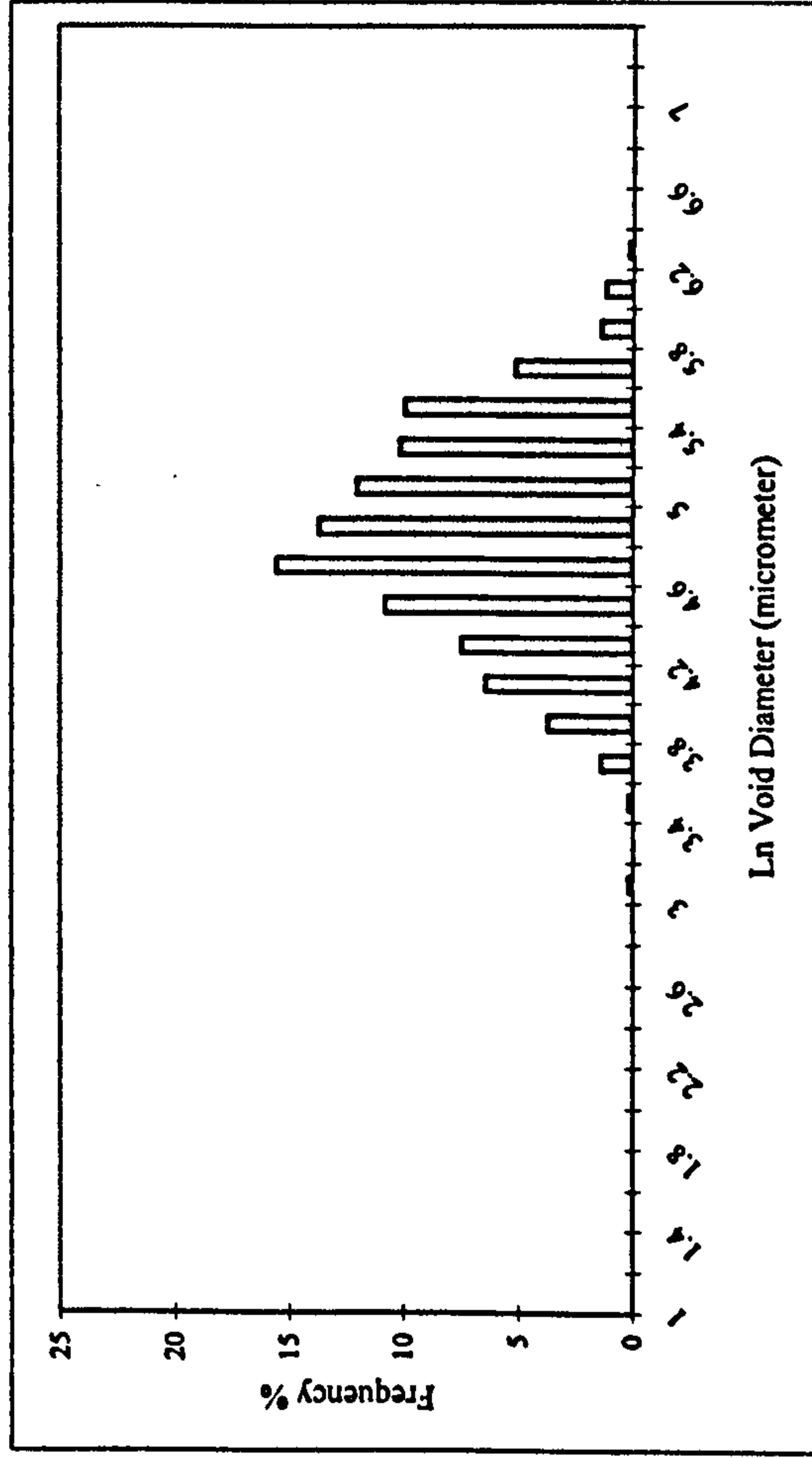
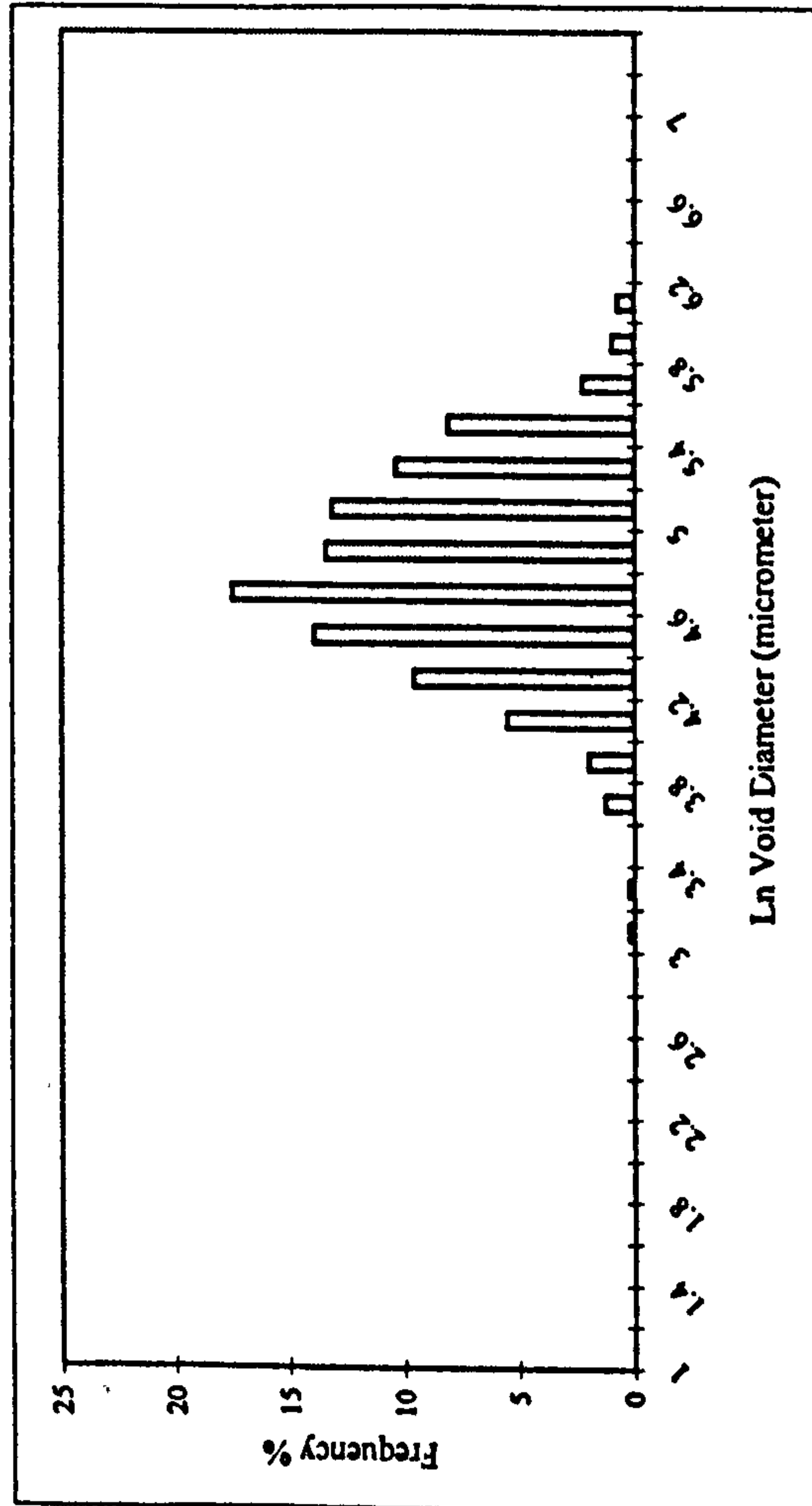


1250 kg/m³ a/c=2

POZZ-FILL



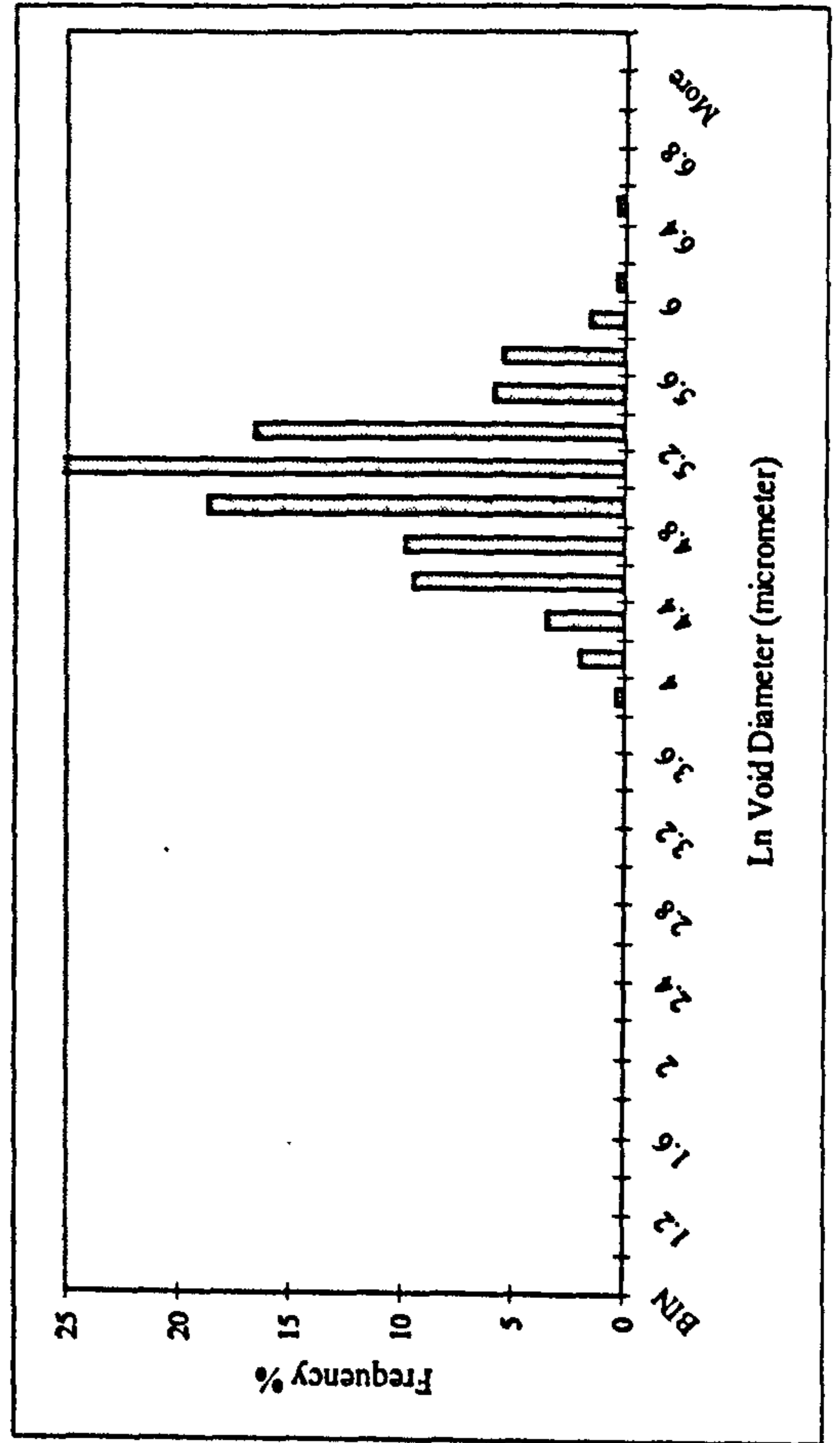
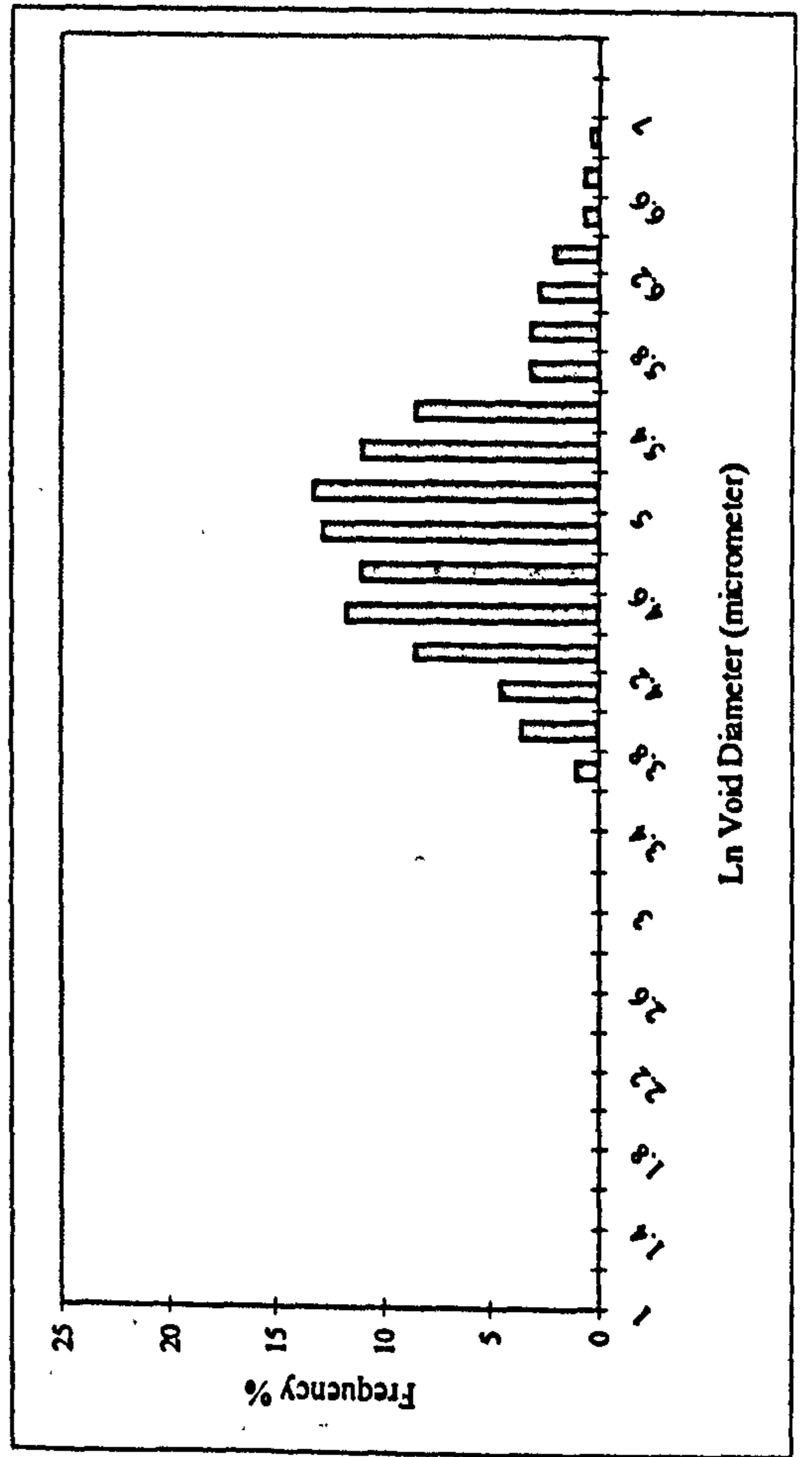
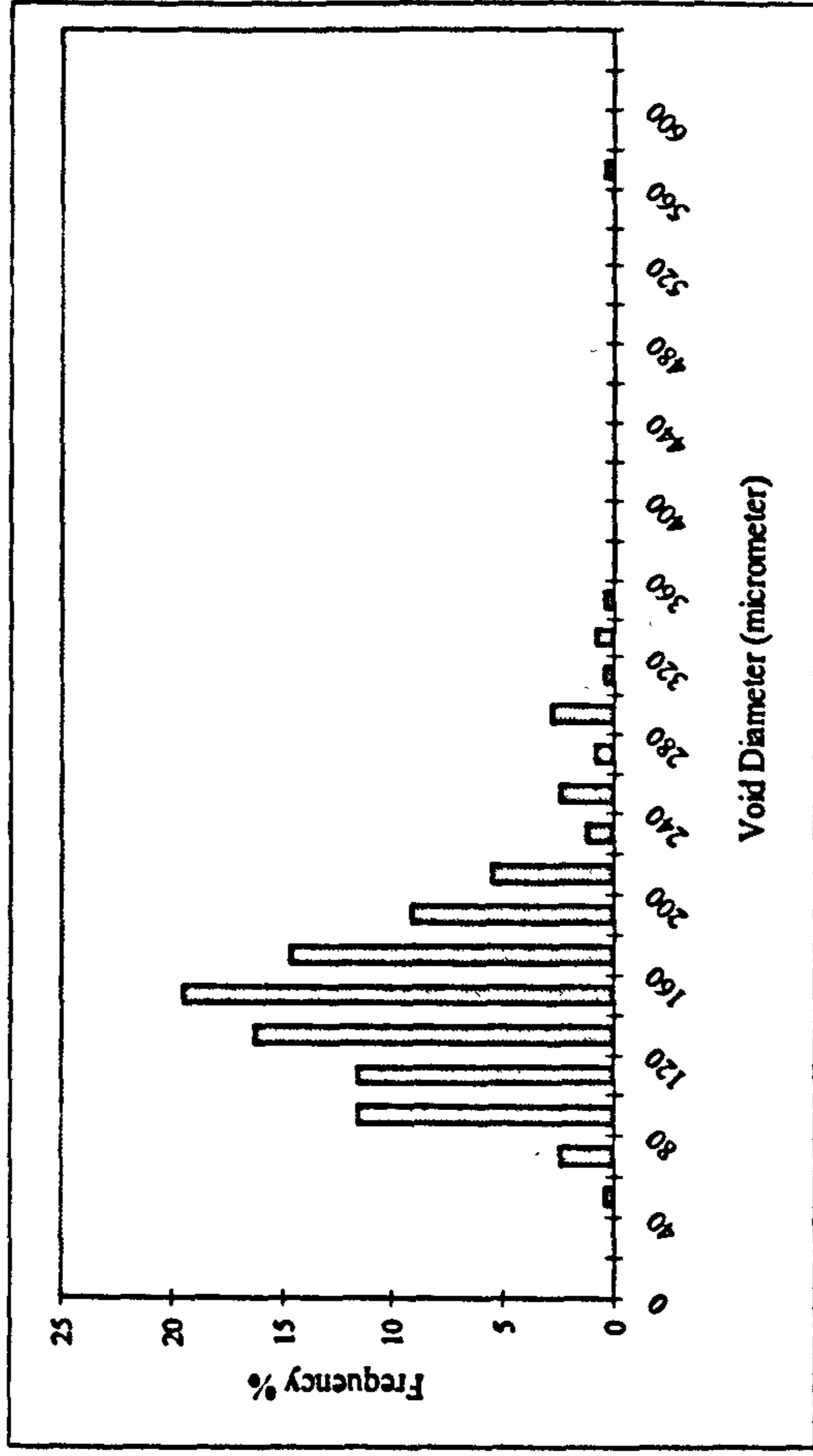
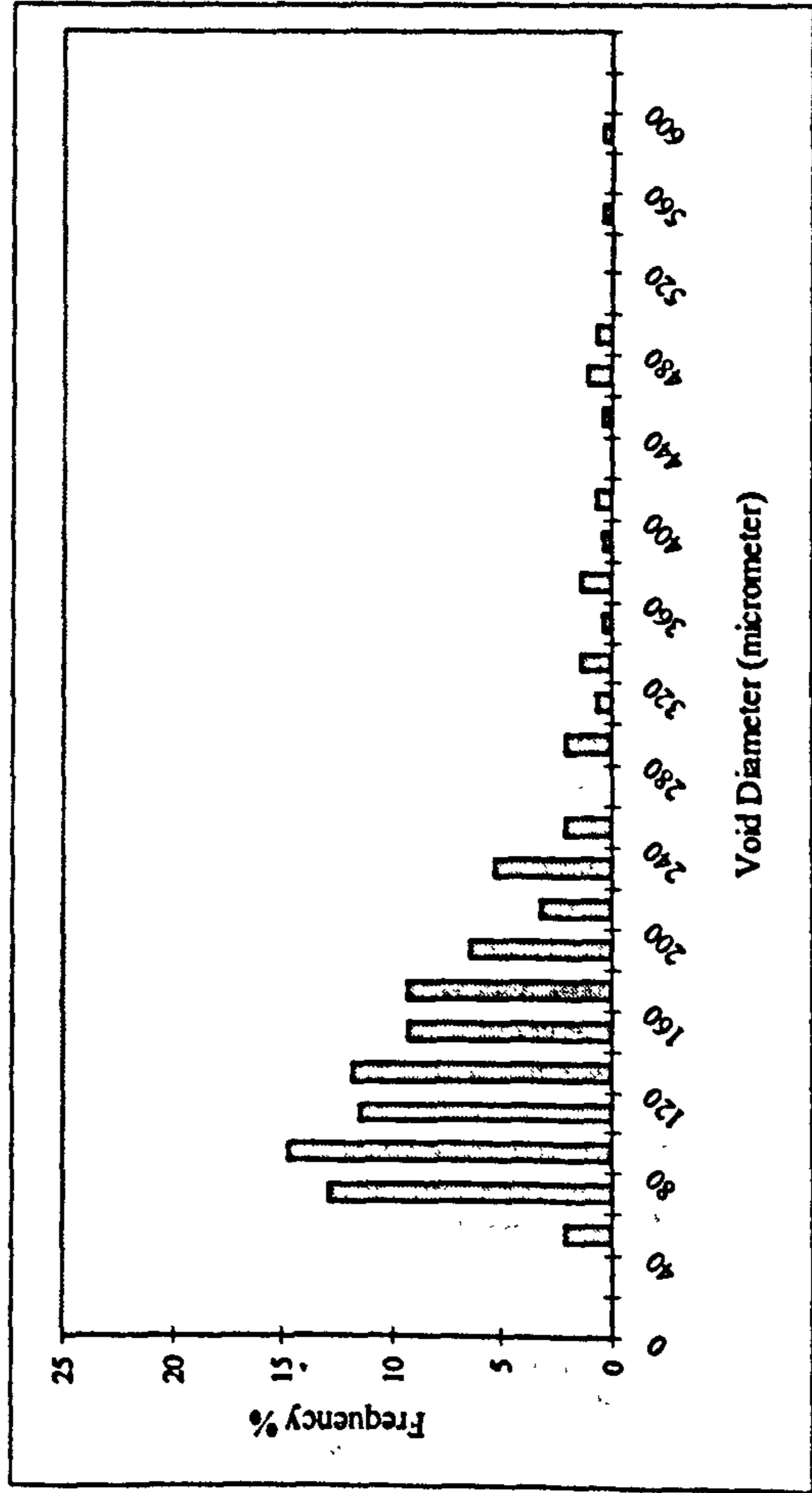
PFA



1250 kg/m³ a/c=3

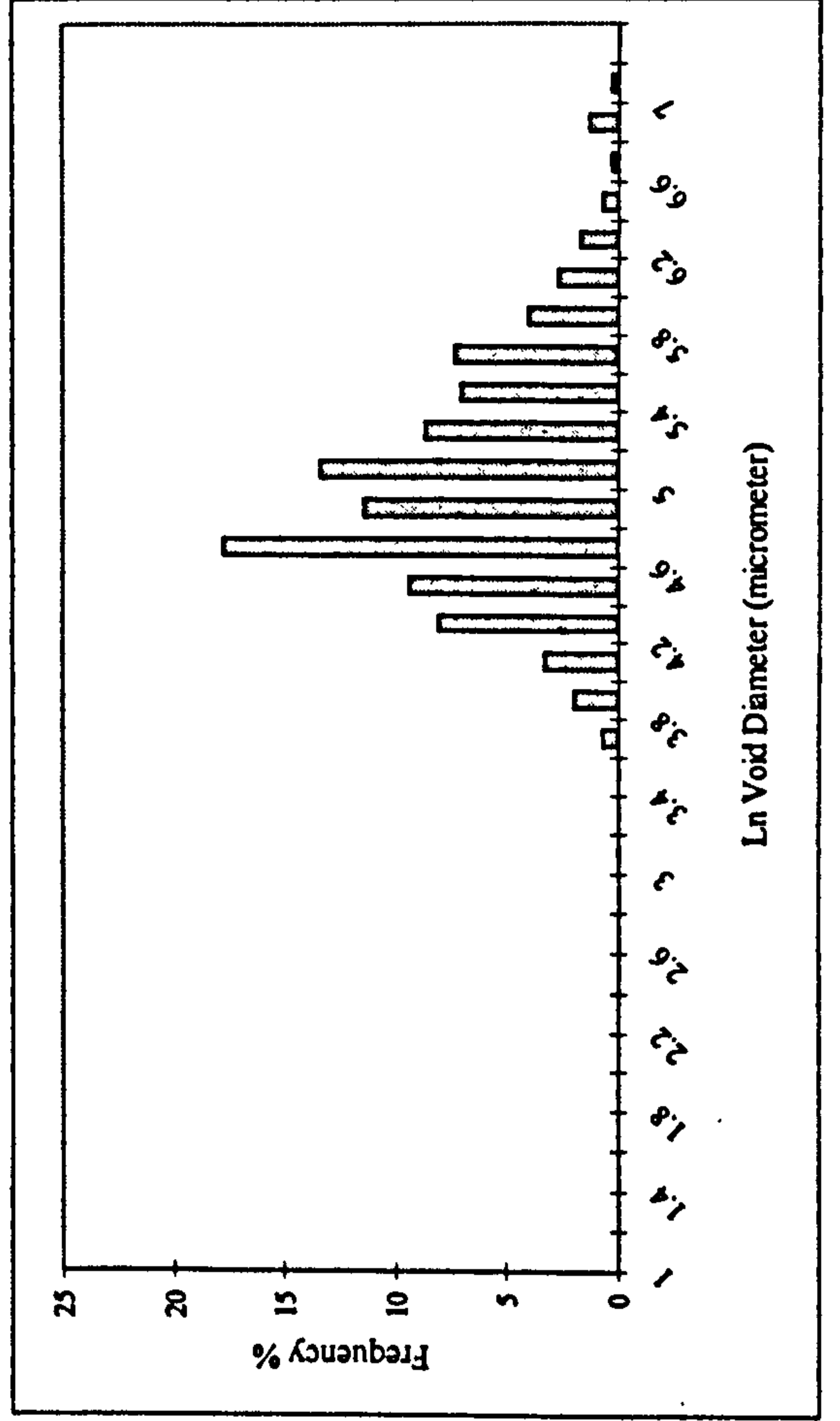
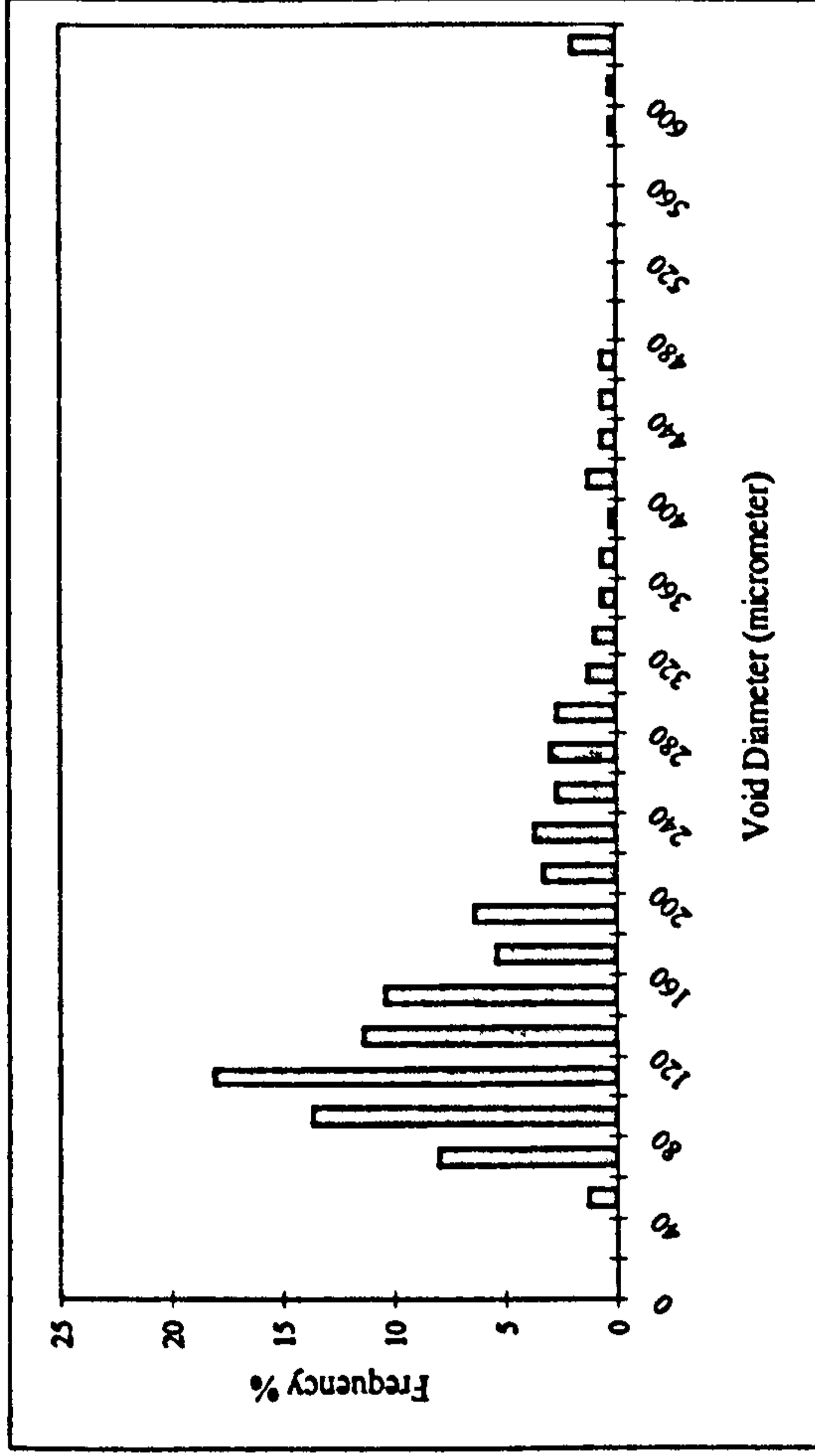
PFA

POZZ-FILL

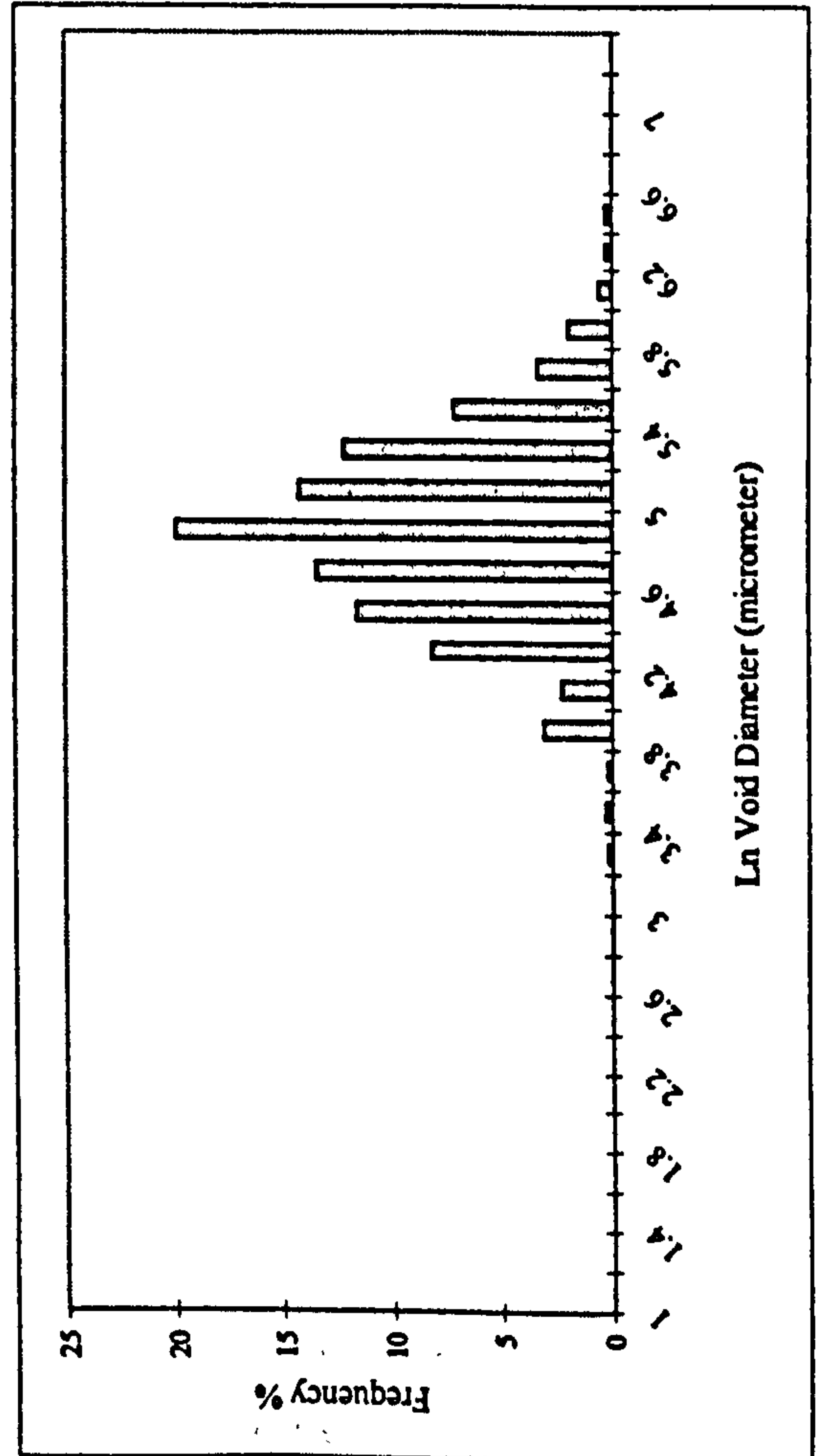
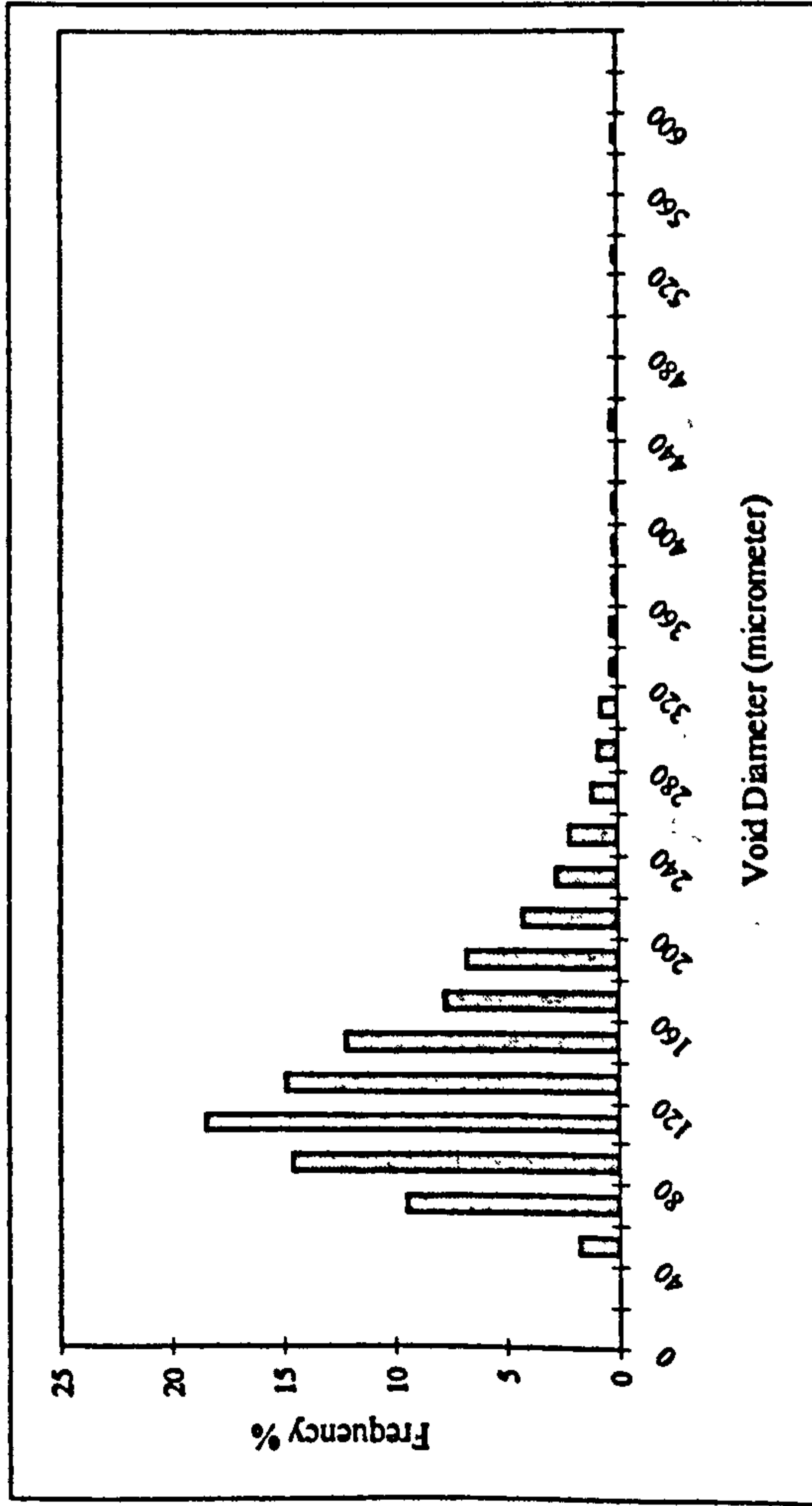


1000 kg/m³ a/c=1

POZZ-FILL



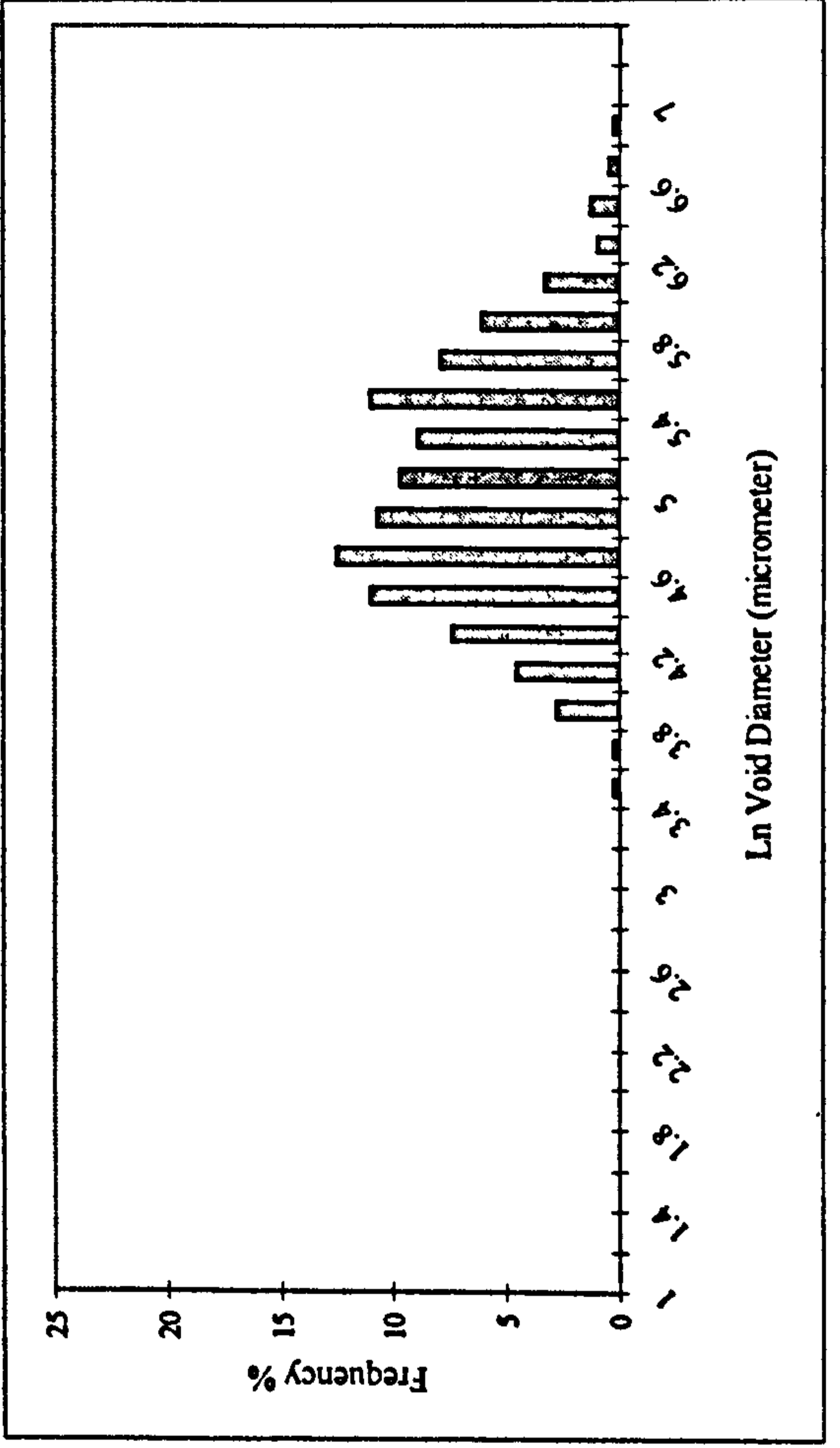
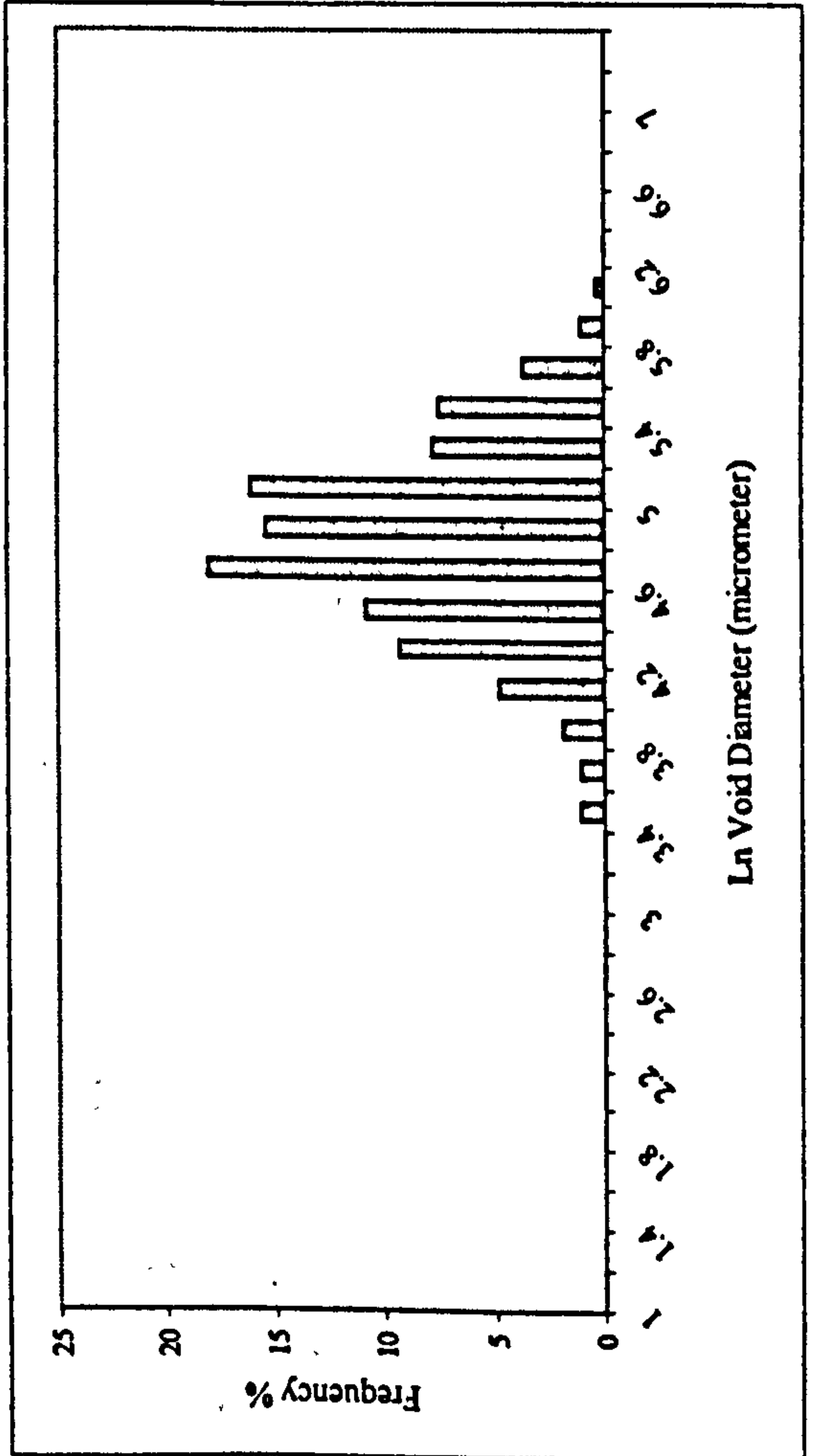
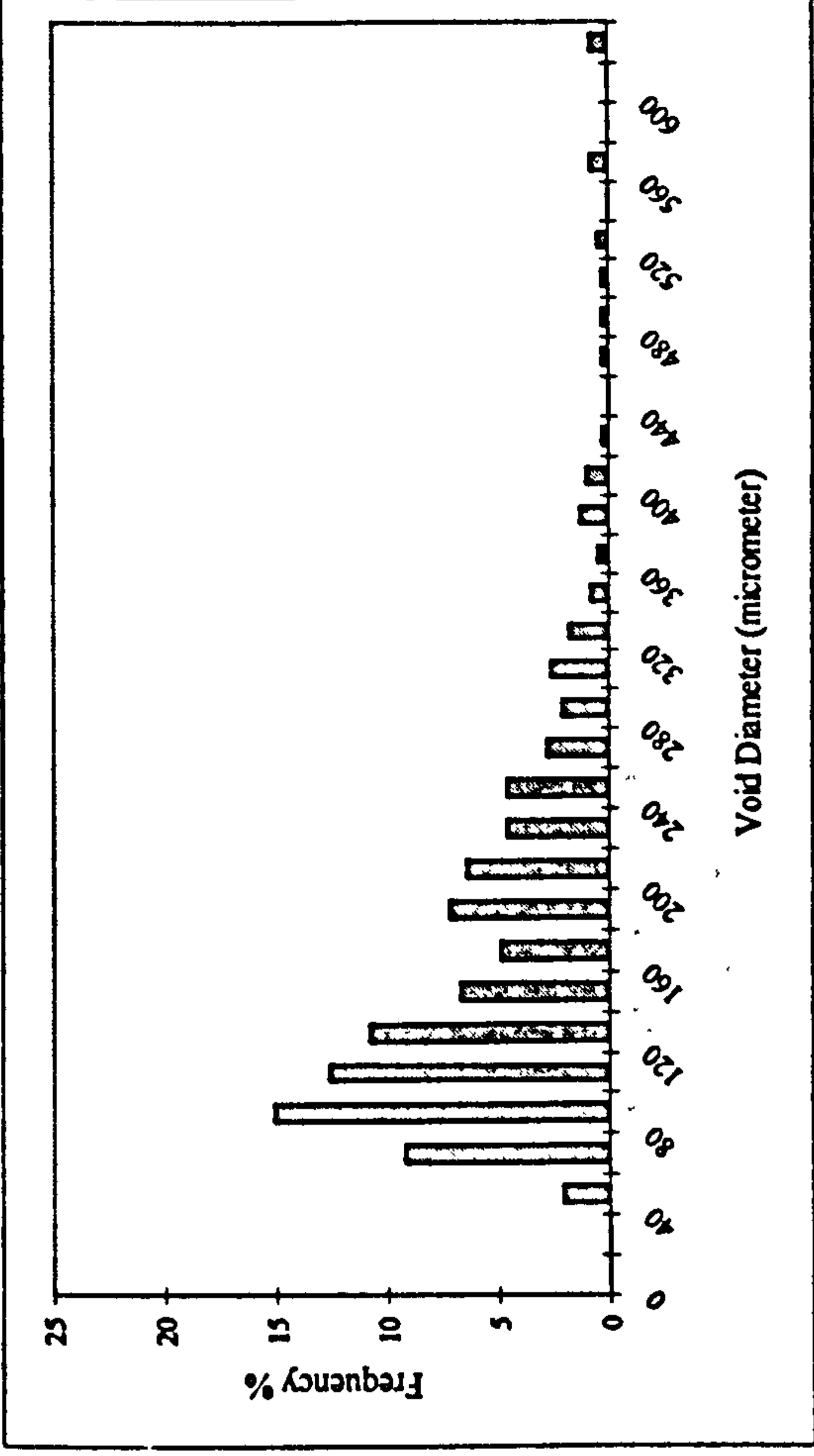
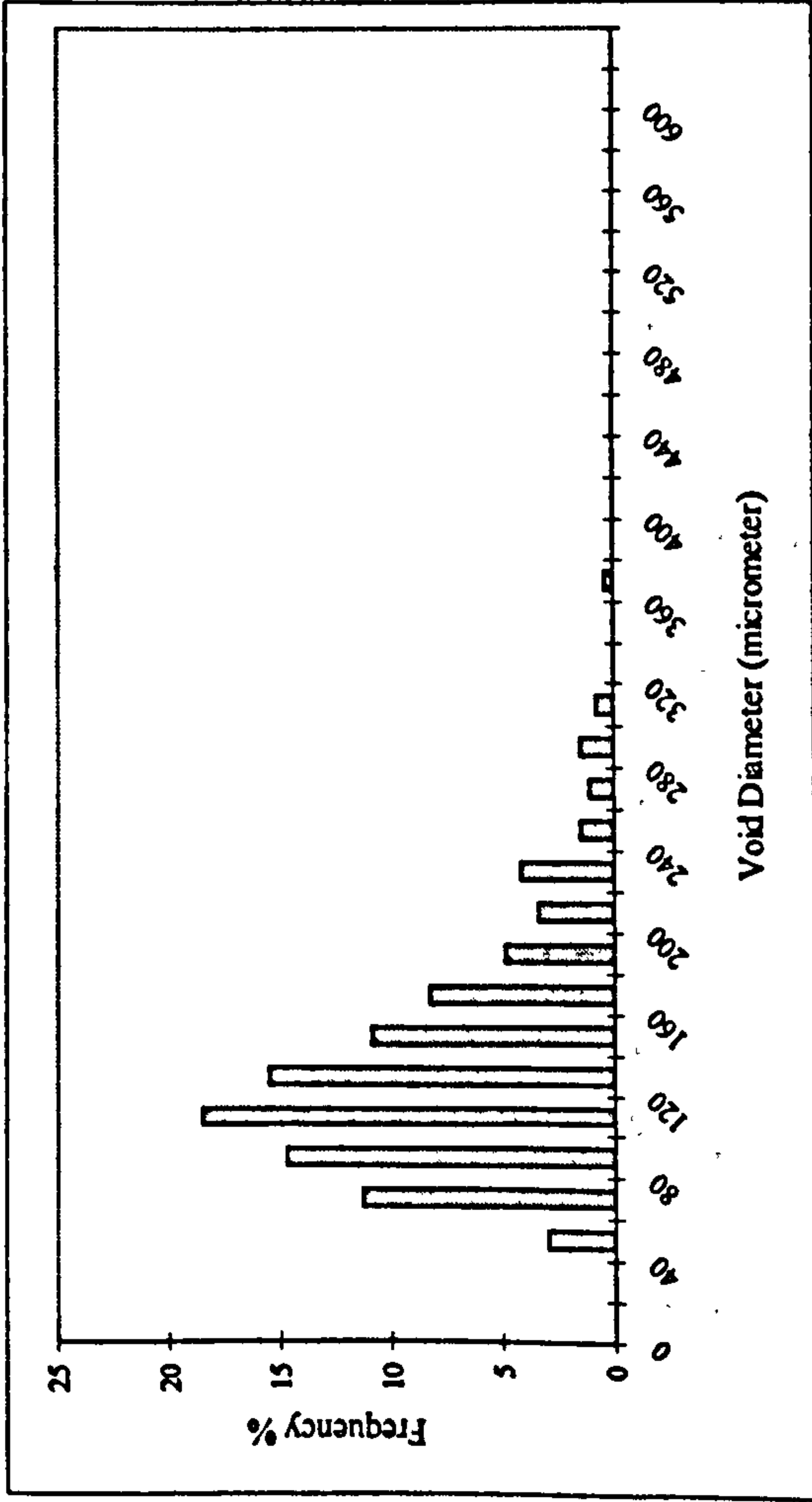
PFA



1000 kg/m³ a/c=2

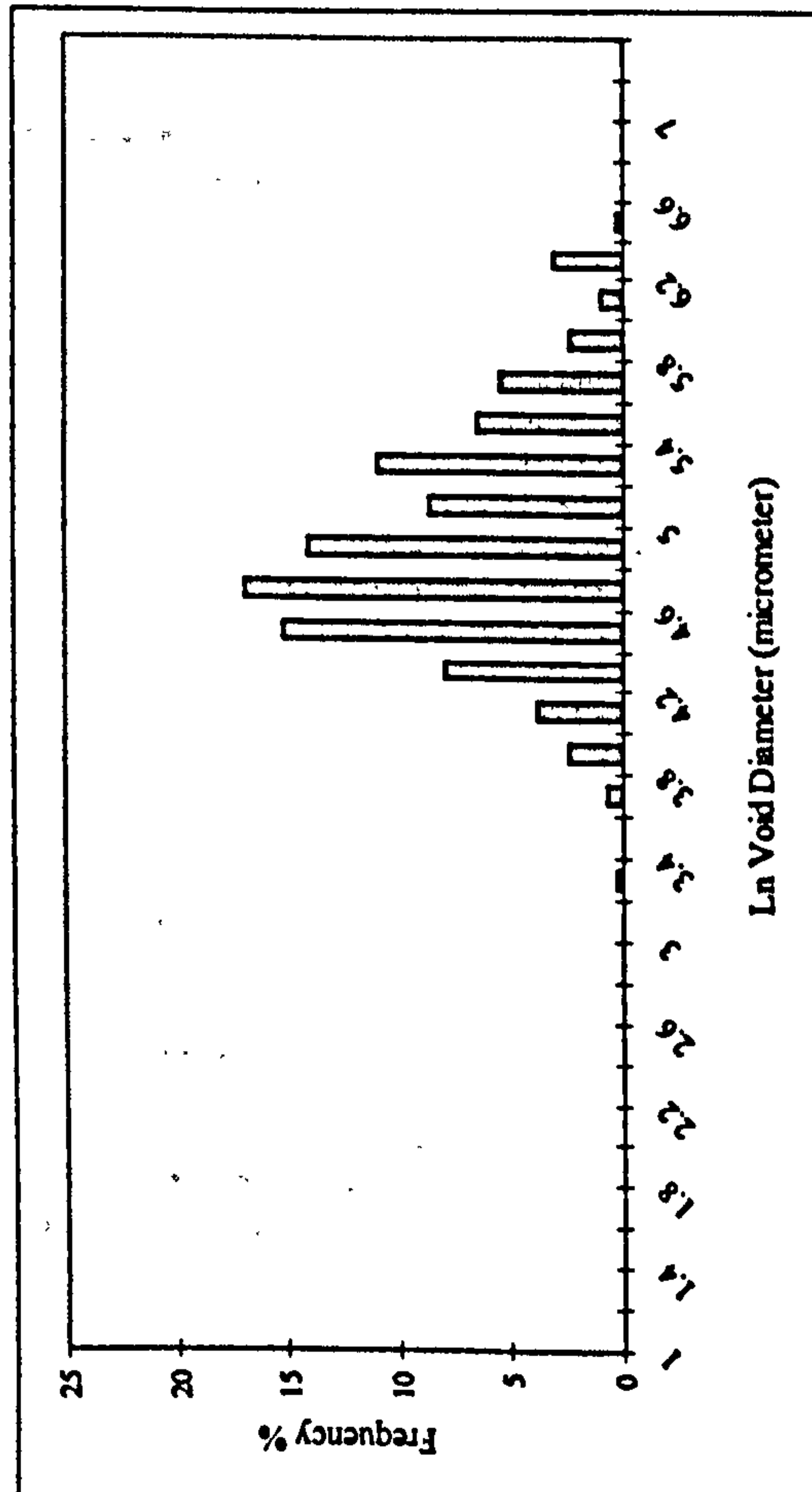
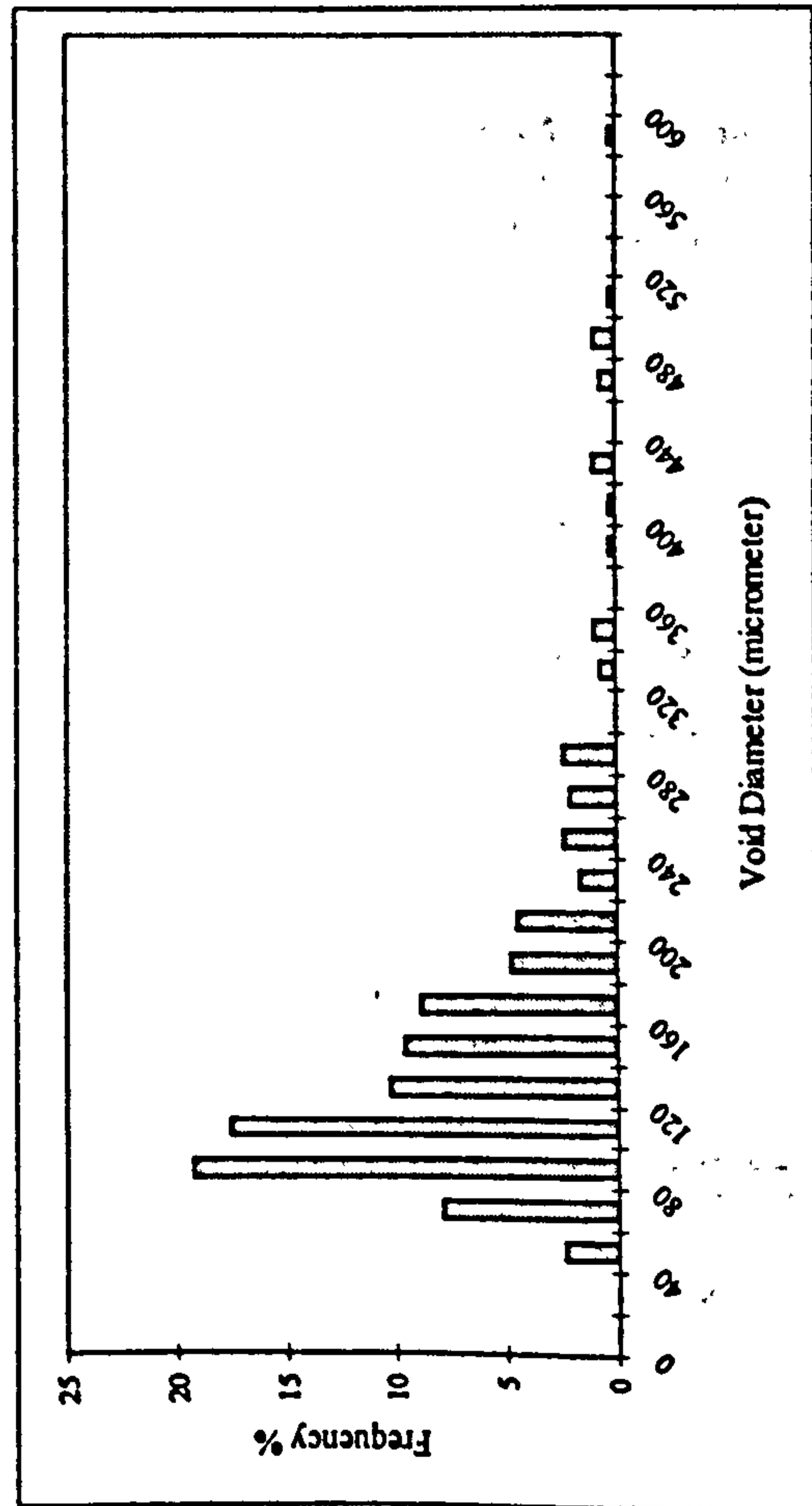
PFA

POZZ-FILL

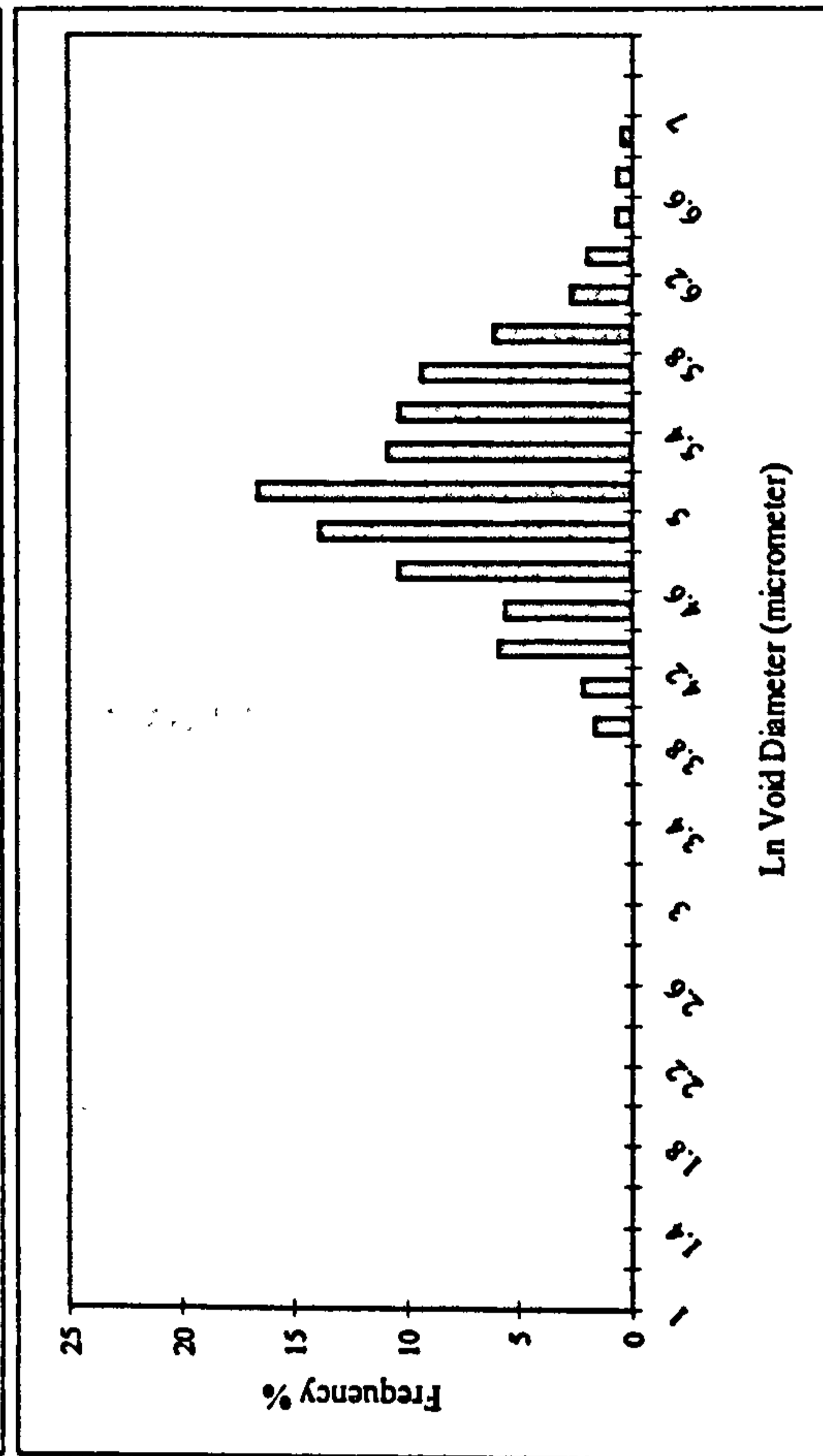
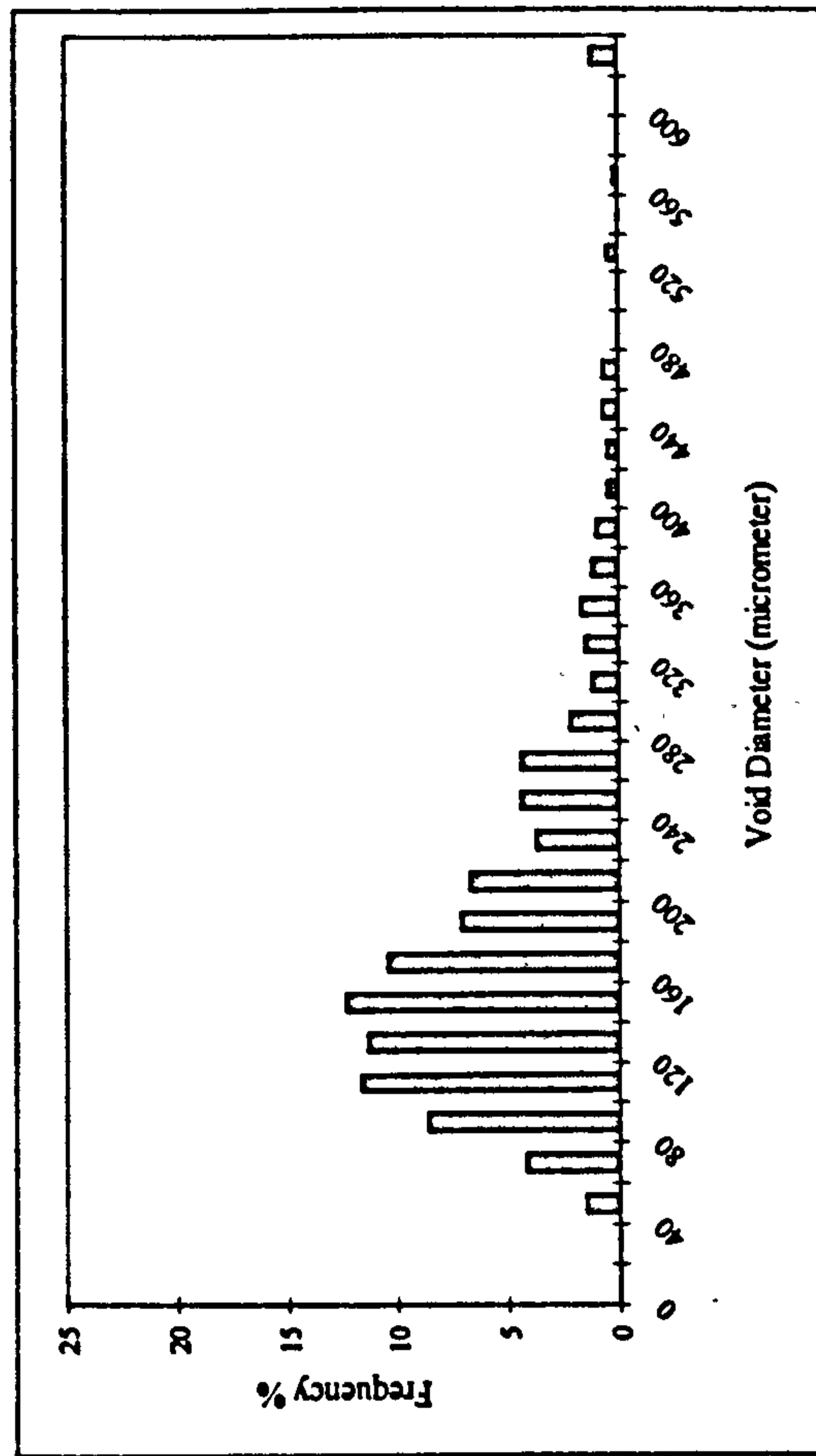


1000 kg/m³ a/c=3

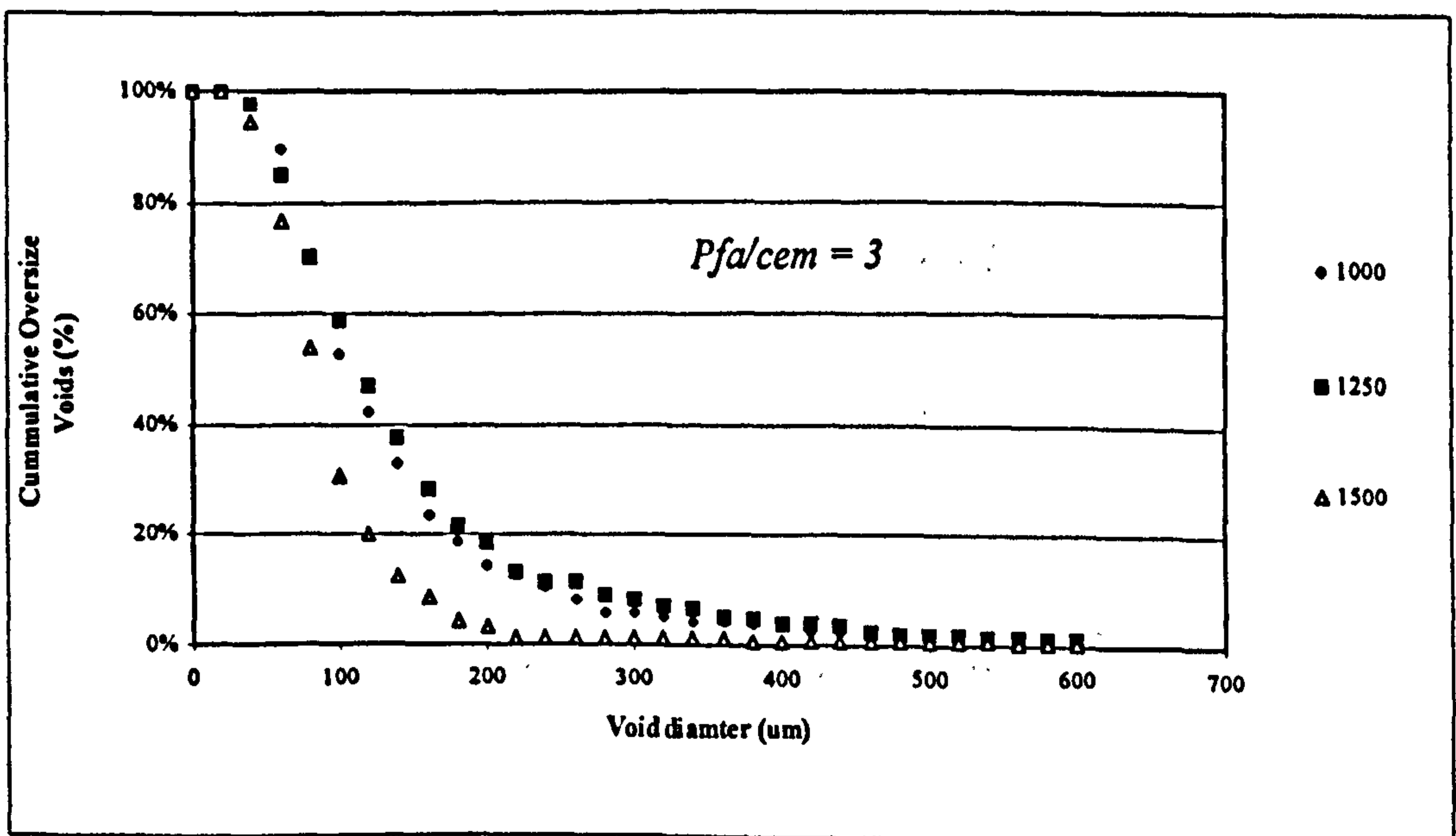
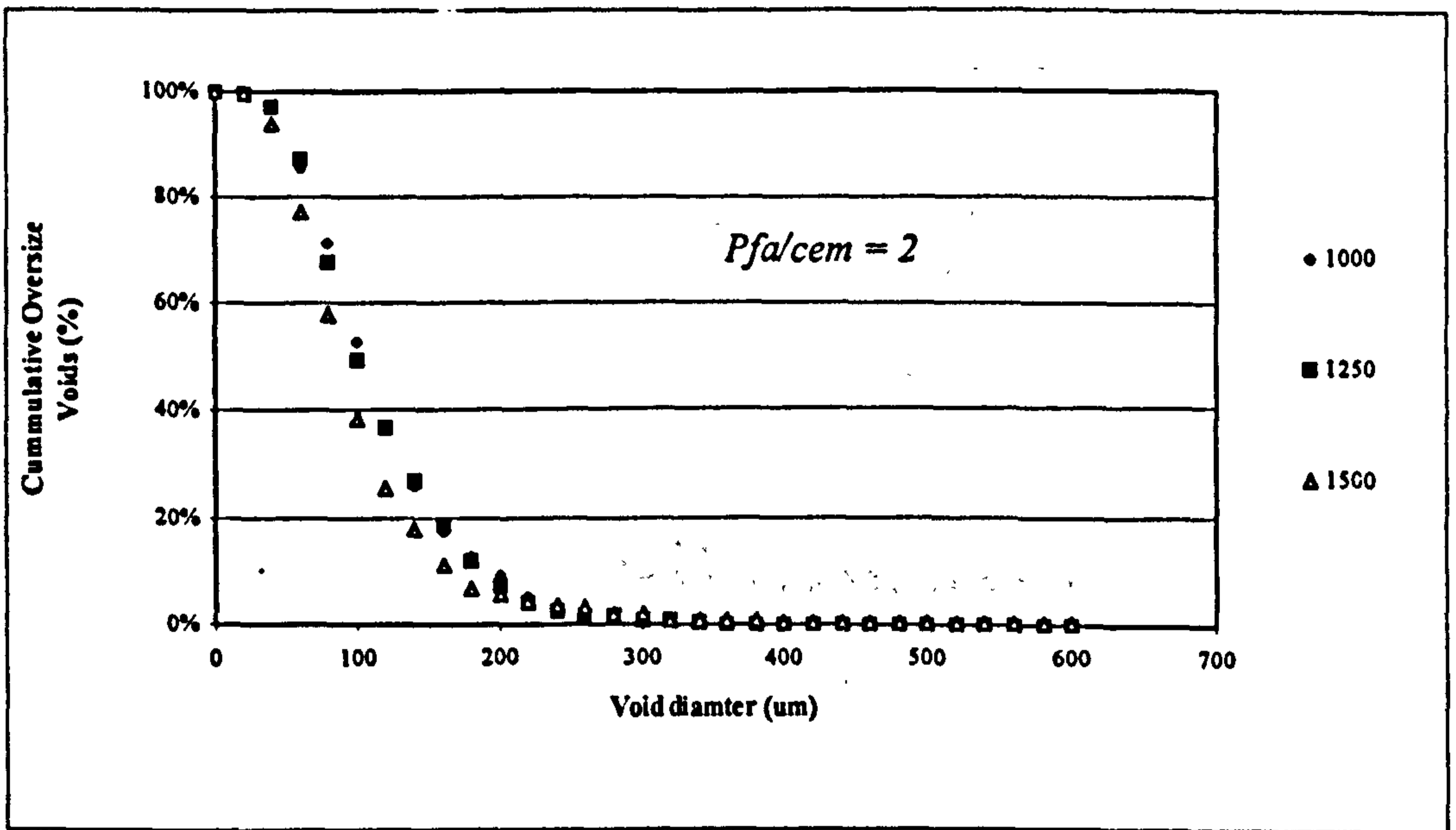
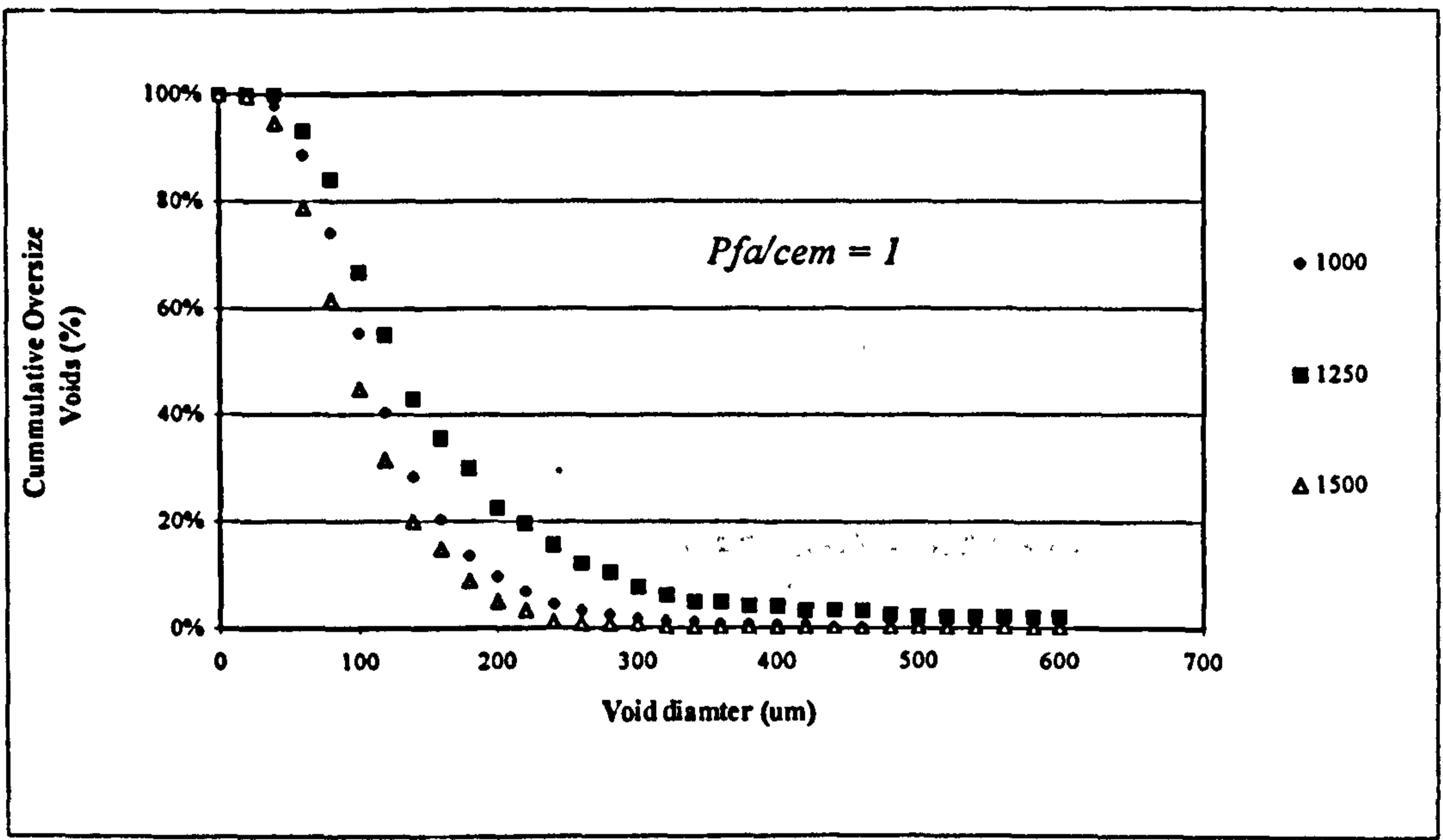
PFA

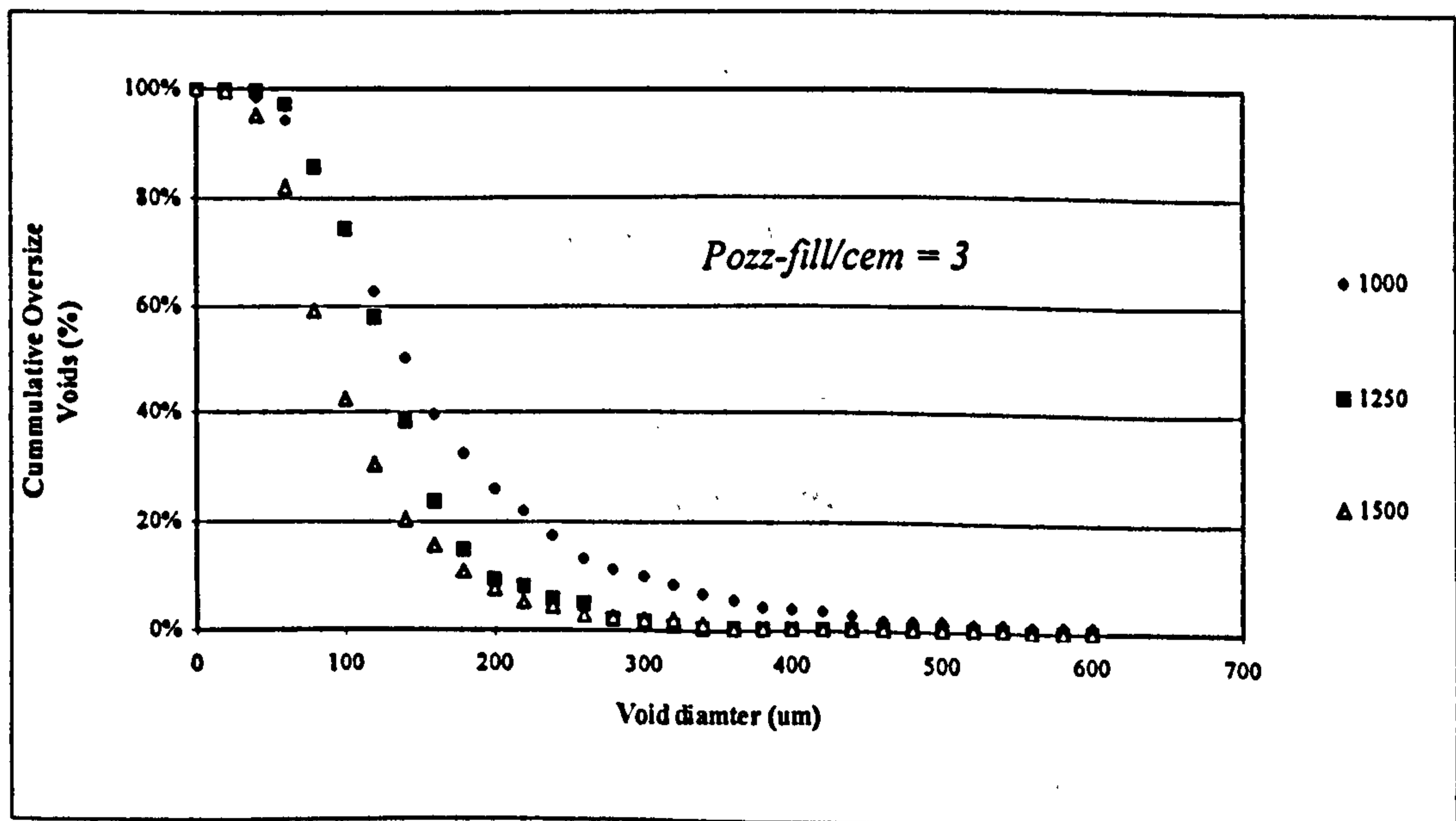
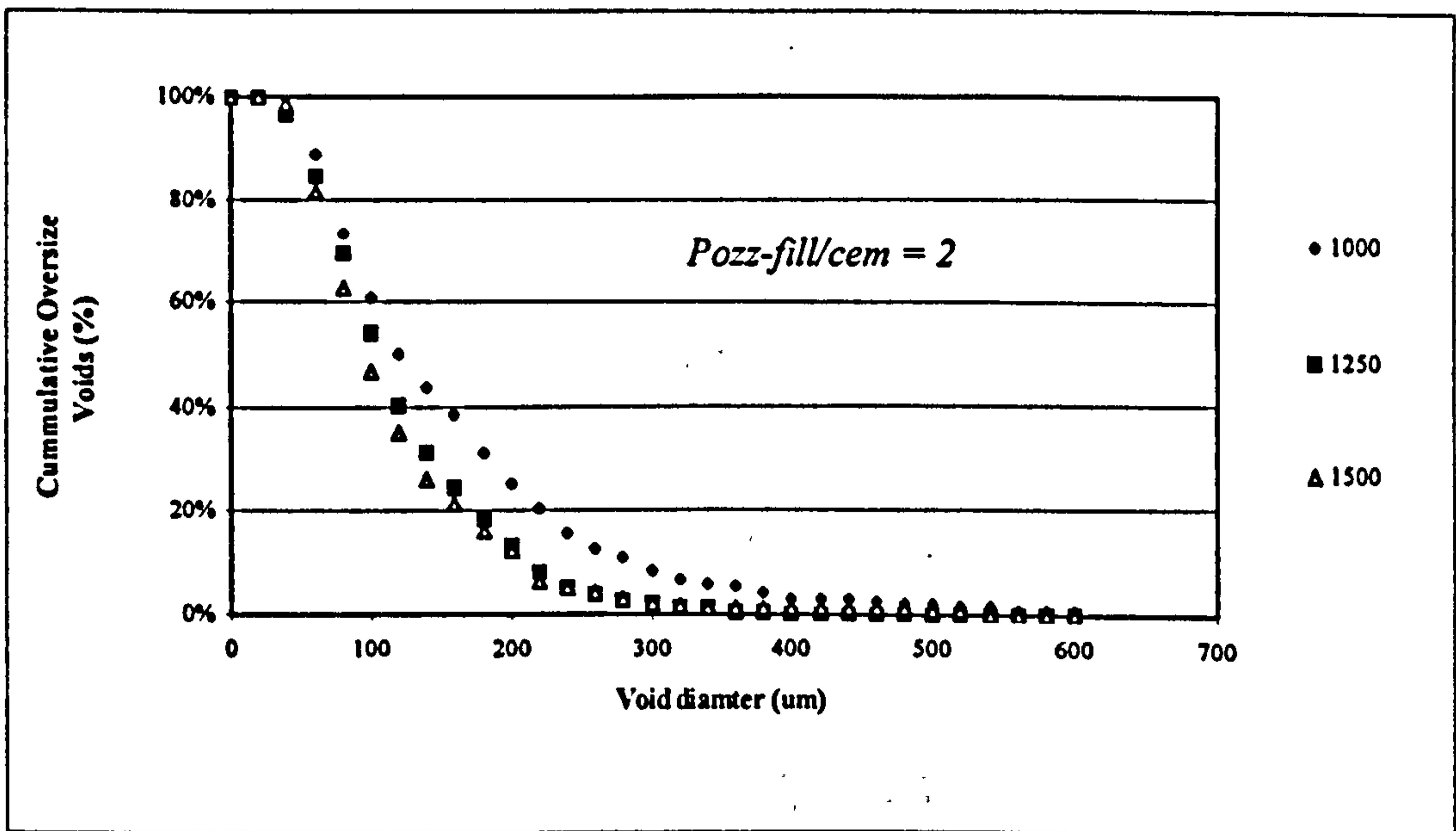
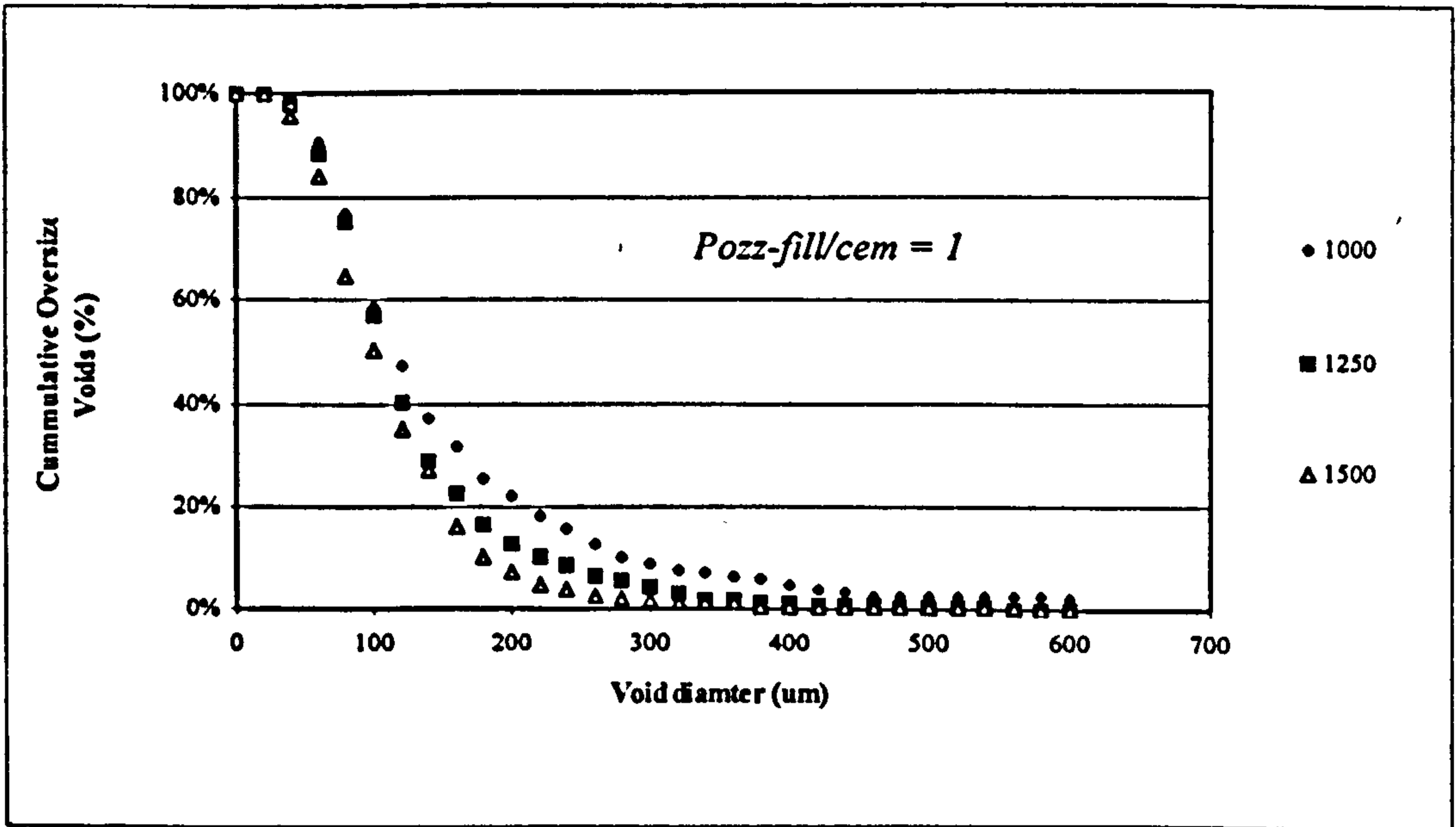


POZZ-FILL



APPENDIX C: CUMULATIVE VOID DIAMETER DISTRIBUTIONS





APPENDIX D: MICROSOFT EXCEL MACRO FOR RECORDING DISTANCES BETWEEN VOIDS

```

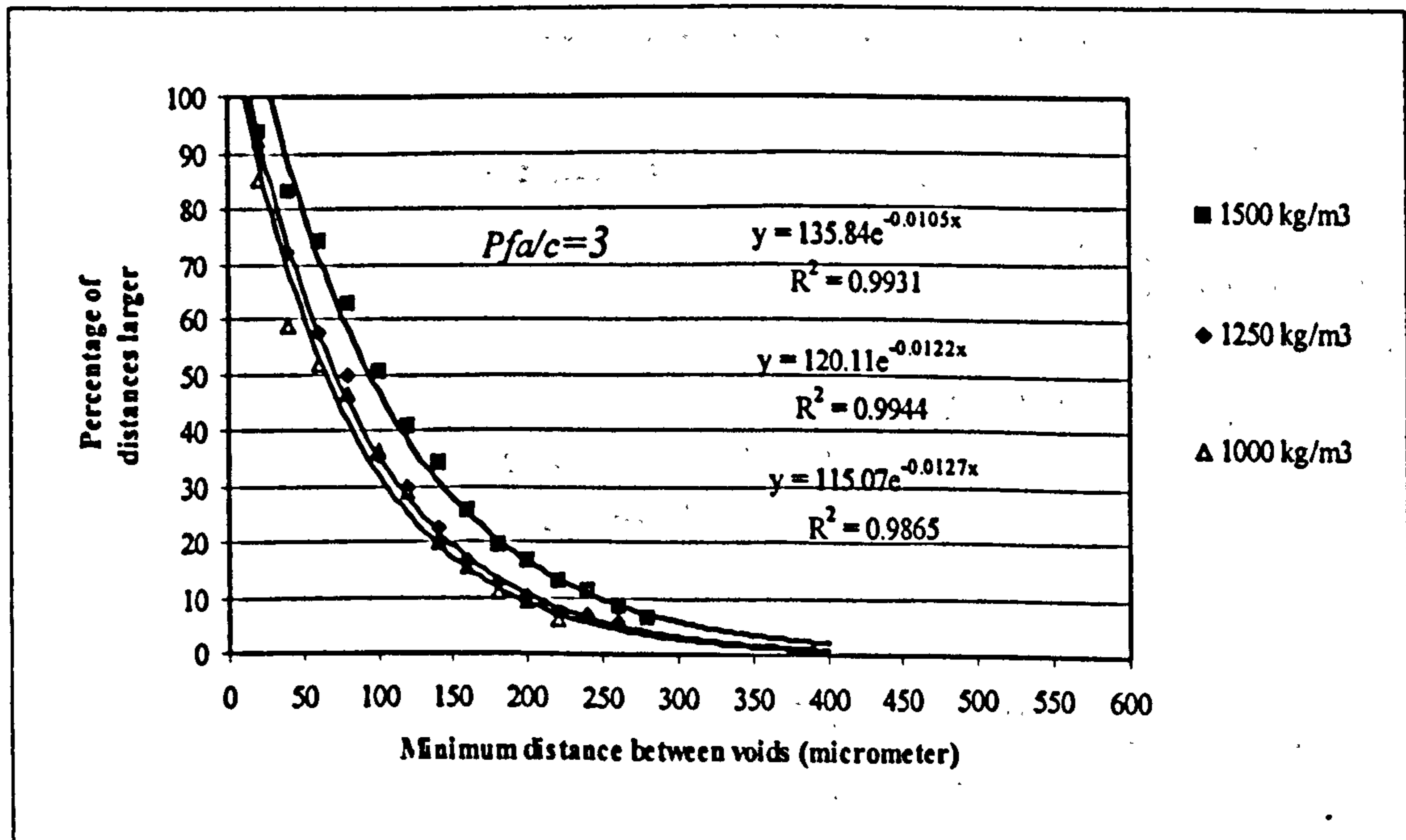
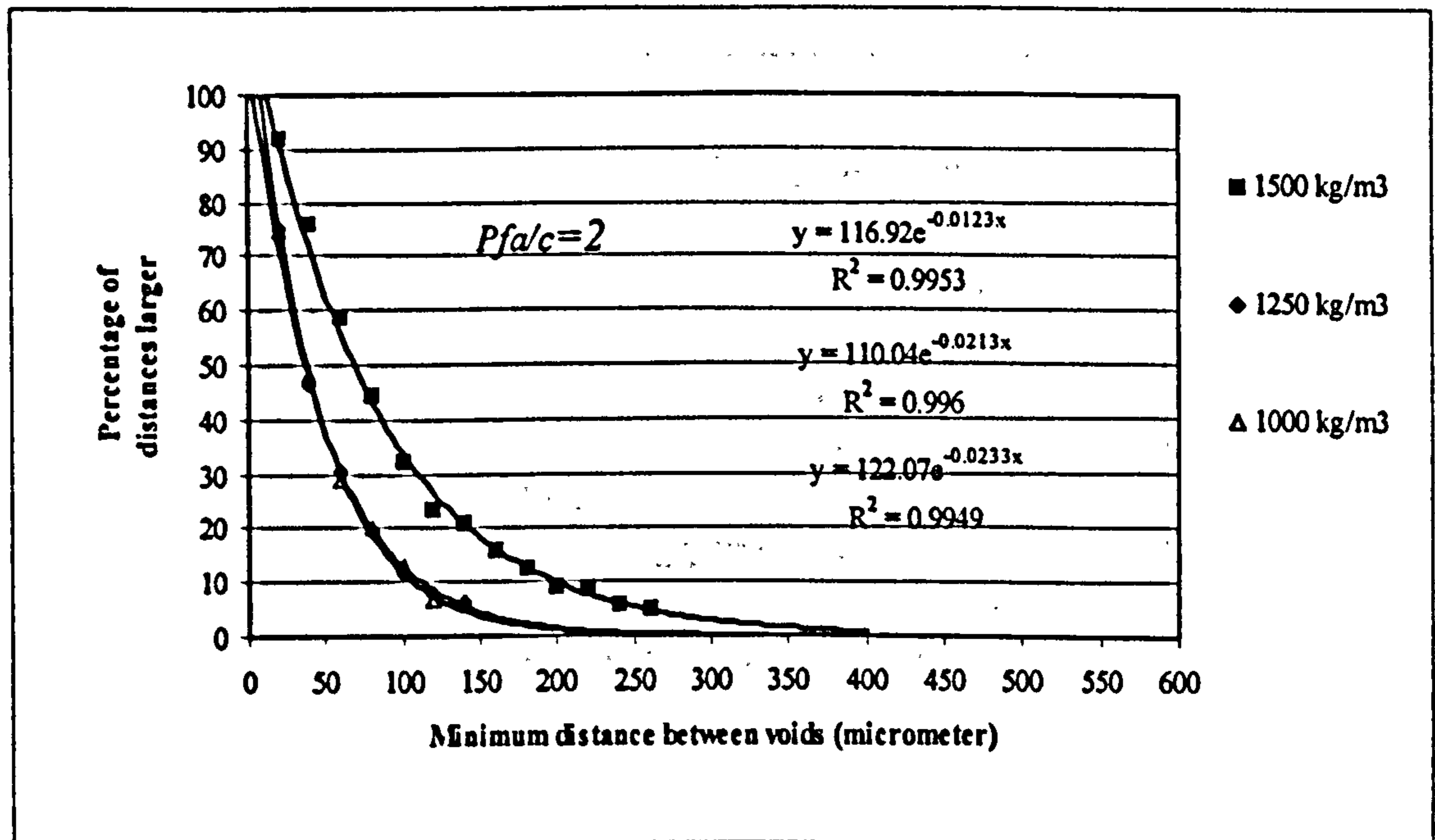
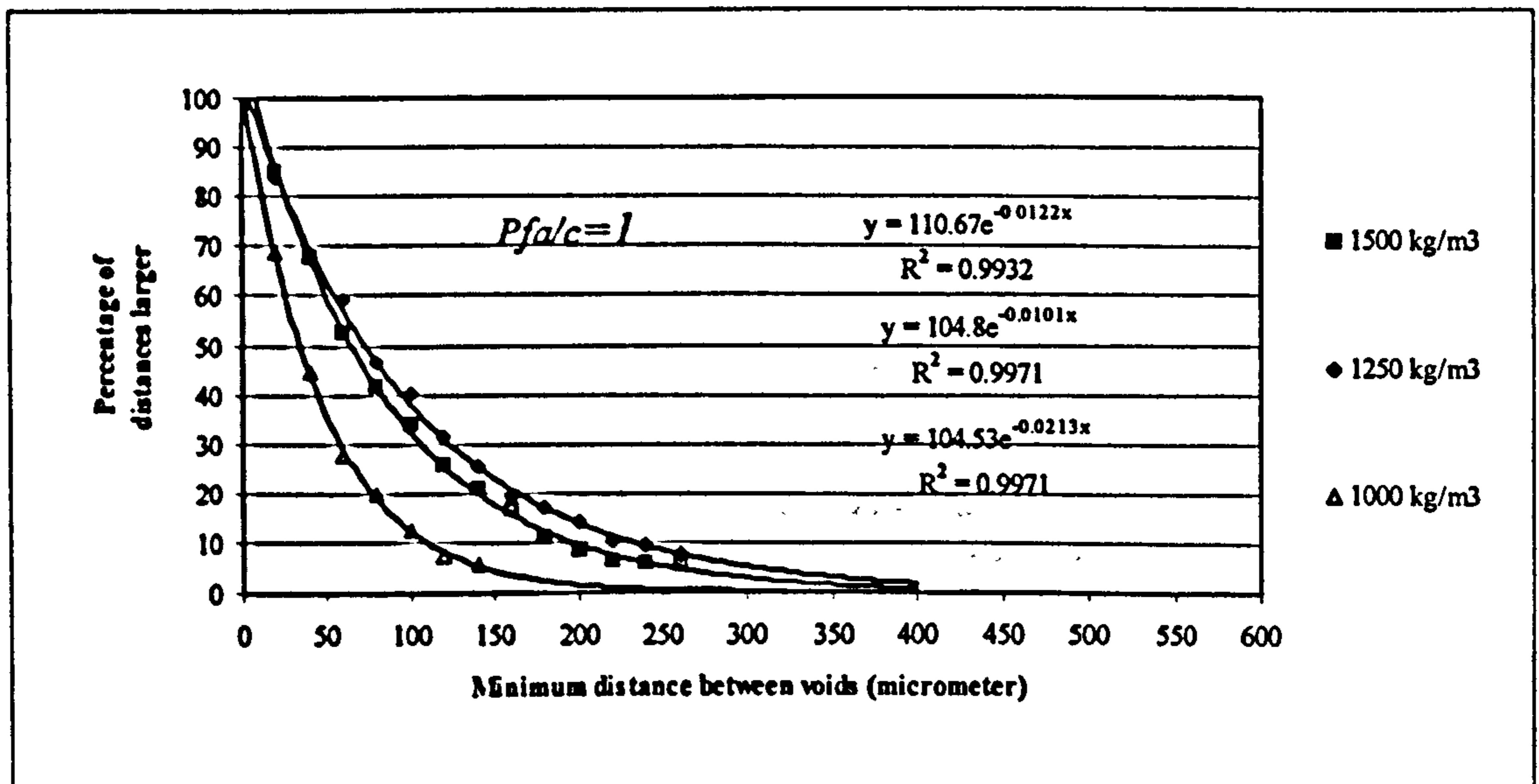
Sub Distance()
'
' distance Macro
' Macro recorded 1999/01/13 by E Kearsley
'

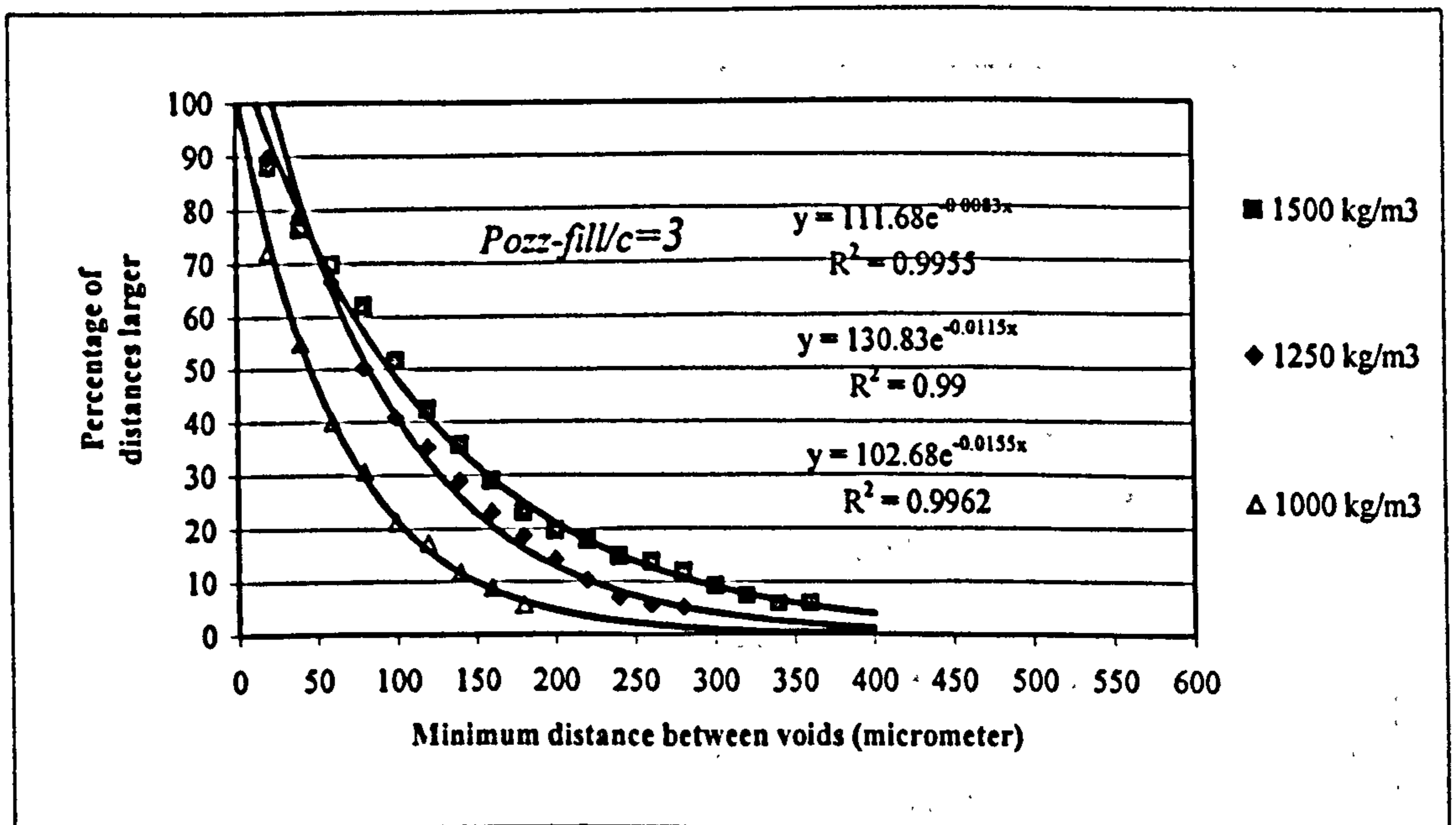
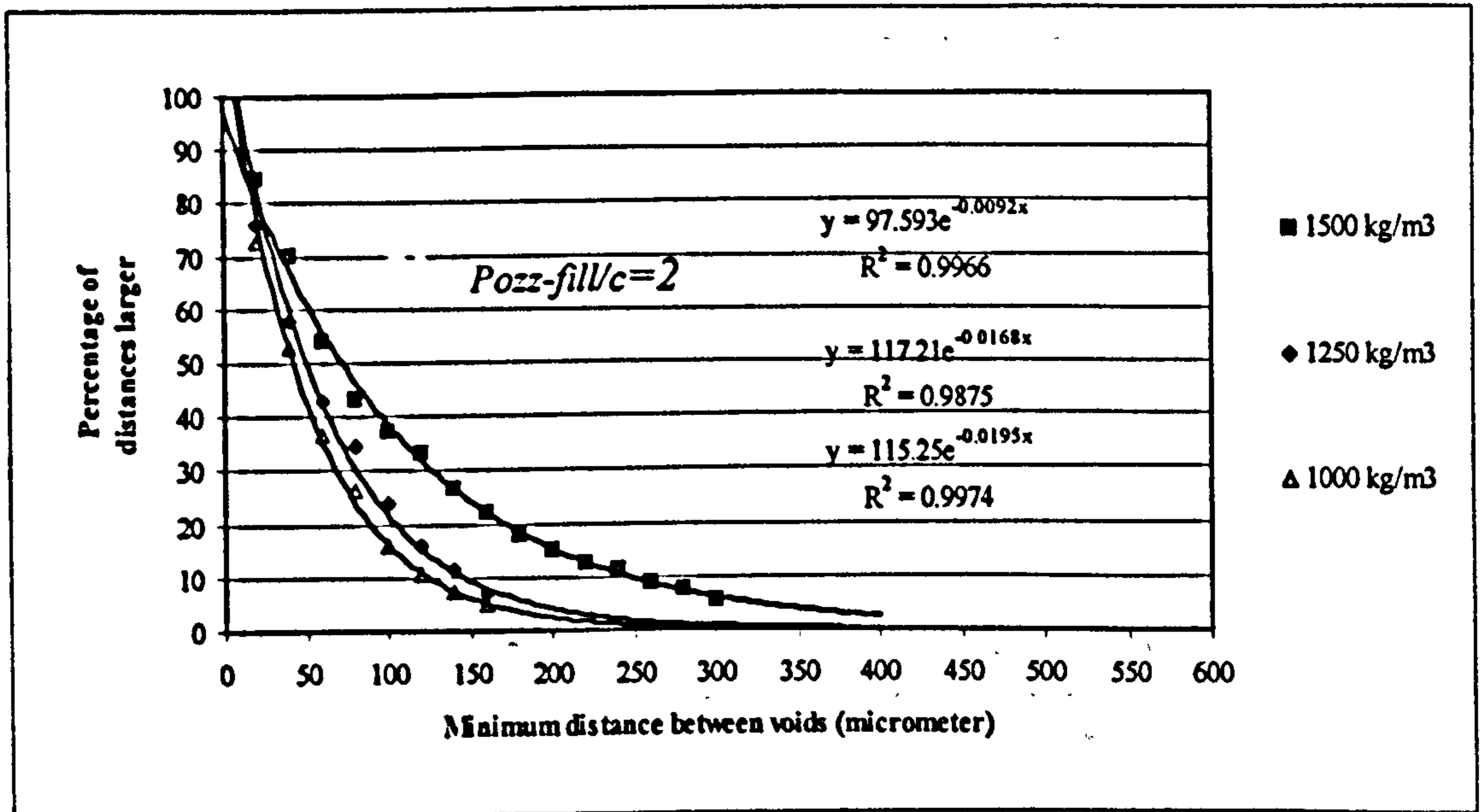
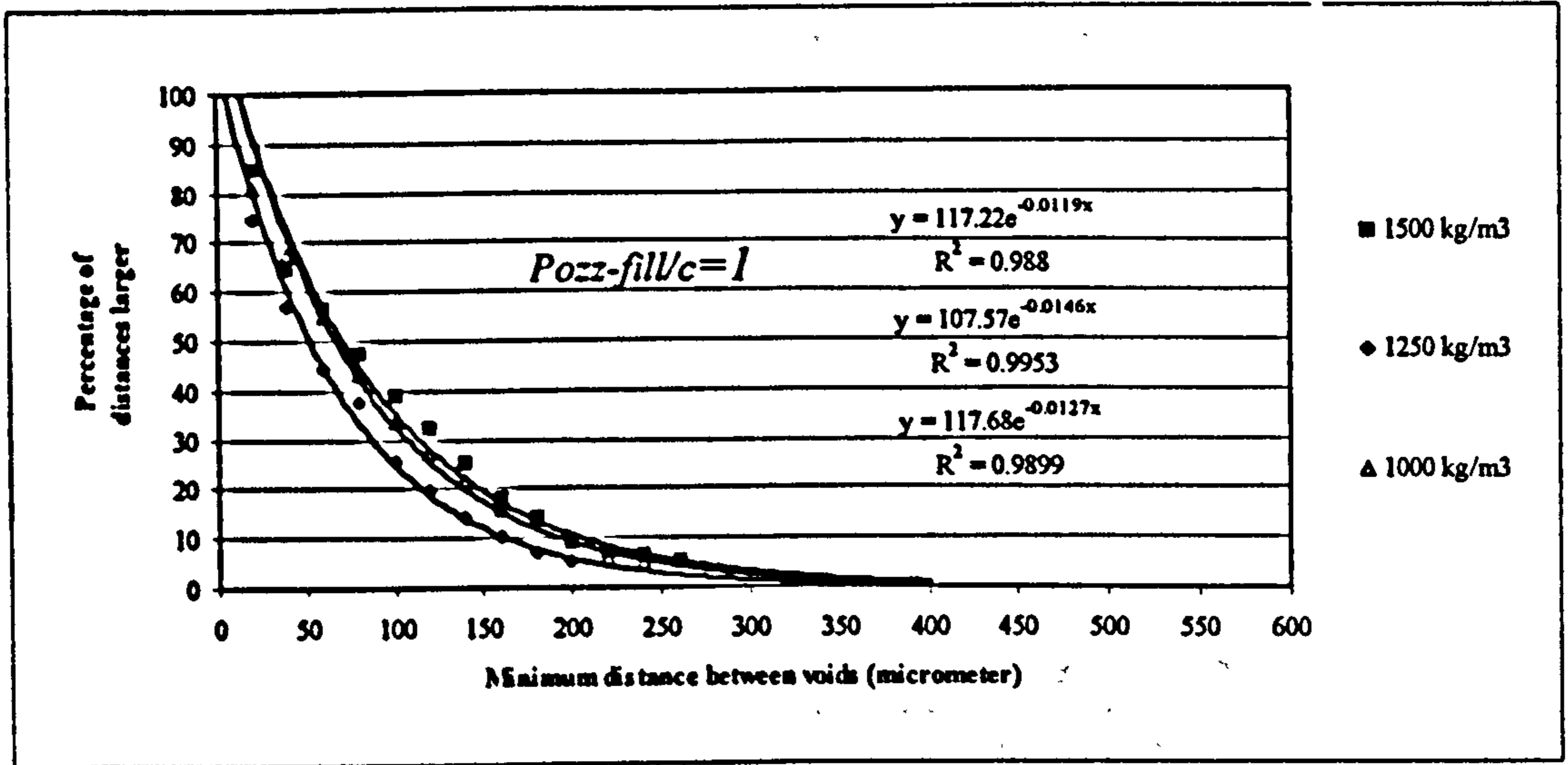
nr = ActiveCell.Value
While nr > 0
For i = 1 To nr
    ActiveCell.Offset(i - 1, 3).Range("A1").Select
    xcord = ActiveCell.Value
    ActiveCell.Offset(0, 1).Range("A1").Select
    ycord = ActiveCell.Value
    ActiveCell.Offset(0, 7).Range("A1").Select
    zcord = ActiveCell.Value
    ActiveCell.Offset(1 - i, 3).Range("A1").Select
    ss = 1000
    For n = 1 To nr
        ActiveCell.Offset(n - 1, -11).Range("A1").Select
        xx = ActiveCell.Value
        ActiveCell.Offset(0, 1).Range("A1").Select
        yy = ActiveCell.Value
        ActiveCell.Offset(0, 7).Range("A1").Select
        zz = ActiveCell.Value
        ActiveCell.Offset(-n + 1, 3).Range("A1").Select
        temp = Dist(xcord, ycord, zcord, xx, yy, zz)
        If temp > 0 Then
            If temp < ss Then
                ss = temp
                ActiveCell.Offset(i - 1, 0).Range("A1").Select
                ActiveCell.FormulaR1C1 = ss
            End If
        End If
    End For
End For
End While
End Sub

```

```
ActiveCell.Offset(0, 1).Range("A1").Select
ActiveCell.FormulaR1C1 = n
ActiveCell.Offset(1 - i, -1).Range("A1").Select
Else
End If
Else
End If
Next
ActiveCell.Offset(0, -14).Range("A1").Select
Next
ActiveCell.Offset(nr, 0).Range("A1").Select
nr = ActiveCell.Value
Wend
End Sub
Function Dist(xcord, ycord, zcord, xx, yy, zz)
    Dist = (Sqr((xcord - xx) ^ 2 + (ycord - yy) ^ 2) - zcord - zz)
End Function
```

APPENDIX E: VOID DISTRIBUTION





APPENDIX F: WATER VAPOUR PERMEABILITY

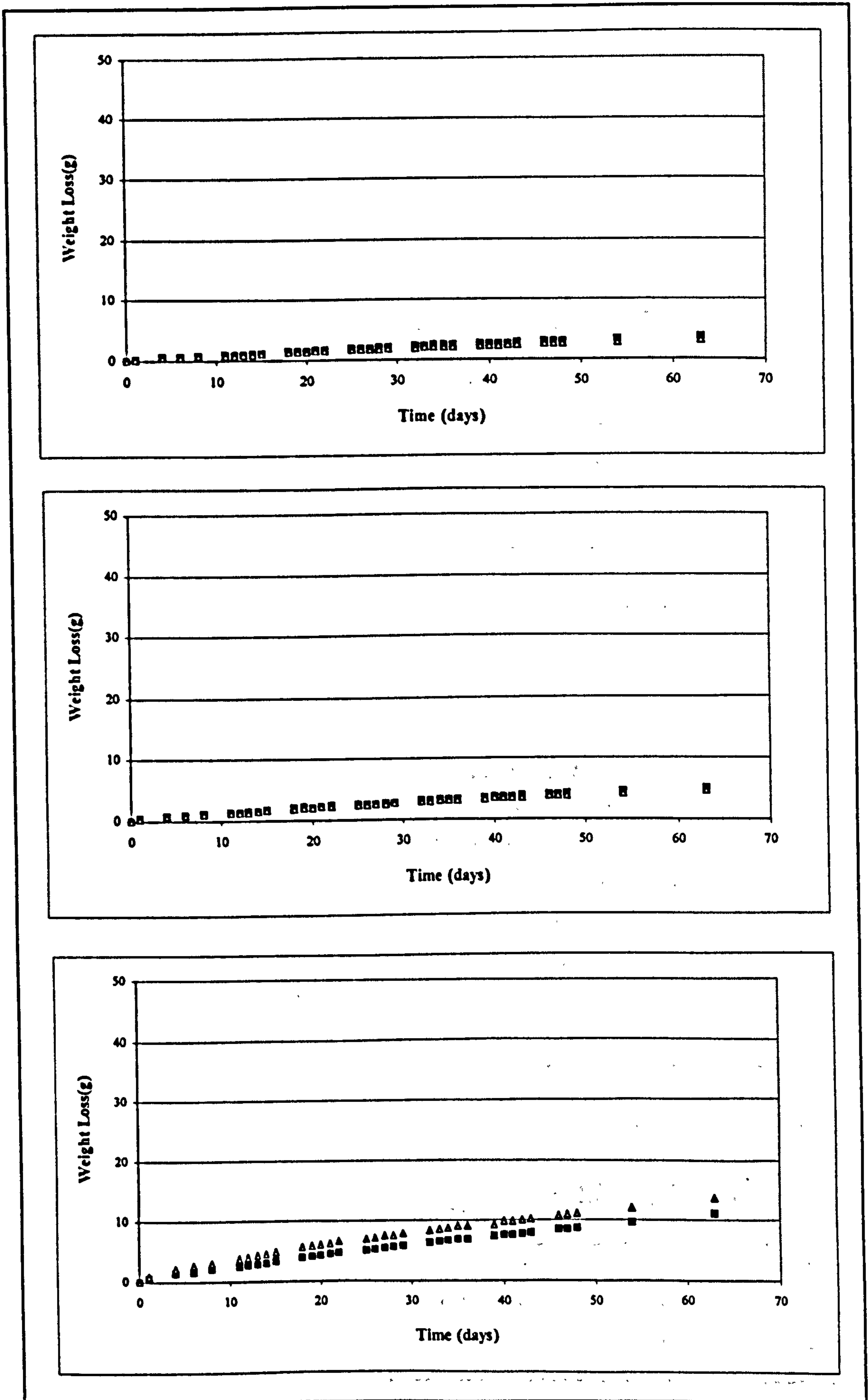


Figure F.1: Weight loss of cement paste with a water/cement ratio of 0.3, 0.4 and 0.6.

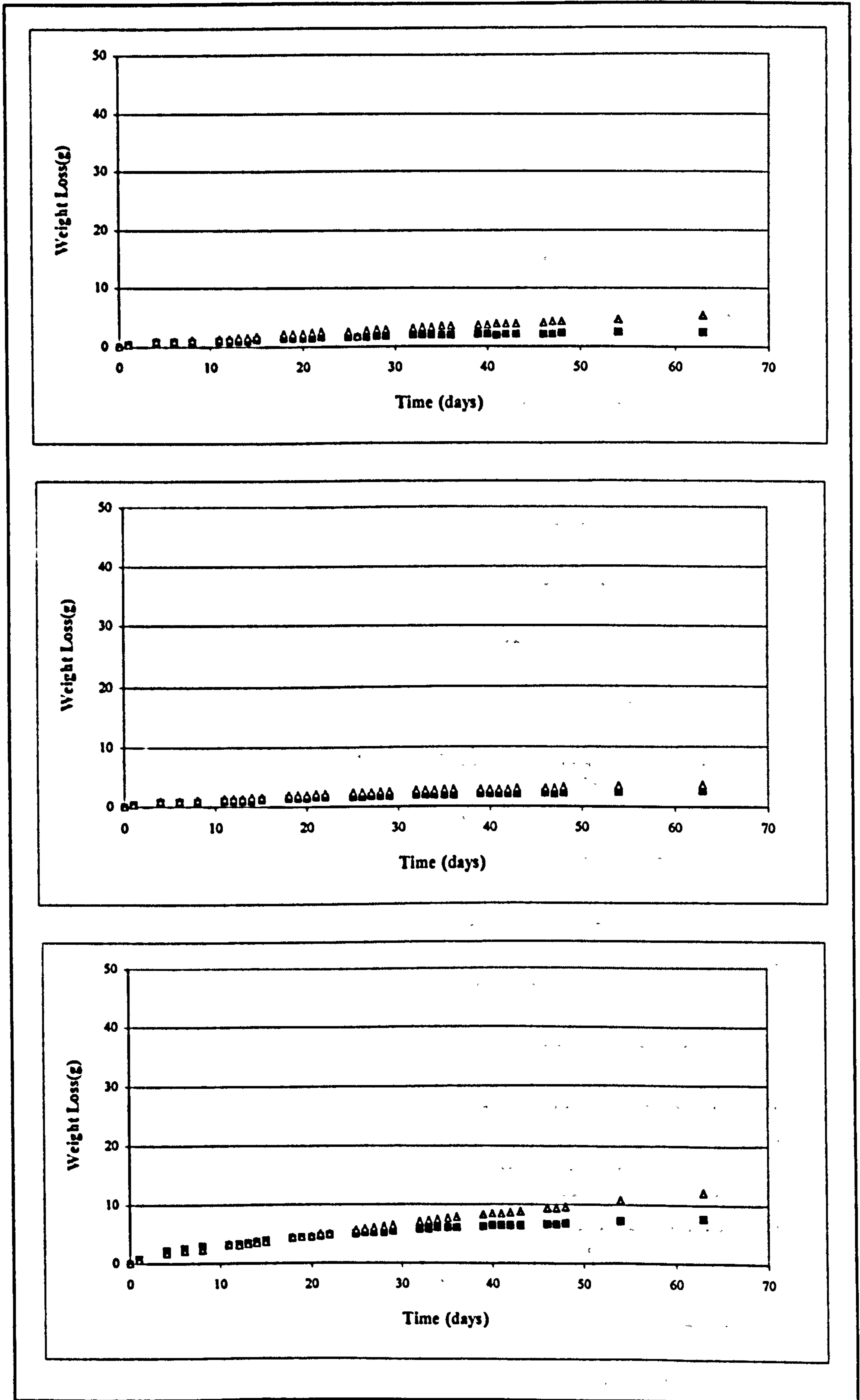


Figure F.2: Weight loss of cement paste with a pfa/cement ratio of 1, 2 and 3.

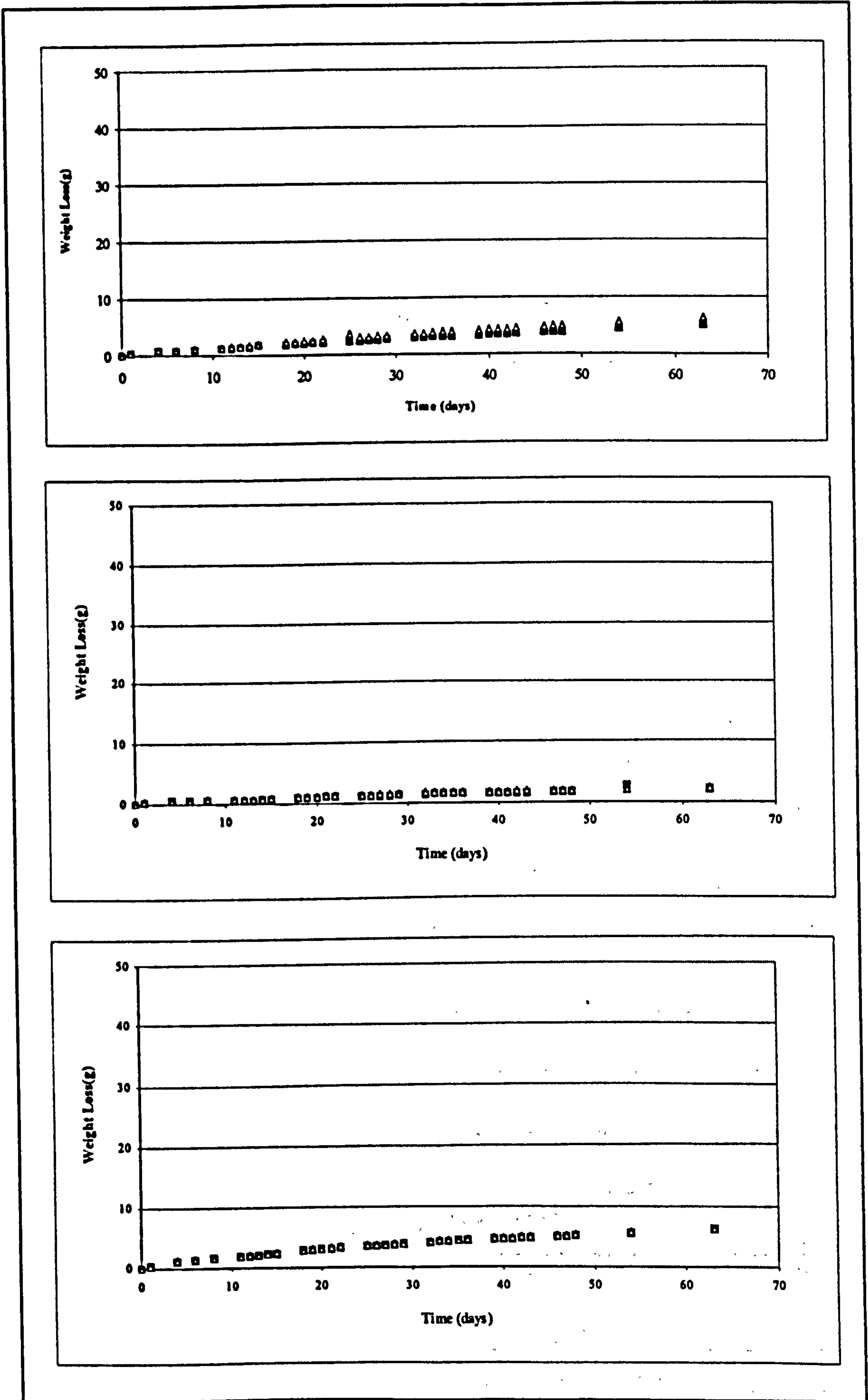


Figure F.3: Weight loss of cement paste with a pozz-fill/cement ratio of 1, 2 and 3.

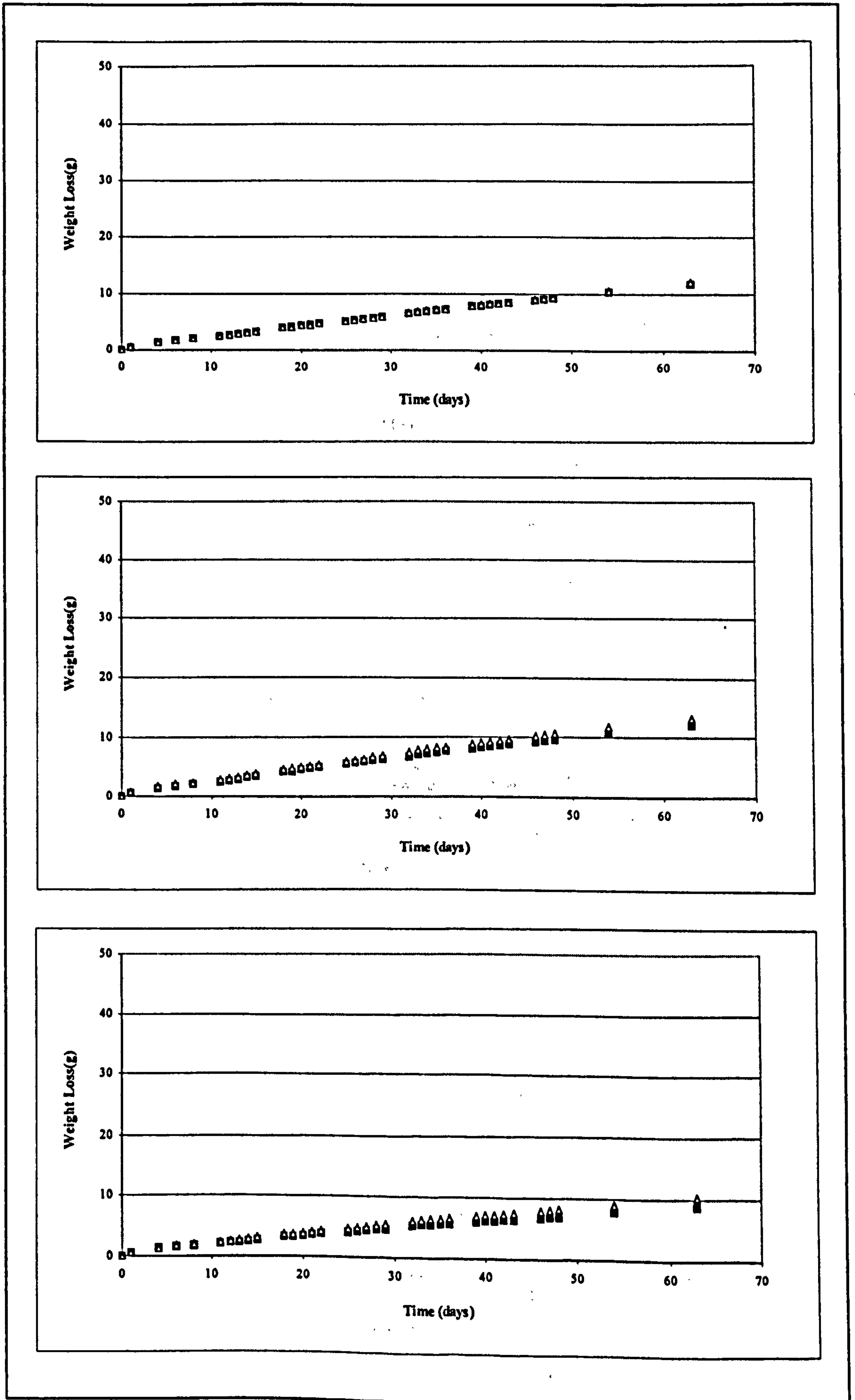


Figure F.4: Weight loss of 1500 kg/m³ foamed concrete with pfa/cement ratios of 1, 2 and 3.

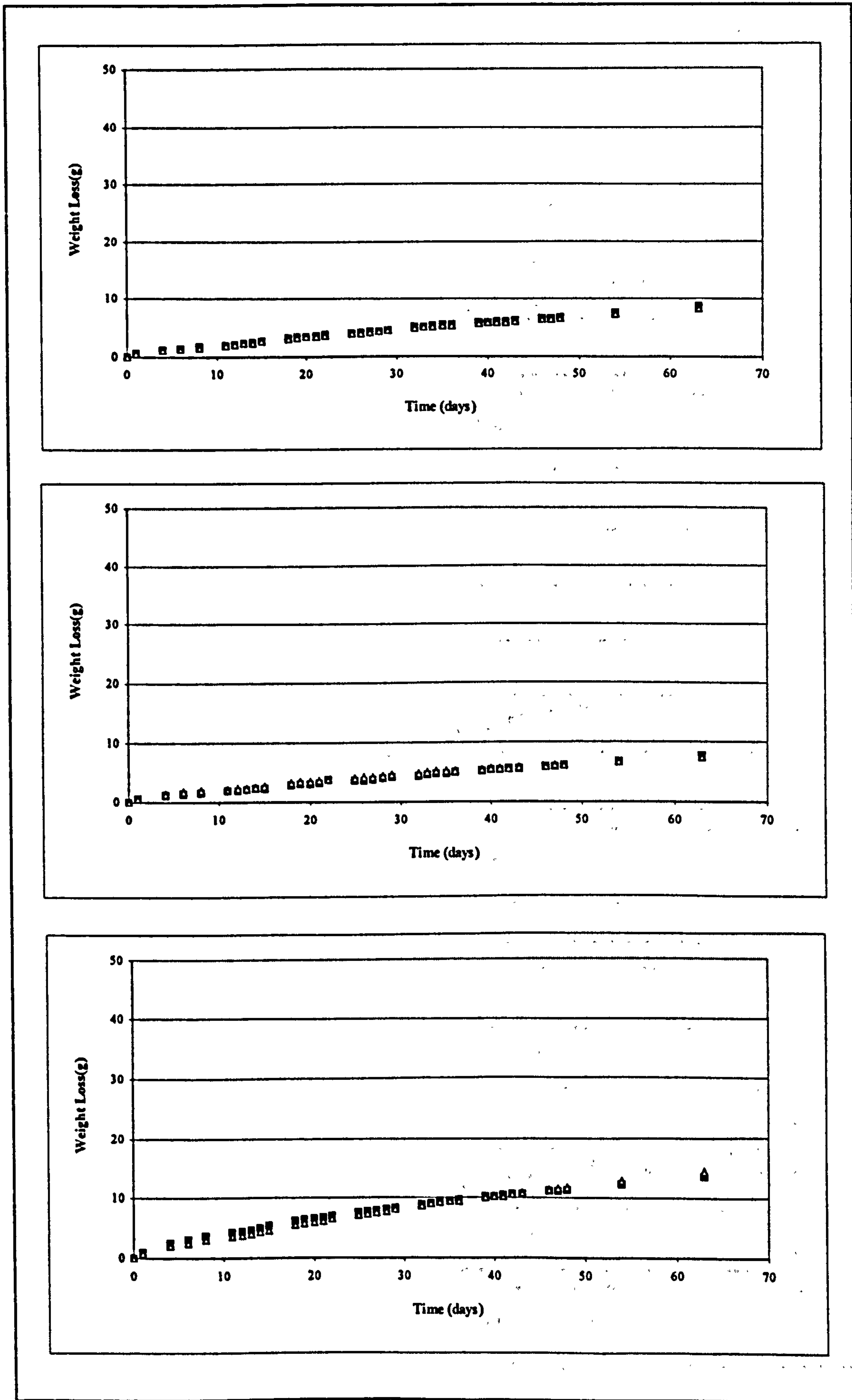


Figure F.5: Weight loss of 1500 kg/m³ foamed concrete with pozz-fill/cement ratios of 1, 2 and 3.

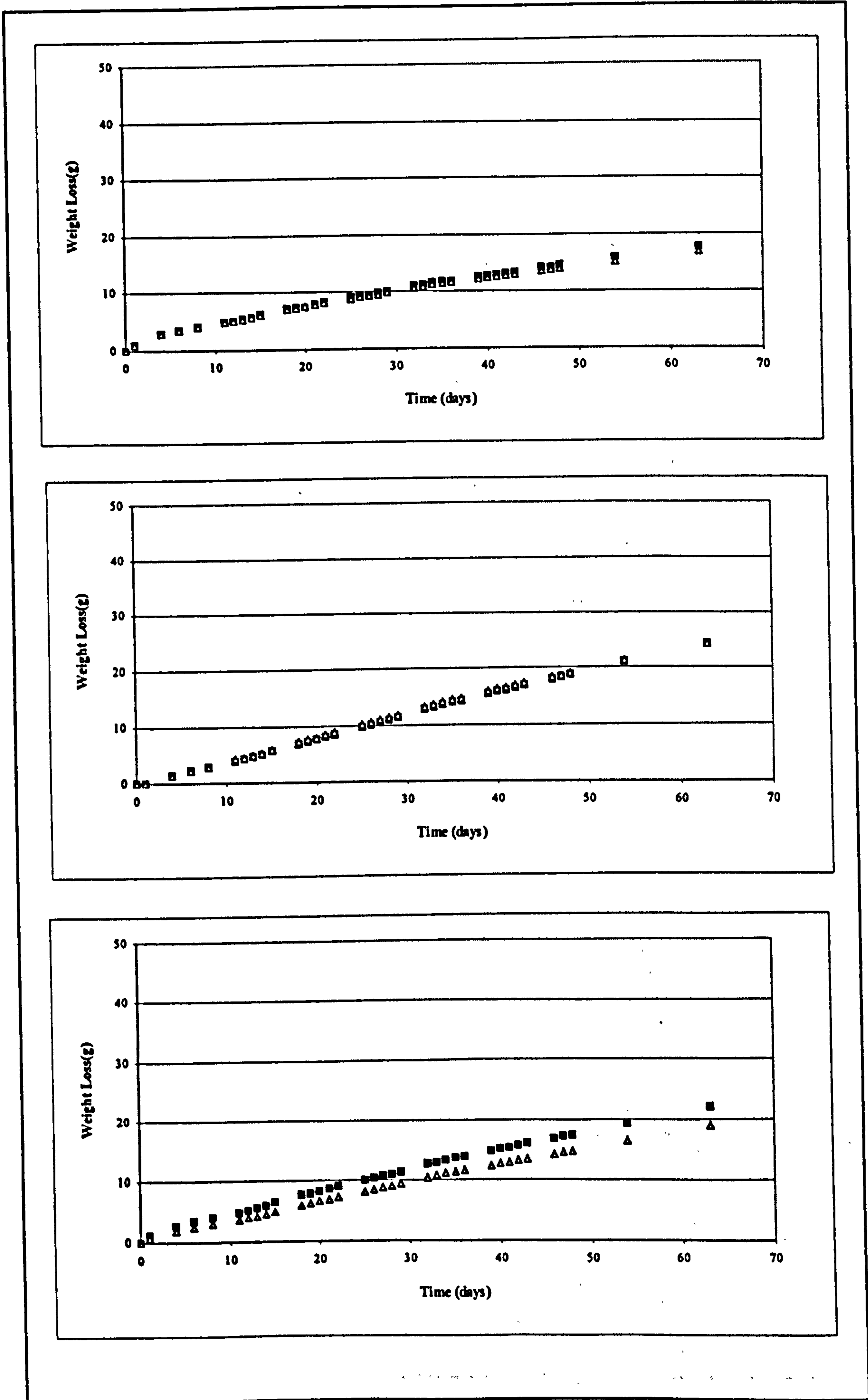


Figure F.6: Weight loss of 1250 kg/m³ foamed concrete with pfa/cement ratios of 1, 2 and 3.

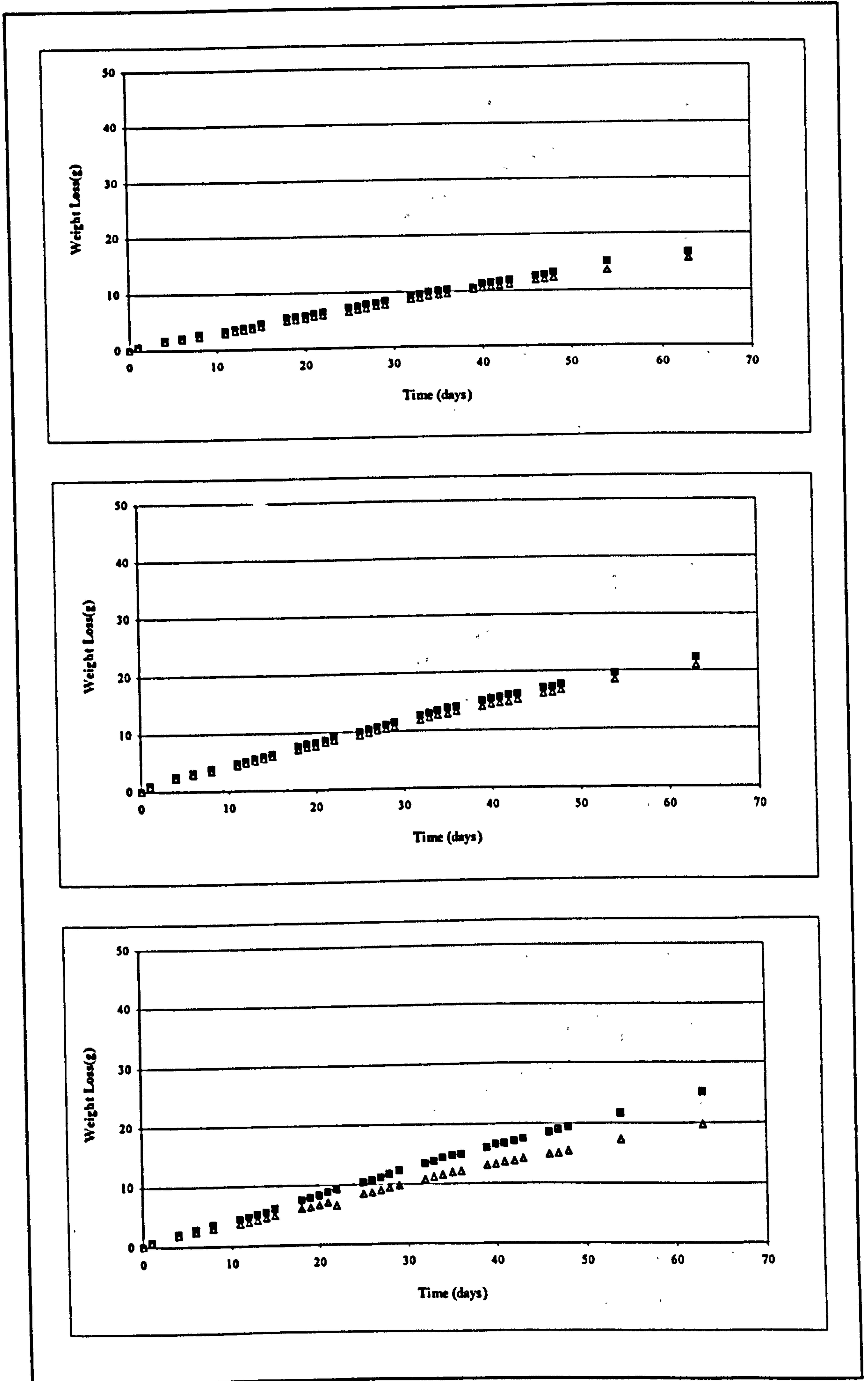


Figure F.7: Weight loss of 1250 kg/m³ foamed concrete with pozz-fill/cement ratios of 1, 2 and 3.

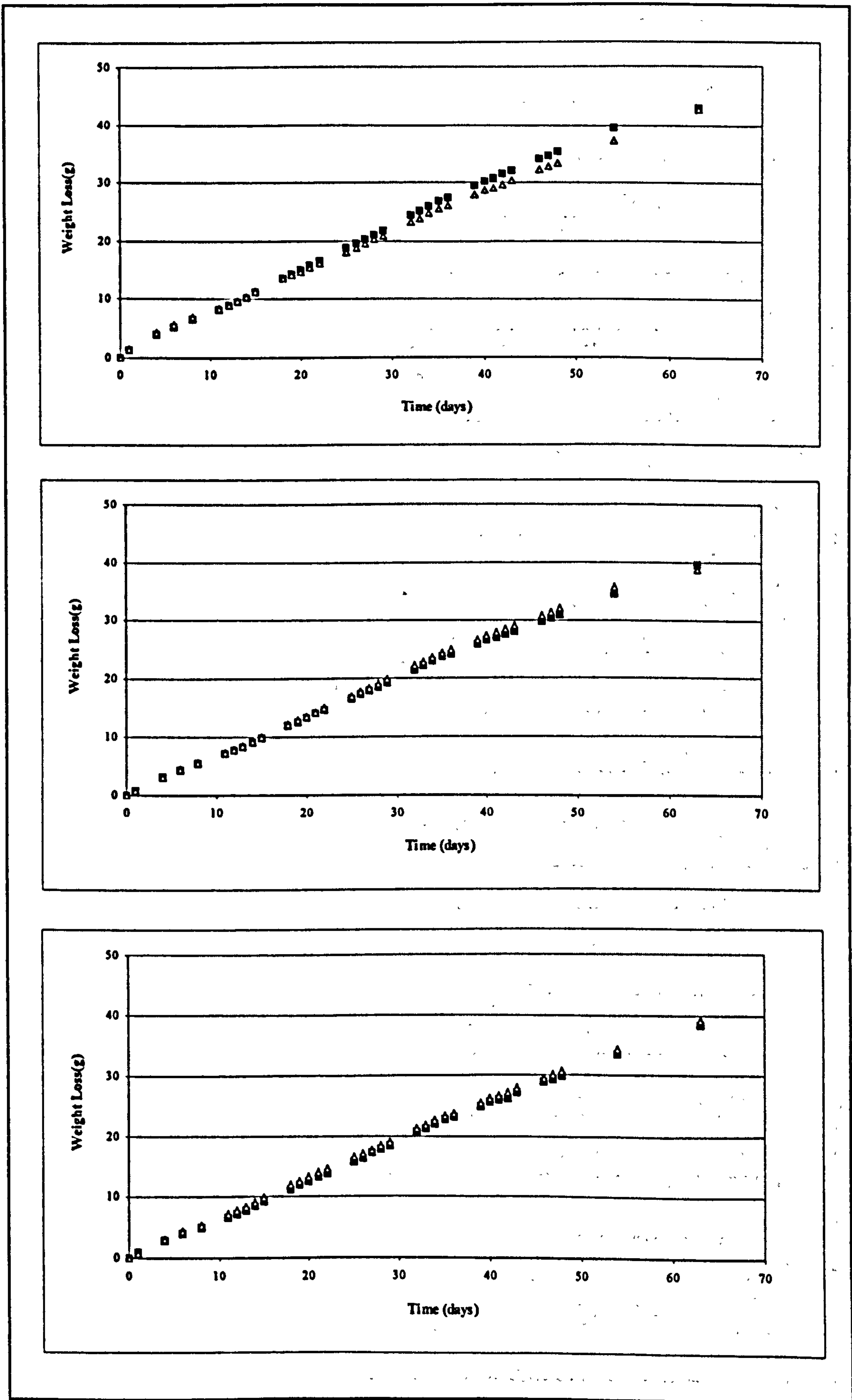


Figure F.8: Weight loss of 1000 kg/m³ foamed concrete with pfa/cement ratios of 1, 2 and 3.

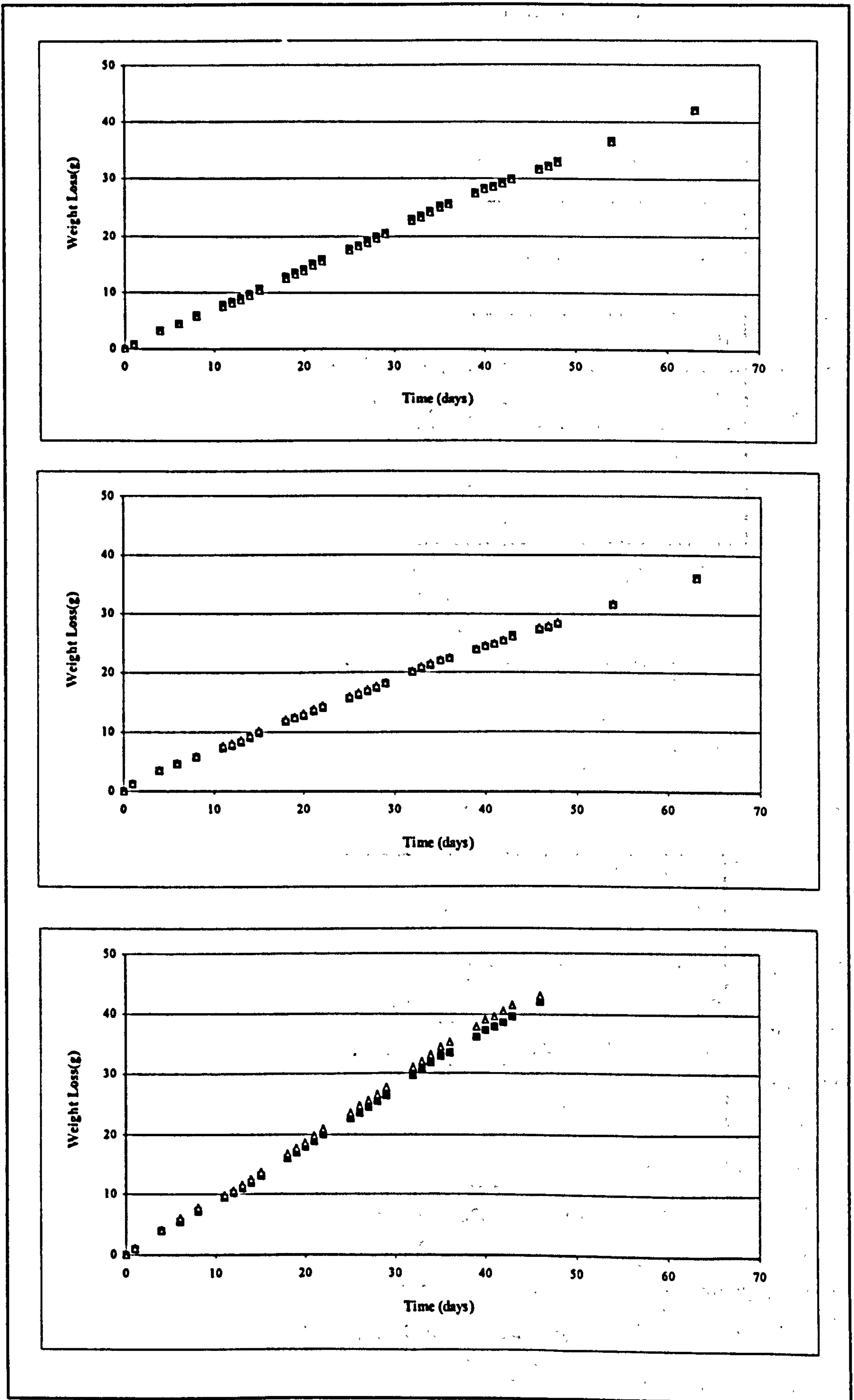
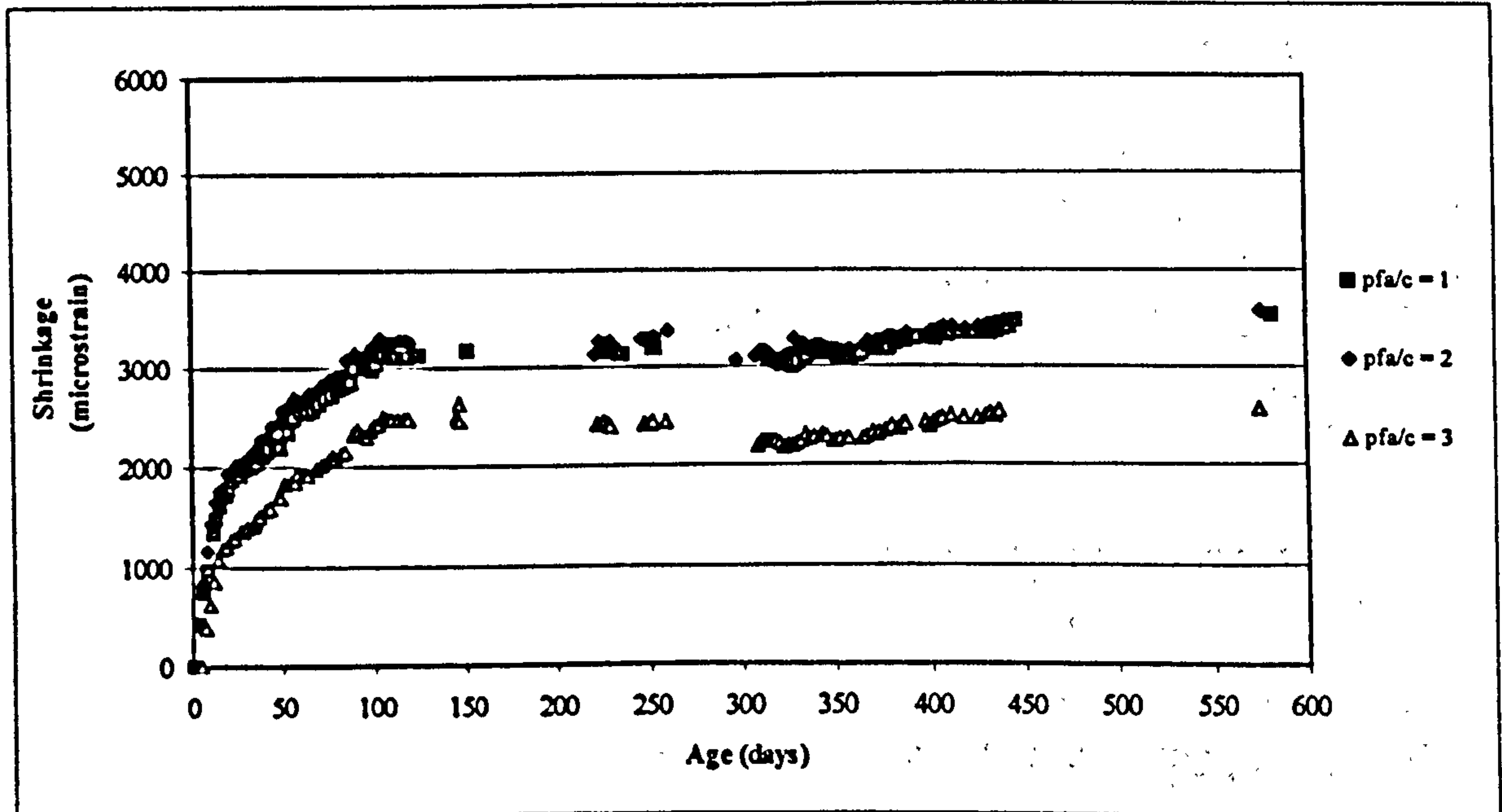
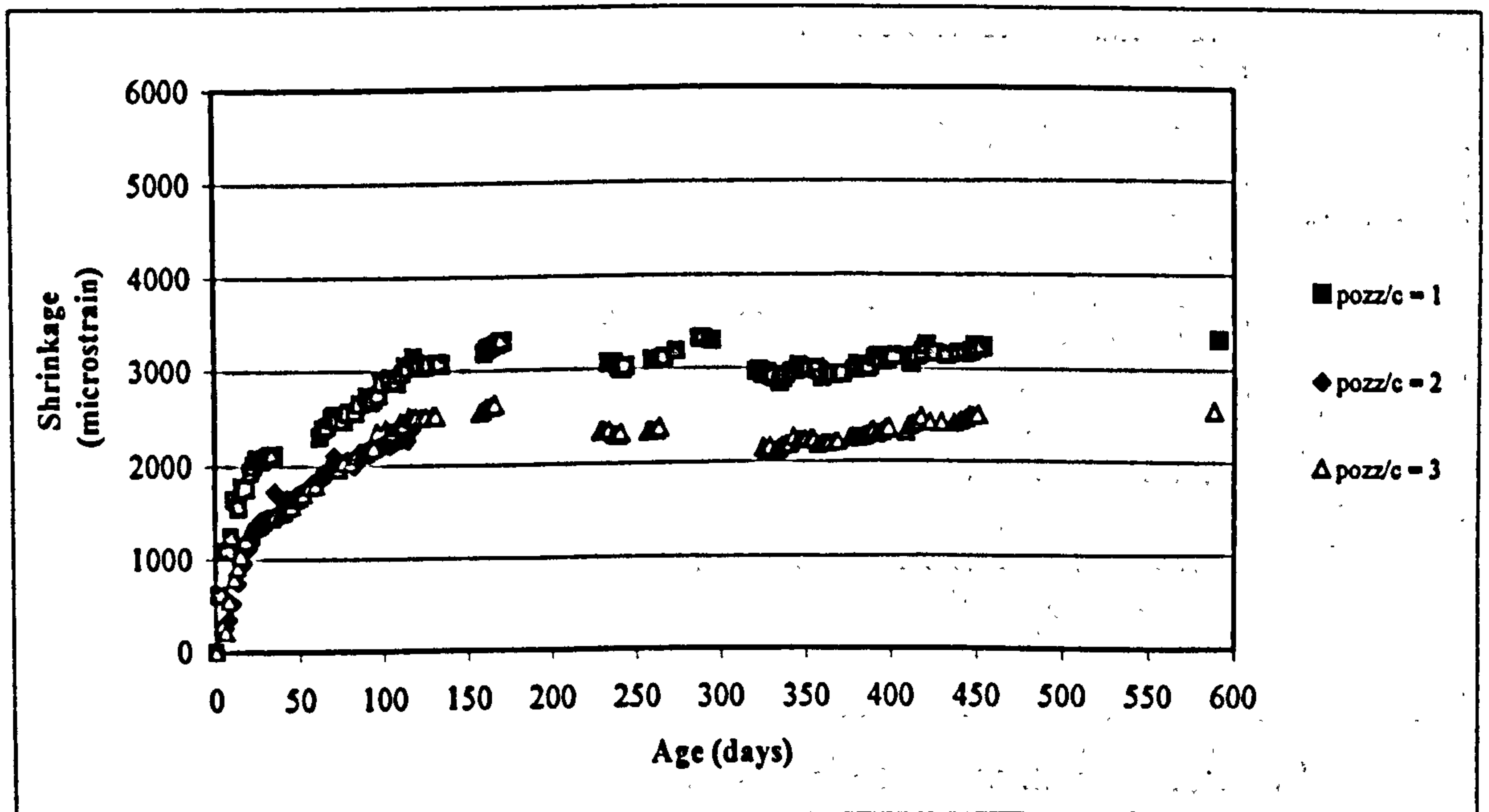


Figure F.9: Weight loss of 1000 kg/m³ foamed concrete with pozz-fill/cement ratios of 1, 2 and 3.

APPENDIX G: SHRINKAGE

Figure G.1: Shrinkage of 1000 kg/m³ foamed concrete containing pfa.Figure G.2: Shrinkage of 1000 kg/m³ foamed concrete containing pozz-fill.

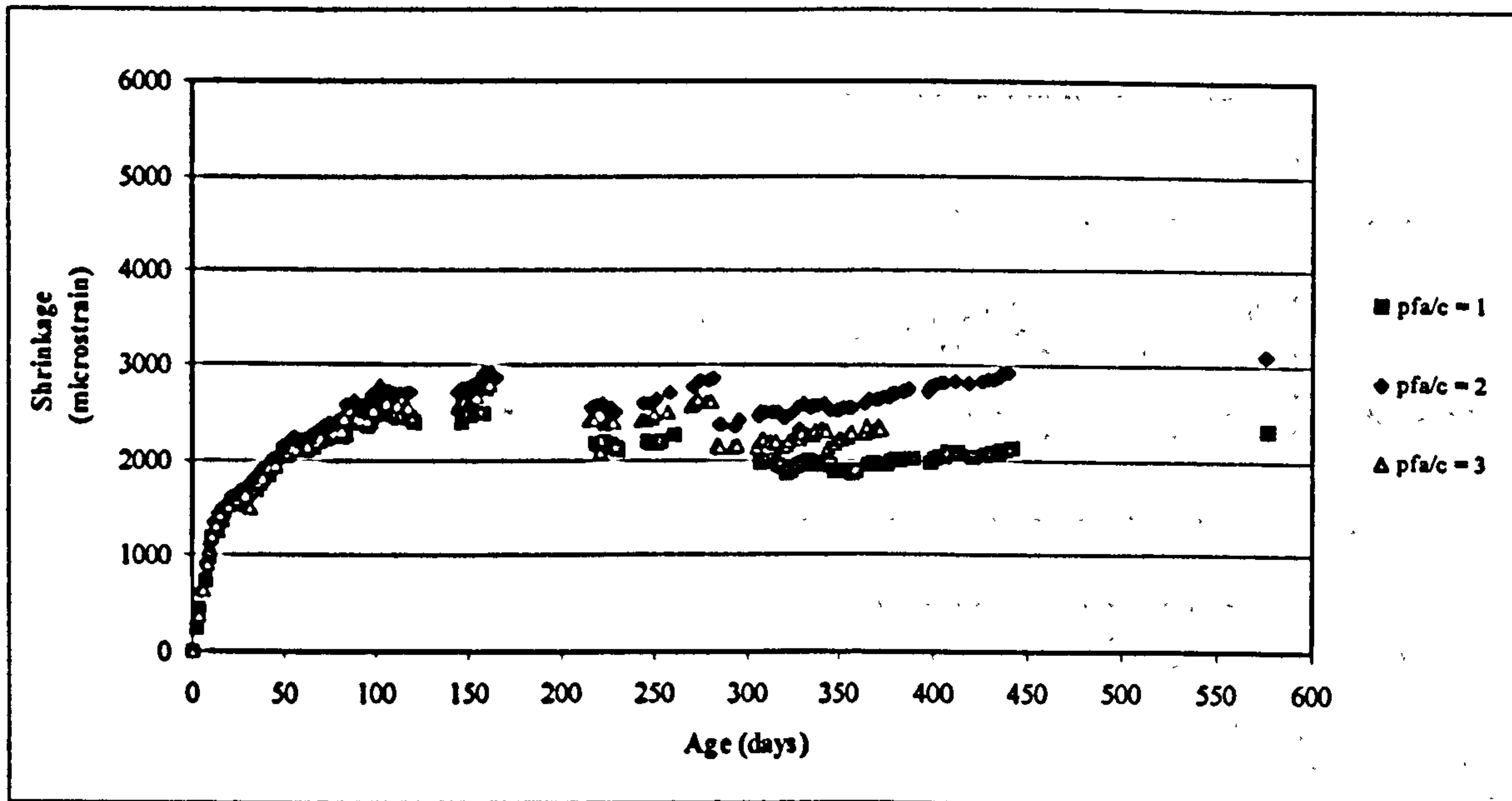


Figure G.3: Shrinkage of 1250 kg/m³ foamed concrete containing pfa.

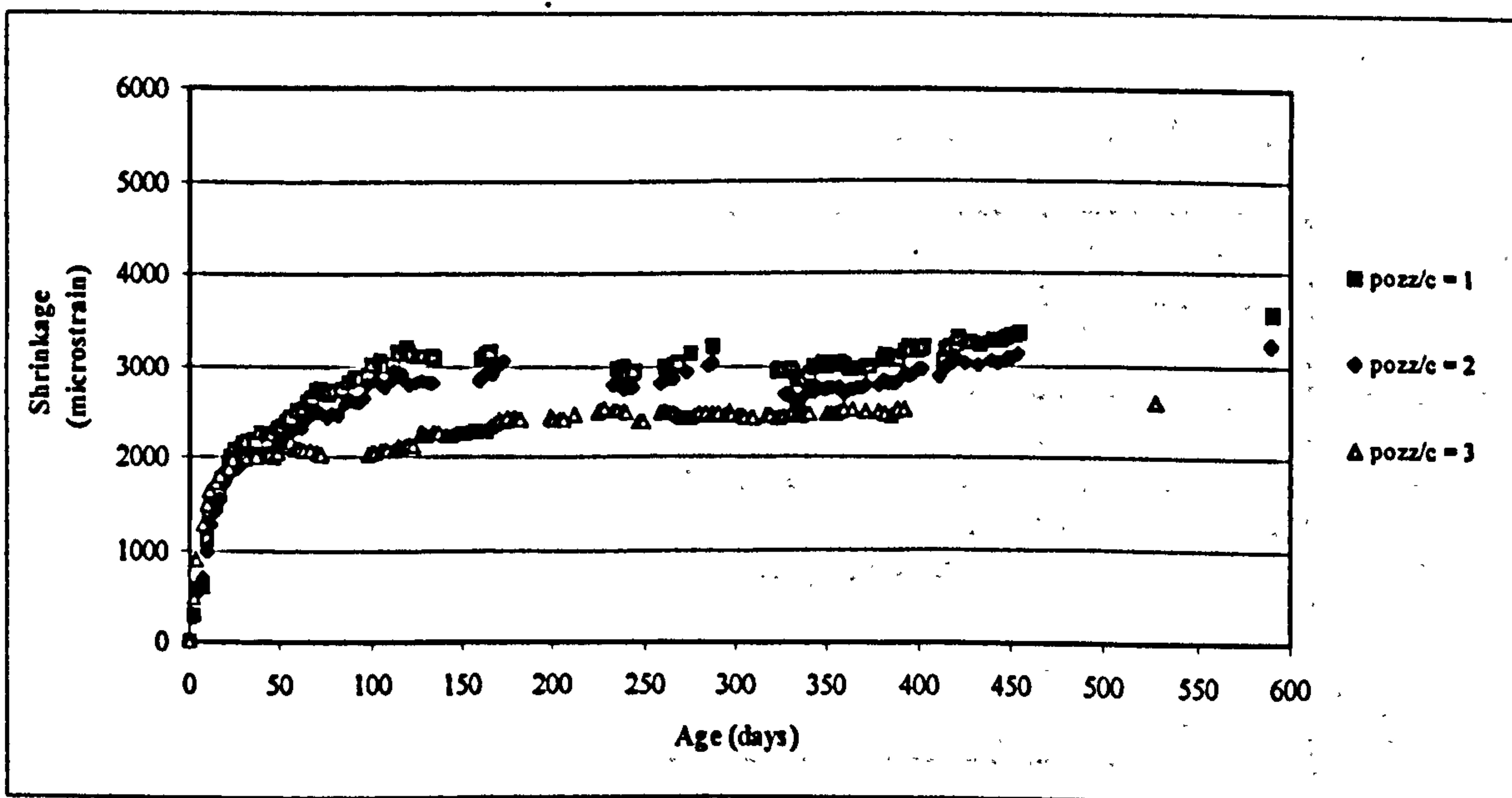


Figure G.4: Shrinkage of 1250 kg/m³ foamed concrete containing pozz-fill.

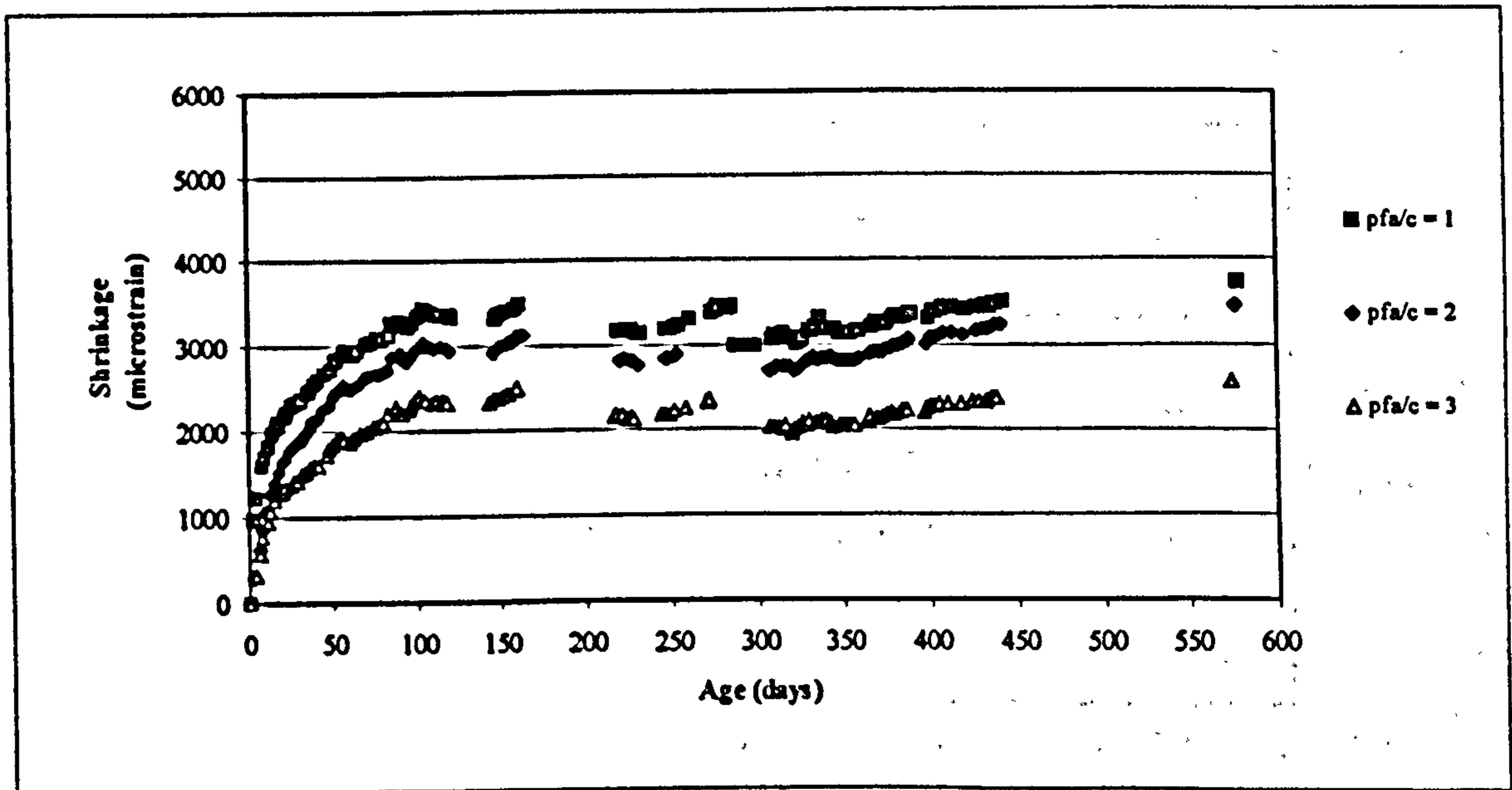


Figure G.5: Shrinkage of 1500 kg/m^3 foamed concrete containing pfa.

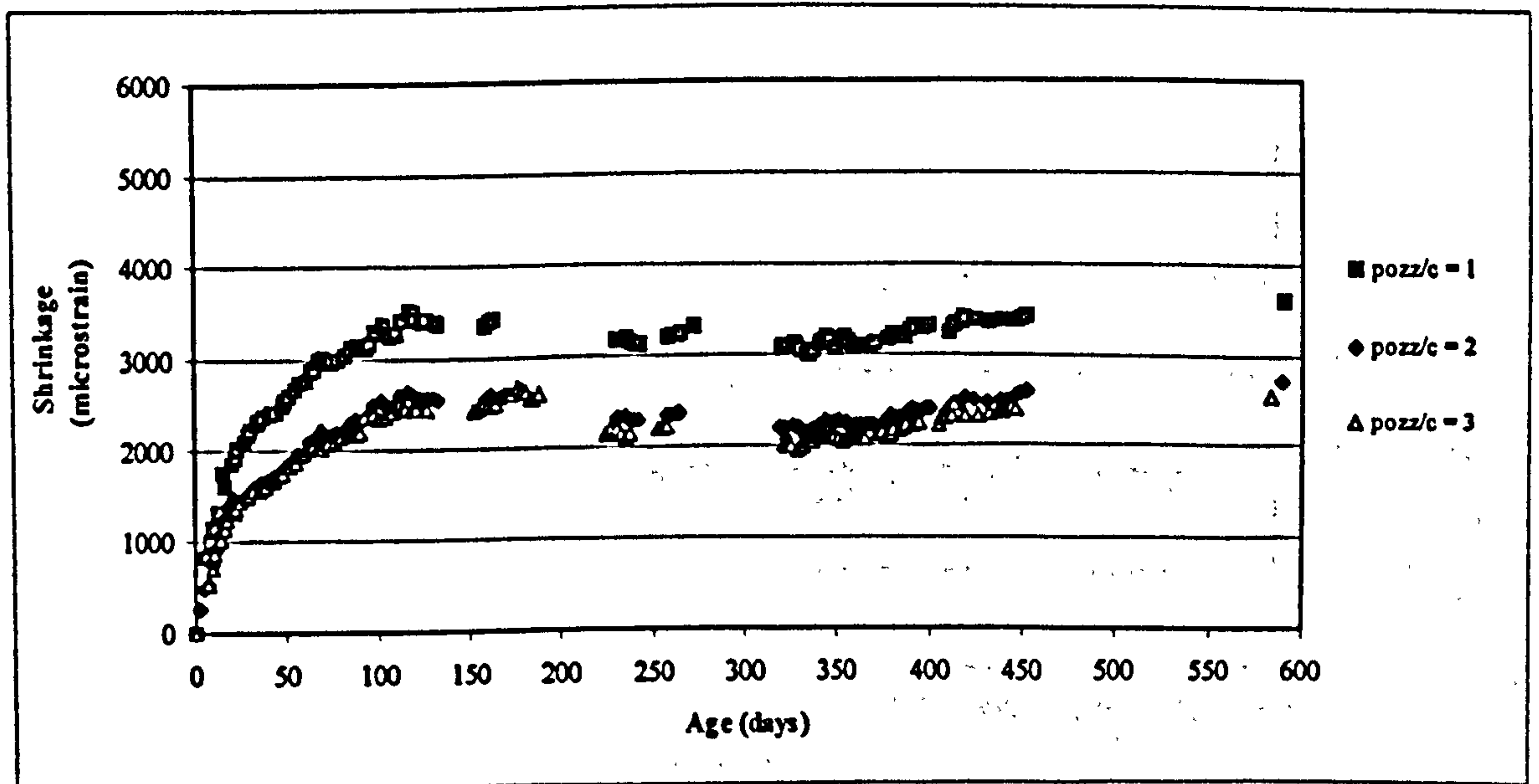


Figure G.6: Shrinkage of 1500 kg/m^3 foamed concrete containing pozz-fill.

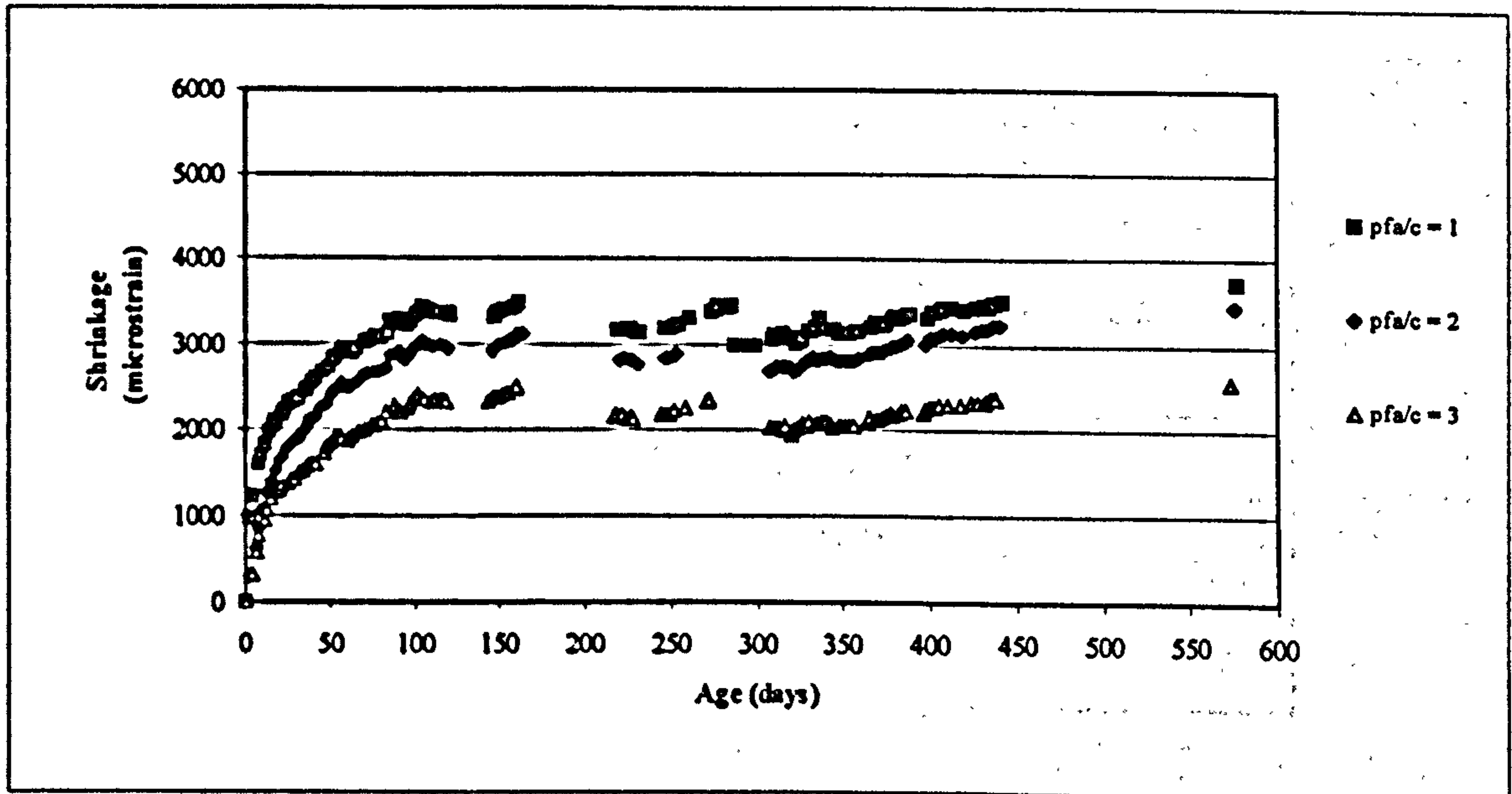


Figure G.5: Shrinkage of 1500 kg/m^3 foamed concrete containing pfa.

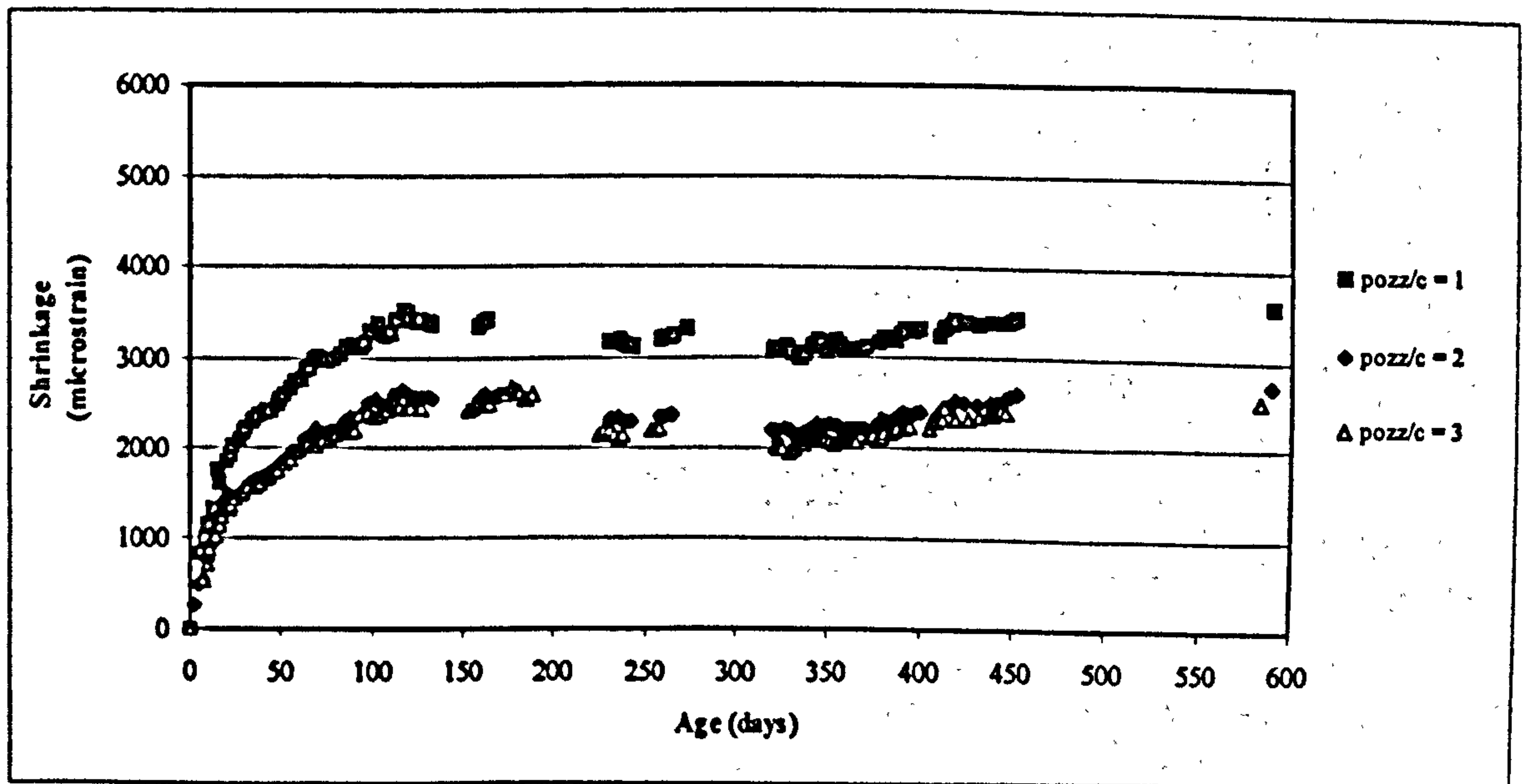


Figure G.6: Shrinkage of 1500 kg/m^3 foamed concrete containing pozz-fill.

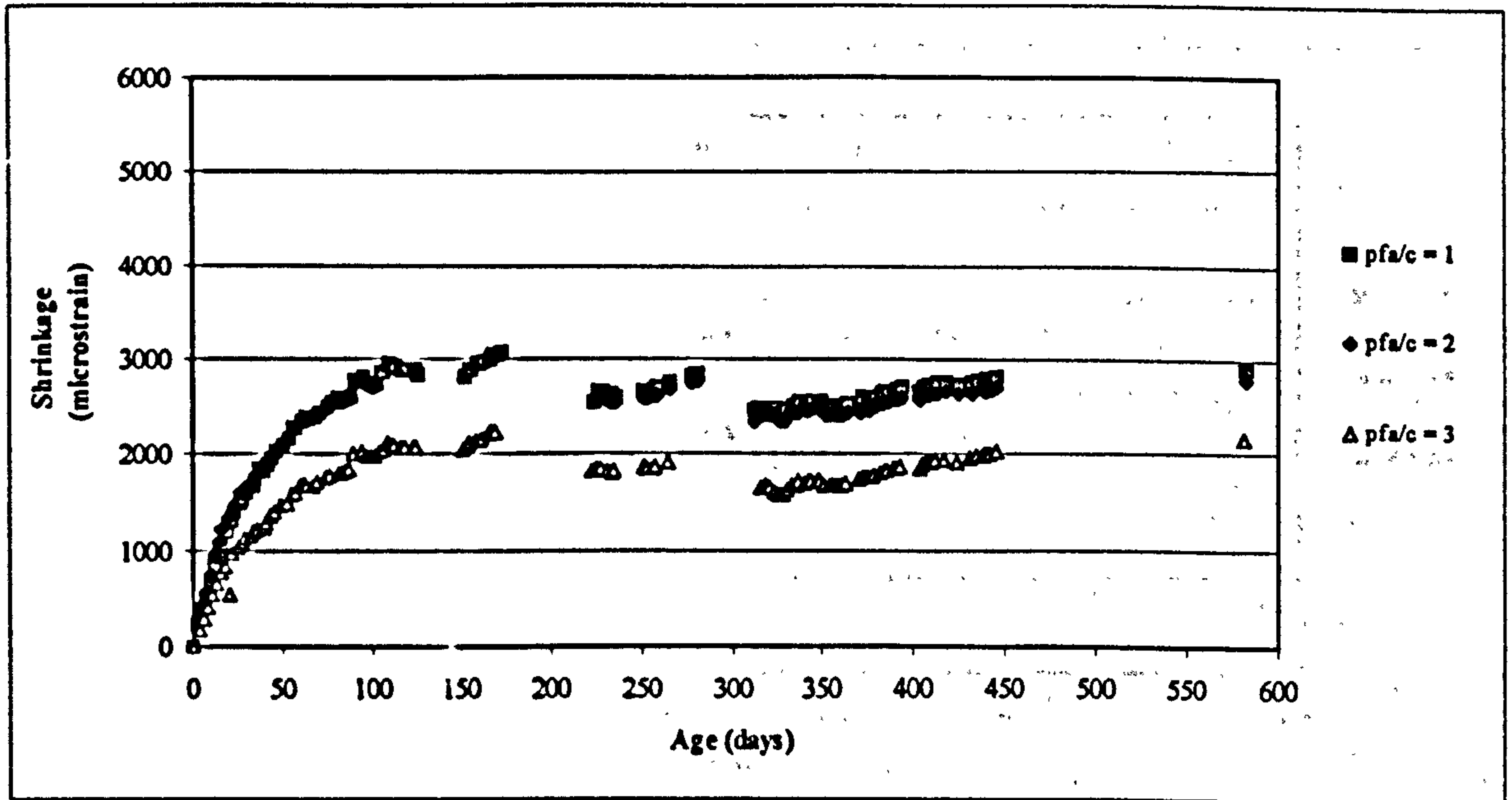


Figure G.7: Shrinkage of cement pastes containing pfa.

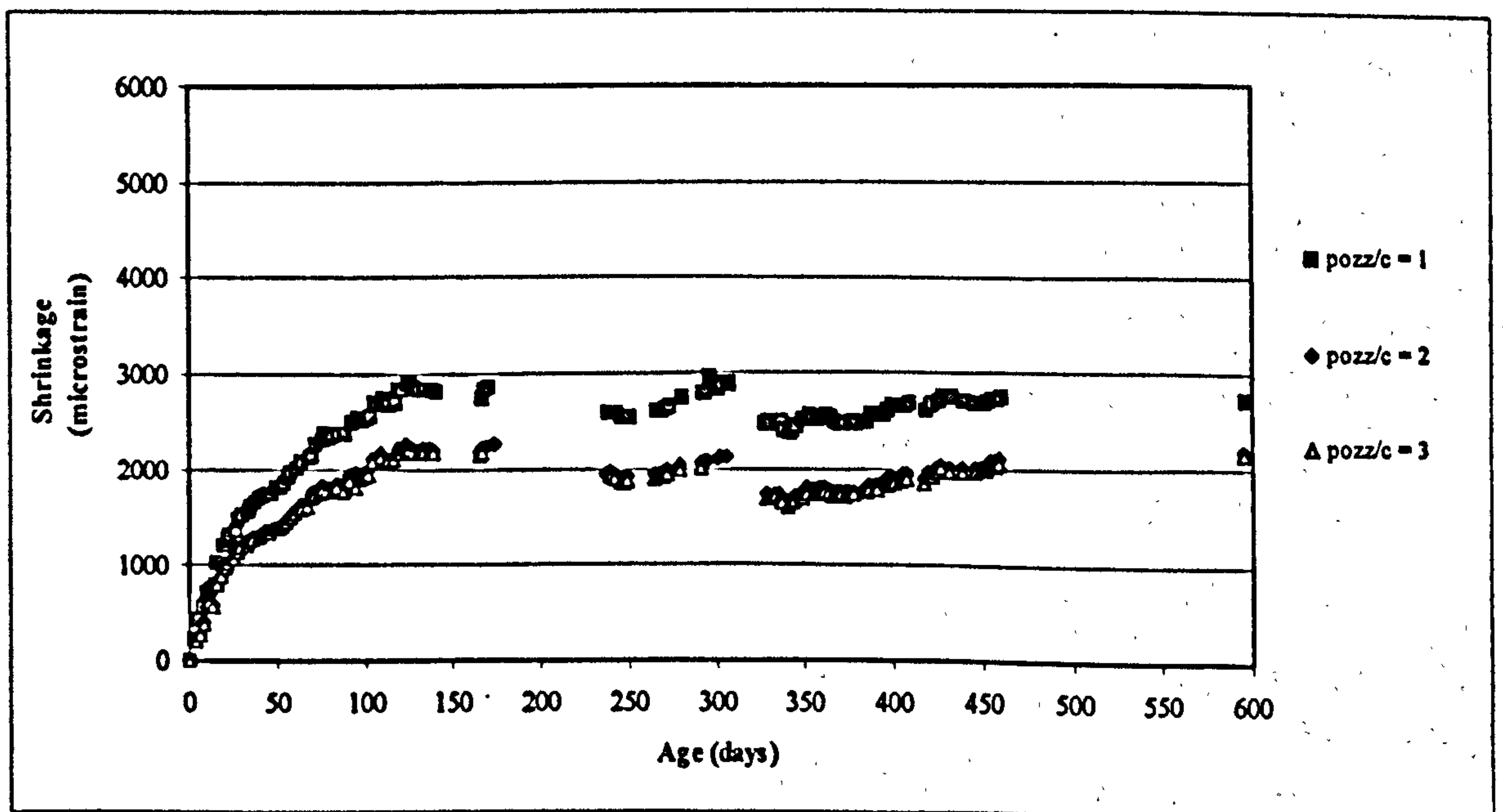


Figure G.8: Shrinkage of cement pastes containing pozz-fill.

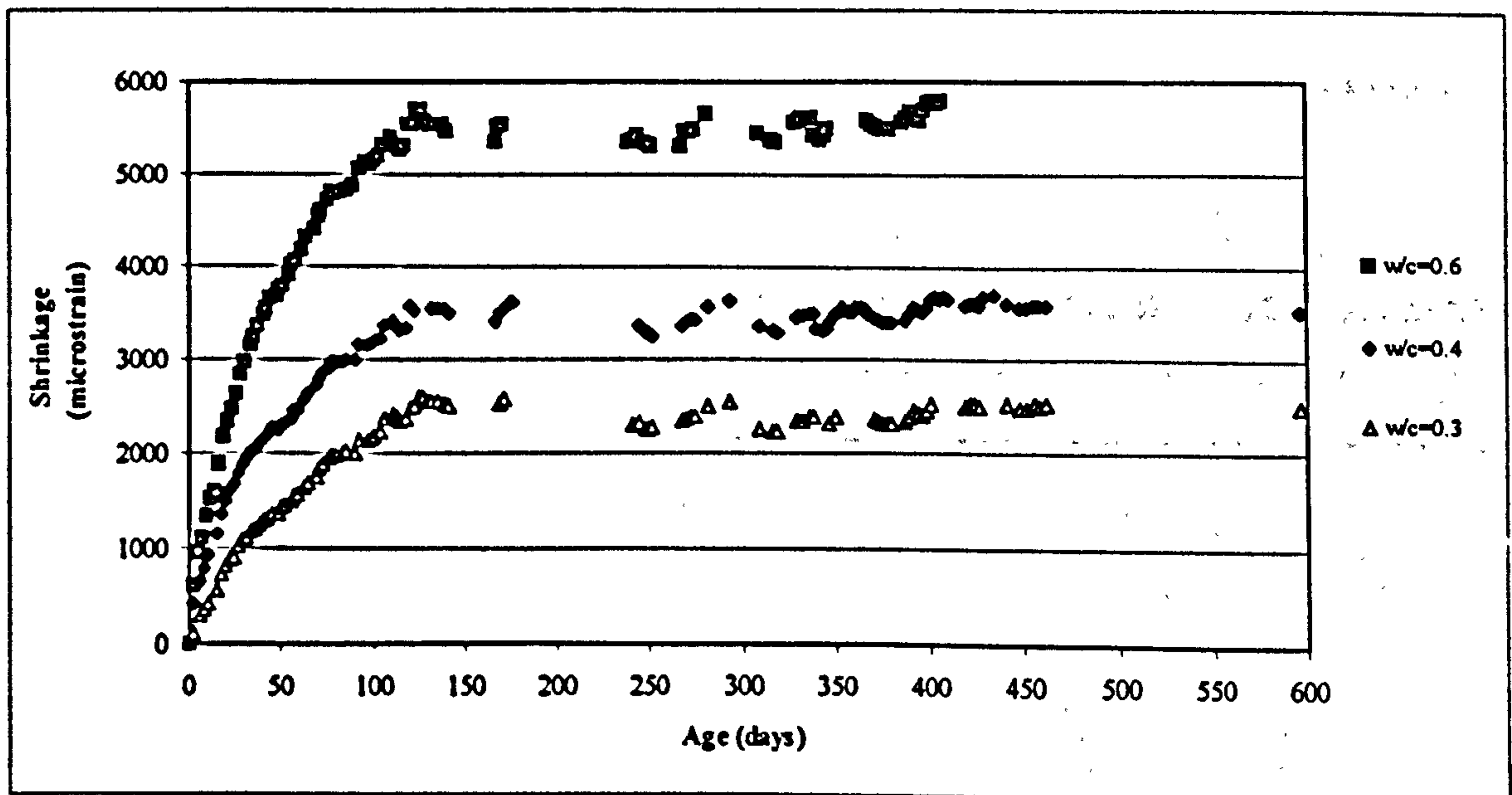


Figure G.9: Shrinkage of cement paste.

APPENDIX H: FORTRAN PROGRAM

H.1 SOURCE CODE

```

C*****
C   MODELA ANALISE
C*****

      IMPLICIT INTEGER*2 (I-N)
      IMPLICIT REAL*8 (A-H,O-Z)

      COMMON/CPARM/ALFA,BETA1,BETA2,BETA3,ZETA1,ZETA2,ZETA3,DAVGY,KFLAG
      COMMON NDATA,AC(189),AGE(189),POROS(189),STRENG(189)
C
C--- OPEN FILE, INITIALIZE-----
      OPEN(2,FILE='MODELA3.RES')
      DO 55 ITYPE=01,02
      GO TO (11,12),ITYPE
11 ALFA=3.700
      BETA1=24.91261
      BETA2=52.89322
      BETA3=-12.27050
      ZETA1=172.84324
      ZETA2=-196.04239
      ZETA3=34.02081
      GO TO 15
12 ALFA=3.700
      BETA1=23.73633
      BETA2=56.77971
      BETA3=-14.31236
      ZETA1=176.88329
      ZETA2=-229.7353
      ZETA3=46.04321
15 DAVGY=0.0
      NAVGY=00
      NDATA=00
      DBEST=1.0D18
C
C--- READ DATA -----
      OPEN(1,FILE='ELSABE.DAT')
20 READ(1,*,END=25)KTYPE,STR,POR,IAC,IAGE
      IF(KTYPE.EQ.00)KTYPE=ITYPE
      IF(KTYPE.NE.ITYPE)GO TO 20
      NDATA=NDATA+01
      STRENG(NDATA)=STR
      POROS(NDATA)=1.0-POR/100.0
      AGE(NDATA)=ALOG(FLOAT(IAGE))

```

```
AC(NDATA)=IAC
DAVGY=DAVGY+STR
NAVGY=NAVGY+01
GO TO 20
25 DAVGY=DAVGY/NAVGY
CLOSE(1)
```

C

C--- SEARCH BEST FIT -----

```
DO 46 IREPT=01,03
30 KFLAG=00
RSTEP=1.0
DO 45 ISTEP=01,20
RSTEP=RSTEP/5.0
DO 45 ISIGN=01,02
RSTEP=-RSTEP
```

C

C--- ADJUST VALUES -----

```
QBETA1=BETA1
31 BETA1=QBETA1+RSTEP
CALL TRYFIT(DBEST,*31)
BETA1=QBETA1
QBETA2=BETA2
32 BETA2=QBETA2+RSTEP
CALL TRYFIT(DBEST,*32)
BETA2=QBETA2
QBETA3=BETA3
33 BETA3=QBETA3+RSTEP
CALL TRYFIT(DBEST,*33)
BETA3=QBETA3
QZETA1=ZETA1
34 ZETA1=QZETA1+RSTEP
CALL TRYFIT(DBEST,*34)
ZETA1=QZETA1
QZETA2=ZETA2
35 ZETA2=QZETA2+RSTEP
CALL TRYFIT(DBEST,*35)
ZETA2=QZETA2
QZETA3=ZETA3
36 ZETA3=QZETA3+RSTEP
CALL TRYFIT(DBEST,*36)
ZETA3=QZETA3
QALFA=ALFA
37 ALFA=QALFA+RSTEP
IF(ALFA.LE.0.0)GO TO 38
CALL TRYFIT(DBEST,*37)
```

```

      38 ALFA=QALFA
C
C--- REPEAT CONTROL -----
      45 CONTINUE
          IF(KFLAG.NE.00)GO TO 30
      46 CONTINUE
C
C--- WRITE RESULTS -----
          CALL REGFIT(DREG)

          WRITE(2,51) ITYPE,ALFA,BETA1,BETA2,BETA3,ZETA1,ZETA2,ZETA3,
          DREG
      51 FORMAT(I20,F20.5/3F20.5/3F20.5/F20.9)
      55 CONTINUE
          STOP
      END
C
C*****
C   PERFORM REGRESSION ANALYSIS AND ACCUMULATE ERROR
C*****

          SUBROUTINE TRYFIT(DBEST,*)
          IMPLICIT INTEGER*2 (I-N)
          IMPLICIT REAL*8 (A-H,O-Z)

          COMMON/CPARM/ALFA,BETA1,BETA2,BETA3,ZETA1,ZETA2,ZETA3,DAVGY,KFLAG
          COMMON NDATA,AC(189),AGE(189),POROS(189),STRENG(189)
C
C--- COMPUTE ERROR -----
          DERR=0.0
          DO 35 IDATA=01,NDATA
          BETA=BETA1+BETA2*AC(IDATA)+BETA3*AC(IDATA)*AC(IDATA)
          ZETA=ZETA1+ZETA2*AC(IDATA)+ZETA3*AC(IDATA)*AC(IDATA)
          D=(ZETA+BETA*AGE(IDATA))*(POROS(IDATA)**ALFA)-
          STRENG(IDATA)
          DERR=DERR+D*D
          35 CONTINUE
C
C--- CHECK IF ERROR REDUCED -----
          IF(DERR.GE.DBEST)RETURN
          DBEST=DERR
CCC  KFLAG=KFLAG+01
CCC  IF(KFLAG.LT.5000)RETURN 1
          WRITE(*,*)DERR
          KFLAG=01
          RETURN 1
          END
C
C*****
C   PERFORM REGRESSION ANALYSIS AND REGRESSION COEFFICIENT
C*****

          SUBROUTINE REGFIT(DREG)
          IMPLICIT INTEGER*2 (I-N)
          IMPLICIT REAL*8 (A-H,O-Z)

```

COMMON/CPARM/ALFA, BETA1, BETA2, BETA3, ZETA1, ZETA2, ZETA3, DAVG
Y, KFLAG

COMMON NDATA, AC(189), AGE(189), POROS(189), STRENG(189)

C

C--- COMPUTE REGRESSION COEFFICIENT -----

DREG=0.0

DERR=0.0

DO 35 IDATA=01, NDATA

BETA=BETA1+BETA2*AC(IDATA)+BETA3*AC(IDATA)*AC(IDATA)

ZETA=ZETA1+ZETA2*AC(IDATA)+ZETA3*AC(IDATA)*AC(IDATA)

S=(ZETA+BETA*AGE(IDATA))*(POROS(IDATA)**ALFA)

D=S-DAVGY

DREG=DREG+D*D

D=S-STRENG(IDATA)

DERR=DERR+D*D

35 CONTINUE

DREG=DREG/(DREG+DERR)

RETURN

END

□□□□□□□□□□□□□□□□

H.2 INPUT DATA

Ash type	Strength	Porosity	Ash/cement	Age
0	63.0667	28.77	0	7
0	47.5667	34.74	0	7
0	20.4667	40.5	0	7
0	78.9667	28.77	0	28
0	58.9667	34.74	0	28
0	31.9667	40.5	0	28
0	80.4	28.77	0	56
0	64.11148	34.74	0	56
0	37.05	40.5	0	56
0	80.4	28.77	0	84
0	62.02682	34.74	0	84
0	38.93333	40.5	0	84
0	84.5	28.77	0	180
0	68.03333	34.74	0	180
0	39.5	40.5	0	180
0	81.6	28.77	0	270
0	68.93333	34.74	0	270
0	43.46666	40.5	0	270
0	85.4	28.77	0	365
0	78.94333	34.74	0	365
0	46.68333	40.5	0	365
1	31.5	34.48	1	7
1	11.9333	45.69	1	7
1	5.5000	52.19	1	7
1	2.1667	66.9	1	7
1	43.3000	34.48	1	28
1	18.1	45.69	1	28
1	9.3	52.19	1	28
1	3.77	66.9	1	28
1	52.63333	34.48	1	56
1	24.975	45.69	1	56
1	5.8	66.9	1	56

1	58.1	34.48	1	84
1	30.83333	45.69	1	84
1	14.13333	52.19	1	84
1	6.2	66.9	1	84
1	69.23333	34.48	1	180
1	29.33333	45.69	1	180
1	15.53333	52.19	1	180
1	9	66.9	1	180
1	84.57333	34.48	1	270
1	36.95	45.69	1	270
1	20.07666	52.19	1	270
1	9.59	66.9	1	270
1	80.26	34.48	1	365
1	39.54666	45.69	1	365
1	19.79666	52.19	1	365
1	9.183333	66.9	1	365
1	23.1	36.71	2	7
1	8.5667	49.87	2	7
1	4.6667	52.39	2	7
1	2.6000	66.32	2	7
1	37.5333	36.71	2	28
1	14.63333	49.87	2	28
1	8.033333	52.39	2	28
1	3.966666	66.32	2	28
1	47.375	36.71	2	56
1	18.54560	49.87	2	56
1	10.625	52.39	2	56
1	4.573245	66.32	2	56
1	58.86666	36.71	2	84
1	26.86666	49.87	2	84
1	13.3	52.39	2	84
1	6.9	66.32	2	84
1	64.73333	36.71	2	180
1	33.16666	49.87	2	180
1	16	52.39	2	180
1	8.166666	66.32	2	180
1	78.30333	36.71	2	270
1	36.11	49.87	2	270
1	18.50666	52.39	2	270
1	8.173333	66.32	2	270
1	81.45	36.71	2	365
1	35.56333	49.87	2	365
1	18.39	52.39	2	365
1	8.59	66.32	2	365
1	9.9	38.08	3	7
1	6.5667	41.8	3	7
1	3.5667	51.14	3	7
1	1.7333	67.4	3	7
1	16.4567	38.08	3	28
1	13.86666	41.8	3	28
1	7.166666	51.14	3	28
1	2.833333	67.4	3	28
1	28.25	38.08	3	56
1	18.03333	41.8	3	56
1	10.3	51.14	3	56
1	5.15	67.4	3	56
1	36.5	38.08	3	84
1	24.63333	41.8	3	84
1	13.6	51.14	3	84
1	5.6	67.4	3	84
1	54.65	38.08	3	180
1	30.76666	41.8	3	180
1	15.2	51.14	3	180
1	7.766666	67.4	3	180
1	61.15666	38.08	3	270
1	33.72333	41.8	3	270
1	18.71333	51.14	3	270
1	7.926666	67.4	3	270

1	58.06	38.08	3	365
1	36.07666	41.8	3	365
1	19.06	51.14	3	365
1	7.07	67.4	3	365
2	35.0333	32.16	1	7
2	14.8667	44.83	1	7
2	7.8667	55.46	1	7
2	2.8967	65.37	1	7
2	45.65781	32.16	1	28
2	19.96666	44.83	1	28
2	9.642071	55.46	1	28
2	4.293333	65.37	1	28
2	52.17195	32.16	1	56
2	23.8	44.83	1	56
2	11.9	55.46	1	56
2	4.975	65.37	1	56
2	55.23333	32.16	1	84
2	29.73333	44.83	1	84
2	14.46666	55.46	1	84
2	6.533333	65.37	1	84
2	68.76666	32.16	1	180
2	33.83333	44.83	1	180
2	16.9	55.46	1	180
2	5.7	65.37	1	180
2	80.1	32.16	1	270
2	39.73333	44.83	1	270
2	19.73333	55.46	1	270
2	6.29	65.37	1	270
2	93.41	32.16	1	365
2	37.01	44.83	1	365
2	19.77333	55.46	1	365
2	6.97	65.37	1	365
2	15.2667	38.79	2	7
2	11.1667	46.17	2	7
2	5.0000	52.91	2	7
2	2.2667	60.81	2	7
2	26.96666	38.79	2	28
2	17.36666	46.17	2	28
2	8.833333	52.91	2	28
2	3.833333	60.81	2	28
2	42.1	38.79	2	56
2	25.55	46.17	2	56
2	11.575	52.91	2	56
2	4.625	60.81	2	56
2	44.73333	38.79	2	84
2	24.83333	46.17	2	84
2	13.96666	52.91	2	84
2	5.6	60.81	2	84
2	65.96666	38.79	2	180
2	35.16666	46.17	2	180
2	15.13333	52.91	2	180
2	6.633333	60.81	2	180
2	75.25333	38.79	2	270
2	39.71	46.17	2	270
2	18.79666	52.91	2	270
2	6.536666	60.81	2	270
2	78.68333	38.79	2	365
2	41.26666	46.17	2	365
2	19.76333	52.91	2	365
2	7.49	60.81	2	365
2	10.2000	34.55	3	7
2	8.5667	40.87	3	7
2	4.6333	50	3	7
2	1.2333	62.31	3	7
2	18.93333	34.55	3	28
2	14.33333	40.87	3	28
2	5.6	50	3	28
2	2.243333	62.31	3	28

H-7

2	30	34.55	3	56
2	21.1	40.87	3	56
2	9.725	50	3	56
2	2.9	62.31	3	56
2	35.16666	34.55	3	84
2	27.2	40.87	3	84
2	12.8	50	3	84
2	4.233333	62.31	3	84
2	48.93333	34.55	3	180
2	30.06666	40.87	3	180
2	15.8	50	3	180
2	5.766666	62.31	3	180
2	59.98333	34.55	3	270
2	36.86666	40.87	3	270
2	18.12666	50	3	270
2	6.143333	62.31	3	270
2	63.13333	34.55	3	365
2	38.81	40.87	3	365
2	17.6	50	3	365
2	5.846666	62.31	3	365

□□□□□□□□□□

H.3 OUTPUT

A1	3.69647	.961293803	
A2	1	3.70000	
	24.91261	52.89322	- 12.27050
	172.84325	-196.04239	34.02081
	.962530615		
	2	3.70000	
	23.73633	56.77971	-14.31236
	176.88329	-229.73531	46.04321
	.958874919		
A3	1	3.70000	
	24.91261	52.89322	-12.27050
	172.84325	-196.04239	34.02081
	.962530615		
	2	3.70000	
	23.73633	56.77971	-14.31236
	176.88329	-229.73531	46.04321
	.958874919		

APPENDIX I: MIXTURES FOR STRENGTH

Table I.1: Mixtures for 28 day Strengths.

		PFA				Pozz-fill				
Strength (MPa)	Approximate Casting Density (kg/m ³)	1750	1500	1250	1000	Approximate Casting Density (kg/m ³)	1750	1500	1250	1000
	Approximate Porosity	30%	40%	50%	60%	Approximate Porosity	30%	40%	50%	60%
5	a/c	3.30 *	3.30 *	3.30 *	2.77	a/c	3.30 *	3.30 *	3.30 *	2.42
	w/c	1.27	1.27	1.27	1.09	w/c	1.27	1.27	1.27	0.98
	water (l)	399	341	282	220	water (l)	399	341	282	218
	cement (kg)	314	268	222	201	cement (kg)	314	268	222	222
	pfa (kg)	1037	884	731	557	pozz-fill (kg)	1037	884	731	537
	foam (l)	29	172	315	463	foam (l)	29	172	315	467
	Cost (R/m ³)	289	254	219	191	Cost (R/m ³)	173	156	138	135
	Density (kg/m ³)	1752	1505	1258	1011	Density (kg/m ³)	1752	1505	1258	1012
10	a/c	3.30 *	3.30 *	3.08		a/c	3.30 *	3.30 *	2.80	
	w/c	1.27	1.27	1.19		w/c	1.27	1.27	1.10	
	water (l)	399	341	279		water (l)	399	341	278	
	cement (kg)	314	268	234		cement (kg)	314	268	252	
	pfa (kg)	1036	884	721		pozz-fill (kg)	1037	884	705	
	foam (l)	29	172	318		foam (l)	29	172	322	
	Cost (R/m ³)	289	254	222		Cost (R/m ³)	173	156	148	
	Density (kg/m ³)	1752	1505	1258		Density (kg/m ³)	1752	1505	1258	
15	a/c	3.30 *	3.30 *	1.87		a/c	3.30 *	3.30 *	1.43	
	w/c	1.27	1.27	0.82		w/c	1.27	1.27	0.70	
	water (l)	399	341	275		water (l)	399	341	278	
	cement (kg)	314	268	335		cement (kg)	314	268	395	
	pfa (kg)	1037	884	625		pozz-fill (kg)	1037	884	562	
	foam (l)	29	172	334		foam (l)	29	172	341	
	Cost (R/m ³)	289	254	243		Cost (R/m ³)	173	156	192	
	Density (kg/m ³)	1752	1505	1259		Density (kg/m ³)	1752	1505	1260	
20	a/c	3.30 *	3.04			a/c	3.30 *	2.75		
	w/c	1.27	1.18			w/c	1.27	1.08		
	water (l)	399	338			water (l)	399	335		
	cement (kg)	314	286			cement (kg)	314	309		
	pfa (kg)	1037	869			pozz-fill (kg)	1037	849		
	foam (l)	29	176			foam (l)	29	181		
	Cost (R/m ³)	289	258			Cost (R/m ³)	173	169		
	Density (kg/m ³)	1752	1505			Density (kg/m ³)	1752	1506		

* - To prevent extrapolation of results, the ash/cement ratio has been limited to within 10% of ratios tested (therefore a/c=3.3 where larger ratios were calculated).

Table I.1 (continue): Mixtures for 28 day Strengths.

		PFA				Pozz-fill				
Strength (MPa)	Approximate Casting Density (kg/m ³)	1750	1500	1250	1000	Approximate Casting Density (kg/m ³)	1750	1500	1250	1000
	Approximate Porosity	30%	40%	50%	60%	Approximate Porosity	30%	40%	50%	60%
25	a/c	3.30 *	2.46			a/c	3.30 *	2.06		
	w/c	1.27	0.99			w/c	1.27	0.88		
	water (l)	399	333			water (l)	399	332		
	cement (kg)	314	335			cement (kg)	314	379		
	pfa (kg)	1037	825			pozz-fill (kg)	1037	782		
	foam (l)	29	185			foam (l)	29	192		
	Cost (R/m ³)	289	269			Cost (R/m ³)	173	191		
	Density (kg/m ³)	1752	1506			Density (kg/m ³)	1752	1506		
30	a/c	3.30 *	1.79			a/c	3.15	1.34		
	w/c	1.27	0.80			w/c	1.22	0.68		
	water (l)	399	333			water (l)	397	337		
	cement (kg)	314	416			cement (kg)	326	493		
	pfa (kg)	1037	744			pozz-fill (kg)	1027	663		
	foam (l)	29	197			foam (l)	32	205		
	Cost (R/m ³)	289	285			Cost (R/m ³)	177	226		
	Density (kg/m ³)	1752	1507			Density (kg/m ³)	1752	1507		
35	a/c	3.06	0.92			a/c	2.77	0.59		
	w/c	1.19	0.58			w/c	1.09	0.51		
	water (l)	396	348			water (l)	393	364		
	cement (kg)	333	595			cement (kg)	359	711		
	pfa (kg)	1020	550			pozz-fill (kg)	997	417		
	foam (l)	34	213			foam (l)	39	220		
	Cost (R/m ³)	293	318			Cost (R/m ³)	188	292		
	Density (kg/m ³)	1752	1508			Density (kg/m ³)	1753	1508		
40	a/c	2.75				a/c	2.39			
	w/c	1.08				w/c	0.97			
	water (l)	393				water (l)	390			
	cement (kg)	362				cement (kg)	401			
	pfa (kg)	995				pozz-fill (kg)	959			
	foam (l)	40				foam (l)	46			
	Cost (R/m ³)	300				Cost (R/m ³)	201			
	Density (kg/m ³)	1753				Density (kg/m ³)	1753			

- - To prevent extrapolation of results, the ash/cement ratio has been limited to within 10% of ratios tested (therefore a/c=3.3 where larger ratios were calculated).

Table I.2: Mixtures for 84 day Strengths.

		PFA				Pozz-fill				
Strength (MPa)	Approximate Casting Density (kg/m ³)	1750	1500	1250	1000	Approximate Casting Density (kg/m ³)	1750	1500	1250	1000
	Approximate Porosity	30%	40%	50%	60%	Approximate Porosity	30%	40%	50%	60%
5	a/c	3.30 *	3.30 *	3.30 *	3.30 *	a/c	3.30 *	3.30 *	3.30 *	3.30 *
	w/c	1.27	1.27	1.27	1.27	w/c	1.27	1.27	1.27	1.27
	water (l)	399	341	282	223	water (l)	399	341	282	223
	cement (kg)	314	268	222	175	cement (kg)	314	268	222	175
	pfa (kg)	1037	884	731	579	pozz-fill (kg)	1037	884	731	579
	foam (l)	29	172	315	458	foam (l)	29	172	315	458
	Cost (R/m ³)	289	254	219	185	Cost (R/m ³)	173	156	138	120
	Density (kg/m ³)	1752	1505	1258	1011	Density (kg/m ³)	1752	1505	1258	1011
10	a/c	3.30 *	3.30 *	3.30 *	1.41	a/c	3.30 *	3.30 *	3.30 *	
	w/c	1.27	1.27	1.27	0.70	w/c	1.27	1.27	1.27	
	water (l)	399	341	282	220	water (l)	399	341	282	
	cement (kg)	314	268	222	314	cement (kg)	314	268	222	
	pfa (kg)	1037	884	731	443	pozz-fill (kg)	1037	884	731	
	foam (l)	29	172	315	478	foam (l)	29	172	315	
	Cost (R/m ³)	289	254	219	213	Cost (R/m ³)	173	156	138	
	Density (kg/m ³)	1752	1505	1258	1012	Density (kg/m ³)	1752	1505	1258	
15	a/c	3.30 *	3.30 *	3.23		a/c	3.30 *	3.30 *	2.96	
	w/c	1.27	1.27	1.25		w/c	1.27	1.27	1.15	
	water (l)	399	341	281		water (l)	399	341	279	
	cement (kg)	314	268	226		cement (kg)	314	268	242	
	pfa (kg)	1037	884	728		pozz-fill (kg)	1037	884	715	
	foam (l)	29	172	316		foam (l)	29	172	319	
	Cost (R/m ³)	289	254	220		Cost (R/m ³)	173	156	144	
	Density (kg/m ³)	1752	1505	1258		Density (kg/m ³)	1752	1505	1258	
20	a/c	3.30 *	3.30 *	2.37		a/c	3.30 *	3.30 *	1.92	
	w/c	1.27	1.27	0.97		w/c	1.27	1.27	0.84	
	water (l)	399	341	275		water (l)	399	341	275	
	cement (kg)	314	268	285		cement (kg)	314	268	328	
	pfa (kg)	1037	884	675		pozz-fill (kg)	1037	884	632	
	foam (l)	29	172	327		foam (l)	29	172	333	
	Cost (R/m ³)	289	254	233		Cost (R/m ³)	173	156	172	
	Density (kg/m ³)	1752	1505	1259		Density (kg/m ³)	1752	1505	1259	

- - To prevent extrapolation of results, the ash/cement ratio has been limited to within 10% of ratios tested (therefore a/c=3.3 where larger ratios were calculated).

Table I.2 (continue): Mixtures for 84 day Strengths.

		PFA				Pozz-fill				
Strength (MPa)	Approximate Casting Density (kg/m ³)	1750	1500	1250	1000	Approximate Casting Density (kg/m ³)	1750	1500	1250	1000
	Approximate Porosity	30%	40%	50%	60%	Approximate Porosity	30%	40%	50%	60%
25	a/c	3.30 *	3.30 *			a/c	3.30 *	3.30		
	w/c	1.27	1.27			w/c	1.27	1.27		
	water (l)	399	341			water (l)	399	341		
	cement (kg)	314	268			cement (kg)	314	268		
	pfa (kg)	1037	884			pozz-fill (kg)	1037	884		
	foam (l)	29	172			foam (l)	29	172		
	Cost (R/m ³)	289	254			Cost (R/m ³)	173	156		
	Density (kg/m ³)	1752	1505			Density (kg/m ³)	1752	1505		
30	a/c	3.30 *	3.19			a/c	3.30 *	2.91		
	w/c	1.27	1.23			w/c	1.27	1.14		
	water (l)	399	339			water (l)	399	336		
	cement (kg)	314	275			cement (kg)	314	296		
	pfa (kg)	1037	878			pozz-fill (kg)	1037	861		
	foam (l)	29	174			foam (l)	29	178		
	Cost (R/m ³)	289	256			Cost (R/m ³)	173	165		
	Density (kg/m ³)	1752	1505			Density (kg/m ³)	1752	1505		
35	a/c	3.30 *	2.79			a/c	3.30 *	2.45		
	w/c	1.27	1.10			w/c	1.27	0.99		
	water (l)	399	335			water (l)	399	333		
	cement (kg)	314	305			cement (kg)	314	336		
	pfa (kg)	1037	852			pozz-fill (kg)	1037	823		
	foam (l)	29	180			foam (l)	29	186		
	Cost (R/m ³)	289	263			Cost (R/m ³)	173	178		
	Density (kg/m ³)	1752	1506			Density (kg/m ³)	1752	1506		
40	a/c	3.30 *	2.28			a/c	3.30 *	1.81		
	w/c	1.27	0.94			w/c	1.27	0.81		
	water (l)	399	332			water (l)	399	332		
	cement (kg)	314	354			cement (kg)	314	413		
	pfa (kg)	1037	807			pozz-fill (kg)	1037	747		
	foam (l)	29	188			foam (l)	29	196		
	Cost (R/m ³)	289	273			Cost (R/m ³)	173	201		
	Density (kg/m ³)	1752	1506			Density (kg/m ³)	1752	1507		

* - To prevent extrapolation of results, the ash/cement ratio has been limited to within 10% of ratios tested (therefore a/c=3.3 where larger ratios were calculated).

Table I.3: Mixtures for 180 day Strengths.

		PFA				Pozz-fill				
Strength (MPa)	Approximate Casting Density (kg/m ³)	1750	1500	1250	1000	Approximate Casting Density (kg/m ³)	1750	1500	1250	1000
	Approximate Porosity	30%	40%	50%	60%	Approximate Porosity	30%	40%	50%	60%
5	a/c	3.30 *	3.30 *	3.30 *	3.30 *	a/c	3.30 *	3.30 *	3.30 *	3.30 *
	w/c	1.27	1.27	1.27	1.27	w/c	1.27	1.27	1.27	1.27
	water (l)	399	341	282	223	water (l)	399	341	282	223
	cement (kg)	314	268	222	175	cement (kg)	314	268	222	175
	pfa (kg)	1037	884	731	579	pozz-fill (kg)	1037	884	731	579
	foam (l)	29	172	315	458	foam (l)	29	172	315	458
	Cost (R/m ³)	289	254	219	185	Cost (R/m ³)	173	156	138	120
	Density (kg/m ³)	1752	1505	1258	1011	Density (kg/m ³)	1752	1505	1258	1011
10	a/c	3.30 *	3.30 *	3.30 *	2.72	a/c	3.30 *	3.30 *	3.30 *	2.36
	w/c	1.27	1.27	1.27	1.07	w/c	1.27	1.27	1.27	0.96
	water (l)	399	341	282	219	water (l)	399	341	282	218
	cement (kg)	314	268	222	204	cement (kg)	314	268	222	226
	pfa (kg)	1037	884	731	554	pozz-fill (kg)	1037	884	731	533
	foam (l)	29	172	315	464	foam (l)	29	172	315	468
	Cost (R/m ³)	289	254	219	191	Cost (R/m ³)	173	156	138	136
	Density (kg/m ³)	1752	1505	1258	1011	Density (kg/m ³)	1752	1505	1258	1012
15	a/c	3.30 *	3.30 *	3.30 *		A/c	3.30 *	3.30 *	3.30 *	
	W/c	1.27	1.27	1.27		W/c	1.27	1.27	1.27	
	Water (l)	399	341	282		Water (l)	399	341	282	
	Cement (kg)	314	268	222		Cement (kg)	314	268	222	
	Pfa (kg)	1037	884	731		Pozz-fill (kg)	1037	884	731	
	Foam (l)	29	172	315		Foam (l)	29	172	315	
	Cost (R/m ³)	289	254	219		Cost (R/m ³)	173	156	138	
	Density (kg/m ³)	1752	1505	1258		Density (kg/m ³)	1752	1505	1258	
20	a/c	3.30 *	3.30 *	3.11		A/c	3.30 *	3.30 *	2.81	
	W/c	1.27	1.27	1.20		W/c	1.27	1.27	1.11	
	Water (l)	399	341	280		Water (l)	399	341	278	
	Cement (kg)	314	268	233		Cement (kg)	314	268	251	
	Pfa (kg)	1037	884	722		Pozz-fill (kg)	1037	884	706	
	Foam (l)	29	172	318		Foam (l)	29	172	321	
	Cost (R/m ³)	289	254	222		Cost (R/m ³)	173	156	147	
	Density (kg/m ³)	1752	1505	1258		Density (kg/m ³)	1752	1505	1258	

*- To prevent extrapolation of results, the ash/cement ratio has been limited to within 10% of ratios tested (therefore a/c=3.3 where larger ratios were calculated).

Table I.3 (continue): Mixtures for 180 day Strengths.

		PFA				Pozz-fill				
Strength (MPa)	Approximate Casting Density (kg/m ³)	1750	1500	1250	1000	Approximate Casting Density (kg/m ³)	1750	1500	1250	1000
	Approximate Porosity	30%	40%	50%	60%	Approximate Porosity	30%	40%	50%	60%
25	a/c	3.30 *	3.30 *	2.32		a/c	3.30 *	3.30 *	1.83	
	w/c	1.27	1.27	0.95		w/c	1.27	1.27	0.81	
	water (l)	399	341	275		water (l)	399	341	275	
	cement (kg)	314	268	289		cement (kg)	314	268	340	
	pfa (kg)	1037	884	671		pozz-fill (kg)	1037	884	620	
	foam (l)	29	172	328		foam (l)	29	172	335	
	Cost (R/m ³)	289	254	234		Cost (R/m ³)	173	156	175	
	Density (kg/m ³)	1752	1505	1259		Density (kg/m ³)	1752	1505	1259	
30	a/c	3.30 *	3.30 *			a/c	3.30 *	3.30 *		
	w/c	1.27	1.27			w/c	1.27	1.27		
	water (l)	399	341			water (l)	399	341		
	cement (kg)	314	268			cement (kg)	314	268		
	pfa (kg)	1037	884			pozz-fill (kg)	1037	884		
	foam (l)	29	172			foam (l)	29	172		
	Cost (R/m ³)	289	254			Cost (R/m ³)	173	156		
	Density (kg/m ³)	1752	1505			Density (kg/m ³)	1752	1505		
35	a/c	3.30 *	3.30 *			a/c	3.30 *	3.09		
	w/c	1.27	1.27			w/c	1.27	1.20		
	water (l)	399	341			water (l)	399	338		
	cement (kg)	314	268			cement (kg)	314	282		
	pfa (kg)	1037	884			pozz-fill (kg)	1037	872		
	foam (l)	29	172			foam (l)	29	176		
	Cost (R/m ³)	289	254			Cost (R/m ³)	173	160		
	Density (kg/m ³)	1752	1505			Density (kg/m ³)	1752	1505		
40	a/c	3.30 *	3.06			a/c	3.30 *	2.76		
	w/c	1.27	1.19			w/c	1.27	1.09		
	water (l)	399	338			water (l)	399	335		
	cement (kg)	314	284			cement (kg)	314	308		
	pfa (kg)	1037	870			pozz-fill (kg)	1037	849		
	foam (l)	29	176			foam (l)	29	181		
	Cost (R/m ³)	289	258			Cost (R/m ³)	173	169		
	Density (kg/m ³)	1752	1505			Density (kg/m ³)	1752	1506		

*- To prevent extrapolation of results, the ash/cement ratio has been limited to within 10% of ratios tested (therefore a/c=3.3 where larger ratios were calculated).

Table I.4: Mixtures for 365 day Strengths.

		PFA				Pozz-fill				
Strength (MPa)	Approximate Casting Density (kg/m ³)	1750	1500	1250	1000	Approximate Casting Density (kg/m ³)	1750	1500	1250	1000
	Approximate Porosity	30%	40%	50%	60%	Approximate Porosity	30%	40%	50%	60%
5	a/c	3.30 *	3.30 *	3.30 *	3.30 *	a/c	3.30 *	3.30 *	3.30 *	3.30 *
	w/c	1.27	1.27	1.27	1.27	w/c	1.27	1.27	1.27	1.27
	water (l)	399	341	282	223	water (l)	399	341	282	223
	cement (kg)	314	268	222	175	cement (kg)	314	268	222	175
	pfa (kg)	1037	884	731	579	pozz-fill (kg)	1037	884	731	579
	foam (l)	29	172	315	458	foam (l)	29	172	315	458
	Cost (R/m ³)	289	254	219	185	Cost (R/m ³)	173	156	138	120
	Density (kg/m ³)	1752	1505	1258	1011	Density (kg/m ³)	1752	1505	1258	1011
10	a/c	3.30 *	3.30 *	3.30 *	3.21	a/c	3.30 *	3.30 *	3.30 *	2.92
	w/c	1.27	1.27	1.27	1.24	w/c	1.27	1.27	1.27	1.14
	water (l)	399	341	282	222	water (l)	399	341	282	220
	cement (kg)	314	268	222	179	cement (kg)	314	268	222	193
	pfa (kg)	1037	884	731	576	pozz-fill (kg)	1037	884	731	564
	foam (l)	29	172	315	459	foam (l)	29	172	315	462
	Cost (R/m ³)	289	254	219	186	Cost (R/m ³)	173	156	138	126
	Density (kg/m ³)	1752	1505	1258	1011	Density (kg/m ³)	1752	1505	1258	1011
15	a/c	3.30 *	3.30 *	3.30 *		A/c	3.30 *	3.30 *	3.30 *	
	W/c	1.27	1.27	1.27		W/c	1.27	1.27	1.27	
	Water (l)	399	341	282		Water (l)	399	341	282	
	Cement (kg)	314	268	222		Cement (kg)	314	268	222	
	Pfa (kg)	1037	884	731		Pozz-fill (kg)	1037	884	731	
	Foam (l)	29	172	315		Foam (l)	29	172	315	
	Cost (R/m ³)	289	254	219		Cost (R/m ³)	173	156	138	
	Density (kg/m ³)	1752	1505	1258		Density (kg/m ³)	1752	1505	1258	
20	a/c	3.30 *	3.30 *	3.30 *		A/c	3.30 *	3.30 *	3.21	
	W/c	1.27	1.27	1.27		W/c	1.27	1.27	1.24	
	Water (l)	399	341	282		Water (l)	399	341	281	
	Cement (kg)	314	268	222		Cement (kg)	314	268	227	
	Pfa (kg)	1037	884	731		Pozz-fill (kg)	1037	884	727	
	Foam (l)	29	172	315		Foam (l)	29	172	316	
	Cost (R/m ³)	289	254	219		Cost (R/m ³)	173	156	140	
	Density (kg/m ³)	1752	1505	1258		Density (kg/m ³)	1752	1505	1258	

*- To prevent extrapolation of results, the ash/cement ratio has been limited to within 10% of ratios tested (therefore a/c=3.3 where larger ratios were calculated).

Table I.4 (continue): Mixtures for 365 day Strengths.

		PFA				Pozz-fill				
Strength (MPa)	Approximate Casting Density (kg/m ³)	1750	1500	1250	1000	Approximate Casting Density (kg/m ³)	1750	1500	1250	1000
	Approximate Porosity	30%	40%	50%	60%	Approximate Porosity	30%	40%	50%	60%
25	a/c	3.30 *	3.30 *	2.98		a/c	3.30 *	3.30 *	2.67	
	w/c	1.27	1.27	1.16		w/c	1.27	1.27	1.06	
	water (l)	399	341	279		water (l)	399	341	277	
	cement (kg)	314	268	240		cement (kg)	314	268	261	
	pfa (kg)	1037	884	716		pozz-fill (kg)	1037	884	697	
	foam (l)	29	172	319		foam (l)	29	172	323	
	Cost (R/m ³)	289	254	224		Cost (R/m ³)	173	156	151	
	Density (kg/m ³)	1752	1505	1258		Density (kg/m ³)	1752	1505	1259	
30	a/c	3.30 *	3.30 *	2.19		a/c	3.30 *	3.30 *		
	w/c	1.27	1.27	0.91		w/c	1.27	1.27		
	water (l)	399	341	275		water (l)	399	341		
	cement (kg)	314	268	301		cement (kg)	314	268		
	pfa (kg)	1037	884	659		pozz-fill (kg)	1037	884		
	foam (l)	29	172	330		foam (l)	29	172		
	Cost (R/m ³)	289	254	237		Cost (R/m ³)	173	156		
	Density (kg/m ³)	1752	1505	1259		Density (kg/m ³)	1752	1505		
35	a/c	3.30 *	3.30 *			a/c	3.30 *	3.30 *		
	w/c	1.27	1.27			w/c	1.27	1.27		
	water (l)	399	341			water (l)	399	341		
	cement (kg)	314	268			cement (kg)	314	268		
	pfa (kg)	1037	884			pozz-fill (kg)	1037	884		
	foam (l)	29	172			foam (l)	29	172		
	Cost (R/m ³)	289	254			Cost (R/m ³)	173	156		
	Density (kg/m ³)	1752	1505			Density (kg/m ³)	1752	1505		
40	a/c	3.30 *	3.30 *			a/c	3.30 *	3.17		
	w/c	1.27	1.27			w/c	1.27	1.23		
	water (l)	399	341			water (l)	399	339		
	cement (kg)	314	268			cement (kg)	314	276		
	pfa (kg)	1037	884			pozz-fill (kg)	1037	877		
	foam (l)	29	172			foam (l)	29	174		
	Cost (R/m ³)	289	254			Cost (R/m ³)	173	158		
	Density (kg/m ³)	1752	1505			Density (kg/m ³)	1752	1505		

*- To prevent extrapolation of results, the ash/cement ratio has been limited to within 10% of ratios tested (therefore a/c=3.3 where larger ratios were calculated).